

**An investigation into the stress response
mechanisms and virulence of the human fungal
pathogen, *Candida albicans*.**

Mèlanie Adaora Céline Ikeh

Thesis submitted in partial fulfilment of the requirements
of the regulations for the degree of Doctor of Philosophy

Faculty of Medical Sciences
Institute of Cell and Molecular Biosciences
Newcastle University

September 2015

Declaration

I certify that this thesis contains my own work, except where acknowledged, and that no part of this material has been previously submitted for a degree or any other qualification at this or any other university.

Abstract

Candida albicans is a major fungal pathogen causing life threatening systemic infections in immunocompromised humans. While in the host *C. albicans* is exposed to a range of stresses during phagocytosis by host innate immune cells, including reactive oxygen species (ROS), cationic fluxes, and fluctuations in pH. The ability of *C. albicans* to adapt to such stresses is essential for survival and pathogenesis. Despite this, however, there is still much to be learnt regarding the stress responsive mechanisms mounted by this major pathogen. Hence, the overarching goal of this project was to provide novel insight into the cellular processes necessary to enable stress adaptation and virulence of *C. albicans*. To facilitate this, quantitative fitness analysis (QFA) of two *C. albicans* deletion libraries was performed using inducers of superoxide, cationic, and alkaline pH stresses. GO term analysis of sensitive genes highlighted distinct and overlapping biological processes, molecular functions, and cellular components enriched during adaptation to each stress. Notably, the importance of ion binding for resistance to cationic and superoxide stress was revealed, whereas cell wall biogenesis was enriched for alkaline pH stress. QFA also identified several regulatory genes not previously implicated in stress responses, including the Pho4 transcription factor.

Cells lacking *PHO4* were acutely sensitive to all three stresses tested and thus the role of Pho4 in mediating stress resistance was investigated further. Additional phenotypic testing revealed *pho4Δ* cells display impaired resistance to several organic and metal cations, and defects in morphogenic switching. Similar to Pho4 function in *S. cerevisiae*, deleting *PHO4* in *C. albicans* completely abolished acquisition and accumulation of phosphate stored as polyphosphate (polyP) in the vacuole. Consistent with stress resistance and nutrient acquisition being important virulence determinants in *C. albicans*, cells lacking *PHO4* were acutely sensitive to macrophage-mediated killing, and displayed attenuated virulence in *Caenorhabditis elegans* and murine models of infection. Further analysis of the role and regulation of Pho4 in stress adaptation in *C. albicans* revealed that in addition to the essential role of Pho4 in phosphate acquisition and storage, which enables survival in phosphate limiting and alkaline pH conditions, Pho4 function is also important for metal ion homeostasis which is essential for cationic and superoxide stress resistance.

As *C. albicans* only causes systemic infections in immunocompromised hosts, the final objective of this study was to explore whether the immune status of the host dictated the importance of key stress regulators in promoting the virulence of this fungal pathogen. Although the Hog1 stress activated protein kinase and the Pho4 transcription factor were demonstrated to be essential for *C. albicans* virulence in the model mini host *C. elegans*, both were dispensable for virulence upon infection of immunocompromised worms. These findings infer that robust stress responses of *C. albicans* may only be required for virulence when immune responses are evoked in an immunocompetent host.

Taken together, the data presented in this thesis highlight that metabolic adaptation is essential for the survival of *C. albicans* to host-imposed stresses, and that the immune status of the host may govern the importance of stress protective mechanisms in mediating the virulence of this major fungal pathogen.

Acknowledgements

I would like to express the deepest appreciation to my supervisor, Prof Jan Quinn who was abundantly helpful and offered invaluable assistance, support and guidance. Because of your exasperating attention to detail I have finally learnt how to properly write gene and protein symbols in a consistent manner! Thanks for sharing your wealth of knowledge. Deepest gratitude are also due to my secondary supervisor, Dr Elizabeth Veal for insightful comments and encouragement. I could not have had a better supervisory team for my PhD study.

This research project would not have been possible without the support and expertise of many people. These are Prof Alister Brown, Prof Lars Erwig, Dr Peter Banks, Dr Carmen Herrero de Dios, Dr Judith Bain, Dr Jeremy Palmer, Dr Julian Rutherford, Prof Brian Morgan, Dr Simon Whitehall, Dr Kevin Waldron, and Stavroula Kastora. Past and current members of the JQ lab, Dr Debbie Smith, Dr Alessandra da Silva Dantas, and Dr Alison Day. Your extensive expertise and willingness to help made this journey a much enriched experience. I would also like to thank my progress review panel, Dr Jeremy Brown and Dr Claudia Schneider for their continued support and encouragement throughout the PhD. Big thanks to Michelle Wray for technical support and willingness to help.

I would also like to acknowledge my fellow PhD students who constantly reminded me there is life outside science; Dr Emma, Dr Ellen, Dr Csenge, Kate, Heather, Clare, Slava, Syatirah, Faye, Faye, Zoe, Johny, and Alex. Thanks for the stimulating discussions, support, good times, and cake. Keep up the hard work, it pays off in the end.

Also I would like to thank my friends, too numerous to mention but you know who you are. Thanks for being there for me, your support and prayers kept me going these last four years. I look forward to catching up with you all.

And most importantly, a massive THANK YOU goes to my parents. Endless gratitude. This work is dedicated to you both for making me who I am. My sisters, Lisa, Jules, Sue, Gela, Sylvia, and Steph for your continuous love and support. Nephews, Terry, Bobby, Ashley, Max, Joey, Micky, and Zara and nieces, Nicole, Michelle, Sammy, Nina, and Serena.

Abbreviations

Ala	Alanine
ALS	Agglutinin-like sequence
AP-1	Activating protein 1
ATP	Adenosine Triphosphate
AP1	Activating protein 1-like
APEC	Avian pathogenic <i>E. coli</i>
B cells	B lymphocytes
BHI	Brain Heart Infusion
bHLH	Basic helix loop helix
BSA	Bovine serum albumin
<i>C. albicans</i>	<i>Candida albicans</i>
<i>C. elegans</i>	<i>Caenorhabditis elegans</i>
cAMP	Cyclic adenosine monophosphate
Cap1	<i>Candida</i> AP-1
CDK	Cyclin dependent kinase
cCRD	C-terminal cysteine rich domain
CGD	Candida Genome Database
CR1-3	Complement receptor 1-3
CSR	Core stress response
Cys	Cysteine
<i>C. neoformans</i>	<i>Cryptococcus neoformans</i>
DAPI	4'-6-diamidino-2-phenylindole
dATP	Deoxyadenosine triphosphate
dCTP	Deoxycytidine triphosphate
dGTP	Deoxyguanosine triphosphate
DMSO	Dimethyl sulphoxide
DNA	Deoxyribonucleic acid
dTTP	Deoxythymidine triphosphate
<i>E. coli</i>	<i>Escherichia coli</i>
ExPEC	Extra-intestinal pathogenic <i>E. coli</i>
g	Gram
GIT3	Glycerophosphodiester transporter
GFP	Green fluorescent protein

Gpx	Glutathione peroxidase
Grx	Glutaredoxin
GSH	Reduced glutathione
GSSH	Oxidised glutathione
GST	Glutathione-S-transferase
GTP	Guanosine triphosphate
HRP	Horse radish peroxidase
H ₂ O ₂	Hydrogen peroxide
ICP-MS	Inductively coupled plasma mass spectrometry
IL	Interleukin
IFN	Interferon
Kb	Kilobase
kDa	Kilodalton
LB	Luria broth
LiAc	Lithium Acetate
LIP	Lipases
Lys	Lysine
M	Molar
μ	Micro
MAPK	Mitogen activated protein kinase
MAPKK	Mitogen activated protein kinase kinase
MAPKKK	Mitogen activated protein kinase kinase kinase
Min	Minute(s)
mM	Millimolar
MR	Mannose receptor
mRNA	Messenger RNA
MW	Molecular weight
NADPH	Nicotinamide adenine dinucleotide
nCRD	N-terminal cysteine rich domain
NF-β	nuclear factor kappa-light-chain-enhancer of activated B cells
NGM_L	Nematode Growth Media Lite
nmol	Nano molar
NO	Nitric oxide
NO•	Nitric oxide radical
NO ₂ -	Nitrite

NOS	Nitric oxide synthase
NS	No stress
O ₂	Molecular oxygen
O ₂ ^{•-}	Superoxide
OD	Optical density
OH [•]	Hydroxyl radical
OH ⁻	Hydroxyl anion
ONOO ⁻	Peroxynitrite
ORF	Open reading frame
OS	Osmotic stress
PAMP	Pathogen associated molecular patterns
Pap1	<i>pombe</i> AP-1
PCR	Polymerase chain reaction
PEG	Polyethyl glycol
Phe	Phenylalanine
PHO	Phosphate
phox	Phagocytic oxidase
Pi	Phosphate
PKA	Protein kinase A
PL	Phospholipases
PLB	Protein lysis buffer
PMSF	Phenylmethyl sulphonyl fluoride
PNMC	Peptone NaCl Magnesium Chloride
Ppn	Endopolyphosphatase
Ppx	Exopolyphosphatase
Pro	Proline
PRR	Pattern recognition receptors
Prx	Peroxiredoxin
PolyP	Polyphosphate
PTM	Post translational modification
QFA	Quantitative Fitness Analysis
RCS	Reactive chlorine species
RHE	Reconstituted human epithelial cells
RNS	Reactive nitrogen species
RNA	Ribonucleic acid

ROS	Reactive oxygen species
rpm	Revolutions per minute
SAP	Secreted aspartyl proteinases
SAPK	Stress activated protein kinase
<i>S. cerevisiae</i>	<i>Saccharomyces cerevisiae</i>
SDS	Sodium dodecyl sulphate
SDS-PAGE	SDS polyacrylamide gel electrophoresis
SIS	Stress Interactive Score
Sod	Superoxide dismutase
SP	Serine-Proline
<i>S. pombe</i>	<i>Schizosaccharomyces pombe</i>
SsDNA	Salmon sperm DNA
SUMO	Sumoylation
T cells	T lymphocytes
<i>T. brucei</i>	<i>Trypanosoma brucei</i>
Th	T helper lymphocytes
TF	Transcription factor
Thr	Threonine
TLR	Toll like receptor
TNF	Tumor necrosis factor
Trr	Thioredoxin reductase
Trx	Thioredoxin
Tyr	Tyrosine
UPEC	Uropathogenic <i>E. coli</i>
VTC	Vacuolar transport chaperone
XS	Oxidative stress
Yap1	Yeast AP-1
Ybp	Yap binding protein
YRE	Yap responsive element
°C	Degrees Celsius
Δ	Gene deletion

Table of Contents

Chapter 1. Introduction.....	1
1.1 <i>Candida albicans</i>	1
1.2 Virulence Determinants of <i>C. albicans</i>	2
1.2.1 Morphogenesis	2
1.2.2 Adhesins	3
1.2.3 Hydrolytic enzymes	4
1.2.4 Adaptation to host environments.....	6
1.3 Immune response of the host against <i>C. albicans</i>	9
1.3.1 Recognition of <i>C. albicans</i> by innate immune cells.....	9
1.3.2 Adaptive immune responses.....	10
1.3.3 Innate Immune responses.....	11
1.4 Stresses encountered within the host.....	13
1.4.1 Oxidative stress.....	13
1.4.1.1 Sources of reactive oxygen species.....	13
1.4.1.2 Cellular effects of oxidative stress.....	13
1.4.1.3 Oxidative stress response.....	14
1.4.2 Cationic stress.....	17
1.4.2.1 Sources of cations.....	17
1.4.2.2 Cellular effects of cationic stress.....	18
1.4.2.3 Cationic stress response.....	18
1.4.3 pH stress.....	19
1.4.3.1 pH diversity in the human host.....	19
1.4.3.2 Cellular effects of pH stress.....	20
1.4.3.3 pH stress response.....	21
1.4.4 Nutrient limitation.....	21
1.4.4.1 Metabolic flexibility.....	22
1.4.4.1.1 Alternative carbon sources.....	22
1.4.4.1.2 Nitrogen limiting conditions.....	22

1.4.4.1.3 Amino acids limiting conditions.....	22
1.4.4.1.4 Phosphate limiting conditions.....	23
1.4.4.2 Nutritional immunity.....	24
1.4.4.2.1 Iron acquisition.....	24
1.4.4.2.2 Zinc acquisition.....	25
1.4.4.2.3 Copper and Manganese acquisition.....	25
1.4.4.3 Nutritional responses and impact on stress resistance and virulence.....	25
1.4.5 Additional stress responses mounted by <i>C. albicans</i> .	
1.4.5.1 Downregulation of the translation machinery	
1.4.5.2 Accumulation of P bodies	
1.5 Stress-responsive signalling pathways and transcription factors.....	26
1.5.1 Cationic stress signalling.....	27
1.5.1.1 SAPK Hog 1 pathway.....	27
1.5.2 Oxidative stress signalling.....	27
1.5.2.1 SAPK Hog 1 pathway.....	27
1.5.2.2 Rad53 DNA damage checkpoint kinase.....	30
1.5.2.3 Cap1 transcription factor	31
1.5.2.4 Skn7 transcription factor	31
1.5.3 pH signalling.....	31
1.5.3.1 Rim101 pH response pathway.....	31
1.5.3.2 Calcineurin/Crz1 pathway.....	35
1.6 Summary and Aims.....	36
Chapter 2. Material and Methods.....	38
2.1 Yeast Techniques.....	38
2.1.1 <i>C. albicans</i> strains, deletion libraries, and growth conditions.....	38
2.1.2 Transformation of <i>C. albicans</i>	38
2.1.3 Yeast Genomic DNA extraction.....	40
2.1.4 <i>C. albicans</i> strain construction.....	41
2.1.4.1 Deletion of <i>VTC1</i> , <i>VTC4</i> , <i>PHM5</i> , <i>PHM7</i> , and <i>PPX1</i>	41

2.1.4.1 Tagging Pho4.....	44
2.2 Phenotypic Tests.....	47
2.2.1 Quantitative Fitness Analysis.....	47
2.2.2 Spot tests.....	48
2.3 <i>Caenorhabditis elegans</i> techniques.....	48
2.3.1 <i>C. elegans</i> strains.....	48
2.3.2 Preparation of Nematode Growth Media Lite (NGML) plates.....	48
2.3.3 Bacterial food source preparation.....	49
2.3.4 Maintenance of <i>C. elegans</i> stock strains.....	49
2.3.5 Synchronicity of nematodes.....	49
2.4 Molecular biology techniques.....	50
2.4.1 Polymerase chain reaction.....	50
2.4.2 Oligonucleotide primer sequences.....	50
2.4.3 Restriction endonuclease digestion, phosphatase treatment and DNA ligation reactions.....	52
2.4.4 Bacterial growth conditions and transformations.....	52
2.4.5 Electrophoresis.....	53
2.4.6 Plasmid DNA extraction.....	53
2.4.7 DNA sequencing.....	54
2.5 RNA analysis.....	54
2.5.1 Growth conditions for RNA preparation.....	54
2.5.2 RNA extraction for Northern blotting.....	54
2.5.3 RNA extraction for RNA Seq analysis.....	54
2.5.4 Northern blotting.....	55
2.5.5 RNA Seq alignment and analysis.....	55
2.6 Protein analysis.....	57
2.6.1 <i>C. albicans</i> protein extraction.....	57
2.6.2 <i>C. elegans</i> protein extraction.....	57
2.6.3 SDS-PAGE and Western blotting.....	58
2.6.4 <i>C. albicans</i> Pho4 phosphorylation assay.....	58
2.6.5 <i>C. albicans</i> Hog1 phosphorylation assay.....	58

2.6.6	<i>C. elegans</i> Pmk1 phosphorylation assay.....	59
2.6.7	Lambda phosphatase treatments.....	59
2.6.8	Sod in-gel activity assay.....	59
2.7	<i>C. albicans</i> polyphosphate (polyP) analysis.....	60
2.7.1	Growth conditions for polyP detection.....	60
2.7.2	PolyP extraction.....	60
2.7.3	PolyP detection by UREA-PAGE and Toluidine Staining.....	60
2.8	Other biochemical techniques used.....	61
2.8.1	Secreted acid phosphatase activity detection assay.....	61
2.8.2	Inductively coupled plasma mass spectrometry (ICP-MS).....	61
2.9	Microscopy.....	61
2.9.1	Pho4 localisation kinetics and fluorescence microscopy.....	62
2.9.2	Yeast to hyphae transition assay.....	62
2.9.3	PolyP detection by Neisser staining.....	62
2.10	Virulence assays.....	63
2.10.1	<i>C. elegans</i> infection assay.....	63
2.10.2	Mouse model of systemic infection.....	63
2.10.3	Macrophage killing assay.....	63
2.10.4	Macrophage live cell video microscopy phagocytosis assay.....	64
 Chapter 3. Global analysis of <i>C. albicans</i> genes required for resistance to physiologically relevant stresses.....		65
3.1	Introduction.....	65
3.2	Results.....	67
3.2.1	Quantitative fitness analysis of genes that confer sensitivity to superoxide, cationic, and alkaline pH resistance.....	67
3.2.1.1	Mutants sensitive to superoxide stress.....	70
3.2.1.2	Mutants sensitive to cationic stress.....	74
3.2.1.3	Mutants sensitive to alkaline pH stress.....	75
3.2.1.4	QFA identifies overlapping genes required for resistance.....	76
3.2.2	Gene Ontology analysis of genes required for superoxide, cationic, and alkaline pH stress resistance.....	79

3.2.2.1 GO analysis of <i>C. albicans</i> homozygous deletion collection....	79
3.3. Discussion.....	91
Chapter 4. The role of Pho4 in phosphate homeostasis in <i>C. albicans</i>.....	97
4.1 Introduction.....	97
4.2 Results.....	98
4.2.1 Sequence alignment of <i>S. cerevisiae</i> Pho4 and <i>C. albicans</i> Pho4 reveals divergence.....	98
4.2.2 Pho4 is required for phosphate acquisition in <i>C. albicans</i>	100
4.2.3 Pho4 is required for phosphate storage and mobilisation in response to phosphate limitation.....	102
4.2.4 Pho4 accumulates in the nucleus in response to Pi limitation.....	102
4.2.5 Nuclear export of Pho4 is regulated by phosphorylation and an additional PTM in phosphate-rich conditions.....	105
4.2.6 Genome-wide analysis to identify genes required for phosphate homeostasis.....	106
4.2.7 Comparison of the transcriptional responses to phosphate limitation between <i>C. albicans</i> and <i>S. cerevisiae</i>	111
4.2.8 Stress resistance is not associated with defective acid phosphatase activity.....	112
4.3 Discussion.....	115
Chapter 5. The role of Pho4 in stress adaptation.....	119
5.1 Introduction.....	119
5.2 Results.....	120
5.2.1 Cells lacking PHO4 display other pleiotropic stress phenotypes.....	120
5.2.2 Pho4 does not accumulate in the nucleus following cationic or superoxide stress.....	122
5.2.3 PolyP is mobilised in response to specific stresses.....	124
5.2.4 PolyP is not required for Pho4-mediated stress resistance.....	128
5.2.5 Pho4 dependent genes and stress phenotypes.....	133
5.2.6 Investigation into the relationship between Hog1 and Pho4 signalling.....	140
5.2.7 Investigating the role of Pho4 in phosphate homeostasis and cationic sensitivity.....	140

5.2.8 Pho4 is required for Superoxide dismutase (Sod1) activity.....	143
5.3 Discussion.....	146
5.3.1 Pho4 mediated phosphate acquisition is vital for alkaline pH resistance.....	146
5.3.2 Polyphosphate and stress resistance in <i>C. albicans</i>	146
5.3.3 Phosphate, metal homeostasis and bioavailability.....	149
Chapter 6. The role of Pho4 in virulence.....	152
6.1 Introduction.....	152
6.2 Results.....	153
6.2.1 Pho4 is required for <i>C. albicans</i> survival following phagocytosis by macrophages.....	153
6.2.2 Pho4 is required for disseminated systemic infection in a mouse model of infection.....	158
6.2.3 Pho4 is required for virulence in an immunocompetent, but not immunocompromised, <i>C. elegans</i> nematode host.....	160
6.2.4 <i>C. elegans</i> Pmk1 is activated and declines over time during <i>C. albicans</i> infection.....	163
6.2.5 <i>C. albicans</i> Hog1 SAPK pathway is activated during <i>C. elegans</i> infection	164
6.3 Discussion.....	165
Chapter 7. Final Discussion.....	170
7.1 Summary.....	170
7.2 Global overview of genes required for stress resistance in <i>C. albicans</i>	170
7.3 Role of Pho4 in phosphate homeostasis in <i>C. albicans</i>	171
7.4 Role of Pho4 in stress resistance in <i>C. albicans</i>	173
7.5 Role of Pho4 in virulence in <i>C. albicans</i>	174
7.6 Concluding Remarks.....	175
Chapter 8. References.....	177
Appendix.....	203

List of Figures

Chapter 1

- Figure 1.1 Diagrammatic representation of the stresses encountered by *C. albicans* in various host niches.....7
- Figure 1.2 Osmotic stress signalling to the Hog1 SAPK pathway in *C. albicans*.....28
- Figure 1.3 Oxidative stress responsive signalling pathways in *C. albicans*.....30
- Figure 1.4 Alkaline pH response pathway in *C. albicans*.....34

Chapter 2

- Figure 2.1 Schematic diagram illustrating strategy used to delete *VTC1*, *VTC4*, *PHM5*, *PHM7*, and *PPX1* in *C. albicans*.....43
- Figure 2.2 Schematic diagram illustrating strategy used to myc-HIS tag *PHO4*.....45
- Figure 2.3 Schematic diagram illustrating the construction of p*PHO4*-GFP.....46

Chapter 3

- Figure 3.1 QFA fitness plots of *C. albicans* deletion collections.....69
- Figure 3.2 Spot test confirmation of sensitive genes identified by QFA.....70
- Figure 3.3 Distinct and overlapping genes required for superoxide, cationic, and alkaline pH stresses.....77
- Figure 3.4 Distribution of enriched functional GO categories of genes required for cationic, superoxide, and alkaline pH8 stresses.....81

Chapter 4

- Figure 4.1 Sequence alignment of *S. cerevisiae* Pho4 and *C. albicans* Pho4.....99
- Figure 4.2 Pho4 is required for phosphate acquisition and storage.....102
- Figure 4.3 Tagging Pho4 in wild-type *C. albicans* does not affect protein functionality103
- Figure 4.4 Pho4 nuclear accumulation and polyP mobilisation.....104
- Figure 4.5 MycHis Tagging Pho4 in wild-type *C. albicans* does not affect protein functionality.....106
- Figure 4.6 Genome response to phosphate limitation in *C. albicans*.....107
- Figure 4.7 Heat map of GO biological processes.....109

Figure 4.8 <i>C. albicans</i> genes containing promoter ScPho4 consensus binding site.....	110
Figure 4.9 Pho4 targets genes in <i>C. albicans</i>	111
Figure 4.10 Identification of genes with defective secreted acid phosphatase activity.....	113

Chapter 5

Figure 5.1 Cells lacking <i>PHO4</i> display pleiotropic stress phenotypes.....	121
Figure 5.2 Pho4 localisation in response to specific stress treatments.....	123
Figure 5.3 Pho4 regulates <i>PHO84</i> induction in response to alkaline pH stress.....	124
Figure 5.4 Poly-P is mobilised in response to specific stresses.....	125
Figure 5.5 PolyP is rapidly mobilized under alkaline pH stress.....	126
Figure 5.6 Poly-P is mobilised in response to hypo osmotic stress.....	127
Figure 5.7 Poly-P is mobilised in response to hyperosmotic stress.....	128
Figure 5.8 The VTC complex proteins (Vtc1 and Vtc4) and Phm5, Phm7, and Ppx1 are involved in polyP metabolism in <i>C. albicans</i>	130
Figure 5.9 PolyP is dispensable for Pho4-dependent stress sensitive phenotypes.....	132
Figure 5.10 Pho4 accumulates in the nucleus in the <i>vtc1</i> and <i>vtc4</i> mutants under phosphate-limiting conditions.....	133
Figure 5.11 Pho4 targets genes in <i>C. albicans</i>	134
Figure 5.12 Processes deregulated in <i>pho4Δ</i> cells under phosphate replete conditions.....	136
Figure 5.13 Cationic stress-induced modification of Pho4.....	138
Figure 5.14 The relationship between Hog1 and Pho4.....	139
Figure 5.15 Loss of Pho4 impacts on cation homeostasis.....	141
Figure 5.16 Expression of <i>ENA2</i> and <i>ENA21</i> under cationic stress are also not dependent on Pho4.....	143
Figure 5.17 Pho4 is required for the activity of the Sod1 superoxide dismutase.....	145

Chapter 6

Figure 6.1 Pho4 is required for virulence in a macrophage model of infection.....	154
Figure 6.2 Uptake of <i>C. albicans</i> cells is not affected by <i>PHO4</i> deletion.....	155
Figure 6.3 J774.1 cells survive co-culture with <i>pho4Δ</i> cells.....	156

Figure 6.4 Defect in hyphal formation associated with Pho4 loss.....	157
Figure 6.5 Deletion of <i>PHO4</i> increases susceptibility to macrophage killing.....	158
Figure 6.6 Pho4 is required for virulence in a mouse model of infection.....	159
Figure 6.7 Pho4 is required for <i>C. albicans</i> virulence in immunocompetent, but not in immunocompromised, <i>C. elegans</i> worms.....	161
Figure 6.8 Hog1 is required for <i>C. albicans</i> virulence in immunocompetent, but not in immunocompromised, <i>C. elegans</i> worms.....	162
Figure 6.9 Phosphorylation status of <i>C. elegans</i> and <i>C. albicans</i> SAPKs following infection.....	164
Figure 6.10 <i>C. albicans</i> Hog1 SAPK is activated during <i>C. elegans</i> infection.....	165

Chapter 7

Figure 7.1 Proposed model of phosphate regulation in <i>C. albicans</i>	173
Figure 7.2 Model depicting the multifaceted roles of Pho4 in mediating stress resistance and virulence.....	176

List of Tables

Chapter 2

Table 2.1 <i>C. albicans</i> strains used in this study.....	38
Table 2.2 Oligonucleotide primers used in the study.....	51
Table 2.3 Oligonucleotide primers used in the study to amplify probes for Northern blotting.....	56

Chapter 3

Table 3.1 Transcription factors required for stress resistance.....	71
Table 3.2 Genes required for stress resistance.....	72
Table 3.3 Genes required to resist all three stress-inducing conditions.....	77
Table 3.4 Overlapping and distinct GO terms required for cationic, superoxide, and alkaline pH stress resistance.....	83
Table 3.5 Distinct biological processes regulated by TFs under cationic, superoxide, and alkaline pH stress.....	89
Table 3.6 Protein kinases, signalling proteins, and GTPases identified by QFA.....	90

Chapter 4

Table 4.1 <i>C. albicans</i> strains with defective acid phosphatase activity.....	114
--	-----

Chapter 1. Introduction

1.1 *Candida albicans*.

Candida albicans typically exists as a benign fungal organism forming part of the human body flora. In most healthy hosts, *C. albicans* is found in various niches such as the skin and mucosal membranes (mouth, genital area, and gastrointestinal tract) which reflects the diverse environments colonised within the host. Under certain conditions, *C. albicans* becomes pathogenic causing both superficial and life threatening systemic infections. The host immune system plays an essential role in preventing *C. albicans* infections. However, when the immune system is suppressed (as seen with transplant or cancer patients) or impaired (for example in AIDS patients) defence mechanisms are defective leading to bloodstream entry and dissemination of the fungus to numerous internal organs (Calderone and Clancy, 2012).

The superficial infections caused by *C. albicans* are usually benign and affect the cutaneous or mucocutaneous tissues and include oropharyngeal candidiasis, vaginitis, conjunctivitis or gastrointestinal candidiasis. These infections occur mainly as a result of any perturbation of the protective bacterial normal flora following, for example antibiotic treatment (Rafii *et al.*, 2008). Increased susceptibility to vaginitis is commonly associated with pregnancy and use of contraceptives (Sobel, 1985). Life threatening systemic infections ensue when the fungus gains access to the bloodstream for instance, following use of indwelling medical devices such as catheters or pace makers, causing a range of infections including endocarditis and disseminated candidiasis (Calandra *et al.*, 1989; Sanchez-Portocarrero *et al.*, 2000).

Superficial infections are easily treated with antifungals, however, this is not the case with systemic infections. Delays in diagnosing candidiasis, limited available antifungals, as well as the emergence of drug resistant *C. albicans* strains, has resulted in an unacceptably high mortality rate of around 40% (Brown *et al.*, 2012; Ostrosky-Zeichner *et al.*, 2003; Cowen *et al.*, 2014). Another major concern is the increase in number of immunocompromised individuals which has contributed significantly to the number of infections due to *C. albicans* (Pfaller and Diekema, 2007 and 2010). In HIV patients alone more than 90% will develop candidiasis (de Repentigny *et al.*, 2004). In addition, this opportunistic pathogen is one of the leading causes of nosocomial infections being the fourth most frequently isolated organism

from blood cultures (Sanchez-Portocarrero *et al.*, 2000; Tabah *et al.*, 2012). Therefore, intensive research into the virulence mechanisms of *C. albicans* is required to enable the development of new antifungal treatments. In this introduction, the major virulence determinants of *C. albicans* are reviewed and an overview of the immune defence mechanisms that operate in healthy individuals to prevent candidiasis is presented. The overall goal of this project was to investigate *C. albicans* stress response mechanisms and their importance in virulence. Thus, a detailed description of host-imposed stresses used to prevent *C. albicans* infection, together with a summary of the current knowledge of how this major fungal pathogen adapts and survives exposure to such host imposed stresses, is also presented.

1.2 Virulence determinants of *C. albicans*.

The ability of *C. albicans* to exist as a commensal or pathogenic organism is attributed to the possession of several determinants that allows it to proliferate and survive in diverse locations within the host. Such virulence determinants include the ability of this fungal pathogen to sense and respond rapidly to changes in the environment, and to adhere to and penetrate host tissues. Loss of these attributes has been shown to prevent proliferation as well as virulence in the host. The subsections below provide brief summaries of the major virulence determinants of *C. albicans*.

1.2.1 Morphogenesis. The ability to switch morphological forms is a major virulent trait of *C. albicans* (Sudbery *et al.*, 2004). *C. albicans* can exist in at least four distinct morphologies: yeast, hyphae, pseudohyphae and hyperpolarised buds. The hyphal form has parallel sided walls with no invagination at the septa while the pseudohyphal forms are elongated cells with invaginations at the septa (Sudbery *et al.*, 2004). Pseudohyphal forms have been suggested to be an intermediate form between the yeast and hyphal forms (Banerjee *et al.*, 2008; Carlisle *et al.*, 2009). Hyperpolarised buds also have invaginated septa but are distinct from the pseudohyphal forms in that the nucleus moves from the mother cell to the polarized bud and results from perturbation of cell cycle progression (Whiteway and Bachewich, 2007).

Various environmental cues trigger the yeast to filamentous transition and include change in pH, CO₂, temperature, nutrient availability, and the presence of serum (Gow *et al.*, 2012). Key regulatory mechanisms governing morphogenesis in *C.*

albicans will be summarised next, however, more detailed descriptions can be found in Sudbery (2011). The signal transduction GTPase Ras1 is involved in the serum-induced transition of yeast to hyphae. During growth in serum Ras1 regulates the transcription factor Efg1 as well as the mitogen activated protein kinase Cek1, which subsequently activates another transcription factor Cph1 (Leberer *et al.*, 2001; Rocha *et al.*, 2001; Feng *et al.*, 1999). Efg1 and Cph1 subsequently activate the expression of hyphal genes (Rocha *et al.*, 2001; Liu *et al.*, 1994). The Rim101 pathway regulates hyphal formation during growth in alkaline pH environments (El Barkani *et al.*, 2000), whereas the DNA checkpoint protein Rad53 regulates the transition to hyperpolarised buds following genotoxic stress (Shi *et al.*, 2007).

Morphogenesis contributes to the pathogenicity of *C. albicans*. The yeast form has been suggested to be required for colonisation and dissemination while the hyphal form is required for tissue penetration and invasion (Berman and Sudbery, 2002; Saville *et al.*, 2003; Thewes *et al.*, 2007). Growth in the hyphal form offer virulent abilities such as penetration of epithelial layers to enter the bloodstream as well as enabling effective colonisation of host tissues. The use of the hyphal form to penetrate host tissues is exquisitely illustrated in *C. albicans* escaping from the phagosome. Following phagocytosis *C. albicans* can be seen to adopt the hyphal form of growth and uses the hyphae to pierce through the phagosomal membrane to escape (Lorenz *et al.*, 2004). The ability to switch between forms is important for pathogenesis as cells locked in one form have been shown to display attenuated virulence *in vivo* (Lo *et al.*, 1997). However, a novel mechanism of escaping the phagosome that is not dependent on filamentation was recently demonstrated in *C. albicans*. In this study, *C. albicans* remodelled its cell surface while in the phagosome thereby inducing macrophage killing by pyroptosis (O'Meara *et al.*, 2015). O-linked glycosylation and mannoproteins were both implicated in mediating this lysing effect (Bain *et al.*, 2014; Netea *et al.*, 2008; Hall and Gow *et al.*, 2013). Although this process was found to not depend on filamentation, some link with morphogenesis exists as mutants defective in filamentation were unable to escape from the phagosome by pyroptosis (Kumamoto and Vices, 2005).

1.2.2 Adhesins. The ability to adhere to host cell surface is another important virulence determinant of *C. albicans* reflected by the fact that *C. albicans* has increased adhesive abilities compared to other *Candida* species (Calderone and Braun, 1991). Adhesion enables host cell invasion and inevitably leads to cell

damage. Adhesion in *C. albicans* is facilitated by the presence of cell-surface mannoproteins and include the agglutinin-like sequence (ALS) family (ALS1 to 7 and ALS9), the hyphal wall protein (HWP) family (Hwp1, Hwp2, and Rbt1), and Iff/Hyr family (Iff1/Rbr3, Iff2/Hyr3, Iff3, Iff5, Iff7/Hyr4, Iff9, Hyr1, and Iff11) (Hoyer *et al.*, 2008; Tsuchimori *et al.*, 2000; Ryan *et al.*, 2012). The best characterised proteins required for adhesion will be briefly described below, a more detailed description of other proteins with adhesive roles in *C. albicans* can be found in the review by Zhu and Filler (2010).

The ALS family, composed of 8 members, have a high level of sequence homology, however each member is differentially expressed depending on the substrate and environment (Hoyer, 2001; Hoyer *et al.*, 2008). For example, to adhere to epithelial cells, *C. albicans* will preferentially use Als4 and 9, and to bind to other host cells will adhere with Als1, 2, 3, and 5 (Hoyer *et al.*, 2008). Als6 enables adhesion to gelatine (Hoyer *et al.*, 2008). The substrate of Als7 has not yet been identified. Certain host niches also determine which ALS is expressed for adhesion. In a model of vaginal candidiasis ALS4 expression was down-regulated in *C. albicans* (Cheng *et al.*, 2005). The role of the ALS family in virulence in *C. albicans* has been demonstrated in several models of infections. Deleting ALS1 attenuates virulence in a mouse model of infection while loss of either ALS3 or ALS2 attenuates virulence in both oral and vaginal reconstituted epithelial models of infection (Hoyer *et al.*, 2008). ALS proteins also enable *C. albicans* to form biofilms on virtually any surface such as catheters, prosthetic cardiac valves, or teeth where *C. albicans* contributes to dental plaque.

The most characterised member of the HWP family, Hwp1, is a GPI-anchored hyphal protein with the potential role as serving as a substrate for mammalian epithelial cell transglutaminase enzymes as the N-terminal sequence shares some homology with that of mammalian cell transglutaminase substrates (Staab *et al.*, 1999).

1.2.3 Hydrolytic enzymes. The ability to invade host tissue following adhesion and acquire nutrients are essential processes required for survival and the pathogenicity of *C. albicans*. Virulence determinants that contribute to these abilities are hydrolytic enzymes and include the family of secreted aspartyl proteases (Saps) and phospholipases (PL). The SAP family is composed of 10 members which exhibit a range of different pH optima, allowing different proteases to be functional within different body niches (Smolenski *et al.*, 1997; Borg-von Zepelin *et al.*, 1998). The

ability of Saps to function in diverse host niches was shown in a study by Aoki *et al.*, (2011) where the 10 members of the Sap family were characterised extensively to determine their biochemical properties. Their findings revealed each Sap has a unique optimal pH and broad substrate specificities which enhances the adaptive ability of *C. albicans* to the diverse host niches (Aoki *et al.*, 2011). Saps1 to 3 have optimal activities at low pH while Saps4 to 6 are active at high pH enabling *C. albicans* occupy acidic and alkaline pH niches respectively (Aoki *et al.*, 2011). Saps have uniquely evolved as virulence determinants in *C. albicans* as the non-pathogenic members of the *Candida* species do not possess Saps (Ruchel *et al.*, 1992). The role of Saps in virulence has been shown extensively using various models of infection. For example, in guinea pig and mouse models of invasive candidiasis, deletions in *SAP1* to *SAP6* lead to attenuated virulence (Hube *et al.*, 1997; Sanglard *et al.*, 1997). Tissue invasion and damage during oral candidiasis is also linked to these hydrolytic enzymes as deleting *SAP1* to *SAP8* prevents tissue damage (Schaller *et al.*, 1998). Saps have also been implicated in vaginitis (vaginal inflammation), as deleting *SAP1* to *SAP3* prevented inflammation (Pericolini *et al.*, 2015).

Less characterised is the family of phospholipases of which four members have been identified in *C. albicans* but only one, *PLB1*, has been shown to be required for virulence in an animal model of candidiasis (Leidich *et al.*, 1998; Ghannoum, 2000). Phospholipases hydrolyse the ester linkages of glycerophospholipids and their activity increases during infection (Ibrahim *et al.*, 1995). Expression of *PLB1* increases during nutrient limitation, change in external pH, and growth phase of *C. albicans* (Schaller *et al.*, 2005).

Another group of uncharacterised enzymes with hydrolytic activity implicated in tissue invasion are the lipase (LIP) family. This family is composed of 10 members involved in lipid metabolism and catalyse the hydrolysis of ester bonds of phospholipids and glycerols. Transcript profiling data has revealed these lipases may also play a role in morphogenesis and potentially in the pathogenicity of *C. albicans* (Hube *et al.*, 2000). Another study demonstrated the role of the secreted lipases of *C. albicans* in inducing cytotoxicity using human macrophages and hepatocytes (Paraje *et al.*, 2008). Phospholipases and lipases as demonstrated above clearly play a vital role in mediating virulence in *C. albicans*, however, the role of lipase activity is not understood.

1.2.4 Adaptation to host environments. The ability of *C. albicans* to rapidly adapt to host-imposed challenges is essential for survival. As shown in Fig 1.1, these challenges include nutrient limitation in various body niches including the phagosome; osmotic stress in the kidney and mouth; pH stress while in the phagosome as well as in the host gastrointestinal and urogenital tracts; and heat shock as a result of increase in body temperature during the inflammatory response induced by the host innate immune system; oxidative and osmotic stress during phagocytosis by innate immune cells (Setiadi *et al.*, 2006; Pierce *et al.*, 2013; Enjalbert *et al.*, 2006; Lorenz *et al.*, 2004)

One of the major stresses encountered by *C. albicans* is oxidative stress mounted by the effector cells of the host innate immune system, the macrophages and neutrophils (Fig 1.1). As a result of the reactive oxidative species generated, *C. albicans* mounts an oxidative stress response as exemplified by the rapid induction of key antioxidant genes such as *CAP1*, *CTA1*, *GPX1*, *GPX3*, and *TRX1* (Lorenz *et al.*, 2004; Fradin *et al.*, 2003; Fradin *et al.*, 2005; Rubin-Bejerano *et al.*, 2003). In addition to oxidative stress within the phagosome, unphagocytosed *C. albicans* cells will experience oxidative stress as phagocytes secrete ROS into the external milieu (Kobayashi *et al.*, 1998; Frohner *et al.*, 2009).

C. albicans is also challenged by the presence of reactive nitrogen species (RNS) while in the phagosome as seen by the induction of the RNS detoxifying enzyme, Yhb1, following phagocytosis by macrophages (Lorenz *et al.*, 2004). Unlike oxidative stress, only *C. albicans* cells that are phagocytosed mount a nitrosative stress response (Miramon *et al.*, 2012). *C. albicans* also experiences nitrosative stress during infection of the epithelial cells as seen by the induced expression of *YHB1*, and other genes required for RNS detoxification, *YBH5* and *SSU1* (Zakikhany *et al.*, 2007; Hromatka *et al.*, 2005).

In addition to oxidative and nitrosative stresses, *C. albicans* will experience cationic stress during phagocytosis as a result of the influx of K^+ used to neutralise the superoxide anions generated (Reeves *et al.*, 2002). *C. albicans* is also likely to be exposed to cationic stress while in the kidney, as the *ENA22* sodium efflux transporter gene was induced during infection (Walker *et al.*, 2009).

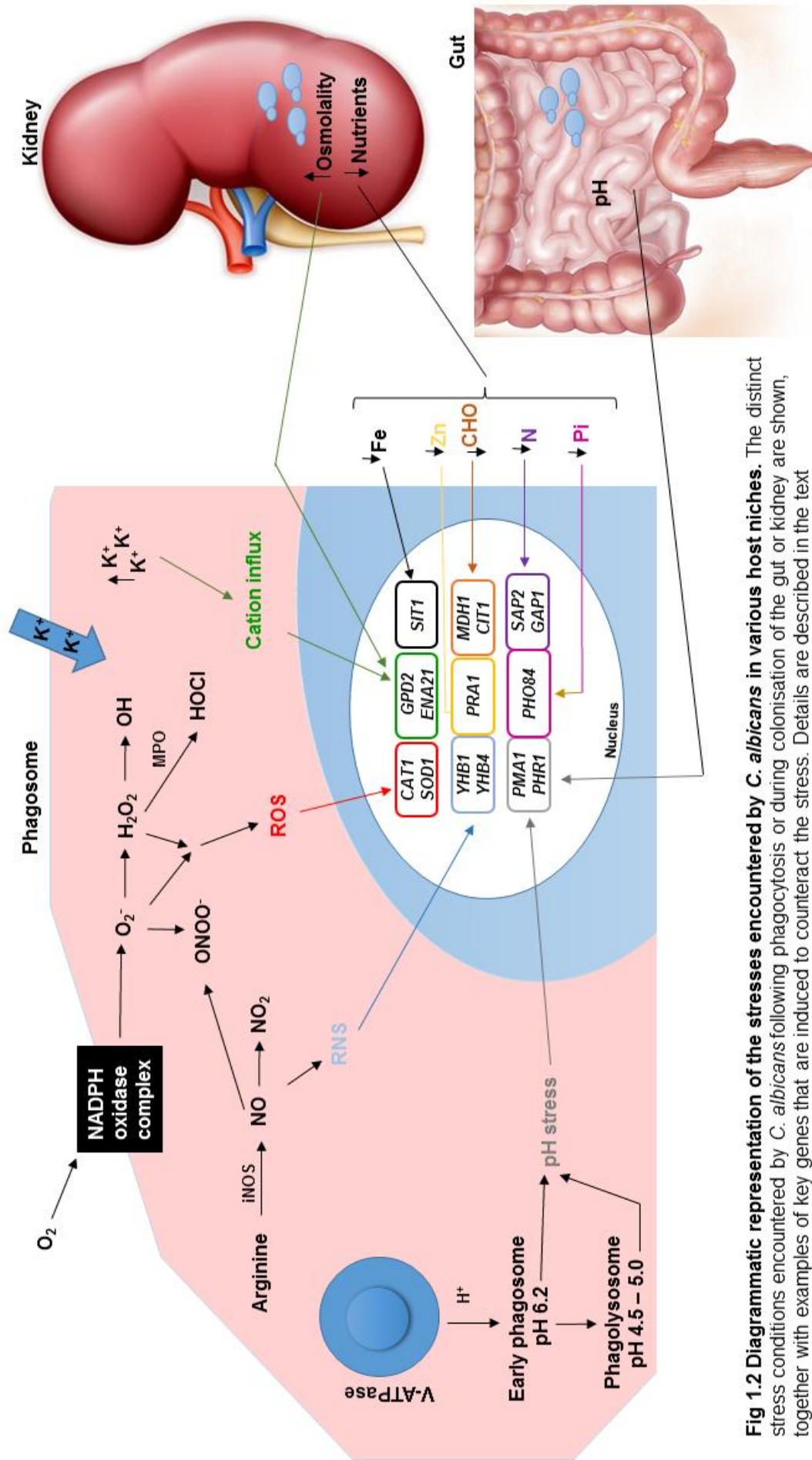


Fig 1.2 Diagrammatic representation of the stresses encountered by *C. albicans* in various host niches. The distinct stress conditions encountered by *C. albicans* following phagocytosis or during colonisation of the gut or kidney are shown, together with examples of key genes that are induced to counteract the stress. Details are described in the text

C. albicans also has to contend with a wide range of pH environments. For instance, a neutral pH environment whilst in the blood stream and acidic pH when in the oral cavity, gut or vagina. In addition, while in the phagosome *C. albicans* will experience fluctuations in pH. pH responsive genes were induced during the invasion of the liver indicating unfavourable pH conditions are encountered in this niche (Thewes *et al.*, 2007).

Although certain host niches are relatively rich in nutrients, *C. albicans* will face nutrient limitation as the fungus will have to compete for these with other host microflora (Brunke and Hube, 2013). In addition, non-preferred carbon sources will be available as most host niches are poor in glucose. For example, in the liver *C. albicans* will have access to glycogen. Furthermore, during invasion of the liver, iron and phosphate transporters are induced in *C. albicans* indicating the liver is limiting in these other essential nutrients (Thewes *et al.*, 2007). Iron availability will not be an issue when *C. albicans* is in the gut due to a surplus supply of iron in this environment (Kortman *et al.*, 2012) however, iron is not readily available in the blood (Amulic *et al.*, 2012). Data from the *C. albicans* transcriptome profiling studies following phagocytosis support the phagosome is a nutrient-limited environment, deficient in both carbohydrates and nitrogen which are both required for growth (Lorenz *et al.*, 2004). In response to carbon limitation, *C. albicans* switches from glycolytic pathway to the glyoxylate cycle to use available carbon sources which include amino acids and lipids (Faro-Trindade and Brown, 2009). In the phagosome, nitrogen starvation responses are activated as shown by the induction of ammonium permeases, genes required for amino acid biosynthesis and transport, and glyoxylate cycle (Fradin *et al.*, 2005; Lorenz *et al.*, 2004; Rubin-Bejerano *et al.*, 2003).

Nutrient immunity, defined as the active sequestering of nutrients by the host from the pathogen, is another major challenge faced by *C. albicans*. Iron is the most abundant metal in the human body, followed by zinc and copper (Bleackley and Macgillivray, 2011). The host however, restricts the availability of these essential nutrients to pathogens (Brunke and Hube, 2013; Mayer *et al.*, 2013). This is because while essential for various physiological functions in the host, excess iron can exacerbate certain fungal diseases, including candidiasis (Iglesias-Osma *et al.*, 1995), therefore the host sequesters iron making it unavailable. Nutrient immunity is also exercised in the phagosome (Frohner *et al.*, 2009). For instance, calprotectin, found in neutrophils and associated with neutrophil extracellular traps (NETs) used to

kill entrapped pathogens, sequesters manganese and zinc, making these essentials nutrients unavailable to *C. albicans* (Urban *et al.*, 2009). Other sequestered essential nutrients include zinc and copper reflected by the up-regulation of uptake systems in *C. albicans* for these metal ions (Lorenz *et al.*, 2004).

1.3 Immune response of the host against *C. albicans*.

The host immune system is an important determinant of *C. albicans* pathogenicity. The epithelial cells, which act as physical barriers, of the mucosal surfaces are the first point of contact between the host innate immune system and *C. albicans* (Moyes and Naglik, 2011; Luo *et al.*, 2013). The epithelial cells have a crucial role of discriminating between the commensal and pathogenic forms of *C. albicans* in order to execute the appropriate response. On bypassing these sentries, the host responds to *C. albicans* systemic infections using both the innate and adaptive branches of the immune system. The innate immune system recognises *C. albicans* and subsequently triggers a rapid response capable of eliminating the fungus and activating the adaptive immune system. Mechanisms employed by innate immune cells to recognise *C. albicans* are described below.

1.3.1 Recognition of *C. albicans* by innate immune cells.

The first line of defence against systemic infection by *C. albicans* is provided by cells of the innate immune system, the dendritic cells, macrophages, and neutrophils, during phagocytosis. Neutrophils are the key players in protecting against *C. albicans* infection (Moyes and Naglik, 2011; Luo *et al.*, 2013). Recognition of pathogenic *C. albicans* by the neutrophils is crucial in recruiting other phagocytes to the site of infection (Netea *et al.*, 2008). Macrophages have the important role of controlling fungal burden at the early stages of infection and in recruiting other phagocytes (Krysan *et al.*, 2014). The other group of innate immune effector cells, the natural killer (NK) cells are not involved in phagocytosis but contribute mainly to *C. albicans* immunity by recruiting other phagocytes as these are less able to kill *C. albicans* (Voigt *et al.*, 2014). More importantly, these immune cells play a vital role in *C. albicans* immunity in immunocompromised patients with defective T- and B-lymphocytes (Quintin *et al.*, 2014). The antigen-presenting dendritic cells (DCs) also have a part to play in *C. albicans* immunity. Like the epithelial cells these provide protection at the mucosal surfaces and present the surface antigens of *C. albicans* via major histocompatibility complex class II molecules thereby linking the innate

immune system with the adaptive branch (d'Ostiani *et al.*, 2000; Cheng *et al.*, 2012). DCs can also distinguish between the yeast and the hyphal forms of phagocytosed *C. albicans* inducing the appropriate T cell differentiation (d'Ostiani *et al.*, 2000; Cheng *et al.*, 2012; Jacobsen *et al.*, 2012).

Recognition is mediated through various pattern recognition receptors (PRRs) such as Toll-like receptors (TLRs), C-type lectin receptors (CLRs) and Nod-like receptors (NLRs). These PRRs recognise specific pathogen-associated molecular patterns (PAMPs) on the surface of *C. albicans* and are restricted to cell wall components. The cell wall of *C. albicans* is a very dynamic and complex structure composed of three layers, an inner chitin layer, an outer layer made up of mannans and glycosylated mannoproteins, and sandwiched between the inner and outer layers is a β -glucan layer (Netea *et al.*, 2008). Mannose residues on the cell wall are recognised by the macrophage via its surface mannose receptor (MR), CLR (Netea *et al.*, 2008). Mannans are recognised by TLR2 and TLR4 (Netea *et al.*, 2006). Dectin-2, a CLR, recognises hyphae while dectin-1 recognises β -glucan structures (Sato *et al.*, 2006; Brown *et al.*, 2002). Recognition of mannose residues by MR and TLR4 in particular is responsible for majority of cytokine and chemokine produced and this is because other PAMPs such as β -glucan which is recognised by dectin-1 is shielded by the outer layer and therefore not accessible (Netea *et al.*, 2006). In addition to recognising *C. albicans* and stimulating cytokine production dectin-1 also plays a role in phagocytosis (Heinsbroek *et al.*, 2008).

1.3.2 Adaptive immune responses. The adaptive immune system is composed of the T lymphocytes, which are the effectors of cellular adaptive immune response, and the B lymphocytes which secrete antibodies making them the effector cells of the humoral adaptive immune system. Upon fungal antigen presentation CD4⁺ T cells differentiate specifically to Th1 and Th17 CD4⁺ T cells responsible for protection against fungi (Weaver *et al.*, 2006; Huang *et al.*, 2004). Th17 cells produce cytokines IL-17A, IL-17F, IL-21, and IL-22 as well as granulocyte-macrophage colony-stimulating factor, chemokines, IL-6, and metalloproteinases, all of which are required for protection against *C. albicans* (Liang *et al.*, 2006; Korn *et al.*, 2007; Nurieva *et al.*, 2007; Zheng *et al.*, 2007; Kolls and Linden, 2004). *In vivo* studies using mice revealed IL-17 production as essential in preventing increase in fungal burden and ensuring survival as mice defective in IL-17 production following *C. albicans* infection were susceptible to infection and showed increased fungal burden

(Huang *et al.*, 2004). B lymphocytes are required to prevent systemic infection. Mice depleted of B cells developed systemic infection following *C. albicans* inoculation (Maiti *et al.*, 1985).

1.3.3 Innate immune responses. The innate immune system is composed of two parts; the immediate acting complement system and the cellular innate immune system, the macrophages and neutrophils. The non-specific complement pathway aids the cellular branch of the innate immune system in the uptake of pathogens. The surface of *C. albicans* triggers **complement** activation which results in the formation of C3 convertase, generation of chemotactic cleavage fragments (C3a, C4a, and C5a) and subsequent opsonisation by C3b and phagocytosis (Kozel, 1996; Kozel *et al.*, 1996). Patients with genetic defects in complement are not more susceptible to *C. albicans* infections, however, observations from *in vivo* studies suggest complement may still play a role in preventing infection. For example, mice unable to generate any of the chemotactic cleavage fragments or their precursors (C3, C4, or C5) are more susceptible to systemic infection (Ashman *et al.*, 1993; Radovanovic *et al.*, 2011; Tsoni *et al.*, 2009). In addition C5 deficiency in mice results in increased levels of pro-inflammatory cytokines (Luo *et al.*, 2013; Mullick *et al.*, 2004).

The initial step in innate-immune cell mediated killing of *C. albicans* involves the internalisation of the pathogen into the phagosome formed by fusion of the cell membrane of the phagocyte around the organism (Fig 1.1). Depending on the phagocyte involved, this step is then followed by fusion with lysozymes to form phagolysosomes (macrophages) or fusion with preformed granules in the cytoplasm (neutrophils). Recognition and engulfment of *C. albicans* triggers the assembly of the **Nicotinamide Adenine Dinucleotide Phosphate (NADPH)** oxidase complex found on the plasma and phagosomal membrane of the phagocyte (Brown and Gordon, 2005; Babior, 1999; Segal *et al.*, 2012). The role of the NADPH oxidase complex in host defence is crucial as individuals with a defective NADPH oxidase system have a severe immunodeficiency known as Chronic Granulomatous disease (CGD), and suffer from recurrent fungal and bacterial infections (Missall *et al.*, 2004; Holland, 2010). Once activated the NADPH oxidase system exerts its defence function by releasing toxic compounds into the phagosome that ultimately kills the engulfed pathogen. These toxic compounds include **reactive oxygen species (ROS)** which spontaneously react with other molecules to generate **reactive nitrogen species (RNS)** and **reactive chlorine species (RCS)**. The first ROS produced by the NADPH

oxidase complex is the **superoxide anion** ($O_2^{\cdot-}$) by the reduction of molecular oxygen with one electron. Superoxide is then dismutated by superoxide dismutase, to **hydrogen peroxide** (H_2O_2) in a multi-step reaction involving the addition of an electron to $O_2^{\cdot-}$ to obtain the peroxide ion O_2^{2-} which is then protonated to form H_2O_2 . H_2O_2 can subsequently be converted to **hydroxyl anions** (OH^-) and **hydroxyl radicals** ($\cdot OH$) via the Haber–Weiss reaction, or to **hypochlorous acid** ($HOCl$) by myeloperoxidase, a lysosomal protein found in the granules of neutrophils. In phagocytic cells, the nitric oxide synthase (NOS_2) generates a range of reactive nitrogen species including the **nitric oxide** (NO) radical and **nitrite** (NO_2^-). NO reacts with superoxide generated by the NADPH oxidase to form **peroxynitrite** ($ONOO^-$). Therefore, the superoxide generated by phagocytic cells leads to the formation of a toxic cocktail of ROS, reactive nitrogen species (RNS), and reactive chlorine species (RCS) which all have deleterious effects on *C. albicans*.

The innate immune system also relies on cationic **antimicrobial peptides** and **hydrolytic enzymes** to kill pathogens including *C. albicans*. The epithelial cells produce a group of **β -defensins** which includes human β - defensins 2 and 3 while neutrophils use **α -defensins** (Duhring *et al.*, 2015). These antifungal agents also act as chemoattractants for monocytes and dendritic cells (Faro-Trindade and Brown, 2009). In addition, the granules of neutrophils contains a family of granule serine proteases which include granulocyte elastase, proteinase 3, azurocidin and cathepsin G. Low levels of granulocyte elastase and cathepsin G can also be found in monocytes. Other antimicrobial peptides used by epithelial cells, monocytes, neutrophils, macrophages, and lymphocytes include **cathelicidin** (hCAP-18) and **LL-37** produced by the cleavage of hCAP-18 (den Hertog *et al.*, 2005; Faro-Trindade and Brown, 2009). The neutrophils also possess **serprocidins** which are cationic serine proteases found in the granules and include protease-3, cathepsin G, and elastase. **Lysozymes** are another group of antimicrobial enzymes with antifungal abilities and these are produced by most phagocytes. The **histatin 5** antimicrobial peptide is transported directly into the cell of the *C. albicans* using its polyamine uptake transporter (Li *et al.*, 2013). Cationic antimicrobial peptides target various macromolecules of the cell including the cytoplasmic membrane and interfere with cellular processes such as DNA and protein synthesis, protein folding, and cell wall synthesis (Nguyen *et al.*, 2011). The exact mechanism used by these peptides is not known, however, they appear to form pores in the membrane lipid bilayers causing

cell lysis (Brogden, 2005). **Hydrolytic enzymes** which have degradative activities include lysozymes, proteases, phospholipases, nucleases, and glycosylases. The lysozyme is one of the well characterised hydrolytic enzyme and a major component of monocytes, macrophages, and leukocytes (Goldstein, 1983). High levels of protons are generated to maintain an acidic phagosome which is required for the optimal activities of hydrolytic enzymes (Pillay *et al.*, 2002; Steinberg *et al.*, 2010). Non phagocytic methods are also employed to eliminate pathogens. One such method involves the production of **extracellular traps** (ETs) which are fibre-like extracellular structures used to trap and kill *C. albicans* (Faro-Trindade and Brown, 2009; Liu *et al.*, 2014). These ETs contain calprotectin, a chemoattractant with antifungal properties (Urban *et al.*, 2009).

1.4 Stresses encountered within the host.

1.4.1 Oxidative stress.

1.4.1.1 Sources of ROS. *C. albicans* is exposed to both endogenous and exogenous sources of ROS. Endogenous ROS is generated within *Candida* cells during aerobic respiration as a result of the activities of the electron transport chain and metal-catalysed reactions. An exogenous source of ROS generated by the NADPH oxidase system occurs during the oxidative burst following phagocytosis as described above. In addition to ROS production within the phagosome, phagocytes secrete ROS into the external milieu (Kobayashi *et al.*, 1998; Frohner *et al.*, 2009). Subsequently, *C. albicans* cells were found to be expressing significantly high levels of the antioxidant genes, *SOD5* and *TRX1*, prior to phagocytosis (Miramon *et al.*, 2012). *C. albicans* will also come in contact with ROS produced by H₂O₂-producing bacteria in the mouth and gut. Several bacteria, for example *Enterococcus faecalis* and *Lactobacillus* species, secrete ROS into their surroundings (Huycke *et al.*, 2001; Fitzsimmons and Berry, 1994).

1.4.1.2 Cellular effects of oxidative stress. Based on observations from *in vitro* experiments, it is predicted that the ROS generated by the NADPH oxidase complex will exert oxidative stress on *C. albicans* by causing irreversible damage to proteins, nucleic acids, and lipids leading to inactivation and loss of function of various cellular components and ultimately death. ROS react with proteins leading to oxidation which affects protein stability and activity (Lu *et al.*, 1999; Kim *et al.*, 2001). ROS can also react with polyunsaturated fatty acids in cell membranes leading to their degradation.

ROS damage DNA by producing single and double strand breaks and various nucleotide modifications (Cadet and Berger, 1985). ROS can affect purine and pyrimidine bases and the phosphodiester DNA backbone producing various mutations (Jackson and Loeb, 2001) such as 8-hydroxyguanine in which the GC component is mutated to TA (Olinski *et al.*, 2002). In addition to 8-hydroxyguanine, oxidation of DNA bases produces urea, hydroxymethyl urea and thymine glycol while sugar modification results in DNA strand breaks (Imlay and Linn, 1988). Unrepaired DNA will lead to mutations, replication errors, genomic instability and death (Klaunig *et al.*, 2010). In *C. albicans*, H₂O₂-mediated DNA damage activates the DNA checkpoint protein kinase, Rad53 resulting in hyperpolarised bud growth (da Silva *et al.*, 2010). *rad53Δ* cells are unable to form hyperpolarised buds in response to H₂O₂ and succumb to the stress (Shi *et al.*, 2007; Loll-Kripplleber *et al.*, 2014). In addition to inducing morphological changes, exposure to H₂O₂ can trigger apoptosis as cells arrest in the G2/M phase of the cell cycle (Philips *et al.*, 2003). Apoptosis in response to H₂O₂ is characterised by loss of cell viability, continuous oxygen consumption and metabolic activity during cell death, production of ROS, condensation of chromatin at the nuclear regions and the accumulation of DNA breaks (Ramsdale, 2008).

1.4.1.3 Oxidative stress response. The genomic response of *C. albicans* to ROS *in vitro* has been extensively characterised by both transcript profiling and proteomic approaches (Enjalbert *et al.*, 2006; Kusch *et al.*, 2007; Yin *et al.*, 2009). Following exposure to H₂O₂, genes that encode antioxidants and detoxifying enzymes are induced (Enjalbert *et al.*, 2006). Importantly, a significant number of the H₂O₂-induced genes and proteins in *C. albicans* are significantly upregulated following phagocytosis by macrophages or neutrophils. However, it is noteworthy that such genes have not been found to be significantly upregulated during infection in other host sites (Thewes *et al.*, 2007; Walker *et al.*, 2009) suggesting that *C. albicans* is only exposed to oxidative stress during phagocytosis. This observation was validated using *C. albicans* cells engineered to express oxidative stress reporter genes. Such reporters were not expressed in *C. albicans* cells infecting mouse kidneys, however expression of these oxidative stress reporter genes occurred following phagocytosis of *C. albicans* cells by neutrophils (Enjalbert *et al.*, 2007). Both phagocytosed and non-phagocytosed fungal cells mount a response to oxidative stress suggesting oxidative stress is imposed both intra- and extracellularly (Miramon *et al.*, 2012).

In response to oxidative stress, *C. albicans* employs both non-enzymatic and enzymatic means for ROS detoxification. Non-enzymatic detoxification mechanisms involve the use of trehalose and glutathione. Trehalose is a non-reducing disaccharide which accumulates in *C. albicans* following oxidative stress via the action of trehalose-6-phosphate synthase, and mutants lacking this enzyme are susceptible to oxidative stress *in vitro* (Alvarez-Peral *et al.*, 2002; Sanchez-Fresneda *et al.*, 2013). Glutathione a tripeptide, exists in both the oxidised (GSSG) form and reduced (GSH) form. Glutathione is oxidised and reduced by glutathione reductase using NADPH as an electron donor (Tillmann *et al.*, 2015). In the reduced form glutathione neutralises ROS by donating an electron (Garcera *et al.*, 2010). Glutathione also protects against irreversible oxidation of proteins by S-thiolation. The reducing activity of glutathione reductase appears to be only required when *C. albicans* is phagocytosed by neutrophils and not macrophages (Miramon *et al.*, 2012; Enjalbert *et al.*, 2007). Glutathione also plays a role in virulence as cells with a defective glutathione reductase activity display attenuated virulence in a murine model of infection (Chaves *et al.*, 2007).

With regard to enzymatic detoxification mechanisms, an important activity is that provided by superoxide dismutases (Sods) which convert the potent superoxide to the less damaging H₂O₂ and molecular oxygen. The importance of such enzymes is demonstrated by the gene expansion in *C. albicans* which contains six different Sods. Two are cytoplasmic; Sod1 and Sod3, Sod2 is mitochondrial, while Sod4, Sod5 and Sod6 are cell surface GPI-anchored cell wall - associated enzymes found in the extracellular environment (Fig 1.1) (Bink *et al.*, 2011; Frohner *et al.*, 2009; Martchenko *et al.*, 2004). Sod1 is a copper- and zinc- containing enzyme (Cu/Zn Sod) while Sod2 contains manganese (Mn Sod) (Martchenko *et al.*, 2004; Frohner *et al.*, 2009). Sod3 is also a manganese-containing Sod but differs from Sod2 in that it also contains iron and localises in the cytoplasm as the mitochondrial transit peptide is absent (Lamarre *et al.*, 2001). Though Sod3 contains iron it only requires manganese for activity (Lamarre *et al.*, 2001). The transition from exponential to stationary phase induces *SOD3* expression and represses that of *SOD1* to ensure continuous protection against oxidative stress (Lamarre *et al.*, 2001). Sod5 is a secreted copper-containing enzyme and acquires Cu directly from the phagosome thus it has no copper chaperone (Gleason *et al.*, 2014). Sod5 is transcriptionally induced during hyphal growth, in the presence of high pH and osmotic stresses

(Nantel *et al.*, 2002; Martchenko *et al.*, 2004) and essential for the detoxification of superoxides secreted outside the phagosome (Frohner *et al.*, 2009). Sod4 and Sod6 are monomeric Sods containing zinc and copper respectively (Martchenko *et al.*, 2004). *SOD4* is transcriptionally induced during growth in the yeast form and together with Sod5 is responsible for the rapid dismutation of superoxide (Heilmann *et al.*, 2011). Possession of surface-associated and intracellular Sods ensures *C. albicans* is protected from both endogenous and exogenous sources of superoxide. The role of superoxide dismutases, responsible for superoxide stress resistance, in virulence has been extensively established in various models of infection including systemic model of disease. Sod1 is essential for surviving exogenous superoxide generated by macrophages and for virulence in a murine model of candidiasis (Chaves *et al.*, 2007; Hwang *et al.*, 2002). Deleting *SOD2* has no impact on the virulence of *C. albicans* and appears to be only required to deal with intracellularly generated superoxide (Hwang *et al.*, 2003). Sod5 eliminates both endogenously and exogenously generated superoxide during the log phase of growth. Sod5 is an interesting Sod in that it is expressed during hyphal growth and following exposure to alkaline pH, high salt and other ROS which are all the conditions *C. albicans* will encounter during phagocytosis (Reeves *et al.*, 2002; Nantel *et al.*, 2002; Martchenko *et al.*, 2004). Inactivating *SOD5* expression attenuates virulence in a mouse model of infection; however the *sod5* mutant displays the same resistance as wild-type cells to phagocytosis (Martchenko *et al.*, 2004). The roles of Sod4 and 6 have yet to be established.

C. albicans also has a suite of enzymes that detoxify H_2O_2 , namely catalase, glutathione peroxidases and thioredoxin peroxidases. Catalase decomposes H_2O_2 to H_2O and molecular oxygen. Expression of *CTA1*, coding for catalase, has been shown to increase during phagocytosis (Fradin *et al.*, 2005; Nakagawa *et al.*, 2003; Enjalbert *et al.*, 2007), and *C. albicans* cells lacking *CTA1* display increased sensitivity to ROS during phagocytosis by neutrophils and attenuated virulence in a mouse model of candidiasis (Wysong *et al.*, 1998; Nakagawa *et al.*, 2003). Another group of enzymes, the glutathione peroxidases (Gpx) catalyse the reduction of H_2O_2 via oxidation of the thiol groups of glutathione (Miramon *et al.*, 2014). Thioredoxin peroxidases, a family of abundant, ubiquitous, redox-regulated thioredoxin peroxidase enzymes which together with thioredoxin and thioredoxin reductase make up the thioredoxin detoxification system, also reduce H_2O_2 . The *C. albicans* 1-Cys

thioredoxin peroxidase, Prx1, is localised in the cytoplasm of yeast cells, however, during morphogenesis the enzyme accumulates in the nucleus of hyphae suggesting a hyphal-specific role (Srinivasa *et al.*, 2012). In contrast the 2-Cys thioredoxin peroxidase Tsa1 is localised in the cytoplasm and nucleus of yeast cells, but redistributes to the cell wall of hyphal cells (Urban *et al.*, 2005). Interestingly, whilst *C. albicans* cells lacking the thioredoxin Trx1 display attenuated virulence in a mouse model of candidiasis (da Silva *et al.*, 2010), cells lacking the thioredoxin peroxidase Tsa1, do not (Urban *et al.*, 2005).

Glutaredoxins are oxidoreductase enzymes activated in response to oxidative, osmotic, and heat stress. They are a group of heat stable proteins also involved in repairing proteins damaged by oxidation (Grant, 2001). In *C. albicans*, four glutaredoxins have been identified however, very little is known about their function. Expression of *GRX2* increased following exposure to oxidative inducing agents and following phagocytosis (Enjalbert *et al.*, 2006; Enjalbert *et al.*, 2007; Fradin *et al.*, 2005; Lorenz *et al.*, 2004). In addition to oxidative stress sensitivity, *C. albicans* cells lacking *GRX2* have morphological defects and reduced virulence in a mouse model of infection (Chaves *et al.*, 2007).

1.4.2 Cationic stress.

1.4.2.1. Sources of cations. It is anticipated that *C. albicans* will be exposed to significant fluctuations in osmolality in certain host niches, including the oral cavity, the kidney, and the gastrointestinal tract. The human kidney can contain extremely high levels of NaCl (600 mmol/L) reaching an osmolality in excess of 1200 mOsm/kg (Ohno *et al.*, 1997; Yancy, 2005). At this concentration, the kidney will be extremely hypertonic being above the normal range 285 – 295 mOsm/Kg found in human serum (Verbalis, 2003), and thus will exert hyperosmotic stress. Sodium concentrations in the gut can increase dramatically, up to 157 mEq/L (milliequivalents of solutes per litre of solvent) in the small intestine, after food consumption (Fordtran and Locklear, 1966). The osmolality of the gut can get as high as 310 mOsm/Kg (milliosmoles per kilogram) following food intake (Fordtran and Locklear, 1966). While in the phagosome *C. albicans* will also experience cationic stress as a result of the influx of potassium ions (K⁺) used to neutralize the negative electron charge created by anionic superoxide radicals within the neutrophil phagosome (Reeves *et al.*, 2002). Concentration of K⁺ ions in the phagosome has been estimated to reach between 200 - 300mM (Reeves *et al.*, 2002) at which cells will experience cationic stress. Neutrophils have been shown

to accumulate high levels of potassium which is mediated by potassium channels (Majander and Wikstrom, 1989; Krause and Welsh, 1990). The presence of potassium may serve as a trigger for the release of granule-associated proteases (Fang, 2004).

1.4.2.2 Cellular effects of cationic stress. Exposure to high concentrations of cations imposes osmotic stress on cells leading to drastic decreases in cell volume and turgor pressure as a result of water loss (Kuhn and Klipp, 2012). The same effect has been observed with *in vitro* experiments in *C. albicans* exposed to high levels of NaCl or Sorbitol (Ene *et al.*, 2015). Cell volume change also induces cell wall biogenesis in *C. albicans* as a result of osmotic shock (Ene *et al.*, 2015). In addition, in yeast cells, the decrease in intracellular water also increases the concentration of solutes within the cell which can have more deleterious effect on the cell (Petelenz-Kurdziel *et al.*, 2011). For instance, high intracellular concentrations of Na⁺ within the cell displaces K⁺ which plays many important physiological roles (Page and Di Cera, 2006). One of the important functions of K⁺ is in maintaining membrane potential in yeast cells, substitution with Na⁺ perturbs membrane potential and leads to damage (Kinclova-Zimmermannva *et al.*, 2006). Also affected by the reduction in intracellular water is the concentration and stability of enzymes which goes on to affect the rate at which biochemical reactions occur in murine mammalian cells (Somero and Yancy, 1997). Another consequence of high external osmolarity observed in yeast cells is growth arrest as a result of the disruption of the actin cytoskeleton (Brewster and Gustin, 1994). During cationic stress, the transport of molecules into the cell is inhibited to restrict uptake of toxic cations, a compromise that will induce other unfavourable effects on the cell. For example, nutrient starvation which occurs as a result of shutting down the activities of nutrient uptake transporters (Norbeck and Blomberg, 1998). Although transcript profiling data have revealed *C. albicans* experiences osmotic stress, none of the above cellular effects of osmotic stress seen in other cells have been demonstrated in *C. albicans*.

1.4.2.3 Cationic stress response. Genome expression studies in *C. albicans* has revealed an osmotic stress response is mounted following exposure to high concentrations of cations (Enjalbert *et al.*, 2006; Smith *et al.*, 2004; Fan *et al.*, 2005). For example, the induction of the putative sodium efflux pump gene, *ENA21* (Enjalbert *et al.*, 2006; Walker *et al.*, 2009). In response to osmotic stress, living cells counter hyperosmotic stress using osmolytes, for example glycerol. Intracellular accumulation of these osmolytes restores turgor pressure enabling cells resume

growth. Like *S. cerevisiae*, *C. albicans* responds to hyperosmotic stress by glycerol accumulation. In *C. albicans*, glycerol is synthesized from the glycolytic intermediate dihydroxyacetone phosphate which is reduced to glycerol-3-phosphate by the enzyme glycerol-3-phosphate dehydrogenase (Gpd1), this is followed by dephosphorylation of glycerol-3-phosphate to release glycerol by glycerol-3-phosphate phosphatase (Rhr2) (Fan *et al.*, 2005). Glycerol is the main osmolyte produced however, other osmolytes are also generated such as D-arabitol, a fungal specific molecule (Kayingo and Wong, 2005). The relevance of D-arabitol accumulation under osmotic stress is not clear.

In addition to the use of osmolytes, yeast and mammalian cells respond to osmotic stress by arresting cell cycle progression and growth and the induction of DNA damage proteins (Kultz *et al.*, 1998; Dmitrieva *et al.*, 2000). To deal with cationic stress *S. cerevisiae* uses cation efflux transporters to restore levels of intracellular cations. These transporters are localised at the plasma membrane and include the H⁺ ATPase, Pma1; the H⁺/Na⁺ antiporter, Nha1; the Na⁺ ATPase, Ena1; and the high-affinity K⁺ transport system, Trk1 and Trk2 (Arino *et al.*, 2010). In *S. cerevisiae* the Ena P-type ATPase and the Nha1 antiporter promote Na⁺ efflux following challenge with a high Na⁺ environment. Cells lacking these pumps are extremely sensitive to cations (Haro *et al.*, 1991; Platara *et al.*, 2006). An orthologue of Ena1 has been identified in *C. albicans* as Ena1 however, no role in cationic stress resistance has been reported. Rather this transporter has been shown to be induced by Rim101 under alkaline conditions and by the iron chelator, Ciclopirox olamine (Bensen *et al.*, 2004; Lee *et al.*, 2005). Another predicted P-type ATPase sodium pump, also an orthologue of Ena2 in *S. cerevisiae*, Ena21 has been identified. This pump, however has been shown to be osmotic-stress induced (Enjalbert *et al.*, 2006). The precise roles these transporters play in cation stress resistance remains to be established.

1.4.3 pH stress.

1.4.3.1 pH diversity in the human host. The pH adaptability of *C. albicans* is reflected by the diverse niches it occurs in the host. The pH in the oral cavity and the digestive tract varies from extremely acidic (pH < 2) to alkaline (pH < 8); pH of human blood and tissues is 7.4, while vaginal pH is around 4. Moreover, the phagosomal environment is maintained at an acidic pH which is the optimal pH for the hydrolytic enzymes (section 1.3.2) however, fluctuations in pH occur during phagocytosis

(Vieira *et al.*, 2002). Following pathogen engulfment the initial neutral pH drops down within 30 mins mainly due to the activity of the vacuolar ATPase (Hackam *et al.*, 1998; Yates and Russell, 2005; Haas, 2007). In neutrophils there is an initial rise in pH followed by drop in pH, a function that is defective in the neutrophils of CGD patients (Segal *et al.*, 1981). The initial alkalinisation occurs during ROS production, due to the high level of proton consumption with the pH rising to 8 during the oxidative burst (Jiang *et al.*, 1997; Segal *et al.*, 1981). Moreover, influx of K⁺ into the phagosome, used to restore the hypertonicity created by superoxide anions present, raises the pH (Reeves *et al.*, 2002). However, the pH rapidly drops to allow the activity of the lysosomes (Segal *et al.*, 1981; Segal, 2005).

1.4.3.2 Cellular effects of pH stress. Changes in environmental pH has profound effects on *C. albicans*. The external surface of *C. albicans* bears the brunt of pH stress as seen by the morphological defects displayed by *C. albicans* cells unable to adjust to external pH (Saporito-Irwin *et al.*, 1995; Popolo and Vai, 1998). Cells unable to adapt are enlarged and round compared to wild-type cells and grow at a slower rate (Saparito-Irwin *et al.*, 1995; Muhlschlegel and Fonzi, 1997). Morphological defects displayed are associated with changes in the polysaccharide content of the cell wall. In cells unable to adjust, chitin levels are raised while levels of glucans and glucan cross-linking become reduced (Popolo and Vai, 1998). Another major challenge of being in an alkaline environment is reduced nutrient availability, as most nutrient molecules become insoluble at high pH. For example, zinc becomes limiting at high pH due to loss of function of the high-affinity zinc transporter, Zrt1 (Bensen *et al.*, 2004). Neutral and alkaline pH also affect iron availability by oxidising the soluble Fe²⁺ to the insoluble form, Fe³⁺. Nutrient uptake across the membrane also becomes impaired under high pH as the proton gradient required is abolished (Davis, 2009). Another consequence of high pH is the inactivation of pH-sensitive proteins such as secreted or surface proteins (Davis, 2009). The ability to adapt to alkaline pH plays a role in the pathogenicity of *C. albicans* as demonstrated in various models of candidiasis. Defective mutants are unable to grow in the bloodstream for example, and are avirulent (Davis *et al.*, 2000). In contrast, the response to acidic stress is not well known. Fungal organisms preferentially grow at acidic pH, however exposure to weak acids can cause death. For example, lactate found in the vagina when dissociated can cross the plasma membrane of the organism causing acidification of the cytoplasm and apoptosis leading to death (Davis, 2009).

1.4.3.3 pH stress response. The ability of *C. albicans* to sense and adapt to changes in environmental pH is essential for survival. As previously mentioned, the major challenge faced by *C. albicans* following pH change is maintaining cell wall strength to ensure support and protection. This is achieved by the action of two differentially expressed glycoproteins, Phr1 and Phr2. These genes encode proteins required for cell wall synthesis with loss of any of these proteins resulting in *C. albicans* being unable to survive and also results in reduced virulence (Ghannoum *et al.*, 1995). *PHR1* is expressed during growth in alkaline pH and encodes for a glycosylphosphatidylinositol-anchored protein involved in cross-linking β -1, 3-glucans with β -1, 6-glucans (Saporito-Irwin *et al.*, 1995; Muhlschlegel and Fonzi, 1997; Fonzi, 1999). In acidic environments, a distinct but functionally related protein coded by *PHR2* mediates growth (Muhlschlegel and Fonzi, 1997). Phr2 was shown to be required for virulence in a vaginal model but not a systemic model of candidiasis (Fonzi, 1999). In the absence of these proteins, β -1, 6-glucans is cross-linked to chitin resulting in a less stable cell wall (Fonzi, 1999). The Pma1 H⁺ ATPase plays a role in restoring intracellular levels of protons during growth under alkaline pH conditions. *PMA1* was upregulated during *C. albicans* infection of the liver (Thewes *et al.*, 2007). In addition to maintaining cell wall integrity and proton extrusion, *C. albicans* modulates the pH of the acidic phagosome by secreting ammonia to raise the pH (Vylkova *et al.*, 2011; Mayer *et al.*, 2013).

1.4.4 Nutrient limitation.

Certain niches within the human host are rich in nutrients but these are not readily available to microbes. Moreover, the host also actively sequesters specific nutrients from the pathogen as a means of preventing infection. For example, *C. albicans* occupies mostly the mucosal surfaces within the host which are abundant in nutrients especially during food consumption, however competing microflora reduce availability (Basson, 2000). The liver and brain are rich in glucose but again the host immune system ensures these nutrient stores are not readily available to pathogens during infection. The bloodstream is also abundantly rich in nutrients as blood is the main transporter of nutrients but the effector cells of the host innate immune system prevent colonisation of the bloodstream by pathogens. However, on circumventing host immune defence during systemic infection, *C. albicans* through adhesion and tissue invasion gains access to the bloodstream and targets these host organs. Successful colonisation of the niches occupied suggests *C. albicans* has evolved

means of acquiring nutrients to ensure growth. The following sections review what is known about how *C. albicans* deals with the availability of key nutrients while in the human host.

1.4.4.1 Metabolic flexibility.

1.4.4.1.1 Alternative carbon sources. When glucose is limiting *C. albicans* switches from the glycolytic pathway to the glyoxylate cycle and gluconeogenesis to enable it use two-carbon compounds as alternative carbon sources (Lorenz *et al.*, 2004). This metabolic shift has been observed in *C. albicans* during nutrient starvation while occupying host niches including the phagosome. Gluconeogenesis enables use of non-fermentable carbon sources to not only generate energy but also to provide sugars used for the biosynthesis of cell wall components and storage compounds. A key enzyme of the gluconeogenesis pathway activated is the phosphoenolpyruvate carboxykinase involved in generating phosphoenolpyruvate from oxaloacetate (Thewes *et al.*, 2007). The presence of oxaloacetate also means the glyoxylate pathway, required to generate oxaloacetate from malate, is also activated in response to non-glucose carbon sources. Other alternative carbon sources include lactate, citrate, glycerol, amino acids, lipids, and fatty acids, of which the key enzyme isocitrate lyase is required for metabolism (Lorenz and Fink, 2001; Barelle *et al.*, 2006; Piekarska *et al.*, 2008; Brock, 2009).

1.4.4.1.2 Nitrogen limiting conditions. Preferable nitrogen sources are equally scarce in the phagosome. *C. albicans* compensates for the nitrogen limiting environment by up-regulating the expression of ammonium permease genes and vacuolar proteases for host protein degradation and turnover (Fradin *et al.*, 2005). Through the hydrolysing activities of the secreted aspartyl proteases, *C. albicans* can also obtain nitrogen from peptides and amino acids released from the damaged host tissues (Brunke and Hube, 2013). A group of peptide transporters (PTR) and oligopeptide transporters (OPT) enable *C. albicans* take up di- and tri- peptides and longer peptides respectively (Dunkel *et al.*, 2013). Deleting the *PTR* genes (*PTR2* and *PTR22*) or the *OPT* ones (*OPT1 – OPT5*) in *C. albicans* prevents growth *in vitro* on medium containing peptides as sole nitrogen source (Dunkel *et al.*, 2013). Deletion has no effect on virulence suggesting that parallel mechanisms exist to obtain nitrogen.

1.4.4.1.3 Amino acids limiting conditions. Through the hydrolysing activities of saps, *C. albicans* can obtain peptides and amino acids released from the damaged host tissues using the PTR and OPT transporters (Brunke and Hube, 2013; Dunkel *et al.*, 2013).

1.4.4.1.4 Phosphate limiting conditions. In the human host most of the phosphate (85%) is stored in bones, 14% in cells and soft tissues, with the remaining 1% found in extracellular fluids (Alon and Chan, 1993). Inorganic phosphate concentration in the serum ranges from 2.5 - 4.5mg/L in adults (Alon and Chan, 1993). Furthermore, the phosphate available in extracellular fluids is bound to proteins. This means phosphate in the host is not readily available to pathogenic organisms during infection. It is therefore vital for cells to possess sophisticated mechanisms to acquire and maintain phosphate homeostasis. Through complex signaling pathways, microorganisms sense phosphate concentration in the environment and trigger a signal transduction cascade accordingly leading to the activation of phosphate-response genes. The transcriptional regulator of the phosphate response in *C. albicans* Pho4, has been identified and shown to be required for growth in phosphate-limiting conditions (Homann *et al.*, 2009; Romanowski *et al.*, 2012). However the PHO pathway in *C. albicans* has not been fully characterised. The phosphate response pathway in the model yeast is one of the best studied signal transduction pathways. The PHO pathway in *S. cerevisiae* is essential for phosphate acquisition and storage. The PHO pathway consists of acid phosphatases, alkaline phosphatases, transporters, polyphosphatases, and kinases that all participate in the acquisition of external phosphate, mobilisation of phosphate from storage, phosphate transportation, and metabolic integration of phosphate (Oshima *et al.*, 1996; Wykoff and O`Shea, 2001). The importance of phosphate availability is further reflected by the presence of intracellular high-molecular weight granules of phosphate stored in the vacuole as a linear polymer referred to as polyphosphate (polyP) (Kulaev *et al.*, 2004; Kornberg, 1999). During *C. albicans* infection, phosphate acquisition is likely important for virulence. For example, the expression of the high-affinity phosphate transporter, *PHO84* is up-regulated during infection of the mammalian liver and kidney tissues (Thewes *et al.*, 2007; Walker *et al.*, 2009), and following phagocytosis (Fradin *et al.*, 2005). Moreover, deletion of *PHO100* and *GIT3*, predicted to be involved in hydrolysing phosphate-containing substrates attenuates virulence

(MacCallum *et al.*, 2009; Bishop *et al.*, 2011). Limiting phosphate conditions, also induces filamentation possibly as a scavenging response (Romanowski *et al.*, 2012).

1.4.4.2 Nutritional immunity. In response to nutrient immunity, the pathogen uses diverse acquisition strategies to obtain these essential nutrients. To acquire sequestered nutrients from the host sites, *C. albicans* has evolved various successful mechanisms and these mechanisms are described below. While the iron acquisition system in *C. albicans* has been best characterised, less is known about how *C. albicans* obtains zinc from the host and even less known about copper and manganese acquisition.

1.4.4.2.1 Iron Acquisition. A complex and dynamic warfare exists between the host and pathogen concerning iron availability. This is not surprising as iron is essential for growth. The human adult body contains 3 - 5 g of iron of which up to 75% is found in erythrocytes bound to heme and used for oxygen transportation (Andrew, 2000). In the host, iron bioavailability is severely restricted to minimize infection. Iron is sequestered from pathogens using storage proteins (e.g., ferritin), carrier proteins (e.g., transferrin), and the senescent red blood cell recycling complex (Ehrensberger and Bird, 2011). To obtain the sequestered iron, fungal pathogens have developed multiple high-affinity iron acquisition systems. These systems include: a reductive iron acquisition (RIA) pathway made up of a permease and a high-affinity iron multicopper oxidase; siderophore transporters that work alongside siderophores; secreted and cell surface reductants; and the endocytic pathway for the endocytosis of haem and a haem oxygenase for iron extraction. *C. albicans* can acquire iron in one of three ways, by secreting hemolysins which act on red blood cells to release iron (Citiulo *et al.*, 2012); by employing siderophores to transport iron (Martin *et al.*, 1987), or by utilising cell-surface ferric reductases (Luo *et al.*, 2001) to obtain iron. *C. albicans* makes use of a RIA pathway that enables iron acquisition from transferrin, ferritin, or other sources (Ftr1/Fet3); a siderophore uptake system that mediates uptake of iron from siderophores (Sit1 transporter); or an uptake system for acquiring iron from haemoglobin and other haem-proteins (Rbt5) (Almeida *et al.*, 2008). The host niche also dictates which system *C. albicans* uses to acquire iron. For instance, in epithelial cells Sit1 mediates iron uptake while the RIA pathway takes over this function during bloodstream infections (Ramanan and Wang, 2000; Almeida *et al.*, 2009). In addition, *C. albicans* also employs non-reductive means of acquiring iron during infection and while receptors for obtaining iron from haemoglobin (Rbt5) or

ferritin (Als3) have been identified, the receptor for transferrin has not yet been identified (Weissman and Kornitzer, 2004; Almeida *et al.*, 2008; Knight *et al.*, 2002).

1.4.4.2.2 Zinc Acquisition. Most of the zinc in humans is intracellular due to its structural and functional roles in macromolecules and enzymes (Tapiero and Tew, 2003; King, 2011). Zinc acquisition *in vivo* in *C. albicans* has been recently detailed and shown to be mediated by a zinc acquisition system which consists of the pH regulated antigen, Pra1 and the zinc transporter, Zrt1 (Citiulo *et al.*, 2012). The zinc acquisition system, referred to as a “zincophore”, was identified using an epithelial model of infection. The proposed mechanism of action of Pra1 is that in alkaline pH environment with limiting zinc Pra1 is secreted into the external milieu where it scavenges and binds host zinc. Zinc uptake into cell is then facilitated by Zrt1 (Citiulo *et al.*, 2012). *C. albicans* also reduces the activities of zinc-dependent enzymes e.g., alcohol dehydrogenases, to ensure zinc is available for storage and transport metalloproteins (Nobile *et al.*, 2009).

1.4.4.2.3 Copper and Manganese acquisition. In contrast to iron and zinc, manganese and copper are found in trace amounts in the human body (Keen *et al.*, 2000; Uauy *et al.*, 2008). Copper is mainly stored in the liver and brain (Uauy *et al.*, 2008; Keen *et al.*, 2000) while manganese is mainly stored in the bones. Ccc1 and Ctr1 are putative transporters identified in *C. albicans* required for the acquisition of manganese and copper respectively (Mayer *et al.*, 2013). The role of these transporters in virulence are currently unknown and requires further exploration.

1.4.4.3 Nutritional responses and impact on stress resistance and virulence.

To overcome this imposed challenge, *C. albicans* has evolved various mechanisms to obtain nutrients from the host. These mechanisms also impact on the virulence of *C. albicans*. For example, the ability of *C. albicans* to invade and subsequently damage endothelial cells was minimised by treating epithelial cells with the iron chelator, Phenanthroline (Fratti *et al.*, 1998). Furthermore, inactivation of any of the iron acquisition mechanisms, described in section 1.4.4.2.1, attenuates the virulence of *C. albicans* (Almeida *et al.*, 2009). *C. albicans* cells lacking Pga7 or Pra1, which play major roles in the scavenging of iron and zinc respectively, exhibit reduced virulence (Hashash *et al.*, 2011; Kuznets *et al.*, 2014). Deleting the zincophore system in *C. albicans* abolishes zinc acquisition thus preventing host cell damage (Citiulo *et al.*, 2012).

In addition to ensuring cell survival, metabolic adaptation to available nutrients has recently been observed to enhance stress resistance and survival in *C. albicans*. For example, cells grown on carbon sources other than glucose were significantly more resistant to osmotic stress and antifungals compared to cells grown on glucose (Ene *et al.*, 2012). Growth on lactate remodels the cell surface of *C. albicans* leading to a more chemically resistant form and in addition enables the fungus avoid immune recognition (Vylkova and Lorenz, 2014). In contrast, growth on glucose actually promotes oxidative stress resistance by an as yet uncharacterised mechanism (Rodaki *et al.*, 2009) while growth on amino acids enables *C. albicans* raise the acidic pH of the phagosome by the extrusion of ammonia (Vylkova and Lorenz, 2014). Metabolic pathways also play a role in mediating virulence in *C. albicans*. For example, the primary enzymes of the glyoxylate cycle, isocitrate lyase and malate synthase, were shown to be required to survive the phagosome environment and for virulence in mice (Lorenz and Fink, 2001; Lorenz *et al.*, 2004). A recent study has also demonstrated that the arginine biosynthetic pathway plays a role in fungal escape from the phagolysosomal environment, as the products of arginine catabolism (CO₂ and urea) neutralize the acidic pH of the phagosome and trigger *C. albicans* filamentation (Vylkova *et al.*, 2011).

1.4.5 Additional stress responses mounted by *C. albicans*.

1.4.5.1 Downregulation of the translation machinery. In response to stress, *C. albicans* upregulates the expression of genes required for adaptation, however, certain genes are downregulated to repress translation. This has been observed in phagocytosed *C. albicans* cells who switch to a starvation mode and upregulate genes that encode proteins of the gluconeogenesis/glyoxylate pathways and downregulate those involved in the translation machinery (Lorenz *et al.*, 2004). This leads to a decrease in ribosomal protein mRNA content. In addition, other genes involved in translation are repressed and these include translation factors, ribosome biogenesis activities, tRNA synthases, and RNA polymerase I and III subunits (Lorenz *et al.*, 2004). Also noteworthy is that the regulatory response of the translation machinery during phagocytosis of *C. albicans* occurs only in the cytoplasm and not the mitochondria (Lorenz *et al.*, 2004).

1.4.5.1 Accumulation of P bodies. Cells also respond to unfavourable environmental conditions by forming P bodies. Also known as stress granules, these

processing bodies are mRNAs associated with protein structures that under certain stress-inducing conditions assemble into non-translating messenger ribonucleoproteins (mRNPs) (Bergues *et al.*, 2005; Kedersha *et al.*, 2005; Parker and Sheth, 2007). The main function assigned to these P bodies is in the formation of high concentration of mRNA degradation components where they are located (Buchan *et al.*, 2008; Buchan and Parker, 2009). The localised mRNA can then be degraded or recycled for translation (Parker and Sheth, 2007; Sheth and Parker, 2006). A set of proteins, conserved from yeast to mammals, exist in these P bodies and include the decapping enzymes Dcp1 and Dcp2; the decapping activators Dhh1/RCK/p54, Pat1, Edc3, and Lsm1 – 7; and the exoribonuclease Kem1/Xrn1 (Buchan and Parker, 2009, Decker *et al.*, 2007; Long and McNally, 2003). In addition, certain components of the P bodies are species- or condition- specific, for example, mammalian P bodies contain the translation initiator factor eIF4E and proteins involved in miRNA-mediated repression and these are absent in P bodies of the model yeast, *S. cerevisiae* (Jung and Kim, 2011). In yeast, stress granules are formed generally following exposure to various stresses that inhibit translation such as heat, glucose deprivation, or ethanol (Buchan *et al.*, 2008; Grousl *et al.*, 2009; and Kato *et al.*, 2011). In *C. albicans*, these stress granules have been identified under stress conditions which include osmotic and oxidative stresses and during transition to the hyphal form of growth (Jung and Kim, 2011).

1.5 Stress-responsive signalling pathways and transcription factors in *C. albicans*.

As described above, *C. albicans* encounters many challenges imposed by the diverse environments colonised during infection. To respond to, and survive, host-imposed stresses, *C. albicans* utilises a number of signalling pathways which are reviewed below.

1.5.1 Cationic stress signalling.

1.5.1.1 Stress Activated Protein Kinase (SAPK) Hog1 pathway. Following exposure to osmotic stress, the Hog1 SAPK is activated by the dual phosphorylation of conserved Thr and Tyr residues by the Pbs2 MAPKK, which is activated by the upstream Ssk2 MAPKKK (Fig 1.2) (Arana *et al.*, 2005; Cheetham *et al.*, 2007; Cheetham *et al.*, 2011). This activates the kinase and triggers its nuclear accumulation where it plays a major role in the activation of osmotic-stress responsive genes (Alonso-Monge *et al.*, 2003; Smith *et al.*, 2004; Enjalbert *et al.*,

2006). Such genes include those necessary for glycerol accumulation (*GPD2* and *RHR2*) and thus activation of Hog1 results in the accumulation of such osmolytes (San Jose *et al.*, 1996) Cells lacking any component for example, Hog1 SAPK, Pbs2 MAPKK, or Ssk2 MAPKKK, of the Hog1 pathway are extremely sensitive to osmotic stress (Fig 1.2). Importantly, inactivation of the pathway attenuates virulence of *C. albicans* in various models of infection, including commensal models (Alonso-Monge *et al.*, 2003; Cheetham *et al.*, 2011; Prieto *et al.*, 2014).

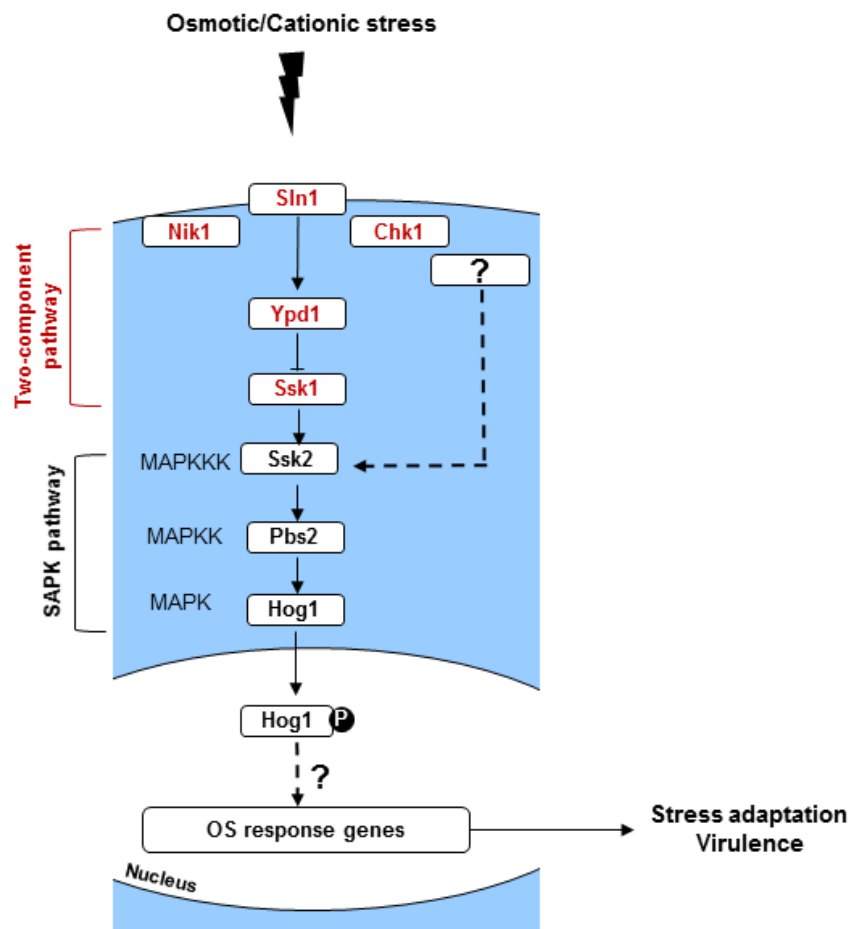


Fig 1.2 Osmotic stress signalling to the Hog1 stress activated protein kinase (SAPK) pathway in *C. albicans*. The Sln1-Ypd1-Ssk1 two component signalling pathway functions redundantly with a second uncharacterised pathway (dashed line) to relay osmotic stress signals to the Hog1 SAPK pathway. This culminates in the phosphorylation and activation of Hog1 which translocates to the nucleus and regulates the induction of osmotic stress protective genes. However, the transcription factor targets of Hog1 that regulate this transcriptional program are unknown.

How osmotic stress signals are sensed by the cell and relayed in the Hog1 SAPK module is not clear, but at least two independent pathways have been indicated (Fig 1.2). One pathway involves a two-component related His-Asp-His-Asp phosphorelay system. In *C. albicans*, this phosphorelay system likely comprises of the Sln1 histidine kinases, Sln1 (Yamada-Okabe *et al.*, 1999), the phosphorelay protein Ypd1

(Calera *et al.*, 2000), and the response regulator Ssk1 (Chauhan *et al.*, 2003; Singh *et al.*, 2004; Bruce *et al.*, 2011). This pathway has been well characterised in *S. cerevisiae*, in which osmotic stress inactivates the Sln1 histidine kinase, which results in the accumulation of unphosphorylated Ssk1 which is a potent activator of the Ssk2 MAPKKK (Nagahashi *et al.*, 1998; Calera and Calderone, 1999; Cheetham *et al.*, 2007). Moreover, as in *S. cerevisiae*, there is a two component independent pathway that regulates osmotic stress mediated activation of Hog1 in *C. albicans*. However, unlike *S. cerevisiae*, this is independent of the Sho1/Msb2 signalling pathways (Roman *et al.*, 2005). In addition to questions regarding the upstream signaling to Hog1, the transcriptional regulator targets of Hog1 that regulate the induction of cationic stress protective genes have not been identified.

1.5.2 Oxidative stress signalling. Much of what is known about oxidative stress response signaling is focused on the response of *C. albicans* to H₂O₂ induced oxidative stress. The pathways that respond to H₂O₂ are detailed below and depicted in Fig.1.3.

1.5.2.1 Stress Activated Protein Kinase (SAPK) Hog1 pathway. Although Hog1 is phosphorylated and accumulates in the nucleus following oxidative stress (Smith *et al.*, 2004), this SAPK does not play a major role in the transcriptional response to H₂O₂ (Luo *et al.*, 2001). Cells lacking Hog1 do however, display significantly impaired resistance to ROS, indicating that Hog1 activation leads to a non-transcriptional response which is vital for the protection of *C. albicans* against oxidative stress (Fig 1.3). A number of studies have explored the mechanisms underlying the H₂O₂-mediated activation of the Hog1 pathway. Deletion of the Ssk1 response regulator results in impaired activation of the Hog1 SAPK in response to oxidative stress (Chauhan *et al.*, 2003; Bruce *et al.*, 2011). Moreover, cells lacking *SSK1* are sensitive to H₂O₂ and display impaired virulence in a mouse model of systemic candidiasis (Chauhan *et al.*, 2003; Calera *et al.*, 2000). However, whether this involves two-component mediated phosphorylation of Ssk1 is not clear, as deletion of the three histidine kinases which regulate Ssk1 phosphorylation, does not impair H₂O₂-mediated Hog1 activation (Roman *et al.*, 2005). In addition to Ssk1, the thioredoxin peroxidase, Tsa1, and the thioredoxin, Trx1, are both required for Hog1 activation specifically in response to H₂O₂ (da Silva *et al.*, 2010). The mechanism behind this is unknown. In addition, the downstream effectors of Hog1 in response to oxidative stress are also unknown.

1.5.2.2 The Rad53 DNA damage checkpoint kinase. Exposure of cells to H₂O₂ triggers the phosphorylation and activation of the Rad53 DNA damage pathway (da Silva *et al.*, 2010). This culminates in cell cycle arrest and the formation of hyperpolarised buds, a filamentous form distinct from hyphae and pseudohyphae but characteristic of other genotoxic stresses that induce cell cycle arrest (Shi *et al.*, 2007; da Silva *et al.*, 2010). The pathway responsible for sensing H₂O₂-mediated DNA damage, and relaying the signal to Rad53, has yet to be elucidated (Fig 1.3).

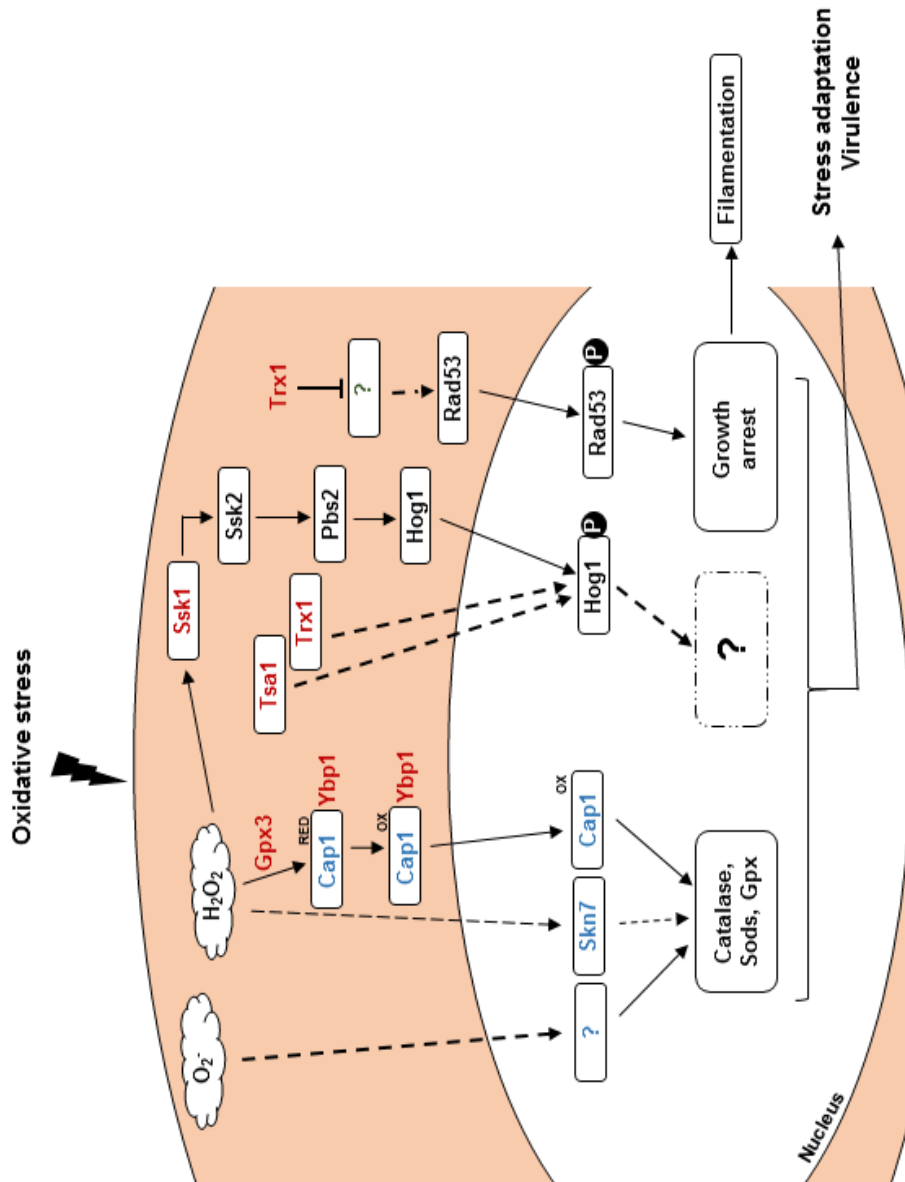


Fig 1.3 Oxidative stress responsive signalling pathways in *C. albicans*. The transcription factor Cap1 is activated by oxidation following H₂O₂ stress, and plays a major role in regulating the transcription response to H₂O₂, with Skn7 also playing a role. In contrast, transcriptional regulators of superoxide (O₂⁻)-induced gene expression are unknown. The Hog1 SAPK and the Rad53 DNA damage checkpoint kinase are activated by phosphorylation in response to H₂O₂. The role of Hog1 in mediating oxidative stress resistance remains unknown, whereas activation of Rad53 induces cell cycle arrest resulting in the formation of hyperpolarised buds. Regulatory proteins known to facilitate the activation of these oxidative stress responsive pathways are shown in red, with dashed lines indicating unknown mechanisms. See text for details.

However, H₂O₂-induced oxidation and inactivation of the thioredoxin protein Trx1 triggers activation of the DNA checkpoint kinase Rad53. Thus, Trx1 is a negative regulator of H₂O₂-induced hyperpolarised bud formation (da Silva *et al.*, 2010). Cells lacking Rad53 are exquisitely sensitive to ROS such as H₂O₂ (da Silva *et al.*, 2010), although the importance of the DNA damage checkpoint kinase in mediating *C. albicans* virulence has not been examined.

1.5.2.3 The Cap1 AP-1-like transcription factor. As described above (section 1.4.1.3) *C. albicans* responds to H₂O₂ by inducing a robust transcriptional response which includes many key antioxidant genes. The major regulator of this anti-oxidant gene expression in *C. albicans* is the AP-1 like transcription factor Cap1 (Wang *et al.*, 2006), and *cap1*Δ cells are extremely sensitive to H₂O₂ (Alarco and Raymond, 1999). Cap1 is a homologue of the well characterised Yap1 and Pap1 transcription factors in *S. cerevisiae* and *S. pombe*, respectively (Moye-Rowley, 2002; Toone *et al.*, 2001). CHiP on chip experiments have shown Cap1 to directly bind to the promoters of genes induced following oxidative stress including antioxidants, genes involved in carbohydrate and energy metabolism, protein degradation, and mitochondrial respiratory function (Znaidi *et al.*, 2009). Cap1, like other yeast AP-1-like factors, is regulated at the level of cellular localisation (Moye-Rowley, 2002; Zhang *et al.*, 2000). Under non-stress conditions, Cap1 can be found dispersed between the cytoplasm and nucleus of the cell. However, following exposure to H₂O₂ Cap1 rapidly accumulates in the nucleus (Fig. 1.3). This is mediated by the H₂O₂-induced oxidation of this transcription factor (da Silva *et al.*, 2010). Following oxidative stress, Cap1 becomes oxidised on redox-sensitive cysteine residues found within two cysteine rich domains located in the middle (n-CRD) and the C-terminus (c-CRD) of protein. This oxidation is predicted to induce structural changes, which masks the nuclear export sequence located within the c-CRD, and thus triggers the nuclear accumulation of Cap1. Recently, Cap1 oxidation has been shown to be mediated by the Gpx3 glutathione peroxidase and a homologue of the *S. cerevisiae* Yap1 binding protein, Ybp1 (Patterson *et al.*, 2013). Furthermore, cells lacking Cap1, Gpx3 or Ybp1 display significantly impaired ability to kill macrophages, and are thus much more susceptible to macrophage mediated killing (Patterson *et al.*, 2013). Strikingly, however, both Cap1 (Patterson *et al.*, 2013; Jain *et al.*, 2013) and its regulatory proteins Ybp1 and Gpx3 (Patterson *et al.*, 2013) are largely dispensable for virulence in a mouse model of systemic candidiasis. Consistent with this differing requirement

for Cap1 in *C. albicans* virulence depending on the infection model, single-cell profiling studies using antioxidant promoter-GFP fusions (Enjalbert *et al.*, 2007), and transcript profiling studies (Thewes *et al.*, 2007; Walker *et al.*, 2009), revealed that whilst anti-oxidant gene expression is clearly induced following phagocytosis by innate immune cells, such genes are not induced during tissue invasion. This indicates that oxidative stress responses may be important to evade initial innate immune defences, but dispensable once the pathogen reaches the kidney or liver. An alternative explanation is that Cap1 mediated oxidative stress responses in *C. albicans* are inhibited in these host niches. Indeed, inhibition of Cap1 mediated antioxidant gene expression has been demonstrated in *C. albicans* cells exposed to combinatorial H₂O₂- and NaCl- induced stresses which led to more rapid killing *in vitro* (Kaloriti *et al.*, 2014). In this scenario, NaCl inhibited the catalase enzyme, required for H₂O₂ detoxification, leading to the accumulation of ROS which inhibited the activity of Cap1 (Kaloriti *et al.*, 2014).

1.5.2.4 Skn7. A homologue of the *S. cerevisiae* Skn7 transcription factor has been characterized in *C. albicans*, and as in *S. cerevisiae*, cells lacking *SKN7* are sensitive to H₂O₂ (Singh *et al.*, 2004). The receiver domain found in response regulator proteins of two-component signal transduction pathways is conserved in the *C. albicans* Skn7 protein. In *S. cerevisiae*, Skn7 functions with the Yap1 transcription factor to regulate stress-response genes (Morgan *et al.*, 1997) however, whether Skn7 is similarly required for Cap1-dependent antioxidant gene expression in *C. albicans* has not been tested. Similar to that reported for *cap1Δ* cells (Patterson *et al.*, 2013), *C. albicans skn7Δ* cells display only mildly attenuated virulence in a mouse model of systemic candidiasis (Singh *et al.*, 2004). Skn7 is clearly involved in oxidative stress resistance in fungi however, its regulatory mechanism is still not understood.

1.5.3 pH signalling.

1.5.3.1 Rim101 pH response pathway. The alkaline pH response mediated via Phr1, Phr2, and Pra1 is regulated by the Rim101 pathway (Fig 1.4) which consists of the transcriptional regulator, Rim101; the β-arrestin-like protein (also referred to as α-arrestin), Rim8; the protease, Rim13; the scaffold protein, Rim20; and the plasma membrane receptors, Rim21 and Dfg16 (Davis *et al.*, 2000). Loss of gene function of any of the components of the pH response pathway affects growth at alkaline pH (Davis *et al.*, 2002). Rim101 pathway is conserved amongst fungi and has been well

characterized in various fungal organisms including *C. albicans* (Fig 1.4). Change in external pH is sensed by Dfg16 and Rim21 (Calcagno-Pizarelli *et al.*, 2007; Castrejon *et al.*, 2006). Neutral-alkaline pH signal received by Dfg16 and Rim21 induces phosphorylation of Rim8 promoting endocytosis (Gomez-Raja and Davis, 2012). These sensor proteins do not function in acidic pH environments. Endocytosis triggers the formation of endosomal-sorting complex (ESCRT) made up of ESCRT-III proteins, Snf7 and Vps20 as well as ESCRT-I and II proteins (Xu *et al.*, 2004). Snf7 initiates Rim13 and Rim20 activity (Xu *et al.*, 2004). Activated Rim20 then binds to the C-terminus of inactive Rim101, a zinc finger transcription factor, which leads to its localization to the endosome (Boysen and Mitchell, 2006). Once in the endosome Snf7 and Rim20 can now activate Rim101 by proteolytic cleavage of the C-terminus allowing its nuclear accumulation and activation of alkaline pH response genes (Davis *et al.*, 2000). Rim101 acts as both activator and repressor of gene expression. Rim101 suppresses the activation of *PHR1*, required for growth at alkaline pH, during growth in acidic conditions and that of *PHR2*, which is required at acidic pH, during alkaline pH (Davis *et al.*, 2000). Adaptation to acidic environment in the host has not been well studied however, preliminary data suggests it is also important.

Rim101 together with another transcription factor, Crz2, may also play a role in acidic pH adaptation. Deleting the *CRZ2* gene in a *rim101* mutant resulted in a growth defect at acidic pH (Kullas *et al.*, 2007). In *C. albicans*, Phr2 is required for growth at acidic pH and essential for infection in a vaginal but not invasive model of candidiasis (Fonzi, 1999; De Bernardis *et al.*, 1998). While the Rim101 pathway has a central role in pH response, other pathways have been implicated in enabling various fungi, including *C. albicans*, adjust to pH changes and include the Ca²⁺-dependent Calcineurin/Crz1 pathway (section 1.5.3.2) (Davis *et al.*, 2002).

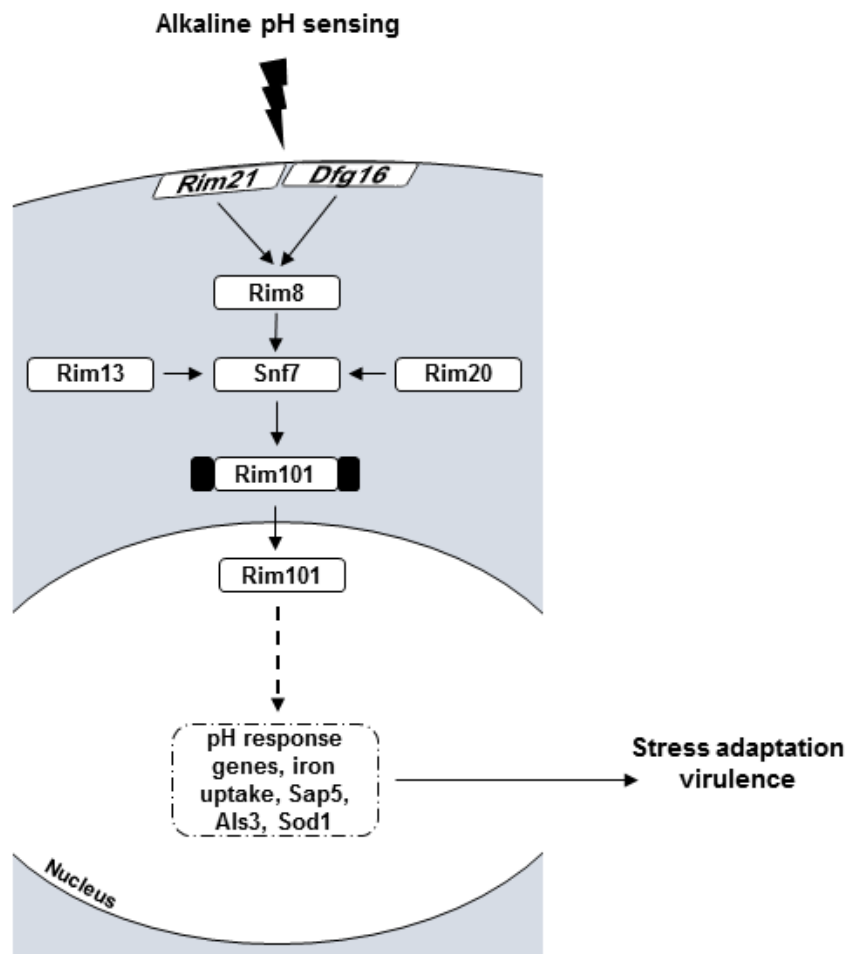


Fig 1.4 Alkaline pH response pathway in *C. albicans*. Growth in alkaline pH environment is sensed by Rim21 and Dfg16 which triggers the ubiquitination of Rim8 and endocytosis. This leads to the recruitment of the ESCRT proteins (eg, Snf7). Snf7 oligomerizes and recruits Rim13 and Rim20 allowing Rim101 processing and activation. Active Rim101 now localises to the nucleus to activate alkaline pH stress response genes. See text for details.

The ability to grow at a given pH is also vital for pathogenesis in *C. albicans*. In the human host, the pH at various locations varies from acidic to alkaline and *C. albicans* must adjust accordingly to establish infection. Both *PHR1* and *PHR2* have been shown to mediate virulence in various models of infection. In a blood model of infection, cells lacking *PHR1* were avirulent (Ghannoum *et al.*, 1995). Contrariwise, *PHR2* is the virulence determinant in acidic environments, this was established using a vaginal and stomach model of infection (De Bernardis *et al.*, 1998; Fonzi, 1999). The Rim101 pathway is also required for virulence in alkaline pH environments. Mutations affecting the pH response regulator Rim101 and members of the pathway, also attenuates virulence but does not prevent killing in a mouse model of infection (Davis *et al.*, 2000). An initial delay in disease onset was observed in mice infected

with *RIM101* pathway deleted *C. albicans* cells however, this was following by rapid disease progression comparable to wild-type cells which lead to death (Davis *et al.*, 2000). This response to infection by *RIM101* pathway mutants is unique and the mechanism involved unknown. Colonisation by these mutants was not affected by deletion suggesting the pathway may play a role in persistence during infection (Davis *et al.*, 2000). The role of Rim101 in virulence has also been demonstrated in other models including oropharyngeal candidiasis and keratitis (Nobile *et al.*, 2008; Yuan *et al.*, 2010) and recently in an intra-abdominal model of candidiasis (Cheng *et al.*, 2013).

As shown in Fig 1.4, besides mediating survival and virulence in alkaline pH niches Rim101 has additional regulatory functions in the pathogenicity of *C. albicans*. *In vitro* and *in vivo* transcriptional profiling studies in *C. albicans* have identified Rim101 dependent genes required for virulence (Bensen *et al.*, 2004; Thewes *et al.*, 2007; Nobile *et al.*, 2008). Rim101 is required for the expression of the adhesin, Als3 involved in host cell invasion (Nobile *et al.*, 2008). No epithelial cell damage occurred with *rim101* mutant cells due to absence of Als3 activity (Nobile *et al.*, 2008). Rim101 also regulates expression of Sap5, a member of the SAP family also required for host tissue invasion (Bensen *et al.*, 2004; Nobile *et al.*, 2008). Rim101 pathway also regulates iron homeostasis at alkaline pH (Bensen *et al.*, 2004; Thewes *et al.*, 2007; Nobile *et al.*, 2008). Rim101 was shown to directly activate expression of genes needed for iron acquisition at alkaline pH. For example, Als3 enables growth on ferritin as iron source during epithelial cell infection (Almeida *et al.*, 2008). Rim101 has also been shown to regulate the expression of *SOD5* under serum-, osmotic-, and alkaline pH- inducing conditions (Martchenko *et al.*, 2004).

1.5.3.2 Calcineurin/Crz1 pathway. In *C. albicans*, Calcineurin, a type 2B protein phosphatase, plays a role in alkaline pH adaptation. This role however, is dependent on Rim101 (Kullas *et al.*, 2007). Calcineurin activates Crz1 by dephosphorylation which prompts its nuclear localisation and activation of pH responsive genes (Karababa *et al.*, 2006). Calcineurin, Crz1, and Crz2 are also required for adaptation to acidic conditions (Kullas *et al.*, 2007). Calcineurin is also essential for virulence in *C. albicans* (Sanglard *et al.*, 2003; Blankenship *et al.*, 2003; Bader *et al.*, 2003).

From the above descriptions, to adapt to host pH niches, *C. albicans* has developed a sophisticated pH sensing and response mechanism. It is also clear that the Rim101

pathway plays a vital role in *C. albicans* virulence but why this is important is not. Interestingly, this pH sensing pathway has additional regulating roles not related to pH adaptation which include adhesion to host cells, tissue invasion, and iron acquisition. In addition, the role of Rim101 in virulence in acidic conditions has not yet been established. There is some indication that Rim101 is required as a double mutation of *RIM101* and *CRZ1* in *C. albicans* cells results in the inability to grow at acidic pH (Davis, 2009). Other regulatory mechanisms for acidic pH adaptation may exist in *C. albicans* but these have not yet been identified.

1.6 Summary and aims

In this introductory chapter, a summary of the major virulence traits of *C. albicans* has been presented, together with a more detailed synopsis of our current understanding of the stress response mechanisms employed by *C. albicans* and their importance in pathogenesis. Whilst there is compelling evidence that stress responses are vital for *C. albicans* to survive within the diverse environments occupied within the host, it is clear that many gaps in our knowledge regarding the stress responses of this major fungal pathogen remain. For example, the transcription factors that mediate gene induction following cationic stress remain elusive. Furthermore, whilst the key role of the Cap1 transcription factor in regulating gene induction following H₂O₂ stress is well established, it is not known which transcription factors regulate *C. albicans* responses to other physiologically relevant ROS, such as superoxide. It is also clear that whilst the pH response pathway has been extensively characterised, not all of the targets of Rim101 may have been identified, and Rim101 independent responses are also evident. It is also noteworthy that whilst transcript profiling studies have identified suites of genes which are induced under particular conditions both *in vitro* and *in vivo*, this does not inform us of the relevant importance of the respective gene products in mediating stress resistance.

Thus a more comprehensive understanding of the cellular processes employed by *C. albicans*, and how these contribute to stress response and virulence, is needed to provide important insight into how *C. albicans* survives successfully as a commensal and a pathogen within the human host. To this end, an initial goal of this project was to provide a global overview of the cellular processes necessary to promote *C. albicans* survival to specific physiologically relevant stresses. This was achieved by screening the *C. albicans* transcription factor deletion collection (Homann *et al.*,

2009) and the most comprehensive deletion collection available (Noble *et al.*, 2010) for genes required for cationic, superoxide, and alkaline pH stress resistance. This provided new insight into both the processes and regulators needed for *C. albicans* stress resistance. Notably, the Pho4 transcription factor was identified as being vital for resisting all three seemingly distinct stresses. Thus subsequent work focused in delineating the role and regulation of the Pho4 transcription factor in mediating stress resistance and virulence in *C. albicans*. Such investigations revealed important links between phosphate metabolism and metal homeostasis in *C. albicans*, providing new evidence that metabolic adaptation is vital to promote *C. albicans* survival in the face of host-imposed stresses.

Chapter 2. Material and Methods

2.1 Yeast Techniques.

2.1.1 *C. albicans* strains, deletion libraries, and growth conditions.

The strains used in this project are listed in Table 2.1. All *C. albicans* strains were grown at 30°C in YPD (yeast extract-peptone-glucose) medium which consists of 2% bacto-peptone, 1% bacto-yeast extract and 2% glucose (Sherman, 2002) in liquid medium or solid with the addition of 2% Bacto-agar. *C. albicans* transformants were grown on SD agar plates (0.67% Bacto-yeast nitrogen base (without amino acids), 2% bacto-agar) supplemented with 2% glucose and appropriate amino acids to allow for selection.

For phosphate limiting conditions strains were grown in YPD - Pi medium made with yeast extract lacking phosphate and supplemented with KCl (ForMedium). For high phosphate growth conditions YPD - Pi medium was supplemented with 10 mM KH₂PO₄ (pH 6).

For detecting secreted acid phosphatase activity PNMC medium (peptone (2.5 g/L), NaCl (3 g/L), MgSO₄ (1 mM), CaCl₂ (1 mM)), supplemented with glucose (20%), ammonium sulphate (5 g/L) was used (Romanowski *et al.*, 2012). When phosphate limiting conditions were required no phosphate was added to the medium (PNMC - Pi) and for studies requiring an enriched phosphate environment the medium was supplemented with 10 mM or 25 mM KH₂PO₄, pH 6 (PNMC + Pi).

Strain		Genotype	Source
SN250	Wt	<i>his1Δ/ his1Δ, leu2Δ:: C. dubliniensis HIS1/leu2Δ::C. maltose LEU2, arg4Δ/arg4, URA3/ura3Δ, IRO1/iro1Δ</i>	Noble <i>et al.</i> , 2005
SN148	Wt	<i>arg4, leu2/leu2, his1/his1, ura3::λimm434/ura3::λimm434, iro1::λimm434/iro1::λimm434</i>	Noble and Johnson, 2005
JC1936	SN250 + Clp10	<i>his1Δ/ his1Δ, leu2Δ::C.dubliniensis HIS1/leu2Δ::C. maltose LEU2, arg4Δ/arg4, ura3/ura3Δ, IRO1 /iro1Δ, Clp10</i>	This study
JC747	SN148 + Clp30	<i>arg4, leu2/leu2, his1/his1, ura3::λimm434/ura3::λimm434, iro1::λimm434/iro1::λimm434, Clp10</i>	Dantas <i>et al.</i> , 2010

$\Delta\Delta orf19.895$	<i>hog1</i> Δ	SN250 <i>his1</i> Δ / <i>his1</i> Δ , <i>leu2</i> Δ :: <i>C. dubliniensis</i> HIS1/ <i>leu2</i> Δ :: <i>C. maltose</i> LEU2, <i>arg4</i> Δ / <i>arg4</i> , URA3/ <i>ura3</i> Δ , IRO1/ <i>iro1</i> Δ <i>hog1</i> Δ :: <i>C. dubliniensis</i> HIS1/ <i>hog1</i> Δ :: <i>C. maltose</i> LEU2	Noble <i>et al.</i> , 2010
JC47	<i>hog1</i> Δ	BWP17 <i>hog1</i> :: <i>loxP</i> -ARG4- <i>ura3-loxP</i> / <i>hog1</i> :: <i>loxP</i> -HIS1- <i>loxP</i>	Enjalbert <i>et al.</i> , 2006
JC75	<i>pbs2</i> Δ	BWP17 <i>pbs2</i> :: <i>loxP</i> -ARG4- <i>ura3-loxP</i> / <i>pbs2</i> :: <i>loxP</i> -HIS1- <i>loxP</i>	Cheetham <i>et al.</i> , 2007
JC482	<i>ssk2</i> Δ	BWP17 <i>ssk2</i> :: <i>loxP</i> -ARG4- <i>ura3-loxP</i> / <i>ssk2</i> :: <i>loxP</i> -HIS1- <i>loxP</i>	Cheetham <i>et al.</i> , 2007
JC50	<i>hog1</i> Δ + Clp20	BWP17 <i>ura3</i> :: <i>limm434/ura3</i> :: <i>limm434</i> , <i>his1</i> :: <i>hisG/his1</i> :: <i>hisG</i> , <i>hog1</i> :: <i>LoxP-ura3-LoxP</i> , <i>hog1</i> :: <i>LoxP-HIS1-LoxP</i> Clp20	Smith <i>et al.</i> , 2004
JC52	<i>hog1</i> Δ + Clp20-HOG1	BWP17 <i>ura3</i> :: <i>limm434/ura3</i> :: <i>limm434</i> , <i>his1</i> :: <i>hisG/his1</i> :: <i>hisG</i> , <i>hog1</i> :: <i>LoxP-ura3-LoxP</i> , <i>hog1</i> :: <i>LoxP-HIS1-LoxP</i> HOG1-Clp20	Smith <i>et al.</i> , 2004
JC63	HOG1-YFP	BWP17 <i>ura3</i> :: <i>limm434/ura3</i> :: <i>limm434</i> , <i>his1</i> :: <i>hisG/his1</i> :: <i>hisG</i> , HOG1-YFP:URA3 HOG1-YFP:HIS1	Smith <i>et al.</i> , 2004
JC1883	PHO4-MH	SN148 PHO4/PHO4-MH:URA3	This study
JC1919	<i>hog1</i> Δ + PHO4-MH	BWP17 <i>hog1</i> :: <i>loxP</i> -ARG4- <i>ura3-loxP</i> / <i>hog1</i> :: <i>loxP</i> -HIS1- <i>loxP</i> /PHO4-MH-URA3	This study
JC1921	<i>pbs2</i> Δ + PHO4-MH	BWP17 <i>pbs2</i> :: <i>loxP</i> -ARG4- <i>ura3-loxP</i> / <i>pbs2</i> :: <i>loxP</i> -HIS1- <i>loxP</i> /PHO4-MH-URA3	This study
JC1923	<i>ssk2</i> Δ + PHO4-MH	BWP17 <i>ssk2</i> :: <i>loxP</i> -ARG4- <i>ura3-loxP</i> / <i>ssk2</i> :: <i>loxP</i> -HIS1- <i>loxP</i> /PHO4-MH-URA3	This study
JC1928	<i>pho4</i> Δ	SN250 <i>his1</i> Δ / <i>his1</i> Δ , <i>leu2</i> Δ :: <i>C. dubliniensis</i> HIS1/ <i>leu2</i> Δ :: <i>C. maltose</i> LEU2, <i>arg4</i> Δ / <i>arg4</i> , <i>ura3/ura3</i> Δ , IRO1/ <i>iro1</i> Δ <i>pho4</i> Δ :: <i>C. dubliniensis</i> HIS1/ <i>pho4</i> Δ :: <i>C. maltose</i> LEU2 Clp10	This study
JC1917	<i>pho4</i> Δ + PHO4	SN250 <i>pho4</i> :: <i>loxP</i> -ARG4- <i>ura3-loxP</i> / <i>pho4</i> :: <i>loxP</i> -HIS1- <i>loxP</i> , Clp10-PHO4	This study
JC1977	PHO4-GFP	SN148 pACT-PHO4-GFP:URA3	This study
JC1983	<i>vtc1</i> Δ	SN148 <i>vtc1</i> :: <i>loxP</i> -ARG4- <i>ura3-loxP</i> / <i>vtc1</i> :: <i>loxP</i> -HIS1- <i>loxP</i> , Clp10	This study
JC1984	<i>vtc4</i> Δ	SN148 <i>vtc4</i> :: <i>loxP</i> -ARG4- <i>ura3-loxP</i> / <i>vtc4</i> :: <i>loxP</i> -HIS1- <i>loxP</i> , Clp10	This study

JC1985	<i>phm5Δ</i>	SN148 <i>phm5::loxP-ARG4-ura3-loxP/phm5::loxP-HIS1-loxP</i> , Clp10	This study
JC1986	<i>phm7Δ</i>	SN148 <i>phm7::loxP-ARG4-ura3-loxP/phm7::loxP-HIS1-loxP</i> , Clp10	This study
JC1991	<i>ppx1Δ</i>	SN148 <i>ppx1::loxP-ARG4-ura3-loxP/ppx1::loxP-HIS1-loxP</i> , Clp10	This study
JC1992	<i>vtc1Δ</i> + PHO4-GFP	SN148 <i>vtc1::loxP-ARG4-ura3-loxP/vtc1::loxP-HIS1-loxP/ PHO4-GFP-URA3</i>	This study
JC1993	<i>vtc4Δ</i> + PHO4-GFP	SN148 <i>vtc4::loxP-ARG4-ura3-loxP/vtc4::loxP-HIS1-loxP/ PHO4 -GFP-URA3</i>	This study
JC2087	<i>vtc4Δ</i> + VTC4	SN148 <i>vtc4::loxP-ARG4-ura3-loxP/vtc4::loxP-HIS1-loxP</i> , Clp10-VTC4	This study
CA-IF003	<i>sod1Δ</i>	SN152, <i>sod1Δ::cmLEU2/ sod1Δ::CdHIS1</i>	Frohner <i>et al.</i> , 2009
CA-IF007	<i>sod2Δ</i>	SN152, <i>sod2Δ::cmLEU2/sod2Δ::CdHIS1</i>	Frohner <i>et al.</i> , 2009
CA-IF0011	<i>sod3Δ</i>	SN152, <i>sod3Δ::cmLEU2/sod3Δ::CdHIS1</i>	Frohner <i>et al.</i> , 2009

Table 2.1 *C. albicans* strains used in this study.

2.1.2 Transformation of *C. albicans*.

The lithium acetate (LiAc) protocol described by Burk Braun (www.sacs.ucsf.edu/home/johnsonlab/burk/transformation) was adopted to transform *C. albicans* cells with exogenous DNA. *C. albicans* strains were grown overnight to an OD₆₆₀ between 1.0 and 3.0 (OD₆₆₀ of 1 is approximately 3.1 x 10⁹ cells/ml). Cells (100 ml) were harvested by centrifugation at 2500 rpm for 2 minutes, pellets washed and resuspended in 40 ml of LiAc/TE solution (100 mM LiAc (pH 7.0), 1x TE [10 mM Tris-HCl pH 7.5, 1 mM EDTA (pH 8.0)]), pelleted again by centrifugation at 2500 rpm for 2 mins and resuspended in 1 ml LiAc/TE. 10 µl of salmon sperm carrier DNA (10 mg/ml) was boiled and cooled prior to addition of exogenous DNA plus 100 µl of LiAc/TE washed *C. albicans* cells and mixed gently. To this mix 750 µl of PEG/LiAc/TE solution (50% PEG 3350, 100 mM LiAc (pH 7.0), 1x TE) was added and mixed gently. The transformation mix was then incubated at 30°C on a shaking platform for 3 h. Cells were then heat shocked at 42°C for 45 mins, following which cells were pelleted by centrifugation at 6,000 rpm for 1 min and resuspended in 200 µl of YPD. Cells were then spread onto SD agar plates containing the appropriate

amino acids for selective growth and grown at 30°C for 2 - 5 days. Colonies recovered from the transformation were then streaked out onto fresh SD agar plates containing the appropriate selective media before genomic DNA extraction for genotype confirmation by polymerase chain reaction (PCR). Positive clones were re-streaked for single colonies on selective SD and YPD agar plates to ensure strain homogeneity and the genotype re-checked by PCR, prior to preparing a 15% glycerol stock in YPD and storage at -80°C.

2.1.3 Yeast genomic DNA extraction.

A large loopful of *C. albicans* cells was scraped from agar plates and washed in 1 ml of distilled H₂O before being resuspended in 200 µl of breakage buffer (10 mM Tris-HCl (pH 8.0), 1 mM EDTA (pH 8.0), 100 mM NaCl, 1% SDS (w/v), 2% Triton X100 (v/v)). Following resuspension 200 µl of phenol-chloroform was added along with approximately 200 µl of glass beads. Cells were disrupted by bead beating for 30 secs in mini bead beater (Biospec Products). Separation of the aqueous DNA containing layer was achieved by centrifugation at 13,000 rpm for 10 mins. DNA was then precipitated by the addition of 2 volumes of 100% ethanol and 1/10th volume of 3 M NaAc (pH 7.0) followed by centrifugation at 13,000 rpm for 15 mins. Pelleted DNA was washed with 70% ethanol and resuspended in 30 µl of sterile nano H₂O. Genomic DNA was stored at -20°C.

2.1.4 *C. albicans* strain construction.

Oligonucleotide primers used for generating the constructs are listed in Table 2.2.

2.1.4.1 Deletion of *VTC1*, *VTC4*, *PHM5*, *PHM7*, and *PPX1*.

To delete *VTC1* in *C. albicans*, disruption cassettes containing either the *HIS1* or *ARG4* gene flanked by *loxP* sites and 91 base pairs upstream and downstream of the *VTC1* open reading frame (ORF), were generated by PCR using *Vtc1del F* and *Vtc1del R* oligonucleotide primers and the plasmid templates pLHL or pLAL (Dennison *et al.*, 2005). Disruption cassettes were then sequentially transformed into SN148 wildtype *C. albicans* cells (Noble and Johnson, 2005) to disrupt both alleles of *VTC1* and generate JC 1970. Disruption of each allele was confirmed by PCR using *Vtc1Ch F* and either *His R* or *Arg2 R* oligonucleotide primers and genomic DNA as template. Loss of *VTC1* was confirmed using the oligonucleotide primers *Vtc1Ch F* and *Vtc1Ch R*. *Clp10* (Murad *et al.*, 2000) was integrated at the *RPS10* locus to create strain JC 1983. This disruption strategy is illustrated in Fig 2.1.

The same disruption strategy was used to delete *VTC4*, *PHM5*, *PHM7*, and *PPX1* genes. *VTC4* alleles were disrupted using *Vtc4del F* and *Vtc4del R* to create strain JC 1973. Disruption of each allele was confirmed by PCR using *Vtc4Ch F* and either *His R* or *Arg2 R* oligonucleotide primers and genomic DNA as template. Loss of *VTC4* was confirmed using the oligonucleotide primers *Vtc4Ch F* and *Vtc4Ch R*. *Clp10* (Murad *et al.*, 2000) was integrated at the *RPS10* locus to create strain JC 1984. *PHM5* alleles were disrupted using *Phm5delF* and *Phm5delR* to create strain JC 1975. Disruption of each allele was confirmed by PCR using *Phm5ChF* and either *His R* or *Arg2 R* oligonucleotide primers and genomic DNA as template. Loss of *PHM5* was confirmed using the oligonucleotide primers *Phm5Ch F* and *Phm5Ch R*. *Clp10* was integrated at the *RPS1* locus to create strain JC1985. *PHM7* alleles were disrupted using *Phm7del F* and *Phm7del R* to create strain JC 1966. Disruption of each allele was confirmed by PCR using *Phm7Ch F* and either *His R* or *Arg2 R* oligonucleotide primers and genomic DNA as template. Loss of *PHM7* was confirmed using the oligonucleotide primers, *Phm7Ch F* and *Phm7Ch R*. *Clp10* was integrated at the *RPS10* locus to create strain JC 1986. *PPX1* alleles were disrupted using *Ppx1del F* and *Ppx1del R* to create strain JC 1964. Disruption of each allele was confirmed by PCR using *Ppx1Ch F* and either *His R* or *Arg2 R* oligonucleotide primers and genomic DNA as template. Loss of *PPX1* was confirmed using the oligonucleotide primers *Ppx1Ch F* and *Ppx1Ch R*. *Clp10* was integrated at the *RPS10* locus to create strain JC 1991.

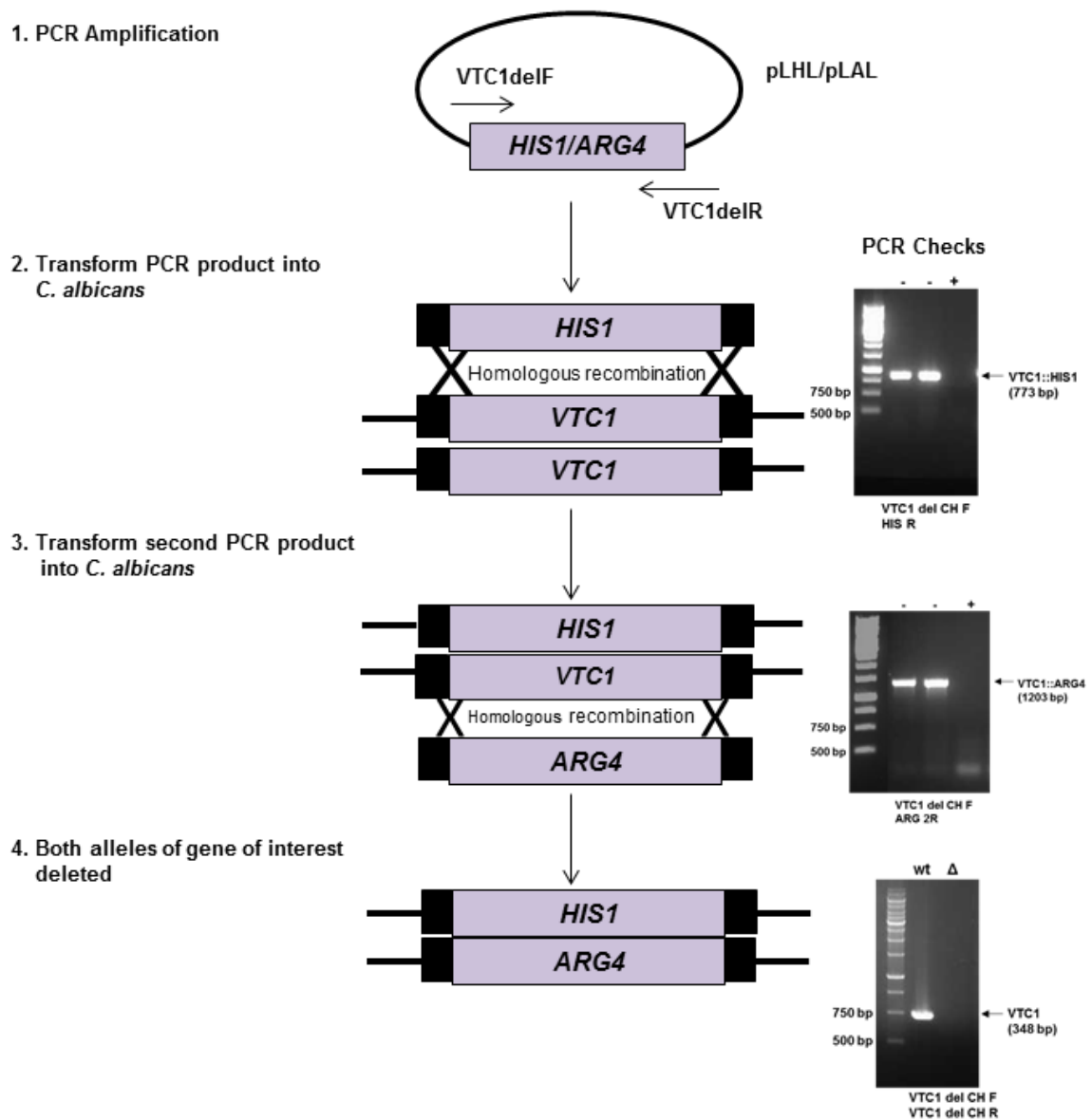


Figure 2.1 Schematic diagram illustrating the strategy employed to delete polyphosphate metabolism genes in *C. albicans*. To delete *gene of interest*, disruption cassettes were generated by PCR using pLHL/pLAL as templates and gene specific deletion oligonucleotide primers. Disruption cassettes consisted of either the *HIS1* or *ARG4* gene flanked by *LoxP* sites at 91 bp of DNA homologous to the regions upstream and downstream of the *gene of interest*. Disruption cassettes were then transformed into SN148 *C. albicans* cells sequentially to disrupt both alleles of the gene. Correct integration was checked by PCR using an oligonucleotide primer upstream of the *gene of interest* with one specific for *HIS1* or *ARG4* using genomic DNA from the *C. albicans* clone (+) or SN148 (-). Gene deletion was also confirmed by PCR using an oligonucleotide primer upstream of the *gene of interest* and one within the *gene of interest* ORF using genomic DNA from SN148 (wt) or the *C. albicans* clone (Δ).

Reintegration of PHO4 and VTC4. To re-integrate *PHO4* into the *pho4* mutant from the deletion library, the *PHO4* ORF plus promoter and terminator sequence was amplified by PCR using the oligonucleotide primers, PHO4BamH1 C1 and PHO4BamH1 C2, and resulting fragment cloned into the integrating plasmid Clp10 (Murad *et al.*, 2000) to generate Clp10-PHO4. Clp10-PHO4 was linearised with *Stu1* and integrated at the *RPS10* locus in a 5 - FOA resistant *pho4Δ* mutant to create JC 1917. The *VTC4* locus plus promoter and terminator sequences was amplified by PCR using the oligonucleotide primers, VTC4BamH1 C1 and VTC4BamH1 C2, and the resulting fragment cloned into the integrating plasmid Clp10 to generate Clp10-VTC4. Clp10-VTC4 was linearised with *Stu1* and integrated at the *RPS10* locus in JC 1973 to create JC 2087. Successful integration of *PHO4* or *VTC4* at the *RPS10* locus was confirmed by PCR using the oligonucleotide primers RSP10 F and PHO4Ch R or VTC4Ch R respectively.

To generate wild-type cells, auxotrophically identical to the *pho4Δ* null (JC 1928) and reintegrated *pho4Δ+PHO4* (JC 1917) strains the deletion library wild-type strain SN250 (Homann *et al.*, 2009) was passed over 5-FOA and Clp10, linearised with *Stu1*, and integrated at the *RPS10* locus to generate JC 1936. Integration at the *RPS10* locus promotes *URA3* expression which negates the influence of *URA3* expression levels on subsequent virulence assays (Brand *et al.*, 2004).

2.1.4.1 Tagging Pho4.

The C-terminus of Pho4 was tagged with 2 copies of the myc-epitope and 6-His residues by amplifying the *PHO4* gene with the oligonucleotide primers Pho4MHSa1 F and Pho4MHSa1 R and genomic DNA as template. The resulting fragment was ligated into the *Pst1* site of Clp-C-MH to generate pPHO4-MH. Correct plasmid construction was confirmed by DNA sequencing. pPHO4-MH was linearised with *Age1* to target integration at the *PHO4* locus in wildtype SN148 cells to generate JC 1883, in *hog1Δ* cells (JC 47) to generate JC 1919, in *pbs2Δ* cells (JC 75) to generate JC 1921, and in *ssk2Δ* cells (JC 482) to generate JC 1923 (Fig 2.2). Chromosomal integration of PHO4-MH was confirmed by PCR using the oligonucleotide primers, Pho4MHTCh F and CycTerm R.

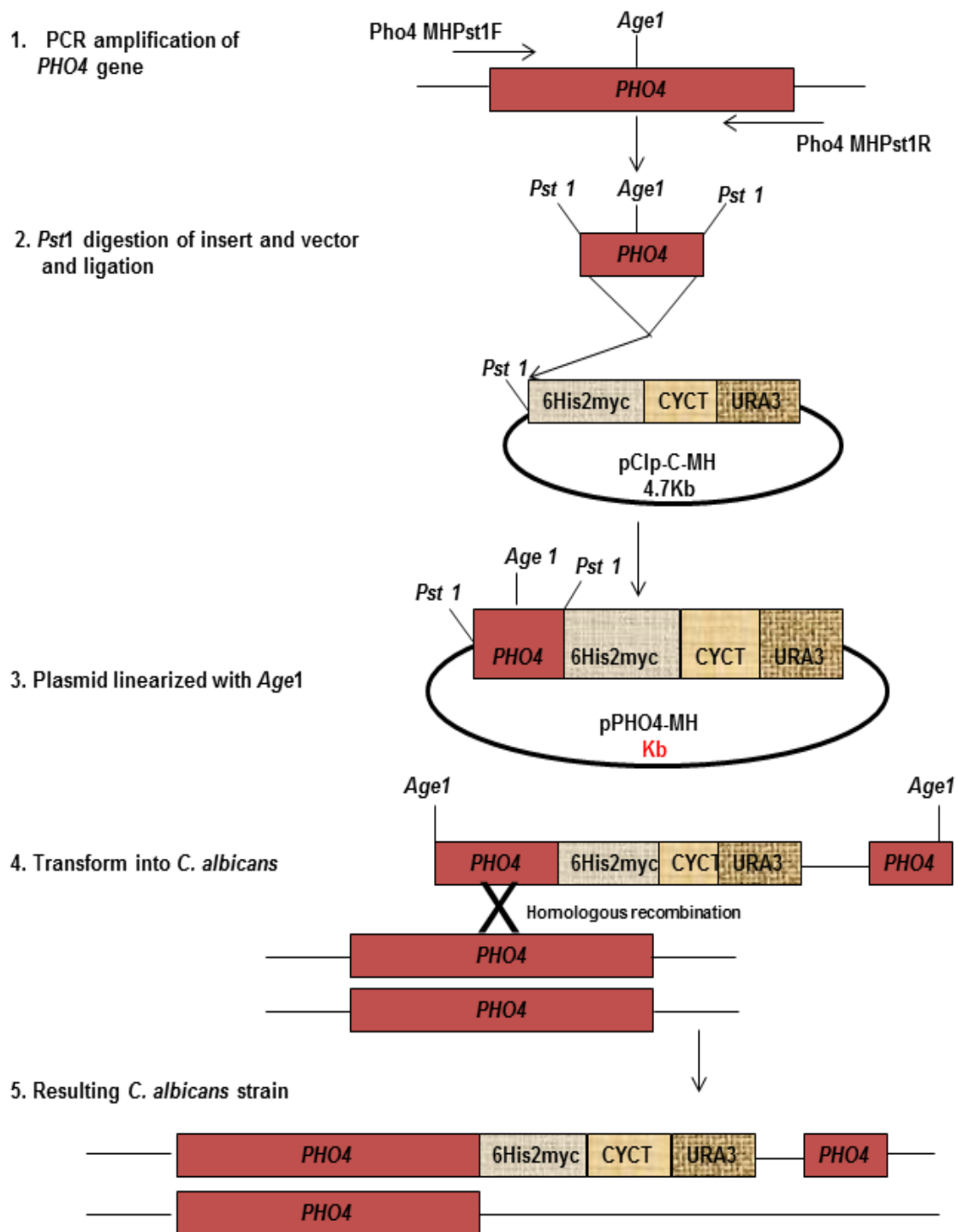


Figure 2.2. Diagram illustrating the myc-HIS tagging of *PHO4* in *C. albicans*. pPHO4-MH was constructed by ligating 308 codons of the *PHO4* ORF into the *Pst*I site of Clp-C-MH (da Silva Dantas *et al*, 2010). The resulting pPHO4-MH was linearised by digestion with *Age*I to direct integration into the chromosome at the native *PHO4* locus to tag Pho4 at the C-terminus with 6His 2myc (Pho4-MH) during transformation of wildtype *C. albicans*.

To tag Pho4 at the C-terminus with GFP the *PHO4* ORF was amplified by PCR using the primers, Pho4ACT1GFP F and GFPACT1 R and ligated into the *Sal1* site of pACT1-GFP (Barelle *et al.*, 2004) to generate pACT-PHO4GFP. The resulting pACT1-*PHO4* plasmid was linearised with *Stu1* and integrated at the *RPS10* locus in wildtype cells to generate JC 1977. DNA sequence and correct integration of plasmid at the *RPS10* locus were confirmed by DNA sequencing and PCR respectively. The same pACT1-*PHO4* plasmid was used to tag Pho4 in *vtc1Δ* and *vtc4Δ* cells to generate JC 1992 and JC 1993 respectively (Fig 2.3).

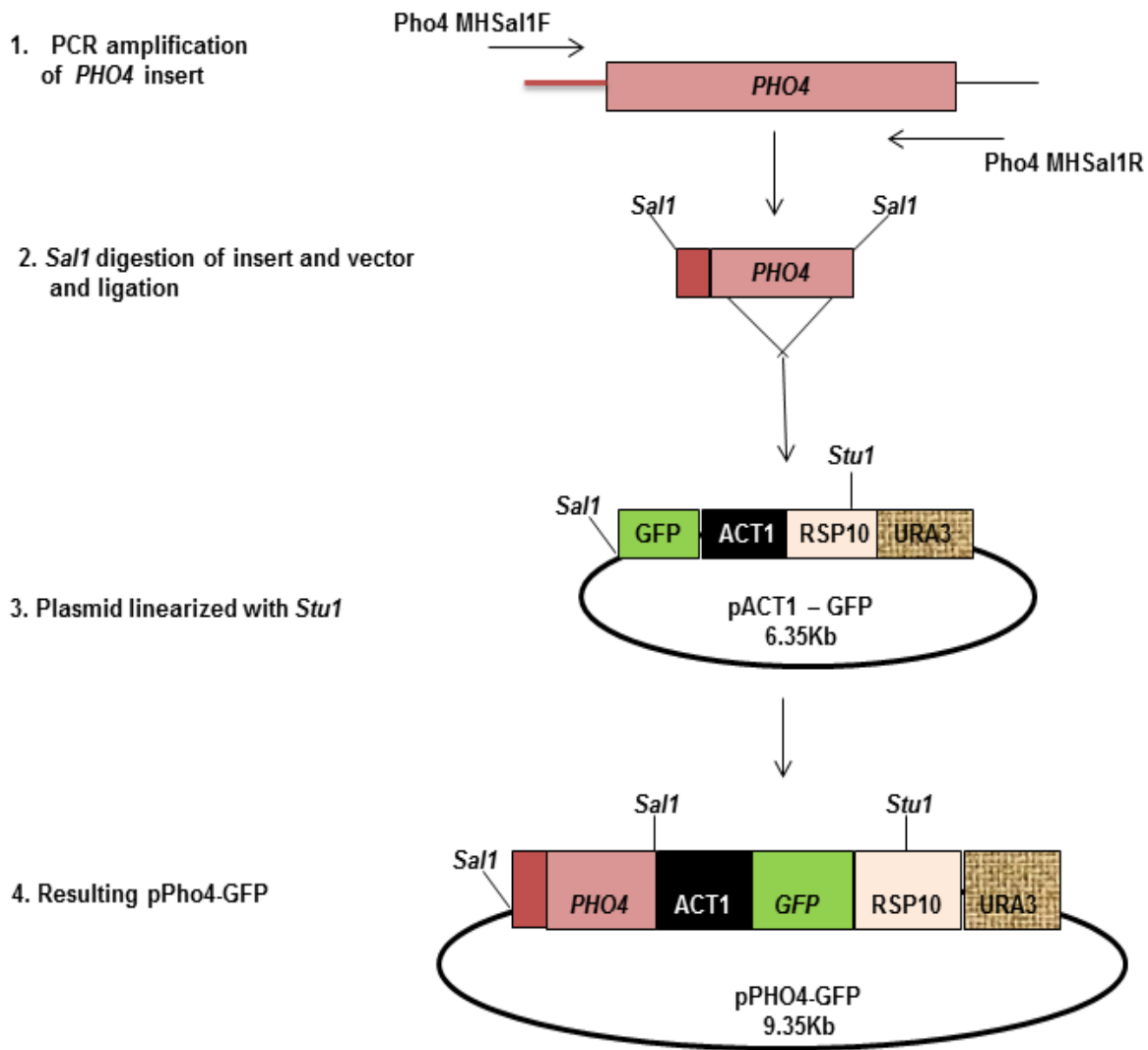


Figure 2.3. Diagram illustrating the construction of pPHO4-GFP. pPHO4-GFP was constructed by ligating the *PHO4* ORF (lacking the STOP codon) and 670bp of the promoter region into the *Sal1* site of pGFP (Barelle *et al.*, 2004). The resulting pPHO4-GFP was then linearised by digestion with *Stu1* which directs integration into the chromosome at the *RPS10* locus in various *C. albicans* strain backgrounds. This plasmid was used to construct JC1977, JC1992, and JC1993.

2.2 Phenotypic tests.

2.2.1 Quantitative Fitness Analysis (QFA).

The *C. albicans* transcription factor deletion collection (Homann *et al.*, 2009) and the most comprehensive deletion collection available (Noble *et al.*, 2010) were screened by QFA to identify genes required for cationic, superoxide, and alkaline pH stress resistance. QFA was carried out by inoculating each strain from the libraries onto solid agar plates and growth of each culture monitored by photography over time. A population growth model was then obtained from the data with the maximum growth rate and maximum doubling potential plotted for each strain. The liquid to solid agar robotic (Biomatrix BM3-SC robot S&P Robotics Inc., Toronto, Canada) spot tests was performed by inoculating colonies from YPD agar plates into 96 - well plates containing YPD medium.

Robotics. Robotics was carried out by Dr Peter Banks, Newcastle University. Resuscitation of frozen strain collections (from liquid to solid agar) was performed on the Biomatrix BM3-SC robot using a 384 - pin (1 mm diameter) tool. Re-array procedures were carried out using the BM3 - SC robot equipped with a 96 - pin rearray pintool. Dilution and spotting of liquid cultures onto solid agar plates was performed on a Biomek FX robot (Beckman Coulter (UK) Limited, High Wycombe, UK) equipped with a pintool magnetic mount and a 96-pin (2 mm diameter) pintool (V&P Scientific, Inc., San Diego, CA, USA). Both the Biomatrix BM3-SC and the Biomek FX were equipped with bar-code readers (Microscan Systems, Inc.) and the bar-codes of plates involved in each experiment were recorded in robot log-files.

Growth assays. Liquid-to-solid agar 384-format robotic spot tests were performed as follows. Individual mutants from the libraries were pinned into 96 - well plates containing 200 ml YPD broth in each well with the Biometrix BM3 - SC robot system (S&P Robotics Inc., Toronto, Canada) using a 96 pin tool. These were grown overnight, without shaking, at 30°C. Cultures were then diluted 1/100 in 200 ml YPD medium and grown without shaking for 8 h at 30°C and spotted onto solid YPD agar plates containing 1 M NaCl, 300 µM menadione, or the pH of YPD adjusted from pH 6 to pH 8 with Tris-HCl (pH 8.25). Plates were incubated at 30°C.

Image analysis and modelling of fitness. This was carried out by Dr Peter Banks, Newcastle University. Solid agar plates were photographed over time on a splmager (S&P Robotics Inc. Toronto, Canada) with an integrated camera. Manual settings of

the camera were as follows: 0.25 s; aperture, F10; white balance, 3700 K; ISO100; image size, large; image quality, fine; image type, .jpg. The image analysis tool, Colonyzer, was used to quantify cell density from captured photographs (<http://research.ncl.ac.uk/colonyzer>) (Lawless *et al*, 2010). Culture density (G) was estimated from captured photographs using the Integrated Optical Density measure of cell density provided by the image-analysis tool Colonyzer (Lawless *et al*, 2010).

GO term analysis. GO term analysis was performed with the Candida Genome Database GO Term Finder looking for enriched cellular processes based on the input of genes represented in both deletion collections.

2.2.2 Spot tests.

Overnight cultures of *C. albicans* grown in YPD were diluted to an OD₆₆₀ of 0.2 in fresh YPD and grown to mid-exponential phase (OD₆₆₀ ~ 0.6). Each culture was then diluted back to an OD₆₆₀ of 0.2 in fresh YPD and 10 - fold serial dilutions were spotted onto YPD plates containing the indicated stress-inducing compounds. Plates were incubated at 30°C for 24 h. Oxidative stress was induced using stock solutions of 30% (w/w) H₂O₂ or 100 mM menadione. To induce osmotic stress a stock solution of 4M sorbitol was used, whereas cationic stress was imposed using 4 M NaCl, or 1 M KCl, CaCl₃, or LiCl or the pH of YPD broth adjusted from pH 6 to pH 8 with a 1 M stock of Tris-HCl (pH 8.25). Cell wall defects were detected using stock solutions of 30 mg/ml Calcoflour white. Sensitivity to heavy metals was assayed using a stock solution of 0.5 M Na₂AsO₃. Polyamine sensitivity was tested for using 1 mg/ml stock of spermidine. Metal toxicity was applied using 1 M stock solutions of CuSO₄, MnCl₂, ZnSO₄, and FeCl₃. Serum sensitivity was tested using 20% (v/v) fetal bovine serum in YPD. All chemicals are either from Sigma or BDH unless stated otherwise.

2.3 Caenorhabditis elegans techniques.

2.3.1 C. elegans strains.

C. elegans strains used in this study are the *glp4 (km25)* and *glp4::sek1 (km25)* from CGC.

2.3.2 Preparation of Nematode Growth Media Lite (NGML) plates.

Nematodes were maintained routinely on Nematode Growth Media-Lite (NGM-L). This medium is composed of 2% (w/v) NaCl, 4% (w/v) Bacto tryptone (BD), 4% (w/v) Bacto agar (BD), 3% (w/v) KH₂PO₄ (BioChemika) and 0.5% K₂HPO₄ (BioChemika).

Following sterilization NGM-L medium was supplemented with 5 mg/ml cholesterol. Freshly prepared plates were either seeded with an *E. coli* OP50 (Brenner, 1974) lawn or kept at 4°C until required. *E. coli* seeded plates were also kept at 4°C until required. All chemicals are either from Sigma unless stated otherwise.

2.3.3 Bacterial food source preparation.

Single colonies of OP50 *E. coli* were generated by streaking out a frozen stock onto a fresh LB solid plate containing 10 µg/ml of streptomycin (Sigma) and incubated overnight at 37°C. A single colony of *E. coli* was then used to inoculate 100 ml of LB liquid medium containing 10 µg/ml of streptomycin and incubated with shaking overnight at 37°C until saturation. Using aseptic techniques NGM-L agar plates were seeded with a thin bacterial lawn of *E. coli* OP50 (approximately 0.7 ml in the middle of each 60mm petri dish). Seeded plates were then allowed to dry at room temperature for at least 48 h and then stored at 4°C until required.

2.3.4 Maintenance of *C. elegans* stock strains.

Stock plates of *C. elegans* were maintained at 15°C in sealed plastic containers (Brenner, 1974). Stocks were transferred to fresh NGM-L plates with a platinum wire pick every week using a stereo microscope (Leica CLS 50x or Zeiss Discovery V8).

2.3.5 Synchronicity of nematodes.

To synchronise nematodes, approximately 20 - 25 L4 larval stage worms were transferred to a seeded NGM-L agar plate. The plate was then starved of food to arrest development of progeny at L1 larval stage. Worms were removed from starved plates using the platinum pick (for the infection assay) or with 2ml of M9 [6% (w/v) Na₂HPO₄ (BDH), 3% (w/v) KH₂PO₄ (BioChemika), 5% (w/v) NaCl (Sigma), 0.25% (w/v) MgSO₄.7H₂O (BDH)] used to aseptically resuspend and transfer worms into a sterile 15 ml polypropylene tube. Any larger larval stage worms were separated from the smaller L1 worms by their rapid sedimentation to the bottom of the tube which occurs between 2 - 3 mins following transfer. The supernatant which contains the L1 larval stage worm was then transferred to a fresh 15ml polypropylene tube. 10 µl of the suspended worms was placed in the centre of a microscope slide (0.8 x 1.0 mm, VWR international) and examined under the microscope (Leica CLS 50x) to confirm synchrony and to determine number of L1 worms per 1.0 µl of suspension. An appropriate volume of the worm suspension was then used to seed fresh NGM-L plates to allow growth to L4 larval stage.

2.4 Molecular biology techniques.

2.4.1 Polymerase chain reaction.

For cloning, DNA fragments were amplified by PCR using the Pfusion PCR system (New England Biolabs). 50 µl reactions mixes containing 0.5 µl template DNA, 200 µM each of dATP, dCTP, dTTP and dGTP, 1x PCR HF buffer (supplied with enzyme), 100 pmol of each oligonucleotide primer and 1.0 µl polymerase enzyme. Reactions were carried using the following conditions: Step (1): 98°C for 30 secs, Step (2): 98°C for 10 secs, Step (3): 50°C for 30 secs, Step (4): 72°C for 30 seconds/kilo base, Steps (2) to (4) repeated for 35 cycles, Step (5): 72°C for 10 mins, Step (6): Held at 4°C.

Diagnostic PCR to check for correct strain construction was used with genomic DNA template and the Simple Red *Taq* polymerase system (Thermoscientific, UK). 50 µl reactions were prepared as above, with the exception that the *Taq* buffer was prepared in house (500 mM KCl, 100 mM Tris (pH 8 - 9), 1% Triton X-100, and 15 mM MgCl₂). Reactions were carried out using the following conditions: Step (1): 94°C for 90 secs, Step (2): 94°C for 30 secs, Step (3): 50°C for 30 secs, Step (4): 72°C for 1 min/kilo base, Steps (2) to (4) repeated for 35 cycles, Step (5): 72°C for 10 mins, Step (6): Held at 4°C.

Disruption cassettes were synthesised using the Simple Red *Taq* polymerase system. 50µl reaction mixes contained 0.5µl template DNA of either the pLHL or pLAL cassettes (Dennison *et al.*, 2005), 400 µM of each dNTP, 1x *Taq* buffer (same as described above), 250 pmol of each oligonucleotide primer and 1 µl polymerase enzyme. PCR was carried out under the following conditions: Step (1): 94°C for 5 mins, Step (2): 94°C for 1 min, Step (3): 50°C for 2 mins, Step (4): 72°C for 2 mins, Step Steps (2) to (4) repeated for 30 cycles, Step (5): 72°C for 18 mins, Step (6): Held at 4°C. All reactions were carried out in a T3 thermocycler (Biometra).

2.4.2 Oligonucleotide Primer Sequences.

Oligonucleotide primers over 40 bp were synthesised by MWG-Biotech (Eurofins MWG Operon, London, UK), and those under 40 bp were synthesised by Eurogentec (Eurogentec, Southampton, UK). Sequences are listed in Table 2.2.

Oligonucleotide	Primer sequence 5' - 3'	Restriction site
PHO4 C1	GCGCGGATCCGGCACGTCTTATTGCAACTAAC	<i>BamH1</i>
PHO4 C2	GCGCGGATCCGCCAATATCATTTCCTGATAGG	<i>BamH1</i>
Pho4 MH Pst1	AATGTCTGCAGCAATGCTACCACGGTCAATGGTAG	<i>Pst1</i>
Pho4 MH Pst2	AATGTCTGCAGCTTCCTTCCTTTCAACTCCTCAAC	<i>Pst1</i>
Pho4 ACT1 GFP F	AGGCGGGTCGACATGGACCAGCAAGTT TGAACCC	
Pho4 ACT1 GFP R	AGGCGGGTCGACTTATTTGTACAATTC ATCCATACCATGGG	
VTC1 del F	ACGTGTGTAGTAATGCGGCTCTCACAAAAAATGTA ACAATAAATTTTGTGCAACTGATAAAAAACAAGTCTTT TTATCACACATTTTTTCTAACCACCCAGGGTTTT CCAGTCACG	
VTC1 del R	CAAACCTCTGCAATAAATAAGGCAATTATATTAGAAG ACATTACTATGTGAAAAGAAAAGTACAAAAAATTT TTTTTTTTGGAGGGGGGCTACACACTCACTAAAGGG AACAAAAGC	
VTC1 Ch F	ATTGGACCCGCCCATCAGCTTGG	
VTC1 Ch R	GGCTCAACTCTAGCTGGTAACGCAAT	
VTC4 del F	GGTCATATCCAGCCTCTCTTTTATCATCCCATTCCC AATATTCCAATTCCTCAACCTACCACTTTTTTTTAAAT AACAACTTTCTATATTTATTTAAGCACCAGGGTTTTCC CCAGTCACG	
VTC4 del R	AAATCAATCTCGTTGAAACAGAATCTACAAAGTATAA TATCTTGTTAGATTAATAAACTTTTCTATTTTTAAAT GACTATACTAGAACCAGTGATACTCACTAAAGGGAA CAAAAGC	
VTC4 Ch F	TGATGATACGGAAGACCCACACGTGG	
VTC4 Ch R	GGACCAAATTTGTCTCCATATGCCACTG	
PHM5 del F	AACAATTAGATCCTTTTGGTTTTTCATTTTCAATTCAAT TTTTAGATTTTTTTTTATTTTCATTTTTTTTGTTTACTT ATACATTTATATATTCAACATAACCAGGGTTTTCCCA GTCACG	
PHM5 del R	AAATGTAAAATTTATATTCGTTACTACATCAAAATAA TCAAAAAATAAAAAATAAAAAATAGAATAATAAAA GTGACCATACAAAATAAAAAATCGCTCACTAAAGGGA ACAAAAGC	
PHM5 Ch F	GCTTTACAACAATTTTATACTGG	
PHM5 Ch R	GGATTCAAATCGGCATAGTAT	

PHM7 del F	ATTTGCTTTCCTAGCTTATTCATTTTCATCTTAACTAAT TAATTGGATTAATTGTTATCATTTATTTTTATTAATCA AGTTTTTTTTTATTAAGAACAGACACCAGGGTTTTCCC AGTCACG	
PHM7 del R	AAAAATACCATTTAAATATACAAAAATCAAAAAAAAA ACCACAACGAACAATGATCTGTTTTGTCTTCTCTTTT TCTTTTTTTATTATAATTATTACTACTAAAGGGAACA AAAGC	
PHM7 Ch F	CGAATGGTAGCAGTTAATCTGC	
PPX1 del F	CGTCATACGTGAAGAGGAAGCACGTTCTATTTAAAG ATATCTTCTCTTTTCATAAAAAATAAAAATCATCTCC AGTAGGGTTGTTCTTAATACTACAGTCCCAGGGTTT TCCCAGTCACG	
PPX1 del R	CATAAACAGTTTAATGCCGGTTTCTATGAGAAGTGT ATCAATTGGTACTGATAATTATTTAATTAGTTATCTAA GCTACACCTAAGGTTATCAATTTCTCACTAAAGGGA ACAAAAGC	
PPX1 Ch F	GGATATTTGTACCACGGC	
PPX1 Ch R	GGCTCCATAAACTTCATTATTGAGT	
Arg2 R	CCCATCTAATAGGTTGAGC	
His R	AATGGTTGCGTAATAAA	
RP10 F	TGTTCCAAGTCCCAGCTCTC	
CycTerm R	CGACAGCCATGTTGTAC	
URA F	GCACTGGAAGTATATTATC	

Table 2.2 Oligonucleotide primers used in strain construction in this study.

2.4.3 Restriction endonuclease digestion, phosphatase treatment and DNA ligation reactions.

Restriction enzymes were supplied by Promega (Southampton, UK) and restriction endonuclease digestion was carried out according to manufacturer's instructions. Phosphatase treatment was carried out using calf intestinal alkaline phosphatase supplied by New England Biolabs (Herts, UK). Reaction mixes were set up according to the manufacturer's instructions, phosphatase treatment was at 37°C for 15 - 20 mins. DNA ligation reactions were carried out using T4 DNA Ligase (supplied by Promega, Southampton, UK), reactions contained a molar ratio of approximately 1 vector (50 ng): 3 insert fragment and incubated at room temperature for 1 h or overnight at 4°C.

2.4.4 Bacterial growth conditions and transformations.

Plasmid transformation was carried out using *Escherichia coli* competent SURE cells (Stratagene, UK) grown at 37°C in liquid Luria Broth (LB) (2% (w/v) Bacto tryptone, 1% (w/v) Bacto yeast extract, and 1% (w/v) NaCl, pH 7.2) or solid LB agar in which 2% (w/v) Bacto agar was added. Selection of *E. coli* SURE cells transformed with plasmids carrying the ampicillin resistance gene was carried out in LB media supplemented with 0.1 mg/ml ampicillin (Sigma, Dorset, UK-Aldrich). 100 ng of plasmid DNA in 0.5 µl was added to 100 µl of competent cells and incubated on ice for 30 minutes. Cells were then heat shocked by incubation at 42°C for 45 secs and followed by 2 mins incubation on ice. 1 ml of LB was added to the cells which were then incubated at 37°C with shaking for 1 h, following which 200 µl of cells were spread onto LB agar containing 0.1 mg/ml ampicillin. Plates were incubated overnight at 37°C.

2.4.5 Electrophoresis.

Analysis of PCR products was carried out by electrophoresis on 1% (w/v) agarose gels containing 0.02% ethidium bromide, prepared and run in 1x TAE buffer (40 mM Tris acetate, 1 mM EDTA [pH 8.0]). PCR products subsequently used for cloning were gel extracted and purified using the QIAquick® Gel extraction Kit (Qiagen, UK) according to the manufacturer's instructions.

2.4.6 Plasmid DNA extraction.

Plasmid DNA was extracted from *E. coli* by the standard alkaline lysis extraction procedure (Birnboim & Doly, 1979). *E. coli* was inoculated into 5 ml LB/Amp and grown at 37°C with shaking overnight. Cells were then pelleted by centrifugation at 13,000 rpm for 1 min. Cell pellets were resuspended in 200 µl of lysis solution 1 (50 mM glucose, 25 mM Tris-HCl (pH 8.0), 10 mM EDTA (pH 8.0)). To this 200 µl of lysis solution 2 was added (0.2 M NaOH, 1% SDS (w/v)) and inverted 6x to mix. Once the solution was clear, 350 µl of a neutralisation solution (3 M KAc, 8% glacial acetic acid (v/v)) was added and inverted 6x to mix. Following this, 400 µl of phenol: chloroform was added to the sample and vortexed to mix. The aqueous layer was separated by centrifugation at 13,000 rpm for 4 mins. Plasmid DNA was precipitated from the aqueous layer by adding 2 volumes of ethanol (100%) and incubating overnight at -20°C. The plasmid DNA was then pelleted by centrifugation at 13,000 rpm for 15 mins, washed with 500 µl of 70% ethanol and then re-suspended in 30 µl of sterile nano H₂O.

Plasmid DNA to be sequenced was prepared using GenElute™ HP Plasmid Miniprep Kit (Sigma, Dorset, UK Aldrich) according to the manufacturer's instructions.

2.4.7 DNA sequencing.

DNA sequencing was carried out by GATC Biotech (GATC Biotech Ltd, London, UK).

2.5 RNA Analysis.

2.5.1 Growth conditions.

C. albicans mid-log samples were collected (25 ml) prior to or following treatment with the specified stress-inducing condition (cationic, superoxide, or alkaline pH) at the specified concentration and times and snap frozen in liquid nitrogen. For phosphate limiting condition, cells were collected (15 ml) prior to or post 14 h of phosphate starvation.

2.5.2 RNA extraction for Northern blotting.

RNA was extracted as described by Blackwell *et al* (2003) with some modifications. Briefly, cell pellets were thawed rapidly at room temperature and resuspended in 200 µl ice cold RNA buffer (100 mM EDTA (pH 8.0), 100 mM NaCl, 50 mM Tris-HCl (pH 8.0) containing 5 µl 20% SDS (w/v). To the cell mix 200 µl of cold phenol: chloroform was added with approximately 1ml of baked glass beads. Cells were disrupted by bead beating for 30 secs, and the aqueous layer containing RNA, separated by centrifugation at 3000 rpm for 15 mins. The aqueous layer was washed twice with an equal volume of phenol: chloroform. RNA was precipitated by the addition of 0.6 volume ice-cold isopropanol and incubation at -80°C overnight. RNA was pelleted by centrifugation at 13,000 rpm for 15 mins, then washed in 70% ethanol and resuspended in 30 µl of nano-pure H₂O by leaving on ice until pellet was completely dissolved. RNA samples were stored at -80°C and, prior to use, concentration was determined by measuring the absorbance at 260nm using a nanodrop spectrophotometer (Nanodrop).

2.5.3 RNA extraction for RNASeq analysis.

For RNA seq analysis, cell pellets were thawed on ice and resuspended in Qiazol (Qiagen). Cells were disrupted by vortexing and the aqueous layer containing RNA separated by centrifugation. RNA was precipitated with isopropanol at room temperature. RNA was pelleted by centrifugation, then washed twice in 70% ethanol and resuspended on ice in DEPC H₂O. Agilent Bioanalyzer was used to check the RNA

integrity and RNA concentration measured with the nanodrop spectrophotometer (Nanodrop). DNAase treatment to remove genomic DNA was done with the TURBO DNA-free kit from Ambion according to the manufacturer`s instructions.

2.5.4 Northern blotting.

RNA at a final concentration of 15 - 25 µg in 10 µl was added to 12 µl of RNA denaturing buffer (2.5 µl 40% glyoxal, 8 µl DMSO and 1.6 µl 100 mM NaPO₄ pH 6.5) and denatured by incubating at 50°C for 15 mins. Denatured RNA was separated on a 1.2% agarose gel prepared in 15 mM NaPO₄ buffer (pH 6.5) at 4 volts/cm² for 3 - 4 h, with buffer re-circulation at approximately 30 mins intervals. RNA was transferred to a Gene Screen membrane (Dupont NEN Research Products, Boston MA); by overnight blotting with 25 mM NaPO₄ buffer (pH 6.5). RNA was then cross-linked onto the membrane using a UV Stratalinker 2400 using the auto crosslink setting.

Prior to RNA detection, the membrane was incubated in a hybridisation solution (QuickHyb (Agilent) containing 100 µg denatured salmon sperm DNA at 68°C for 10 - 20 mins. Gene specific probes were amplified by PCR using genomic DNA as a template and the oligonucleotide primers listed in Table 2.3. Probes were labelled with [α -³²P] dCTP (supplier) with a Prime-a-Gene labelling kit (Promega, Southampton, UK,) according to the manufacturer`s instructions and then incubated with the membrane and hybridisation solution at 68°C for 1 h with rotation. The membrane was washed with 2X SSPE + 0.01% SDS for 10 mins and then with 1X SSPE + 0.01% SDS for 5 mins, and mRNA levels visualised by exposing the membrane to a phosphorimager plate and phosphorimaging using the Bio-imaging analyser Fuji Film Bas - 1500 and quantification performed using ImageQuant software. In addition, autoradiographs were obtained by exposing the membrane to film (Fuji Medical X-ray film- SuperRX) for 1 - 12 h at -80°C before manual developing.

2.5.5 RNASeq alignment and analysis.

Samples were processed through the Ion Torrent Proton sequencer (CGEBM University of Aberdeen Genomics facility). RNA Seq alignment and analysis was performed by Stavroula Kastora, University of Aberdeen. Raw fastq files were successively processed in the following order through Fastqc (v.10.1), Trimalore (v. 3.1), Samtools (v.1.19), STAR aligner (v. 2.4) and Htseq (v. 5.4). Genome alignment was conducted against the C_albicans_SC5314_version_A21-s02-m09-r08

chromosomes file provided by Candida Genome Database. Gene expression analysis was performed using Partek® Genomics Suite® software, version 6.6
Copyright ©; 2015.

Oligonucleotide	Sequence 5' - 3'
SOD3 NP F	CCTTACCCAAGATTGATTGG
SOD3 NP R	AGCCCAGTTGATCACGTTCC
PHO84 NP F	ACCGCTTTCAAAGATTATTTGG
PHO84 NP R	CGACTTTATCGGCAATAGAACC
ENA2 NP F2	GCTGACTAAAGAGAATTCG
ENA2 NP R2	CGATGGTTAATCTGTATGC
ENA21 NP F	CTGGTGAATCATTACCAGTGG
ENA21 NP R	CCAGTTTTATCTGAACAAAT
SOD1 NP F	GCTGGTATGTAATTCAATGC
SOD1 NP R	CCAGCATGACCAGTAGTTTT
GPD 2 F	TGTATTGTCGGTCCGGTAACTGG
GPD 2 R	CTTTAACATTTCTACCACCTGAGC
RHR2 F	GACAAAGACTCAACAACCAG
RHR2 R	CCTTGAATTCGTCAGTTTCC
PHO4 ChF	ACAACAAAGCGTGTTAGG
PHO4 MHPst1R	AATGTCTGCAGCTTCCTCCTTTCAACTCCTCAAC
PHO100 NP F	ACCAACGATGATGGTTGG
PHO100 NP R	GGTAATGAACAGTCACCATT
FGR2 NP F	CTCATGATGAAGATACTTTGGCC
FGR2 NP F	TTGGTAAAATGCATATGCTAATGC
PMA1 NP F	AAAAC TTGGTTCTTAAATTCG
PMA1 NP R	GGTAGTACCAATACCGTTCA
ACT1 F	GATGAAGCCAATCCAAAAG
ACT1 R	GGAGTTGAAAGTGGTTTGGT

Table 2.3 Oligonucleotide primers used to amplify probes for Northern blotting.

2.6 Protein analysis.

2.6.1 *C. albicans* protein extraction.

Samples were collected from mid-exponential phase *C. albicans* cultures, either with or without stress treatment as indicated. Cells were harvested by centrifugation at 2500 rpm for 2 mins prior to being snap frozen in liquid nitrogen. Cell pellets were thawed on ice, washed in 700 µl of ice-cold protein lysis buffer (50 mM Tris-HCl pH 7.5, 150 mM NaCl, 0.5% NP₄O (v/v), and 10 mM imidazole) containing protease (0.1% leupeptin (v/v), 0.1% pepstatin A (v/v), 1% aprotinin (v/v), 1% phenylmethanesulfonyl fluoride (PMSF) (v/v)) and phosphatase inhibitors (0.2% Na₃VO₄ (v/v) and 5% NaF (v/v)). All the chemicals were obtained from Sigma unless stated otherwise. For samples to be subsequently treated with phosphatase, Na₃VO₄ and NaF were omitted from the lysis buffer. Cells were resuspended in 150 µl of the ice-cold protein lysis buffer mix and approximately 2 ml of cold glass beads added. Cells were disrupted by vortexing with a bead beater machine for 2x 25 seconds with 2 mins on ice between vortexing. Extracts were collected and cell debris was removed by centrifugation at 13,000 rpm for 10 mins at 4°C. Protein concentration was determined by Bradford protein assay (Bradford, 1976) (Pierce) according to the manufacturer's instructions. Samples were prepared to the desired protein concentration, as indicated, and 2x SDS loading dye (62.5 mM Tris pH 6.7, 2% SDS (w/v), 50% Glycerol) added and stored at -20°C.

2.6.2 *C. elegans* protein extraction.

Approximately 3000 worms were washed off NGM-L or BHI agar plates seeded with *E. coli* OP50 or *C. albicans* respectively as described above (section 2.3.5) with 3 – 5 ml of M9 into a sterile 15 ml polypropylene tube. Worms were allowed to sediment to the bottom of the tube following which the supernatant was removed and worm pellets snap frozen in liquid nitrogen. 200 µl of ice-cold lysis buffer (same composition as that described in section 2.6.1) was added to the rapidly thawed worm pellets which were then transferred to ribolyser polypropylene tube (Greiner Bio-One) containing 1 ml of chilled 0.5 mm glass beads (Biospec Products). The worms were broken up with a bead beater for 15 secs. The bottom of the tube was pierced and worm lysate gathered by centrifugation at 2500 rpm for 2 mins at 4°C (Harrier 18/8 Sanyo). Protein lysates were cleared by centrifugation in a micro centrifuge at 13, 000rpm for 10 mins at 4°C (Hawk 15/05 Sanyo). The supernatant was transferred to a fresh Eppendorf tube and total protein concentration determined

using Bradford reagent (Thermoscientific) using the absorbance of 595nm. Loading dye of 4x sample buffer (0.5% (w/v) Bromophenol blue, 10% (v/v) SDS (BioChemika), 625 mM Tris-HCl pH 6.8, 50% (v/v) glycerol (BDH), 10% (v/v) β -mercaptoethanol) was added to each sample and boiled for 5 mins at 100°C prior to SDS polyacrylamide gel electrophoresis (SDS-PAGE). All chemicals were from Sigma unless stated otherwise.

2.6.3 SDS - PAGE and Western blotting.

Protein samples were analysed by electrophoresis using 8% or 10% SDS polyacrylamide gels (Laemmli, 1970). Following electrophoresis proteins were transferred to nitrocellulose membrane (Protran®, Schleicher & Schuell Bioscience, DE), and blocked with bovine serum albumin (BSA) (10% BSA (w/v) in TBST; 1x TBS (1 mM Tris HCl (pH 8), 15 mM NaCl, 0.01% Tween 20). Membranes were probed with the appropriate primary antibodies overnight at 4°C. Membrane was then probed with the secondary antibodies at room temperature. Membrane development was done using the ECL™ Western blotting detection system (Amersham Pharmacia Biotech) and Fuji Medical X-ray film.

2.6.4 Detection of Pho4 phosphorylation.

C. albicans cells expressing 2-myc 6His tagged Pho4 (Pho4 - MH) were grown to an OD₆₆₀ of 0.5 - 0.6 and treated with the appropriate stress-inducing agents at the specified concentrations and times. Cells were harvested by centrifugation at 2500 rpm for 2 mins and snap frozen. Protein extraction was carried as detailed above. Proteins were subsequently analysed by 8% SDS - PAGE and western blotting. Pho4 - myc tagged was detected with an anti-myc mouse monoclonal primary antibody (9E10, Sigma, Dorset, UK) and HRP-conjugated anti-mouse secondary antibody (Sigma, Dorset, UK).

2.6.5 Hog1 phosphorylation assay.

C. albicans cells were grown to an OD₆₆₀ of 0.5 - 0.6 and treated with the appropriate stress-inducing agents at the specified concentrations and times. Cells were harvested by centrifugation at 2500 rpm for 2 mins and snap frozen. Protein extraction was carried as detailed above and 30 – 50 μ g of protein extracts subsequently analysed by 8% SDS - PAGE and western blotting. Phosphorylated Hog1 was detected with an anti-phospho-p38 antibody (New England Biolabs) and HRP-conjugated anti-rabbit secondary antibody (Sigma, Dorset, UK). Total Hog1

levels were determined by stripping blots and probing with an anti-Hog1 antibody (Santa Cruz Biotechnology) and HRP-conjugated anti-rabbit secondary antibody (Sigma, Dorset, UK). Equal loading of protein samples were also determined by probing with an anti-tubulin antibody (DSHB, University of Iowa) HRP-conjugated anti-mouse secondary antibody (Sigma, Dorset, UK).

2.6.6 *C. elegans* Pmk1 phosphorylation assay.

Protein extraction was carried as detailed above and 8 – 10 µg of protein extracts subsequently analysed by 10% SDS-PAGE and western blotting. Phosphorylated PMK1 was detected with an anti-phospho-p38 antibody (New England Biolabs). Equal loading of protein samples were also determined by stripping blots and probing with an anti-tubulin antibody (E7) (Developmental Studies Hydridoma Bank, University of Iowa) and HRP-conjugated anti-mouse secondary antibody (Sigma, Dorset, UK).

2.6.7 Lambda phosphatase treatments.

Protein extracts were performed as previously described omitting phosphatase inhibitors from the protein lysis buffer. Protein samples were incubated at 30°C for 30 mins with lambda protein phosphatase (New England Biolabs, Herts, UK). 2x SDS loading dye was added to the phosphatase treated protein lysates and samples were stored at -20°C. Proteins were subsequently analysed by 10% SDS - PAGE and western blotting.

2.6.8 Sod in-gel activity assay.

Mid-exponential phase *C. albicans* cells (OD₆₆₀ 0.5-0.6), with or without the addition of menadione or copper as indicated, were harvested by centrifugation at 2500 rpm for 2 mins and snap frozen in liquid nitrogen prior to protein extraction. Duplicate whole cell lysates were prepared using lysis buffer containing 10 mM sodium phosphate, pH 7.8, 5 mM EDTA, 5 mM EGTA, 50 mM NaCl, 0.45% (v/v) NP - 40 and 10% (v/v) glycerol (Aguirre *et al.*, 2013). Cells were lysed with a bead beater and then clarified by centrifugation at 13,000rpm for 10 mins at 4°C. Protein concentration was determined by the Bradford protein assay. For native-PAGE gel electrophoresis the method described by Weydert and Cullen (2010) was used with a few modifications. One set of lysate protein (50µg) samples was subjected to electrophoresis on 12% native gel for 360 mins at 4°C. Prior to use the gel was pre-ran for 120 mins at 4°C. Sod activity was assayed by Nitro blue tetrazolium (NBT)

staining as described by Kuo *et al* (2013). After electrophoresis, gel was washed 3x in distilled water prior to incubation with NBT solution in the dark with gentle shaking for 30 mins at room temperature (RT). This was followed by 1 wash in distilled water (in the dark) and incubation with riboflavin solution in the dark with gentle shaking for 30 mins at RT. Gel was washed with distilled water 3 times prior to illumination under white light and kept in water during the illumination period (1 – 24 h). Gel was then imaged on a flatbed scanner when the gel turned blue/purple with clear white bands appearing where the Sod enzymes are present in the gel. The remaining set of protein lysate (50 µg) samples was used to confirm equal loading of protein samples by 10% SDS-PAGE, Western blotting and Ponceau-S staining of the membrane.

2.7 *C. albicans* polyphosphate (polyP) analysis.

2.7.1 Growth conditions for polyP detection.

For PolyP detection exponentially growing cells (OD₆₆₀ 1 - 3) in YPD were harvested by centrifugation at 2500 rpm for 2 mins and snap frozen in liquid nitrogen. For PolyP mobilisation assay following stress cells were grown to an OD₆₆₀ 0.7 - 0.8, the appropriate stress-inducing agent added and cells collected by centrifugation at 2,500 rpm for 2 mins at the indicated times.

2.7.2 PolyP extraction.

The same method as that employed for RNA extraction was used (section 2.5.2), however the wash step prior to snap freezing in liquid nitrogen was omitted.

2.7.3 PolyP detection by UREA-PAGE and Toluidine Staining.

PolyP (20 µg of total RNA) was resolved by electrophoresis using 15% polyacrylamide TBE-UREA (7M) pre-cast gels from Bio-Rad (Hercules, CA, USA). Electrophoresis was at 100 V for 150 mins and the running buffer was made up of Tris (89 mM), borate (89 mM), and EDTA (2 mM) at pH 8. 6x loading dye contained 6x TBE, 15% Ficoll (Sigma), and 0.025% xylene cyanol FF (Sigma). Gels were then fixed in solution consisting of methanol (25%) and glycerol (5%) for 15 mins with gentle agitation, then stained with toluidine blue (0.05%) (Sigma) in fixative solution for 15 mins with gentle agitation and destained with gentle agitation over 3 h in three changes of fixative solution (Smith and Morrissey, 2007). Gels were imaged on a flatbed scanner.

2.8 Other biochemical techniques used.

2.8.1 Secreted acid phosphatase activity detection assay.

To detect secreted acid phosphatase activity overnight cultures of *C. albicans* grown in YPD at 30°C were diluted to an OD₆₆₀ of 0.2 in fresh PNMC + 2 mM Pi and grown to mid-exponential phase (OD₆₆₀ ~ 0.6). Cells were then washed twice in PNMC - Pi and re-suspended in PNMC - Pi to an OD₆₆₀ 0.5 and spotted onto PNMC agar plates without phosphate or with 10mM Pi. Spotted plates were incubated for 24 h at 30°C. Secreted acid phosphatase activity was detected on plates by agar-overlay coloration (Schurr and Yagil, 1971) as follows. Agar plates with *C. albicans* colonies were covered with melted agar solution (1%) containing sodium acetate (50 mM, pH4), naphthyl phosphate (18.65 µM Sigma), and Fast blue salt dye (105.2 µM Sigma) and incubated at 30°C for 30 - 60mins. *C. albicans* cells positive for secreted acid phosphatase activity stain red when grown in no phosphate medium.

2.8.2 Inductively coupled plasma mass spectrometry (ICP-MS).

This was performed by Dr Kevin Waldron and Dr Emma Tarrant, Newcastle University. Exponentially growing cells, grown in YPD at 30°C, were harvested by centrifugation, washed twice with 25 ml of Tris buffer (50 mM Tris, pH 7.5) then incubated in the same buffer containing 10 mM EDTA for 5 min at room temperature to remove surface-bound metal, and then washed twice with 25 ml of the same buffer without EDTA. Washed pellets were digested in 1 ml of 65% (w/v) HNO₃ (Merck) and incubated for >48 h at room temperature. The triplicate digested samples were centrifuged (13,000 *g*, 20 min), and the supernatants were diluted 1:10 with 2% (w/v) HNO₃ solution which contained 20 µg/L Ag and Pt as internal standards, and analysed by ICP-MS essentially as previously described (Tottey *et al.*, 2008). Each sample was analysed for sodium (²³Na), phosphorus (³¹P), manganese (⁵⁵Mn), iron (⁵⁶Fe), copper (⁶⁵Cu) and zinc (⁶⁶Zn), as well as silver (¹⁰⁷Ag) and platinum (¹⁹⁵Pt), using a Thermo X-series ICP-MS operating in collision cell mode (3.0 ml min⁻¹ of 8% H₂ in He as collision gas). Each isotope was analysed in peak-jump mode 100 times, with 25 ms dwell time on 3 channels with 0.02 atomic mass units separation, each in triplicate. Metal concentrations were calculated by comparison to matrix-matched elemental standards (containing 0 - 100 µg/L of each element) which were analysed within the same analytical run and were normalized according to the OD₆₆₀ recorded for each culture.

2.9 Microscopy.

2.9.1 Pho4 localisation kinetics and fluorescence microscopy.

For Pho4 localisation following phosphate limitation, *C. albicans* cells expressing GFP-tagged Pho4 were depleted of polyP stores and starved of phosphate over time. Phosphate (10 mM KH₂PO₄) was added back at the indicated times. At each time point 9 ml of cells was collected. For Pho4 localization following stress, cells were grown to mid-exponential phase (OD₆₆₀ 0.5 - 0.6) and 9 ml of cells collected before and after treatment with stress-inducing compound at the indicated concentration and times. Cells were fixed in 3% final volume para-formaldehyde solution made in PEM (100 mM piperazine-1, 4 - bis (2-ethanesulfonic acid) (PIPES), 1.0 mM EGTA pH 8.0, 1 mM MgSO₄), and then washed 3x in PEM. Cells were spread onto Poly-L-lysine-coated slides, fixed by incubating in ice cold methanol for 6 mins and acetone for 30 secs, and cover slips mounted using Vectashield® mounting medium containing 1.5 mg/ml DAPI (4'-6-diamidino-2-phenylindole; Vector Laboratories). GFP fluorescence and DAPI were captured by exciting cells with 365 - and 450 - 490nm wavelengths, respectively, using a Zeiss Axioscope, with a 63x oil immersion objective and AxioVision imaging system.

2.9.2 Yeast to hyphae transition assay.

To induce morphogenesis stationary phase cells were diluted 1:10 in fresh YPD liquid medium containing 10% fetal calf serum and incubated at 37°C for 6 h with shaking (180 rpm). 9 ml of cells was collected and fixed as described for fluorescence microscopy. Differential interference contrast (DIC) images were then captured using a Zeiss Axioscope, with a 63x oil immersion objective, and Axiovision imaging system.

2.9.3 PolyP detection by neisser staining.

The presence of intracellular polyP granules was determined by light microscopy by Neisser staining of *C. albicans* cells (Gurr, 1965). Paraformaldehyde fixed cells (Enjalbert *et al.*, 2006) were mounted onto a slide and stained with freshly prepared solution A (Methylene blue 0.1%, Glacial acetic acid 5%, ethanol 5%), and solution B (Crystal violet 10% in ethanol) for 10 – 15 secs. Slides were rinsed with water and solution C (Chrysoidin Y 1%) added for 45 secs, rinsed off and allowed to dry. Differential interference contrast (DIC) images were captured using a Zeiss Axioscope, with a 63x oil immersion objective, and Axiovision imaging system.

2.10 Virulence assays.

2.10.1 *C. elegans* infection assay.

For the infection assay, 60 - 70 age - synchronised young adult worms were transferred from *E. coli* plates to fresh plates seeded with *C. albicans* cells. Plates were incubated at 25°C and monitored daily for viability. Death was confirmed when there was no response to touch and no pharynx contraction observed. The survival of animals was monitored using the Binocular Stereo zoom Microscope (Nikon SMZ1000, Japan). Differences in *C. elegans* survival was determined by the log-rank test. A *P* value of <0.05 in all experiments was considered significant.

2.10.2 Mouse model of systemic infection.

The murine intravenous challenge model of *C. albicans* infection (MacCallum *et al.*, 2009 and MacCallum *et al.*, 2010) was employed to determine the impact of deleting *PH04* on virulence. This was carried out by Dr Donna MacCallum, University of Aberdeen. *C. albicans* strains were grown overnight at 30°C and harvested in sterile saline and cell counts adjusted to deliver a challenge dose of 3×10^4 CFU/g body weight. BALB/c female mice were infected intravenously via a lateral tail vein. Body weights were recorded daily. 72 h post challenge the animals were weighed, humanely terminated and kidneys removed aseptically. Fungal burdens were measured by viable counts for two half kidneys per animal; the other half kidneys were fixed, embedded and stained for histopathological examination. Virulence of the challenge strains was assessed by fungal kidney burdens at 72 h, and by percent weight change over 72 h, from which an outcome score was calculated (MacCallum *et al.*, 2009 and MacCallum *et al.*, 2010). Differences between mean body weight changes and mean kidney burdens were tested statistically by the Mann-Whitney *U* test. All animal experimentation conformed to the requirements of United Kingdom Home Office legislation and of the Ethical Review Committee of the University of Aberdeen.

2.10.3 Macrophage killing assay.

J774.1 macrophages were seeded at a density of 2×10^5 cells in six well plates for 24 h. Overnight culture of *C. albicans* cells was added to the macrophages at an MOI of 3:1 macrophage/candida ratio, or to media without macrophages. Cells were co-incubated for 6 h at 37°C following which unphagocytosed macrophages were washed off and macrophages lysed with Triton X-100 (1%) to release *C. albicans* cells. Cells

were plated onto YPD plates and incubated overnight at 30°C, and percentage survival calculated as $\text{CFUs} + \text{macrophages} / \text{CFUs} - \text{macrophages} \times 100$. Mean values and standard deviations were calculated for all phagocytosis assays. Differences were tested for statistical significance by one-way analysis of variance, ANOVA (** $P < 0.01$).

2.10.4 Macrophage live cell video microscopy phagocytosis assay.

The method described in Bain *et al* (2014) was used as follows. The J774.1 mouse macrophage cell line was maintained at 37°C and 5% CO₂ in Dulbecco's modified Eagle's medium (DMEM) (Lonza, Braine-l'Alleud, Belgium) supplemented with 10% heat-activated fetal calf serum (FCS) (Biosera, Ringmer, United Kingdom). Cells were seeded at 1.2×10^5 cells/well in an 8-well slide and incubated overnight at 37°C and 5% CO₂. Overnight cultures of *C. albicans* strains grown in YPD were washed 3x in sterile phosphate-buffered saline (PBS) (pH 7.4) and resuspended 1:100 in sterile PBS with cell numbers adjusted to 1×10^6 cells/μl with a haemocytometer. Candida cells were co-cultured with the J774.1 cells at a MOI of 3:1 respectively. Prior to co-incubation growth medium in wells was replaced with prewarmed CO₂-independent medium containing 10% FCS (Invitrogen) and 1 μm of LysoTracker Red DND - 99 (Invitrogen) added for phagosome maturation experiments. DIC images of co-cultured cells were taken every minute for 6 h. Phagocytosis assays were imaged using an Ultra VIEW VoX spinning-disk microscope (Nikon, Surrey, United Kingdom) with Volocity software used for data analysis (Improvision, PerkinElmer, Coventry, United Kingdom). Captured images were also used to determine macrophage survival/killing by candida and candida hyphal growth during phagocytosis. Data were analysed by one-way analysis of variance (ANOVA) with Bonferonni's post hoc comparisons.

Chapter 3. Global analysis of *C. albicans* genes required for resistance to physiologically relevant stresses

3.1 Introduction.

Previous genome-wide expression studies have demonstrated that following exposure to host-imposed stresses *C. albicans* induces the expression of suites of genes (reviewed in Wilson *et al.*, 2009). A limited number of *in vivo* and *in vitro* studies have been performed to establish the role of some of these stress responsive genes. For example, following oxidative stress imposed by H₂O₂, the gene encoding the Cap1 transcription factor is highly induced (Enjalbert *et al.*, 2006). Subsequent studies revealed that cells lacking Cap1, which is the major regulator of H₂O₂-induced antioxidant genes, are unable to escape phagocytosis (Jain *et al.*, 2013; Patterson *et al.*, 2013). It has also been shown that inactivation of genes regulated by Cap1, such as *CAT1* which encodes catalase also affects the ability of *C. albicans* to survive phagocytosis and attenuates virulence in a mouse model of systemic infection (Wysong *et al.*, 1998). However, there are many more stress responsive genes identified from microarray studies that have not been examined further, with regard to their contribution to stress resistance and virulence of *C. albicans*.

In addition, there are still many gaps in our knowledge regarding the transcriptional regulators of the stress-responsive genes. For example, whilst the role of Cap1 in mediating the transcription response to H₂O₂-induced oxidative stress is well documented (Wang *et al.*, 2006), the transcription factor(s) that regulates superoxide-induced gene expression is not known. Likewise, little is known regarding the mechanisms employed by *C. albicans* to adapt to acidic environments, and whereas the regulation of the Rim101 transcription factor in response to alkaline pH is well studied (reviewed in Davis, 2009), less is known regarding downstream effectors. Furthermore, although the Hog1 stress activated protein kinase is required for resistance to a multitude of host-imposed challenges including cationic and oxidative stresses (San Jose *et al.*, 1996; Alonso-Monge *et al.*, 1999; Smith *et al.*, 2004) and is essential for virulence in all models of infection tested (Alonso-Monge *et al.*, 2003; Arana *et al.*, 2007; Prieto *et al.*, 2014), the transcription factor targets for Hog1 remain largely unknown.

Clearly, therefore, there are many gaps in our knowledge regarding the stress response mechanisms of *C. albicans* and their contribution to the virulence of this

major fungal pathogen. As discussed in Chapter 1 the main goal of this study was to provide new insight into the cellular processes and mechanisms required for *C. albicans* adaptation to specific physiologically relevant stresses. To achieve this, the *C. albicans* transcription factor (TF) deletion collection, comprising of 143 TF deletion strains (Homann *et al.*, 2009), and the more comprehensive deletion collection comprising of 674 deletion strains (Noble *et al.*, 2010), were screened by quantitative fitness analysis (QFA) against superoxide (300 μ M menadione), cationic (1 M NaCl), and alkaline pH (pH 8) stress-inducing compounds.

The *C. albicans* transcription factor (TF) deletion collection was originally created to phenotypically characterise transcriptional regulators in an effort to identify novel biological roles relevant to pathogenicity (Homann *et al.*, 2009). This phenotypic screen identified new regulators involved in morphogenesis, antifungal drug resistance, biofilm formation, and iron acquisition (Homann *et al.*, 2009). Moreover, a number of factors were found to be necessary for resistance to the cationic stress imposed by 0.3 M lithium chloride, the Cap1 transcription factor was required for resistance to superoxide stress imposed by 90 μ M menadione, and the Rim101 transcription factor together with the iron acquisition factors Hap43 and Sef1, were identified as being required for resistance to an alkaline pH environment of 10.5. The larger deletion collection, however, has yet to be screened against such stresses (Noble *et al.*, 2010). Moreover, we reasoned that the conditions employed in the transcription factor library screen may not accurately represent the cationic, superoxide and alkaline pH stresses encountered by *C. albicans* during infection of the human host. For example, lithium is only present as a trace element within the human body, whereas *C. albicans* is expected to be exposed to high levels of sodium cations in the kidney, or potassium cations following phagocytosis. Indeed, Reeves *et al.* (2002) calculated the concentration of K^+ in the phagosome to be in the range of 300 mM. Moreover, neutrophils produce high levels of superoxide anions, ranging between 1 (Hampton *et al.*, 1998) and 4 M/l (Reeves *et al.*, 2002) within the phagocytic vacuole. Thus, the amount of the superoxide generating compound (90 μ M menadione) used to screen the transcription factor deletion library may not represent the concentration of superoxide produced within the phagosome. Finally, regarding pH stress, a pH of 10.5 was employed to provide an alkaline environment yet at this pH *C. albicans* struggles to grow (M. Ikeh and J. Quinn, unpublished), and it is not clear which niche within the human host would have such a high pH.

Therefore, to facilitate the aim to identify novel proteins required for stress adaptation in *C. albicans*, screens were performed in this study using more physiologically relevant stress conditions. For example, the screen for alkaline pH sensitive mutants was performed at pH 8, as the mammalian host environment can generally be considered to be slightly alkaline (Davis, 2009). Furthermore, for the reasons discussed above, we chose to use sodium chloride rather than lithium chloride to impose cationic stress and to employ a higher concentration of the superoxide generating drug menadione. In addition, we also employed quantitative fitness analysis, which detects even slight changes in strain fitness following stress, and we screened the larger *C. albicans* deletion collection (674 genes) in addition to the transcription factor library. The data obtained from the screens performed in this study are presented in this chapter.

3.2 Results.

3.2.1 Quantitative fitness analysis of genes required for superoxide, cationic, and alkaline pH stress resistance.

To identify genes whose deletion confers sensitivity to the aforementioned stresses, the two deletion collections were screened by quantitative fitness analysis (QFA) for mutants with impaired resistance to cationic (NaCl), superoxide (menadione), and alkaline pH (pH8) stresses. QFA was carried out at the High-throughput screening facility at Newcastle University using the method described in Banks *et al* (2012) with a few modifications (Materials and Methods). Robotics was done by Dr Peter Banks, Newcastle University. Each strain was spot inoculated, by a robot system, onto rich YPD agar and YPD supplemented with NaCl (1M) to induce cationic stress; or menadione (300 μ M) to induce superoxide stress; or the pH of YPD adjusted from pH 6 to pH 8 with Tris-HCl (pH 8.25). Growth on solid agar plates was monitored by photography over time. Quantitative growth parameters were then determined by generating measurements from the images captured. Measurements were used to create growth curves from which the maximum doubling rate (MDR, population doublings/day) and the maximum doubling potential (MDP, population doublings) were calculated. Growth fitness was defined as the product of the MDP and MDR values (Fitness, F , population doubling²/day). However, the superoxide and cationic stresses employed in this study result in reduced fitness of the reference wild-type strain. Thus a multiplicative model of fitness was applied in which fitness predictions

of the mutant strains are made based on the reduction of fitness of wild-type cells following either cationic or superoxide stress. This linear prediction is shown as the solid grey line. Deviations from this line generates a Stress Interaction Score (SIS), with the larger the deviation below the line indicative of greater impaired fitness to the stress condition in question. Lists of the SIS for each mutant under the specific stress condition were compiled and strains ranked accordingly. Only mutants with a SIS number ≤ -0.05 were used for GO term analysis. Fitness plots generated from the analysis are shown in Fig 3.1.

To validate the QFA screen the top ten most sensitive strains to either menadione or NaCl were selected for spot test assay. Spot test results support the QFA findings for the superoxide stress (Fig 3.2), however such an assay was not sufficiently sensitive to visualise the growth defects induced by NaCl in strains with higher SIS (Fig 3.2). Due to time constraints the hits from the alkaline pH screen could not be validated.

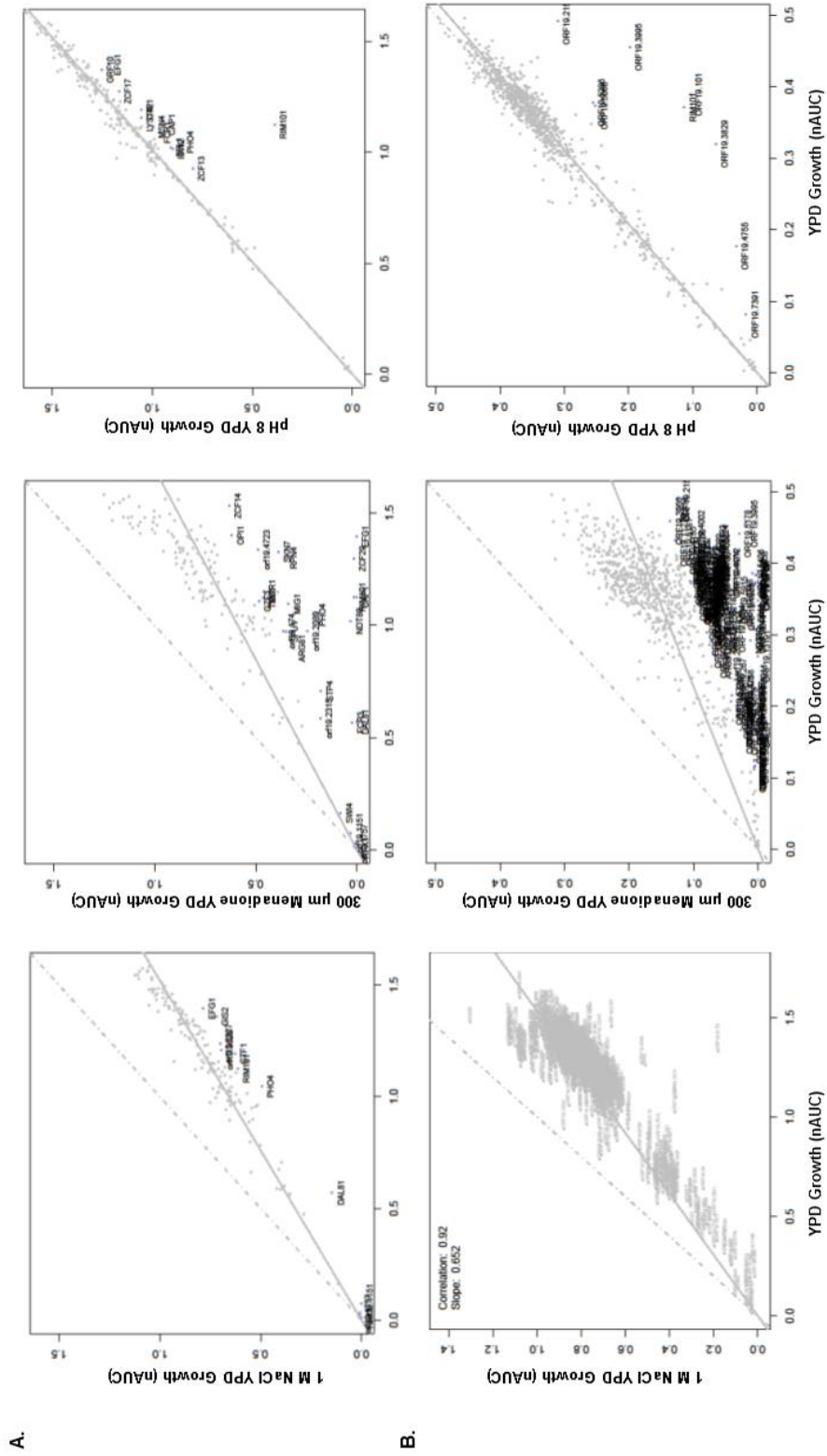


Fig 3.1 Quantitative fitness analysis plots of the transcription factor deletion library (A) and the homozygous deletion collection (B) grown on media containing 1 M NaCl, 300 μM menadione or pH adjusted from 6 to 8. Highlighted in A are genes with the lowest SIS. These could not be highlighted in B (NaCl and Menadione) due to the number of genes.

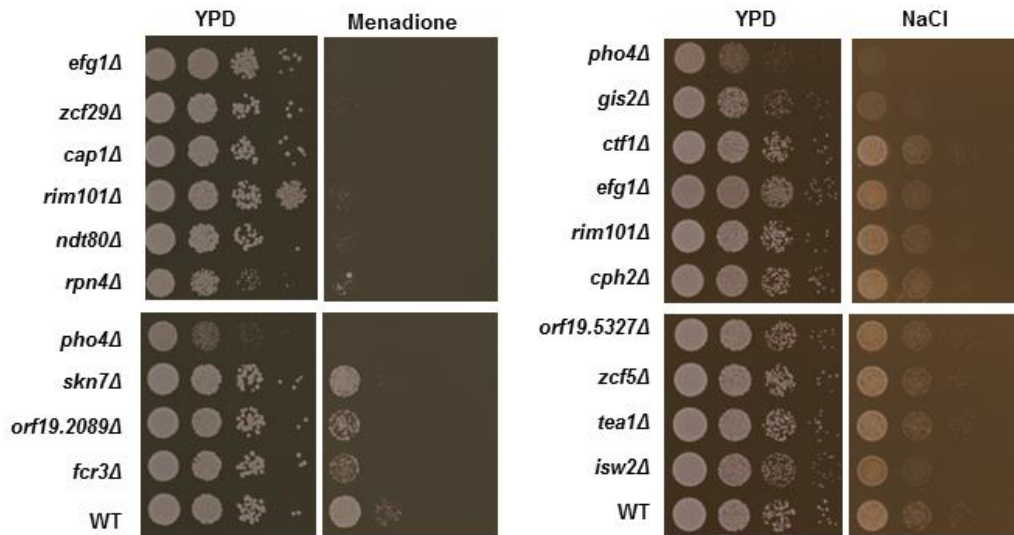


Fig 3.2 Spot test confirmation of sensitive genes identified by QFA. 10^{-7} and 10^{-8} fold dilutions thereof of exponentially-growing wild-type and respective mutant strains were spotted onto agar plates containing either 300 μ M Menadione or 1M NaCl. Plates were incubated at 30 $^{\circ}$ C for 24 h. Data shown is representative of two biological replicates.

3.2.1.1 Mutants sensitive to superoxide stress.

The screen against the superoxide-generating compound menadione, identified 269 *C. albicans* deletion strains, of which 51 were deleted of a specific transcriptional regulator, with reduced fitness compared to wild-type cells. Table 3.1 shows the 10 most sensitive TF mutants while Table 3.2 shows the 20 most sensitive mutants from the Noble deletion collection. A comprehensive list of all sensitive strains can be found in Appendix 1A. Among the transcription factor mutants, cells lacking *CAP1*, *SKN7*, and *ZCF29*, previously implicated in oxidative stress resistance (Homann *et al.*, 2009) were sensitive to menadione thus validating the results from the QFA. Of particular interest however, was the identification of three transcription factors not previously implicated in superoxide stress resistance, namely *Pho4*, *Rpn4*, *Rim101* and *Dpb4* (Table 3.1). Whilst *Rim101* has well characterised role in pH regulation, this has not previously been implicated in oxidative stress resistance. Screening of the Noble deletion library also identified uncharacterised genes whose gene products have no previously documented role in superoxide stress resistance (Table 3.2). These include *Pkh2*, a protein kinase involved in endocytosis; *orf19.7086*, orthologues of which have roles in TF nuclear import; *Ktr4*, a mannosyltransferase induced during cell wall regeneration; and members of the pH response pathway, *Rim9* and *Rim13* (Table 3.2). In addition, the multicopper oxidases (*FET99* and

FET3) and genes regulated by the Hap43 transcription factor (ZCF29) are also necessary for superoxide stress adaptation (Table 3.1; Table 3.2; Appendix 1A).

Gene	SIS	Function
Superoxide stress		
<i>EFG1</i>	-0.82282	Required for hyphal growth
<i>ZCF29</i>	-0.75071	Required for caffeine and menadione resistance; Hap43-repressed
<i>CAP1</i>	-0.66091	Oxidative stress response regulator
<i>RIM101</i>	-0.64918	Alkaline pH response regulator
<i>NDT80</i>	-0.56936	Meiosis-specific TF; activator of CDR1 induction by antifungal drugs
<i>RPN4</i>	-0.40951	Putative regulator of proteasome genes
<i>PHO4</i>	-0.40382	Regulates phosphate homeostasis
<i>SKN7</i>	-0.39617	Required for resistance to H ₂ O ₂
<i>DAL81</i>	-0.33632	Involved in the regulation of nitrogen-degradation genes
<i>DPB4</i>	-0.33	Putative DNA polymerase epsilon subunit D
Cationic stress		
<i>PHO4</i>	-0.194368	Regulates phosphate homeostasis
<i>GIS2</i>	-0.455203	Induced in high iron; null exhibits sensitivity to sorbitol
<i>CTF1</i>	-0.157821	Activates genes required for fatty acid degradation; induced by oleate; null mutant displays carbon source utilization defects and slightly reduced virulence
<i>EFG1</i>	-0.133175	Required for hyphal growth
<i>RIM101</i>	-0.127529	Alkaline pH response regulator
<i>CPH2</i>	-0.116837	Promotes hyphal growth
<i>orf19.5326</i>	-0.116117	Putative transcription factor with zinc finger DNA-binding motif; possible ortholog of <i>S. cerevisiae</i> Mig2p
<i>ZCF5</i>	-0.109325	colony morphology-related gene regulation by Ssn6
<i>TEA1</i>	-0.106443	Putative transcription factor; has similarity to <i>S. cerevisiae</i> Tea1p; Hap43p-repressed gene
<i>ISW2</i>	-0.400764	An ATPase involved in chromatin remodelling; Hap43-induced gene; repressed by high-level peroxide
Alkaline pH stress		
<i>EFG1</i>	-1.22501	Required for hyphal growth
<i>SKN7</i>	-1.15977	Required for resistance to H ₂ O ₂
<i>RIM101</i>	-0.8086	Protein required for alkaline pH response via the Rim101 signaling pathway
<i>GZF3</i>	-0.73742	oxidative stress-induced via Cap1; mutant has abnormal colony morphology and altered sensitivity to fluconazole, LiCl, and copper
<i>SEF1</i>	-0.66057	regulates iron uptake; promotes virulence in mice; mutants display decreased colonization of mouse kidneys
<i>CUP9</i>	-0.59558	represses SOK1 expression in response to farnesol inhibition

<i>FCR1</i>	-0.47498	Repressor of fluconazole /ketoconazole/ brefeldin A resistance
<i>NDT80</i>	-0.46316	Meiosis-specific TF; activator of CDR1 induction by antifungal drugs
<i>CPH2</i>	-0.4594	Promotes hyphal growth; required for colonization of the mouse GI tract
<i>PHO4</i>	-0.27625	Regulates phosphate homeostasis

Table 3.1. Transcription factors required for stress resistance. Red – Uncharacterised, or have not previously been implicated in the stress studied.

Gene	SIS	Gene function
Superoxide stress		
<i>RIM13</i>	-0.781	Protease of the pH response pathway
<i>SNQ2</i>	-0.76698	member of PDR subfamily of ABC family
<i>ORF19.4658</i>	-0.76246	RING finger and CHY zinc finger domain-containing protein
<i>PST3</i>	-0.75271	Putative flavodoxin
<i>ORF19.5406</i>	-0.72223	Predicted plasma membrane associated protein phosphatase
<i>ORF19.4292</i>	-0.66384	Orthologs have SNAP receptor activity
<i>PHO15</i>	-0.6458	4-nitrophenyl phosphatase induced in core stress response; cadmium stress induced by Hog1
<i>SNT1</i>	-0.59438	an NAD-independent histone deacetylase
<i>VPS41</i>	-0.56158	Involved in vacuole organization and biogenesis; induced by amino acid starvation
<i>ORF19.6348</i>	-0.54122	Predicted cysteine proteinase domain
<i>ORF19.4474</i>	-0.50704	Orthologs have cytoplasm, nucleus localization
<i>PKH2</i>	-0.5047	Putative protein kinase; predicted role in sphingolipid-mediated signaling pathway (endocytosis)
<i>SNF4</i>	-0.49942	Ortholog of <i>S. cerevisiae</i> Snf4, the activating gamma subunit of the AMP-activated Snf1p kinase
<i>FET99</i>	-0.49754	Multicopper oxidase family protein
<i>DUR35</i>	-0.49721	Putative urea transporter
<i>SIN3</i>	-0.46055	Transcriptional corepressor involved in histone deacetylase recruitment
<i>ORF19.4193</i>	-0.45457	Ortholog(s) have Arp2/3 complex binding activity, role in actin cortical patch assembly
<i>ORF19.7086</i>	-0.45388	Ortholog(s) have protein transporter activity, role in transcription factor import
<i>RIM9</i>	-0.43879	Protein required for alkaline pH response via the Rim101 signaling pathway
<i>KTR4(MNT4)</i>	-0.4345	Mannosyltransferase; induced during cell wall regeneration; fungal-specific
Cationic stress		
<i>ENA21</i>	-0.68911	Predicted P-type ATPase sodium pump
<i>STT4</i>	-0.34513	Putative phosphatidylinositol-4-kinase

<i>KIS1</i>	-0.30266	Snf1p complex scaffold protein; mutants hypersensitive to caspofungin and H ₂ O ₂ ; Hap43p-repressed
<i>RHO3</i>	-0.29303	Putative Rho family GTPase
<i>DAC1</i>	-0.28638	N-acetylglucosamine-6-phosphate (GlcNAcP) deacetylase; required for wild-type hyphal growth and virulence in mouse systemic infection
<i>ORF19.12247</i>	-0.17928	Protein of unknown function
<i>ORF19.13064</i>	-0.17356	Protein of unknown function
<i>SPF1</i>	-0.17049	P-type calcium-transporting ATPase, involved in control of calcium homeostasis, response to ER stress, hyphal growth, biofilm formation and virulence
<i>ORF19.1267</i>	-0.16752	Ortholog of <i>S. cerevisiae</i> CAJ1, a nuclear type II heat shock protein
<i>CLB4</i>	-0.16154	B-type mitotic cyclin; nonessential; negative regulator of pseudohyphal growth;
<i>GPD2</i>	-0.14965	glycerol 3 dehydrogenase; induced by cell wall regeneration, macrophage/pseudohyphal growth, core stress response
<i>ORF19.2821</i>	-0.13681	Protein of unknown function; Hap43-repressed gene; repressed by nitric oxide
<i>CTA2</i>	-0.13531	Putative transcription factor; Med2 mediator domain; repressed by Efg1; Tbf1-induced
<i>SIN3</i>	-0.13393	Protein similar to <i>S.cerevisiae</i> Sin3p, a transcriptional corepressor involved in histone deacetylase recruitment
<i>SAP8</i>	-0.13173	Secreted aspartyl protease; prominent role in biofilms
<i>KIN2</i>	-0.12702	Protein with similarity to <i>S.cerevisiae</i> Kin2p, transcription is positively regulated by Tbf1
<i>ORF19.194</i>	-0.11916	Ortholog of <i>C. dubliniensis</i> CD36
<i>PBS2</i>	-0.11606	MAPKK; role in osmotic and oxidative stress responses, required for stress regulation of Hog1p
<i>ORF19.2500</i>	-0.11464	Has domain(s) with predicted transferase activity and role in biosynthetic process
<i>PCL2</i>	-0.11306	Cyclin homolog; reduced expression observed upon depletion of Cln3; farnesol regulated; periodic mRNA expression, peak at cell-cycle G1/S phase; Hap43-induced
Alkaline pH stress		
<i>PHR1</i>	-0.82388	Cell surface glycosidase; may act on cell-wall beta-1,3-glucan prior to beta-1,6-glucan linkage; role in systemic, not vaginal virulence; high pH or filamentation induced;
<i>RIM13</i>	-0.67826	Protease of the pH response pathway
<i>KEX2</i>	-0.46804	Protease (proprotein convertase); processes aspartyl proteins
<i>DAC1</i>	-0.38228	N-acetylglucosamine-6-phosphate deacetylase; required for wild-type hyphal growth and virulence in mouse systemic infection; gene and protein are GlcNAcP-induced
<i>YCP4</i>	-0.3705	Putative flavodoxin
<i>IRE1</i>	-0.33608	Putative protein kinase; role in cell wall regulation; mutant is hypersensitive to caspofungin

<i>OCH1</i>	-0.27098	Alpha-1,6-mannosyltransferase; initiates N-glycan outer chain branch addition; required for wild-type virulence in mouse intravenous infection; fungal-specific
<i>ORF19.13064</i>	-0.22299	Protein of unknown function
<i>DUN1</i>	-0.2041	Protein similar to <i>S. cerevisiae</i> Dun1p, which is a serine-threonine protein kinase involved in DNA damage cell-cycle checkpoint; induced under Cdc5p depletion
<i>SSK2</i>	-0.19922	MAPKKK; regulates Hog1 activation and signaling
<i>APM1</i>	-0.19858	Ortholog of <i>S. cerevisiae/S. pombe</i> Apm1; a clathrin-associated protein complex (AP-1) subunit; phosphorylated protein; Tn mutation affects filamentous growth
<i>ORF19.12247</i>	-0.18609	Protein of unknown function; induced during chlamydospore formation in both <i>C. albicans</i>
<i>ORF19.6736</i>	-0.18502	Protein required for mitochondrial ribosome small subunit biogenesis; role in maturation of SSU-rRNA
<i>COX4</i>	-0.18159	Putative cytochrome c oxidase subunit IV; Mig1-regulated; macrophage or pseudohyphal-induced gene; macrophage-induced protein; repressed by nitric oxide; 5'-UTR intron; Hap43-repressed
<i>ORF19.1267</i>	-0.16964	Ortholog of <i>S. cerevisiae</i> CAJ1gis
<i>ORF19.3854</i>	-0.14652	Ortholog of <i>S. cerevisiae</i> Sat4; amphotericin B induced; clade-associated gene expression
<i>PBS2</i>	-0.13932	MAPK kinase (MAPKK); role in osmotic and oxidative stress responses, oxidative stress adaptation; required for stress regulation of Hog1p localization and activity
<i>ORF19.2115</i>	-0.13411	Putative molybdopterin-converting factor; fungal-specific
<i>KRE62</i>	-0.132	Putative subunit of glucan synthase; macrophage-induced gene
<i>ORF19.2484</i>	-0.11662	Has domain(s) with predicted peptidase activity and role in proteolysis

Table 3.2. Genes required for stress resistance. Red – Uncharacterised or have not previously been implicated in the stress studied.

3.2.1.2 Mutants sensitive to cationic stress.

The screen against the cationic stress inducer, NaCl, identified 168 *C. albicans* deletion strains, of which 22 were deleted of a specific transcriptional regulator, with reduced fitness compared to wild-type cells. Table 3.1 shows the 10 most sensitive TF mutants while Table 3.2 shows the 20 most sensitive mutants from the Noble deletion collection. The comprehensive list of all NaCl-sensitive strains can be found in Appendix 1B. An examination of the TF mutants revealed that the transcription factor Gis2, previously reported to be required for resistance to the osmotic stress inducer, sorbitol (Homann *et al.*, 2009), was also sensitive to NaCl (Fig 3.2) which can impose osmotic in addition to cationic stresses. Interestingly, the *pho4Δ* transcription factor mutant, found to be superoxide sensitive was also sensitive to NaCl (Table 3.1, Fig 3.2). In addition, from the Noble deletion library, genes

previously reported to be required for cationic stress resistance were identified. For example, QFA identified the important osmotic stress regulator, the Hog1 SAPK, and upstream components of the Hog1 pathway, Pbs2 and Ssk2. The most sensitive mutant (lowest SIS score) to NaCl was found to be the predicted P-type ATPase sodium pump, Ena21 (Table 3.2). Also of interest was the identification of Ypt72 involved in vacuolar biogenesis, filamentous growth, and virulence (Johnston *et al.*, 2009). The vacuole by providing a component where ions are sequestered for elimination has an essential role in ion stress resistance and adaptation. Another interesting find was the identification of the Ras1 GTPase which regulates the cAMP-dependent PKA pathway (Leberer *et al.*, 2001), as the predicted transcription factor target of this pathway Efg1 was also sensitive to cationic stress. Several uncharacterised genes were also pulled out of the screen (Table 3.2). In addition to being sensitive to superoxide anions, the multicopper oxidases (Fet99 and Fet3) and the copper-containing Sod6 were found to be required for resistance to NaCl (Appendix 1B). The presence of high levels of NaCl may also induce iron-limiting conditions as Hap43 regulated genes were identified in the screen (Table 3.1; Table 3.2; Appendix 1B).

3.2.1.3 Mutants sensitive to alkaline pH.

Raising the pH of the growth medium from 6 to 8 isolated 113 *C. albicans* mutants, of which 27 were deleted for a specific transcriptional regulator, that displayed reduced fitness compared to wild-type cells. Table 3.1 shows the 10 most sensitive TF mutants while Table 3.2 shows the 20 most sensitive mutants from the Noble deletion collection. The comprehensive list of all alkaline pH sensitive strains can be found in Appendix 1C. An examination of the TF mutants identified a number of genes previously implicated in pH adaptation, such as Rim101, and Efg1 which regulates hyphal formation under alkaline growth conditions (Table 3.1; Table 3.2). This screen also revealed that the transcription factor Skn7, in addition to oxidative stress resistance, may have additional roles in alkaline pH stress resistance (Table 3.1). Intriguingly, the *pho4Δ* mutant, which is acutely sensitive to superoxide- and cationic-stress inducing agents (Fig 3.2), was also unable to grow at pH 8 (Table 3.1). The *FCR1* gene previously implicated in drug resistance in *C. albicans* (Talibi and Raymond, 1999), was also identified in this screen as also being necessary for growth at pH 8 (Table 3.1). Moreover, the impact of alkalinisation on nutrient availability was also indicated by the identification of Sef1, the transcriptional

regulator of iron uptake (Table 3.1). From the Noble deletion library, genes in the pH response pathway such as *RIM13* and *PHR1*, were as predicted found to be sensitive to alkaline pH. Also identified, and of interest, were the macrophage-induced genes, *COX4* and *KRE62*, whose roles in mediating phagocytosis resistance remain unknown (Table 3.2). A DNA damage cell cycle check point gene, *DUN1*, was also found to be alkaline pH sensitive (Table 3.2). Moreover, all three components of the Hog1 pathway (Hog1, Pbs2, Ssk2) were found to be required for alkaline pH resistance (Table 3.2; Appendix 3), which strongly implies a novel role of Hog1 in pH adaptation. Consistent with the importance of the cell wall in mediating pH resistance, genes involved in cell wall synthesis (*OCH1*, *KRE62*) were also identified as being sensitive to alkaline pH (Table 3.2).

3.2.1.4 QFA identifies overlapping genes required for resistance.

A Venn diagram was constructed to illustrate the overlapping and distinct genes required for fitness to superoxide, cationic, and alkaline pH stresses in *C. albicans* (Fig 3.3). A larger number of genes was required specifically for superoxide stress resistance (170), compared to cationic stress (66) and alkaline pH stress (60) (Fig 3.3). 48 genes were sensitive to both menadione and NaCl; 30 genes were sensitive to both NaCl and pH8 resistance; whereas 22 were sensitive to both pH 8 and menadione stresses. In addition, a set of 26 genes were identified that were found to be required for stress resistance to all three stresses tested (Fig 3.3; Table 3.3), and of these eight were transcription factors. Two of these are the well characterised Rim101 and Efg1 factors with established roles in pH adaptation and morphogenesis, respectively. However, important roles in superoxide or cationic stress have not previously been reported for either transcription factor. Furthermore, the Pho4 transcriptional regulator, predicted to be important for phosphate homeostasis, was also acutely sensitive to all three stress conditions (Table 3.3). Interesting non-transcription factor targets, sensitive to all three stresses, included the Inp51 putative phosphatidylinositol-4, 5-bisphosphate phosphatase which has previously been implicated in hyphal growth, cell integrity, and virulence (Badrane *et al.*, 2008), and the putative cytochrome c oxidase subunit IV which has been shown to be induced during phagocytosis. In addition, the identification that the α -1, 6-mannosyltransferase, Och1, involved in the synthesis of outer chain N-glycans (Bates *et al.*, 2006), further emphasises the importance of cell wall integrity in promoting stress resistance.

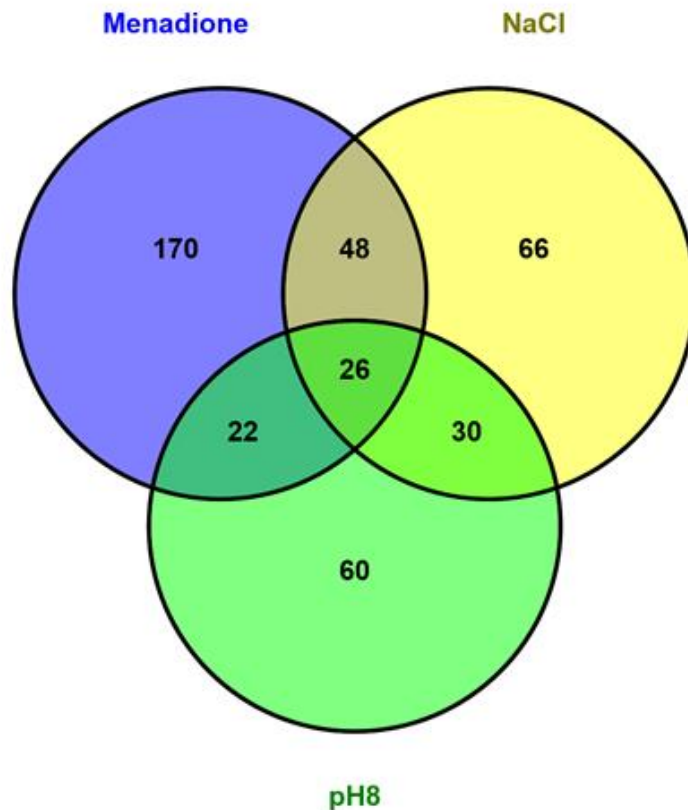


Fig 3.3 Distinct and overlapping genes required for superoxide, cationic, and alkaline pH stresses. Venn diagram illustrating genes required for resistance to all three stresses; genes specifically required for each stress; and genes required for resistance to two of the three stresses.

ORF	Gene	Function
Transcription factors		
ORF19.7247	<i>RIM101</i>	Transcription factor; alkaline pH response; required for alkaline-induced hyphal growth; role in virulence in mice; activated by C-terminal proteolytic cleavage; mediates both positive and negative regulation
ORF19.6011	<i>SIN3</i>	Protein similar to <i>S. cerevisiae</i> Sin3p (transcriptional corepressor involved in histone deacetylase recruitment); has paired amphipathic helix PAH1 domain; interacts with ScOpi1p, not CaOpi1p
ORF19.3182	<i>GIS2</i>	Translational activator for mRNAs with internal ribosome entry sites; induced in high iron; repressed by yeast-hypha switch; null exhibits sensitivity to sorbitol, 5-fluorocytosine, and cold temperatures
ORF19.6817	<i>FCR1</i>	Transcription factor; repressor of fluconazole/ketoconazole/brefeldin A resistance; Tn mutation enhances filamentation; partially rescues <i>S. cerevisiae</i> pdr1 pdr3 fluconazole sensitivity
ORF19.1253	<i>PHO4</i>	bHLH transcription factor of the myc-family; required for growth in medium lacking phosphate and for resistance to copper and Phloxine B; induced by Mnl1 under weak acid stress
ORF19.610	<i>EFG1</i>	bHLH transcription factor; required for white-phase cell type, hyphal growth, cell-wall gene regulation; roles in adhesion,

		virulence; Cph1 and Efg1 have role in host cytokine response; binds E-box
ORF19.3252	<i>DAL81</i>	Zn(II)2Cys6 transcription factor; ortholog of <i>S. cerevisiae</i> Dal81, involved in the regulation of nitrogen-degradation genes; required for yeast cell adherence to silicone substrate
ORF19.4312	<i>ORF19.4312</i>	Ortholog(s) have TBP-class protein binding, transcription cofactor activity
Non transcriptional regulators		
ORF19.1471	<i>COX4</i>	Putative cytochrome c oxidase subunit IV; Mig1-regulated; macrophage/pseudohyphal-induced gene; macrophage-induced protein; repressed by nitric oxide; 5'-UTR intron; Hap43-repressed
ORF19.3449	<i>ORF19.3449</i>	Ortholog(s) have ubiquitin-protein ligase activity
ORF19.7391	<i>OCH1</i>	Alpha-1, 6-mannosyltransferase; initiates N-glycan outer chain branch addition; similar to <i>S. cerevisiae</i> Och1p; required for wild-type virulence in mouse intravenous infection; fungal-specific
ORF19.3470	<i>ORF19.3470</i>	Putative flavodoxin; similar to <i>S. cerevisiae</i> Tyw1, an iron-sulfur protein required for synthesis of wybutosine modified tRNA; predicted Kex2p substrate
ORF19.30	<i>SPF1</i>	P-type calcium-transporting ATPase, involved in control of calcium homeostasis, response to ER stress, hyphal growth, biofilm formation and virulence
ORF19.194	<i>ORF19.194</i>	Ortholog of <i>C. dubliniensis</i> CD36 : Cd36_19300, <i>C. parapsilosis</i> CDC317 : CPAR2_209720, <i>Candida tenuis</i>
ORF19.7388	<i>PBS2</i>	MAPK kinase (MAPKK); role in osmotic and oxidative stress responses, oxidative stress adaptation; required for stress regulation of Hog1p localization and activity; functional homolog of <i>S. cerevisiae</i> Pbs2p
ORF19.1373	<i>INP51</i>	Putative phosphatidylinositol-4, 5-bisphosphate phosphatase; involved in maintenance of phosphoinositide levels; affects hyphal growth, virulence, cell integrity; interacts with Lrs4p
ORF19.3453	<i>ORF19.3453</i>	Ortholog(s) have cellular bud tip, cytoplasm localization
ORF19.5207	<i>ORF19.5207</i>	Predicted diphthamide biosynthesis protein
ORF19.2157	<i>DAC1</i>	N-acetylglucosamine-6-phosphate (GlcNAcP) deacetylase; N-acetylglucosamine utilization; required for wild-type hyphal growth and virulence in mouse systemic infection; gene and protein are GlcNAc-induced
ORF19.5559	<i>RAV2</i>	Protein similar to <i>S. cerevisiae</i> Rav2; a regulator of (H+)-ATPase in vacuolar membrane; transposon mutation affects filamentous growth
ORF19.7401	<i>ISW2</i>	Ortholog of <i>S. cerevisiae</i> Isw2; an ATPase involved in chromatin remodelling; required for chlamyospore formation; Hap43-induced gene; repressed by high-level peroxide stress
ORF19.909	<i>STP4</i>	C2H2 transcription factor; induced in core caspofungin response; colony morphology-related gene regulation by Ssn6; induced by 17-beta-estradiol, ethynyl estradiol
ORF19.4766	<i>ARG81</i>	Zn(II)2Cys6 transcription factor; required for utilization of ornithine as a nitrogen source and for wild-type resistance to caffeine; required for yeast cell adherence to silicone substrate
ORF19.1567	<i>ORF19.1567</i>	Ortholog(s) have Rab guanyl-nucleotide exchange factor activity, phosphatidylinositol binding activity

ORF19.3534	<i>RHO3</i>	Putative Rho family GTPase; possible substrate of protein farnesyltransferase and geranylgeranyl transferase type I; greater transcription in hyphal form than yeast form; plasma membrane-localized
ORF19.101	<i>RIM9</i>	Protein required for alkaline pH response via the Rim101 signaling pathway

Table 3.3 Genes required to resist all three stress-inducing conditions. Highlighted in red are uncharacterised, or have not previously been implicated in stress response.

3.2.2 Gene Ontology analysis of genes required for superoxide, cationic, and alkaline pH stress resistance.

Gene Ontology (GO) analysis was carried out to determine biological processes, molecular functions, and cellular components enriched during cationic, superoxide, and alkaline pH stresses. The GO term Finder tool in the *Candida* Genome Database (CGD) was used looking for cellular processes enriched against the input of genes represented in the Noble deletion collection (Noble *et al.*, 2010). Only GO terms significantly enriched (False discovery rate (FDR) ≤ 0.05) were used for further analyses. Functional enrichment analysis using GO annotations of sensitive strains showed both overlapping and distinct requirements for resistance to each stress-inducing compound.

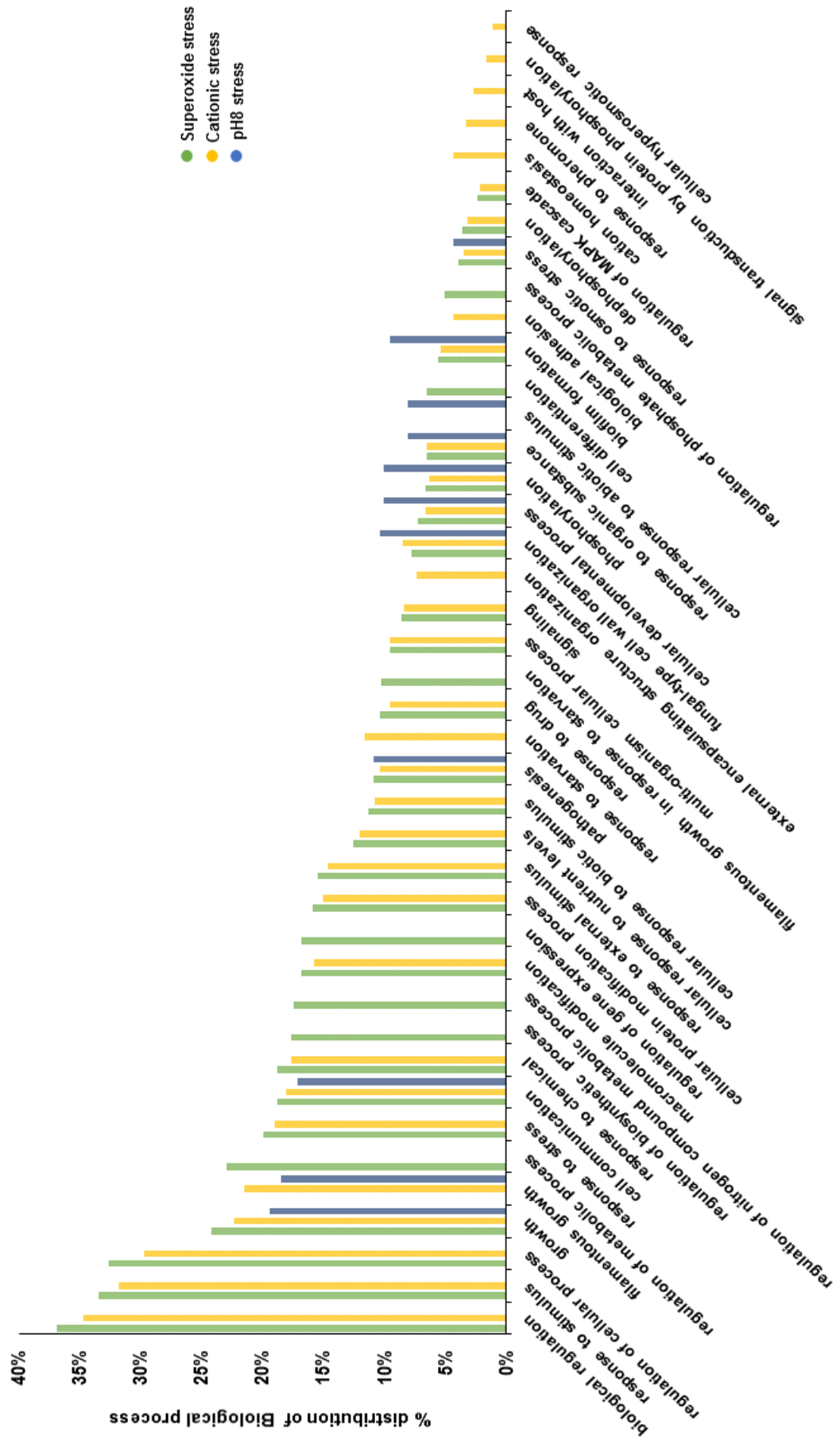
3.2.2.1 GO analysis of *C. albicans* homozygous deletion collection.

GO analysis of the stress sensitive genes from the *C. albicans* homozygous deletion collection (Noble *et al.*, 2010), identified 75 biological processes to be significantly enriched. The genes required for cationic and superoxide stress were aligned to 33 and 31 biological processes, respectively, compared to 11 for alkaline pH stress (Fig 3.4A). GO analysis for biological processes significantly enriched following superoxide stress identified the terms, biological regulation (36.9%), response to stimulus (33.5%), regulation of cellular process (32.6%), growth (24.2%), and regulation of metabolic process (22.9%) (Fig 3.4A). Similarly, GO analysis for biological processes required for cationic stress assigned most genes to biological regulation (34.7%), response to stimulus (31.8%), regulation of cellular process (29.7%), and growth (22.3%), however regulation of metabolic process was not enriched (Fig 3.4A). In contrast, genes involved in biological regulation and regulation of cellular process were not significantly enriched for alkaline pH stress. Furthermore, although the broad GO term “response to stimulus” was not enriched for alkaline pH, the child term “response to abiotic stress” was enriched (Fig 3.4A). However, growth,

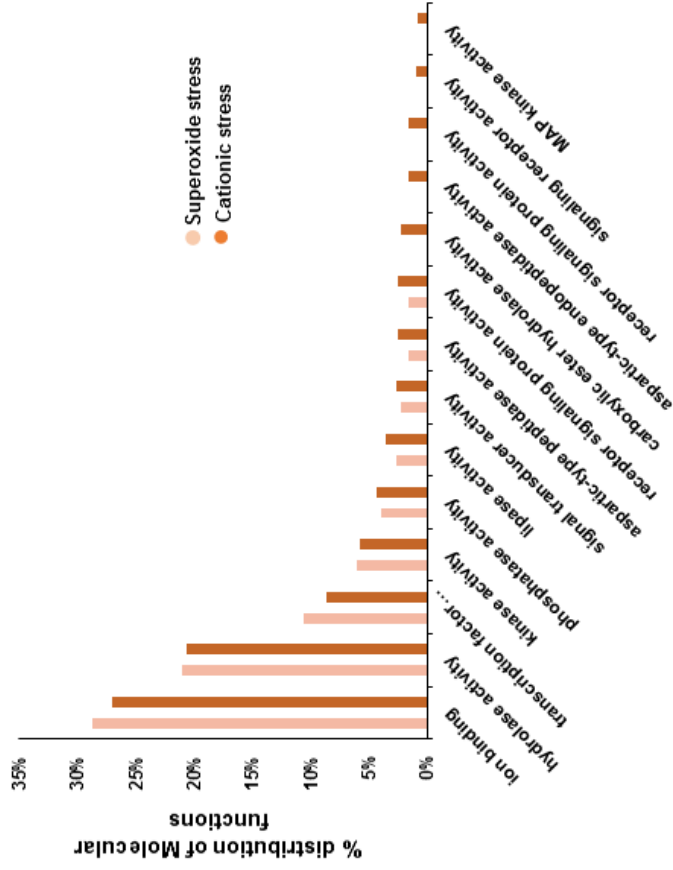
filamentous growth, pathogenesis, and cell communication were all significantly enriched for all three stresses (Fig 3.4A). Resistance to all three stress conditions also appears to require an intact cell wall, as indicated by the number of stress sensitive genes being involved in the biosynthesis of the macromolecules that make up the cell wall under the GO term “fungal cell-wall organisation” (Fig 3.4A). Notably, a greater fraction of the pH 8 response genes came up in this category followed by cationic stress and then superoxide stress (Table 3.4). A further biological process enriched for all three challenges is phosphorylation (Fig 3.4A). More protein kinase genes were assigned to cationic stress compared to superoxide and alkaline pH stress adaptation (Table 3.4). Other processes enriched across all three stresses include growth, cell communication, response to organic substance, biofilm formation, and response to osmotic stress (Fig 3.4A).

Distinct biological processes were also enriched for each stress. As expected the biological processes “cation homeostasis” and “cellular hyperosmotic response” were enriched specifically for cationic stress (Fig 3.4A; Table 3.4). Other processes uniquely enriched in the cationic stress sensitive genes include “response to pheromone”, “interaction with host”, “signal transduction by protein phosphorylation”, “response to starvation”, external encapsulating structure organisation”, and “biological adhesion” (Fig 3.4; Table 3.4). For the superoxide stress sensitive genes adaptation the following biological processes were enriched “regulation of metabolic process” which includes the child term “regulation of phosphate metabolic process”, “regulation of biosynthetic processes”, “regulation of gene expression”, “filamentous growth in response to starvation”, and “cell differentiation” (Fig 3.4A; Table 3.4). However, the category “cellular response to abiotic stimulus” was the only biological processes unique to alkaline pH stress (Fig 3.4A; Table 3.4).

A.



B.



C.

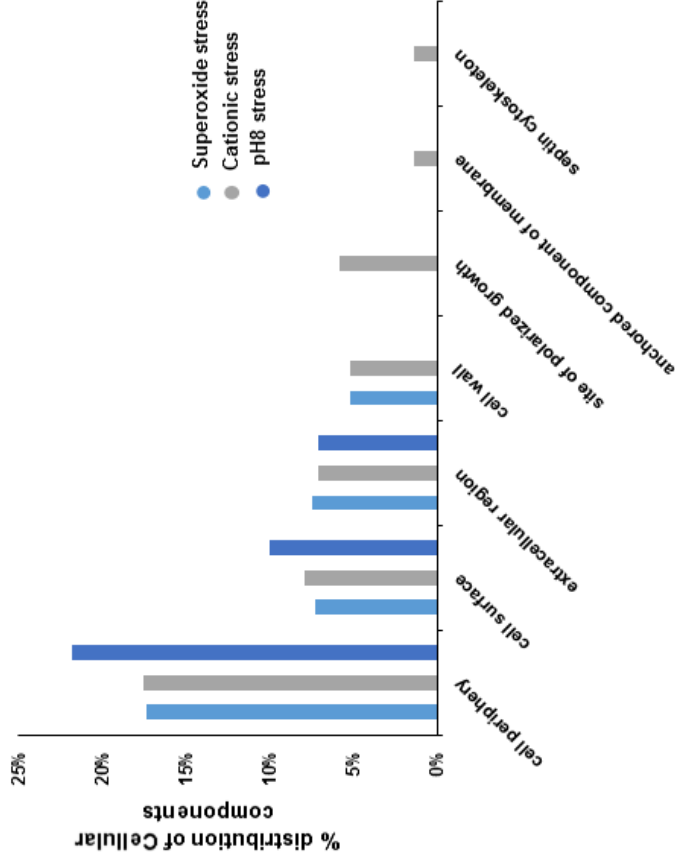


Fig 3.4 Distribution of enriched functional GO categories of genes required for cationic, superoxide, and alkaline pH8 stresses. Charts show the ranked distribution of genes identified as significantly sensitive (SIS cut-off ≤ -0.05) within enriched significant GO categories (False discovery rate cut-off ≤ 0.05) for biological processes (A), Molecular functions (B), and Cellular Components (C) gene ontologies. For each set of genes used for the analysis, the percentages of genes associated with each GO term was used to rank the distribution.

Common biological processes			
Go term	Superoxide stress	Cationic stress	Alkaline pH stress
Pathogenesis	<i>AHR1, BRG1, CLA4, CST20, DAC1, GLN3, GYP1, HOG1, HSX11, IFF11, INP51, MKC1, MTLA1, MTS1, NIK1, NUO1, NUO2, PEP7, PHO100, PTC1, RBE1, RBT4, RIM101, RIM13, SAP3, SAP5, SET3, SIT4, SPF1</i>	<i>MAD2, SIT4, SAP7, BRG1, CHS7, RBT4, CPH1, PHO100, IRE1, KEX2, PTC1, LIP2, MTS1CPP1, CLA4, TYE7, RBE1, SET3, RIM101, CHK1, HOG1, STE11, SPF1, YPT722, INP51RAS1, IFF11, UTR2, MNT1, GPA2, SLD1, NUO2, SAP3, CRZ1, AHR1, PGA7, PEP7, CAS5, HSX11, HWP2, RBT1, PHR1, PPG1, CEK1, MTLA1, CST20, HSL1, HEX1, GLN3, RIM13, HET1, SAP6, SAP5, SAP1, NAG1, DAC1, NIK1, LIP8, NRG1, MKC1, IFF4, CDC10, ACE2, YHB1, NUO1</i>	<i>DAC1, HET1, HEX1, HOG1, INP51, IRE1, KEX2, PGA7, PHR1, RBT1, RIM101, RIM13, SIT4, SPF1, YHB1, YPT722, ZCF6</i>
Cell wall biogenesis	<i>PGA5, C1_03470C_A, ENG1, MNS1, KTR4, SIT4, CHS7, SMI1, IRE1, KEX2, SSU81, PKH2, PGA13, C1_13530W_A, CSK1, RIM101, MSB2, CHK1, HOG1, STE11, DCK1, CHS5, KIC1, SPF1, PIR1, CDA2, C2_08920W_A, YEA4, INP51, RAS1, CMK2, MNT1, KRE5, SAP9, RHB1, CHS4, CRZ1, PBS2, OCH1, C3_07470W_A, C4_00190W_A, CAS5, RBT1, SAP10, PHR1, MNN22, CEK1, CST20, MID1, CRH12, PGA4, ACF2, YPS7, MKC1, CR_02800C_A, HST7, CDC10, ACE2, TSC11, CR_09340W_A</i>	<i>ACF2, C2_08920W_A, CDC10, HOG1, INP51, KIC1, MID1, OCH1, PBS2, PGA5, RAS1, RBT1, RHB1, RIM101, SPF1, TUS1</i>	<i>ACF2, SPF1, C2_08920W_A, HOG1, HST7, INP51, IRE1, KEX2, MID1, MSB2, OCH1, PBS2, PGA5, PHR1, RBT1, RIM101, SIT4</i>
Phosphorylation	<i>BUR2, CLA4, COX4, CR_06040W_A, CST20, DUN1, HOG1, KIS1, MKC1, NIK1, NPR1, PBS2,</i>	<i>EHD3, C1_03470C_A, C1_04090C_A, SIT4, C1_04780C_A, NPR1, C1_07640C_A, IRE1, CLA4, GIN4,</i>	<i>C1_07640C_A, CEK1, COX4, CR_06040W_A, DUN1, EHD3, HOG1,</i>

	<i>PKH2, SIT4, SNF4, SSK2, SSN3, STT4</i>	<i>PKH2, CSK1, COX4, CHK1, HOG1, PDK2, C2_03760C_A, STE11, SSN3, KIC1, KIS1, CMK2, C3_05420W_A, PBS2, SSK2, CEK1, CST20, BUR2, HSL1, DUN1, SNF4, NIK1, PRR2, MKC1, KIN2, PRK1, HST7, CEK2, CR_06040W_A, STT4</i>	<i>HST7, IRE1, PBS2, SIT4, SSK2</i>
Distinct biological processes			
Go term	Superoxide stress	Cationic stress	Alkaline pH stress
Cation homeostasis		<i>CTR2, C1_09780C_A, SFU1, C2_02200W_A, GDT1, SPF1, YPT722, ZSF1, GPA2, CCC1, CRZ1, FRP1, PGA7, RBT5, ECM7, PGA10, TOK1, CFL2, CSA2, ZRT1, PRA1, RAV2, CSA1, SEF1, CR_06040W_A, PPZ1, CR_06640C_A</i>	
Interaction with host		<i>CPH1, KEX2, HYR1, RIM101, CDC19, RAS1, CAP1, SAP9, SAP3, CTA4, PHR1, PRA1, RIM13, SAP6, SAP1, ALS5, YHB1</i>	
Response to pheromone		<i>C1_03960C_A, STE3, CPH1, PTC1, CPP1, CLA4, STE11, IFF6, RAS1, GPA2, CRZ1, CEK1, CST20, GRR1, CAG1, FIG1, FAR1, YPS7, KAR4, HST7, STE2</i>	
Signal transduction by phosphorylation		<i>EHD3, PKH2, HOG1, STE11, PBS2, SSK2, CEK1, CST20, MKC1, HST7</i>	

Response to starvation		<p>SIN3, C1_03870C_A, SIT4, BRG1, CPH1, VPS41, CPP1, SFU1, CLA4, SNT1, SET3, RIM101, ESC4, FGR22, HOG1, DCK2, DCK1FGR51, KIC1, CDC19, TSC11, C2_07100W_A, BUD20, KAR3, C2_09870W_A, RAS1, GPA2, C3_02760C_A, KRE5, NPR2, FCY2, C3_03680W_A, PEP8, RDI1, RHB1, CRZ1, AHR1, OCH1, FCR1, ECM29, MAL2, SSU1, C3_07670W_A, FRP1, PEP7, ADR1, UBR1, CEK1, CST20, HSL1, FGR27, CHT2, GLN3, APM1, VID27, RIM9, RAV2, FGR17, SNQ2, SNF4, DAC1, FGR2, NIK1, ERG5, HST7, STE13, C7_03860W_A, NRG1, MKC1, PIN4, ECM4, CEK2, CR_08430W_A</p>	
External encapsulating structure organisation		<p>PGA5, C1_03470C_A, SIT4, TUS1, CPH1, IRE1, KEX2, SSU81, CSK1, MSB2, HOG1, DCK1, CHS5, KIC1, SPF1, PIR1, TSC11, PGA13, C2_08920W_A, INP51, CMK2, UTR2, MNT1KRE5, SAP9, RHB1, CRZ1, PBS2, C3_07470W_A, C4_00190W_A, CAS5, RBT1, SAP10, PHR1, CEK1, CST20, MID1, CRH12, PGA4, YPS7, MKC1, CDA2, HST7, CDC10, ACE2, CR_09340W_A</p>	
Biological adhesion		<p>HYR1, SPF1, YWP1, KIS1, RAS1, UTR2, MNT1, C3_02870C_A, SAP9, SAP3, AHR1, AAF1, RBT5, PEP7, HWP2, SAP10, PHR1, PRA1, SAP6, SAP5, SAP1, ALS5, IFF4,</p>	

		CDC10, BCR1, STE2, ACE2	
Regulation of phosphate metabolic process	C1_04090C_A, SIT4, PCL2, PTC1, CPP1, SNT1, TYE7, MSB2, STE11, C2_09870W_A, RAS1, GAL4, GPA2, PBS2, OSH3, SSK2, CEK1, CST20, BUR2, MID1, CAG1, PTP3 C7_00840C_A, CLB4, PHO81, PTC2, HST7, CR_08430W_A,		
Regulation of gene expression	SIN3, SIZ1, EHD3, PDK2, PTP3, C1_03470C_A, MNN22, SSK2, C1_03600W_A, MNS1, MNT4, C1_03920C_A, KTR4, SIT4, RAD32, C1_04090C_A, C1_04640W_A, C1_04780C_A, NPR1, PHO15, C1_07640C_A, IRE1, C1_08700W_A, PTC1, C1_09790C_A, CPP1, CLA4, GIN4, SNT1, PKH2, SET3, C1_12650C_A, OCA6, CSK1, STE11, C1_14170W_A, ATS1 C2_00170C_A, TOM1, CHK1, HOG1, C2_03760C_A, C2_03780C_A, SSN3, KIC1, VAN1, C2_05840W_A, SPF1, KIS1, CMK2, MNT1, KRE5, PTC7, C3_04420W_A, PTC5, C3_05420W_A, MNN14, PBS2, OCH1, C3_05680W_A, C3_06990W_A, C4_00260W_A, C4_00580W_A, C4_03600C_A, CEK1, DOT4, RAD18, PTP1, C4_07010C_A, CST20, MNN13, HST7, BUR2, SNF4, PPZ1, C5_02400W_A, C5_02900W_A, GRR1, DUN1, PEX4, C6_01350W_A, C6_02290C_A,		

	<p>C7_00840C_A, C7_02110W_A, PRR2, MKC1, CR_00370W_A, KIN2, CR_01170W_A, PTC2, PPH3, ULP2, CR_06040W_A,</p>		
<p>Filamentous growth in response to starvation</p>	<p>MAD2, RBT4, SMI1, IRE1, CLA4, GIN4, RIM101, KIC1, CNT, KIS1, SGT1, DAG7, C2_09860C_A, C2_10540W_A, CAP1, KRE5, NPR2, FCY2, RHB1, TEA1, CRZ1, AHR1, FCR1, MRR2, ECM7, SNQ2, GDE1, C4_00610W_A, ARL1, C4_01090C_A, CAS5, OPT6, PHR1, CEK1, GIS2, MID1, C5_04120C_A, GLN3, CAG1, PGA4, VID27, CPH2, FET3, C6_01870C_, C7_01170C_A, PRR2, NRG1, MKC1, CR_02510W_A, CR_02800C_A, GZF3, PPH3, HST7, CR_06040W_A, ACE2, PTC5, PDK2, CR_09830W_A</p>		
<p>Regulation of biosynthetic processes</p>	<p>SIN3, SWI4, EHD3, BRG1, C1_03870C_A, MAD2, SIT4, IRE1, KEX2, SSU81, PTC1, VPS41, CPP1, SFU1, CLA4, C1_12650C_A, TYE7, CUP2, SET3, RIM101, MSB2, CHK1, HOG1, RAD32, STE11, CAP1, GPA2, C2_03780C_A, SSU1, DCK1, KIC1, CDC1, MEC3, KAR3, C2_09870W_A, RAS1, CMK2, C3_00570C_A, C3_02760C_A, KRE5, NPR2, FCY2, MAL2, C3_03680W_A, PEP8, RDI1, RHB1, CRZ1, AHR1, PBS2, OCH1, FCR1, ECM29, C3_07670W_A, FRP1, PEP7, CAS5, ADR1, FGR3, CSR1, FGR10, SSK2, C4_06020C_A, C4_07010C_A, GIS2,</p>		

	<i>CST20, FGR27, CHT2, GLN3, GRR1, DUN1, APM1, VID27, CPH2, RIM9, CIP1, RAD18, FPG1, RAV2, FGR17, SNQ2, SNF4, DAC1, FGR2, NIK1, ERG5, C7_03860W_A, NRG1, MKC1, PHO81, PIN4, PTC2, ECM4, RFG1, GZF3, PPH3, HST7, STE13, CR_06040W_A, BCR1, TSC11, YHB1, CEK1, CR_08430W_A,</i>		
Cell differentiation	<i>C1_03960C_A, IRE1, PTC1, CPP1, CLA4, RTG3, HST7, GZF3, C2_02520W_A, CHK1, HOG1, STE11, PTC2, C2_03780C_A, IFF6, RAS1, CAP1, GPA2, CRZ1, CTA4, ADR1, AGO1, CEK1, CST20, GLN3, GRR1, CAG1, C6_01460C_A, DAC1, FAR1, YPS7, NIK1, NRG1, MKC1, KAR4, CR_02510W_A,</i>		
Cellular response to abiotic stimulus			<i>SIN3, CTA9, SEP7, SIT4, CPH1, KEX2, VPS41, GIN, RIM101, MSB2, HOG1, DCK2, FGR51, RHO3, YPT72, DFG10, INP51, RAS1, UTR2MNT1, PBS2, OCH1, BEM3, ADR1, OSH3, FGR3, PHR1, MID1, RIM13, APM1, RIM9, RAV2, DAC1, SEF1, GZF3, HST7, CEK2, BCR1, YHB1</i>

Table 3.4 Overlapping and distinct GO terms required for cationic, superoxide, and alkaline pH stress resistance.

GO analysis looking at enriched molecular functions was also explored. No significantly enriched molecular function was identified for alkaline pH stress response however, 9 and 14 molecular functions were enriched respectively within the gene sets required for superoxide and cationic stress resistance (Fig 3.4B). The most significantly enriched molecular functions for both of these stresses were ion binding and hydrolase activity (Fig 3.4B).

For all three stresses studied, significantly enriched cellular component terms were identified by GO analysis. Genes annotated to the cell periphery, cell surface and

extracellular region GO terms were significantly enriched for all three stresses (Fig 3.4C). The cell wall GO term was also enriched within the genes required for cationic and superoxide stress resistance, whereas the terms polarised growth, anchored component of membrane, and septin cytoskeleton were only enriched in the cationic-stress resistance genes (Fig 3.4C).

Biological process	Superoxide stress	Cationic stress	Alkaline pH stress
Transcriptional activity	<i>RTG1, MSN4, RTG3, CTA4, MNL1, TAC1, RPN4, CAP1, PHO4, CZF1, C1_05750C_A, DPB4, ISW2, GRF10, TEC1, MAC1, SFL1, EFG1, TUP1, UPC2, RIM101, NDT80, SNF4, C2_08540C_A, ASH1, LYS144, AHR1, CAS5, GAT1, NRG1</i>	<i>CAP1, CRZ1, CAS5, GIS2, BCR1, RTG1, CTA4, MNL1, RIM101, CTF1, C2_08540C_A, ASH1, LYS144, AHR1, NRG1, EFG1, SNF4</i>	<i>RIM101, NDT80, GZF3, MSN4, CAP1, SKN7, MSN4, C1_05750C_A, MSN4, ROB1, DPB4, ISW2, ASH1, CPH2, EFG1</i>
Protein kinase activity	<i>C1_03470C_A, C1_04780C_A, NPR1, C1_07640C_A, IRE1, CLA4, GIN4, PKH2, CSK1, CHK1, HOG1, C2_03760C_A, STE11, SSN3, KIC1, KIS1, CMK2, C3_05420W_A, PBS2, SSK2, CEK1, CST20, DUN1, NIK1, PRR2, MKC1, KIN2, HST7, CR_06040W_A, PDK2</i>	<i>C1_03470C_A, C1_04780C_A, NPR1, C1_07640C_A, IRE1, CLA4, GIN4, PKH2, CSK1, CHK1, HOG1, C2_03760C_A, STE11, SSN3, KIC1, KIS1, CR_06040W_A, CMK2, PDK2, C3_05420W_A, PBS2, SSK2, CEK1, CST20, HSL1, DUN1, NIK1, PRR2, MKC1, KIN2, PRK1, HST7, CEK2,</i>	<i>C1_03470C_A, C1_07640C_A, IRE1, GIN4, HOG1, C2_03760C_A, PBS2, SSK2, DUN1, PRR2, HST7, CEK2, CR_06040W_A</i>
GTPases	<i>RHO3, CRL1, ARL3, YPT722, RAS1, GLO3, ARL1, RGA2, BEM3, MTG2</i>	<i>RHO3, CRL1, ARL3, YPT722, RAS1, GLO3, ARL1, RGA2, BEM3, MTG2</i>	

Table 3.5 Distinct biological processes regulated by TFs under cationic, superoxide, and alkaline pH stress.

Protein kinases	
Npr1 - Predicted serine/threonine protein kinase, involved in regulation of ammonium transport; induced in core stress response; Hap43p-repressed gene	Ire1 - Putative protein kinase; role in cell wall regulation; mutant is hypersensitive to caspofungin
C1_03470C_B - Ortholog(s) have protein kinase activity, role in activation of bipolar cell growth, ascospore wall assembly, protein phosphorylation and cell division	C1_04780C_A - Ortholog(s) have clathrin-coated vesicle, cytoplasm localization
C1_07640C_A - Protein with predicted serine/threonine kinase and tyrosine kinase domains; possibly an essential gene, disruptants not obtained by UAU1 method	Cla4 - Ste20p family Ser/Thr kinase required for wild-type filamentous growth, organ colonization and virulence in mouse systemic infection; role in chlamydospore formation; functional homolog of <i>S. cerevisiae</i> Cla4p;
Gin4 - Autophosphorylated kinase; role in pseudohyphal-hyphal switch and cytokinesis; phosphorylates Cdc11p on S395; necessary for septin ring within germ tube but not for septin band at mother cell junction; physically associates with septins. Oxidative stress resistance: decreased	Pkh2 - Putative serine/threonine protein kinase; predicted role in sphingolipid-mediated signaling pathway that controls endocytosis; mRNA binds She3 and is localized to hyphal tips
Csk1 - Putative mitogen-activated protein (MAP) kinase with an unknown role; null mutant produces wrinkled colonies; similar to <i>S. cerevisiae</i> Smk1p, which is a protein kinase required for sporulation	C2_03760C_B - Predicted protein kinase similar to <i>S. cerevisiae</i> Nnk1; implicated in proteasome function in <i>S. cerevisiae</i> ; induced by Mnl1 under weak acid stress
Ste11 - Protein similar to <i>S. cerevisiae</i> Ste11p; mutants are sensitive to growth on H ₂ O ₂ medium	Ssn3 - Putative cyclin-dependent protein kinase; mutants are sensitive to growth on H ₂ O ₂ medium
Kic1 - Member of the GCK-III subfamily of eukaryotic Ste20p kinases; in RAM cell wall integrity signaling network; role in cell separation, azole sensitivity; required for hyphal growth; constitutive expression is MTL, white-opaque independent	Kis1 - Snf1p complex scaffold protein; similar to <i>S. cerevisiae</i> Gal83p and Sip2p with regions of similarity to Sip1p (ASC and KIS domain); interacts with Snf4p; mutants are hypersensitive to caspofungin and H ₂ O ₂ ; Hap43p-repressed gene
Crnk2 - Putative calcium/calmodulin-dependent protein kinase II; expression regulated upon white-opaque switching; biochemically purified Ca ²⁺ /CaM-dependent kinase is soluble, cytosolic, monomeric, and serine-autophosphorylated; Hap43p-repressed	C3_05420W_B - Has domain(s) with predicted ATP binding, protein tyrosine kinase activity and role in protein phosphorylation
Cst20 - Protein kinase of Ste20p/p65PAK family, required for wild-type mating efficiency and virulence in a mouse model; Cst20p-Hst7p-Cek1p-Cph1p MAPK pathway regulates some hyphal growth; involved in Cdc42p growth regulation	Dun1 - Protein similar to <i>S. cerevisiae</i> Dun1p, which is a serine-threonine protein kinase involved in DNA damage cell-cycle checkpoint; induced under Cdc5p depletion
Nik1 - Histidine kinase involved in a two-component signaling pathway that regulates cell wall biosynthesis; required for wild-type virulence in mouse systemic infection but not for wild-type growth or drug sensitivity/resistance; 9 HAMP domains. Decreased resistance to oxidative stress.	Prr2 - Putative serine/threonine protein kinase; mutation confers resistance to 5-fluorocytosine
Mkc1 - MAP kinase; role in biofilm formation, contact-induced invasive filamentation, systemic virulence in mouse, cell wall structure/maintenance, caspofungin response; phosphorylated on surface contact, membrane perturbation, or cell wall stress	Kin2 - Protein with similarity to <i>S. cerevisiae</i> Kin2p, transcription is positively regulated by Tbf1
Hst7 - MAPKK involved in mating and hyphal growth signal transduction pathways; wild-type virulence in mouse systemic infection; functional homolog of <i>S. cerevisiae</i> Ste7p; mutants are hypersensitive to caspofungin	Pdk2 - Putative pyruvate dehydrogenase kinase; mutation confers hypersensitivity to amphotericin B

Prk1 - Putative protein serine/threonine kinase; mutant is sensitive to growth on H ₂ O ₂	Cek2 - MAP kinase required for wild-type efficiency of mating; component of the signal transduction pathway that regulates mating; ortholog of <i>S. cerevisiae</i> Fus3; induced by Cph1
Proteins with signal transducer activity	
Ssu81 - Predicted adaptor protein involved in activation of MAP kinase-dependent signaling pathways; links response to oxidative stress to morphogenesis and cell wall biosynthesis; caspofungin repressed	Ste3 - Protein similar to <i>S. cerevisiae</i> Ste3p, the receptor for a-factor mating pheromone; alpha mating-type-specific transcription
Msb2 - Mucin family adhesin-like protein; cell wall damage sensor; required for Cek1 phosphorylation by cell wall stress; Rim101-repressed	Ste11 - Protein similar to <i>S. cerevisiae</i> Ste11p; mutants are sensitive to growth on H ₂ O ₂ medium
Gpa2 - G-protein alpha subunit; regulates filamentous growth, copper resistance; involved in cAMP-mediated glucose signaling; reports differ on role in cAMP-PKA pathway, MAP kinase cascade; Gpr1 C terminus binds Gpa2; regulates HWP1 and ECE1	Cag1 - heterotrimeric G protein alpha subunit; positive role in mating pheromone response; opaque-enriched transcript; transcript repressed by MTL α 1-MTL α 2; regulated by hemoglobin-responsive Hbr1 via MTL genes; rat catheter biofilm repressed
Ste2 - Receptor for alpha factor mating pheromone, MF α ; required for a-type cells to respond to alpha factor, for opaque a-form mating and white a-form response; possible Kex2p substrate	
GTPases	
Crl1 - Predicted GTPase of RHO family; CAAX motif geranylgeranylated; expression in <i>S. cerevisiae</i> causes dominant-negative inhibition of pheromone response	Glo3 - Ortholog(s) have ARF GTPase activator activity and role in COPI coating of Golgi vesicle, ER to Golgi vesicle-mediated transport, retrograde vesicle-mediated transport, Golgi to ER
Arl3 - Uncharacterised, Putative Ras superfamily GTPase; induced by nitric oxide independent of Yhb1p	Arl1 - Putative GTPase; mutation confers dose-dependent sensitivity to Brefeldin A
Rho3 - Putative Rho family GTPase; possible substrate of protein farnesyltransferase and geranylgeranyl transferase type I; greater transcription in hyphal form than yeast form; plasma membrane-localized	Bem3 - Putative GTPase-activating protein (GAP) for Rho-type GTPase Cdc42p; involved in cell signaling pathways that control cell polarity; similar to <i>S. cerevisiae</i> Bem3p
Rga2 - Putative GTPase-activating protein (GAP) for Rho-type GTPase Cdc42p; involved in cell signaling pathways controlling cell polarity; similar to <i>S. cerevisiae</i> Rga2p; induced upon low-level peroxide stress; late-stage biofilm-induced	Mtg2 - Putative Obg family GTPase member; peripheral protein of the mitochondrial inner membrane; associates with the large ribosomal subunit; required for mitochondrial translation; rat catheter biofilm repressed

Table 3.6 Protein kinases, signalling proteins, and GTPases identified by QFA.

3.3 Discussion.

Successful adaptation to host-imposed challenges is paramount to the survival of *C. albicans*. The response to stress is tightly regulated by several key proteins, some of which have been studied extensively to understand the cellular processes involved in stress adaptation in this major pathogen. However, there is still much to be learnt about how *C. albicans* responds to physiologically relevant stresses. In this chapter,

two *C. albicans* deletion collections were analysed by QFA to define the genetic determinants and cellular processes of stress resistance in *C. albicans*.

The effects of the cationic stress agent, NaCl, on the cellular responses of the model yeast *S. cerevisiae* have been extensively studied. Exposure to high concentrations of external NaCl induces both cationic and osmotic stress and leads to drastic decrease in cell volume and turgor pressure as a result of water loss (Kuhn and Klipp, 2012). In *C. albicans* the transcriptional response to cationic stress is mediated by the action of the Hog1 SAPK, which is phosphorylated and accumulates in the nucleus following NaCl exposure, to activate cationic stress response genes (Smith *et al.*, 2004; Enjalbert *et al.*, 2006). Activation of cationic stress response genes prompts glycerol accumulation which restores turgor pressure and cell survival. Cells lacking Hog1 are extremely sensitive to osmotic and cationic stresses (San Jose *et al.*, 1996; Smith *et al.*, 2004), and display highly attenuated virulence in neutrophil, systemic and commensal models of infection (Alonso-Monge *et al.*, 2003; Arana *et al.*, 2007; Prieto *et al.*, 2014). The importance of a fully functioning Hog1 pathway for stress resistance was reiterated by the results from this study. Deleting any of the genes that make up the Hog1 pathway (Hog 1 MAPK, Pbs2 MAPKK, and Ssk2 MAPKKK) resulted in sensitivity to all three stress conditions. However, whilst roles for Hog1 signalling in response to NaCl and menadione stress have previously been reported (Smith *et al.*, 2004), this is the first demonstration that Hog1 is important for resistance to alkaline pH stress. Interestingly, the histidine kinases, Nik1 and Chk1, predicted to relay stress signals to the Hog1 module, were also sensitive to all stresses tested. With regard to important downstream targets of Hog1, this study identified the Ena21 predicted P-type ATPase sodium pump to be the most sensitive mutant to NaCl imposed cationic stress. Previous *in vitro* transcript profiling studies identified *ENA21* to be induced following cationic stress in a Hog1-dependent manner (Enjalbert *et al.*, 2006), and *in vivo* transcriptional profiling found *ENA21* to be upregulated following *C. albicans* infection of the in the kidney (Walker *et al.*, 2009). To deal with high levels of NaCl, *S. cerevisiae* uses the homologous P-type ATPase sodium efflux pump, Ena1 and cells lacking *ENA1* are sensitive to cations (Haro *et al.*, 1991). We also found that *C. albicans ena21Δ* cells are also sensitive to alkaline pH, suggesting this efflux pump may also be required to pump out protons to lower the pH of the environment. Further characterisation of this predicted sodium pump and its role stress resistance are warranted.

Although the Hog-1 regulated transcriptome in response to osmotic stress has been characterised (Enjalbert *et al.*, 2006), the transcriptional regulator(s) that mediate this response have remained elusive. In this study, the transcriptional factor, Gis2 was found to be required for cationic stress resistance. Gis2 is a putative transcription factor whose expression was reported to increase during growth in high iron medium and de-regulated during the yeast to hyphae switch (Lan *et al.*, 2004; Nantel *et al.*, 2002). In the original screen of the transcription factor deletion collection (Homann *et al.*, 2009), cells lacking *GIS2* were also reported to be sensitive to the osmotic stress inducing agent sorbitol. Hog1 is also essential for sorbitol-induced osmotic stress resistance (Smith *et al.*, 2004), and moreover high levels of NaCl impose an osmotic stress on the cell in addition to cationic stress. Thus it is tempting to speculate that Gis2 may be a transcription factor of Hog1 to regulate osmotic and cationic stress-protective genes. Further investigations to test this hypothesis are necessary. However, other transcription factors with roles in cationic stress resistance were identified in this study. Unexpectedly, the transcription factor Pho4, which has predicted roles in phosphate homeostasis, was found to exhibit the strongest cationic stress sensitive phenotype of all the *C. albicans* mutants tested in this study. Such a role has not been reported for the analogous Pho4 transcription factor in *S. cerevisiae*, which raised the possibility that the function of this transcription factor may have been reassigned in *C. albicans*. In addition, to our knowledge no role for cationic resistance has been reported for the transcription factor Cas5, yet was identified by QFA in this study. However, *C. albicans* cells lacking *CAS5* have cell wall defects, are sensitive to caspofungin, and have reduced virulent abilities in a mouse model of infection (Chamilos *et al.*, 2009). Thus the stress sensitivities seen with *cas5Δ* cells may be due to cell wall defects.

In agreement with the findings of Homann *et al.* (2009), we found the transcriptional regulator Cap1 to be essential for menadione-imposed stress. This indicates that this transcription factor, in addition to regulating responses to H₂O₂ (Patterson *et al.*, 2013), also contributes to the transcriptional response to menadione-induced superoxide stress. This is consistent with superoxide being rapidly dismutated to H₂O₂ via the action of the superoxide dismutase enzymes. Screening the Noble deletion collection for mutants sensitive to menadione in this study, has also revealed the importance of iron availability in facilitating superoxide stress adaptation. Mutants in *FET3*, *FET31*, and *FET99* (Table 3.2) which encode multicopper oxidases

required for growth in iron-limiting environments (Erk *et al.*, 1999; Chen *et al.*, 2011), were all sensitive to menadione-imposed superoxide stress. Fet99 is regulated by the transcription factors, Tup1 and Rim101 (Knight *et al.*, 2002; Ramon and Fonza, 2003). Rim101 is the transcriptional regulator at the heart of the pH response pathway which regulates the response to alkaline pH (Ramon *et al.*, 1999). However, in addition to alkaline pH response, Rim101 has reported additional roles in iron acquisition, and the activation of the superoxide dismutase Sod5 (section 1.5.3.1). Thus, our findings here, that the *rim101Δ* mutant is acutely sensitive to menadione, could be linked to roles in the pH response pathway in iron acquisition and activation of *SOD5*. Indeed, mutants in other components of the pH response pathway, *rim13Δ* and *rim9Δ*, were also found to be sensitive to menadione. Interesting, we also found that cells lacking the Pho4 transcription factor were extremely sensitive to menadione. This was of interest, because similar to the cationic stress sensitivity of *pho4Δ* cells, a role for Pho4 in superoxide resistance has not previously been reported in *C. albicans* or the model yeast *S. cerevisiae*. In addition, as the potential Pho4-dependent gene, *PHO15* was also found to be required for superoxide resistance, this implied that the role of Pho4 in phosphate homeostasis may be important.

The ability to adapt to the diverse pH niches in the host is achieved in *C. albicans* by the pH response pathway Rim101 which governs the expression of pH response genes. Consistent with this, Rim101 and other components of the pH response pathway Rim13 and Rim9 were identified as being required for alkaline pH adaptation in this study. Moreover, the Crz1 transcription factor shown to be sensitive to alkaline pH in this study, has previously been shown to play a role in the alkaline pH response (Liang *et al.*, 2011). Cells lacking *PHO4* were also extremely sensitive to alkaline pH. However, whilst Pho4 has not been implicated in cationic or superoxide stress resistance in yeasts including *C. albicans*, a role in promoting survival to alkaline pH environments has been indicated in *S. cerevisiae* (Serrano *et al.*, 2002). This, however, has not previously been reported in *C. albicans*.

To summarise the key stress regulators that contribute to the cellular response to cationic, superoxide, and alkaline pH stresses in *C. albicans*, the transcription factors, protein kinases, proteins with signalling transducer activity, and GTPases identified by QFA in this study are listed in Table 3.5. Protein kinases play essential roles in signal transduction enabling adaptation and survival. One aim of this study

was to identify such stress regulators not previously implicated in stress resistance. These include, *CSK1*, which encodes for a putative mitogen-activated protein kinase and *PKH2*, which has a predicted role in sphingolipid-mediated signaling pathway that controls endocytosis (Pastor-Flores *et al.*, 2013), both of which are required for cationic and superoxide stress resistance. Other kinases required for both cationic and superoxide stress resistance include, Npr1 induced during the core stress response (Enjalbert *et al.*, 2006) which governs the function of ammonium permeases in response to nitrogen limitation (Neuhauser *et al.*, 2011), Ire1, previously found to be sensitive to caspofungin and involved in cell wall integrity (Blankenship *et al.*, 2010), and *ORF19.3049* which encodes for an uncharacterised protein with kinase activity (Table 3.5; 3.6). Further characterisation of these kinases could potentially identify signalling pathways needed for cationic and superoxide stress resistance in *C. albicans*. Cmk2 is a putative Ca²⁺/calmodulin-dependent protein kinase that has been recently shown to be involved in cell wall integrity and oxidative stress response (Ding *et al.*, 2014) (Table 3.5; 3.6). Data from this study show Cmk2 may also be involved in cationic stress response (Table 3.5; 3.6). Previously, cells lacking the Ste11 kinase have been reported to demonstrate impaired resistance to H₂O₂ (Blankenship *et al.*, 2010), this study demonstrated deletion also affects the ability to resist superoxide anions and cations. Furthermore, whilst the Cst20 kinase has been implicated in *C. albicans* virulence (Csank *et al.*, 1998) the mechanism behind this role is not known. However, we found cells lacking *CST20* displayed increased sensitivity to both cations and superoxide anions, both of which will be encountered in the phagosome, which may underlie the impaired ability of *cst20Δ* cells to cause infection.

GTPases are a large family of hydrolases that bind and hydrolyse GTP, and have essential roles in signal transduction, protein biosynthesis, and transportation. In *C. albicans*, the GTPases identified from the screen have diverse predicted functions (Table 3.5; 3.6). Of interest was the identification of Ypt72 involved in vacuolar biogenesis, filamentous growth, and virulence (Johnston *et al.*, 2009). Another interesting finding is the Ras1 GTPase which regulates both the cAMP dependent PKA and the Cek1 MAP kinase pathways to trigger the yeast to hyphal switch, also plays a role in cation resistance. This is particularly compelling in light of the unanticipated finding that the PKA regulated transcription factor Efg1 was required for resistance to all three stresses examined in this study. Several other GTPases

were also identified and intriguingly, include Rga2 and Bem3 with predicted roles in cell signaling pathways that govern cell polarity (Table 3.5; 3.6).

Taken together, therefore, the QFA screens performed in this study have identified proteins not previously implicated in stress resistance, or have revealed novel stress protective roles. A prime example of this is the transcription factor Pho4 which was found to be critical for *C. albicans* resistance to all three stress conditions investigated. The analogous Pho4 transcription factor in *S. cerevisiae* plays a central role in phosphate acquisition and homeostasis, but roles in cationic and superoxide resistance have not previously been reported. Based on these findings, we decided to investigate further the molecular mechanisms underlying the role of Pho4 in mediating such pleiotropic stress resistance phenotypes in the fungal pathogen *C. albicans*.

Chapter 4. The role of Pho4 in phosphate homeostasis

4.1 Introduction

Transcription factors play essential roles in the response of *C. albicans* to various stresses. For example, Cap1 activates the expression of anti-oxidant genes following exposure to ROS during phagocytosis (Alonso-Monge *et al.*, 2003; Enjalbert *et al.*, 2006). Given the results from the QFA screen, presented in Chapter 3, which identified the transcription factor Pho4 in *C. albicans* as essential for resistance to cationic and superoxide stresses, and adapting to alkaline pH, the next objective of this study was to investigate this novel role of Pho4 in stress adaptation.

In *S. cerevisiae*, Pho4 has essential roles in regulating phosphate acquisition and storage as polyP and has never been implicated in mediating superoxide and cationic stress resistance. Its role in enabling yeast cells grow in alkaline pH environments has been attributed to regulating phosphate availability under such conditions (Arino *et al.*, 2010). The phosphate response mechanism in *S. cerevisiae* has been extensively characterised. Briefly, the PHO pathway is composed of three important components: (1) an acquisition system made up of phosphatases and phosphate transporters to enable phosphate acquisition over a wide range of concentrations and substrates; (2) a phosphate reservoir polyP, which can be mobilised during phosphate limitation; and (3) and the signalling cascade that senses extra and intracellular phosphate concentrations and initiates the appropriate response (Oshima, 1996; Persson *et al.*, 2003; Lenburg and O`Shea, 1996). During growth in phosphate-rich conditions, Pho4 is phosphorylated by the CDK complex Pho80-Pho85 and kept out of the nucleus. The inhibitory effect of Pho80-Pho85 during phosphate-poor conditions is ablated by the CDK inhibitor, Pho81 (O`Neil *et al.*, 1996; Schneider *et al.*, 1994). Under low phosphate conditions the phosphorylation of Pho4 is prevented by the inhibitory effect of the Pho81 on Pho80-Pho85 complex, and Pho4 accumulates in the nucleus to activate phosphate response genes (O`Neil *et al.*, 1996; Schneider *et al.*, 1994). These phosphate-response genes also include polyP metabolism genes (Ogawa *et al.*, 2000). Both intracellular and extracellular concentrations of phosphate influence the activity of Pho4 (Auesukaree *et al.*, 2004).

Less is known about phosphate regulation in *C. albicans*. CaPho4, like that of *S. cerevisiae*, is a bHLH transcription factor of the myc-family implicated in enabling

growth in phosphate limiting conditions (Homann *et al.*, 2009; Romanowski *et al.*, 2012). In *S. cerevisiae*, the activation of *PHO* genes by Pho4 is mediated also by another transcription factor, Pho2 (Barbaric *et al.*, 1996). Pho2 is specifically required for the co-activation of the acid phosphatase, Pho5 (Barbaric *et al.*, 1998). The homologue of Pho2, Grf1 in *C. albicans* however, is not involved in phosphate homeostasis (Homann *et al.*, 2009). This difference in transcriptional regulation suggests the role of Pho4 may not be conserved in *C. albicans*. More convincing is the sequence divergence between the two transcription factors. As can be seen in Fig 4.1, sequence alignment of the Pho4 transcription factors in *S. cerevisiae* and *C. albicans* revealed very little homology apart from the DNA binding domains at the C-terminus. The N-terminal regulatory region of the two sequences exhibits significant divergence with that of *C. albicans* more extended compared to ScPho4 (Fig 4.1). In particular, the phosphorylation sites, with the exception of one, of ScPho4 (in yellow) which regulates cellular localisation and DNA binding are largely non-conserved in CaPho4 (Fig. 4.1). Hence, we wondered if the function of Pho4 in *C. albicans* had been reassigned. Therefore, before investigating the role of Pho4 in stress resistance the next objective was to establish the role of Pho4 in phosphate homeostasis in *C. albicans*.

4.2 Results.

4.2.1 Sequence alignment of *S. cerevisiae* Pho4 and *C. albicans* Pho4 reveals divergence.

As previously mentioned, sequence alignment of the Pho4 transcription factors in *S. cerevisiae* and *C. albicans* revealed very little homology apart from the DNA binding domains at the C-terminus with the N-terminal regulatory region of the two sequences exhibiting significant divergence (Fig 4.1). In particular, the phosphorylation sites of ScPho4 (in yellow) which regulates cellular localisation and DNA binding are largely non-conserved in CaPho4 (Fig. 4.1).

```

CaPho4 MDQQVWNPIFSPSGTTPGKSPSYNE LAPQSQSHISNQDPQLPLQTQHRLFHIDGGSNH
ScPho4 -----MGRTTSEGIHGFVDDLEPKS-SILDKVGFITVNTKRH-----
          . ** . . : : * * * * * : : . : : : * : *

CaPho4 STPSGNIQLPSSSQNTPHIVSNTPTAFADSDQVFLQHMEMYDNQQHTNQSAAGNTPGPIS
ScPho4 -----DGRED-----
                                     * .

CaPho4 FHNHNPNLQQASQQPHQHISPHLNNQQQHSQQPYQHCHSRSHIDSEAPSANDTPTSSG
ScPho4 FNEQND-----ELNSQENHN-----SSENGNENENEQDS-
          * : : * . * * * : * . * * . * : . *

CaPho4 ALGMAPQPPLLSSTNPQSFDLGLDTIGFIIPEELNFDTPNHISSAFPPQLPADQTPSL
ScPho4 -----

CaPho4 LAVDKLKQLQQQQQQQQRQQDPLSELSSPVLPQNDQSYNPHHYHRQSSNSVVFVAGKN
ScPho4 LALDDLDR-----AFELVEGMDMDWMMPSHAHHS-----
          * : * * . : : * : : * * * *

CaPho4 TGSSVSAPSQHVRPDAVFTPLVSPVVAPLDTNGKADKENGNSGGHNSHSSSFSPQPAV
ScPho4 ----PATTATIKPRLLYSPLIH-----TQSAV
          . * . : : * : : * * *

CaPho4 QISFEPLTSPALNAEPSTIKSKGGKKNHKETDRRRRSTSSAYAPSKDENKQYKRRTPHGT
ScPho4 PVTISPNLVATATSTTSANKVTKNKSNSSPYLNKRRGKPGPDS-----AT
          : : : * . : : . * : * . * * . : : * * * . :

CaPho4 PILQGHTSNATTVNGSGKPYKSPITKNGKNSQKQDFSTNQFEKLPESTITVKSEPMETS
ScPho4 SLFELPDSVIPTPKPKPKPKQYPKVILPSNSTR-----VSPVTAKTS-----
          . : : * . * : . * * : * . * * : : * : * * .

CaPho4 VEPPLAPQGGQQDDSNPMLPPNGKPFVEITGAPLMGFTMGKLAEGGAGTVADKKSARKAGA
ScPho4 ----SSAEGVVVASESPVIAPHGS-----
          : : * . . * * : : * * .

CaPho4 NNGKLSRKPSYSKRNRSVSSSSDESSTASSTSPKMLANNGTNSGKRSEKPKATKKASHK
ScPho4 ----SHSRSLSKRRSSGALVDDD-----KRESHK
          * : . * * * * * : . * : * * *

CaPho4 LAEQGRRNRMNNAVQELGRLI PQSY--HDEVSI PSKATTVELASKYITALLKEVEELKGR
ScPho4 HAEQARRNRLAVALHELASLI PAEWKQQNVSAAPSKATTVEAACRYIRHLQQNVST----
          * * * * * : * : * * . * * * . : : : * * * * * * * * * * * : : * .

```

Fig 4.1. Alignment of *C. albicans* and *S. cerevisiae* Pho4 reveals sequence divergence. The basic helix-loop-helix DNA binding domain (in red) is conserved between ScPho4 and CaPho4. In contrast the N-terminal regulatory region exhibits significant divergence. In particular, the phosphorylation sites of ScPho4 (in yellow) which regulate cellular localisation and DNA binding are not conserved in CaPho4. Sequences of ScPho4 and CaPho4 were aligned using ClustalW. Dashes indicate single nucleotide gaps introduced to maximise alignment. Identical nucleotides in both sequences are indicated by *.

4.2.2 *Pho4* is required for phosphate acquisition in *C. albicans*.

Given the lack of homology between ScPho4 and CaPho4 and the absence of similar stress phenotypes in *S. cerevisiae*, whether Pho4 in *C. albicans* was required for phosphate acquisition was first investigated. Activation of the PHO pathway during growth in low phosphate medium can be detected by the activity of secreted acid phosphatases using a colorimetric assay (To *et al.*, 1973). Wild-type, *pho4Δ*, and *pho4Δ+PHO4* candida cells were grown on Peptone NaCl Magnesium Chloride (PNMC) agar plates plus or minus phosphate and then overlaid with soft agar containing a phosphate substrate and dye. Cells with phosphatase activity in response to phosphate limitation appear dark in colour. From the assay it was discovered that cells lacking *PHO4* are defective at secreting phosphatases in response to limiting phosphate (Fig 4.2A). This result strongly suggests Pho4 is required for phosphate acquisition from external sources.

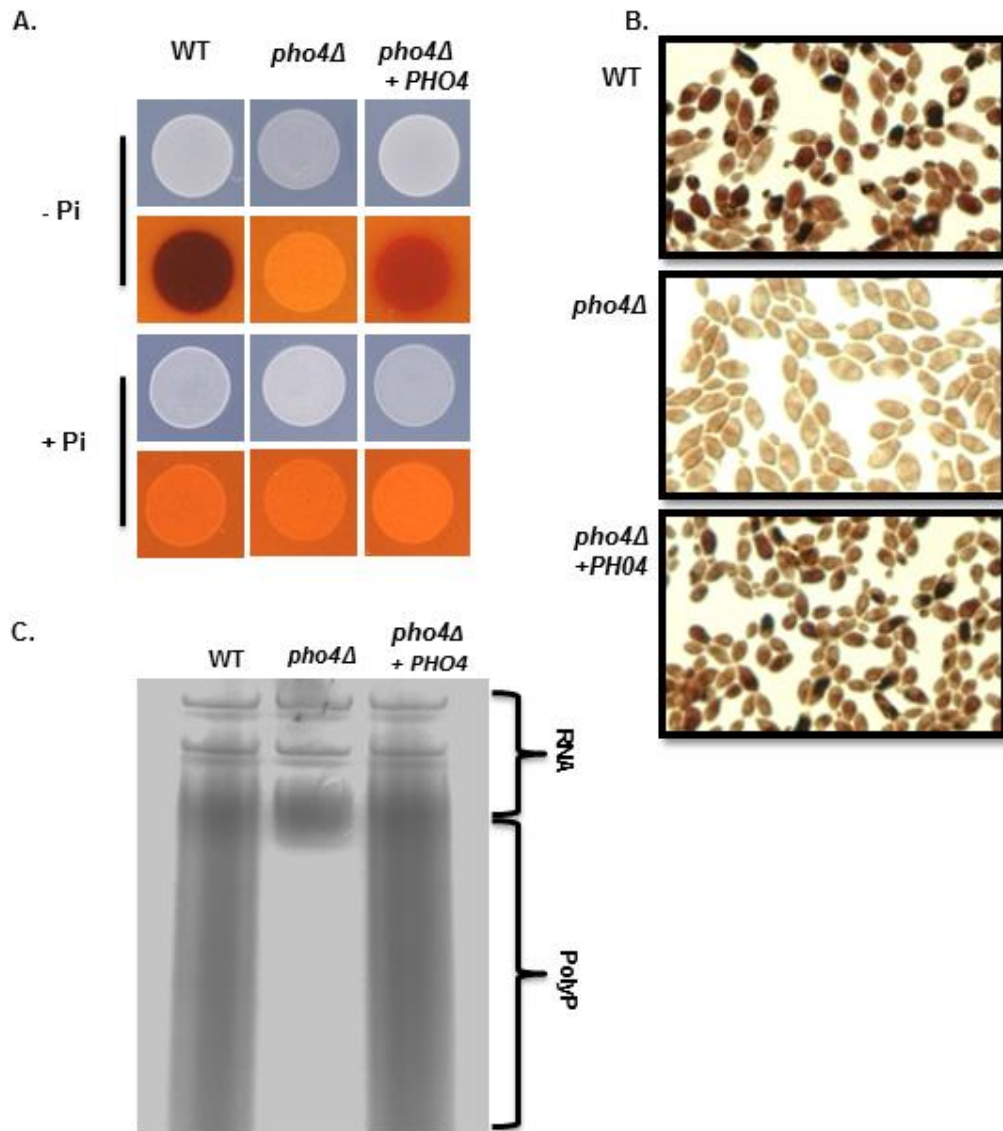


Fig. 4.2. Pho4 is required for phosphate acquisition and storage. (A). Cells lacking *PHO4* have no detectable acid phosphatase activity. 2×10^3 cells, and 10-fold dilutions thereof, of exponentially-growing wild-type, *pho4Δ*, *pho4Δ+PHO4* strains were spotted onto PNMC (Peptone, NaCl, MgSO₄, and CaCl₂) agar plates, with or without Pi. Plates were incubated at 30°C for 24 h following which colonies were overlaid with p-nitrophenylphosphate and fast blue salt B and incubated for 30 mins. Dark colour on minus Pi plates indicates phosphatase activity (B) Cells lacking *PHO4* have no polyP inclusions. Exponentially-growing wild-type, *pho4Δ*, *pho4Δ+PHO4* strains were fixed by paraformaldehyde and then stained by Neisser staining (C) No polyP detected in the *pho4Δ* cells. PolyP on a toluidine blue stained UREA-PAGE gel showing polyP content. 20 μg of total RNA extracted from wildtype, *pho4Δ*, *pho4Δ+PHO4* cells was loaded onto a 12% UREA-PAGE gel. The experiment was repeated twice, a representative gel is shown.

4.2.3 *Pho4* is required for phosphate storage and mobilisation in response to phosphate limitation.

In addition to regulating the production of secreted acid phosphatases following phosphate limitation, ScPho4 also regulates the induction of genes necessary for PolyP synthesis. Thus, the role of CaPho4 in polyP synthesis was investigated. Two different methods were used to detect the presence of polyP granules in *C. albicans*. Neisser staining involves staining paraformaldehyde fixed cells with basic dyes such as methylene blue. With this method, polyP can be visualised as purple-black stained granules against yellowish-brown background in the fixed cells (Bartholomew, 1981). The other method used requires electrophoresis of polyP extracted from cells on urea-polyacrylamide gels followed by staining of the gel with another basic dye, toluidine blue (Robinson *et al.*, 1984; Clark and Woods, 1987). Both RNA and polyP are extracted as these are both anionic molecules but the two run through the gel quite differently. Using both methods the presence of polyP granules in wild-type, *pho4Δ*, and *pho4Δ+PHO4* cells grown in YPD were examined. Neisser staining showed the polyP granules in wild-type and *pho4Δ+PHO4* reintegrated cells however, no polyP was detected in the *pho4Δ* cells (Fig 4.2B). The same result was obtained using gel electrophoresis to analyse polyP content (Fig 4.2C). Taken together, these results illustrate that despite sequence divergence, the *C. albicans* Pho4 transcription factor does play key roles in phosphate acquisition and storage, similar to that of *S. cerevisiae*.

4.2.4 *Pho4* accumulates in the nucleus in response to phosphate limitation.

Having established that Pho4 governs phosphate homeostasis in *C. albicans*, the cellular localisation and post-translational modification of Pho4 under phosphate-rich and phosphate-limiting conditions were examined. The kinetics of Pho4 localisation was monitored over time following transfer from phosphate-rich medium to no-phosphate medium using wild-type cells expressing a Pho4-green fluorescent protein (GFP) fusion. Tagging Pho4 at the C-terminus with GFP does not affect Pho4 function as *pho4Δ/PHO4-GFP* cells in which the single remaining copy of Pho4 has been tagged with GFP have the same stress phenotypes as wild-type cells (Fig 4.3A). In phosphate-rich medium, Pho4-GFP was seen dispersed throughout the cells (Fig 4.4A). However, upon transfer to phosphate-lacking medium Pho4 was marginally localised in the nucleus within 4 h of transferring cells (Fig 4.4A). There was marginal accumulation at the earlier time points with more robust accumulation occurring as a result of polyP mobilisation (Fig 4.4B & C). Nuclear accumulation of

Pho4 was sustained for up to 14 h in no-phosphate medium, however 5 mins following phosphate addition Pho4 could no longer be detected in the nucleus (Fig 4.4A).

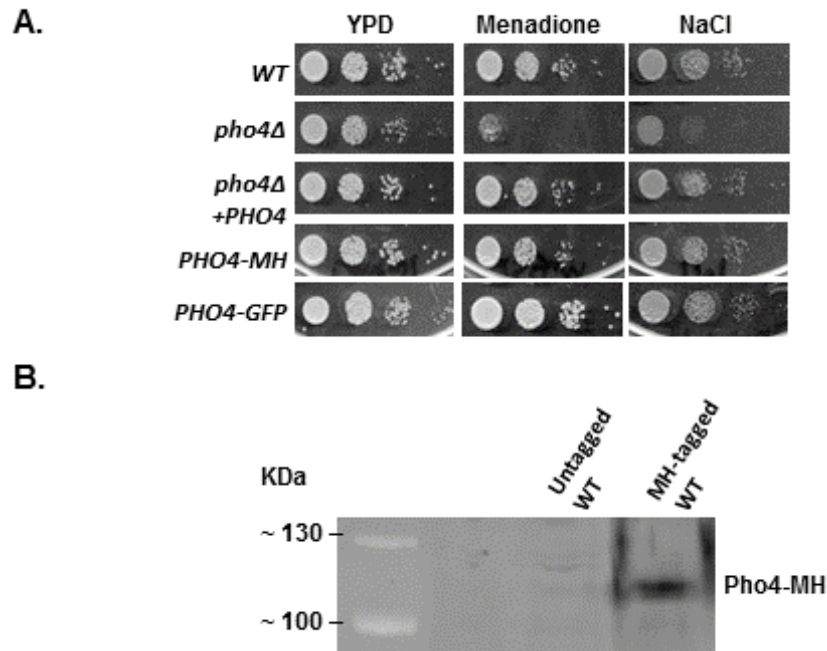


Fig 4.3 Tagging Pho4 in wild-type *C.albicans* does not affect protein functionality (A) Exponentially growing wild-type cells expressing Pho4-MH or Pho-GFP were diluted and spotted in serial dilutions onto YPD agar plates containing 300 μ M menadione or 1M NaCl. Plates were incubated for 24 h at 30°C (B) Confirmation of Pho4 myc His tag in wild-type cells. Samples of exponentially growing wild-type cells and wild-type cells expressing Pho4 - MH grown in YPD were harvested. Protein was extracted and subjected to non-reducing SDS - PAGE and Western blotting using anti-Myc antibody.

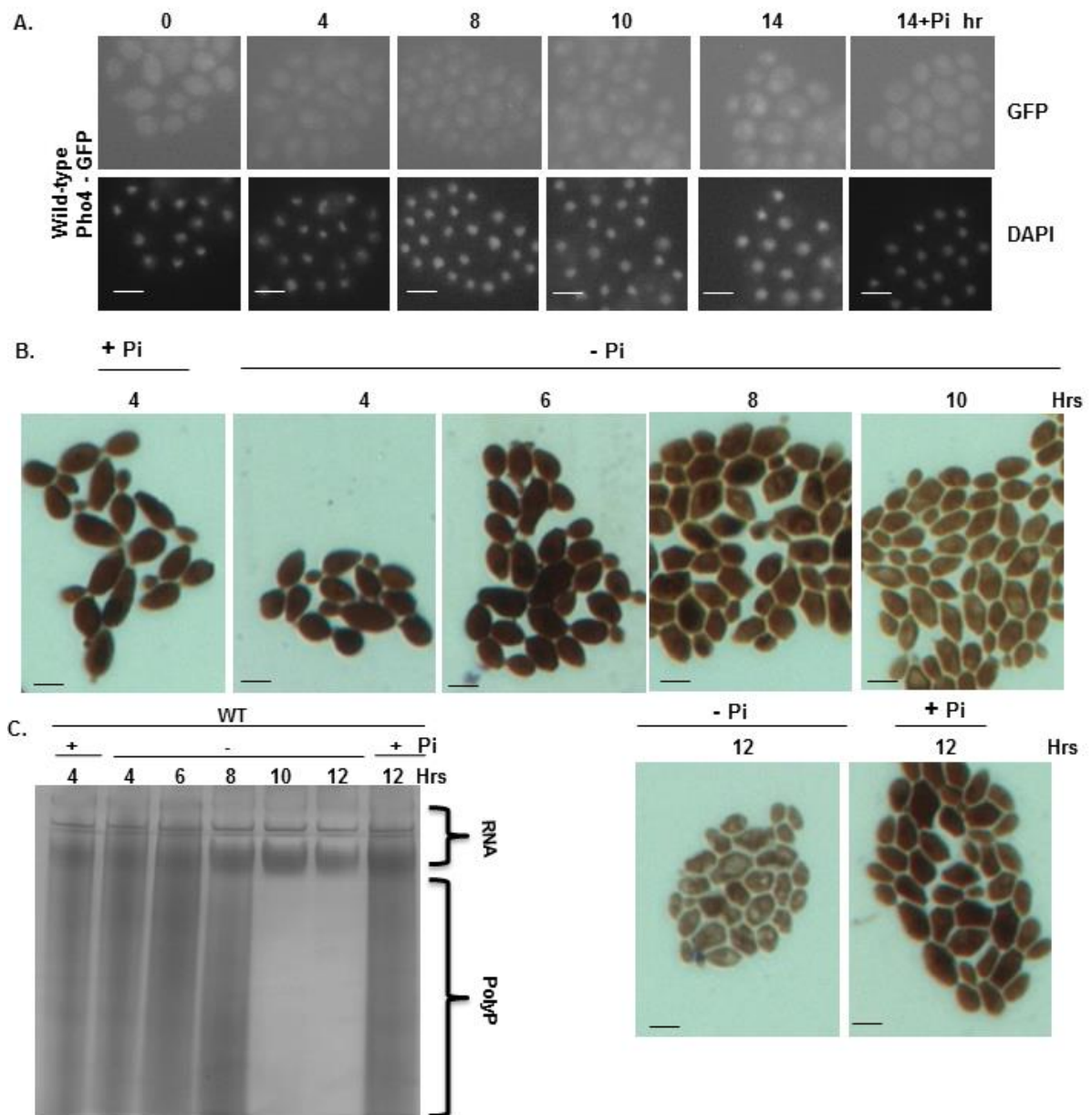


Fig. 4.4 Pho4 nuclear accumulation and polyP mobilisation (A) Pho4 accumulates in the nucleus under phosphate limiting conditions. Under phosphate-limiting conditions Pho4 accumulates in the nucleus. Cells expressing Pho4 - GFP were transferred to YPD minus phosphate medium, and localisation was determined by fluorescence microscopy over a 14 h time course. + Pi indicates the localisation of Pho4 on phosphate addition to the 14h - Pi sample. DAPI staining indicates nuclear position **(B) PolyP is mobilised during phosphate limitation.** The kinetics of polyP mobilisation during growth in phosphate-limiting conditions was monitored by Neisser staining. Exponentially-growing wild-type and mutant strains were fixed by paraformaldehyde and stained by Neisser staining **(C) PolyP mobilisation was also monitored on a toluidine blue stained UREA-PAGE gel.** 20 μ g of total RNA/polyP extracted from wild-type cells at the indicated time points was loaded onto a 12% UREA-PAGE gel. This experiment was repeated at least twice, representative images and gel are shown. Scale bar 10 μ m.

4.2.5 Nuclear export of Pho4 is regulated by phosphorylation and an additional PTM in phosphate-rich conditions.

In *S. cerevisiae*, phosphate limitation triggers the inhibitory action of Pho81 on Pho80-Pho85 CDK complex thereby preventing phosphorylation of Pho4 and allowing nuclear accumulation. As the regulatory phosphorylation sites are not conserved in CaPho4, the regulatory mechanism involved was explored next. Prior to this, successful tagging as well as effect of tagging on protein functionality was validated. The Pho4 protein was detected in the wild-type 2myc 6His tagged strain (Pho4-MH) and not in the untagged strain (Fig 4.3B). In addition, tagging Pho4 at the C-terminus with 2myc 6His does not affect Pho4 function as *pho4Δ/PHO4-MH* cells in which the single remaining copy of Pho4 has been tagged have the same stress resistant phenotypes as wild-type cells (Fig 4.3A). To determine how Pho4 is modified in *C. albicans* in response to phosphate levels, the mobility of Pho4 extracted from *C. albicans* Pho4-MH wild-type cells grown in minus phosphate and plus phosphate was monitored on SDS-PAGE. As shown in Fig 4.5B, Pho4-MH ran with a reduced mobility following the addition of phosphate to the growth medium, compared with the mobility of Pho4-MH under phosphate starvation conditions. To explore whether this reduced mobility was due to the increased phosphorylation of Pho4 under phosphate replete conditions, samples were treated with lambda phosphatase prior to gel electrophoresis. Intriguingly, the mobility of Pho4 was increased following lambda phosphatase treatment, both under phosphate replete and starvation conditions. This indicates that Pho4 in *C. albicans* is phosphorylated irrespective of external phosphate concentrations. This seemingly contrasts with Pho4 regulation in *S. cerevisiae* in which the lack of phosphorylation of Pho4 following phosphate starvation triggers its nuclear accumulation (Kaffman *et al.*, 1994). Strikingly, the slower mobility of Pho4 observed in *C. albicans* under phosphate replete conditions is resistant to phosphatase treatment, which suggests that Pho4 may be subject to a different modification in this fungal pathogen. Due to time constraints this extra PTM has not yet been identified. Taken together, these data indicate that Pho4 is phosphorylated during growth in phosphate-rich as well as phosphate-deplete conditions. During growth in phosphate-limiting conditions, Pho4 accumulates in the nucleus and following phosphate addition is exported out of the nucleus by two regulatory modifications.

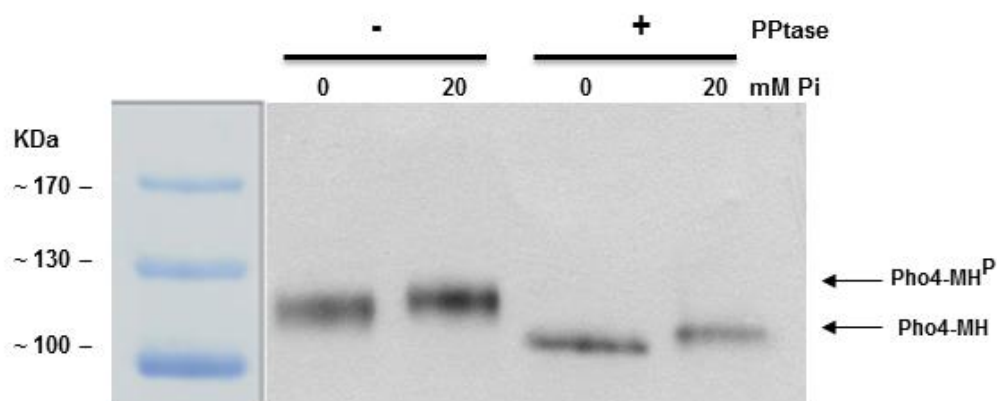


Fig 4.5 Tagging Pho4 in wild-type *C.albicans* does not affect protein functionality (A) Exponentially growing wild-type cells expressing Pho4-MH or Pho-GFP were diluted and spotted in serial dilutions onto YPD agar plates containing 300 μ M menadione or 1M NaCl. Plates were incubated for 24 hrs at 30°C (B) Confirmation of Pho4 myc His tag in wild-type cells. Samples of exponentially growing wild-type cells and wild-type cells expressing Pho4-MH grown in YPD were harvested. Protein was extracted and subjected to non-reducing SDS-PAGE and Western blotting using anti-Myc antibody.

4.2.6 Genome-wide analysis to identify genes required for phosphate homeostasis in *C. albicans*.

To identify Pho4 targets, RNA seq analysis was performed to generate genome-wide transcriptional profiles of *C. albicans* wild-type and *pho4* Δ cells grown in phosphate-depleted and phosphate-replete conditions. Cells were starved of phosphate for 16 hrs and harvested, following which phosphate (10 mM) was added to the phosphate starved cells and samples harvested 2 hrs later. Fluorescent microscopy had confirmed that Pho4 is in the nucleus under these minus phosphate conditions and out following phosphate addition (Fig 4.6A). Under these conditions genes whose expressions change depending on phosphate level and Pho4 dependent were identified. Three independent experiments were performed for each condition. Bioinformatics analysis of the data generated by RNA seq analysis was done by Stavroula Kastora, Aberdeen fungal group, Aberdeen University. The complete data set is presented in Appendix 2.

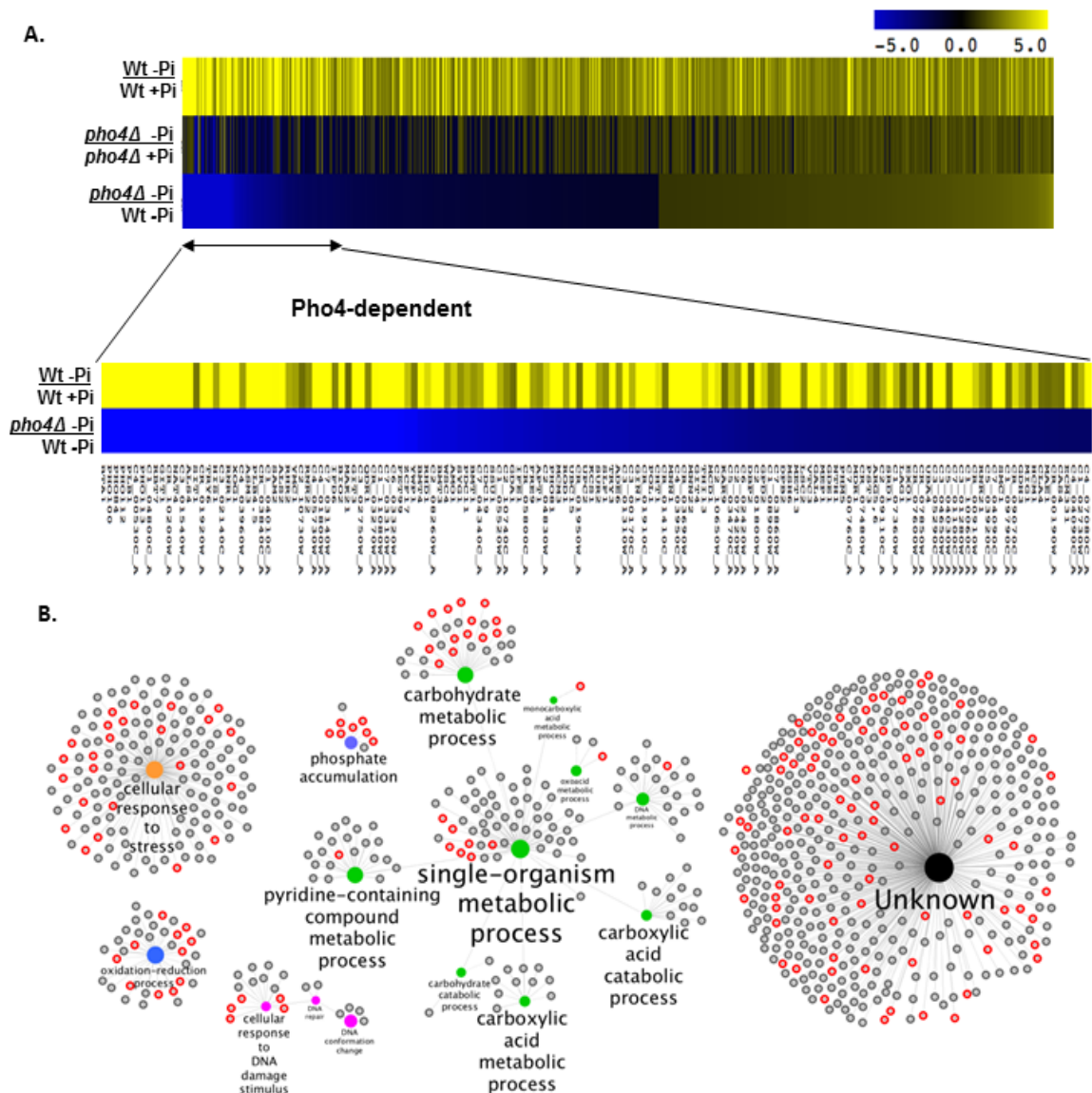


Fig 4.6. Genome response to phosphate limitation in *C. albicans*. (A). Heat map showing the fold induction of genes induced (>2 fold) in wild-type cells following phosphate limitation (top column), and the fold-expression of these genes in *pho4Δ* cells (middle column), as measured by RNA seq analysis. Of the 822 genes significantly induced in wild-type cells, 150 genes displayed a decrease of 2 fold or lower in *pho4Δ* cells upon comparing the expression ratio *pho4Δ* -Pi/Wt -Pi (lower column). These are designated as Pho4-dependent genes. (B). Cytoscape network illustrating all 822 upregulated genes in wild-type cells following phosphate limitation. Those that display Pho4-dependency are shown in red. GO term family members are represented in the same colour while the size of each node representing each GO term corresponds to its gene enrichment level. Genes that were mapped according to CGD as “Biological process unknown” are clustered in the category “Unknown”.

A heat map showing the fold induction of genes that display significant increase in gene expression following Pi limitation in wild-type cells (2 fold or more), and their fold induction in *pho4Δ* cells, is shown in Fig 4.6A. Genes which displayed a decrease of -2 fold or lower in *pho4Δ* cells compared to wild-type cells were classified as Pho4-dependent targets. From this analysis, 822 genes were found to

be significantly upregulated in wild-type cells in minus Pi compared to plus Pi conditions, and of these 150 displayed Pho4 dependency for their induction (Appendix 2). A cytoscape network of all genes induced under phosphate-limiting, illustrating both the significantly enriched functional categories (GO terms) and the contribution of Pho4 is shown in Fig 4.6B. Genes in the functional categories of response to single organism, metabolic processes, cellular response to stress, oxidation/reduction processes, cellular response to DNA damage stimulus, and phosphate accumulation, were significantly enriched in the gene pool that was upregulated in wild-type cells following phosphate limitation (Fig. 4.7). Pho4 contributes to several of these functional categories upregulated in wild-type cells following Pi limitation including phosphate accumulation, oxidation-reduction processes, and cellular response to stress (Fig. 4.7).

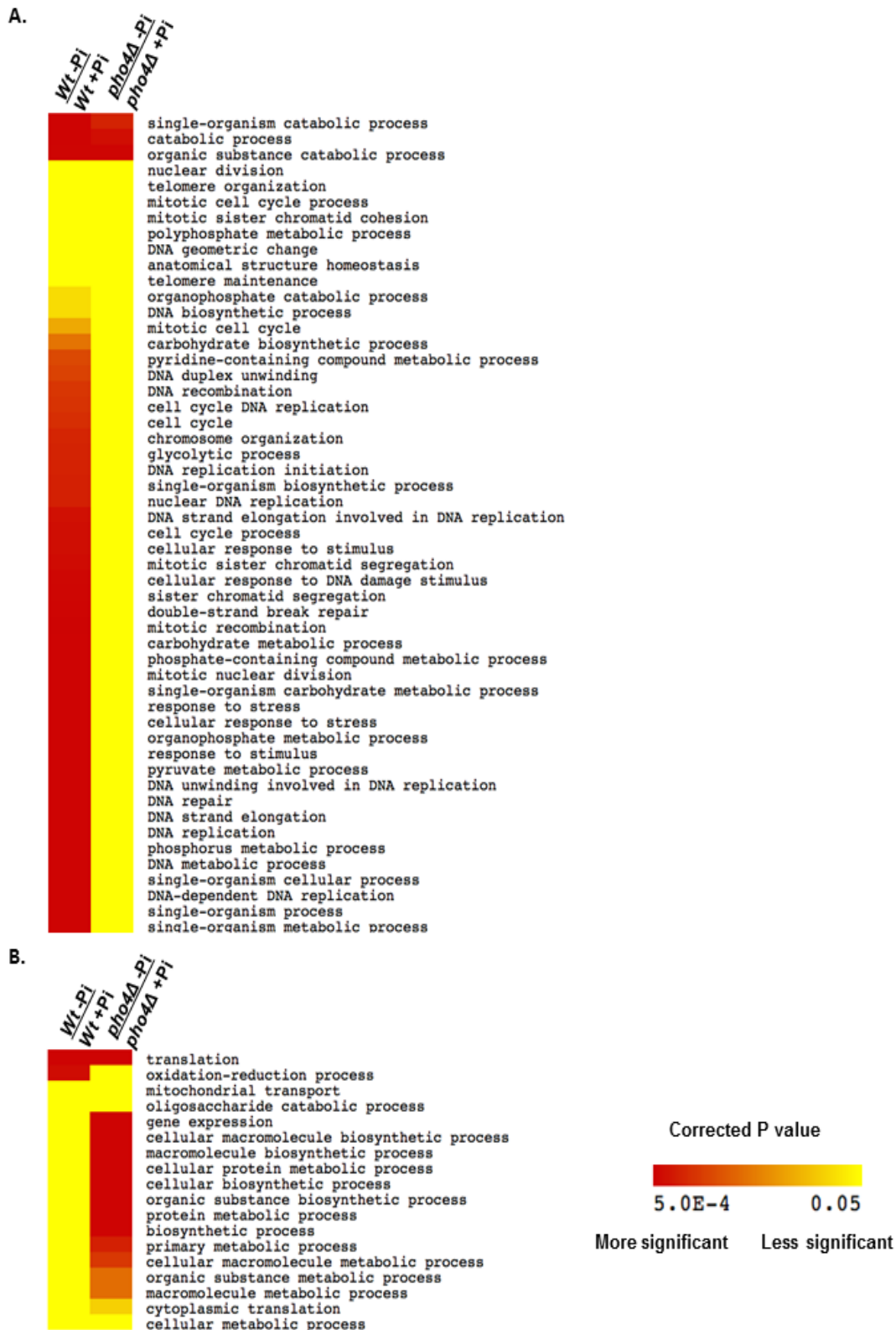


Fig 4.7. Heatmap of GO Biological processes upregulated (A) or downregulated (B) in wild-type cells following phosphate limitation, and their behaviour in *pho4Δ* cells.

A closer look at the genes predicted to have roles in phosphate acquisition and storage revealed that Pho4 was required for the expression of the high affinity phosphate transporter *PHO84*, several acid phosphatase genes *PHO100*, *PHO112*

and *PHO113*, and the *VTC1* and *VTC3* genes. The Pho4-dependency of *PHO84* and *PHO100* expressions was confirmed by Northern blotting (Fig. 4.9) and supports the role of Pho4 in phosphate sensing, accumulation, and storage (Fig 4.2; Fig 4.4). As previously reported, Pho4 was also seen to be required for the induction of genes encoding glycerophosphodiester transporters, *GIT1 – 3*, as well as that of a glycerophosphocholine phosphodiesterase, *GDE1* (Bishop *et al.*, 2013; Bishop *et al.*, 2011). These proteins enable *C. albicans* use glycerophosphodiester generated from phospholipids as a source of phosphate (Bishop *et al.*, 2011). Consistent with this finding was the up-regulation of phospholipases required to generate glycerophosphodiester from phospholipids (Appendix 2).

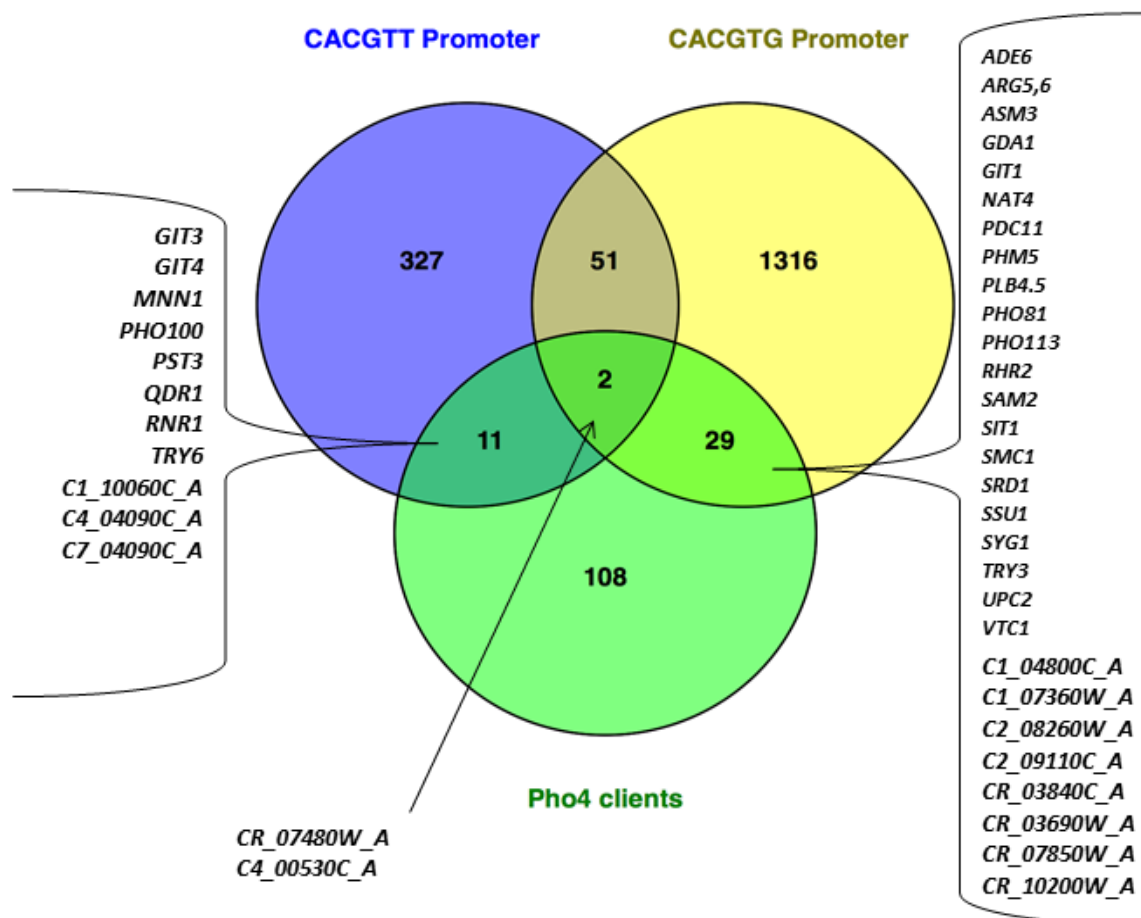


Fig 4.8. *C. albicans* genes containing promoter ScPho4 consensus binding site(s). The identification of genes containing consensus binding sites CACGTG/CACGTT within promoter regions was performed using CGD PatMatch (ORF, DNA, genomic sequences, plus 1000bp up- and downstream; DNA-A22). No mismatch was allowed and search limited to ~ 500bp upstream of each gene.

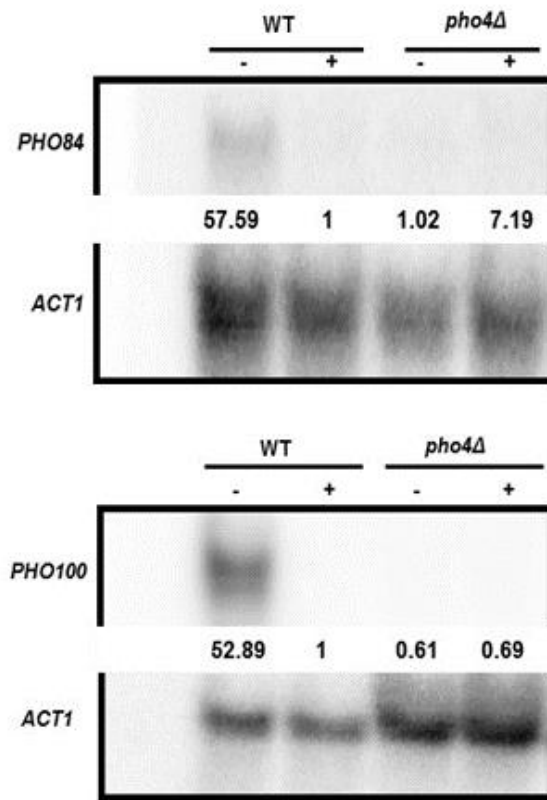


Fig. 4.9. Pho4 targets genes in *C. albicans*. Validation of gene expression profiles observed in RNA-Seq analysis. Northern blot analysis of RNA isolated from wild-type and *pho4Δ* cells using the same – Pi and + Pi conditions used for RNA-Seq experiments. Blots were analysed with probes specific for the indicated genes, with *ACT1* as a loading control. Fold induction compared to Wt cells + Pi is shown.

4.2.7 Comparison of the transcriptional responses to phosphate limitation between *C. albicans* and *S. cerevisiae*.

The Pho4-dependent genes identified from the RNA-seq analysis performed in this study were compared to that previously identified in *S. cerevisiae*. Using microarray analysis, 81 genes were identified as significantly induced following phosphate starvation in *S. cerevisiae*, of these 26 were Pho4-dependent (Zhou and O`Shea, 2011). Therefore, more genes were identified as being upregulated under phosphate-limiting conditions (822), of which 150 are Pho4-dependent compared to RNA-seq used in this study identified a lot more genes (822) with 150 Pho4 dependent compared to *S. cerevisiae*. However, this difference in number of genes identified could be accounted for by the different gene profiling methods, as well as the different minus-phosphate growth conditions, used by both studies. Nonetheless, the data obtained from this study was cross-referenced with the Candida Genome Database (CGD) and revealed that 20 of the Pho4 regulated genes in *S. cerevisiae* have orthologues in *C. albicans* with 10 dependent on Pho4 for activation under

phosphate limiting conditions. These include the high-affinity transporter *PHO84*, the acid phosphatases *PHO112* and *PHO113*, the polyP synthase components *VTC1* and *VTC3* as well as *GIT3* and *GDE3* involved in glycerophosphodiester utilisation as phosphate source. The gene coding for the CDK complex inhibitor *PHO81*, which enables Pho4 nuclear accumulation in *S. cerevisiae* in response to phosphate limitation, was also identified. Also suggestive of a link between phosphate and iron homeostasis was the identification of a transporter of ferrichrome siderophores, *SIT1/ARN4* involved in iron homeostasis which was found up-regulated under phosphate limitation in a Pho4 dependent manner in both *C. albicans* and *S. cerevisiae*.

To identify putative direct targets of Pho4, a systematic promoter (500bp upstream) analysis of each gene was performed by searching for the core DNA-binding motifs of Pho4 in *S. cerevisiae*, CACGTG and CACGTT, against *C. albicans* phosphate genes without mismatch allowance (Fig 4.8). Forty-two of the Pho4-dependent genes contained a binding motif, and several of these have been validated as Pho4 targets including *PHO100* (Fig 4.8) and the *GIT* genes (Bishop *et al.*, 2013). Some Pho4-dependent genes however, did not have either of the Pho4 binding motifs, for example *PHO84*, suggesting additional factors dictate Pho4-dependency for activation other than presence of the DNA-binding motif in the promoter of the gene.

4.2.8 Stress resistance is not associated with defective acid phosphatase activity.

Gene profiling analysis however, does not explain the Pho4-dependent stress phenotypes identified from the QFA screen so we wondered if acid phosphatase activity was important for stress resistance. To identify *C. albicans* mutants with defective acid phosphatase activity, the *C. albicans* deletion libraries were screened under phosphate-rich and phosphate-deplete conditions. Cells were grown to exponential phase in 96 well plates without shaking and then spot inoculated onto solid agar plates using a 96-pin tool. After overnight growth at 30°C, the agar plates were overlaid with soft agar containing phosphate substrate and dye. Experiment was performed alongside a wild-type *C. albicans* strain as positive control and the *pho4* mutant as the negative control. Screen identified 9 mutant strains with no detectable phosphatase activity and 15 with a partial defect (Fig 4.10A; Table 4.1). Positive strains were confirmed by a more quantitative method where optical densities (OD) of exponentially-grown cells were measured and adjusted to OD₆₆₀ ~

0.5 and 10- fold serial dilutions carried out (Fig 4.10B). Of the 24 acid phosphatase defective mutants identified, only the *pho100* mutant is Pho4-dependent (Fig 4.10A; Table 4.1). Interestingly, several of the mutant strains with defect in phosphatase activity appear to be under the control of the iron-response regulator, the transcription factor Hap43, strongly suggesting phosphate limitation has an impact on iron availability (Table 4.1). Perturbations in phosphate homeostasis in yeast has been shown to create iron starvation response supporting the above finding (Rosenfeld *et al.*, 2010). In conclusion, the screen performed supports the role of Pho100 as an acid phosphatase required for phosphate scavenging and also supports a link exists between phosphate and iron homeostasis.

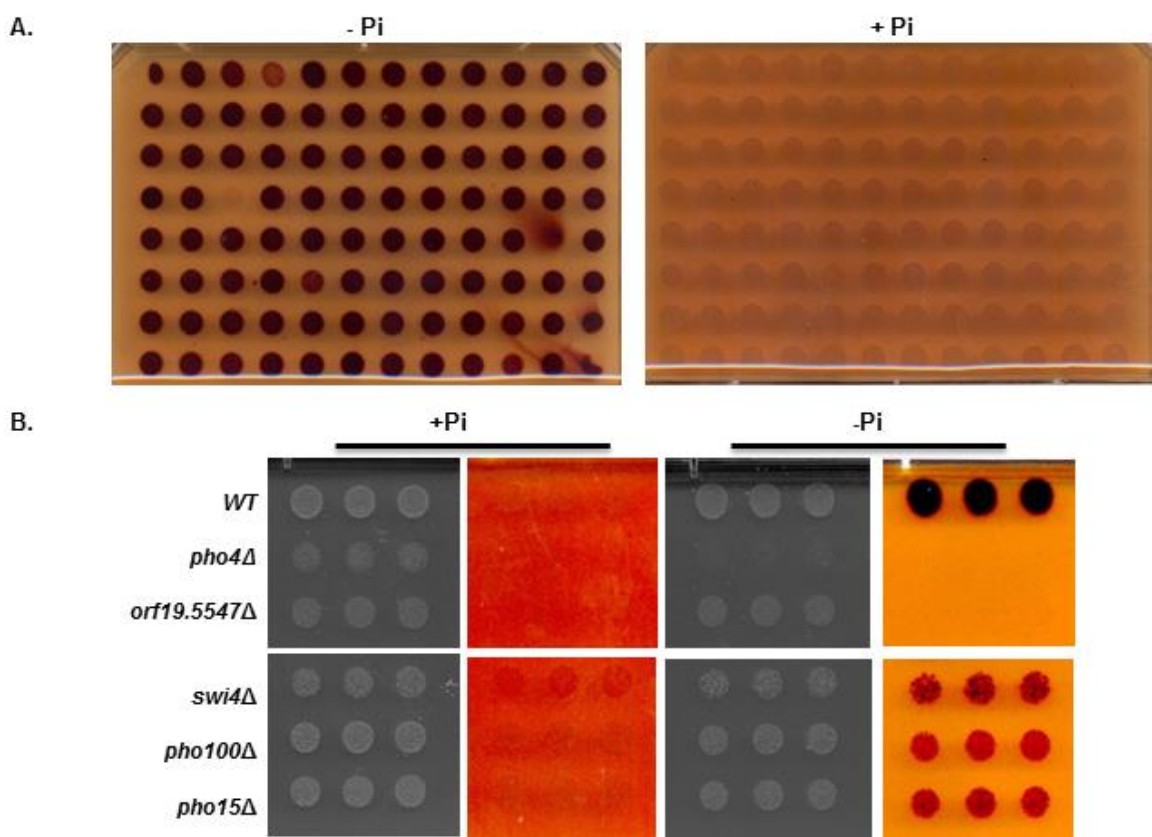


Fig. 4.10. Identification of genes with defective secreted acid phosphatase activity. Colorimetric plate phosphatase screen of *C. albicans* deletion libraries. Dark colour indicates phosphatase activity (A) Examples of scanned images of phosphatase plate assay demonstrating secreted acid phosphatase activity. Same method as Fig 4.2A (B) Quantitative validation of phosphatase activity defects. 2×10^3 cells, and 10-fold dilutions thereof, of exponentially-growing wild-type and mutant strains were spotted onto agar plates, with or without Pi. Plates were incubated at 30°C for 24 h following which colonies were overlaid with p-nitrophenylphosphate and fast blue salt B and incubated at 30°C for 30 mins.

Defective acid phosphatase activity	Partial acid phosphatase activity
<i>PHO4</i> - bHLH transcription factor of the myc-family; required for growth in medium lacking phosphate and for resistance to copper and Phloxine B; induced by Mnl1 under weak acid stress	<i>FPG1</i> - Formamidopyrimidine DNA glycosylase, involved in repair of gamma-irradiated DNA; <u>Hap43p-repressed gene</u>
<i>DAL81</i> - Zn(II)2Cys6 transcription factor; ortholog of <i>S. cerevisiae</i> Dal81, involved in the regulation of nitrogen-degradation genes	<i>ORF19.2838</i> - Protein of unknown function; mutation confers hypersensitivity to amphotericin B; flow model biofilm induced
<i>ORF19.287</i> - Putative NADH-ubiquinone oxidoreductase subunit; <u>Hap43p-repressed gene</u> ; repressed by nitric oxide	<i>ORF19.2850</i> - Protein of unknown function; induced by nitric oxide independent of Yhb1p
<i>ORF19.1625</i> - Putative ubiquinone oxidoreductase; repressed by nitric oxide; <u>Hap43p-repressed</u>	<i>SWI4</i> - Putative component of the SBF transcription complex involved in G1/S cell-cycle progression
<i>ORF19.1710</i> - Putative NADH-ubiquinone oxidoreductase; in detergent-resistant membrane fraction (possible lipid raft component); predicted N-terminal acetylation	<i>PHO100</i> - Putative inducible acid phosphatase; DTT-extractable and observed in culture supernatant in low-phosphate conditions; slight effect on murine virulence
<i>PWP1</i> - Putative rRNA processing protein; <u>Hap43-induced</u> ; repressed in core stress response	<i>PHO15</i> - 4-nitrophenyl phosphatase, possible histone H2A phosphatase; involved in regulation of white-opaque switch; hyphal repressed; induced in core stress response; induced by cadmium stress via Hog1
<i>MCI4</i> - Putative NADH-ubiquinone dehydrogenase; <u>Hap43p-repressed gene</u>	<i>ORF19.2500</i> - Has domain(s) with predicted transferase activity
<i>ORF19.4758</i> - Putative reductase or dehydrogenase; <u>Hap43-repressed gene</u> ; alkaline repressed	<i>ORF19.7590</i> - Putative NADH-ubiquinone oxidoreductase; identified in detergent-resistant membrane fraction
<i>ORF19.5547</i> - Protein of unknown function; <u>Hap43-repressed gene</u>	<i>GIN4</i> - Autophosphorylated kinase; role in pseudohyphal-hyphal switch and cytokinesis
	<i>ORF19.3029</i> - Predicted 3-hydroxyisobutyryl-CoA hydrolase; mitochondrially localized
	<i>CCN1</i> - G1 cyclin; required for hyphal growth maintenance (not initiation); cell-cycle regulated transcription (G1/S); Cdc28p-

	Ccn1p initiates Cdc11p S394 phosphorylation on hyphal induction
	SAP5 - Secreted aspartyl proteinase; sap4,5,6 triple null defective in utilization of protein as N source; virulence role effected by URA3; expressed during infection
	COX4 - Putative cytochrome c oxidase subunit IV; Mig1-regulated; macrophage/pseudohyphal-induced gene; macrophage-induced protein; repressed by nitric oxide; 5'-UTR intron; <u>Hap43-repressed</u>
	ASG1 - Gal4p family zinc-finger transcription factor with similarity to <i>S. cerevisiae</i> Asg1p
	ORF19.6607 - Ortholog(s) have role in mitochondrial respiratory chain complex I assembly

Table 4.1 *C. albicans* strains with defective acid phosphatase activity.

4.3 Discussion

While the response to phosphate limitation has been extensively characterised in the model yeast, *S. cerevisiae*, very little is known about phosphate response in the fungal pathogen, *C. albicans*. This part of the study established the role of CaPho4 in phosphate homeostasis and found similarities as well as deviations in the regulatory mechanism of Pho4 between *S. cerevisiae* and *C. albicans*.

The first deviation identified was in the sequence of CaPho4 which was found to diverge significantly from that of ScPho4. More significant was the observation that most of the phosphorylation sites of ScPho4, which regulates cellular localisation and DNA binding, are not conserved in CaPho4 (Fig 4.1). ScPho4 sequence has five Serine-Proline (SP1 to SP4 and SP6) sites phosphorylated by the CDK complex Pho80-Pho85 (O'Neill *et al.*, 1996). Each site plays a distinct role in the regulation of Pho4 activity. Phosphorylation at SP2 and SP3 ensures Pho4 nuclear export while phosphorylation at SP4 promotes its import, and interaction with Pho2, the co-transcription factor, during phosphate-rich growth is prevented by phosphorylation at SP6 (Komeili and O'Shea, 1999). In addition, it was noted that some of the Pho4-dependent genes did not have either of the Pho4 binding motifs, for example *PHO84*,

suggesting additional factors dictate Pho4-dependency for activation other than the presence of the DNA-binding motif in the promoter of the gene. In *S. cerevisiae*, Pho4 transcriptional specificity for PHO genes is regulated at the promoter level by the presence of nucleosomes and another transcription factor that recognises the same binding motif as Pho4 (Zhou and O`Shea, 2011). During growth in phosphate-rich environment, nucleosomes prevent Pho4 binding and at sites where there are no nucleosomes Cbf1, which is more abundantly present as phosphorylated Pho4 would be exported out of the nucleus, outcompetes Pho4 for these nucleosome-free sites (Zhou and O`Shea, 2011). During low-phosphate nuclear levels of unphosphorylated Pho4 increase so Pho4 can now outcompete Cbf1 (Zhou and O`Shea, 2011). This ensures Pho4 only binds to PHO genes and only during phosphate-limiting conditions.

Based on the sequence divergence observed, the regulation and localisation of CaPho4 in wild-type cells in response to phosphate concentration was then examined. In a manner similar to that of ScPho4, the Pho81 CDK inhibitor, necessary for Pho4 activation in *S. cerevisiae*, is also induced in *C. albicans* under phosphate-limiting conditions which indicates this part of the regulatory mechanism is conserved. In addition, under phosphate-limiting conditions, CaPho4 was found to accumulate in the nucleus (Fig 4.4A). An orthologue of Pho80 (C6_03810W_B), the cyclin-dependent protein kinase has been identified in *C. albicans* but its role in regulating Pho4 has not been validated. CaPho85 however, has been shown to complement a *pho85Δ* in *S. cerevisiae* suggesting the function of this protein kinase may be conserved in *C. albicans* (Miyakawa, 2000). The next objective then was to examine if CaPho4 activity during growth in minus or plus phosphate was also regulated by phosphorylation. In contrast to ScPho4, CaPho4 is phosphorylated under both phosphate replete and deplete conditions however, if phosphorylated sites change in response to phosphate concentrations could not be determined (Fig 4.5). On the other hand, it was discovered that an additional post translational modification appears to regulate CaPho4 (Fig 4.5D). This extra PTM requires further investigation. Pho4 may be modified by ubiquitin-like modifier such as SUMO as sumoylation of certain transcription factors, for example Tec1 required for invasive growth in yeast cells (Wang *et al.*, 2009) has been shown to regulate nuclear localisation.

While in the nucleus, Pho4 activates the expression of key genes for example, secreted acid phosphatases. In *S. cerevisiae*, the expression of an acid phosphatase, *PHO5* which is Pho4-dependent, increases during growth in phosphate-limiting conditions in *S. cerevisiae* (Kaffman *et al.*, 1994). Phosphate scavenging is facilitated by the action of secreted acid phosphatases which hydrolyse phosphate-containing compounds to release phosphate. Acid and alkaline phosphatase activities were first demonstrated in clinical isolates of *C. albicans* and reported to be low or delayed however, a recent study confirmed phosphate starvation triggers a robust induction of phosphatase activity (Chattaway *et al.*, 1971; Smith *et al.*, 1973; Romanowski *et al.*, 2012). This robust response was found to be CaPho4 dependent. The role of Pho4 and phosphatase activity in response to phosphate limitation is further corroborated by findings from this study. No acid phosphatase activity was detected in cells lacking *PHO4* under phosphate-limiting conditions (Fig 4.2A). RNA-seq experiments also revealed that under phosphate starvation cells respond by massive induction of various phosphatases including acid phosphatases, phospholipases, and glycerophosphocholine phosphodiesterases (Appendix 2; Fig 4.9). In *S. cerevisiae*, deleting *PHO84* results in growth defects under low-phosphate conditions, little polyP synthesis as well as the constitutive expression of PHO response genes (Wykoff *et al.*, 2007). Another key protein up-regulated during phosphate limitation as identified by the RNA-seq analysis, in *C. albicans* was the high-affinity phosphate transporter, Pho84.

PolyP functions mainly as a phosphate reservoir in virtually all living cells with around 99% of the polymer found in the vacuole (Kornberg, 1999). The remaining fraction of polyP is found in the nucleus, cytoplasm, mitochondria, and cell wall (Secco *et al.*, 2012). The proteins involved in synthesising polyP have been identified in yeast. Deleting the genes that encode for these proteins completely abolishes polyP synthesis (Ogawa *et al.*, 2000). Genes required for polyP synthesis as well as mobilisation during growth in phosphate-limiting conditions are under the regulation of ScPho4 (Ault-Riche *et al.*, 1998; Oshima, 1997; Ogawa *et al.*, 2000). In most living cells, phosphate availability is ensured by the mobilisation of internal polyP stores during growth under conditions of limiting external phosphate. In this study this mechanism was found to be conserved in *C. albicans* (Fig 4.4A; Fig 4.4B).

Collectively these data strongly indicate the role of Pho4 in regulating the response to phosphate limitation is conserved in *C. albicans*. Therefore in *C. albicans*, Pho4 plays

a crucial role in the acquisition and storage of phosphate essential for various cellular processes and growth. During growth in phosphate-rich conditions, Pho4 is phosphorylated, possibly by the conserved Pho85-Pho80 protein kinases, and dispersed throughout the cell. Following phosphate depletion, Pho81 inhibits further phosphorylation of Pho4 thereby triggering its nuclear accumulation. In the nucleus, Pho4 activates the expression of genes involved in phosphate acquisition which include the acid phosphatases, *PHO100*, *PHO112*, and *PHO113*, the high-affinity phosphate transporter, *PHO84* and genes involved in polyP hydrolysis, *VTC1*, *VTC3*, *VTC4*, and *PHM5*. Also activated are the *GIT* genes, *GIT3* and *GDE3*, to enable phosphate acquisition from glycerophosphodiester. During phosphate uptake, genes involved in polyP synthesis, for example *VTC1*, are activated to synthesise polyP from phosphate to replenish depleted polyP stores in the vacuole.

Having established the role of Pho4 in phosphate homeostasis, the next aim of the project was to analyse whether this role of Pho4 was extended to mediating pleiotropic stress resistance in *C. albicans*.

Chapter 5: The role of Pho4 in stress adaptation

5.1. Introduction

Although *C. albicans* is known to successfully adapt to the diverse environments encountered in the host there is still much to be learnt about the mechanisms employed in stress adaptation. Following phagocytosis, microorganisms are exposed to high levels of the potent superoxide anions generated by the NADPH oxidase system (Reeves *et al.*, 2002). In addition, the resulting accumulation of anionic charge is compensated for by an influx of potassium ions into the phagosome thereby creating cationic stress on the engulfed organism (Reeves *et al.*, 2002). The phagosome is acidic to enable the hydrolytic activities of lysosomes however, microbes will experience fluctuations in pH particularly at the onset of phagocytosis (Segal *et al.*, 1981; Segal, 1985). Very little is known about the regulators required for resistance to these phagocyte-imposed stresses in *C. albicans*. Capturing the *C. albicans* transcriptome following phagocytosis also revealed that the phagosome is a nutrient-limited environment, deficient in both carbohydrates and nitrogen which are both required for growth. To counter this during phagocytosis, *C. albicans* induces the expression of genes encoding proteins that allow the utilisation of alternative carbon sources such as enzymes of glyoxylate cycle, gluconeogenesis, and β -oxidation of fatty acids, and represses genes encoding enzymes involved in protein synthesis and glycolysis (Lorenz *et al.*, 2004). Nutritional immunity by the host is also extended to metals, lack of which impacts on the pathogen's ability to adapt to stress and cause infection. However, nutrient availability within the diverse host niches during infection has not been clearly defined. For example, aside from studies showing that the inactivation of iron acquisition mechanisms in *C. albicans* leads to attenuated virulence (Almeida *et al.*, 2009), little is known about how the host limits iron availability.

The QFA screen of *C. albicans* mutants deleted of transcriptional regulators performed in this study identified the Pho4 transcription factor as essential for resisting menadione-induced superoxide, NaCl-induced cationic, and alkaline pH stress resistance in *C. albicans*. In *S. cerevisiae*, Pho4 is essential for phosphate acquisition and storage as polyP and apart from alkaline pH stress has never been implicated in superoxide and cationic stress resistance. The role of Pho4 in

phosphate homeostasis in *C. albicans* was initially investigated in Chapter 4 and similar to that of *S. cerevisiae* shown to regulate phosphate homeostasis. Therefore, the additional roles Pho4 plays in *C. albicans* were then investigated to determine the molecular mechanisms of stress resistance.

5.2 Results

5.2.1 Cells lacking *PHO4* display other pleiotropic stress phenotypes.

As Pho4 was required for resistance to the seemingly distinct stresses imposed by menadione, cationic stress and alkaline pH stress (Fig 5.1A), an extensive phenotypic analysis of the *pho4* mutant was carried out to identify any other additional stress-protective roles in *C. albicans*. Interestingly, cells lacking *PHO4* are specifically sensitive to cationic stress and not osmotic stress as these were not more sensitive to sorbitol (Fig 5.1B). Similarly, *pho4Δ* cells were as resistant to hydrogen peroxide as wildtype cells, indicating a specific role of Pho4 in superoxide stress resistance (Fig 5.1B). However, additional requirements for Pho4 in *C. albicans* were identified. Consistent with the role of Pho4 in cationic stress protection, *pho4Δ* cells were also sensitive to organic cations, such as the polyamine spermidine, and also to a range of different metal cations including calcium, iron, manganese and as reported recently (Urralde *et al*, 2015) to the heavy metalloid arsenite (Fig 5.1A). Cells lacking *PHO4* were also resistant to copper, as reported previously (Homann *et al.*, 2009), and also to the cell wall perturbing agent Calcoflour white indicating that *pho4Δ* cells may have cell wall defects (Fig 5.1A). Finally, also noted was that cells lacking *PHO4* were notably sensitive to media containing serum (Fig 5.1A), and possibly as a consequence of this, serum-induced filamentation was significantly delayed (Fig 5.1D). Most importantly, these stress phenotypes of *pho4Δ* cells are reversed by the addition of a copy of *PHO4* back into the mutant strain (Fig 5.1A). Taken together, such phenotypic profiling in *C. albicans*, has revealed a number of environmental conditions that require Pho4-mediated responses.

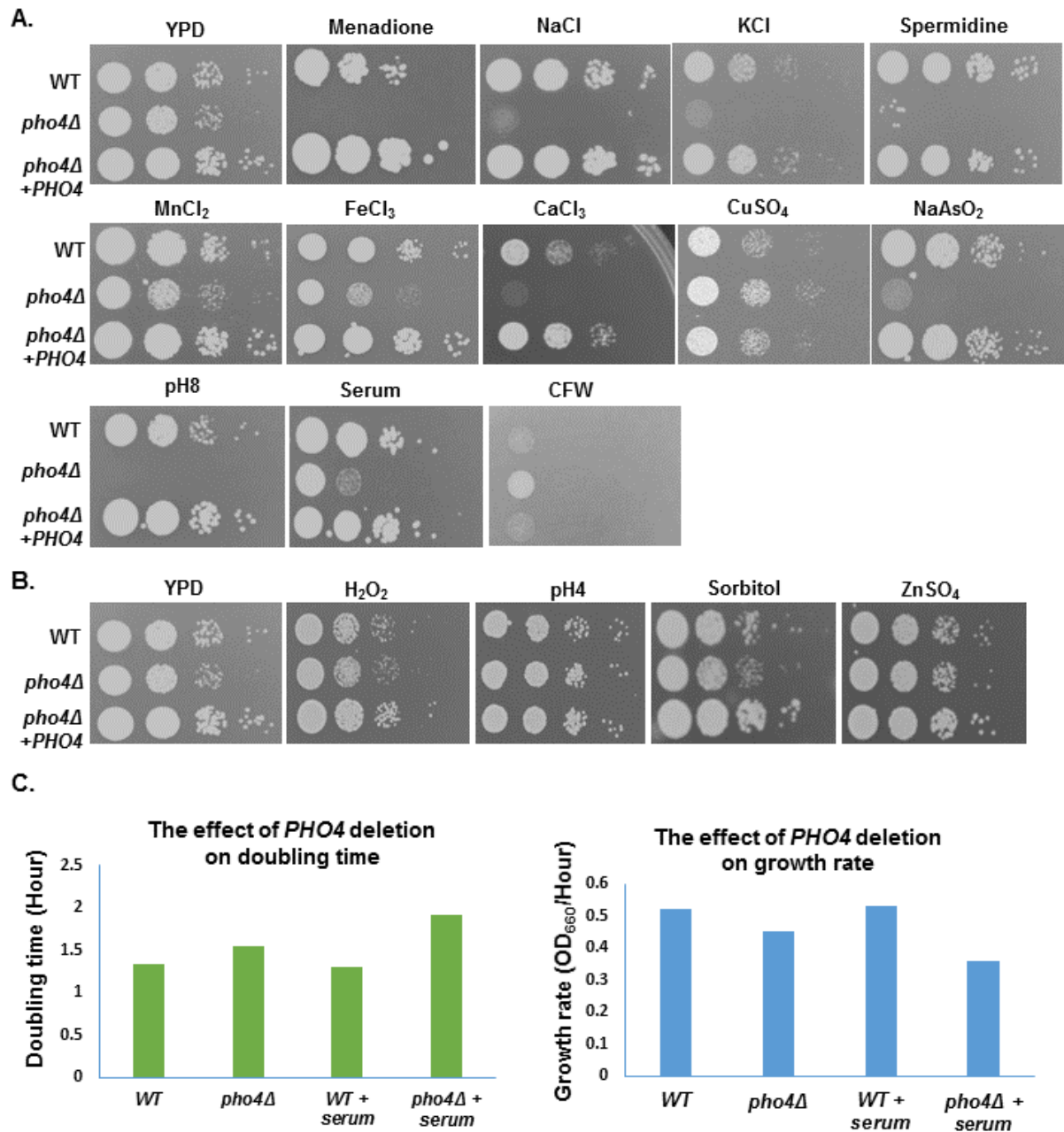


Fig 5.1 Cells lacking *PHO4* display pleiotropic stress phenotypes (A). Exponentially growing strains were spotted in serial dilutions onto YPD plates containing 1 M NaCl, 0.6 M KCl, 300 μ M menadione, 0.32 μ g/ml spermidine, 5 mM MnCl₂, 5 mM FeCl₂, 450 mM CaCl₂, 2 mM NaAsO₂, 5 mM CuSO₄, 30 μ g/ml Calcoflour white, 20% fetal bovine serum. For pH 8 media, the pH of YPD was adjusted using 1M Tris-HCl (pH 8.25). Plates were incubated for 24 hrs at 30°C. **(B)** Stress resistance not impaired by Pho4 loss. Exponentially growing strains were spotted in serial dilutions onto YPD plates and YPD plates containing 5 mM H₂O₂, 1.2 M Sorbitol, 3 mM ZnSO₄, or on YPD plates adjusted to pH 4 by the addition of succinic acid. Plates were incubated for 24 hrs at 30°C.

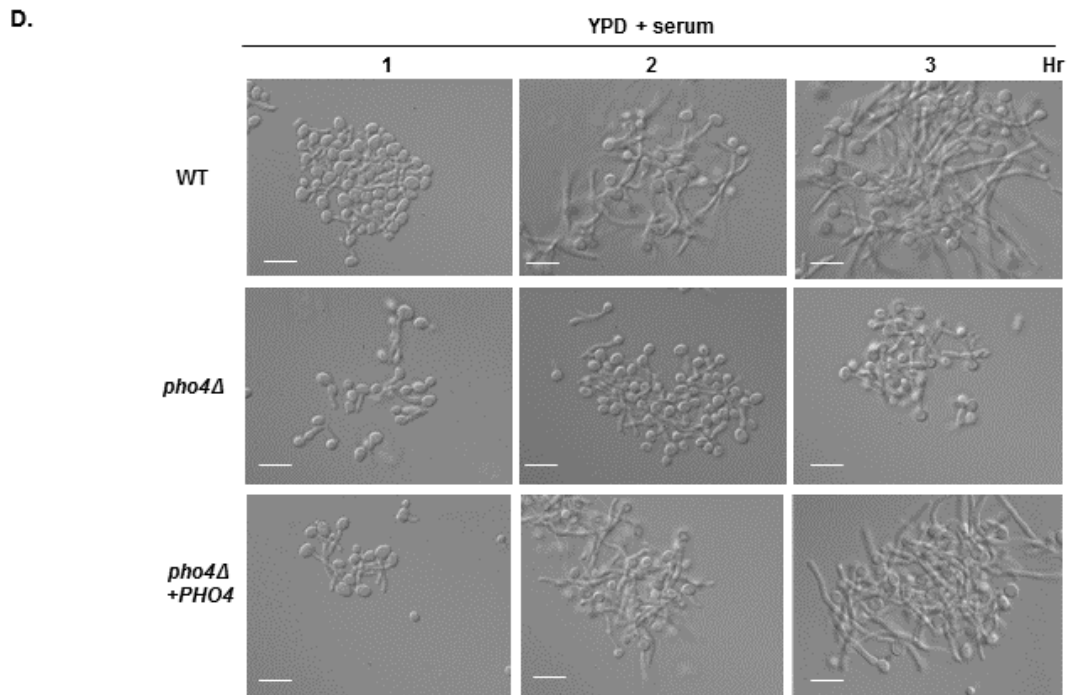


Fig 5.1 Contd. Cells lacking *PHO4* display pleiotropic stress phenotypes *Pho4Δ* cells display delayed serum-induced growth (C) and (D) Growth of *pho4Δ* cells is reduced compared to wild-type cells in YPD or YPD containing 20% fetal bovine serum. Kinetics of serum induced hyphal formation are delayed in *pho4Δ* cells. Stationary phase cells were diluted 1:10 in YPD medium containing 10% fetal bovine serum and incubated at 37°C for the times indicated.

5.2.2 *Pho4* does not accumulate in the nucleus following cationic or superoxide stress.

As *Pho4* in *C. albicans* is required for resistance to a range of distinct stress conditions (Fig 5.1) in addition to phosphate uptake and storage (Fig 4.2), experiments were performed to explore whether the stress phenotypes displayed by *pho4Δ* cells are dependent or independent of the roles of *Pho4* in phosphate homeostasis. As *Pho4* accumulates in the nucleus following phosphate starvation (Fig 4.4), initially experiments were performed to determine whether *Pho4* similarly accumulates in the nucleus following cationic, superoxide or alkaline pH stress. Similar to phosphate limitation, *Pho4* rapidly accumulated in the nucleus within minutes of raising pH but changes in the cellular localisation of *Pho4* were not evident following cationic or superoxide stress (Fig 5.2). Consistent with *Pho4* nuclear localisation following alkaline pH stress, the expression of *PHO84*, the *Pho4*-dependent high-affinity phosphate transporter, was upregulated (Fig 5.3) suggesting *Pho4* may play a direct role in activating alkaline pH stress response genes. In *S. cerevisiae*, the H⁺ ATPase efflux pump *Pma1*, restores intracellular levels of protons

during growth in alkaline pH (Arino *et al.*, 2010). Interestingly, *PMA1* in *C. albicans* was activated following alkaline pH stress but in a Pho4-independent manner indicating cells are specifically responding to a phosphate-limiting condition (Fig 5.3). The lack of nuclear accumulation following cationic or superoxide stress suggested that Pho4 may play an indirect role in mediating resistance to these stresses.

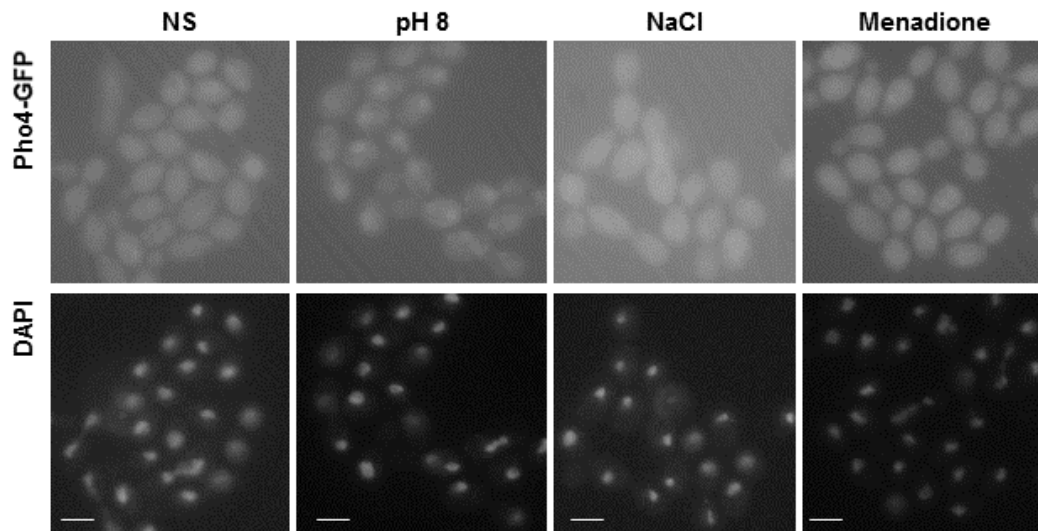


Fig 5.2 Pho4 localisation in response to specific stress treatments. Pho4 only accumulates in the nucleus following exposure to alkaline pH. *C. albicans* cells expressing Pho4-GFP were grown in YPD pH 8 (10 min), or exposed to 1M NaCl (10 min), or 300 μ M menadione (10 min) and Pho4 localisation imaged using fluorescent microscopy. DAPI staining illustrates nuclear positioning.

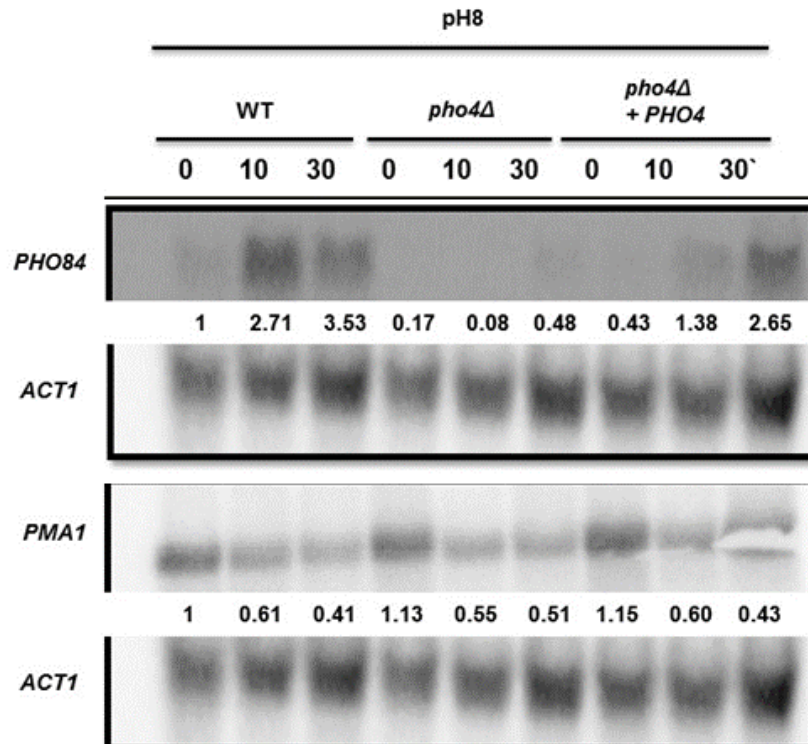


Fig 5.3 Pho4 regulates *PHO84* induction in response to alkaline pH stress. Northern blot analyses of RNA extracted from exponentially grown wild-type, *pho4Δ*, and *pho4Δ+PHO4* cells. Gene-specific probes were used to detect RNA transcripts from the indicated genes. For loading control, a gene-specific probe for *ACT1* transcripts was used. Relative intensities (to wild type) are shown below each of the genes investigated. Phosphoimager analysis was carried with a GE Typhoon FLA9500 and quantification was performed with ImageQuant software.

5.2.3 PolyP is mobilised in response to specific stresses.

Notably polyP, in addition to roles in phosphate and energy storage, has also been implicated in stress adaptation and osmoregulation in both bacteria and lower eukaryotic species such as yeast, fungi and trypanosomes (reviewed in Moreno and Docampo, 2013). Hence, it was possible that the role of Pho4 in polyP synthesis (Fig 4.2B; C) was a key determinant in mediating Pho4-dependent stress resistance. To investigate this, polyP mobilisation in response to alkaline, menadione or cationic stresses was examined. Neisser staining and PAGE revealed polyP was mobilised during alkaline pH and osmotic stresses with no obvious difference observed during superoxide stress exposure (Fig 5.4). A more detailed analysis of the impact of alkaline pH and osmotic stresses on polyP levels was then carried out. Specifically, the kinetics of polyP mobilisation during growth in stress conditions over time was investigated. As it has been shown in higher eukaryotes, for example *Trypanosoma cruzi*, that both hyper-osmotic and hypo-osmotic stresses trigger polyP mobilisation

we also examined the effect of hypo-osmotic exposure on polyP levels in *C. albicans*. Neisser staining and UREA-PAGE analysis illustrated that, like in phosphate-limiting conditions (Fig 4.2D) there was a rapid decrease in polyP levels following alkaline pH stress (Fig 5.5) while polyP levels also appeared to be reduced following hypo and hyper osmotic stress (Fig 5.6; Fig 5.7). More polyP was mobilised for alkaline pH and hypo-osmotic stress compared to hyper-osmotic stress. Taken together, these results revealed polyP in *C. albicans* is mobilised during alkaline pH and osmotic stresses.

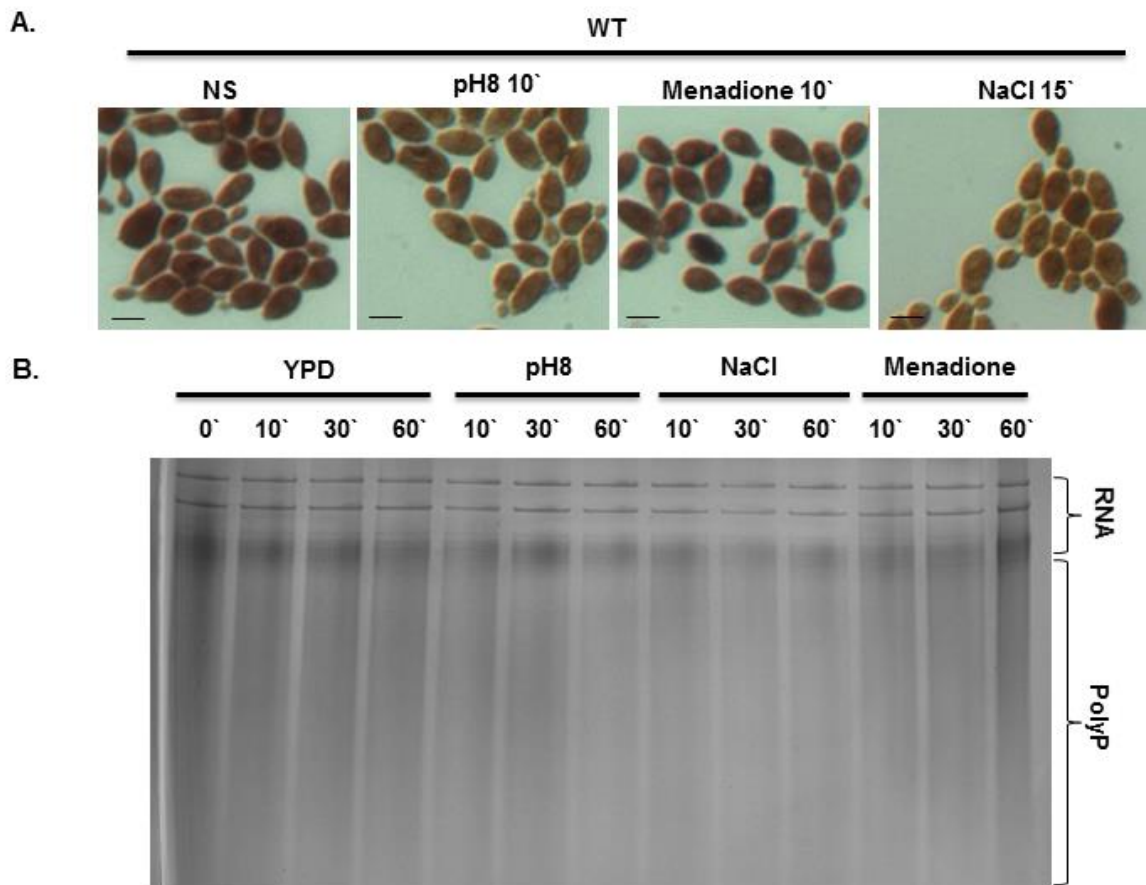


Fig 5.4 Poly-P is mobilised in response to specific stresses (A) Neisser staining of cells treated as described in Fig 4.2C (B) Toluidine blue staining of RNA/polyP extracts following electrophoresis on urea-polyacrylamide gels from cells grown in YPD pH 8, or YPD containing 1M NaCl or 300 μ m menadione for the indicated times. 20 μ g of RNA extracted from wildtype cells at each indicated time point was loaded onto a 12% UREA-PAGE gel. The experiment was repeated 3 times and a representative gel is shown.

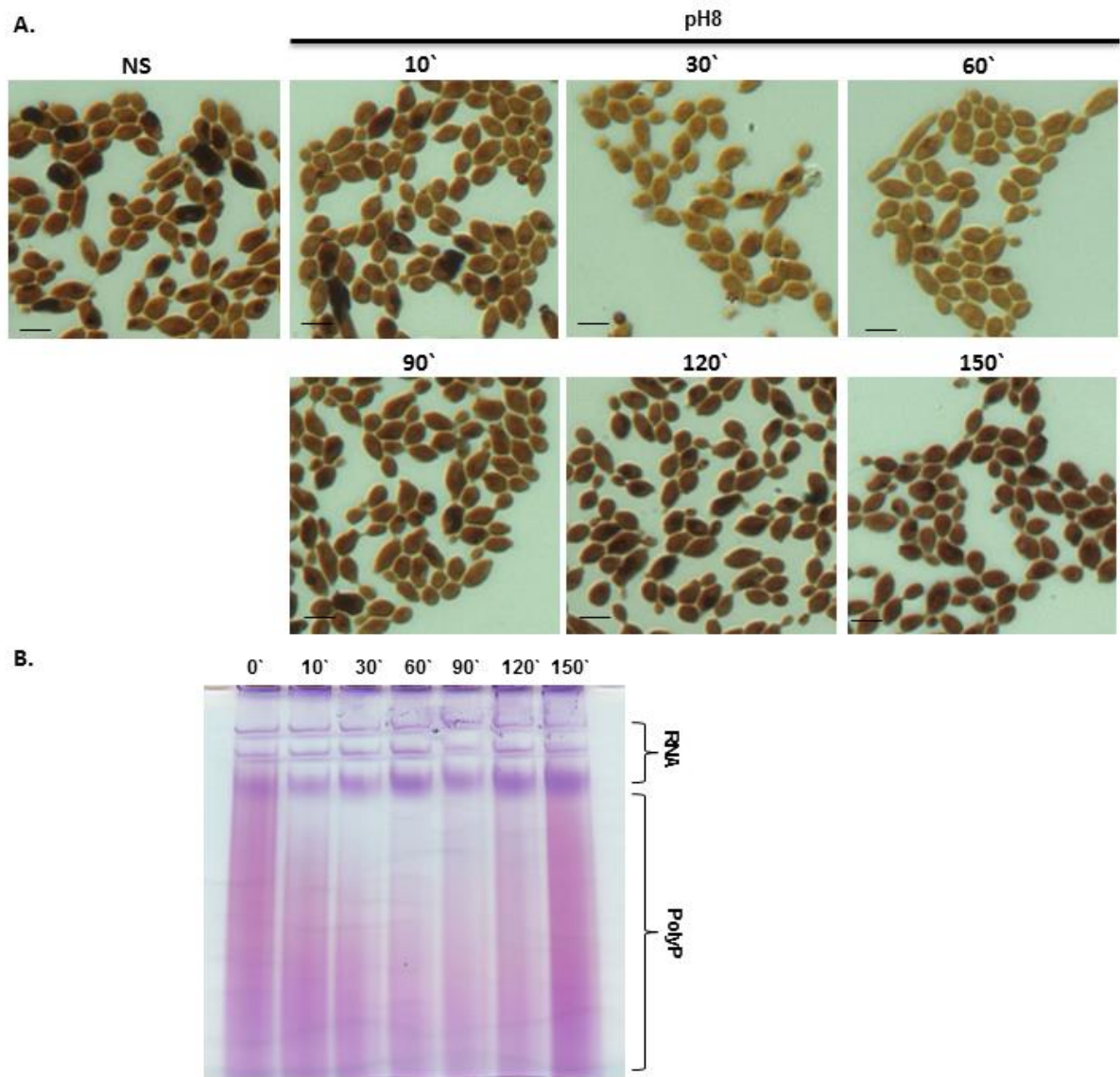


Fig 5.5 PolyP is rapidly mobilized under alkaline pH stress. Kinetics of polyP mobilisation in response to alkaline pH stress **(A)** Neisser staining of cells treated as described in Fig 4.2C **(B)** Toluidine blue staining of RNA/polyP extracts following electrophoresis on urea-polyacrylamide gels from cells grown in YPD pH 8. 20 μ g of RNA extracted from wildtype cells at each indicated time point was loaded onto a 12% UREA-PAGE gel. These experiments were repeated 3 times, representative images and gel are shown.

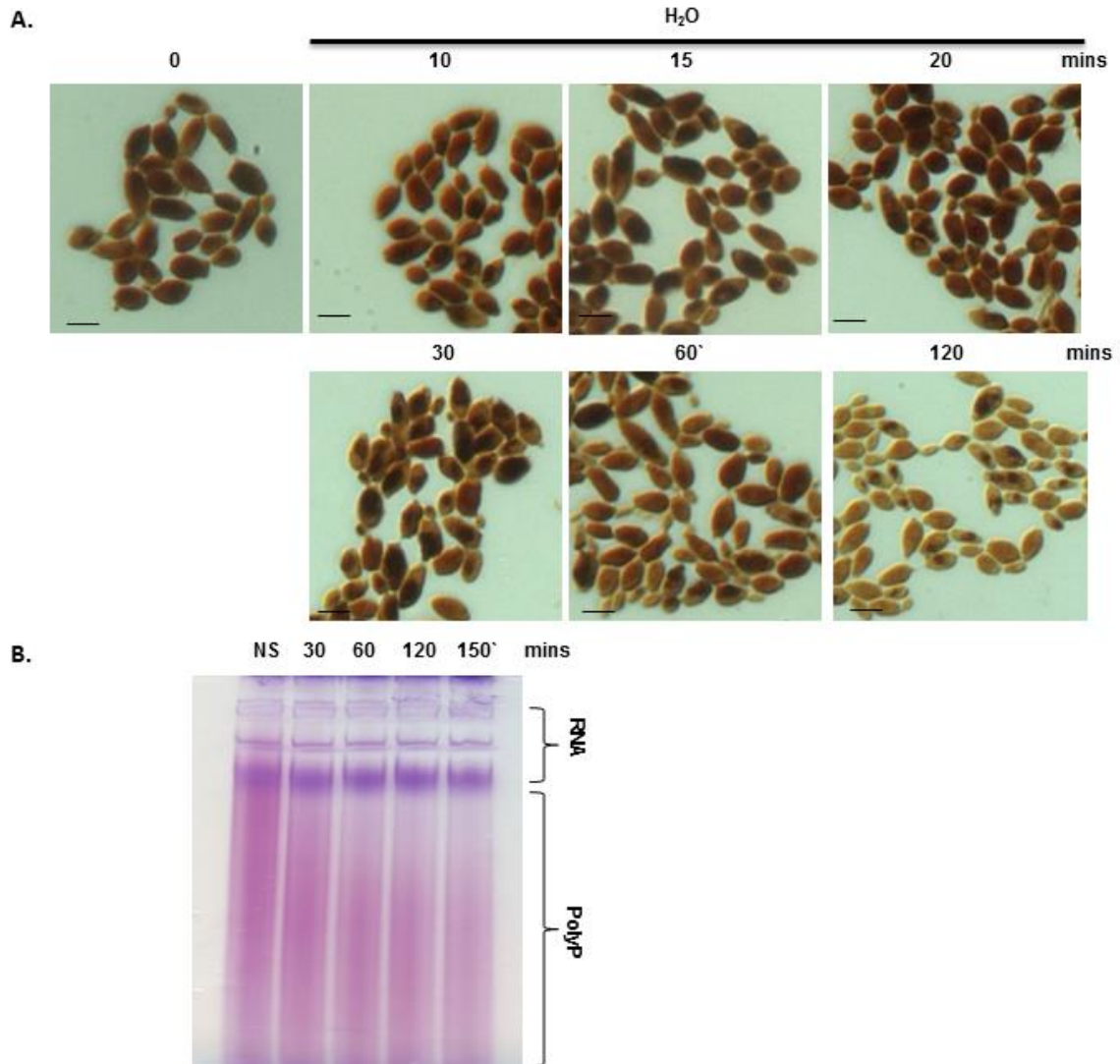


Fig 5.6 Poly-P is mobilised in response to hypo osmotic stress (A) Neisser staining of cells treated as described in Fig 4.2C **(B)** Toluidine blue staining of RNA/polyP extracts following electrophoresis on urea-polyacrylamide gels from cells grown in YPD, washed and resuspended in distilled water for the indicated times. 20 µg of RNA extracted from wildtype cells at each indicated time point was loaded onto a 12% UREA-PAGE gel. The experiment was repeated 3 times and a representative gel is shown.

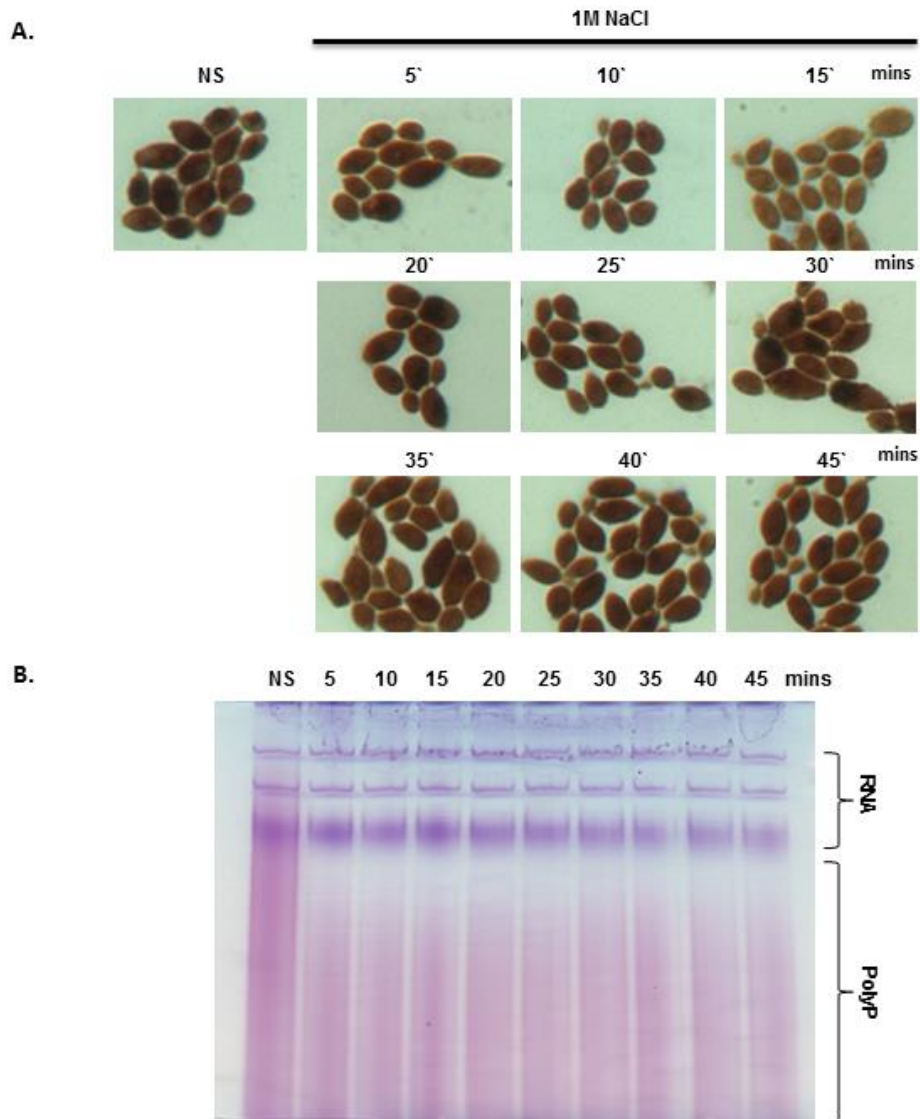


Fig 5.7 Poly-P is mobilised in response to hyperosmotic stress (A) Neisser staining of cells treated as described in Fig 4.2C **(B)** Toluidine blue staining of RNA/polyP extracts following electrophoresis on urea-polyacrylamide gels from cells grown in YPD containing 1 M NaCl for the indicated times. 20 μ g of RNA extracted from wildtype cells at each indicated time point was loaded onto a 12% UREA-PAGE gel. The experiment was repeated 3 times and a representative gel is shown.

5.2.4 PolyP is not required for Pho4-mediated stress resistance.

As polyP is mobilised following alkaline pH stress, and to a lesser extent following cationic stress, we asked whether the physical presence of polyP provided stress resistance in *C. albicans*.

Initially, polyP metabolism in *C. albicans* was explored further to identify proteins involved and establish role. In *S. cerevisiae*, polyP synthesis is dependent on the yeast vacuolar transporter chaperone (VTC) complex, which is a membrane protein assembly comprising of the Vtc1 - 4 proteins. Vtc4 has been identified as the polyP

polymerase within the VTC complex (Hothorn *et al.*, 2009), and *S. cerevisiae vtc4Δ* and *vtc1Δ* null mutants lack detectable polyP (Ogawa *et al.*, 2000; Hothorn *et al.*, 2009). In contrast, polyP processing to release Pi is regulated by the Ppx1 exopolyphosphatase and the Ppn1 endo-/exopolyphosphatase enzymes (Ogawa *et al.*, 2000).

Homologues of the proteins involved in polyP metabolism in *S. cerevisiae* were identified in *C. albicans* and knock out deletion strains of *VTC1*, *VTC4*, *PHM5*, *PHM7*, and *PPX1* created to validate the role of these genes in *C. albicans*. Specifically, the precise function each protein plays in polyP metabolism was investigated. Investigation was started off by looking at the effect of gene deletion on polyP metabolism which was assessed by looking at polyP content using Neisser staining and Urea-PAGE analysis of cells grown in phosphate-rich conditions. This method identified strains unable to synthesis polyP in phosphate-rich conditions. PolyP synthesis was completely abolished in the *vtc1Δ* and *vtc4Δ* cells (Fig 5.8A; B). Both Neisser staining and gel electrophoretic analysis revealed the *phm7Δ* cells have less polyP compared to wild-type cells (Fig 5.8A; B). From the Neisser stained images, the *phm5Δ* and *ppx1Δ* cells appear to have more polyP compared to wild-type cells however, the gel electrophoresis analysis suggests the mutants have less polyP (Fig 5.8A; B). Also observed from the neisser stained images are morphological defects in *phm5Δ* and *ppx1Δ* cells (Fig 5.8A). Both mutants are significantly bigger than wild-type, *vtc1Δ* and *vtc4Δ* cells and also grow at a slower rate suggesting the activities of polyphosphatases might be required for normal cell cycle progression (Fig 5.8B; C). However, taken together, this study identified proteins involved in polyP synthesis in *C. albicans* and although contrasting results were obtained for the mutants with putative roles in polyP hydrolysis, findings suggest normal polyP content or distribution and cell cycle progression may have been affected by gene deletion and also suggest there may be compensatory roles for the polyphosphatases.

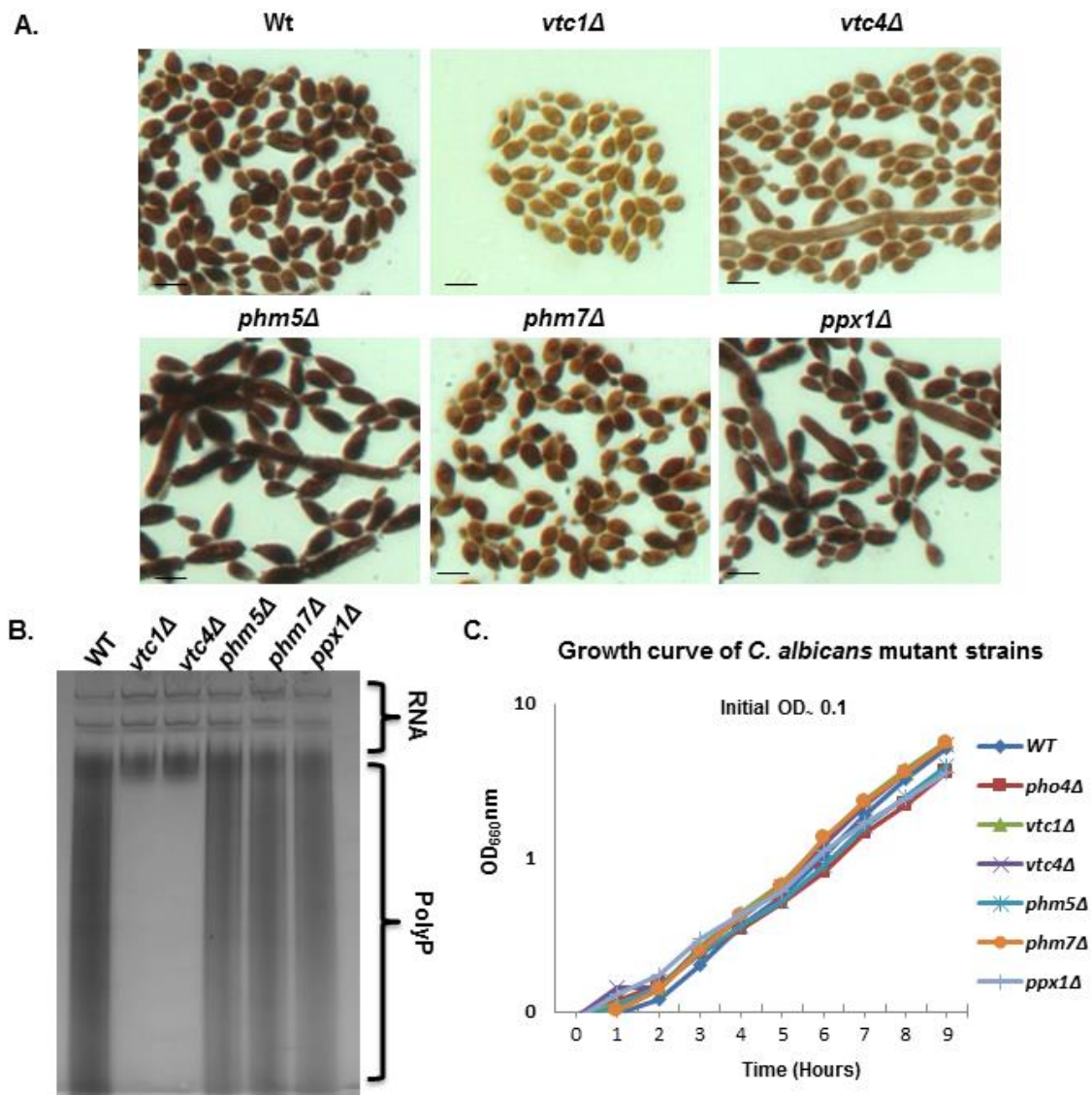


Fig. 5.8 The VTC complex proteins (Vtc1 and Vtc4) and Phm5, Phm7, and Ppx1 are involved in polyP metabolism in *C. albicans* (A) Gene deletion impacts polyP metabolism and cell morphology. No polyP detected in the *vtc1Δ* and *vtc4Δ* strains while *phm5Δ* and *ppx1Δ* strains appear to have more polyP compared to wild-type and also display morphological defects. Exponentially-growing wild-type and mutant strains were fixed by paraformaldehyde and stained by Neisser staining (B). PolyP gel electrophoresis confirms lack of polyP in the *vtc1* and *vtc4* mutants. With this method, the *phm5Δ* and *ppx1Δ* have less polyP compared to wild-type cells. PolyP on a toluidine blue stained gel showing polyP content. Urea-Page 20 μg of total RNA extracted from wildtype and mutant strains was loaded onto a 12% UREA-PAGE gel. The experiment was repeated twice, a representative gel is shown. (C). Deletion of *PHO4*, *PHM5*, or *PPX1* results in a slow growth phenotype. Growth curves of wild-type, *pho4Δ*, *vtc1Δ*, *vtc4Δ*, *phm5Δ*, *phm7Δ*, and *ppx1Δ* cells growing exponentially in YPD.

With proteins involved in polyP metabolism established in *C. albicans*, the role of polyP in stress resistance was examined. An extensive analysis of the *C. albicans* *vtc1Δ* and *vtc4Δ* mutants, defective in polyP synthesis, revealed little overlap with the cationic, menadione and alkaline pH stress-sensitive phenotypes exhibited by *pho4Δ* cells (Fig 5.9A). However, the polyP deficient *vtc1Δ* and *vtc4Δ* cells did display similar impaired resistance as the *pho4Δ* mutant to manganese (Fig 5.9A), but not to any other metals tested (Fig 5.9A). This suggests that in *C. albicans*, polyP functions as a reservoir for this particular transition metal. Cells lacking the endo- and exo-polyphosphatases similarly did not display significant stress-sensitive phenotypes to most of the conditions tested, with the exception of calcium (Fig 5.9A). Thus polyP mobilisation may be important to counteract an influx of calcium ions into the cell. Taken together, these results indicate that the drastic reduction of polyP levels in *pho4Δ* cells does not underlie the majority of the stress-sensitive phenotypes associated with loss of the Pho4 transcription factor. Perhaps, related to this, is the observation that Pho4 nuclear accumulation following phosphate limitation is not impaired in *vtc1Δ* and *vtc4Δ* cells lacking polyP (Fig 5.10). Hence, cells lacking polyP but containing Pho4 should be able to acquire external sources of phosphate.

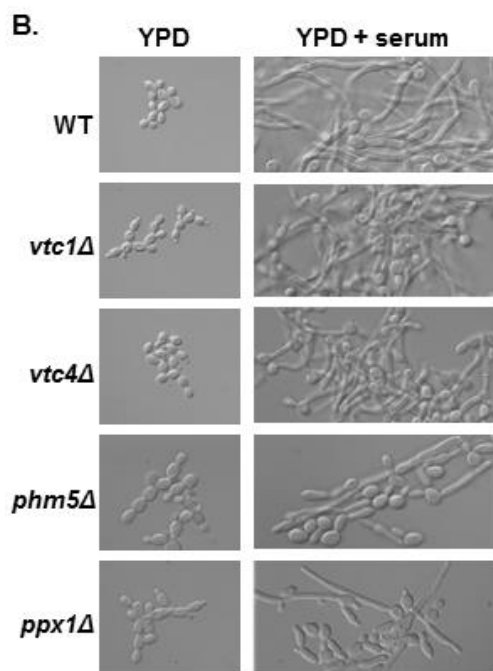
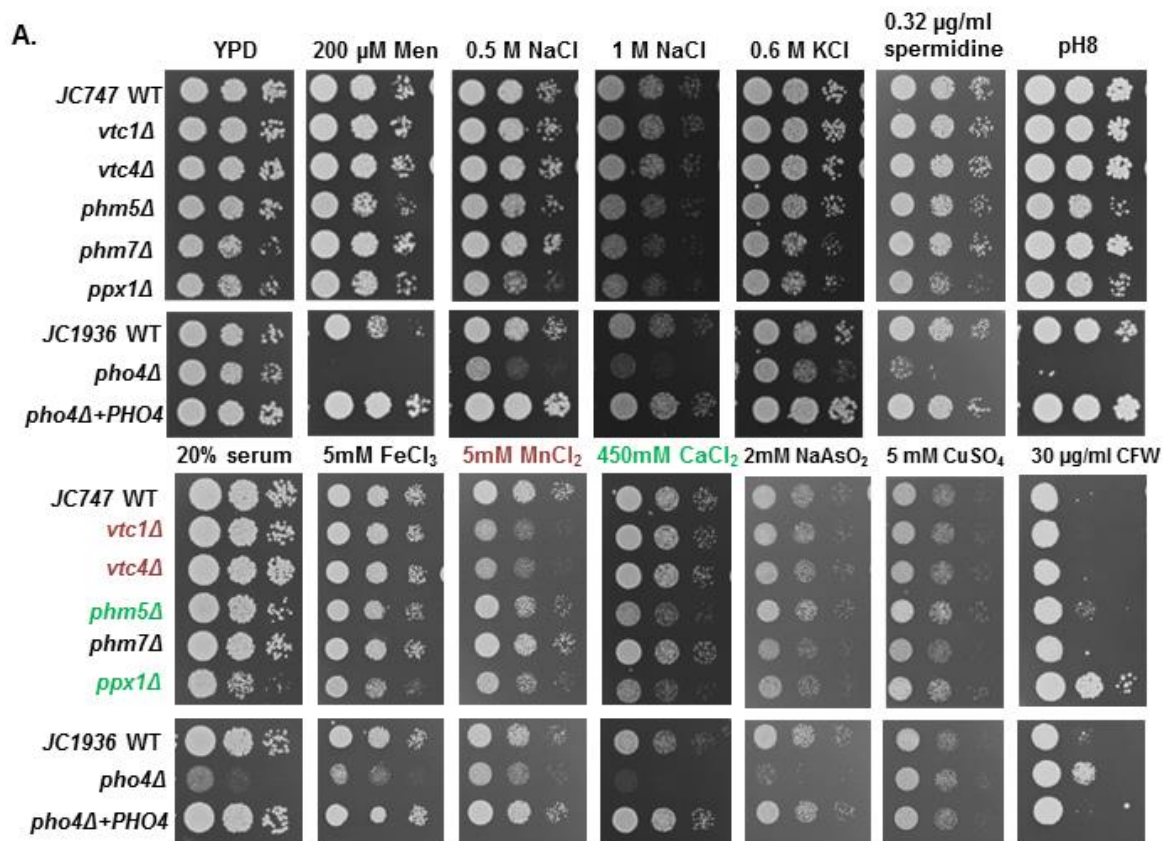


Fig 5.9 PolyP is largely dispensable for Pho4-associated stress sensitive phenotypes. Exponentially growing strains were spotted in serial dilutions onto YPD plates containing the indicated additives. Plates were incubated for 24 hrs at 30°C. (B) Serum induced hyphal formation. Stationary phase cells were diluted 1:10 in YPD medium containing 10% fetal bovine serum and incubated at 37°C for 4 h.

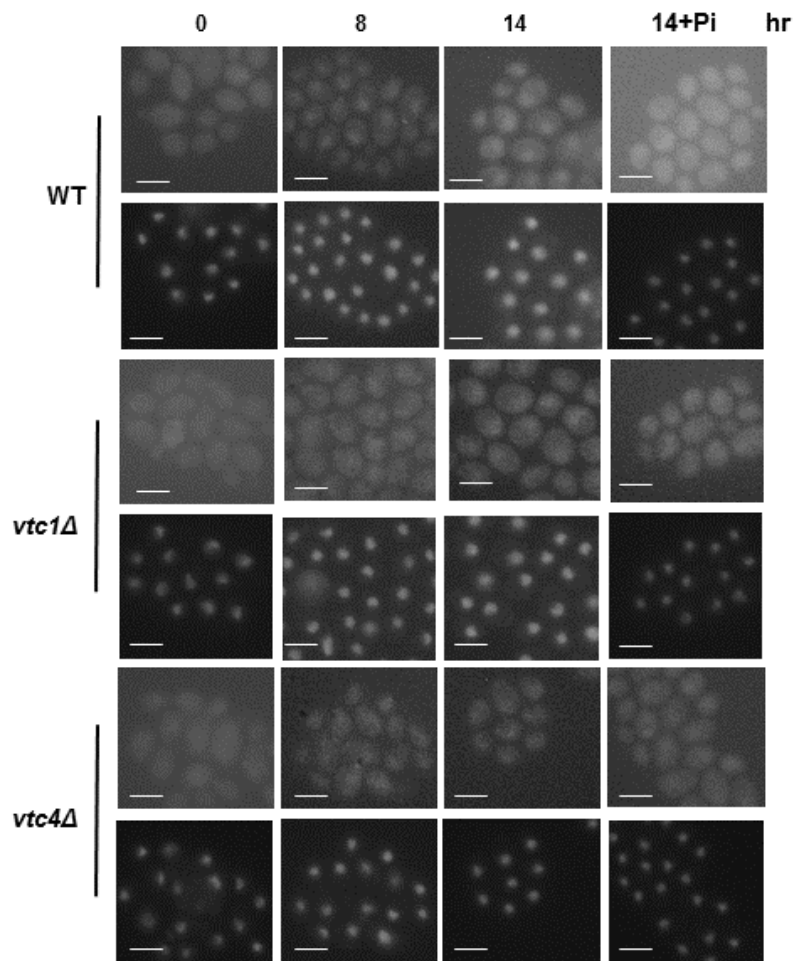


Fig 5.10 Pho4 accumulates in the nucleus in the *vtc1* and *vtc4* mutants under phosphate-limiting conditions. Under phosphate limiting conditions Pho4 accumulates in the nucleus in the *vtc1Δ* and *vtc4Δ*. Cells expressing Pho4-GFP were transferred to YPD media lacking phosphate, and localisation determined by fluorescence microscopy over a 14 h time course. +Pi indicates the localisation of Pho4 following addition of phosphate (10 min) to the 14 h sample. DAPI staining illustrates nuclear positioning.

5.2.5 Pho4 dependent genes and stress phenotypes.

As the role of Pho4 in polyP synthesis appears dispensable for stress phenotypes displayed by *pho4Δ* cells, we revisited the RNA-seq dataset described in Chapter 4 to explore whether genes deregulated in *pho4Δ* cells could relate to the diverse stress phenotypes associated with loss of Pho4 (Fig 4.6). GO term analysis of the 150 Pho4 dependent genes identified under minus Pi conditions did not identify terms associated with stress resistance (Fig 4.7). However, as *C. albicans* cells lacking Pho4 are very sensitive to cationic stress, we wondered whether any of the 150 Pho4 dependent genes were also upregulated in *C. albicans* following cationic stress using the previous microarray data generated by the JQ lab (Enjalbert *et al.*, 2006). Only 5 genes were common to both datasets, *C3_01540W_A*, *C3_02140C_A*,

C6_03320W_A, *GPD2* and *RHR2*. Three are of unknown function however, *GPD2* and *RHR2* work alongside each other to dephosphorylate glycerol phosphate, generating both an osmo-protectant and a source of phosphate. Northern blotting validated the role of Pho4 in the induction of these genes following phosphate limitation (Fig 5.11).

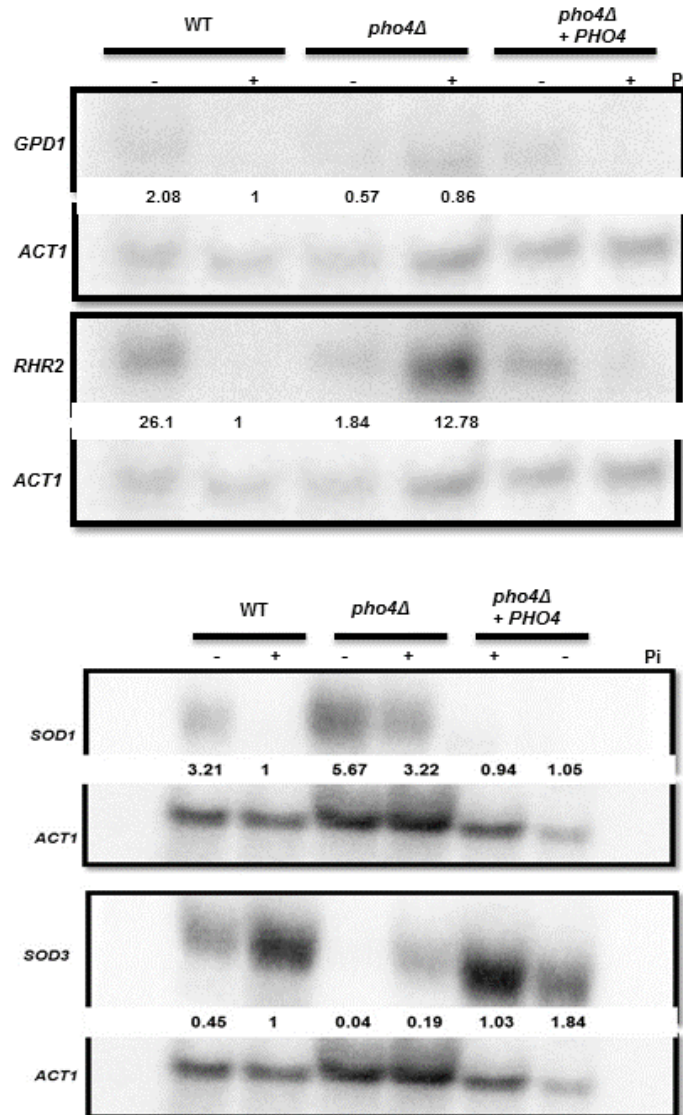


Fig. 5.11 Pho4 targets genes in *C. albicans*. Validation of gene expression profiles observed in RNA-Seq analysis. Northern blot analysis of RNA isolated from wild-type and *pho4Δ* cells using the same –Pi and +Pi conditions used for RNA-Seq experiments. Blots were analysed with probes specific for the indicated genes, with *ACT1* as a loading control. Fold induction compared to Wt cells +Pi is shown.

In addition, the genes deregulated in *pho4Δ* cells compared to wildtype cells under phosphate replete conditions were also examined. A large number of genes (<1300) were upregulated 2 fold or greater in *pho4Δ* cells compared to wild-type cells, whereas 49 genes were downregulated. Thus loss of Pho4 clearly has a significant impact on the *C. albicans* transcriptome. Significantly enriched functional categories up-regulated in *pho4Δ* cells include processes involved in DNA metabolism, DNA repair and response to DNA damage, cell cycle, and response to stress (Fig 5.12). These may reflect the high Pi requirement of DNA replication, and that phosphate regulation is linked with cell cycle progression in *S. cerevisiae* (Menoyo *et al.*, 2013). However, cross reference of the genes upregulated in *pho4Δ* cells with the cationic stress induced regulon (Enjalbert *et al.*, 2006), again revealed little overlap (23 genes), with no cellular processes significantly enriched. Thus no significant connection between Pho4 dependent and cationic stress-induced genes in *C. albicans* was discovered. However, relevant to the superoxide stress-sensitive phenotype of *pho4Δ* cells is the upregulation of three of the four copper/zinc-containing superoxide dismutase genes, *SOD1*, *SOD5* and *SOD6*, in this mutant. In contrast, the transcription of the manganese-dependent *SOD3* gene is downregulated (Appendix 2). The impact of Pho4 loss on *SOD1* and *SOD3* levels was validated by Northern blotting (Fig 5.11). The induction of the copper-dependent *SOD* genes could reflect a compensatory mechanism to allow cells to adapt to the superoxide stress sensitivity of *pho4Δ* cells, whereas the repression of the manganese-dependent *SOD3* may be linked to the sensitivity of *pho4Δ* cells to this metal. Finally, also noted was that processes involved in metal homeostasis and oxidative-reduction processes were significantly downregulated in *pho4Δ* cells compared to wild-type cells (Fig 5.12). Specifically, genes involved in iron (*FTR2*, *FET3*), zinc (*ZRT2*, *CSR1*) and copper (*CTR1*, *FRE7*) acquisition were all downregulated in cells lacking Pho4. This suggested a role for Pho4 in maintaining metal homeostasis, which could underlie the altered stress resistance exhibited by *pho4Δ* cells to a number of metals (Fig 5.1).

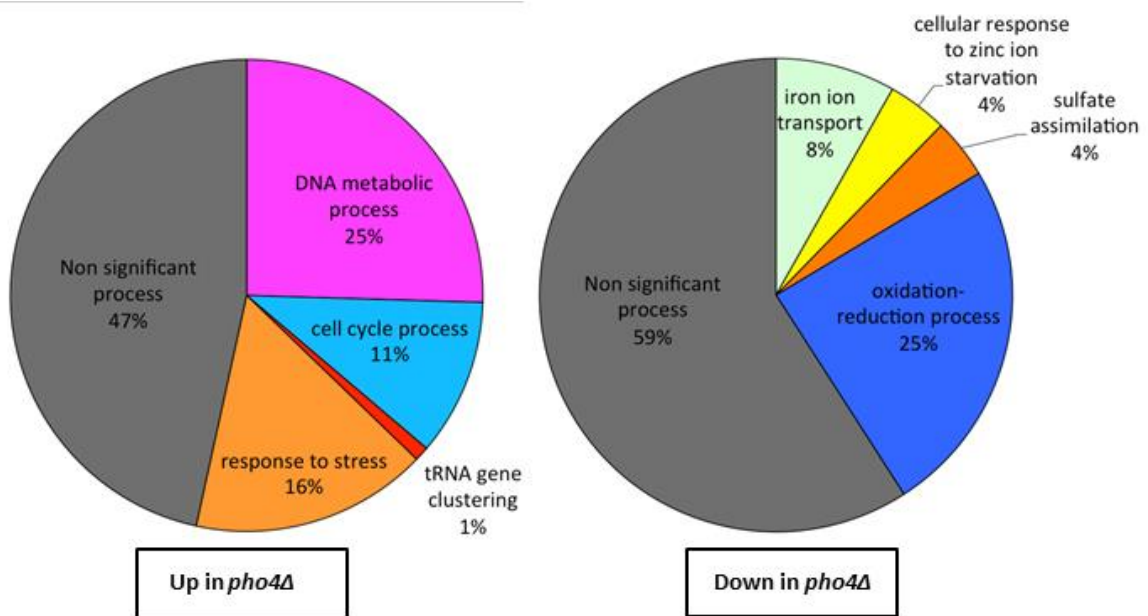


Fig 5.12 Processes deregulated in *pho4Δ* cells under phosphate replete conditions. Pie charts illustrating the GO processes that are deregulated in *pho4Δ* cells compared to wild-type cells when grown in media containing Pi. In the pie chart displaying biological processes upregulated in *pho4Δ* cells, DNA metabolic process incorporates significant terms, in respect to p-value, that have emerged from the initial GO term analysis. These terms include DNA packaging (2.4%), DNA repair (6.4%), and cellular response to DNA damage (7.4%). The non-significant process category presented in both pie charts includes all additional processes that have been retrieved from GO term analysis but did not pass the p-value criteria as well as the term “Unknown Biological Process”.

5.2.6 Investigation into the relationship between Hog1 and Pho4 signalling.

The RNA Seq dataset revealed that the genes, *GPD2* and *RHR2*, previously shown to be induced by cationic stress (Enjalbert *et al.*, 2006) are also upregulated following phosphate limitation in a Pho4-dependent manner. Previously, the NaCl-induced induction of *GPD2* and *RHR2* had been shown to be dependent on the Hog1 SAPK (Enjalbert *et al.*, 2006). Thus it was reasoned that Pho4 could be a transcription factor target of the Hog1 kinase which regulates the induction of such Hog1-dependent genes. Consistent with this, it was found that Pho4 is robustly phosphorylated following exposure to NaCl stress (Fig 5.13A). However, further investigations revealed that this cationic-stress induced phosphorylation of Pho4 occurs independently of Hog1 (Fig 5.13B). Moreover, although Pho4 contributes to the induction of Hog1 targets, *GPD2* and *RHR2*, following phosphate limitation, this transcription factor is dispensable for their induction following cationic stress (Fig 5.13C). Unexpectedly, it was found that Pho4 levels were significantly reduced in cells lacking either Hog1 or the upstream Pbs2 MAPKK and Ssk2 MAPKKK of the

Hog1 pathway (Fig 5.14A). Thus a basal level of Hog1 signalling appears to be vital to promote Pho4 levels. Indeed, as a consequence of this, *hog1Δ* cells display some phenotypes indicative of low Pho4 levels such as reduced acid phosphatase activity (Fig 5.14B), and lower levels of polyphosphate (Fig 5.14C). It is interesting to speculate that some of the stress phenotypes exhibited by *hog1Δ* cells may be due to a reduction in Pho4 levels. For example, both *hog1Δ* and *pho4Δ* cells display sensitivity to menadione (Fig 5.14D), but Hog1 is only marginally activated by this stress (Smith *et al.*, 2004). Taken together, however, the role of Pho4 in cationic stress resistance is independent of regulating the induction of Hog1-target genes.

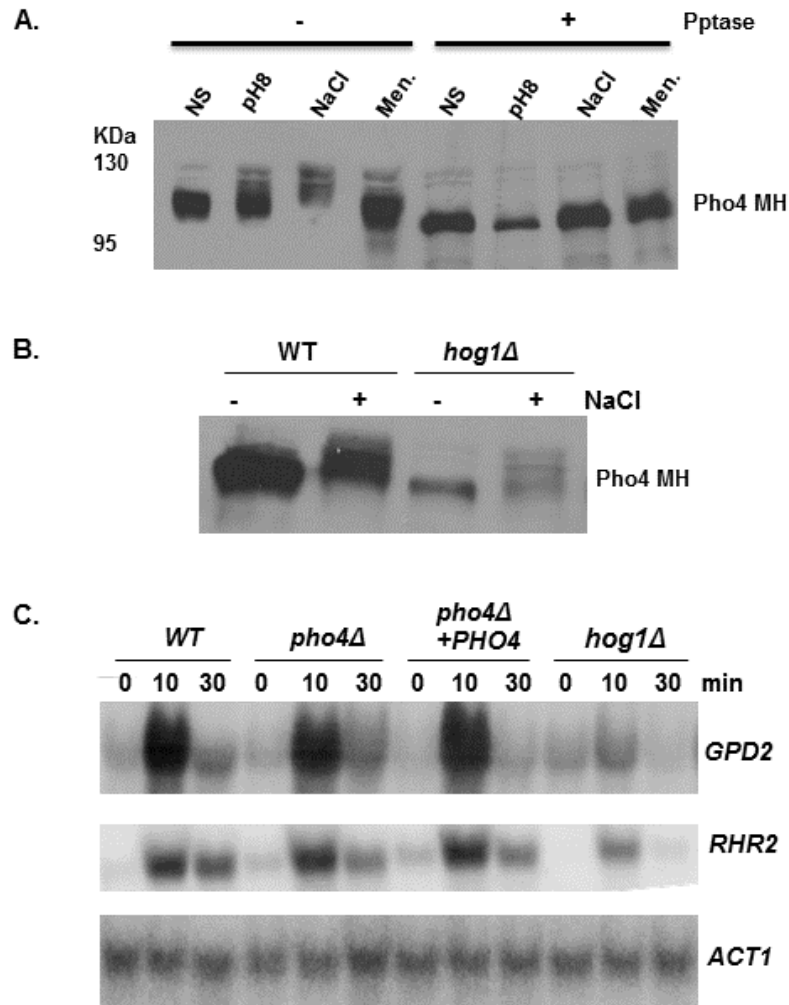


Fig 5.13 Cationic stress-induced modification of Pho4 (A) Pho4 is phosphorylated following cationic but not alkaline pH and menadione stresses. Western blot analysis of whole cell extracts isolated from cells expressing Pho4-MH following treatment with the indicated stresses. Blots were probed for Pho4-MH using an anti-myc antibody **(B)** The cationic stress-induced phosphorylation of Pho4 is independent of Hog1. Western blot analysis of whole cell extracts isolated from *WT* and *hog1Δ* cells expressing Pho4-MH, as described above **(C)** Pho4 is dispensable for cationic stress induced gene expression. Northern blot analysis of RNA isolated from the indicated strains following exposure to 0.3 M NaCl. Blots were analysed with probes specific for *GPD2* and *RHR2*, with *ACT1* as a loading control.

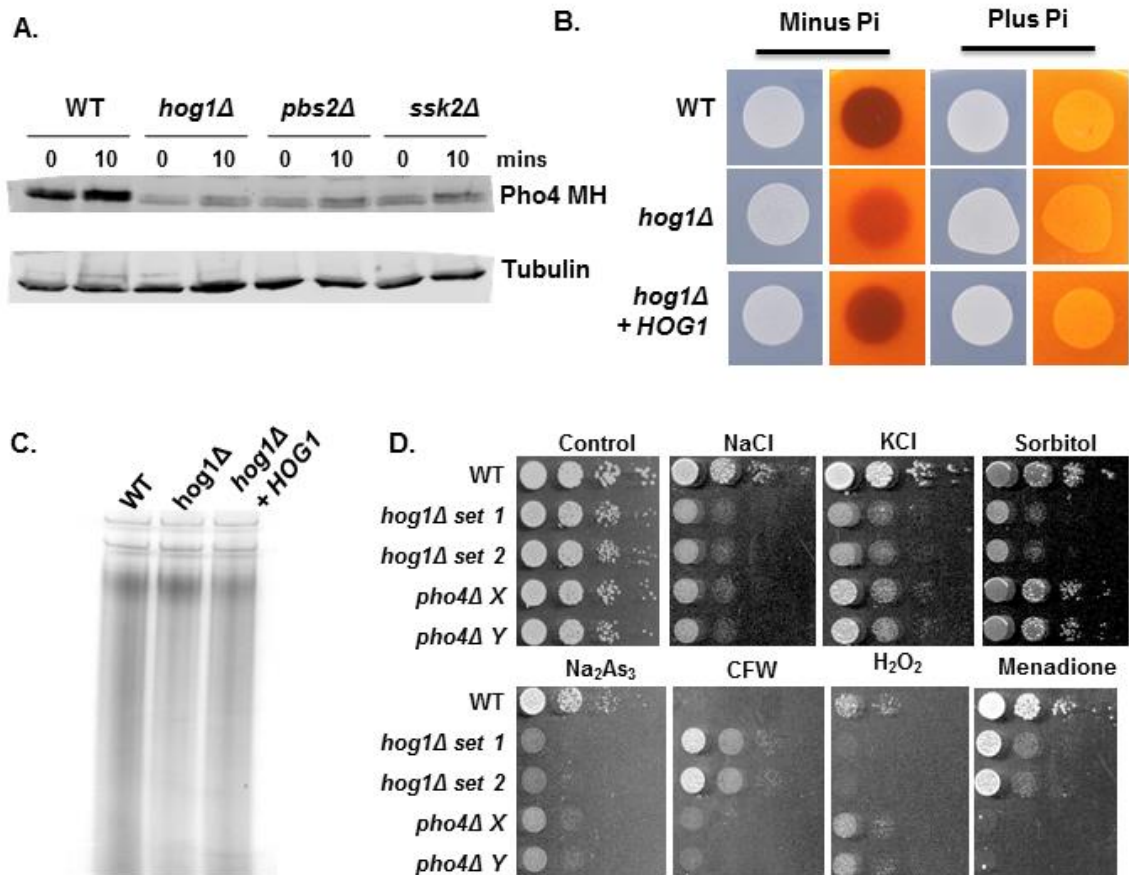
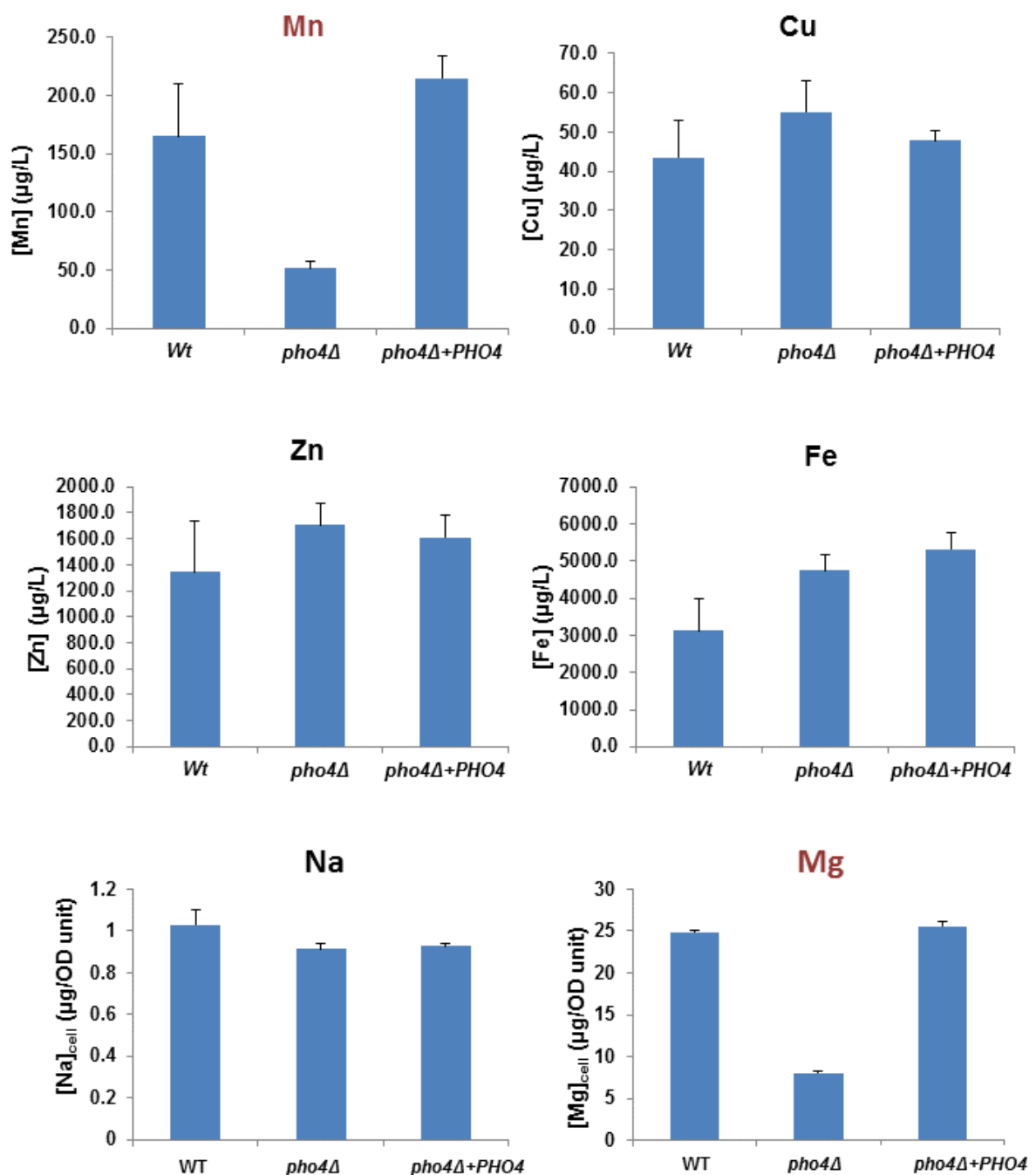


Fig 5.14 The relationship between Hog1 and Pho4 (A) Pho4 protein levels are dependent on Hog1 SAPK pathway components. Western blot analysis of whole cell extracts isolated from *Wt*, *hog1Δ*, *pbs2Δ* and *ssk2Δ* cells expressing Pho4-MH. Blots were probed for Pho4-MH using an anti-myc antibody, and an anti-tubulin antibody was used as a loading control (B) Cells lacking *HOG1* display reduced acid phosphatase activity. Strains grown on PNMC agar plates, with or without Pi, were subjected to an agar-overlay colouration assay in which secreted acid phosphatase activity is visualised by a dark red colouration (C) Cells lacking *HOG1* have lower polyP levels. Toluuidine blue staining of RNA/polyP extracts from the indicated strains following electrophoresis on urea-polyacrylamide gels (D) Apart from cationic stress the *pho4Δ* strain shares no other stress phenotype with the *hog1Δ*. Spot tests were carried out as per Fig 5.1A

5.2.7. Investigating the role of Pho4 in phosphate homeostasis and cationic sensitivity.

Next we wondered if there was a link between the role of Pho4 in regulating intracellular phosphate levels and cation sensitivity. In support of this, a recent report in *C. neoformans*, revealed that deletion of all three phosphate transporters *PHO84*, *PHO840* and *PHO89*, resulted in significantly higher intracellular sodium levels compared to wild-type cells (~300%), and such cells displayed increased sensitivity to NaCl-imposed cationic stress (Kretschmer *et al.*, 2014). Increased levels of iron (~130%) and zinc (~153%) were also noted in the triple *C. neoformans* mutant (Kretschmer *et al.*, 2014). In addition, disruption of phosphate control in *S. cerevisiae*, via deletion of the cyclin *PHO80*, caused a wide range of metal homeostasis defects (Rosenfeld *et al.*, 2010). Based on these findings, inductively coupled plasma mass spectrometry (ICP-MS) was employed to determine whether loss of *PHO4* in *C. albicans* impacted on metal cation homeostasis. ICP-MS was performed by Dr Emma Tarrant and Dr Kelvin Waldron, Newcastle University. *C. albicans pho4Δ* cells contained significantly lower levels (~16% of wild-type) of manganese than wild-type and reconstituted strains (Fig 5.15), which is consistent with the findings that polyP may function as a reservoir for this metal. Similar effects were observed for magnesium (30% of wild-type cells) levels, and consistent with the role of Pho4 in phosphate homeostasis, phosphate content was also lower in *pho4Δ* cells (Fig 5.15). Unexpectedly, levels of sodium were not dramatically increased in *pho4Δ* cells (Fig 5.14) which contrasts with that reported for the *C. neoformans* phosphate transporter triple mutant (Kretschmer *et al.*, 2014). In fact, sodium and potassium levels were significantly lower (89% and 80% respectively) in the *pho4Δ* cells (Fig 5.15). However, analyses of other metal cations revealed other differences; levels of zinc and iron were higher in *pho4Δ* cells (123% and 125% respectively) than wild-type cells (Fig 5.15). These findings propose that the significant lack of phosphate homeostasis in cells lacking *PHO4* may underline the acute sensitivity of *pho4Δ* cells to cationic stress imposed by manganese, magnesium, and possibly, sodium. In *S. cerevisiae*, excess NaCl in the cell is exported out of the cell by ion transporters, for example the P-type ATPase, Ena1 (Hohmann, 2002). In an effort to determine the role of Pho4 in NaCl-induced cationic stress, the expression of the predicted sodium efflux pumps identified in *C. albicans*, *ENA2* and *ENA21*, as well as Pho4-dependency was examined. Northern blot analysis revealed these genes are

activated in response to NaCl-induced cationic stress but in a Pho4-independent manner (Fig 5.16). These pumps may have a reduced ability to pump out excess Na⁺ in the *pho4Δ* cells during exposure to high NaCl as these pumps use energy from a variety of sources including ATP and polyP, of which phosphate is a precursor and unavailable in *pho4Δ* cells (Achbergerova and Nahalka, 2011; Trilisenko and Kulakovskaya, 2014). In spite of the unresolved role of Pho4 in cationic stress adaptation, these findings support the concept that phosphate metabolism plays an important role in metal cation homeostasis in *C. albicans*. However, the precise role of Pho4 in cationic stress induced by NaCl remains unknown.



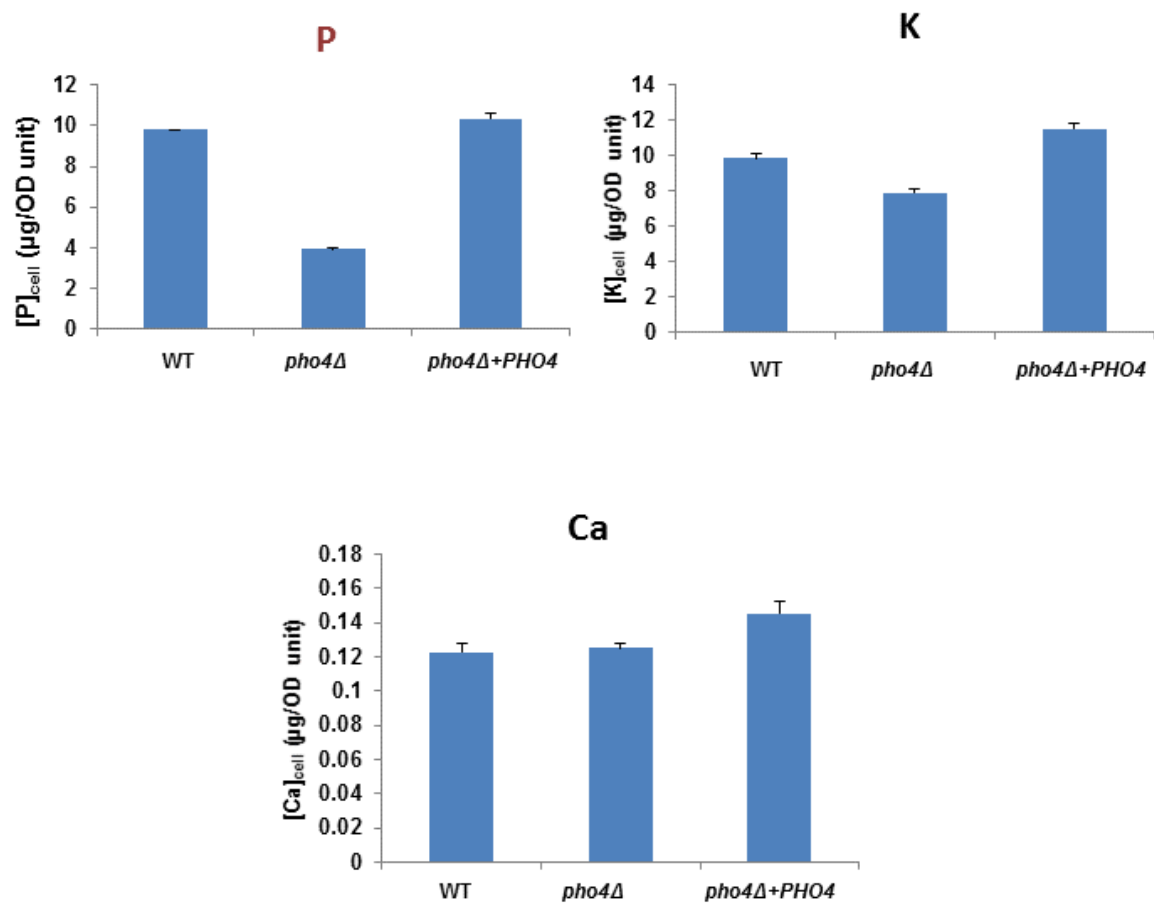


Fig 5.15 Loss of Pho4 impacts on cation homeostasis. Whole-cell nitric acid digests of *WT* and *pho4* Δ cells grown in YPD were analysed by inductively coupled plasma mass spectroscopy (ICP-MS). The results for the indicated elements are shown as the mean \pm the standard deviation.

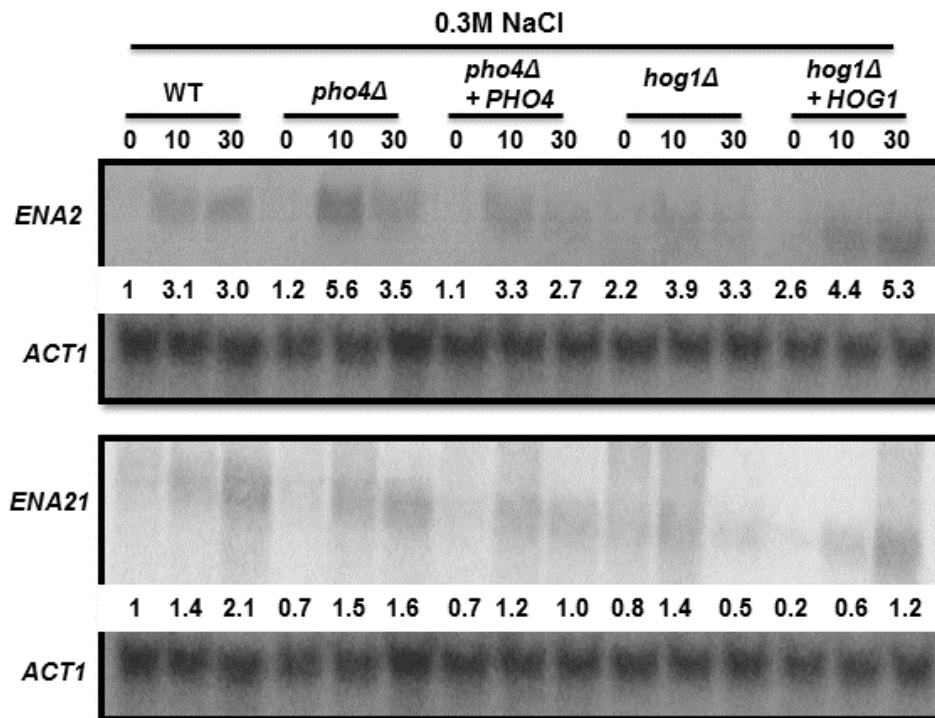


Fig 5.16 Expression of *ENA2* and *ENA21* under cationic stress are also not dependent on *Pho4*. Northern blot analyses of RNA extracted from exponentially grown wild-type, *pho4Δ*, and *pho4Δ+PHO4*, *hog1Δ*, *hog1Δ + HOG1* cells. Gene-specific probes were used to detect RNA transcripts from the indicated genes. For loading control a gene-specific probe for *ACT1* transcripts was used. Relative intensities (to wild type) are shown below each of the genes investigated. Phosphoimager analysis was conducted using a GE Typhoon FLA9500 and quantification was performed with ImageQuant software.

5.2.8 *Pho4* is required for Superoxide dismutase (*Sod1*) activity.

As described above, the RNA Seq dataset revealed a number of superoxide dismutase encoding genes were deregulated in *C. albicans pho4Δ* cells. Specifically, the copper-containing Sods, *SOD1*, *SOD5* and *SOD6* were all significantly induced in cells lacking *Pho4* under normal growth conditions. This observation raised the important question of why there is no protection against superoxide stress in the *pho4Δ* cells. To investigate this, an in-gel Sod activity assay was carried out to explore whether the increase in *SOD* transcripts was reflected by increase in activity. Strikingly, the amount of *Sod1* activity was noticeably less in *pho4Δ* cells compared to the wild-type and the *pho4Δ+PHO4* reconstituted strains (Fig 5.17A). This was even more apparent after subjecting the cells to menadione (Fig 5.17A). In contrast, the activity of the manganese-containing *Sod2* enzyme was not impaired in cells lacking *Pho4* (Fig 5.17A). The observation that three of the four copper-containing

SODs are deregulated in *pho4Δ* cells, together with the copper resistant phenotype of cells lacking Pho4 (Fig 5.1B), suggested that copper was either limiting, or its bioavailability reduced, in *pho4Δ* cells. However, no significant difference in copper levels were detected by ICP-MS analysis in *pho4Δ* cells (Fig 5.14), suggesting therefore that the bioavailability of this metal is reduced. Studies in *S. cerevisiae* have revealed that defects in delivery of copper to Sods for example, due to the inactivation of the Ccs1 copper chaperone, can be overcome by the addition of excess copper to the growth media (Rae *et al.*, 1999). Based on this observation in yeast cells, it was explored whether the Pho4-dependent defect in Sod1 activity, and menadione sensitivity, could be rescued by supplementing the growth media with copper. Strikingly, Sod1 activity was restored to wild-type levels in *pho4Δ* cells in the presence of excess copper (Fig 5.17B). Consistent with this, exposure of *pho4Δ* cells to menadione in the presence of copper, completely rescued the sensitivity of such cells (Fig 5.17C). Supplementation of the growth media with zinc could also partially rescue superoxide sensitive phenotype of *pho4Δ* cells, whereas manganese had no impact (Fig 5.17C). Taken together, these results indicate that the exquisite sensitivity of *pho4Δ* cells to superoxide is due to a role of Pho4 in regulating the bioavailability of copper, an essential metal co-factor of the copper/zinc Sod enzymes. These findings further highlight the link between phosphate metabolism and metal homeostasis in *C. albicans*.

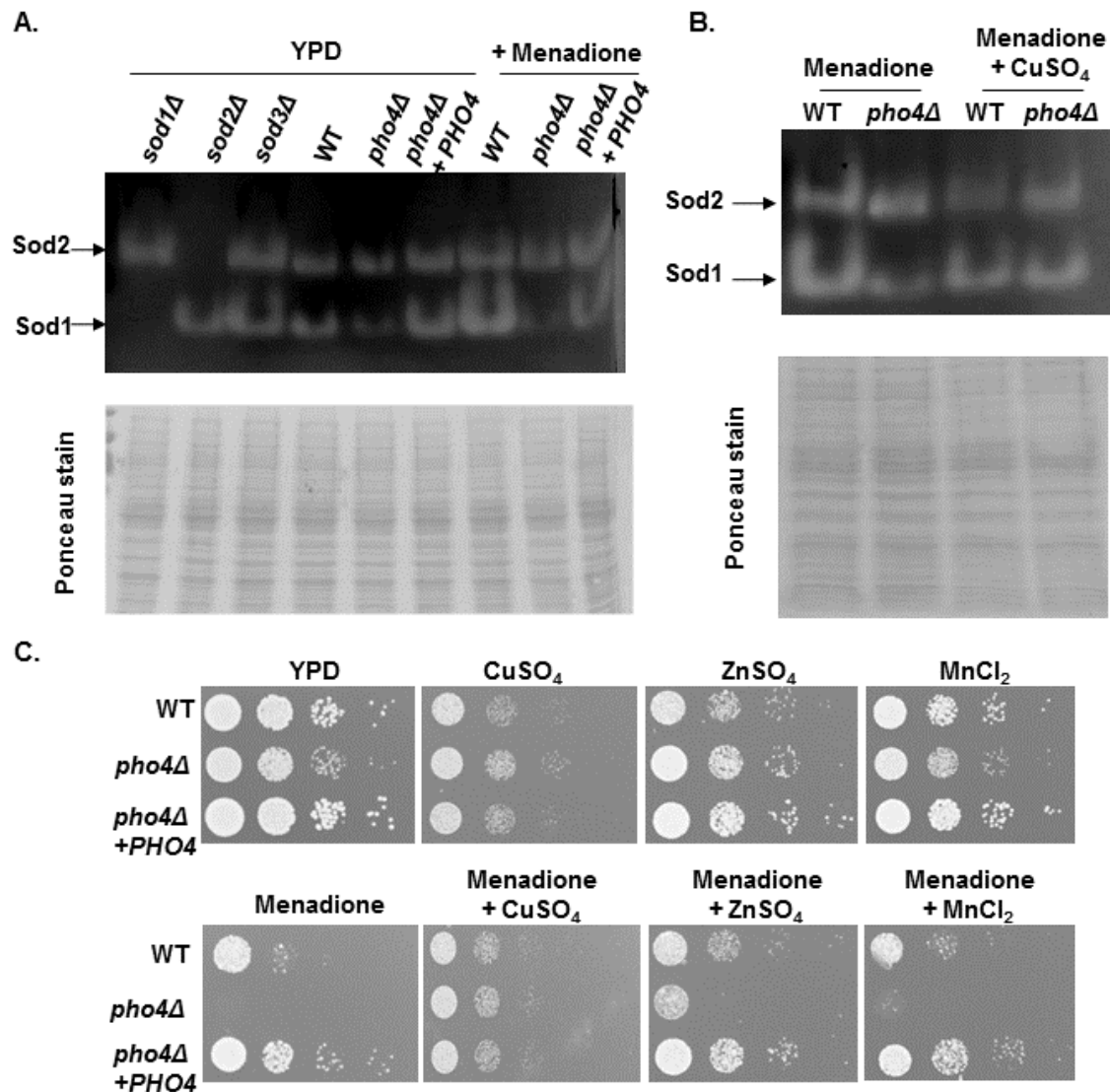


Fig 5.17 Pho4 is required for the activity of the Sod1 superoxide dismutase (A) Sod1 activity is reduced in cells lacking *pho4Δ*. Native extracts from the indicated strains, before and after treatment with 300 μM menadione for 1 h, were assayed for superoxide dismutase activity using nitro blue tetrazolium staining. Duplicates samples were subjected to SDS-PAGE, and following transfer membranes were stained with Ponceau S to assess protein loading. **(B)** Supplementation of media with copper rescues the menadione sensitivity of *pho4Δ* cells. Exponentially growing strains were spotted in serial dilutions onto YPD plates with or without 300 μM menadione, and containing 5 mM CuSO_2 , 1 mM ZnSO_4 or 5 mM MnCl_2 . Plates were incubated for 24 hrs at 30°C. **(C)** Supplementation of media with copper restores Sod1 activity in *pho4Δ* cells. Native extracts from the indicated strains following treatment with 300 μM menadione for 1 h in the presence or absence of 5 mM CuSO_2 , were assayed for superoxide dismutase activity as in (A).

5.3 Discussion.

In this chapter, the role of Pho4 in stress adaptation in *C. albicans* was investigated. Based on findings, a connection between phosphate acquisition and metal homeostasis was discovered.

5.3.1 Pho4 mediated phosphate acquisition is vital for alkaline pH resistance.

In addition to phosphate-limiting conditions, Pho4 was found to rapidly accumulate in the nucleus following exposure to alkaline pH stress suggesting Pho4 plays a direct role in this stress response. Exposure to pH 8 also triggered rapid mobilisation of polyP stores. Alkalinisation of growth medium mimicking phosphate limitation has been previously reported in yeast and in *C. albicans*. Expression of genes involved in phosphate transport and polyP synthesis were upregulated under alkaline growth conditions in *S. cerevisiae* while in *C. albicans* the phosphate transporter genes *PHO84* and *PHO89* were induced however, only the expression of *PHO84* was found to be completely Pho4-dependent (Serrano *et al.*, 2002; Bensen *et al.*, 2004). The activation of phosphate response genes is most likely a secondary effect of the alkaline pH environment. At pH 8 the preferred uptake form of phosphate, which is as ions, becomes unavailable therefore cells respond by activating expression of phosphate acquisition genes (Goodman and Rothstein, 1957). This explanation is consistent with the finding from this study that one of the key targets of Pho4 under limiting phosphate, the high-affinity transporter, *PHO84* was also induced under alkaline pH stress (Fig 5.10). In addition, under alkaline pH the phosphate uptake activity of Pho84 would be submaximal as this transporter has an acidic pH optima (Goodman and Rothstein, 1957). Taken together, these findings suggests that the critical role Pho4 plays in *C. albicans* during alkaline pH stress is in phosphate acquisition.

5.3.2 Polyphosphate and stress resistance in *C. albicans*.

In addition, the presence of certain metabolites in the cell has been shown to enable stress adaptation. For example, in some lower eukaryotes polyphosphate, the stored form of phosphate, which is the only negatively charged anion present in the vacuole and acidocalcisome has great buffering capacities playing a role in overall cell charge, pH regulation and osmoregulation (Weiss *et al.*, 1991; Docampo *et al.*, 2010). In higher eukaryotes, polyP has been found to function as a potent regulator of blood coagulation (Docampo *et al.*, 2014). PolyP function has been most extensively studied in bacteria, where it is linked to multiple processes including

growth, stress responses, development, biofilm formation and virulence. These complex and diverse phenotypes regulated by polyP may be linked to recent findings that polyP functions as a protein chaperone in bacteria (Gray *et al.*, 2014). Less is known however, about polyP function in eukaryotic cells.

One of the many functions attributed to PolyP is in pH buffering. The proposed mechanism for this function in alga for example, is that high pH triggers the rapid hydrolysis of vacuolar polyP to release sequestered protons needed to neutralise alkali ions (Pick and Weiss, 1991). Yeast cells have also been shown to have shorter chains of polyP, indicative of polyP hydrolysis, under high alkaline pH conditions (Greenfield *et al.*, 1987). These shorter lengths of polyP are further hydrolysed to release phosphate which results in the accumulation of sugar phosphates and subsequent restoration of the acidic environment in the cytoplasm (Castrol *et al.*, 1999). It was suggested that the hydrolysis of glycogen to generate acid and ATP may be dependent on polyP hydrolysis in yeast cells (Castrol *et al.*, 1999). Less is known about polyP mobilisation in response to stress in yeast. Two polyphosphatases have been identified in yeast. An exopolyphosphatase, Ppx1 and an endopolyphosphatase, Phm5 (also referred to as Ppn1) (Wurst *et al.*, 1995; Ogawa *et al.*, 2000). Deleting the genes coding for these polyphosphatases did not affect polyP hydrolysis suggesting there are other polyphosphatases present (Lichko *et al.*, 2008). However, *phm5Δ* cells displayed a growth defect which was attributed to the presence of long chains of polyP in the cells (Ogawa *et al.*, 2000; Sethuraman *et al.*, 2001). Interestingly, from this study, *C. albicans* cells lacking the polyphosphatases Ppx1 and Phm5, also had slower growth rate compared to wild-type cells and were significantly larger than the wildtype cells and the *vtc1Δ* and *vtc4Δ* mutants which lack polyP (Fig 5.8). In particular, the *ppx1Δ* mutant displayed a pseudohyphal growth morphology regardless of the growth conditions (Fig 5.8A). These morphological defects observed suggest a defect in cell cycle progression in the *ppx1Δ* and *phm5Δ* cells. In *S. cerevisiae*, *PHO* genes are specifically induced during M phase to meet the metabolic demands of phosphate requirement during mitosis (Neef and Kladdle, 2003). Moreover, the cell-cycle induction of *PHO* genes coincides with decrease in polyP levels. This observation has also revealed that polyP functions as a phosphate reservoir and only once depleted does the cell initiate acquisition of phosphate from external sources. Indeed, polyP has been shown to negatively regulate the PHO pathway during mitosis (Neef and Kladdle, 2003).

Therefore, an inability to effectively mobilise polyP stores, as seen in cells lacking *PPX1* and *PHM5*, may interfere with phosphate acquisition induced during cell cycle thus resulting in defects in cell cycle progression (Fig 5.8C).

In this study, polyP was mobilised in response to alkaline pH stress in wild type *C. albicans* cells (Fig 5.5) however, polyP was dispensable for alkaline pH resistance as inactivating the genes required for polyP synthesis, *VTC1* and *VTC4*, did not impair stress resistance (Fig 5.9A). However, unlike the *C. albicans pho4Δ* cells, phosphate acquisition is not impaired in these mutants (Fig 5.10) which suggests that cells that can acquire phosphate are able to adapt to alkaline pH stress. On the other hand, cells lacking this ability, as seen with *pho4Δ* cells, are extremely sensitive to alkaline pH stress.

Another important function assigned to polyP is in osmoregulation. Studies in trypanosomatid parasites, have established strong links between polyP and osmotic stress responses within these eukaryotic microbes. Exposure of *Trypanosoma cruzi* to hypo-osmotic stress results in the rapid mobilisation of polyP, whereas hyperosmotic stress triggers an increase in poly-P levels (Ruiz *et al.*, 2001). Again as observed for alkaline pH stress, no osmotic stress sensitive phenotypes associated with the *C. albicans* mutants involved in polyP metabolism. In fact, apart from MnCl₂ sensitivity these mutants have no other overlapping stress phenotypes with the *pho4Δ* cells (Fig 5.9). PolyP mobilisation was also noted in *C. albicans* following hypo-osmotic stress (Fig 5.6) however, polyP was also mobilised following hyper-osmotic stress induced by NaCl (Fig 5.7). Nonetheless, none of the results obtained support a physiological role for polyP in *C. albicans* in mediating osmotic stress resistance. PolyP may however, play a role in sequestering Mn²⁺ in *C. albicans* as the *vtc1Δ* and *vtc4Δ* mutants lacking polyP are sensitive to MnCl₂ (Fig 5.9). Consistent with this, *pho4Δ* cells which lack polyP specifically have lower levels of this cation (Fig 5.15).

Finally, in the maize pathogen, *Ustilago maydis*, polyP has been implicated in filamentous growth, as *vtc4Δ* null cells exhibited a constitutively filamentous phenotype (Boyce *et al.*, 2006). However, the analogous *vtc4Δ* mutant in *C. albicans* was not hyper filamentous and, moreover, it was found that polyP synthesis and mobilisation was also dispensable for serum-induced filamentation in this human pathogen (Fig 5.9B).

5.3.3 Phosphate, metal homeostasis and bioavailability.

Metals have essential roles in cell signalling, structure, and enzymatic activities however, in high concentrations within the cell these can be toxic. Very little however, is known about metal homeostasis. What is known is that metals interact with proteins and other organic macromolecules. However, as negatively charged inorganic compounds such as phosphate can also bind metal cations, it is emerging that metal-phosphate interactions play important mechanistic roles in regulating cellular metal homeostasis (Rosenfeld *et al.*, 2010). Based on this, the role of phosphate in metal homeostasis in *C. albicans* was explored extensively in this study. Data generated demonstrate that phosphate accumulation affects metal ion homeostasis in *C. albicans*. Furthermore, this negative impact was found to be responsible for several of the stress-sensitive phenotypes exhibited by *pho4Δ* cells. It was observed that cells lacking Pho4, which cannot accumulate Pi, display altered resistance to a number of metals including alkali and alkaline earth metals (sodium, potassium, and calcium) and transition metals (manganese, iron, and copper). GO term analysis of the genes involved in phosphate homeostasis, identified by the RNA seq analysis carried out in Chapter 4, revealed the GO terms, iron ion transport, and cellular response to zinc ion starvation, were significantly enriched in the gene-set downregulated in *pho4Δ* cells compared to wild-type cells (Fig 5.12). In addition, ICP-MS analysis revealed that the levels of manganese and magnesium (as well as phosphate) are significantly lower in *pho4Δ* cells (Fig 5.15). As discussed above, the role of Pho4 in mediating tolerance to manganese is likely related to the role of polyP in sequestering this metal. Deregulation of phosphate accumulation has been shown to result in defects in ion homeostasis in other fungi. In *S. cerevisiae*, cells lacking the Pho4 negative regulator, the Pho80 cyclin, have constitutively high cytosolic phosphate levels and this has widespread effects on metal cation accumulation, bioavailability and toxicity (Rosenfeld *et al.*, 2010). In particular, the *pho80Δ*-mediated high intracellular phosphate levels resulted in increased intracellular levels of many metal cations, most notably sodium. Consistent with this, a recent study in *C. neoformans* revealed that a triple phosphate transporter mutant (*pho84Δ/pho840Δ/pho89Δ*), exhibited low intracellular phosphate but high intracellular sodium levels, which was attributed to the high sensitivity of this mutant to cationic stress (Kretschmer *et al.*, 2012). In contrast, it was found that lower intracellular phosphate levels has no impact on sodium levels in *C. albicans* (Fig 5.15). Clearly, therefore, the relationship between phosphate accumulation and

intracellular metal levels is complicated. However an emerging theme from these studies is that disruption of an abundant anion such as phosphate can have dramatic effects on the homeostasis of biologically important metals. This strongly underlies the critical role of the Pho4 transcription factor in mediating resistance to metal cations in *C. albicans*.

Results obtained also show intracellular phosphate levels affects the bioavailability of certain metals. In particular, the acute sensitivity of *pho4Δ* cells to the superoxide generating drug menadione, was found to be connected to defects in the activity of the copper/zinc superoxide dismutase Sod1. Both the *CTR1* copper transporter and *FRE7* cupric reductase encoding genes, which together form a high-affinity copper import system, are downregulated in *pho4Δ* cells compared to wild-type cells under phosphate replete conditions. Indeed, in contrast to other cations, cells lacking Pho4 appear resistant to copper compared to wild-type cells (Homann *et al.*, 2009). Strikingly, however, ICP-MS analysis revealed that there are actually slightly higher levels of copper in *pho4Δ* cells (127%) compared to wild-type cells. Despite the presence of copper, the activity of the Sod1 superoxide dismutase is impaired in *pho4Δ* cells. Moreover, the cells appear to adapt to this by increasing the expression of three of the four copper-containing *C. albicans* SOD genes, *SOD1*, *SOD5* and *SOD6*. As the major target for copper in eukaryotic cells is the Sod1 copper/zinc superoxide dismutase (Nevitt *et al.*, 2012), it appears that although copper is present in cells lacking *PHO4*, its bioavailability is restricted. This hypothesis is supported by the observations that supplementation of the growth media with excess copper restores both Sod1 activity and resistance to menadione in *pho4Δ* cells.

Yeast cells tightly regulate copper uptake and storage due to the ability of copper to participate in redox reactions and to compete with zinc or iron-sulphur clusters for cysteine-rich metal binding sites. In *C. albicans*, as in *S. cerevisiae*, copper limiting conditions triggers activation of the Mac1 transcription factor which drives the expression of copper acquisition genes such as *CTR1* and *FRE7* (Marvin *et al.*, 2004). Resistance to excess copper is provided by the Crp1 P1-type ATPase copper transporter, and the copper metallothioneins Cup1 and Crd2 (Riggle and Kumamoto, 2000; Weissman *et al.*, 2000). The expression of *CRP1* and *CUP1* is induced in high copper environments, whereas *CRD2* expression is seemingly insensitive to copper levels (Riggle and Kumamoto, 2000; Weissman *et al.*, 2000). As intracellular copper levels are maintained at extremely low levels, copper chaperones are necessary to

deliver copper to target enzymes and, in *C. albicans*, the Ccs1 copper-chaperone transfers copper to the copper containing Sod1 enzyme (Gleason *et al.*, 2014). The RNA-Seq data generated in this study was examined to see whether any of the aforementioned genes involved in copper homeostasis are deregulated in *pho4Δ* cells. As described above, the *CTR1* and *FRE7* genes, necessary for high affinity copper transport, are both downregulated in the *pho4Δ* mutant compared to wild-type cells. Intriguingly, although these genes are dependent on the Mac1 transcription factor, a slight (2 fold) increase in *MAC1* transcript levels was seen in cells lacking *PHO4*. Perhaps most significant, however, is the upregulation of the *CRD2* copper metallothionein gene (4.7 fold) in *pho4Δ* cells. This could possibly provide a mechanism underlying the apparent biological unavailability of copper in *C. albicans pho4Δ* cells. Further investigations into the relationship between phosphate and copper homeostasis are clearly warranted, as whilst copper is vital for important fungal proteins such as copper containing Sods, iron transporters and cytochrome c oxidase, the fact that excess copper is highly toxic to the cell is exploited by phagocytes as an antimicrobial defense mechanism (Ding *et al.*, 2014).

In conclusion, this study has revealed that the Pho4 transcription factor in the major fungal pathogen, *C. albicans* plays multifaceted essential roles in promoting resistance to superoxide, cationic, and alkaline pH stresses. The role of Pho4 in phosphate acquisition is essential for adapting to alkaline pH while its role in phosphate homeostasis enables cells adapt adequately to superoxide and cationic stress. More importantly, as many of the Pho4-attributed phenotypes relate to the role of phosphate in regulating metal homeostasis, this study has uncovered a further layer of regulation in this process in *C. albicans*. Based on these important roles for Pho4 in stress resistance the next major objective was to explore whether this stress protective role was extended to mediating virulence in *C. albicans*.

Chapter 6. The role of Pho4 in virulence

6.1 Introduction.

The role of phosphate signalling pathways in virulence has been established in bacterial pathogens such as *Shigella* and *Salmonella* (Kim *et al.*, 2002). In pathogenic *E. coli*, the PhoR-PhoB regulon governs the expression of virulence determinants (Lamarche *et al.*, 2008). In eukaryotic pathogens such as *Trypanosoma brucei*, deleting *VTC4* which encodes the enzyme responsible for synthesizing polyP, reduces cellular polyP content and the capacity of this parasite to infect mice (Lander *et al.*, 2013). A recent study in the fungal pathogen *Cryptococcus neoformans*, further illustrates that phosphate acquisition is essential for virulence as deleting three the phosphate transporters significantly prevented infection in a mouse model of cryptococcosis (Kretschmer *et al.*, 2014).

In the human host, most phosphate (85%) is stored in bones, 14% in cells and soft tissues, with the remaining 1% found in extracellular fluids (Alon and Chan, 1993). Inorganic phosphate concentration in the serum ranges from 2.5 - 4.5 mg/L in adults (Alon and Chan, 1993). Furthermore the phosphate available in extracellular fluids is bound to proteins. Thus, phosphate in the host is not readily available to pathogenic organisms during infection. It is therefore vital for cells to possess sophisticated mechanisms to acquire and maintain phosphate homeostasis. It is not surprising therefore that pathogenic microorganisms have evolved several strategies to obtain phosphate from the host during infection. For example, in *C. albicans*, using *in vivo* and *ex vivo* comparative genome - wide transcriptional profiling experiments, the expression of *PHO84*, involved in phosphate acquisition was upregulated during infection of the liver and in reconstituted human oral epithelium (RHE) model of infection (Thewes *et al.*, 2007; Zakikhany *et al.*, 2007). This is further supported by *in vivo* experiment where *PHO100* and *GIT3*, required for external phosphate scavenging, were required for virulence in a mouse model of infection (MacCallum *et al.*, 2009; Bishop *et al.*, 2013).

This study identified and established a role for the *C. albicans* Pho4 transcription factor in phosphate metabolism which in turn was found to impact on metal homeostasis and stress resistance in this major fungal pathogen. However, the importance of this transcription factor in mediating *C. albicans* virulence is unknown.

Therefore, the role of Pho4 in mediating virulence in *C. albicans* was extensively investigated using a range of infection models. A further objective of this chapter was to use the model mini host *C. elegans* to examine whether the immune status of the host impacted on the stress-protective virulence requirements of the pathogen.

6.2 Results.

6.2.1 Pho4 is required for *C. albicans* survival following phagocytosis by macrophages.

As cells lacking Pho4 are exquisitely sensitive to stresses encountered following phagocytosis, such as superoxide anions, cationic fluxes, and pH fluctuations, the impact of *PHO4* loss upon *C. albicans* - macrophage interactions was initially investigated. First, a role of Pho4 in promoting *C. albicans* survival following phagocytosis by J774.1 macrophages was examined. Cells lacking *PHO4* were exquisitely sensitive to macrophage-mediated killing compared to the wild-type cells ($p < 0.01$) (Fig 6.1). Despite being taken up at the same rate (Fig 6.2), less than 20% of *pho4Δ* cells survived phagocytosis by J774.1 cells compared to wild-type and reconstituted *pho4Δ+PHO4* cells (Fig 6.1A). Also significant, was the full restoration of virulence capacity on re-integrating *PHO4* into the mutant strain (Fig 6.1). To further explore the importance of Pho4 in mediating *C. albicans* survival following phagocytosis, a detailed analysis of the interaction of macrophages co-cultured with wild-type, *pho4Δ* or *pho4Δ+PHO4* *C. albicans* cells was performed using live cell video microscopy. This technology allows minute by minute analysis of the interaction of macrophages with *C. albicans* cells providing details about the rate at which the cells were engulfed by macrophages, hyphal formation inside the phagosome, as well as the ability of the engulfed cell to lyse the macrophage. From the data generated, no significant differences were found between the migration rate of J774.1 macrophages towards wild-type (mean \pm SEM; 0.65 ± 1.01 $\mu\text{m}/\text{min}$) or the *pho4Δ* mutant (0.63 ± 0.99 $\mu\text{m}/\text{min}$) cells (Fig 6.2A), or in fungal uptake (Fig 6.2B). In fact, cells lacking *PHO4* were engulfed slightly more quickly than wild-type cells (Fig 6.2C). The ability to kill macrophages was then determined by calculating the percentage of macrophages lysed by each strain. Looking at survival, 80% of the J774.1 macrophages survived co-culture with *pho4Δ* cells compared to wild-type and *pho4Δ+PHO4* cells (Fig 6.3).

As cells lacking the Pho4 transcription factor are extremely sensitive to macrophage killing (Fig 6.1), the ability of *pho4Δ* cells to filament, an important virulence determinant, within the macrophage was explored. The *pho4Δ* yeast cells had a reduced ability to form hyphal filaments within the phagosome (Figs 6.4A, B & C). An additional observation made, was that in a small number of cases, the hyphae formed by *pho4Δ* cells seemed very flexible and, rather than pierce the macrophage, appeared to be easily bent by the macrophage (Fig 6.5). For every 100 macrophage/*C. albicans* events examined this occurred 5 times (5%) with *pho4Δ* cells, once (1%) with the *pho4Δ+PHO4* reconstitute, but was never observed with wild type cells. Collectively, therefore, these results show that cells lacking *PHO4* are unable to survive macrophage-mediated killing, and cannot effectively form hyphae following phagocytosis.

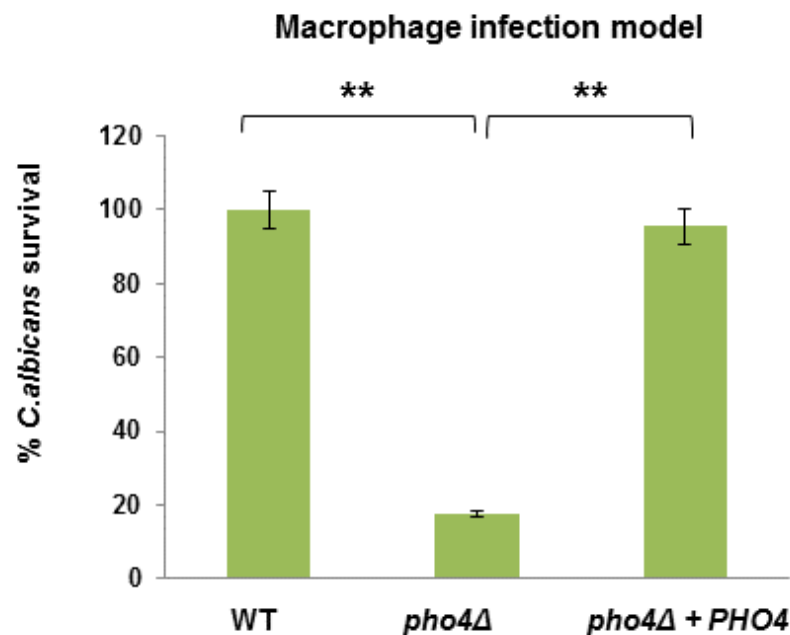


Fig 6.1 Pho4 is required for virulence in a macrophage model of infection. Macrophage model of infection. Percent of *C. albicans* killed following co-incubation with J774.1 macrophages. Data were obtained in triplicate from 3 separate biological replicates and ANOVA was used to determine statistical significance (** $P < 0.01$).

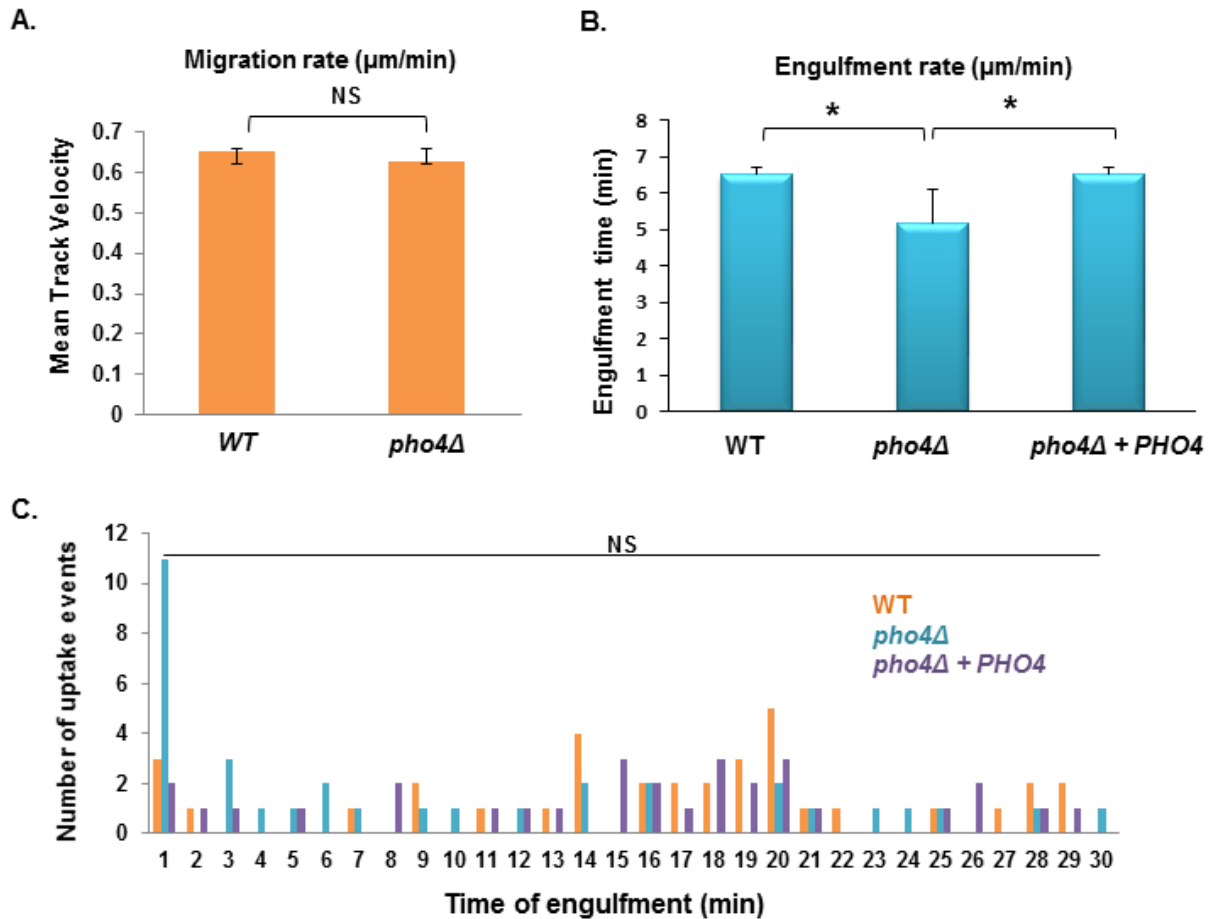


Fig 6.2 Uptake of *C. albicans* cells is not affected by *PHO4* deletion. (A) The migration rate of macrophages toward *pho4* Δ cells is not impaired by gene deletion. (B) Loss of *PHO4* enhanced the rate of engulfment of *pho4* Δ cells by macrophages. (C) Percentage of uptake events during a 30 min incubation period of J774.1 macrophages with *Wt*, *pho4* Δ and *pho4* Δ +*PHO4* cells. Individual J774.1 macrophages were co-cultured with *Wt*, *pho4* Δ , or *pho4* Δ +*PHO4* cells and tracked using Volocity 6.3 software. ANOVA was used to determine statistical significance (* $P \leq 0.05$), NS = no significant difference.

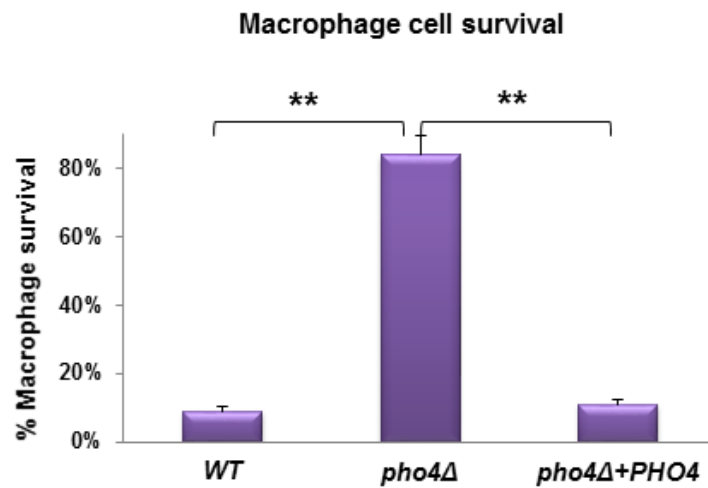


Fig 6.3 J774.1 cells survive co-culture with *pho4Δ* cells. Macrophage survival. This was determined by detecting the number of ruptured macrophages following co-culture with the *pho4Δ* mutant and wild-type and reintegrand controls. ANOVA was used to determine statistical significance (** $P \leq 0.01$).

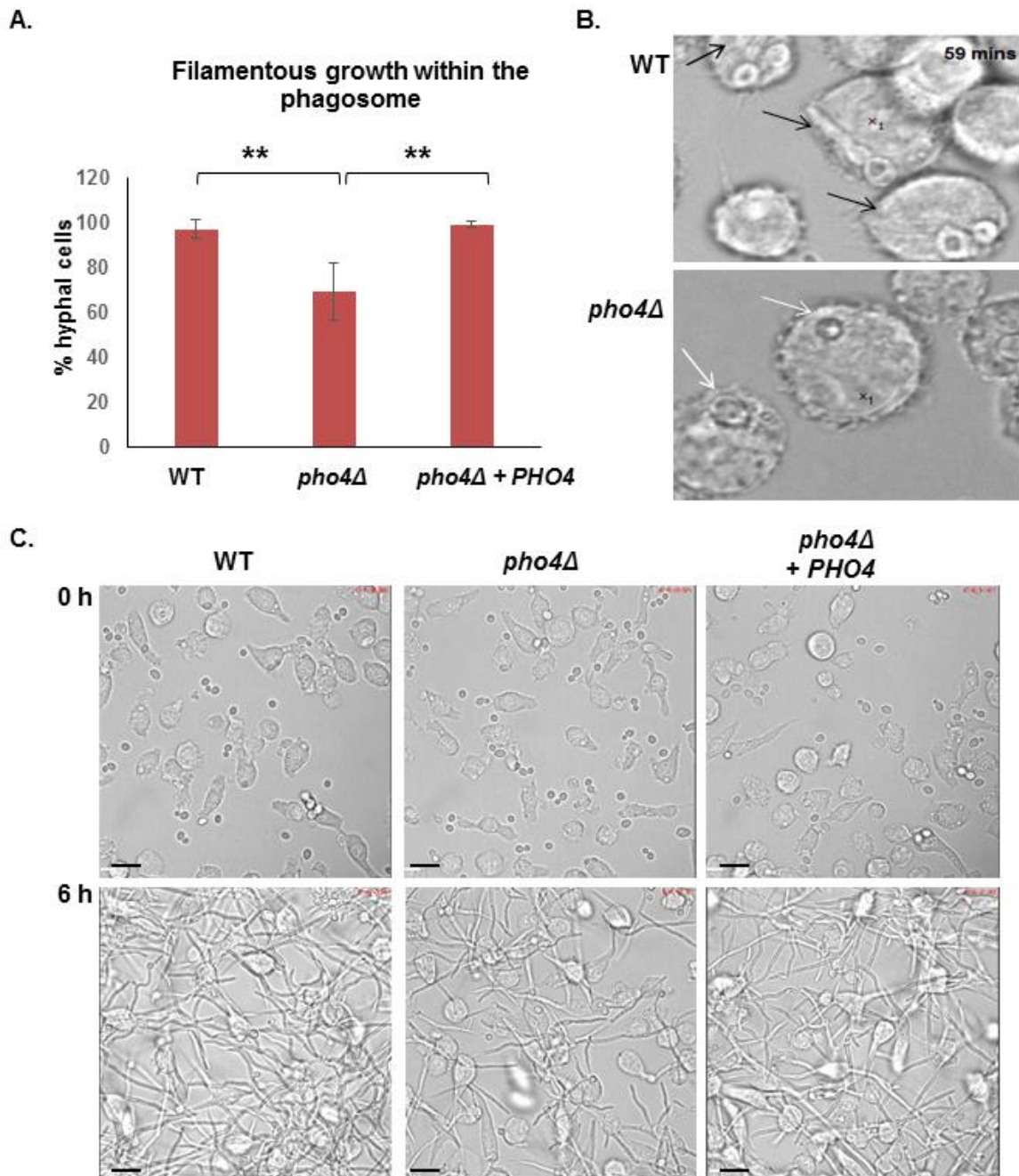


Fig 6.4 Defect in hyphal formation associated with Pho4 loss (A) Percentage of *C. albicans* cells that undergo filamentation following phagocytosis. (** $P \leq 0.01$). **(B)** Cells lacking *PHO4* display defective intracellular hyphal formation following phagocytosis. Images were taken from videos made using a spinning-disk confocal microscope. The numbers in the upper right corner of each image show the time of the phagocytic events. Black arrows indicate the positioning of *C. albicans* hyphal cells within the macrophage, whereas white arrows indicate non-filamentous *C. albicans* cells. **(C)** Less hyphal formation by the *pho4Δ* cells 6 h post co-incubation with J774.1 macrophages. Scale bar 17μm.

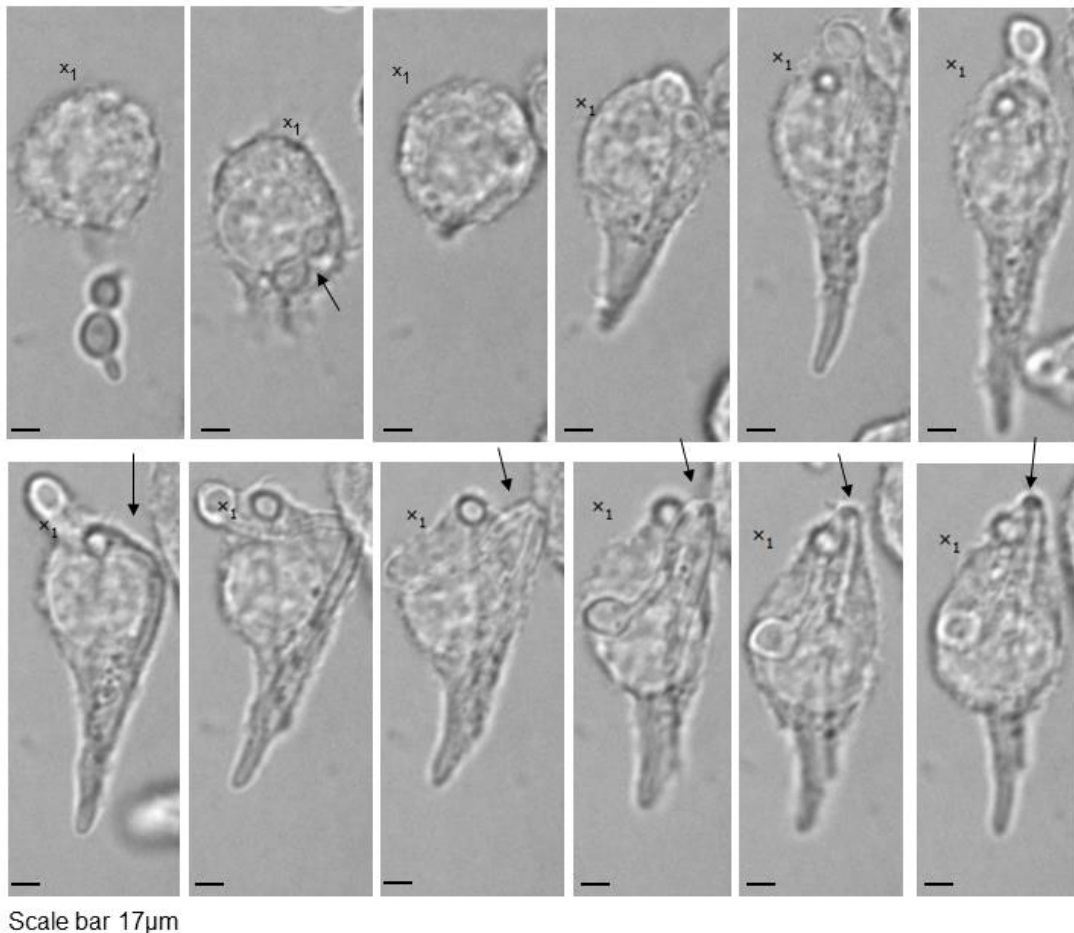


Fig 6.5 Deletion of *PHO4* in *C. albicans* increases susceptibility to macrophage killing. The J774.1 macrophages were able to bend the hyphae formed by *pho4* mutant. Arrows show the process of bending the hyphae of a *pho4*Δ cell.

6.2.2 *Pho4* is required for disseminated systemic infection in a mouse model of infection.

Following the finding that Pho4 was required for survival following phagocytosis by macrophages, the role of Pho4 in *C. albicans* virulence in a systemic model of infection was examined using the three day murine intravenous challenge model (MacCallum *et al.*, 2009; MacCallum *et al.*, 2010). Experiments were carried out by Dr Donna MacCallum, Aberdeen University. This model combines weight loss and kidney fungal burden measurements following 3 days of infection to give an ‘outcome score’. A higher outcome score is indicative of greater virulence. Mice infected with *pho4*Δ cells had a significantly lower outcome score than *Wt* cells ($p < 0.01$) (Fig 6.4A). However, this virulence defect was only partially restored in mice infected with the *pho4*Δ+*PHO4* reconstituted strain (Fig 6.4A). This is possibly due to haploid insufficiency, as reintroduction of *PHO4* only partially rescued the acid phosphatase defect of *pho4*Δ cells (Fig 5.2). It was also observed that loss of *PHO4* had an impact on weight loss but did not significantly affect fungal burdens in the kidney of mice (Fig

6.4B & C). Interestingly, similar findings were recently reported in *C. neoformans*, in which cells defective in phosphate acquisition displayed attenuated virulence in a murine model of cryptococcosis yet the fungal load in lungs and brain was comparable to that of wild-type cells (Kretschmer *et al.*, 2014). However, these results demonstrate Pho4 is required for virulence in macrophage and mouse models of infection strongly indicating this transcription factor has an important role in the pathogenesis of *C. albicans*.

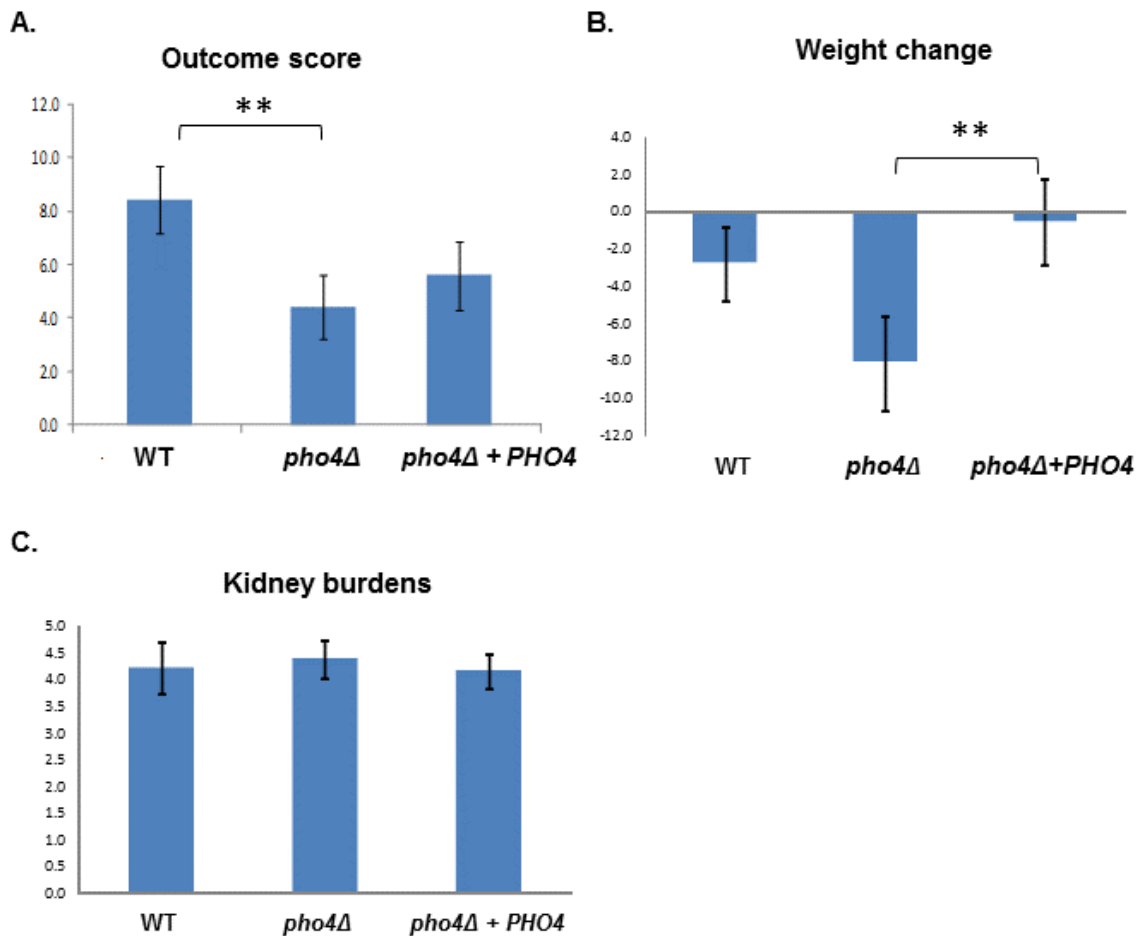


Fig 6.6 Pho4 is required for *C. albicans* virulence in a mouse model of infection. Outcome score measurements of mice (n=6) infected with the indicated strains. Comparison of *Wt* and *pho4Δ* infected groups by Kruskal-Wallis statistical analysis demonstrated a significant difference with *pho4Δ* infected mice giving a significantly lower outcome score (A), percentage weight loss (B), and kidney fungal burden measurements (C) of mice infected with *Wt*, *pho4Δ*, or *pho4Δ+PHO4* cells. Pairwise comparisons (Mann-Whitney U) demonstrates significant differences between *Wt* and *pho4Δ* cells for weight loss and outcome score but not kidney fungal burden measurements. (** $P < 0.01$).

6.2.3 *Pho4* is required for virulence in an immunocompetent, but not immunocompromised, *C. elegans* nematode host.

The above investigations revealed *Pho4* is required for virulence in mouse systemic model of infection which may be attributed to *pho4Δ* cells being sensitive to macrophage killing. Consistent with this is the exquisite sensitivity of *pho4Δ* cells to the chemical defences employed by the innate immune system. Therefore, we explored whether *Pho4* was required for virulence in an immunocompromised host. The model chosen to explore whether the status of the host's innate immune defences determined the importance of stress resistance in promoting fungal virulence was the nematode *C. elegans* due to its ease of use in the lab. Furthermore, typical characteristics associated with *C. albicans* infection in the human host are displayed during worm infection. For example, *C. albicans* grows in the filamentous form and is capable of piercing and damaging worm tissue leading to its death and also grows in the yeast form to disseminate from point of entry (the mouth) to the mucosal surfaces in the worm where proliferation causes massive distension of the worm body (Pukkila-Worley *et al.*, 2009). The p38 MAPK pathway which governs the innate immune defense against infection in mammals is conserved in this nematode (Pukkila-Worley *et al.*, 2012; Kruz and Tan, 2004). *C. elegans* response to infection depends upon the activity of PMK1, the worm homologue of p38 MAPK leading to the activation of antifungal innate immune effector genes for example, *FIPR-22/23*, *CNC-4*, and *CNC-7* (Pukkila-Worley *et al.*, 2012; Kruz and Tan, 2004). The *C. elegans* p38 MAP kinase pathway consists of NSY1 (MAPKKK), SEK1 (MAPKK), and PMK1 (MAPK), and previous studies have shown that the *C. elegans* PMK1 pathway is essential for defence against pathogens. Being genetically tractable, immunocompromised *C. elegans* worms have been created in which either *SEK1*, responsible for activating PMK1 or *PMK1* has been deleted. *C. elegans pmk1* mutants are extremely susceptible to infection with microbial pathogens, *C. albicans* included (Iraozqui *et al.*, 2010; Aballay *et al.*, 2003; Pukkila-Worley *et al.*, 2012).

Age-synchronised L4 stage young adult wild-type sterile worms (*glp-4*) or immunocompromised mutant worms lacking a functional PMK1 pathway (*glp-4::sek-1*) were transferred from lawns of the *E. coli* strain OP50, which is the normal laboratory food, to lawns of wild-type, *pho4Δ*, or *pho4+PHO4* cells grown on solid Brain Heart Infusion (BHI) agar media, and monitored daily for viability. As illustrated in Fig 6.7A, the survival rate of immunocompetent *glp-4 C. elegans* was significantly

higher in worms fed the *pho4Δ* cells compared to those fed the wild-type and reconstituted strains ($P < 0.001$). Thus Pho4, similar to that seen in the murine infection models described above, is important for *C. albicans* virulence in the *C. elegans* model of infection. Strikingly however, Pho4 was dispensable for *C. albicans* virulence upon infecting immunocompromised *sek-1* mutant worms; here similar survival kinetics were observed upon infection with wild-type, *pho4Δ*, or *pho4+PHO4* reconstituted *C. albicans* cells (Fig 6.7B). These findings, therefore, illustrate that whilst Pho4 is required for virulence in immunocompetent worms, in equivalent immunocompromised hosts *pho4Δ* cells are equally as virulent as wild-type *C. albicans*.

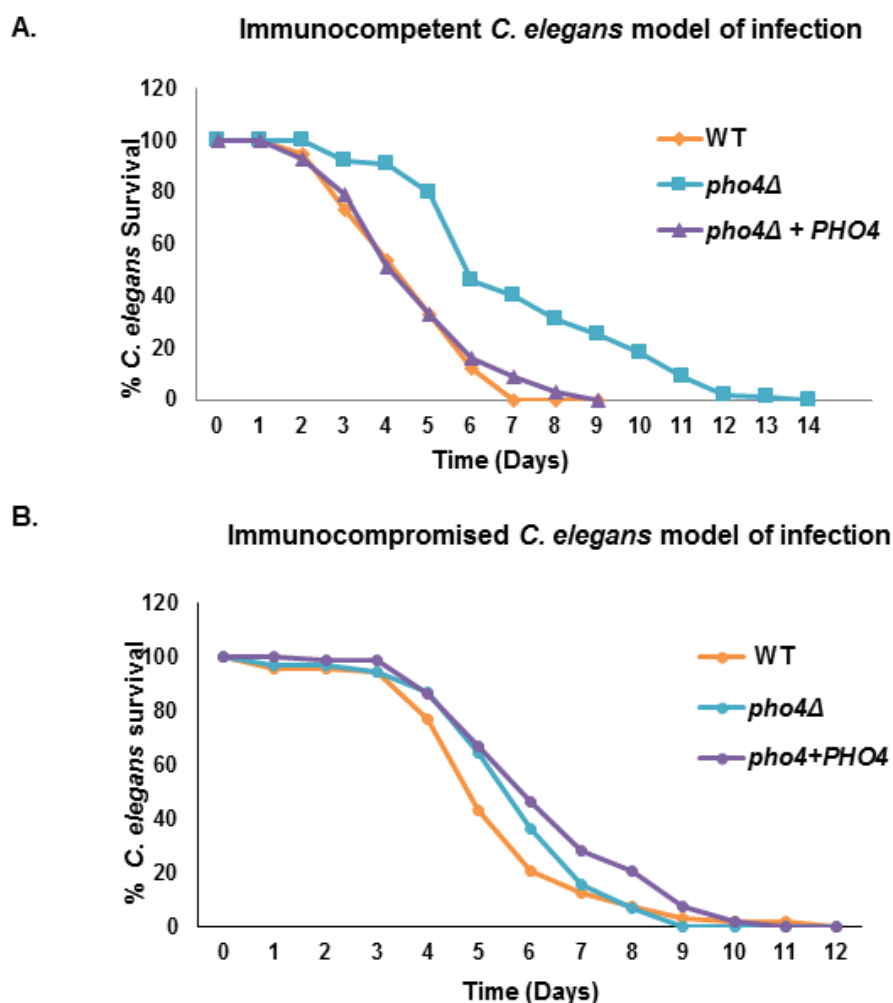


Fig 6.7 Pho4 is required for *C. albicans* virulence in immunocompetent, but not in immunocompromised, *C. elegans* worms. (A) In an immunocompetent *C. elegans* (*glp4*) host, *C. albicans* cells lacking *PHO4* displayed significantly reduced killing of the nematodes compared to Wt and reconstituted strains ($P < 0.001$) **(B)** In an immunocompromised *C. elegans* (*glp4 sek1*) host, Pho4 was dispensable for virulence. 60 – 70 nematodes were infected with the indicated strains and survival monitored daily. These data are from a single experiment representative of three independent biological replicates.

Based on this finding we wondered if the immune status of the host determined the importance of virulence determinants in the pathogen. And if yes, another question raised was is this outcome restricted to Pho4 or extended to other stress regulators. To explore this, the role of SAPK Hog1, required for virulence in various models of immunocompetent hosts, was examined in an immunocompromised host. Survival of wild-type *C. elegans* worms was significantly prolonged when maintained on *hog1Δ* cells compared to both wild-type and *hog1Δ+HOG1* reconstituted strains (Fig 6.8A). In contrast, *sek-1* mutant worms displayed similar survival kinetics when fed with wild-type, *hog1Δ* or *hog1Δ+HOG1* cells (Fig 6.8B). Therefore, like Pho4, Hog1 was only required to kill the immunocompetent worms (Fig 6.8A).

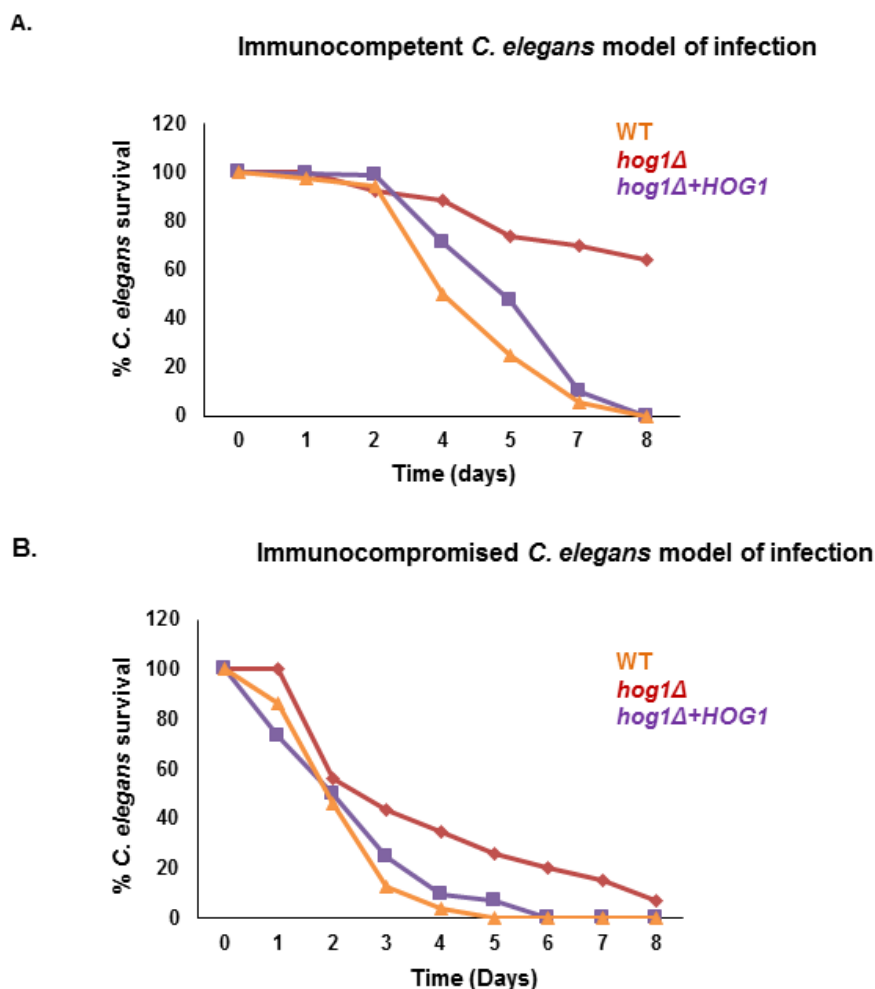


Fig 6.8 Hog1 is required for *C. albicans* virulence in immunocompetent, but not in immunocompromised, *C. elegans* worms. (A) In an immunocompetent *C. elegans* (*glp4*) host, cells lacking *HOG1* displayed significantly reduced killing of the nematodes compared to WT and reconstituted strains ($P < 0.001$) (B) In an immunocompromised *C. elegans* (*glp4 sek1*) host, Hog1 was dispensable for virulence. 60 – 70 nematodes were infected with the indicated strains and survival monitored daily. These data are from a single experiment representative of three independent biological replicates.

6.2.4 *C. elegans* Pmk1 is activated and declines over time during *C. albicans* infection.

Following the finding that the stress protective regulators Hog1 and Pho4 were only required for virulence in immunocompetent but not immunocompromised worms, we explored activation of innate immune responses in the worm following *C. albicans* infection. Specifically, the activation of *C. elegans* PMK1, which can be detected via phosphorylation on the conserved TGY motif, can be easily monitored using antibodies raised against the phosphorylated mammalian p38 SAPK. Western blotting of whole cell extracts from *C. elegans* maintained on *C. albicans* revealed that phosphorylated PMK-1 can be detected following infection with *C. albicans* (Fig 6.9A). However, the level of phosphorylated PMK1 appears to decrease over the time course of infection (Fig 6.9A). This contrasts to that seen in *C. elegans* worms maintained on the non-pathogenic food source *E. coli* OP50 (Fig 6.9B), as the levels of phosphorylated PMK-1 do not fluctuate throughout the course of the experiment. As previously stated, the PMK1 pathway plays an important role in protecting *C. elegans* from *C. albicans* infection. We found that the levels of active PMK1 appeared to decline during the time course of infection studied which may explain the increased killing of *C. elegans* seen at the later time points during infection (Fig 6.7 & 6.8). More precisely, we see reduced levels of PMK1 by day 3 of *C. albicans* infection (Fig 6.9A) which coincides with the significant increase in worm killing seen by day 3 of the survival curves (Fig 6.7; Fig 6.8). More importantly, this also explains the more rapid killing of the worms lacking a functional PMK1 protein kinase (Fig 6.7B; Fig 6.8B).

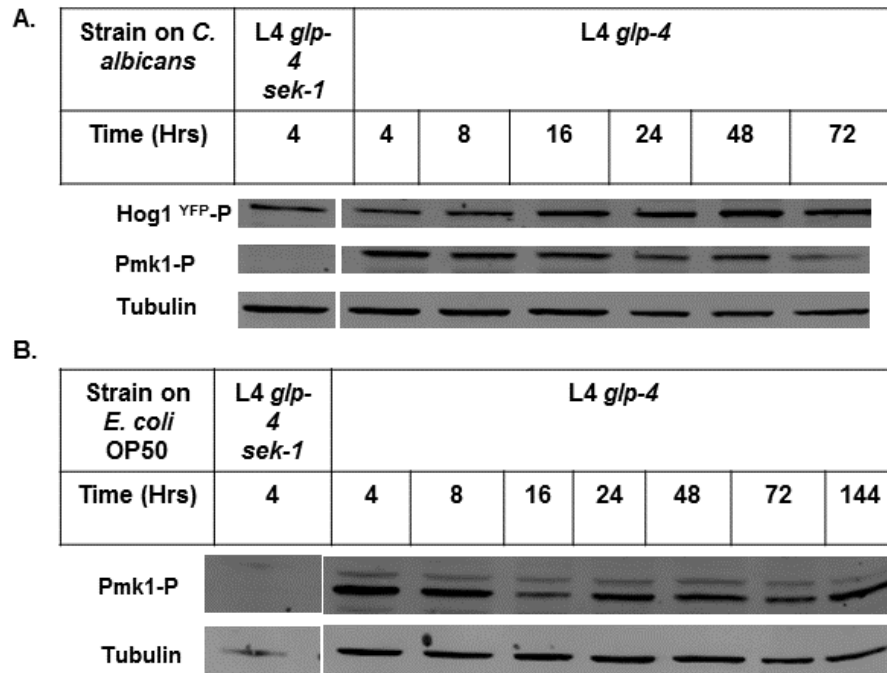


Fig 6.9 Phosphorylation status of *C. elegans* and *C. albicans* SAPKs following infection. (A) Phosphorylated Pmk1 levels in worms maintained on *C. albicans* demonstrate a reduction in Pmk-1-P levels following infection. Western blot analysis of whole cell extracts isolated from L4 *glp-4* (*km4*) worms fed *C. albicans* wild-type cells expressing Hog1^{YFP} at the indicated times. Blots were probed with an anti-phospho p-38 antibody which recognises the phosphorylated form of *C. albicans* Hog1^{YFP} (Hog1^{YFP}-P) and the phosphorylated form of *C. elegans* Pmk1 (Pmk1-P). *Glp4 sek-1* (*km25*) worms provided a negative control for Pmk1-P, and a worm anti-tubulin antibody was used as a loading control. (B) Phosphorylated Pmk1 levels in worms maintained on *E. coli* OP50 cells do not decline over time. Western blots

6.2.5 *C. albicans* Hog1 SAPK pathway is activated during *C. elegans* infection

Following the finding that Hog1 SAPK is only required for virulence in immunocompetent *C. elegans* we examined whether Hog1 was activated during infection. Hog1, rather than Pho4, was chosen because like PMK1 Hog1 activation via phosphorylation can be monitored with the same antibody raised against the phosphorylated mammalian p38 MAPK. However, as the *C. albicans* Hog1 and *C. elegans* PMK1 SAPKs are very similar in size, worms were fed with *C. albicans* cells expressing a YFP-tagged Hog1 fusion protein which has a significantly greater molecular weight. This size difference allows the phosphorylation status of the nematode and *C. albicans* SAPKs to be detected concurrently. Previous work in the Quinn lab confirmed the functionality of the Hog1-YFP fusion (Smith *et al.*, 2004).

As shown in Fig 6.10 (left panel), *C. albicans* Hog1 SAPK was phosphorylated during the time course of the experiment. However, the possibility that the maintenance of *C. albicans* on the BHI agar plates prior to exposure to *C. elegans* may be stressing the fungus leading to Hog1 activation. To test this, Hog1 activation in *C. albicans* cells maintained under exactly the same conditions only that this set had not been exposed to *C. elegans* was examined first. As shown in Fig 6.10 (right panel), only in the presence of *C. elegans* is the *C. albicans* Hog1 SAPK activated. This indicates that *C. albicans* is responding to infection of *C. elegans* by activating the Hog1 SAPK pathway, which is consistent with the data shown in Fig 6.8 that Hog1 SAPK is essential for virulence in an immunocompetent nematode. However, a functional PMK1 pathway appears dispensable for Hog1 SAPK phosphorylation as Hog1 is activated in the *sek1* mutant worms (Fig 6.9A).

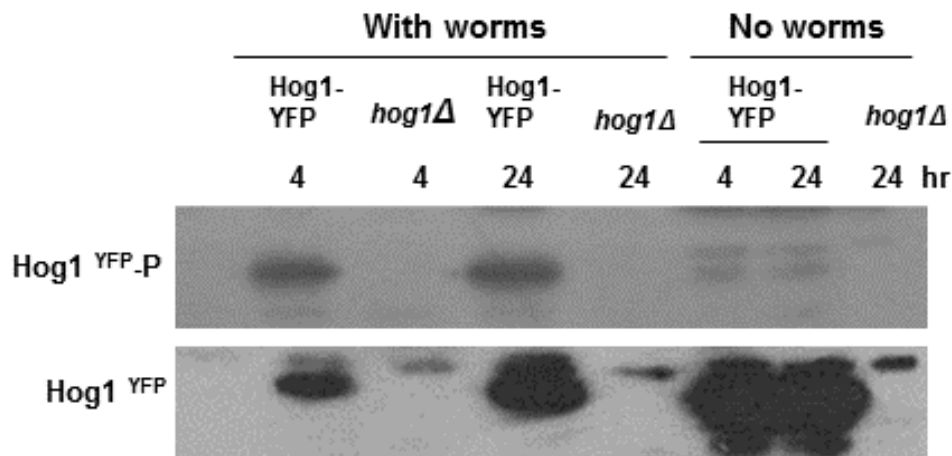


Fig 6.10 *C. albicans* Hog1 SAPK is activated during *C. elegans* infection. *C. albicans* Hog1 is phosphorylated in the presence of *C. elegans*. Protein extracts were prepared from *C. elegans* worms fed *C. albicans* cells and *C. albicans* cells not exposed to *C. elegans*. These were analysed by Western blotting as in Fig 6.9. Blots were probed with an anti-phospho p-38 antibody, stripped and then probed with an anti-Hog1 antibody which recognises both phosphorylated and unphosphorylated forms of Hog1.

Taken together, these preliminary investigations indicate that both Pho4 and Hog1 play an active role in mediating virulence in an invertebrate model of infection and moreover, that robust stress responses of *C. albicans* may only be required for virulence when the host has a fully functional immune system.

6.3 Discussion.

In line with the importance of phosphate acquisition in both bacterial and eukaryotic pathogens, here we report, using a suite of infection models that the Pho4 transcription factor is important for virulence in the major human fungal pathogen, *C. albicans*. This was important as little is known about the role of phosphate acquisition in stress adaptation and virulence in *C. albicans*. For example, we know the genes required for phosphate scavenging, *PHO100* and *GIT3*, are required for virulence in a mouse model of systemic infection but the role of phosphate in virulence is not known (MacCallum *et al.*, 2009; Bishop *et al.*, 2013). This important role of phosphate regulators in virulence has been recently demonstrated in another important human fungal pathogen, *C. neoformans* (Kretschmer *et al.*, 2014). Deleting the three phosphate transporters was required to impede growth on phosphate limiting medium and deletions also resulted in reduced formation of capsule and melanin, both of which are virulence traits in *C. neoformans* (Kretschmer *et al.*, 2014). In addition, the triple mutant was unable to survive phagocytosis by macrophages and displayed attenuated virulence in a mouse model of infection (Kretschmer *et al.*, 2014).

C. albicans is able to survive phagocytosis by macrophages. The *pho4Δ* cells were extremely sensitive to stresses encountered within the phagosome and unable to survive phagocytosis by macrophages therefore, the potential role of Pho4 in enabling this ability was examined. Despite being taken up at the same rate as wild type and reconstituted strains, the *pho4Δ* cells were unable to survive phagocytosis by murine macrophages. In the reciprocal experiment, the majority of the macrophages were able to survive infection with *pho4Δ* cells. Following macrophage engulfment, one of the mechanisms used to escape the phagosome is hyphal formation with which *C. albicans* pierces through the macrophage (Lorenz *et al.*, 2004). On closer examination at hyphal formation in the *pho4Δ* cells while in the phagosome, it was observed that this ability was impaired compared to wild type and reconstituted strains which possibly explains the impaired killing displayed by *pho4Δ* cells. This is consistent with the finding that *pho4Δ* cells display impaired serum-induced hyphal formation *in vitro* (Fig 5.1). Although hyphal formation is not the only mechanism of escape and killing macrophages, hyphal length can make it more difficult for macrophages to engulf candida cells (Lewis *et al.*, 2012) and whilst in the phagosome, *C. albicans* hyphae can stretch the macrophage resulting in lysis (Seider *et al.*, 2010; Gow *et al.*, 2012). Video microscopy revealed *pho4Δ* cells could

not effectively form hyphae while in the phagosome however, when the *pho4* mutant did form hyphae these were bent effectively regardless of hyphal length, an event that never occurred with wild type candida cells. The ease in bending candida hyphae could be as a result of *pho4Δ* possessing a weaker cell wall. The *pho4Δ* cells were specifically resistant to CFW (Fig 5.1) suggesting there is less chitin in the cell wall which may impact on the strength of the cell wall. Cell wall composition and impact on phagocytosis has been demonstrated in another study looking at the glycosylation state of *C. albicans* cell wall. In this case, modification in cell wall composition affected the rate of engulfment of *C. albicans* by mouse macrophages. O-linked and N-linked mannan deficient *C. albicans* mutants were taken up at a faster rate than wildtype and reconstituted strains and also displayed impaired macrophage killing (McKenzie *et al.*, 2010). Cell wall remodelling and impact on macrophage killing has also been recently demonstrated by O`Meara *et al.*, (2015) showing exposing cell-wall glycosylated proteins on the surface of phagocytosed *C. albicans* induced macrophage lysis.

The Pho4 target gene *PHO84* found slightly upregulated (1.8x) during phagocytosis by macrophages (Fradin *et al.*, 2005) provides further evidence that Pho4 is required for surviving the phagosome environment. The phagosome as a phosphate-limiting environment has been implicated in other studies looking at the gene expression of intraphagosomal *Mycobacterium tuberculosis* in which the phosphate transport system was found upregulated (Rengarajan *et al.*, 2005). However, as other Pho4 target genes were not found to be significantly induced following phagocytosis (Fradin *et al.*, 2005), it is likely that it is the essential requirement of Pho4 in regulating phosphate homeostasis that is important to resist high levels of superoxides and cations. This is further supported by the finding that Sod1, which this study found requires Pho4 function for activity, is important for *C. albicans* survival following phagocytosis (Hwang *et al.*, 2002). Collectively, these results demonstrate Pho4 through its vital roles is required to survive phagocytosis.

Extensive investigations also revealed this transcription factor to be essential in mediating virulence in both nematode and mouse models of infection. This is consistent with previous studies demonstrating that the Pho4 target genes, *GIT3* and *PHO100*, are required for full virulence in murine systemic models of candidiasis (Bishop *et al.*, 2013; MacCallum *et al.*, 2009). Interestingly, a recent study which also employed the nematode infection model, reported that loss of Pho4 enhanced the

virulence of *C. albicans*. However, this previous study employed low phosphate growth conditions, which triggered enhanced filamentation in *pho4Δ* cells (Romanowski *et al.*, 2012) (Romanowski *et al.*, 2012) (Romanowski *et al.*, 2012) (Romanowski *et al.*, 2012) (Romanowski *et al.*, 2012) (Romanowski *et al.*, 2012). As filamentation is a virulence determinant in *C. elegans* infection model (Pukkila-Worley *et al.*, 2009), it is likely that this enhanced filamentation underlies the reported enhanced virulence of *pho4Δ* cells (Romanowski *et al.*, 2012). In this study, under phosphate-rich conditions, *pho4Δ* cells clearly demonstrated reduced virulence in the *C. elegans* infection model (Fig 6.7A). More importantly, data from this study has revealed phosphate homeostasis impacts on the ability of *C. albicans* to resist physiologically relevant stresses which include superoxide, cationic, and alkaline pH stresses.

The host innate immune system is responsible for protection against disseminated candidiasis. Therefore a compromised immune system increases the risk for developing candidiasis. The role of the innate immune system in preventing *C. albicans* infection has been demonstrated using various models in which one aspect of the innate immune response has been modified. These models on the other hand, also provide details of *C. albicans* response to defense mounted by the host. During infection, proteomic studies using oral and vaginal epithelial cells have provided evidence that the mammalian p38 MAPK and NF- β (nuclear factor kappa-light-chain-enhancer of activated B cells) signalling pathways are activated in the presence of candida cells (Moyes *et al.*, 2010; Moyes *et al.*, 2011). Activation of these immune response signaling pathways led to neutrophil recruitment and protection against *C. albicans* infection (Schaller *et al.*, 2006).

In this study the importance of the host innate immune defence in determining the virulence factor repertoire required for *C. albicans* infection was explored. Specifically, if innate immune defences were diminished would robust stress responses still be required in the fungus to survive. To study the interplay between host immune system and pathogenic organisms, most studies have used immunocompetent host models. In the *C. elegans* infection model, previous work has demonstrated that a specific immune response to *C. albicans* infection is initiated by upregulating the expression of antifungal genes and repressing those involved in antibacterial defense (Pukkila-Worley *et al.*, 2012). Repression of antibacterial genes was suggested to be mediated directly by *C. albicans* and not by *C. elegans* (Pukkila-

Worley *et al.*, 2012), possibly to increase virulence. Data obtained from this study suggests that a robust immune system is required to combat *C. albicans* infection as the immunocompromised *sek-1* worms were more rapidly killed compared to immunocompetent worms. Even the *pho4Δ* and *hog1Δ* cells which lacked the ability to kill immunocompetent worms were able to kill the immunocompromised ones at a similar rate to wild type and reconstituted strains. This finding is particularly significant as this provides the first evidence that the immune status of the host may impact on stress-associated virulence factors.

In trying to decipher the mechanism behind this impaired immune protection it was observed that activated PMK1 seemed to decline in *C. elegans* during *C. albicans* infection and this may be responsible for the increased susceptibility of the worms to *C. albicans* infection. This decline in PMK1 function has been observed in aging *C. elegans*, which is attributed to play a major contribution to the mechanism underlying immunosenescence, and the increased susceptibility of elderly worms to bacterial infection (Youngman *et al.*, 2011). The decline in PMK1 levels may be a direct consequence of *C. albicans* infection which could be mediated by stress regulators of *C. albicans*, for example Hog1 SAPK shown to be essential for virulence. We see Hog1 SAPK activated in both immunocompetent and immunocompromised worms but in the immunocompromised worms Hog1 activation may only be required at the initial stages of the infection and therefore is not sustained as infection progresses due to lack of host immune defence. However, more studies are required to establish the role of stress regulators in pathogenesis, for example will the decline in PMK1 levels over the course of infection still occur in worms infected with *C. albicans* *hog1Δ* cells.

In conclusion, this study has uncovered a significant finding in that the stress regulators, in this case, Pho4 and Hog1 SAPK, in *C. albicans* are only required for virulence in immunocompetent hosts. This is particularly significant because systemic infections caused by *C. albicans* are life-threatening in immunocompromised hosts therefore more investigations could potentially identify ways of boosting the host immune system to prevent infection.

Chapter 7. Final Discussion

7.1 Summary

The overall aim of this study was to identify novel stress response mechanisms, and define their importance in virulence, in the major human fungal pathogen *C. albicans*. This was facilitated by screening two available *C. albicans* deletion collections for cationic, superoxide, and alkaline pH stress-sensitive mutants. GO term analysis of the stress-sensitive mutants identified revealed that both distinct and overlapping cellular processes are employed by *C. albicans* in dealing with these physiologically relevant stresses. Importantly, the QFA screens also identified genes not previously implicated in stress responses, such as the Pho4 transcription factor which was extremely sensitive to all three stress conditions. Further characterisation of Pho4 revealed the transcription factor to be vital for phosphate homeostasis in *C. albicans* which, in turn, impacts on the ability of *C. albicans* to survive a wide range of stresses encountered within the human host. Moreover, this study uncovered links between phosphate metabolism and metal homeostasis in *C. albicans*, which underlies many of the stress sensitive phenotypes exhibited by *pho4Δ* cells. Consistent with the diverse stress sensitive phenotypes displayed by *pho4Δ* cells, this transcription factor was shown to be an important virulence determinant of *C. albicans* in multiple infection models. Finally, studies in the model mini host *C. elegans*, revealed that the competency of innate immune defences plays an important role in defining the importance of stress regulators such as Pho4 in mediating *C. albicans* virulence.

7.2 Global overview of genes required for stress resistance in *C. albicans*.

The characterisation of *C. albicans* responses to physiologically relevant stresses, such as superoxide, cationic, and pH, is challenging due to the overlapping and diverse mechanisms that are likely to be employed. To address these challenges, this study employed an unbiased genome-wide phenotypic screen. Using quantitative fitness analysis two *C. albicans* deletion collections were screened for stress-sensitive mutants and then GO analysis performed to identify enriched cellular processes. This provided a comprehensive overview of the cellular processes that are enriched during the responses of *C. albicans* to cationic, superoxide and alkaline pH stresses. The screens also uncovered many stress regulators, including transcription factors, protein kinases, and GTPases, as having previously

uncharacterised roles in stress resistance, which now provides a framework to define novel stress signalling pathways in *C. albicans*.

For example, an examination of the top ten most sensitive transcription factor mutants revealed that cells lacking Efg1, Rim101, and Pho4 were sensitive to all three stresses examined in this study. Here we have performed an extensive study of Pho4, but an examination into the role of Efg1 and Rim101 in mediating stress resistance warrants further investigation. Efg1 has well characterised roles in regulating hyphal growth (Stoldt *et al.*, 2007), whereas Rim101 is important for the alkaline pH response (Davis *et al.*, 2000a). Data obtained in this thesis revealed that cells in an alkaline pH environment quickly become depleted of internal phosphate stores. Thus the inability of cells lacking Rim101 to adapt to an alkaline environment may result in a sustained defect in phosphate homeostasis which would in turn, based on results in this thesis, result in pleiotropic stress sensitive phenotypes. Further experiments however, are needed to explore this hypothesis. The importance of Efg1 in stress resistance is consistent with studies in both *C. albicans* (Wilson *et al.*, 2007) and *S. cerevisiae* (Park *et al.*, 2005) linking cAMP dependent signalling and stress resistance. However, further investigations are needed to uncover the precise mechanism underlying the stress sensitive phenotypes of *efg1* Δ cells.

7.3 Role of Pho4 in phosphate homeostasis in *C. albicans*.

In this study we chose to focus our investigations on the role of the Pho4 transcription factor which, as stated above, was one of three transcription factors that was highly sensitive to the cationic, superoxide, and alkaline pH stresses employed in this study. Such stress-protective roles of Pho4 were unanticipated, as the Pho4 orthologue in the model yeast *S. cerevisiae*, whilst important for phosphate acquisition and storage (Ogawa *et al.*, 2000), has not been implicated in cationic and superoxide stress resistance. Notably, however, the sequence of *C. albicans* Pho4 is highly divergent to Pho4 in *S. cerevisiae*, with only the DNA-binding domain showing a significant level of conservation (Chapter 3). This prompted the question therefore whether Pho4 in *C. albicans* played any role in phosphate metabolism, or whether this factor had been functionally reassigned to respond to diverse stress conditions in this pathogenic fungus. However, despite the lack of sequence conservation, data presented in this thesis clearly illustrate that Pho4 in *C. albicans*, like that in *S. cerevisiae*, plays a central role in phosphate homeostasis (Chapter 3). *C. albicans*

Pho4 was shown to accumulate in the nucleus under phosphate limiting conditions and activate a suite of phosphate responsive genes, including acid phosphatases, phosphate transporters and genes that regulate polyP synthesis.

Despite the conservation of function of Pho4 in *S. cerevisiae* and *C. albicans*, Pho4 regulation by post-translational modification (PTM) appears to differ between these two species. In *S. cerevisiae*, Pho4 is phosphorylated under phosphate-rich conditions by the Pho80-Pho85 CDK complex which prevents the nuclear accumulation of Pho4. When external phosphate becomes limiting the activity of the CDK complex is inhibited by the CDK inhibitor Pho81, which results in the dephosphorylation of Pho4 allowing its nuclear accumulation and the subsequent activation of phosphate-response genes. In this study, our RNA seq analysis revealed *PHO81* to be induced following phosphate limitation, suggesting that the regulatory role of Pho81 CDK inhibitor in activating Pho4 may be conserved in *C. albicans*. Despite this, however, the CDK target sites on *S. cerevisiae* Pho4 are largely not conserved in the *C. albicans* protein. Moreover, we find that Pho4 is phosphorylated under both phosphate replete and phosphate limiting conditions in *C. albicans*. Strikingly, an additional, phosphatase resistant, PTM is observed under phosphate replete conditions, but not when phosphate levels are limiting. Based on these findings a model of Pho4 regulation and phosphate acquisition and storage in *C. albicans* is proposed (Fig 7.1).

Taken together, the results presented in this study suggest that a distinct mechanism involving a novel PTM regulates the cellular localisation of Pho4 following phosphate limitation in *C. albicans*. Further investigations are required to test this hypothesis, such as an assessment of the role of Pho80, Pho85 and Pho81 in regulating Pho4, and mass spectroscopy coupled with genetic approaches to identify the differing post translational modifications of Pho4 under phosphate replete and limiting conditions.

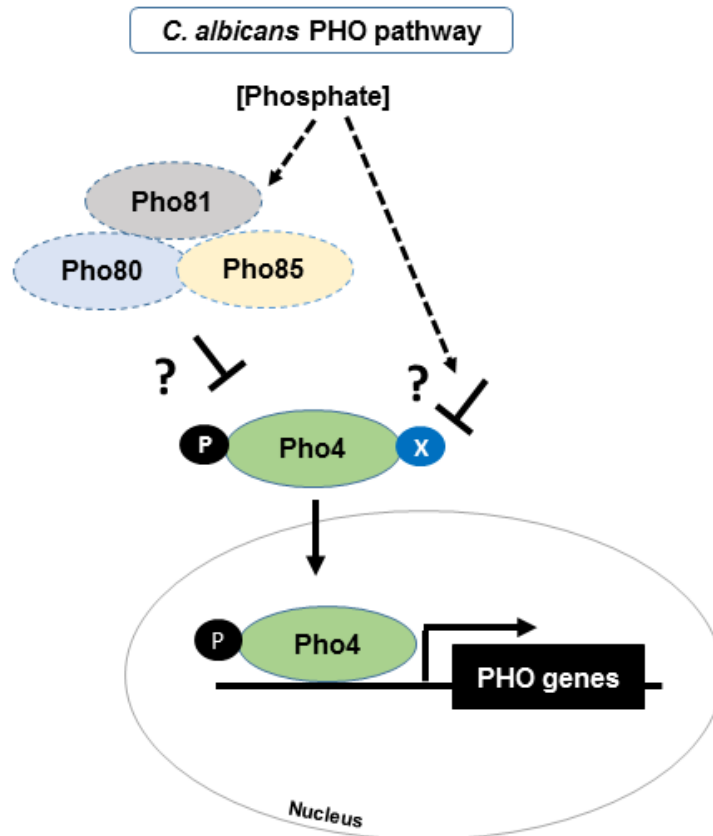


Fig 7.1 Proposed model of phosphate regulation in *C. albicans*. When both internal and external phosphate becomes limiting in *C. albicans*, Pho4 accumulates in the nucleus where it regulates the induction of PHO response genes such as *PHO84*, *PHO100*, *VTC1*, and *GIT3*. In *S. cerevisiae*, Pho4 nuclear accumulation is triggered by its de-phosphorylation, mediated by the inhibitory action of Pho81 on the Pho80/Pho85 CDK complex. In *C. albicans*, *PHO81* is induced following phosphate limitation yet Pho4 remains phosphorylated. However, Pho4 is subjected to an additional, phosphatase resistant, modification (X) in *C. albicans* which is lost following phosphate limitation. Thus *C. albicans* Pho4 may be regulated differently to Pho4 in *S. cerevisiae*.

7.4 Role of Pho4 in stress resistance in *C. albicans*.

Several major conclusions can be made based on the investigations in this study to dissect the role of Pho4 in mediating stress resistance. Firstly, the critical role of the *C. albicans* Pho4 transcription factor to allow survival in both phosphate limiting and alkaline environments, is to induce a gene expression program to allow phosphate acquisition. Secondly, the role of Pho4 in polyP synthesis is largely dispensable for Pho4-mediated stress resistance. Indeed, the only role that could be attributed to polyP from the investigations in this thesis is one of manganese storage. Thirdly, depletion of an abundant anion such as phosphate can affect the homeostasis of biologically important metals. This, we suggest, underlies the critical role of the Pho4

transcription factor in mediating resistance to metal cations in *C. albicans*. Finally, intracellular phosphate levels also impact on the bioavailability of metals such as copper. This is manifested in *C. albicans* by the observation that Pho4 is important for the activity of the copper/zinc Sod1 superoxide dismutase by mediating copper bioavailability, which in turn underlies the acute sensitivity of the *pho4Δ* mutant to superoxide stress.

Thus this study has revealed that many of the unanticipated stress-sensitive phenotypes exhibited by *pho4Δ* cells relate to the impact of phosphate metabolism on metal homeostasis. This is a relatively new concept. In *S. cerevisiae*, constitutive activation of Pho4 was found to cause widespread effects on metal cation accumulation, bioavailability, and toxicity (Rosenfeld *et al.*, 2010). More recently, an analysis of a triple phosphate transporter mutant in *C. neoformans* also revealed multiple effects on intracellular metal levels and toxicity (Kretschmer *et al.*, 2012). As metal acquisition and detoxification strategies are vital for fungal survival at the host/pathogen interface (Ding *et al.*, 2014), the emerging role of phosphate in metal homeostasis clearly warrants further investigation in *C. albicans* and other eukaryotic pathogens.

7.5 Role of Pho4 in virulence in *C. albicans*.

In bacterial pathogens, the PHO pathway has been extensively shown to be essential for phosphate homeostasis and the expression of virulence traits (Lamarche *et al.*, 2008). For example, transcriptional profiling of *Bacillus anthracis* while in the alveolar macrophage indicated genes coding phosphate transporters were upregulated supporting the phagosome as a phosphate limiting environment (Bergman *et al.*, 2007), but more importantly phosphate starvation triggered the expression of virulence traits thereby enhancing the virulence of *B. anthracis* (Aggarwal *et al.*, 2015). In the pathogenic *E. coli* strain, the PhoR-PhoB regulon governs the expression of virulence determinants (Lamarche *et al.*, 2008). Deleting the phosphate transport system (Pst) in various pathogenic strains of *E. coli* (Extra-intestinal pathogenic *E. coli* (ExPEC), Avian pathogenic *E. coli* (APEC), and Uropathogenic *E. coli* (UPEC)) affected resistance to oxidative stress, serum, production of type 1 fimbriae and attenuated virulence (Chekabab *et al.*, 2014). The role of phosphate signalling pathways in virulence has additionally been studied and established in

other important bacterial pathogens such as *Shigella* and *Salmonella* (Kim *et al.*, 2002).

In contrast to the wealth of knowledge linking phosphate homeostasis and virulence in bacterial pathogens, there are relatively few studies exploring this in eukaryotic pathogens. However a recent study in *C. neoformans*, revealed that deleting three phosphate transporters resulted in reduced formation of capsule and melanin, both of which are important virulence traits in this fungal pathogen *C. neoformans* (Kretschmer *et al.*, 2014). Indeed, the triple mutant was unable to survive phagocytosis by macrophages and displayed attenuated virulence in a mouse model of infection (Kretschmer *et al.*, 2014). In contrast, polyP is largely dispensable for virulence in *C. neoformans*, which contrasts with findings in the higher eukaryotic pathogen *Trypanosoma brucei*, in which polyP synthesis was found to be required for full virulence (Lander *et al.*, 2013). In this study, we also demonstrate that phosphate homeostasis is vital for the virulence of the *C. albicans* human fungal pathogen. *C. albicans* cells lacking Pho4, which are unable to accumulate and store phosphate, are acutely sensitive to macrophage-mediated killing, and also display attenuated virulence in both nematode and mouse models of infection. Based on these findings, future investigations could focus on the regulators of Pho4, or downstream targets of this transcription factor, as potential targets for novel antifungal therapies. In this regard it is interesting to note that the *PHO84* phosphate transporter gene, which we show in this study to be regulated by Pho4, has been found to be induced in every experimental infection model reported to date.

Finally, our observations using *C. elegans* as a model host, that stress regulatory proteins such as Pho4 and the Hog1 SAPK, are only vital for virulence in immunocompetent hosts clearly warrants further study. Can such findings be replicated in mammalian infection model systems for example? The concept that the immune status of the host impacts on the virulence determinants of the pathogen is especially important in opportunistic pathogens such as *C. albicans*, as these in general only cause life-threatening systemic infections in immunocompromised hosts.

7.6 Concluding remarks.

C. albicans is exposed to a range of stresses during phagocytosis by host innate immune cells, including reactive oxygen species, cationic fluxes, and fluctuations in

pH. Adaptation to such hostile environments by *C. albicans* requires robust stress responses to ensure survival and pathogenesis. Despite this, however, there is still much to be learnt regarding the stress responsive mechanisms mounted by this major pathogen. In this study we have furthered our knowledge by illustrating that phosphate metabolism, governed by Pho4, impacts on stress responses and the pathogenicity of *C. albicans*. A model summarising the multifaceted roles of Pho4 in mediating stress responses and virulence is shown in Fig 7.2. These findings provide a novel example of how metabolic adaptation promotes *C. albicans* survival in the face of host-imposed stresses, which will hopefully open new avenues for the development of new antifungal therapies.

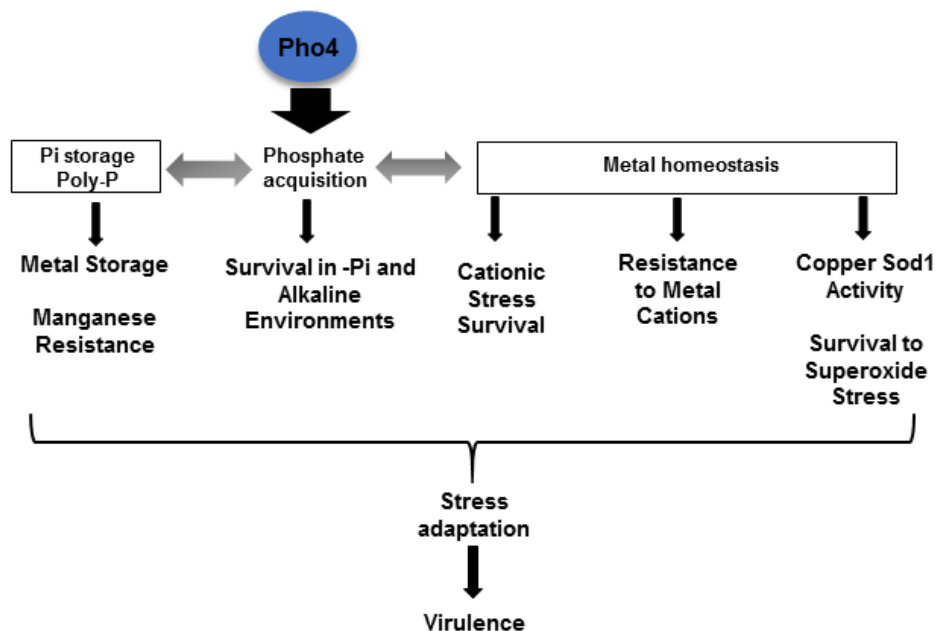


Fig 7.2 Model depicting the multifaceted roles of Pho4 in mediating stress resistance and virulence. See text for details.

Chapter 8. References

- Aballay, A., Drenkard, E., Hilbun, L.R. and Ausubel, F.M. (2003) '*Caenorhabditis elegans* innate immune response triggered by *Salmonella enterica* requires intact LPS and is mediated by a MAPK signaling pathway', *Curr Biol*, 13(1), pp. 47-52.
- Achbergerova, L. and Nahalka, J. (2011) 'Polyphosphate--an ancient energy source and active metabolic regulator', *Microb Cell Fact*, 10, p. 63.
- Aggarwal, S., Somani, V.K. and Bhatnagar, R. (2015) 'Phosphate starvation enhances the pathogenesis of *Bacillus anthracis*', *International Journal of Medical Microbiology*, 305(6), pp. 523-531.
- Aguirre, J.D., Clark, H.M., McIlvin, M., Vazquez, C., Palmere, S.L., Grab, D.J., Seshu, J., Hart, P.J., Saito, M. and Culotta, V.C. (2013) 'A manganese-rich environment supports superoxide dismutase activity in a Lyme disease pathogen, *Borrelia burgdorferi*', *J Biol Chem*, 288(12), pp. 8468-78.
- Alarco, A.M. and Raymond, M. (1999) 'The bZip transcription factor Cap1p is involved in multidrug resistance and oxidative stress response in *Candida albicans*', *J Bacteriol*, 181(3), pp. 700-8.
- Almeida, R.S., Brunke, S., Albrecht, A., Thewes, S., Laue, M., Edwards, J.E., Filler, S.G. and Hube, B. (2008) 'the hyphal-associated adhesin and invasin Als3 of *Candida albicans* mediates iron acquisition from host ferritin', *PLoS Pathog*, 4(11), p. e1000217.
- Alonso-Monge, R., Navarro-García, F., Román, E., Negredo, A.I., Eisman, B., Nombela, C. and Pla, J. (2003) 'The Hog1 Mitogen-Activated Protein Kinase Is Essential in the Oxidative Stress Response and Chlamydospore Formation in *Candida albicans*', *Eukaryot Cell*, 2(2), pp. 351-61.
- Alon, U. and Chan, J.C.M. (1993) Introduction. In Phosphate in paediatric health and disease. CRC press, Inc., pp. 2.
- Alvarez-Peral, F.J., Zaragoza, O., Pedreno, Y. and Arguelles, J.C. (2002) 'Protective role of trehalose during severe oxidative stress caused by hydrogen peroxide and the adaptive oxidative stress response in *Candida albicans*', *Microbiology*, 148(Pt 8), pp. 2599-606.
- Amulic, B., Cazalet, C., Hayes, G.L., Metzler, K.D. and Zychlinsky, A. (2012) 'Neutrophil function: from mechanisms to disease', *Annu Rev Immunol*, 30, pp. 459-89.
- Andrews, N.C. (2000) 'Iron homeostasis: insights from genetics and animal models', *Nat Rev Genet*, 1(3), pp. 208-17.
- Aoki, W., Kitahara, N., Miura, N., Morisaka, H., Yamamoto, Y., Kuroda, K. and Ueda, M. (2011) 'Comprehensive characterization of secreted aspartic proteases encoded by a virulence gene family in *Candida albicans*', *J Biochem*, 150(4), pp. 431-8.
- Arana, D.M., Nombela, C., Alonso-Monge, R. and Pla, J. (2005) 'The Pbs2 MAP kinase kinase is essential for the oxidative-stress response in the fungal pathogen *Candida albicans*', *Microbiology*, 151(Pt 4), pp. 1033-49.
- Arino, J., Ramos, J. and Sychrova, H. (2010) 'Alkali metal cation transport and homeostasis in yeasts', *Microbiol Mol Biol Rev*, 74(1), pp. 95-120.

- Ashman, R.B., Bolitho, E.M. and Papadimitriou, J.M. (1993) 'Patterns of resistance to *Candida albicans* in inbred mouse strains', *Immunol Cell Biol*, 71 (Pt 3), pp. 221-5.
- Auesukaree, C., Homma, T., Tochio, H., Shirakawa, M., Kaneko, Y. and Harashima, S. (2004) 'Intracellular phosphate serves as a signal for the regulation of the PHO pathway in *Saccharomyces cerevisiae*', *J Biol Chem*, 279(17), pp. 17289-94.
- Ault-Riche, D., Fraley, C.D., Tzeng, C.M. and Kornberg, A. (1998) 'Novel assay reveals multiple pathways regulating stress-induced accumulations of inorganic polyphosphate in *Escherichia coli*', *J Bacteriol*, 180(7), pp. 1841-7.
- Bader, T., Bodendorfer, B., Schroppel, K. and Morschhauser, J. (2003) 'Calcineurin is essential for virulence in *Candida albicans*', *Infect Immun*, 71(9), pp. 5344-54.
- Badrane, H., Nguyen, M.H., Cheng, S., Kumar, V., Derendorf, H., Iczkowski, K.A. and Clancy, C.J. (2008) 'The *Candida albicans* phosphatase Inp51p interacts with the EH domain protein Irs4p, regulates phosphatidylinositol-4,5-bisphosphate levels and influences hyphal formation, the cell integrity pathway and virulence', *Microbiology*, 154(Pt 11), pp. 3296-308.
- Bain, J.M., Louw, J., Lewis, L.E., Okai, B., Walls, C.A., Ballou, E.R., Walker, L.A., Reid, D., Munro, C.A., Brown, A.J., Brown, G.D., Gow, N.A. and Erwig, L.P. (2014) '*Candida albicans* hypha formation and mannan masking of beta-glucan inhibit macrophage phagosome maturation', *MBio*, 5(6), p. e01874.
- Banerjee, M., Thompson, D.S., Lazzell, A., Carlisle, P.L., Pierce, C., Monteagudo, C., Lopez-Ribot, J.L. and Kadosh, D. (2008) 'UME6, a novel filament-specific regulator of *Candida albicans* hyphal extension and virulence', *Mol Biol Cell*, 19(4), pp. 1354-65.
- Banks, A.P., Lawless, C. and Lydall, D.A. (2012) 'A quantitative fitness analysis workflow', *J Vis Exp*, (66).
- Barbaric, S., Munsterkotter, M., Goding, C. and Horz, W. (1998) 'Cooperative Pho2-Pho4 interactions at the PHO5 promoter are critical for binding of Pho4 to UASp1 and for efficient transactivation by Pho4 at UASp2', *Mol Cell Biol*, 18(5), pp. 2629-39.
- Barelle, C.J., Manson, C.L., MacCallum, D.M., Odds, F.C., Gow, N.A. and Brown, A.J. (2004) 'GFP as a quantitative reporter of gene regulation in *Candida albicans*', *Yeast*, 21(4), pp. 333-40.
- Basson, M.D. (2000) 'Microscopy and the gut mucosa: into the next millennium', *Microsc Res Tech*, 51(2), p. 111.
- Bates, S., Hughes, H.B., Munro, C.A., Thomas, W.P., MacCallum, D.M., Bertram, G., Atrih, A., Ferguson, M.A., Brown, A.J., Odds, F.C. and Gow, N.A. (2006) 'Outer chain N-glycans are required for cell wall integrity and virulence of *Candida albicans*', *J Biol Chem*, 281(1), pp. 90-8.
- Bensen, E.S., Martin, S.J., Li, M., Berman, J. and Davis, D.A. (2004) 'Transcriptional profiling in *Candida albicans* reveals new adaptive responses to extracellular pH and functions for Rim101p', *Mol Microbiol*, 54(5), pp. 1335-51.
- Bergman, N.H., Anderson, E.C., Swenson, E.E., Janes, B.K., Fisher, N., Niemeyer, M.M., Miyoshi, A.D. and Hanna, P.C. (2007) 'Transcriptional profiling of *Bacillus anthracis* during infection of host macrophages', *Infect Immun*, 75(7), pp. 3434-44.
- Berman, J. and Sudbery, P.E. (2002) '*Candida Albicans*: a molecular revolution built on lessons from budding yeast', *Nat Rev Genet*, 3(12), pp. 918-30.

- Bink, A., Vandenbosch, D., Coenye, T., Nelis, H., Cammue, B.P. and Thevissen, K. (2011) 'Superoxide dismutases are involved in *Candida albicans* biofilm persistence against miconazole', *Antimicrob Agents Chemother*, 55(9), pp. 4033-7.
- Bishop, A.C., Ganguly, S., Solis, N.V., Cooley, B.M., Jensen-Seaman, M.I., Filler, S.G., Mitchell, A.P. and Patton-Vogt, J. (2013) 'Glycerophosphocholine utilization by *Candida albicans*: role of the Git3 transporter in virulence', *J Biol Chem*, 288(47), pp. 33939-52.
- Bishop, A.C., Sun, T., Johnson, M.E., Bruno, V.M. and Patton-Vogt, J. (2011) 'Robust utilization of phospholipase-generated metabolites, glycerophosphodiester, by *Candida albicans*: role of the CaGit1 permease', *Eukaryot Cell*, 10(12), pp. 1618-27.
- Blackwell, C., Russell, C.L., Argimon, S., Brown, A.J. and Brown, J.D. (2003) 'Protein A-tagging for purification of native macromolecular complexes from *Candida albicans*', *Yeast*, 20(15), pp. 1235-41.
- Blankenship, J.R., Wormley, F.L., Boyce, M.K., Schell, W.A., Filler, S.G., Perfect, J.R. and Heitman, J. (2003) 'Calcineurin is essential for *Candida albicans* survival in serum and virulence', *Eukaryot Cell*, 2(3), pp. 422-30.
- Bartholomew, J. W. (1981) Stains for Microorganisms in Smears. In G. Clark (Ed.), *Staining Procedures*, 4th Edn, Williams and Wilkins, Baltimore, MA, USA, pp. 375–440.
- Bleackley, M.R. and Macgillivray, R.T. (2011) 'Transition metal homeostasis: from yeast to human disease', *Biometals*, 24(5), pp. 785-809.
- Borg-von Zepelin, M., Beggah, S., Boggian, K., Sanglard, D. and Monod, M. (1998) 'The expression of the secreted aspartyl proteinases Sap4 to Sap6 from *Candida albicans* in murine macrophages', *Mol Microbiol*, 28(3), pp. 543-54.
- Boyce, K.J., Kretschmer, M. and Kronstad, J.W. (2006) 'The *vtc4* gene influences polyphosphate storage, morphogenesis, and virulence in the maize pathogen *Ustilago maydis*', *Eukaryot Cell*, 5(8), pp. 1399-409.
- Boysen, J.H. and Mitchell, A.P. (2006) 'Control of Bro1-domain protein Rim20 localization by external pH, ESCRT machinery, and the *Saccharomyces cerevisiae* Rim101 pathway', *Mol Biol Cell*, 17(3), pp. 1344-53.
- Brand, A., MacCallum, D.M., Brown, A.J., Gow, N.A. and Odds, F.C. (2004) 'Ectopic expression of URA3 can influence the virulence phenotypes and proteome of *Candida albicans* but can be overcome by targeted reintegration of URA3 at the RPS10 locus', *Eukaryot Cell*, 3(4), pp. 900-9.
- Brenner, S. (1974) 'The genetics of *Caenorhabditis elegans*', *Genetics*, 77(1), pp. 71-94.
- Brewster, J.L. and Gustin, M.C. (1994) 'Positioning of cell growth and division after osmotic stress requires a MAP kinase pathway', *Yeast*, 10(4), pp. 425-39.
- Brock, M. (2009) 'Fungal metabolism in host niches', *Current Opinion in Microbiology*, 12(4), pp. 371-376.
- Brogden, K.A. (2005) 'Antimicrobial peptides: pore formers or metabolic inhibitors in bacteria?', *Nat Rev Microbiol*, 3(3), pp. 238-50.
- Brown, G.D., Denning, D.W. and Levitz, S.M. (2012) 'Tackling human fungal infections', *Science*, 336(6082), p. 647.

- Brown, G.D., Taylor, P.R., Reid, D.M., Willment, J.A., Williams, D.L., Martinez-Pomares, L., Wong, S.Y. and Gordon, S. (2002) 'Dectin-1 is a major beta-glucan receptor on macrophages', *J Exp Med*, 196(3), pp. 407-12.
- Bruce, C.R., Smith, D.A., Rodgers, D., da Silva Dantas, A., MacCallum, D.M., Morgan, B.A. and Quinn, J. (2011) 'Identification of a novel response regulator, Crr1, that is required for hydrogen peroxide resistance in *Candida albicans*', *PLoS One*, 6(12), p. e27979.
- Brunke, S. and Hube, B. (2013) 'Two unlike cousins: *Candida albicans* and *C. glabrata* infection strategies', *Cell Microbiol*, 15(5), pp. 701-8.
- Cadet, J. and Berger, M. (1985) 'Radiation-induced decomposition of the purine bases within DNA and related model compounds', *Int J Radiat Biol Relat Stud Phys Chem Med*, 47(2), pp. 127-43.
- Calandra, T., Bille, J., Schneider, R., Mosimann, F. and Francioli, P. (1989) 'Clinical significance of *Candida* isolated from peritoneum in surgical patients', *Lancet*, 2(8677), pp. 1437-40.
- Calcagno-Pizarelli, A.M., Negrete-Urtasun, S., Denison, S.H., Rudnicka, J.D., Bussink, H.J., Munera-Huertas, T., Stanton, L., Hervas-Aguilar, A., Espeso, E.A., Tilburn, J., Arst, H.N., Jr. and Penalva, M.A. (2007) 'Establishment of the ambient pH signaling complex in *Aspergillus nidulans*: PalH assists plasma membrane localization of PalH', *Eukaryot Cell*, 6(12), pp. 2365-75.
- Calderone, R.A. and Braun, P.C. (1991) 'Adherence and receptor relationships of *Candida albicans*', *Microbiol Rev*, 55(1), pp. 1-20.
- Calderone RA, Clancy CJ. **Candida** and Candidiasis: ASM Press, Washington, DC, 2012.
- Calera, J.A., Herman, D. and Calderone, R. (2000a) 'Identification of *YPD1*, a gene of *Candida albicans* which encodes a two-component phosphohistidine intermediate protein', *Yeast*, 16(11), pp. 1053-9.
- Calera, J.A., Zhao, X.J. and Calderone, R. (2000b) 'Defective hyphal development and avirulence caused by a deletion of the *SSK1* response regulator gene in *Candida albicans*', *Infect Immun*, 68(2), pp. 518-25.
- Carlisle, P.L., Banerjee, M., Lazzell, A., Monteagudo, C., Lopez-Ribot, J.L. and Kadosh, D. (2009) 'Expression levels of a filament-specific transcriptional regulator are sufficient to determine *Candida albicans* morphology and virulence', *Proc Natl Acad Sci U S A*, 106(2), pp. 599-604.
- Castrejon, F., Gomez, A., Sanz, M., Duran, A. and Roncero, C. (2006) 'The RIM101 pathway contributes to yeast cell wall assembly and its function becomes essential in the absence of mitogen-activated protein kinase Slt2p', *Eukaryot Cell*, 5(3), pp. 507-17.
- Castrol, C.D., Koretsky, A.P. and Domach, M.M. (1999) 'NMR-Observed phosphate trafficking and polyphosphate dynamics in wild-type and *vph1-1* mutant *Saccharomyces cerevisiae* in response to stresses', *Biotechnol Prog*, 15(1), pp. 65-73.
- Chamilos, G., Nobile, C.J., Bruno, V.M., Lewis, R.E., Mitchell, A.P. and Kontoyiannis, D.P. (2009) '*Candida albicans* Cas5, a regulator of cell wall integrity, is required for virulence in murine and toll mutant fly models', *J Infect Dis*, 200(1), pp. 152-7.

- Chattaway, F.W., Odds, F.C. and Barlow, A.J. (1971) 'An examination of the production of hydrolytic enzymes and toxins by pathogenic strains of *Candida albicans*', *J Gen Microbiol*, 67(3), pp. 255-63.
- Chauhan, N., Inglis, D., Roman, E., Pla, J., Li, D., Calera, J.A. and Calderone, R. (2003) '*Candida albicans* response regulator gene *SSK1* regulates a subset of genes whose functions are associated with cell wall biosynthesis and adaptation to oxidative stress', *Eukaryot Cell*, 2(5), pp. 1018-24.
- Chaves, G.M., Bates, S., Maccallum, D.M. and Odds, F.C. (2007) '*Candida albicans* *GRX2*, encoding a putative glutaredoxin, is required for virulence in a murine model', *Genet Mol Res*, 6(4), pp. 1051-63.
- Chaves, G.M. and da Silva, W.P. (2012) 'Superoxide dismutases and glutaredoxins have a distinct role in the response of *Candida albicans* to oxidative stress generated by the chemical compounds menadione and diamide', *Mem Inst Oswaldo Cruz*, 107(8), pp. 998-1005.
- Cheetham, J., MacCallum, D.M., Doris, K.S., da Silva Dantas, A., Scorfield, S., Odds, F., Smith, D.A. and Quinn, J. (2011) 'MAPKKK-independent regulation of the Hog1 stress-activated protein kinase in *Candida albicans*', *J Biol Chem*, 286(49), pp. 42002-16.
- Cheetham, J., Smith, D.A., da Silva Dantas, A., Doris, K.S., Patterson, M.J., Bruce, C.R. and Quinn, J. (2007) 'A single MAPKKK regulates the Hog1 MAPK pathway in the pathogenic fungus *Candida albicans*', *Mol Biol Cell*, 18(11), pp. 4603-14.
- Chekabab, S.M., Harel, J. and Dozois, C.M. (2014) 'Interplay between genetic regulation of phosphate homeostasis and bacterial virulence', *Virulence*, 5(8), pp. 786-93.
- Chen, C., Pande, K., French, S.D., Tuch, B.B. and Noble, S.M. (2011) 'An iron homeostasis regulatory circuit with reciprocal roles in *Candida albicans* commensalism and pathogenesis', *Cell Host Microbe*, 10(2), pp. 118-35.
- Cheng, G., Wozniak, K., Wallig, M.A., Fidel, P.L., Jr., Trupin, S.R. and Hoyer, L.L. (2005) 'Comparison between *Candida albicans* agglutinin-like sequence gene expression patterns in human clinical specimens and models of vaginal candidiasis', *Infect Immun*, 73(3), pp. 1656-63.
- Cheng, S., Clancy, C.J., Xu, W., Schneider, F., Hao, B., Mitchell, A.P. and Nguyen, M.H. (2013) 'Profiling of *Candida albicans* gene expression during intra-abdominal candidiasis identifies biologic processes involved in pathogenesis', *J Infect Dis*, 208(9), pp. 1529-37.
- Cheng, S.C., Joosten, L.A., Kullberg, B.J. and Netea, M.G. (2012) 'Interplay between *Candida albicans* and the mammalian innate host defense', *Infect Immun*, 80(4), pp. 1304-13.
- Citiulo, F., Jacobsen, I.D., Miramon, P., Schild, L., Brunke, S., Zipfel, P., Brock, M., Hube, B. and Wilson, D. (2012) '*Candida albicans* scavenges host zinc via Pra1 during endothelial invasion', *PLoS Pathog*, 8(6), p. e1002777.
- Clark, J.E. and Wood, H.G. (1987) 'Preparation of standards and determination of sizes of long-chain polyphosphates by gel electrophoresis', *Anal Biochem*, 161(2), pp. 280-90.

- Cowen, L.E., Sanglard, D., Howard, S.J., Rogers, P.D. and Perlin, D.S. (2015) 'Mechanisms of Antifungal Drug Resistance', *Cold Spring Harb Perspect Med*, 5(7), p. a019752.
- Csank, C., Schroppel, K., Leberer, E., Harcus, D., Mohamed, O., Meloche, S., Thomas, D.Y. and Whiteway, M. (1998) 'Roles of the *Candida albicans* mitogen-activated protein kinase homolog, Cek1p, in hyphal development and systemic candidiasis', *Infect Immun*, 66(6), pp. 2713-21.
- d'Ostiani, C.F., Del Sero, G., Bacci, A., Montagnoli, C., Spreca, A., Mencacci, A., Ricciardi-Castagnoli, P. and Romani, L. (2000) 'Dendritic cells discriminate between yeasts and hyphae of the fungus *Candida albicans*. Implications for initiation of T helper cell immunity in vitro and in vivo', *J Exp Med*, 191(10), pp. 1661-74.
- da Silva Dantas, A., Patterson, M.J., Smith, D.A., Maccallum, D.M., Erwig, L.P., Morgan, B.A. and Quinn, J. (2010) 'Thioredoxin regulates multiple hydrogen peroxide-induced signaling pathways in *Candida albicans*', *Mol Cell Biol*, 30(19), pp. 4550-63.
- Davis, D., Wilson, R.B. and Mitchell, A.P. (2000) 'RIM101-dependent and-independent pathways govern pH responses in *Candida albicans*', *Mol Cell Biol*, 20(3), pp. 971-8.
- Davis, D.A. (2009) 'How human pathogenic fungi sense and adapt to pH: the link to virulence', *Curr Opin Microbiol*, 12(4), pp. 365-70.
- Davis, D.A., Bruno, V.M., Loza, L., Filler, S.G. and Mitchell, A.P. (2002) '*Candida albicans* Mds3p, a conserved regulator of pH responses and virulence identified through insertional mutagenesis', *Genetics*, 162(4), pp. 1573-81.
- De Bernardis, F., Muhlschlegel, F.A., Cassone, A. and Fonzi, W.A. (1998) 'The pH of the host niche controls gene expression in and virulence of *Candida albicans*', *Infect Immun*, 66(7), pp. 3317-25.
- de Repentigny, L., Lewandowski, D. and Jolicoeur, P. (2004) 'Immunopathogenesis of oropharyngeal candidiasis in human immunodeficiency virus infection', *Clin Microbiol Rev*, 17(4), pp. 729-59.
- den Hertog, A.L., van Marle, J., van Veen, H.A., Van't Hof, W., Bolscher, J.G., Veerman, E.C. and Nieuw Amerongen, A.V. (2005) 'Candidacidal effects of two antimicrobial peptides: histatin 5 causes small membrane defects, but LL-37 causes massive disruption of the cell membrane', *Biochem J*, 388(Pt 2), pp. 689-95.
- Dennison, P.M., Ramsdale, M., Manson, C.L. and Brown, A.J. (2005) 'Gene disruption in *Candida albicans* using a synthetic, codon-optimised Cre-loxP system', *Fungal Genet Biol*, 42(9), pp. 737-48.
- Ding, X., Yu, Q., Zhang, B., Xu, N., Jia, C., Dong, Y., Chen, Y., Xing, L. and Li, M. (2014) 'The type II Ca²⁺/calmodulin-dependent protein kinases are involved in the regulation of cell wall integrity and oxidative stress response in *Candida albicans*', *Biochem Biophys Res Commun*, 446(4), pp. 1073-8.
- Dmitrieva, N., Kultz, D., Michea, L., Ferraris, J. and Burg, M. (2000) 'Protection of renal inner medullary epithelial cells from apoptosis by hypertonic stress-induced p53 activation', *J Biol Chem*, 275(24), pp. 18243-7.
- Docampo, R. (2014) 'Polyphosphate: a target for thrombosis attenuation', *Blood*, 124(22), pp. 3177-8.

- Docampo, R., Ulrich, P. and Moreno, S.N. (2010) 'Evolution of acidocalcisomes and their role in polyphosphate storage and osmoregulation in eukaryotic microbes', *Philos Trans R Soc Lond B Biol Sci*, 365(1541), pp. 775-84.
- Dühring, S., Germerodt, S., Skerka, C., Zipfel, P.F., Dandekar, T. and Schuster, S. (2015) 'Host-pathogen interactions between the human innate immune system and *Candida albicans*—understanding and modeling defense and evasion strategies', *Front Microbiol*, 6.
- Dunkel, N., Hertlein, T., Franz, R., Reuß, O., Sasse, C., Schäfer, T., Ohlsen, K. and Morschhäuser, J. (2013) 'Roles of Different Peptide Transporters in Nutrient Acquisition in *Candida albicans*', *Eukaryot Cell*, 12(4), pp. 520-8.
- Eck, R., Hundt, S., Hartl, A., Roemer, E. and Kunkel, W. (1999) 'A multicopper oxidase gene from *Candida albicans*: cloning, characterization and disruption', *Microbiology*, 145 (Pt 9), pp. 2415-22.
- Ehrensberger, K.M. and Bird, A.J. (2011) 'Hammering out details: regulating metal levels in eukaryotes', *Trends Biochem Sci*, 36(10), pp. 524-31.
- El Barkani, A., Kurzai, O., Fonzi, W.A., Ramon, A., Porta, A., Frosch, M. and Muhlschlegel, F.A. (2000) 'Dominant active alleles of RIM101 (PRR2) bypass the pH restriction on filamentation of *Candida albicans*', *Mol Cell Biol*, 20(13), pp. 4635-47.
- Ene, I.V., Walker, L.A., Schiavone, M., Lee, K.K., Martin-Yken, H., Dague, E., Gow, N.A., Munro, C.A. and Brown, A.J. (2015) 'Cell Wall Remodeling Enzymes Modulate Fungal Cell Wall Elasticity and Osmotic Stress Resistance', *MBio*, 6(4).
- Enjalbert, B., MacCallum, D.M., Odds, F.C. and Brown, A.J. (2007) 'Niche-specific activation of the oxidative stress response by the pathogenic fungus *Candida albicans*', *Infect Immun*, 75(5), pp. 2143-51.
- Enjalbert, B., Smith, D.A., Cornell, M.J., Alam, I., Nicholls, S., Brown, A.J. and Quinn, J. (2006) 'Role of the Hog1 stress-activated protein kinase in the global transcriptional response to stress in the fungal pathogen *Candida albicans*', *Mol Biol Cell*, 17(2), pp. 1018-32.
- Fan, J., Whiteway, M. and Shen, S.H. (2005) 'Disruption of a gene encoding glycerol 3-phosphatase from *Candida albicans* impairs intracellular glycerol accumulation-mediated salt-tolerance', *FEMS Microbiol Lett*, 245(1), pp. 107-16.
- Fang, F.C. (2004) 'Antimicrobial reactive oxygen and nitrogen species: concepts and controversies', *Nat Rev Microbiol*, 2(10), pp. 820-32.
- Faro-Trindade I, Brown G D (2009). Interaction of *Candida albicans* with phagocytes, in Phagocyte-Pathogen Interactions: Macrophages and the Host Response to Infection, eds Russell D. G., Gordon S., editors. (Washington, DC: ASM Press), 437–451.
- Feng, Q., Summers, E., Guo, B. and Fink, G. (1999) 'Ras signaling is required for serum-induced hyphal differentiation in *Candida albicans*', *J Bacteriol*, 181(20), pp. 6339-46.
- Fitzsimmons, N. and Berry, D.R. (1994) 'Inhibition of *Candida albicans* by *Lactobacillus acidophilus*: evidence for the involvement of a peroxidase system', *Microbios*, 80(323), pp. 125-33.

- Fonzi, W.A. (1999) 'PHR1 and PHR2 of *Candida albicans* Encode Putative Glycosidases Required for Proper Cross-Linking of β -1,3- and β -1,6-Glucans', *J Bacteriol*, 181(22), pp. 7070-9.
- Fordtran, J.S. and Locklear, T.W. (1966) 'Ionic constituents and osmolality of gastric and small-intestinal fluids after eating', *Am J Dig Dis*, 11(7), pp. 503-21.
- Fradin, C., De Groot, P., MacCallum, D., Schaller, M., Klis, F., Odds, F.C. and Hube, B. (2005) 'Granulocytes govern the transcriptional response, morphology and proliferation of *Candida albicans* in human blood', *Mol Microbiol*, 56(2), pp. 397-415.
- Fradin, C., Kretschmar, M., Nichterlein, T., Gaillardin, C., d'Enfert, C. and Hube, B. (2003) 'Stage-specific gene expression of *Candida albicans* in human blood', *Mol Microbiol*, 47(6), pp. 1523-43.
- Fratti, R.A., Belanger, P.H., Ghannoum, M.A., Edwards, J.E., Jr. and Filler, S.G. (1998) 'Endothelial cell injury caused by *Candida albicans* is dependent on iron', *Infect Immun*, 66(1), pp. 191-6.
- Frohner, I.E., Bourgeois, C., Yatsyk, K., Majer, O. and Kuchler, K. (2009) '*Candida albicans* cell surface superoxide dismutases degrade host-derived reactive oxygen species to escape innate immune surveillance', *Mol Microbiol*, 71(1), pp. 240-52.
- Garcera, A., Casas, C. and Herrero, E. (2010) 'Expression of *Candida albicans* glutathione transferases is induced inside phagocytes and upon diverse environmental stresses', *FEMS Yeast Res*, 10(4), pp. 422-31.
- Ghannoum, M.A. (2000) 'Potential role of phospholipases in virulence and fungal pathogenesis', *Clin Microbiol Rev*, 13(1), pp. 122-43, table of contents.
- Ghannoum, M.A., Spellberg, B., Saporito-Irwin, S.M. and Fonzi, W.A. (1995) 'Reduced virulence of *Candida albicans* PHR1 mutants', *Infect Immun*, 63(11), pp. 4528-30.
- Gleason, J.E., Li, C.X., Odeh, H.M. and Culotta, V.C. (2014) 'Species-specific activation of Cu/Zn SOD by its CCS copper chaperone in the pathogenic yeast *Candida albicans*', *J Biol Inorg Chem*, 19(4-5), pp. 595-603.
- Goldstein, E. (1983) 'Hydrolytic enzymes of alveolar macrophages', *Rev Infect Dis*, 5(6), pp. 1078-92.
- Gomez-Raja, J. and Davis, D.A. (2012) 'The β -Arrestin-Like Protein Rim8 Is Hyperphosphorylated and Complexes with Rim21 and Rim101 To Promote Adaptation to Neutral-Alkaline pH', *Eukaryot Cell*, 11(5), pp. 683-93.
- Goodman, J. and Rothstein, A. (1957) 'The active transport of phosphate into the yeast cell', *J Gen Physiol*, 40(6), pp. 915-23.
- Gow, N.A., van de Veerdonk, F.L., Brown, A.J. and Netea, M.G. (2012) '*Candida albicans* morphogenesis and host defence: discriminating invasion from colonization', *Nat Rev Microbiol*, 10(2), pp. 112-22.
- Grant, C.M. (2001) 'Role of the glutathione/glutaredoxin and thioredoxin systems in yeast growth and response to stress conditions', *Mol Microbiol*, 39(3), pp. 533-41.
- Gray, M.J., Wholey, W.Y., Wagner, N.O., Cremers, C.M., Mueller-Schickert, A., Hock, N.T., Krieger, A.G., Smith, E.M., Bender, R.A., Bardwell, J.C. and Jakob, U. (2014) 'Polyphosphate is a primordial chaperone', *Mol Cell*, 53(5), pp. 689-99.

- Greenfield, N.J., Hussain, M. and Lenard, J. (1987) 'Effects of growth state and amines on cytoplasmic and vacuolar pH, phosphate and polyphosphate levels in *Saccharomyces cerevisiae*: a ³¹P-nuclear magnetic resonance study', *Biochim Biophys Acta*, 926(3), pp. 205-14.
- Haas, A. (2007) 'The phagosome: compartment with a license to kill', *Traffic*, 8(4), pp. 311-30.
- Hackam, D.J., Rotstein, O.D., Zhang, W., Gruenheid, S., Gros, P. and Grinstein, S. (1998) 'Host resistance to intracellular infection: mutation of natural resistance-associated macrophage protein 1 (Nramp1) impairs phagosomal acidification', *J Exp Med*, 188(2), pp. 351-64.
- Hall, R.A. and Gow, N.A. (2013) 'Mannosylation in *Candida albicans*: role in cell wall function and immune recognition', *Mol Microbiol*, 90(6), pp. 1147-61.
- Haro, R., Garciadeblas, B. and Rodriguez-Navarro, A. (1991) 'A novel P-type ATPase from yeast involved in sodium transport', *FEBS Lett*, 291(2), pp. 189-91.
- Hashash, R., Younes, S., Bahnan, W., El Koussa, J., Maalouf, K., Dimassi, H.I. and Khalaf, R.A. (2011) 'Characterisation of Pga1, a putative *Candida albicans* cell wall protein necessary for proper adhesion and biofilm formation', *Mycoses*, 54(6), pp. 491-500.
- Heilmann, C.J., Sorgo, A.G., Siliakus, A.R., Dekker, H.L., Brul, S., de Koster, C.G., de Koning, L.J. and Klis, F.M. (2011) 'Hyphal induction in the human fungal pathogen *Candida albicans* reveals a characteristic wall protein profile', *Microbiology*, 157(Pt 8), pp. 2297-307.
- Heinsbroek, S.E., Taylor, P.R., Martinez, F.O., Martinez-Pomares, L., Brown, G.D. and Gordon, S. (2008) 'Stage-specific sampling by pattern recognition receptors during *Candida albicans* phagocytosis', *PLoS Pathog*, 4(11), p. e1000218.
- Hohmann, S. (2002) 'Osmotic adaptation in yeast--control of the yeast osmolyte system', *Int Rev Cytol*, 215, pp. 149-87.
- Holland, S.M. (2010) 'Chronic granulomatous disease', *Clin Rev Allergy Immunol*, 38(1), pp. 3-10.
- Homann, O.R., Dea, J., Noble, S.M. and Johnson, A.D. (2009) 'A phenotypic profile of the *Candida albicans* regulatory network', *PLoS Genet*, 5(12), p. e1000783.
- Hothorn, M., Neumann, H., Lenherr, E.D., Wehner, M., Rybin, V., Hassa, P.O., Uttenweiler, A., Reinhardt, M., Schmidt, A., Seiler, J., Ladurner, A.G., Herrmann, C., Scheffzek, K. and Mayer, A. (2009) 'Catalytic core of a membrane-associated eukaryotic polyphosphate polymerase', *Science*, 324(5926), pp. 513-6.
- Hoyer, L.L. (2001) 'The ALS gene family of *Candida albicans*', *Trends Microbiol*, 9(4), pp. 176-80.
- Hoyer, L.L., Green, C.B., Oh, S.H. and Zhao, X. (2008) 'Discovering the secrets of the *Candida albicans* agglutinin-like sequence (ALS) gene family--a sticky pursuit', *Med Mycol*, 46(1), pp. 1-15.
- Hromatka, B.S., Noble, S.M. and Johnson, A.D. (2005) 'Transcriptional response of *Candida albicans* to nitric oxide and the role of the YHB1 gene in nitrosative stress and virulence', *Mol Biol Cell*, 16(10), pp. 4814-26.
- Hube, B., Sanglard, D., Odds, F.C., Hess, D., Monod, M., Schafer, W., Brown, A.J. and Gow, N.A. (1997) 'Disruption of each of the secreted aspartyl proteinase genes

SAP1, SAP2, and SAP3 of *Candida albicans* attenuates virulence', *Infect Immun*, 65(9), pp. 3529-38.

Hube, B., Stehr, F., Bossenz, M., Mazur, A., Kretschmar, M. and Schafer, W. (2000) 'Secreted lipases of *Candida albicans*: cloning, characterisation and expression analysis of a new gene family with at least ten members', *Arch Microbiol*, 174(5), pp. 362-74.

Huycke, M.M., Moore, D., Joyce, W., Wise, P., Shepard, L., Kotake, Y. and Gilmore, M.S. (2001) 'Extracellular superoxide production by *Enterococcus faecalis* requires demethylmenaquinone and is attenuated by functional terminal quinol oxidases', *Mol Microbiol*, 42(3), pp. 729-40.

Hwang, C.S., Baek, Y.U., Yim, H.S. and Kang, S.O. (2003) 'Protective roles of mitochondrial manganese-containing superoxide dismutase against various stresses in *Candida albicans*', *Yeast*, 20(11), pp. 929-41.

Hwang, C.S., Rhie, G.E., Oh, J.H., Huh, W.K., Yim, H.S. and Kang, S.O. (2002) 'Copper- and zinc-containing superoxide dismutase (Cu/ZnSOD) is required for the protection of *Candida albicans* against oxidative stresses and the expression of its full virulence', *Microbiology*, 148(Pt 11), pp. 3705-13.

Ibrahim, A.S., Mirbod, F., Filler, S.G., Banno, Y., Cole, G.T., Kitajima, Y., Edwards, J.E., Jr., Nozawa, Y. and Ghannoum, M.A. (1995) 'Evidence implicating phospholipase as a virulence factor of *Candida albicans*', *Infect Immun*, 63(5), pp. 1993-8.

Iglesias-Osma, C., Gonzalez-Villaron, L., San Miguel, J.F., Caballero, M.D., Vazquez, L. and de Castro, S. (1995) 'Iron metabolism and fungal infections in patients with haematological malignancies', *J Clin Pathol*, 48(3), pp. 223-5.

Imlay, J.A. and Linn, S. (1988) 'DNA damage and oxygen radical toxicity', *Science*, 240(4857), pp. 1302-9.

Irazaqui, J.E., Troemel, E.R., Feinbaum, R.L., Luhachack, L.G., Cezairliyan, B.O. and Ausubel, F.M. (2010) 'Distinct pathogenesis and host responses during infection of *C. elegans* by *P. aeruginosa* and *S. aureus*', *PLoS Pathog*, 6, p. e1000982.

Jackson, A.L. and Loeb, L.A. (2001) 'The contribution of endogenous sources of DNA damage to the multiple mutations in cancer', *Mutat Res*, 477(1-2), pp. 7-21.

Jacobsen, I.D., Wilson, D., Wachtler, B., Brunke, S., Naglik, J.R. and Hube, B. (2012) '*Candida albicans* dimorphism as a therapeutic target', *Expert Rev Anti Infect Ther*, 10(1), pp. 85-93.

Jain, C., Pastor, K., Gonzalez, A.Y., Lorenz, M.C. and Rao, R.P. (2013) 'The role of *Candida albicans* AP-1 protein against host derived ROS in in vivo models of infection', *Virulence*, 4(1), pp. 67-76.

Jiang, Q., Griffin, D.A., Barofsky, D.F. and Hurst, J.K. (1997) 'Intraphagosomal chlorination dynamics and yields determined using unique fluorescent bacterial mimics', *Chem Res Toxicol*, 10(10), pp. 1080-9.

Johnston, D.A., Eberle, K.E., Sturtevant, J.E. and Palmer, G.E. (2009) 'Role for endosomal and vacuolar GTPases in *Candida albicans* pathogenesis', *Infect Immun*, 77(6), pp. 2343-55.

- Kaffman, A., Herskowitz, I., Tjian, R. and O'Shea, E.K. (1994) 'Phosphorylation of the transcription factor PHO4 by a cyclin-CDK complex, PHO80-PHO85', *Science*, 263(5150), pp. 1153-6.
- Kaloriti, D., Jacobsen, M., Yin, Z., Patterson, M., Tillmann, A., Smith, D.A., Cook, E., You, T., Grimm, M.J., Bohovych, I., Grebogi, C., Segal, B.H., Gow, N.A., Haynes, K., Quinn, J. and Brown, A.J. (2014) 'Mechanisms underlying the exquisite sensitivity of *Candida albicans* to combinatorial cationic and oxidative stress that enhances the potent fungicidal activity of phagocytes', *MBio*, 5(4), pp. e01334-14.
- Karababa, M., Valentino, E., Pardini, G., Coste, A.T., Bille, J. and Sanglard, D. (2006) 'CRZ1, a target of the calcineurin pathway in *Candida albicans*', *Mol Microbiol*, 59(5), pp. 1429-51.
- Kayingo, G. and Wong, B. (2005) 'The MAP kinase Hog1p differentially regulates stress-induced production and accumulation of glycerol and d-arabitol in *Candida albicans*', *Microbiology*, 151(9), pp. 2987-2999.
- Keen, C.L., Ensunsa, J.L. and Clegg, M.S. (2000) 'Manganese metabolism in animals and humans including the toxicity of manganese', *Met Ions Biol Syst*, 37, pp. 89-121.
- Kim, K.S., Rao, N.N., Fraley, C.D. and Kornberg, A. (2002) 'Inorganic polyphosphate is essential for long-term survival and virulence factors in *Shigella* and *Salmonella* spp', *Proc Natl Acad Sci U S A*, 99(11), pp. 7675-80.
- Kinclova-Zimmermannova, O., Gaskova, D. and Sychrova, H. (2006) 'The Na⁺,K⁺/H⁺ -antiporter Nha1 influences the plasma membrane potential of *Saccharomyces cerevisiae*', *FEMS Yeast Res*, 6(5), pp. 792-800.
- King, J.C. (2011) 'Zinc: an essential but elusive nutrient', *Am J Clin Nutr*, 94(2), pp. 679s-84s.
- Klaunig, J.E., Kamendulis, L.M. and Hocevar, B.A. (2010) 'Oxidative stress and oxidative damage in carcinogenesis', *Toxicol Pathol*, 38(1), pp. 96-109.
- Knight, S.A., Lesuisse, E., Stearman, R., Klausner, R.D. and Dancis, A. (2002) 'Reductive iron uptake by *Candida albicans*: role of copper, iron and the TUP1 regulator', *Microbiology*, 148(Pt 1), pp. 29-40.
- Kobayashi, T., Robinson, J.M. and Seguchi, H. (1998) 'Identification of intracellular sites of superoxide production in stimulated neutrophils', *J Cell Sci*, 111 (Pt 1), pp. 81-91.
- Kolls, J.K. and Linden, A. (2004) 'Interleukin-17 family members and inflammation', *Immunity*, 21(4), pp. 467-76.
- Komeili, A. and O'Shea, E.K. (1999) 'Roles of phosphorylation sites in regulating activity of the transcription factor Pho4', *Science*, 284(5416), pp. 977-80.
- Korn, T., Bettelli, E., Gao, W., Awasthi, A., Jager, A., Strom, T.B., Oukka, M. and Kuchroo, V.K. (2007) 'IL-21 initiates an alternative pathway to induce proinflammatory T(H)17 cells', *Nature*, 448(7152), pp. 484-7.
- Kornberg, A. (1999) 'Inorganic polyphosphate: a molecule of many functions', *Prog Mol Subcell Biol*, 23, pp. 1-18.

- Kortman, G.A., Boleij, A., Swinkels, D.W. and Tjalsma, H. (2012) 'Iron availability increases the pathogenic potential of *Salmonella typhimurium* and other enteric pathogens at the intestinal epithelial interface', *PLoS One*, 7(1), p. e29968.
- Kozel, T.R. (1996) 'Activation of the complement system by pathogenic fungi', *Clin Microbiol Rev*, 9(1), pp. 34-46.
- Kozel, T.R., Weinhold, L.C. and Lupan, D.M. (1996) 'Distinct characteristics of initiation of the classical and alternative complement pathways by *Candida albicans*', *Infect Immun*, 64(8), pp. 3360-8.
- Krause, K.H. and Welsh, M.J. (1990) 'Voltage-dependent and Ca²⁺-activated ion channels in human neutrophils', *J Clin Invest*, 85(2), pp. 491-8.
- Kretschmer, M., Reiner, E., Hu, G., Tam, N., Oliveira, D.L., Caza, M., Yeon, J.H., Kim, J., Kastrup, C.J., Jung, W.H. and Kronstad, J.W. (2014) 'Defects in phosphate acquisition and storage influence virulence of *Cryptococcus neoformans*', *Infect Immun*, 82(7), pp. 2697-712.
- Krysan, D.J., Sutterwala, F.S. and Wellington, M. (2014) 'Catching fire: *Candida albicans*, macrophages, and pyroptosis', *PLoS Pathog*, 10(6), p. e1004139.
- Kuhn, C. and Klipp, E. (2012) 'Zooming in on yeast osmoadaptation', *Adv Exp Med Biol*, 736, pp. 293-310.
- Kulaev, I.S., Vagabov, V. M. and Kulakovskaya, T. V. (2004) 'The Biochemistry of Inorganic Polyphosphates'. Chichester, UK. : John Wiley & Sons, Ltd.
- Kullas, A.L., Martin, S.J. and Davis, D. (2007) 'Adaptation to environmental pH: integrating the Rim101 and calcineurin signal transduction pathways', *Mol Microbiol*, 66(4), pp. 858-71.
- Kultz, D., Madhany, S. and Burg, M.B. (1998) 'Hyperosmolality causes growth arrest of murine kidney cells. Induction of GADD45 and GADD153 by osmosensing via stress-activated protein kinase 2', *J Biol Chem*, 273(22), pp. 13645-51.
- Kumamoto, C.A. and Vices, M.D. (2005) 'Contributions of hyphae and hypha-co-regulated genes to *Candida albicans* virulence', *Cell Microbiol*, 7(11), pp. 1546-54.
- Kuo, W.Y., Huang, C.H. and Jinn, T.L. (2013) 'Chaperonin 20 might be an iron chaperone for superoxide dismutase in activating iron superoxide dismutase (FeSOD)', *Plant Signal Behav*, 8(2), p. e23074.
- Kurz, C.L. and Tan, M.W. (2004) 'Regulation of aging and innate immunity in *C. elegans*', *Aging Cell*, 3(4), pp. 185-93.
- Kusch, H., Engelmann, S., Albrecht, D., Morschhauser, J. and Hecker, M. (2007) 'Proteomic analysis of the oxidative stress response in *Candida albicans*', *Proteomics*, 7(5), pp. 686-97.
- Kuznets, G., Vigonsky, E., Weissman, Z., Lalli, D., Gildor, T., Kauffman, S.J., Turano, P., Becker, J., Lewinson, O. and Kornitzer, D. (2014) 'A relay network of extracellular heme-binding proteins drives *C. albicans* iron acquisition from hemoglobin', *PLoS Pathog*, 10(10), p. e1004407.
- Laemmli, U.K. (1970) 'Cleavage of structural proteins during the assembly of the head of bacteriophage T4', *Nature*, 227(5259), pp. 680-5.

- Lamarche, M.G., Wanner, B.L., Crepin, S. and Harel, J. (2008) 'The phosphate regulon and bacterial virulence: a regulatory network connecting phosphate homeostasis and pathogenesis', *FEMS Microbiol Rev*, 32(3), pp. 461-73.
- Lamarre, C., LeMay, J.D., Deslauriers, N. and Bourbonnais, Y. (2001) '*Candida albicans* expresses an unusual cytoplasmic manganese-containing superoxide dismutase (SOD3 gene product) upon the entry and during the stationary phase', *J Biol Chem*, 276(47), pp. 43784-91.
- Lan, C.Y., Rodarte, G., Murillo, L.A., Jones, T., Davis, R.W., Dungan, J., Newport, G. and Agabian, N. (2004) 'Regulatory networks affected by iron availability in *Candida albicans*', *Mol Microbiol*, 53(5), pp. 1451-69.
- Lander, N., Ulrich, P.N. and Docampo, R. (2013) '*Trypanosoma brucei* vacuolar transporter chaperone 4 (TbVtc4) is an acidocalcisome polyphosphate kinase required for in vivo infection', *J Biol Chem*, 288(47), pp. 34205-16.
- Lawless, C., Wilkinson, D.J., Young, A., Addinall, S.G. and Lydall, D.A. (2010) 'Colonyzer: automated quantification of micro-organism growth characteristics on solid agar', *BMC Bioinformatics*, 11, pp. 287-287.
- Leberer, E., Harcus, D., Dignard, D., Johnson, L., Ushinsky, S., Thomas, D.Y. and Schroppe, K. (2001) 'Ras links cellular morphogenesis to virulence by regulation of the MAP kinase and cAMP signalling pathways in the pathogenic fungus *Candida albicans*', *Mol Microbiol*, 42(3), pp. 673-87.
- Lee, R.E., Liu, T.T., Barker, K.S., Lee, R.E. and Rogers, P.D. (2005) 'Genome-wide expression profiling of the response to ciclopirox olamine in *Candida albicans*', *J Antimicrob Chemother*, 55(5), pp. 655-62.
- Leidich, S.D., Ibrahim, A.S., Fu, Y., Koul, A., Jessup, C., Vitullo, J., Fonzi, W., Mirbod, F., Nakashima, S., Nozawa, Y. and Ghannoum, M.A. (1998) 'Cloning and disruption of caPLB1, a phospholipase B gene involved in the pathogenicity of *Candida albicans*', *J Biol Chem*, 273(40), pp. 26078-86.
- Lenburg, M.E. and O'Shea, E.K. (1996) 'Signaling phosphate starvation', *Trends Biochem Sci*, 21(10), pp. 383-7.
- Lewis, L.E., Bain, J.M., Lowes, C., Gillespie, C., Rudkin, F.M., Gow, N.A. and Erwig, L.P. (2012) 'Stage specific assessment of *Candida albicans* phagocytosis by macrophages identifies cell wall composition and morphogenesis as key determinants', *PLoS Pathog*, 8(3), p. e1002578.
- Li, R., Kumar, R., Tati, S., Puri, S. and Edgerton, M. (2013) '*Candida albicans* flu1-mediated efflux of salivary histatin 5 reduces its cytosolic concentration and fungicidal activity', *Antimicrob Agents Chemother*, 57(4), pp. 1832-9.
- Liang, S.C., Tan, X.Y., Luxenberg, D.P., Karim, R., Dunussi-Joannopoulos, K., Collins, M. and Fouser, L.A. (2006) 'Interleukin (IL)-22 and IL-17 are coexpressed by Th17 cells and cooperatively enhance expression of antimicrobial peptides', *J Exp Med*, 203(10), pp. 2271-9.
- Liang, Y., Zhang, B., Zheng, W., Xing, L. and Li, M. (2011) 'Alkaline stress triggers an immediate calcium fluctuation in *Candida albicans* mediated by Rim101p and Crz1p transcription factors' *FEMS Yeast Res*, 11(5), 1567-1364.
- Lichko, L.P., Kulakovskaya, T.V., Kulakovskaya, E.V. and Kulaev, I.S. (2008) 'Inactivation of PPX1 and PPN1 genes encoding exopolyphosphatases of

- Saccharomyces cerevisiae* does not prevent utilization of polyphosphates as phosphate reserve', *Biochemistry (Mosc)*, 73(9), pp. 985-9.
- Liu, H., Kohler, J. and Fink, G.R. (1994) 'Suppression of hyphal formation in *Candida albicans* by mutation of a STE12 homolog', *Science*, 266(5191), pp. 1723-6.
- Lo, H.J., Kohler, J.R., DiDomenico, B., Loebenberg, D., Cacciapuoti, A. and Fink, G.R. (1997) 'Nonfilamentous *C. albicans* mutants are avirulent', *Cell*, 90(5), pp. 939-49.
- Loll-Krippelber, R., d'Enfert, C., Feri, A., Diogo, D., Perin, A., Marcet-Houben, M., Bougnoux, M.E. and Legrand, M. (2014) 'A study of the DNA damage checkpoint in *Candida albicans*: uncoupling of the functions of Rad53 in DNA repair, cell cycle regulation and genotoxic stress-induced polarized growth', *Mol Microbiol*, 91(3), pp. 452-71.
- Lorenz, M.C., Bender, J.A. and Fink, G.R. (2004) 'Transcriptional response of *Candida albicans* upon internalization by macrophages', *Eukaryot Cell*, 3(5), pp. 1076-87.
- Lorenz, M.C. and Fink, G.R. (2001) 'The glyoxylate cycle is required for fungal virulence', *Nature*, 412(6842), pp. 83-6.
- Lu, H.S., Fausset, P.R., Narhi, L.O., Horan, T., Shinagawa, K., Shimamoto, G. and Boone, T.C. (1999) 'Chemical modification and site-directed mutagenesis of methionine residues in recombinant human granulocyte colony-stimulating factor: effect on stability and biological activity', *Arch Biochem Biophys*, 362(1), pp. 1-11.
- Luo, G., Samaranayake, L.P. and Yau, J.Y. (2001) '*Candida* species exhibit differential in vitro hemolytic activities', *J Clin Microbiol*, 39(8), pp. 2971-4.
- Luo, S., Skerka, C., Kurzai, O. and Zipfel, P.F. (2013) 'Complement and innate immune evasion strategies of the human pathogenic fungus *Candida albicans*', *Mol Immunol*, 56(3), pp. 161-9.
- MacCallum, D.M., Castillo, L., Nather, K., Munro, C.A., Brown, A.J., Gow, N.A. and Odds, F.C. (2009) 'Property differences among the four major *Candida albicans* strain clades', *Eukaryot Cell*, 8(3), pp. 373-87.
- MacCallum, D.M., Coste, A., Ischer, F., Jacobsen, M.D., Odds, F.C. and Sanglard, D. (2010) 'Genetic dissection of azole resistance mechanisms in *Candida albicans* and their validation in a mouse model of disseminated infection', *Antimicrob Agents Chemother*, 54(4), pp. 1476-83.
- Maiti, P.K., Kumar, A., Kumar, R. and Mohapatra, L.N. (1985) 'Role of antibodies and effect of BCG vaccination in experimental candidiasis in mice', *Mycopathologia*, 91(2), pp. 79-85.
- Majander, A. and Wikstrom, M. (1989) 'The plasma membrane potential of human neutrophils. Role of ion channels and the sodium/potassium pump', *Biochim Biophys Acta*, 980(2), pp. 139-45.
- Martchenko, M., Alarco, A.M., Harcus, D. and Whiteway, M. (2004) 'Superoxide dismutases in *Candida albicans*: transcriptional regulation and functional characterization of the hyphal-induced *SOD5* gene', *Mol Biol Cell*, 15(2), pp. 456-67.
- Martin, R.B., Savory, J., Brown, S., Bertholf, R.L. and Wills, M.R. (1987) 'Transferrin binding of Al³⁺ and Fe³⁺', *Clin Chem*, 33(3), pp. 405-7.

- Mayer, F.L., Wilson, D. and Hube, B. (2013) '*Candida albicans* pathogenicity mechanisms', *Virulence*, 4(2), pp. 119-28.
- McKenzie, C.G., Koser, U., Lewis, L.E., Bain, J.M., Mora-Montes, H.M., Barker, R.N., Gow, N.A. and Erwig, L.P. (2010) 'Contribution of *Candida albicans* cell wall components to recognition by and escape from murine macrophages', *Infect Immun*, 78(4), pp. 1650-8.
- Miramon, P., Dunker, C., Windecker, H., Bohovych, I.M., Brown, A.J., Kurzai, O. and Hube, B. (2012) 'Cellular responses of *Candida albicans* to phagocytosis and the extracellular activities of neutrophils are critical to counteract carbohydrate starvation, oxidative and nitrosative stress', *PLoS One*, 7(12), p. e52850.
- Missall, T.A., Lodge, J.K. and McEwen, J.E. (2004) 'Mechanisms of resistance to oxidative and nitrosative stress: implications for fungal survival in mammalian hosts', *Eukaryot Cell*, 3(4), pp. 835-46.
- Miyakawa, Y. (2000) 'Identification of a *Candida albicans* homologue of the *PHO85* gene, a negative regulator of the PHO system in *Saccharomyces cerevisiae*', *Yeast*, 16(11), pp. 1045-51.
- Moreno, S.N. and Docampo, R. (2013) 'Polyphosphate and its diverse functions in host cells and pathogens', *PLoS Pathog*, 9(5), p. e1003230.
- Morgan, B.A., Banks, G.R., Toone, W.M., Raitt, D., Kuge, S. and Johnston, L.H. (1997) 'The Skn7 response regulator controls gene expression in the oxidative stress response of the budding yeast *Saccharomyces cerevisiae*', *Embo j*, 16(5), pp. 1035-44.
- Moye-Rowley, W.S. (2002) 'Transcription factors regulating the response to oxidative stress in yeast', *Antioxid Redox Signal*, 4(1), pp. 123-40.
- Moyes, D.L. and Naglik, J.R. (2011) 'Mucosal immunity and *Candida albicans* infection', *Clin Dev Immunol*, 2011, p. 346307.
- Moyes, D.L., Runglall, M., Murciano, C., Shen, C., Nayar, D., Thavaraj, S., Kohli, A., Islam, A., Mora-Montes, H., Challacombe, S.J. and Naglik, J.R. (2010) 'A biphasic innate immune MAPK response discriminates between the yeast and hyphal forms of *Candida albicans* in epithelial cells', *Cell Host Microbe*, 8(3), pp. 225-35.
- Muhlschlegel, F.A. and Fonzi, W.A. (1997) '*PHR2* of *Candida albicans* encodes a functional homolog of the pH-regulated gene *PHR1* with an inverted pattern of pH-dependent expression', *Mol Cell Biol*, 17(10), pp. 5960-7.
- Mullick, A., Elias, M., Picard, S., Bourget, L., Jovcevski, O., Gauthier, S., Tuite, A., Harakidas, P., Bihun, C., Massie, B. and Gros, P. (2004) 'Dysregulated inflammatory response to *Candida albicans* in a C5-deficient mouse strain', *Infect Immun*, 72(10), pp. 5868-76.
- Murad, A.M., Lee, P.R., Broadbent, I.D., Barelle, C.J. and Brown, A.J. (2000) 'Clp10, an efficient and convenient integrating vector for *Candida albicans*', *Yeast*, 16(4), pp. 325-7.
- Nagahashi, S., Mio, T., Ono, N., Yamada-Okabe, T., Arisawa, M., Bussey, H. and Yamada-Okabe, H. (1998) 'Isolation of *CaSLN1* and *CaNIK1*, the genes for osmosensing histidine kinase homologues, from the pathogenic fungus *Candida albicans*', *Microbiology*, 144 (Pt 2), pp. 425-32.

- Nakagawa, Y., Kanbe, T. and Mizuguchi, I. (2003) 'Disruption of the human pathogenic yeast *Candida albicans* catalase gene decreases survival in mouse-model infection and elevates susceptibility to higher temperature and to detergents', *Microbiol Immunol*, 47(6), pp. 395-403.
- Nantel, A., Dignard, D., Bachewich, C., Harcus, D., Marcil, A., Bouin, A.P., Sensen, C.W., Hogues, H., van het Hoog, M., Gordon, P., Rigby, T., Benoit, F., Tessier, D.C., Thomas, D.Y. and Whiteway, M. (2002) 'Transcription profiling of *Candida albicans* cells undergoing the yeast-to-hyphal transition', *Mol Biol Cell*, 13(10), pp. 3452-65.
- Neef, D.W. and Kladde, M.P. (2003) 'Polyphosphate loss promotes SNF/SWI- and Gcn5-dependent mitotic induction of PHO5', *Mol Cell Biol*, 23(11), pp. 3788-97.
- Netea, M.G., Brown, G.D., Kullberg, B.J. and Gow, N.A. (2008) 'An integrated model of the recognition of *Candida albicans* by the innate immune system', *Nat Rev Microbiol*, 6(1), pp. 67-78.
- Neuhauser, B., Dunkel, N., Satheesh, S.V. and Morschhauser, J. (2011) 'Role of the Npr1 kinase in ammonium transport and signaling by the ammonium permease Mep2 in *Candida albicans*', *Eukaryot Cell*, 10(3), pp. 332-42.
- Nevitt, T., Ohrvik, H. and Thiele, D.J. (2012) 'Charting the travels of copper in eukaryotes from yeast to mammals', *Biochim Biophys Acta*, 1823(9), pp. 1580-93.
- Nguyen, L.T., de Boer, L., Zaat, S.A. and Vogel, H.J. (2011) 'Investigating the cationic side chains of the antimicrobial peptide tritrypticin: hydrogen bonding properties govern its membrane-disruptive activities', *Biochim Biophys Acta*, 1808(9), pp. 2297-303.
- Nobile, C.J., Nett, J.E., Hernday, A.D., Homann, O.R., Deneault, J.S., Nantel, A., Andes, D.R., Johnson, A.D. and Mitchell, A.P. (2009) 'Biofilm matrix regulation by *Candida albicans* Zap1', *PLoS Biol*, 7(6), p. e1000133.
- Nobile, C.J., Solis, N., Myers, C.L., Fay, A.J., Deneault, J.S., Nantel, A., Mitchell, A.P. and Filler, S.G. (2008) '*Candida albicans* transcription factor Rim101 mediates pathogenic interactions through cell wall functions', *Cell Microbiol*, 10(11), pp. 2180-96.
- Noble, S.M., French, S., Kohn, L.A., Chen, V. and Johnson, A.D. (2010) 'Systematic screens of a *Candida albicans* homozygous deletion library decouple morphogenetic switching and pathogenicity', *Nat Genet*, 42(7), pp. 590-8.
- Noble, S.M. and Johnson, A.D. (2005) 'Strains and strategies for large-scale gene deletion studies of the diploid human fungal pathogen *Candida albicans*', *Eukaryot Cell*, 4(2), pp. 298-309.
- Norbeck, J. and Blomberg, A. (1998) 'Amino acid uptake is strongly affected during exponential growth of *Saccharomyces cerevisiae* in 0.7 M NaCl medium', *FEMS Microbiology Letters*, 158(1), pp. 121-126.
- Nurieva, R., Yang, X.O., Martinez, G., Zhang, Y., Panopoulos, A.D., Ma, L., Schluns, K., Tian, Q., Watowich, S.S., Jetten, A.M. and Dong, C. (2007) 'Essential autocrine regulation by IL-21 in the generation of inflammatory T cells', *Nature*, 448(7152), pp. 480-3.
- O'Meara, T.R., Veri, A.O., Ketela, T., Jiang, B., Roemer, T. and Cowen, L.E. (2015) 'Global analysis of fungal morphology exposes mechanisms of host cell escape', *Nat Commun*, 6, p. 6741.

O'Neill, E.M., Kaffman, A., Jolly, E.R. and O'Shea, E.K. (1996) 'Regulation of PHO4 nuclear localization by the PHO80-PHO85 cyclin-CDK complex', *Science*, 271(5246), pp. 209-12.

O'Meara, T.R., Veri, A.O., Ketela, T., Jiang, B., Roemer, T. and Cowen, L.E. 'Global analysis of fungal morphology exposes mechanisms of host cell escape', *Nat Commun*, 6.

Ogawa, N., DeRisi, J. and Brown, P.O. (2000) 'New components of a system for phosphate accumulation and polyphosphate metabolism in *Saccharomyces cerevisiae* revealed by genomic expression analysis', *Mol Biol Cell*, 11(12), pp. 4309-21.

Ohno, A., Muller, E., Fraek, M.L., Thurau, K. and Beck, F. (1997) 'Solute composition and heat shock proteins in rat renal medulla', *Pflugers Arch*, 434(1), pp. 117-22.

Olinski, R., Gackowski, D., Foksinski, M., Rozalski, R., Roszkowski, K. and Jaruga, P. (2002) 'Oxidative DNA damage: assessment of the role in carcinogenesis, atherosclerosis, and acquired immunodeficiency syndrome', *Free Radic Biol Med*, 33(2), pp. 192-200.

Oshima, Y., Ogawa, N. and Harashima, S. (1996) 'Regulation of phosphatase synthesis in *Saccharomyces cerevisiae*-a review', *Gene*, 179(1), pp. 171-7.

Ostrosky-Zeichner, L., Marr, K.A., Rex, J.H. and Cohen, S.H. (2003) 'Amphotericin B: time for a new "gold standard"', *Clin Infect Dis*, 37(3), pp. 415-25.

Page, M.J. and Di Cera, E. (2006) 'Role of Na⁺ and K⁺ in enzyme function', *Physiol Rev*, 86(4), pp. 1049-92.

Paraje, M.G., Correa, S.G., Renna, M.S., Theumer, M. and Sotomayor, C.E. (2008) '*Candida albicans*-secreted lipase induces injury and steatosis in immune and parenchymal cells', *Can J Microbiol*, 54(8), pp. 647-59.

Park, H., Myers, C.L., Sheppard, D.C., Phan, Q.T., Sanchez, A.A., J, E.E. and Filler, S.G. (2005) 'Role of the fungal Ras-protein kinase A pathway in governing epithelial cell interactions during oropharyngeal candidiasis', *Cell Microbiol*, 7(4), pp. 499-510.

Pastor-Flores, D., Schulze, J.O., Bahi, A., Giacometti, R., Ferrer-Dalmau, J., Passeron, S., Engel, M., Suss, E., Casamayor, A. and Biondi, R.M. (2013) 'PIF-pocket as a target for *C. albicans* Pkh selective inhibitors', *ACS Chem Biol*, 8(10), pp. 2283-92.

Patterson, M.J., McKenzie, C.G., Smith, D.A., da Silva Dantas, A., Sherston, S., Veal, E.A., Morgan, B.A., MacCallum, D.M., Erwig, L.P. and Quinn, J. (2013) 'Ybp1 and Gpx3 Signaling in *Candida albicans* Govern Hydrogen Peroxide-Induced Oxidation of the Cap1 Transcription Factor and Macrophage Escape', *Antioxid Redox Signal*, 19(18), pp. 2244-60.

Pericolini, E., Gabrielli, E., Amacker, M., Kasper, L., Roselletti, E., Luciano, E., Sabbatini, S., Kaeser, M., Moser, C., Hube, B., Vecchiarelli, A. and Cassone, A. (2015) 'Secretory Aspartyl Proteinases Cause Vaginitis and Can Mediate Vaginitis Caused by *Candida albicans* in Mice', *MBio*, 6(3).

Persson, B.L., Lagerstedt, J.O., Pratt, J.R., Pattison-Granberg, J., Lundh, K., Shokrollahzadeh, S. and Lundh, F. (2003) 'Regulation of phosphate acquisition in *Saccharomyces cerevisiae*', *Curr Genet*, 43(4), pp. 225-44.

- Petelenz-Kurdziel, E., Eriksson, E., Smedh, M., Beck, C., Hohmann, S. and Goksoor, M. (2011) 'Quantification of cell volume changes upon hyperosmotic stress in *Saccharomyces cerevisiae*', *Integr Biol (Camb)*, 3(11), pp. 1120-6.
- Pfaller, M.A. and Diekema, D.J. (2007) 'Epidemiology of invasive candidiasis: a persistent public health problem', *Clin Microbiol Rev*, 20(1), pp. 133-63.
- Pfaller, M.A. and Diekema, D.J. (2010) 'Epidemiology of invasive mycoses in North America', *Crit Rev Microbiol*, 36(1), pp. 1-53.
- Phillips, A.J., Sudbery, I. and Ramsdale, M. (2003) 'Apoptosis induced by environmental stresses and amphotericin B in *Candida albicans*', *Proc Natl Acad Sci U S A*, 100(24), pp. 14327-32.
- Pick, U. and Weiss, M. (1991) 'Polyphosphate Hydrolysis within Acidic Vacuoles in Response to Amine-Induced Alkaline Stress in the Halotolerant Alga *Dunaliella salina*', *Plant Physiol*, 97(3), pp. 1234-40.
- Piekarska, K., Hardy, G., Mol, E., van den Burg, J., Strijbis, K., van Roermund, C., van den Berg, M. and Distel, B. (2008) 'The activity of the glyoxylate cycle in peroxisomes of *Candida albicans* depends on a functional beta-oxidation pathway: evidence for reduced metabolite transport across the peroxisomal membrane', *Microbiology*, 154(Pt 10), pp. 3061-72.
- Pierce, J.V., Dignard, D., Whiteway, M. and Kumamoto, C.A. (2013) 'Normal adaptation of *Candida albicans* to the murine gastrointestinal tract requires Efg1p-dependent regulation of metabolic and host defense genes', *Eukaryot Cell*, 12(1), pp. 37-49.
- Pillay Cé, S., Elliott, E. and Dennison, C. (2002) 'Endolysosomal proteolysis and its regulation', *Biochem J*, 363(Pt 3), pp. 417-29.
- Platara, M., Ruiz, A., Serrano, R., Palomino, A., Moreno, F. and Arino, J. (2006) 'The transcriptional response of the yeast Na⁺ ATPase ENA1 gene to alkaline stress involves three main signaling pathways', *J Biol Chem*, 281(48), pp. 36632-42.
- Popolo, L. and Vai, M. (1998) 'Defects in assembly of the extracellular matrix are responsible for altered morphogenesis of a *Candida albicans phr1* mutant', *J Bacteriol*, 180(1), pp. 163-6.
- Prieto, D., Roman, E., Correia, I. and Pla, J. (2014) 'The HOG pathway is critical for the colonization of the mouse gastrointestinal tract by *Candida albicans*', *PLoS One*, 9(1), p. e87128.
- Pukkila-Worley, R. and Ausubel, F.M. (2012) 'Immune defense mechanisms in the *Caenorhabditis elegans* intestinal epithelium', *Curr Opin Immunol*, 24(1), pp. 3-9.
- Pukkila-Worley, R., Peleg, A.Y., Tampakakis, E. and Mylonakis, E. (2009) '*Candida albicans* hyphal formation and virulence assessed using a *Caenorhabditis elegans* infection model' *Eukaryot cell*, 8(11), p1750-8.
- Quintin, J., Cheng, S.C., van der Meer, J.W. and Netea, M.G. (2014) 'Innate immune memory: towards a better understanding of host defense mechanisms', *Curr Opin Immunol*, 29, pp. 1-7.
- Radovanovic, I., Mullick, A. and Gros, P. (2011) 'Genetic control of susceptibility to infection with *Candida albicans* in mice', *PLoS One*, 6(4), p. e18957.

- Rafii, F., Sutherland, J.B. and Cerniglia, C.E. (2008) 'Effects of treatment with antimicrobial agents on the human colonic microflora', *The Clin Risk Manag*, 4(6), pp. 1343-58.
- Ramanan, N. and Wang, Y. (2000) 'A high-affinity iron permease essential for *Candida albicans* virulence', *Science*, 288(5468), pp. 1062-4.
- Ramon, A.M. and Fonzi, W.A. (2003) 'Diverged binding specificity of Rim101p, the *Candida albicans* ortholog of PacC', *Eukaryot Cell*, 2(4), pp. 718-28.
- Ramon, A.M., Porta, A. and Fonzi, W.A. (1999) 'Effect of environmental pH on morphological development of *Candida albicans* is mediated via the PacC-related transcription factor encoded by PRR2', *J Bacteriol*, 181(24), pp. 7524-30.
- Ramsdale, M. (2008) 'Programmed cell death in pathogenic fungi', *Biochim Biophys Acta*, 1783(7), pp. 1369-80.
- Reeves, E.P., Lu, H., Jacobs, H.L., Messina, C.G., Bolsover, S., Gabella, G., Potma, E.O., Warley, A., Roes, J. and Segal, A.W. (2002) 'Killing activity of neutrophils is mediated through activation of proteases by K⁺ flux', *Nature*, 416(6878), pp. 291-7.
- Rengarajan, J., Bloom, B.R. and Rubin, E.J. (2005) 'Genome-wide requirements for *Mycobacterium tuberculosis* adaptation and survival in macrophages', *Proc Natl Acad Sci U S A*, 102(23), pp. 8327-32.
- Riggle, P.J. and Kumamoto, C.A. (2000) 'Role of a *Candida albicans* P1-type ATPase in resistance to copper and silver ion toxicity', *J Bacteriol*, 182(17), pp. 4899-905.
- Robinson, N.A., Goss, N.H. and Wood, H.G. (1984) 'Polyphosphate kinase from *Propionibacterium shermanii*: formation of an enzymatically active insoluble complex with basic proteins and characterization of synthesized polyphosphate', *Biochem Int*, 8(6), pp. 757-69.
- Rocha, C.R., Schroppel, K., Harcus, D., Marcil, A., Dignard, D., Taylor, B.N., Thomas, D.Y., Whiteway, M. and Leberer, E. (2001) 'Signaling through adenylyl cyclase is essential for hyphal growth and virulence in the pathogenic fungus *Candida albicans*', *Mol Biol Cell*, 12(11), pp. 3631-43.
- Rodaki, A., Bohovych, I.M., Enjalbert, B., Young, T., Odds, F.C., Gow, N.A.R. and Brown, A.J.P. (2009) 'Glucose Promotes Stress Resistance in the Fungal Pathogen *Candida albicans*', *Mol Biol Cell*, 20(22), pp. 4845-55.
- Roman, E., Nombela, C. and Pla, J. (2005) 'The Sho1 adaptor protein links oxidative stress to morphogenesis and cell wall biosynthesis in the fungal pathogen *Candida albicans*', *Mol Cell Biol*, 25(23), pp. 10611-27.
- Romanowski, K., Zaborin, A., Valuckaite, V., Rolfes, R.J., Babrowski, T., Bethel, C., Olivas, A., Zaborina, O. and Alverdy, J.C. (2012) '*Candida albicans* isolates from the gut of critically ill patients respond to phosphate limitation by expressing filaments and a lethal phenotype', *PLoS One*, 7(1), p. e30119.
- Rosenfeld, L., Reddi, A.R., Leung, E., Aranda, K., Jensen, L.T. and Culotta, V.C. (2010) 'the effect of phosphate accumulation on metal ion homeostasis in *Saccharomyces cerevisiae*', *J Biol Inorg Chem*, 15(7), pp. 1051-62.
- Rubin-Bejerano, I., Fraser, I., Grisafi, P. and Fink, G.R. (2003) 'Phagocytosis by neutrophils induces an amino acid deprivation response in *Saccharomyces cerevisiae* and *Candida albicans*', *Proc Natl Acad Sci U S A*, 100(19), pp. 11007-12.

- Ruchel, R., de Bernardis, F., Ray, T.L., Sullivan, P.A. and Cole, G.T. (1992) 'Candida acid proteinases', *J Med Vet Mycol*, 30 Suppl 1, pp. 123-32.
- Ryan, O., Shapiro, R.S., Kurat, C.F., Mayhew, D., Baryshnikova, A., Chin, B., Lin, Z.Y., Cox, M.J., Vizeacoumar, F., Cheung, D., Bahr, S., Tsui, K., Tebbji, F., Sellam, A., Istel, F., Schwarzmuller, T., Reynolds, T.B., Kuchler, K., Gifford, D.K., Whiteway, M., Giaever, G., Nislow, C., Costanzo, M., Gingras, A.C., Mitra, R.D., Andrews, B., Fink, G.R., Cowen, L.E. and Boone, C. (2012) 'Global gene deletion analysis exploring yeast filamentous growth', *Science*, 337(6100), pp. 1353-6.
- San José, C., Monge, R.A., Pérez-Díaz, R., Pla, J. and Nombela, C. (1996) 'The mitogen-activated protein kinase homolog *HOG1* gene controls glycerol accumulation in the pathogenic fungus *Candida albicans*', *J Bacteriol*, 178(19), pp. 5850-2.
- Sanchez-Fresneda, R., Guirao-Abad, J.P., Arguelles, A., Gonzalez-Parraga, P., Valentin, E. and Arguelles, J.C. (2013) 'Specific stress-induced storage of trehalose, glycerol and D-arabitol in response to oxidative and osmotic stress in *Candida albicans*', *Biochem Biophys Res Commun*, 430(4), pp. 1334-9.
- Sanchez-Portocarrero, J., Perez-Cecilia, E., Corral, O., Romero-Vivas, J. and Picazo, J.J. (2000) 'The central nervous system and infection by *Candida* species', *Diagn Microbiol Infect Dis*, 37(3), pp. 169-79.
- Sanglard, D., Hube, B., Monod, M., Odds, F.C. and Gow, N.A. (1997) 'A triple deletion of the secreted aspartyl proteinase genes *SAP4*, *SAP5*, and *SAP6* of *Candida albicans* causes attenuated virulence', *Infect Immun*, 65(9), pp. 3539-46.
- Sanglard, D., Ischer, F., Marchetti, O., Entenza, J. and Bille, J. (2003) 'Calcineurin A of *Candida albicans*: involvement in antifungal tolerance, cell morphogenesis and virulence', *Mol Microbiol*, 48(4), pp. 959-76.
- Saporito-Irwin, S.M., Birse, C.E., Sypherd, P.S. and Fonzi, W.A. (1995) '*PHR1*, a pH-regulated gene of *Candida albicans*, is required for morphogenesis', *Mol Cell Biol*, 15(2), pp. 601-13.
- Sato, K., Yang, X.L., Yudate, T., Chung, J.S., Wu, J., Luby-Phelps, K., Kimberly, R.P., Underhill, D., Cruz, P.D., Jr. and Ariizumi, K. (2006) 'Dectin-2 is a pattern recognition receptor for fungi that couples with the Fc receptor gamma chain to induce innate immune responses', *J Biol Chem*, 281(50), pp. 38854-66.
- Saville, S.P., Lazzell, A.L., Monteagudo, C. and Lopez-Ribot, J.L. (2003) 'Engineered control of cell morphology in vivo reveals distinct roles for yeast and filamentous forms of *Candida albicans* during infection', *Eukaryot Cell*, 2(5), pp. 1053-60.
- Schaller, M., Schafer, W., Korting, H.C. and Hube, B. (1998) 'Differential expression of secreted aspartyl proteinases in a model of human oral candidosis and in patient samples from the oral cavity', *Mol Microbiol*, 29(2), pp. 605-15.
- Schaller, M., Zakikhany, K., Naglik, J.R., Weindl, G. and Hube, B. (2006) 'Models of oral and vaginal candidiasis based on in vitro reconstituted human epithelia', *Nat Protoc*, 1(6), pp. 2767-73.
- Schneider, K.R., Smith, R.L. and O'Shea, E.K. (1994) 'Phosphate-regulated inactivation of the kinase PHO80-PHO85 by the CDK inhibitor PHO81', *Science*, 266(5182), pp. 122-6.

- Secco, D., Wang, C., Shou, H. and Whelan, J. (2012) 'Phosphate homeostasis in the yeast *Saccharomyces cerevisiae*, the key role of the SPX domain-containing proteins', *FEBS Lett*, 586(4), pp. 289-95.
- Segal, A.W. (2005) 'How neutrophils kill microbes', *Annu Rev Immunol*, 23, pp. 197-223.
- Segal, A.W., Geisow, M., Garcia, R., Harper, A. and Miller, R. (1981) 'The respiratory burst of phagocytic cells is associated with a rise in vacuolar pH', *Nature*, 290(5805), pp. 406-9.
- Seider, K., Heyken, A., Luttich, A., Miramon, P. and Hube, B. (2010) 'Interaction of pathogenic yeasts with phagocytes: survival, persistence and escape', *Curr Opin Microbiol*, 13(4), pp. 392-400.
- Serrano, R., Ruiz, A., Bernal, D., Chambers, J.R. and Arino, J. (2002) 'The transcriptional response to alkaline pH in *Saccharomyces cerevisiae*: evidence for calcium-mediated signalling', *Mol Microbiol*, 46(5), pp. 1319-33.
- Sethuraman, A., Rao, N.N. and Kornberg, A. (2001) 'The endopolyphosphatase gene: essential in *Saccharomyces cerevisiae*', *Proc Natl Acad Sci U S A*, 98(15), pp. 8542-7.
- Setiadi, E.R., Doedt, T., Cottier, F., Noffz, C. and Ernst, J.F. (2006) 'Transcriptional response of *Candida albicans* to hypoxia: linkage of oxygen sensing and Efg1p-regulatory networks', *J Mol Biol*, 361(3), pp. 399-411.
- Sherman, F. (2002) 'Getting started with yeast', *Methods Enzymol*, 350, pp. 3-41.
- Shi, Q.M., Wang, Y.M., Zheng, X.D., Lee, R.T. and Wang, Y. (2007) 'Critical role of DNA checkpoints in mediating genotoxic-stress-induced filamentous growth in *Candida albicans*', *Mol Biol Cell*, 18(3), pp. 815-26.
- Singh, P., Chauhan, N., Ghosh, A., Dixon, F. and Calderone, R. (2004) 'SKN7 of *Candida albicans*: mutant construction and phenotype analysis', *Infect Immun*, 72(4), pp. 2390-4.
- Smith, D.A., Nicholls, S., Morgan, B.A., Brown, A.J.P. and Quinn, J. (2004) 'A Conserved Stress-activated Protein Kinase Regulates a Core Stress Response in the Human Pathogen *Candida albicans*', *Mol Biol Cell*, 15(9), pp. 4179-90.
- Smith, R.F., Blasi, D. and Dayton, S.L. (1973) 'Phosphatase activity among *Candida* species and other yeasts isolated from clinical material', *Appl Microbiol*, 26(3), pp. 364-7.
- Smith, S.A. and Morrissey, J.H. (2007) 'Sensitive fluorescence detection of polyphosphate in polyacrylamide gels using 4',6-diamidino-2-phenylindol', *Electrophoresis*, 28(19), pp. 3461-5.
- Smolenski, G., Sullivan, P.A., Cutfield, S.M. and Cutfield, J.F. (1997) 'Analysis of secreted aspartic proteinases from *Candida albicans*: purification and characterization of individual Sap1, Sap2 and Sap3 isoenzymes', *Microbiology*, 143 (Pt 2), pp. 349-56.
- Spellberg B, Marr K, Filler SG. *Candida*: What Should Clinicians and Scientists Be Talking About? In: Calderone RA, Clancy, C.J., ed. *Candida and Candidiasis*: ASM Press, Washington, DC, pp. 225-242., 2012.

- Sobel, J.D. (1985) 'Epidemiology and pathogenesis of recurrent vulvovaginal candidiasis', *Am J Obstet Gynecol*, 152(7 Pt 2), pp. 924-35.
- Somero G N, Yancey P. In: Osmolytes and Cell Volume Regulation: Physiological and Evolutionary Principles. Hoffmann J F, Jamieson J D, editors. Washington, DC: Am. Physiol. Soc.; 1997. pp. 441–484.
- Srinivasa, K., Kim, N.R., Kim, J., Kim, M., Bae, J.Y., Jeong, W., Kim, W. and Choi, W. (2012) 'Characterization of a putative thioredoxin peroxidase prx1 of *Candida albicans*', *Mol Cells*, 33(3), pp. 301-7.
- Staab, J.F., Bradway, S.D., Fidel, P.L. and Sundstrom, P. (1999) 'Adhesive and mammalian transglutaminase substrate properties of *Candida albicans* Hwp1', *Science*, 283(5407), pp. 1535-8.
- Steinberg, B.E., Huynh, K.K., Brodovitch, A., Jabs, S., Stauber, T., Jentsch, T.J. and Grinstein, S. (2010) 'A cation counterflux supports lysosomal acidification', *J Cell Biol*, 189(7), pp. 1171-86.
- Stoldt, V.R., Sonneborn, A., Leuker, C.E. and Ernst, J.F. (1997) 'Efg1p, an essential regulator of morphogenesis of the human pathogen *Candida albicans*, is a member of a conserved class of bHLH proteins regulating morphogenetic processes in fungi', *Embo j*, 16(8), pp. 1982-91.
- Sudbery, P., Gow, N. and Berman, J. (2004) 'The distinct morphogenic states of *Candida albicans*', *Trends Microbiol*, 12(7), pp. 317-24.
- Sudbery, P.E. (2011) 'Growth of *Candida albicans* hyphae', *Nat Rev Microbiol*, 9(10), pp. 737-48.
- Tabah, A., Koulenti, D., Laupland, K., Misset, B., Valles, J., Bruzzi de Carvalho, F., Paiva, J.A., Cakar, N., Ma, X., Eggimann, P., Antonelli, M., Bonten, M.J., Csomos, A., Krueger, W.A., Mikstacki, A., Lipman, J., Depuydt, P., Vesin, A., Garrouste-Orgeas, M., Zahar, J.R., Blot, S., Carlet, J., Brun-Buisson, C., Martin, C., Rello, J., Dimopoulos, G. and Timsit, J.F. (2012) 'Characteristics and determinants of outcome of hospital-acquired bloodstream infections in intensive care units: the EUROBACT International Cohort Study', *Intensive Care Med*, 38(12), pp. 1930-45.
- Talibi, D. and Raymond, M. (1999) 'Isolation of a putative *Candida albicans* transcriptional regulator involved in pleiotropic drug resistance by functional complementation of a *pdv1 pdv3* mutation in *Saccharomyces cerevisiae*', *J Bacteriol*, 181(1), pp. 231-40.
- Tapiero, H. and Tew, K.D. (2003) 'Trace elements in human physiology and pathology: zinc and metallothioneins', *Biomed Pharmacother*, 57(9), pp. 399-411.
- Thewes, S., Kretschmar, M., Park, H., Schaller, M., Filler, S.G. and Hube, B. (2007) 'In vivo and ex vivo comparative transcriptional profiling of invasive and non-invasive *Candida albicans* isolates identifies genes associated with tissue invasion', *Mol Microbiol*, 63(6), pp. 1606-28.
- Tillmann, A.T., Strijbis, K., Cameron, G., Radmaneshfar, E., Thiel, M., Munro, C.A., MacCallum, D.M., Distel, B., Gow, N.A. and Brown, A.J. (2015) 'Contribution of Fdh3 and Glr1 to Glutathione Redox State, Stress Adaptation and Virulence in *Candida albicans*', *PLoS One*, 10(6), p. e0126940.

- To, E.A., Ueda, Y., Kakimoto, S.I. and Oshima, Y. (1973) 'Isolation and characterization of acid phosphatase mutants in *Saccharomyces cerevisiae*', *J Bacteriol*, 113(2), pp. 727-38.
- Toone, W.M., Morgan, B.A. and Jones, N. (2001) 'Redox control of AP-1-like factors in yeast and beyond', *Oncogene*, 20(19), pp. 2336-46.
- Tottey, S., Waldron, K.J., Firbank, S.J., Reale, B., Bessant, C., Sato, K., Cheek, T.R., Gray, J., Banfield, M.J., Dennison, C. and Robinson, N.J. (2008) 'Protein-folding location can regulate manganese-binding versus copper- or zinc-binding', *Nature*, 455(7216), pp. 1138-42.
- Trilisenko, L.V. and Kulakovskaya, T.V. (2014) 'Polyphosphates as an energy source for growth of *Saccharomyces cerevisiae*', *Biochemistry (Mosc)*, 79(5), pp. 478-82.
- Tsoni, S.V., Kerrigan, A.M., Marakalala, M.J., Srinivasan, N., Duffield, M., Taylor, P.R., Botto, M., Steele, C. and Brown, G.D. (2009) 'Complement C3 plays an essential role in the control of opportunistic fungal infections', *Infect Immun*, 77(9), pp. 3679-85.
- Tsuchimori, N., Sharkey, L.L., Fonzi, W.A., French, S.W., Edwards, J.E., Jr. and Filler, S.G. (2000) 'Reduced virulence of HWP1-deficient mutants of *Candida albicans* and their interactions with host cells', *Infect Immun*, 68(4), pp. 1997-2002.
- Uauy, R., Maass, A. and Araya, M. (2008) 'Estimating risk from copper excess in human populations', *The American Journal of Clinical Nutrition*, 88(3), pp. 867S-871S.
- Urban, C., Xiong, X., Sohn, K., Schroppel, K., Brunner, H. and Rupp, S. (2005) 'The moonlighting protein Tsa1p is implicated in oxidative stress response and in cell wall biogenesis in *Candida albicans*', *Mol Microbiol*, 57(5), pp. 1318-41.
- Verbalis, J.G. (2003) 'Disorders of body water homeostasis', *Best Pract Res Clin Endocrinol Metab*, 17(4), pp. 471-503.
- Vieira, O.V., Botelho, R.J. and Grinstein, S. (2002) 'Phagosome maturation: aging gracefully', *Biochem J*, 366(Pt 3), pp. 689-704.
- Voigt, J., Hunniger, K., Bouzani, M., Jacobsen, I.D., Barz, D., Hube, B., Löffler, J. and Kurzai, O. (2014) 'Human natural killer cells acting as phagocytes against *Candida albicans* and mounting an inflammatory response that modulates neutrophil antifungal activity', *J Infect Dis*, 209(4), pp. 616-26.
- Vylkova, S., Carman, A.J., Danhof, H.A., Collette, J.R., Zhou, H. and Lorenz, M.C. (2011) 'The fungal pathogen *Candida albicans* autoinduces hyphal morphogenesis by raising extracellular pH', *MBio*, 2(3), pp. e00055-11.
- Vylkova, S. and Lorenz, M.C. (2014) 'Modulation of phagosomal pH by *Candida albicans* promotes hyphal morphogenesis and requires Stp2p, a regulator of amino acid transport', *PLoS Pathog*, 10(3), p. e1003995.
- Walker, L.A., Maccallum, D.M., Bertram, G., Gow, N.A., Odds, F.C. and Brown, A.J. (2009) 'Genome-wide analysis of *Candida albicans* gene expression patterns during infection of the mammalian kidney', *Fungal Genet Biol*, 46(2), pp. 210-9.
- Wang, Y., Abu Irqeba, A., Ayalew, M. and Suntay, K. (2009) 'Sumoylation of transcription factor Tec1 regulates signaling of mitogen-activated protein kinase pathways in yeast', *PLoS One*, 4(10), p. e7456.

- Wang, Y., Cao, Y.Y., Jia, X.M., Cao, Y.B., Gao, P.H., Fu, X.P., Ying, K., Chen, W.S. and Jiang, Y.Y. (2006) 'Cap1p is involved in multiple pathways of oxidative stress response in *Candida albicans*', *Free Radic Biol Med*, 40(7), pp. 1201-9.
- Weaver, C.T., Harrington, L.E., Mangan, P.R., Gavrieli, M. and Murphy, K.M. (2006) 'Th17: an effector CD4 T cell lineage with regulatory T cell ties', *Immunity*, 24(6), pp. 677-88.
- Weiss, M., Bental, M. and Pick, U. (1991) 'Hydrolysis of polyphosphates and permeability changes in response to osmotic shocks in cells of the halotolerant alga *dunaliella*', *Plant Physiol*, 97(3), pp. 1241-8.
- Weissman, Z. and Kornitzer, D. (2004) 'A family of *Candida* cell surface haem-binding proteins involved in haemin and haemoglobin-iron utilization', *Mol Microbiol*, 53(4), pp. 1209-20.
- Weydert, C.J. and Cullen, J.J. (2010) 'Measurement of superoxide dismutase, catalase and glutathione peroxidase in cultured cells and tissue', *Nat Protoc*, 5(1), pp. 51-66.
- Whiteway, M. and Bachewich, C. (2007) 'Morphogenesis in *Candida albicans*', *Annu Rev Microbiol*, 61, pp. 529-53.
- Wilson, D., Thewes, S., Zakikhany, K., Fradin, C., Albrecht, A., Almeida, R., Brunke, S., Grosse, K., Martin, R., Mayer, F., Leonhardt, I., Schild, L., Seider, K., Skibbe, M., Slesiona, S., Waechter, B., Jacobsen, I. and Hube, B. (2009) 'Identifying infection-associated genes of *Candida albicans* in the postgenomic era', *FEMS Yeast Res*, 9(5), pp. 688-700.
- Wilson, D., Tutulan-Cunita, A., Jung, W., Hauser, N.C., Hernandez, R., Williamson, T., Piekarska, K., Rupp, S., Young, T. and Stateva, L. (2007) 'Deletion of the high-affinity cAMP phosphodiesterase encoded by *PDE2* affects stress responses and virulence in *Candida albicans*', *Mol Microbiol*, 65(4), pp. 841-56.
- Wurst, H., Shiba, T. and Kornberg, A. (1995) 'The gene for a major exopolyphosphatase of *Saccharomyces cerevisiae*', *J Bacteriol*, 177(4), pp. 898-906.
- Wykoff, D.D. and O'Shea, E.K. (2001) 'Phosphate transport and sensing in *Saccharomyces cerevisiae*', *Genetics*, 159(4), pp. 1491-9.
- Wykoff, D.D., Rizvi, A.H., Raser, J.M., Margolin, B. and O'Shea, E.K. (2007) 'Positive feedback regulates switching of phosphate transporters in *S. cerevisiae*', *Mol Cell*, 27(6), pp. 1005-13.
- Wysong, D.R., Christin, L., Sugar, A.M., Robbins, P.W. and Diamond, R.D. (1998) 'Cloning and sequencing of a *Candida albicans* catalase gene and effects of disruption of this gene', *Infect Immun*, 66(5), pp. 1953-61.
- Xu, W., Smith, F.J., Jr., Subaran, R. and Mitchell, A.P. (2004) 'Multivesicular body-ESCRT components function in pH response regulation in *Saccharomyces cerevisiae* and *Candida albicans*', *Mol Biol Cell*, 15(12), pp. 5528-37.
- Yamada-Okabe, T., Mio, T., Ono, N., Kashima, Y., Matsui, M., Arisawa, M. and Yamada-Okabe, H. (1999) 'Roles of three histidine kinase genes in hyphal development and virulence of the pathogenic fungus *Candida albicans*', *J Bacteriol*, 181(23), pp. 7243-7.

- Yancey, P.H. (2005) 'Organic osmolytes as compatible, metabolic and counteracting cytoprotectants in high osmolarity and other stresses', *J Exp Biol*, 208(Pt 15), pp. 2819-30.
- Yates, R.M. and Russell, D.G. (2005) 'Phagosome maturation proceeds independently of stimulation of toll-like receptors 2 and 4', *Immunity*, 23(4), pp. 409-17.
- Yin, Z., Stead, D., Walker, J., Selway, L., Smith, D.A., Brown, A.J. and Quinn, J. (2009) 'A proteomic analysis of the salt, cadmium and peroxide stress responses in *Candida albicans* and the role of the Hog1 stress-activated MAPK in regulating the stress-induced proteome', *Proteomics*, 9(20), pp. 4686-703.
- Youngman, M.J., Rogers, Z.N. and Kim, D.H. (2011) 'A decline in p38 MAPK signaling underlies immunosenescence in *Caenorhabditis elegans*', *PLoS Genet*, 7(5), p. e1002082.
- Yuan, X., Mitchell, B.M., Hua, X., Davis, D.A. and Wilhelmus, K.R. (2010) 'The RIM101 signal transduction pathway regulates *Candida albicans* virulence during experimental keratomycosis', *Invest Ophthalmol Vis Sci*, 51(9), pp. 4668-76.
- Zakikhany, K., Naglik, J.R., Schmidt-Westhausen, A., Holland, G., Schaller, M. and Hube, B. (2007) 'In vivo transcript profiling of *Candida albicans* identifies a gene essential for interepithelial dissemination', *Cell Microbiol*, 9(12), pp. 2938-54.
- Zhang, X., De Micheli, M., Coleman, S.T., Sanglard, D. and Moye-Rowley, W.S. (2000) 'Analysis of the oxidative stress regulation of the *Candida albicans* transcription factor, Cap1p', *Mol Microbiol*, 36(3), pp. 618-29.
- Zheng, Y., Danilenko, D.M., Valdez, P., Kasman, I., Eastham-Anderson, J., Wu, J. and Ouyang, W. (2007) 'Interleukin-22, a T(H)17 cytokine, mediates IL-23-induced dermal inflammation and acanthosis', *Nature*, 445(7128), pp. 648-51.
- Zhou, X. and O'Shea, E.K. (2011) 'Integrated approaches reveal determinants of genome-wide binding and function of the transcription factor Pho4', *Mol Cell*, 42(6), pp. 826-36.
- Zhu, W. and Filler, S.G. (2010) 'Interactions of *Candida albicans* with epithelial cells', *Cell Microbiol*, 12(3), pp. 273-82.
- Znaidi, S., Barker, K.S., Weber, S., Alarco, A.M., Liu, T.T., Boucher, G., Rogers, P.D. and Raymond, M. (2009) 'Identification of the *Candida albicans* Cap1p regulon', *Eukaryot Cell*, 8(6), pp. 806-20.

Appendix

Superoxide stress sensitive mutants		
Transcription factor mutants		
ORF	Gene	SIS
ORF19.610	<i>EFG1</i>	-0.82282
ORF19.5133	<i>ZCF29</i>	-0.75071
ORF19.1623	<i>CAP1</i>	-0.66091
ORF19.7247	<i>RIM101</i>	-0.64918
ORF19.2119	<i>NDT80</i>	-0.56936
ORF19.1069	<i>RPN4</i>	-0.40951
ORF19.1253	<i>PHO4</i>	-0.40382
ORF19.971	<i>SKN7</i>	-0.39617
ORF19.3252	<i>DAL81</i>	-0.33632
ORF19.2088	<i>orf19.2089</i>	-0.33
ORF19.3193	<i>FCR3</i>	-0.30926
ORF19.4318	<i>MIG1</i>	-0.30739
ORF19.4722	<i>orf19.4723</i>	-0.3
ORF19.7401	<i>ISW2</i>	-0.29454
ORF19.6121	<i>MNL1</i>	-0.28467
ORF19.723	<i>BCR1</i>	-0.27534
ORF19.2647	<i>ZCF14</i>	-0.27263
ORF19.909	<i>STP4</i>	-0.23973
ORF19.4869	<i>SFU1</i>	-0.22361
ORF19.7372	<i>MRR1</i>	-0.21954
ORF19.4766	<i>ARG81</i>	-0.21644
ORF19.173	<i>orf19.174</i>	-0.21063
ORF19.1543	<i>OPI1</i>	-0.20711
ORF19.5908	<i>TEC1</i>	-0.19889
ORF19.454	<i>SFL1</i>	-0.17774
ORF19.2842	<i>GZF3</i>	-0.16989
ORF19.2315	<i>orf19.2315</i>	-0.16627
ORF19.5343	<i>ASH1</i>	-0.15274
ORF19.7436	<i>AAF1</i>	-0.13638
ORF19.6817	<i>FCR1</i>	-0.13422
ORF19.5910	<i>orf19.5911</i>	-0.11645
ORF19.7381	<i>AHR1</i>	-0.11391
ORF19.6985	<i>TEA1</i>	-0.11234
ORF19.1926	<i>SEF2</i>	-0.10197
ORF19.4767	<i>ZCF28</i>	-0.10129
ORF19.3182	<i>GIS2</i>	-0.09652
ORF19.5338	<i>GAL4</i>	-0.09501
ORF19.4778	<i>LYS142</i>	-0.08534
ORF19.4670	<i>CAS5</i>	-0.08414
ORF19.3986	<i>PPR1</i>	-0.0822
ORF19.7150	<i>NRG1</i>	-0.08153

ORF19.1685	<i>ZCF7</i>	-0.07823
ORF19.1497	<i>ZCF6</i>	-0.07819
ORF19.391	<i>UPC2</i>	-0.0771
ORF19.3625	<i>orf19.3626</i>	-0.07658
ORF19.6109	<i>TUP1</i>	-0.07464
ORF19.4000	<i>GRF10</i>	-0.07314
ORF19.1973	<i>HAP5</i>	-0.06788
ORF19.3127	<i>CZF1</i>	-0.06658
ORF19.6781	<i>ZFU2</i>	-0.06639
ORF19.4752	<i>MSN4</i>	-0.05572
ORF19.1275	<i>GAT1</i>	-0.05483

Noble deletion library mutants		
ORF	Gene	SIS
ORF19.7247	<i>RIM101</i>	-0.79001
ORF19.3995	<i>ORF19.3995</i>	-0.781
ORF19.5759	<i>ORF19.5759</i>	-0.76698
ORF19.4658	<i>ORF19.4658</i>	-0.76246
ORF19.5285	<i>ORF19.5285</i>	-0.75271
ORF19.5406	<i>ORF19.5406</i>	-0.72223
ORF19.1623	<i>CAP1</i>	-0.7217
ORF19.5178	<i>ORF19.5178</i>	-0.7002
ORF19.4292	<i>ORF19.4292</i>	-0.66384
ORF19.4444	<i>ORF19.4444</i>	-0.6458
ORF19.5241	<i>ORF19.5241</i>	-0.59438
ORF19.4859	<i>ORF19.4859</i>	-0.56158
ORF19.6348	<i>ORF19.6348</i>	-0.54122
ORF19.4474	<i>ORF19.4474</i>	-0.50704
ORF19.5224	<i>ORF19.5224</i>	-0.5047
ORF19.13191	<i>ORF19.13191</i>	-0.49942
ORF19.4212	<i>FET99</i>	-0.49754
ORF19.5915	<i>ORF19.5915</i>	-0.49721
ORF19.6011	<i>ORF19.6011</i>	-0.46055
ORF19.4193	<i>ORF19.4193</i>	-0.45457
ORF19.7086	<i>ORF19.7086</i>	-0.45388
ORF19.101	<i>ORF19.101</i>	-0.43879
ORF19.4475	<i>ORF19.4475</i>	-0.4345
ORF19.6202	<i>ORF19.6202</i>	-0.42129
ORF19.4084	<i>ORF19.4084</i>	-0.41624
ORF19.3534	<i>ORF19.3534</i>	-0.41057
ORF19.5968	<i>ORF19.5968</i>	-0.40694
ORF19.6411	<i>ORF19.6411</i>	-0.40406
ORF19.1814	<i>ORF19.1814</i>	-0.40201
ORF19.6738	<i>ORF19.6738</i>	-0.39924
ORF19.4002	<i>ORF19.4002</i>	-0.38943
ORF19.1567	<i>ORF19.1567</i>	-0.38627

ORF19.6607	<i>ORF19.6607</i>	-0.37909
ORF19.5892	<i>ORF19.5892</i>	-0.37858
ORF19.1625	<i>ORF19.1625</i>	-0.37549
ORF19.4284	<i>ORF19.4284</i>	-0.37452
ORF19.4089	<i>ORF19.4089</i>	-0.37167
ORF19.7313	<i>ORF19.7313</i>	-0.35649
ORF19.4056	<i>BRG1</i>	-0.35308
ORF19.7381	<i>AHR1</i>	-0.3516
ORF19.4036	<i>ORF19.4036</i>	-0.34674
ORF19.4772	<i>ORF19.4772</i>	-0.33973
ORF19.4655	<i>ORF19.4655</i>	-0.33653
ORF19.4758	<i>ORF19.4758</i>	-0.33549
ORF19.328	<i>ORF19.328</i>	-0.3318
ORF19.4707	<i>ORF19.4707</i>	-0.33142
<i>ORF19.4211</i>	<i>FET31</i>	-0.33111
ORF19.6232	<i>ORF19.6232</i>	-0.31631
ORF19.4242	<i>ORF19.4242</i>	-0.31624
ORF19.4496	<i>ORF19.4496</i>	-0.31328
ORF19.2157	<i>ORF19.2157</i>	-0.30772
ORF19.5588	<i>ORF19.5588</i>	-0.30606
ORF19.4195	<i>ORF19.4195</i>	-0.30335
ORF19.6553	<i>ORF19.6553</i>	-0.30198
ORF19.5760	<i>ORF19.5760</i>	-0.29381
ORF19.6038	<i>UGA32</i>	-0.2922
ORF19.287	<i>ORF19.287</i>	-0.29066
ORF19.4678	<i>ORF19.4678</i>	-0.28604
ORF19.6324	<i>ORF19.6324</i>	-0.28386
ORF19.6376	<i>ORF19.6376</i>	-0.28215
ORF19.267	<i>ORF19.267</i>	-0.2812
ORF19.4362	<i>ORF19.4362</i>	-0.28113
ORF19.5874	<i>ORF19.5874</i>	-0.28022
ORF19.794	<i>ORF19.794</i>	-0.27932
ORF19.5181	<i>ORF19.5181</i>	-0.27859
ORF19.6365	<i>ORF19.6365</i>	-0.27384
ORF19.5485	<i>ORF19.5485</i>	-0.26227
ORF19.5662	<i>ORF19.5662</i>	-0.26213
ORF19.6358	<i>ORF19.6358</i>	-0.25903
ORF19.4843	<i>ORF19.4843</i>	-0.25726
ORF19.2821	<i>ORF19.2821</i>	-0.25368
ORF19.5207	<i>ORF19.5207</i>	-0.25309
ORF19.4869	<i>SFU1</i>	-0.24595
ORF19.5559	<i>ORF19.5559</i>	-0.24485
ORF19.11257	<i>ORF19.11257</i>	-0.24475
ORF19.4182	<i>ORF19.4182</i>	-0.24224
ORF19.5547	<i>ORF19.5547</i>	-0.23943
ORF19.3966	<i>ORF19.3966</i>	-0.23901

ORF19.2500	<i>ORF19.2500</i>	-0.2371
ORF19.7475	<i>ORF19.7475</i>	-0.2336
ORF19.5994	<i>ORF19.5994</i>	-0.23105
ORF19.4135	<i>ORF19.4135</i>	-0.22954
ORF19.4567	<i>ORF19.4567</i>	-0.22743
ORF19.7329	<i>ORF19.7329</i>	-0.22432
ORF19.6948	<i>ORF19.6948</i>	-0.21905
ORF19.5600	<i>ORF19.5600</i>	-0.21808
ORF19.3203	<i>ORF19.3203</i>	-0.21686
ORF19.5634	<i>ORF19.5634</i>	-0.21411
ORF19.5673	<i>ORF19.5673</i>	-0.21308
ORF19.6530	<i>ORF19.6530</i>	-0.21307
ORF19.4933	<i>ORF19.4933</i>	-0.21283
ORF19.4376	<i>ORF19.4376</i>	-0.20991
ORF19.5020	<i>ORF19.5020</i>	-0.20953
ORF19.4805	<i>ORF19.4805</i>	-0.20874
ORF19.5585	<i>ORF19.5585</i>	-0.20566
ORF19.5338	<i>GAL4</i>	-0.2041
ORF19.4831	<i>ORF19.4831</i>	-0.20367
ORF19.5736	<i>ORF19.5736</i>	-0.20362
ORF19.4729	<i>ORF19.4729</i>	-0.20289
ORF19.1471	<i>ORF19.1471</i>	-0.20263
ORF19.5200	<i>ORF19.5200</i>	-0.20228
ORF19.11270	<i>ORF19.11270</i>	-0.20172
ORF19.6018	<i>ORF19.6018</i>	-0.20072
ORF19.4407	<i>ORF19.4407</i>	-0.19964
ORF19.3611	<i>ORF19.3611</i>	-0.19896
ORF19.5001	<i>CUP2</i>	-0.19632
ORF19.3449	<i>ORF19.3449</i>	-0.19362
ORF19.7224	<i>ORF19.7224</i>	-0.18992
ORF19.2805	<i>ORF19.2805</i>	-0.18759
ORF19.7391	<i>ORF19.7391</i>	-0.18104
ORF19.7320	<i>ORF19.7320</i>	-0.17783
ORF19.3470	<i>ORF19.3470</i>	-0.17466
ORF19.10080	<i>ORF19.10080</i>	-0.17433
ORF19.4014	<i>ORF19.4014</i>	-0.16889
ORF19.6219	<i>ORF19.6219</i>	-0.16883
ORF19.4248	<i>ORF19.4248</i>	-0.16677
ORF19.4459	<i>ORF19.4459</i>	-0.16333
ORF19.4982	<i>ORF19.4982</i>	-0.15923
ORF19.1710	<i>ORF19.1710</i>	-0.15785
ORF19.5644	<i>ORF19.5644</i>	-0.15747
ORF19.7096	<i>ORF19.7096</i>	-0.15685
ORF19.4012	<i>ORF19.4012</i>	-0.15634
ORF19.4185	<i>ORF19.4185</i>	-0.15562
ORF19.5942	<i>ORF19.5942</i>	-0.15423

ORF19.6182	<i>ZCF34</i>	-0.15337
ORF19.7328	<i>ORF19.7328</i>	-0.15152
ORF19.5247	<i>ORF19.5247</i>	-0.15028
ORF19.4471	<i>ORF19.4471</i>	-0.14884
ORF19.2836	<i>ORF19.2836</i>	-0.14714
ORF19.5729	<i>FGR17</i>	-0.1471
ORF19.4592	<i>ORF19.4592</i>	-0.14608
ORF19.7221	<i>ORF19.7221</i>	-0.14503
ORF19.6736	<i>ORF19.6736</i>	-0.14502
ORF19.3811	<i>ORF19.3811</i>	-0.14341
ORF19.4649	<i>ZCF27</i>	-0.14284
ORF19.4041	<i>ORF19.4041</i>	-0.14013
ORF19.4603	<i>ORF19.4603</i>	-0.13817
ORF19.4916	<i>ORF19.4916</i>	-0.13783
ORF19.3854	<i>ORF19.3854</i>	-0.13745
ORF19.7590	<i>ORF19.7590</i>	-0.13476
ORF19.6420	<i>ORF19.6420</i>	-0.13272
ORF19.3720	<i>ORF19.3720</i>	-0.13167
ORF19.4975	<i>ORF19.4975</i>	-0.13034
ORF19.7186	<i>ORF19.7186</i>	-0.1302
ORF19.30	<i>SPF1</i>	-0.12991
ORF19.7282	<i>ORF19.7282</i>	-0.12858
ORF19.7349	<i>ORF19.7349</i>	-0.127
ORF19.5782	<i>ORF19.5782</i>	-0.1264
ORF19.7318	<i>ORF19.7318</i>	-0.12426
ORF19.6318	<i>ORF19.6318</i>	-0.12423
ORF19.6035	<i>ORF19.6035</i>	-0.12403
ORF19.5975	<i>TRY4</i>	-0.12079
ORF19.194	<i>ORF19.194</i>	-0.12014
ORF19.6653	<i>ORF19.6653</i>	-0.11982
ORF19.564	<i>ORF19.564</i>	-0.1188
ORF19.6313	<i>ORF19.6313</i>	-0.1186
ORF19.5593	<i>ORF19.5593</i>	-0.11766
ORF19.2570	<i>ORF19.2570</i>	-0.11602
ORF19.7347	<i>ORF19.7347</i>	-0.11552
ORF19.3290	<i>ORF19.3290</i>	-0.11541
ORF19.1573	<i>ORF19.1573</i>	-0.11469
ORF19.7218	<i>ORF19.7218</i>	-0.11367
ORF19.7388	<i>ORF19.7388</i>	-0.11357
ORF19.6514	<i>CUP9</i>	-0.11164
ORF19.4785	<i>ORF19.4785</i>	-0.1106
ORF19.4566	<i>ORF19.4566</i>	-0.10642
ORF19.3710	<i>ORF19.3710</i>	-0.10512
ORF19.7228	<i>ORF19.7228</i>	-0.10342
ORF19.3201	<i>ORF19.3201</i>	-0.10333
ORF19.4188	<i>ORF19.4188</i>	-0.102

ORF19.4844	<i>ORF19.4844</i>	-0.10164
ORF19.4412	<i>ORF19.4412</i>	-0.10141
ORF19.3374	<i>ORF19.3374</i>	-0.0994
ORF19.6245	<i>ORF19.6245</i>	-0.09907
ORF19.757	<i>ORF19.757</i>	-0.09895
ORF19.4350	<i>ORF19.4350</i>	-0.09735
ORF19.5342	<i>ORF19.5342</i>	-0.09481
ORF19.5661	<i>ORF19.5661</i>	-0.09474
ORF19.1373	<i>ORF19.1373</i>	-0.09397
ORF19.6927	<i>ORF19.6927</i>	-0.09042
ORF19.4183	<i>ORF19.4183</i>	-0.08996
ORF19.895	<i>ORF19.895</i>	-0.08985
ORF19.4312	<i>ORF19.4312</i>	-0.08515
ORF19.7330	<i>ORF19.7330</i>	-0.08487
ORF19.5848	<i>ORF19.5848</i>	-0.08479
ORF19.4545	<i>SWI4</i>	-0.08417
ORF19.1860	<i>ORF19.1860</i>	-0.08277
ORF19.7523	<i>ORF19.7523</i>	-0.07753
ORF19.6592	<i>ORF19.6592</i>	-0.07744
ORF19.4984	<i>ORF19.4984</i>	-0.07731
ORF19.6001	<i>ORF19.6001</i>	-0.07698
ORF19.5352	<i>ORF19.5352</i>	-0.07439
ORF19.6606	<i>ORF19.6606</i>	-0.07411
ORF19.7206	<i>ORF19.7206</i>	-0.07376
ORF19.3982	<i>ORF19.3982</i>	-0.07329
ORF19.2063	<i>ORF19.2063</i>	-0.07295
ORF19.10841	<i>ORF19.10841</i>	-0.0728
ORF19.4640	<i>ORF19.4640</i>	-0.07207
ORF19.5776	<i>ORF19.5776</i>	-0.07206
ORF19.4593	<i>ORF19.4593</i>	-0.07112
ORF19.5903	<i>ORF19.5903</i>	-0.07083
ORF19.3488	<i>ORF19.3488</i>	-0.06915
ORF19.2463	<i>ORF19.2463</i>	-0.06726
ORF19.3453	<i>ORF19.3453</i>	-0.06602
ORF19.4890	<i>ORF19.4890</i>	-0.06582
ORF19.4424	<i>ORF19.4424</i>	-0.06579
ORF19.3912	<i>GLN3</i>	-0.06397
ORF19.3315	<i>ORF19.3315</i>	-0.06251
ORF19.7497	<i>ORF19.7497</i>	-0.06097
ORF19.7049	<i>ORF19.7049</i>	-0.06015
ORF19.6053	<i>ORF19.6053</i>	-0.05933
ORF19.2133	<i>ORF19.2133</i>	-0.05616
ORF19.5399	<i>ORF19.5399</i>	-0.05579
ORF19.5170	<i>ORF19.5170</i>	-0.05546
ORF19.4765	<i>ORF19.4765</i>	-0.05415
ORF19.3412	<i>ORF19.3412</i>	-0.05274

ORF19.5643	<i>ORF19.5643</i>	-0.05228
ORF19.4524	<i>ZCF24</i>	-0.05222
ORF19.783	<i>ORF19.783</i>	-0.05103

Appendix 1A. Superoxide stress sensitive *C. albicans* mutants.

Cationic stress sensitive mutants		
Transcription factor mutants		
ORF	Gene	SIS
ORF19.3252	<i>DAL81</i>	-0.229363
ORF19.1253	<i>PHO4</i>	-0.194368
ORF19.3182	<i>GIS2</i>	-0.175201
ORF19.1499	<i>CTF1</i>	-0.157821
ORF19.610	<i>EFG1</i>	-0.133175
ORF19.7247	<i>RIM101</i>	-0.127529
ORF19.1187	<i>CPH2</i>	-0.116837
ORF19.5326	<i>orf19.5327</i>	-0.116117
ORF19.1255	<i>ZCF5</i>	-0.109325
ORF19.6985	<i>TEA1</i>	-0.106443
ORF19.7401	<i>ISW2</i>	-0.102407
ORF19.3625	<i>orf19.3626</i>	-0.0991469
ORF19.723	<i>BCR1</i>	-0.080001
ORF19.5251	<i>ZCF30</i>	-0.0724415
ORF19.909	<i>STP4</i>	-0.0700823
ORF19.6817	<i>FCR1</i>	-0.070011
ORF19.2961	<i>orf19.2962</i>	-0.0685469
ORF19.4670	<i>CAS5</i>	-0.0583105
ORF19.5133	<i>ZCF29</i>	-0.0570857
ORF19.4766	<i>ARG81</i>	-0.0538952
ORF19.4778	<i>LYS142</i>	-0.0538742
ORF19.517	<i>HAP31</i>	-0.0538441
ORF19.4662	<i>RLM1</i>	-0.0512116

Noble deletion library mutants		
ORF	Gene	SIS
ORF19.5170	<i>ENA21</i>	-0.68911
ORF19.1814	<i>ORF19.1814</i>	-0.34513
ORF19.3182	<i>GIS2</i>	-0.31257
ORF19.4084	<i>ORF19.4084</i>	-0.30266
ORF19.3534	<i>ORF19.3534</i>	-0.29303
ORF19.2157	<i>ORF19.2157</i>	-0.28638
ORF19.12247	<i>ORF19.12247</i>	-0.17928
ORF19.13064	<i>ORF19.13064</i>	-0.17356
ORF19.30	<i>ORF19.30</i>	-0.17049
ORF19.1267	<i>ORF19.1267</i>	-0.16752
ORF19.7186	<i>ORF19.7186</i>	-0.16154
ORF19.101	<i>ORF19.101</i>	-0.1577

ORF19.691	<i>ORF19.691</i>	-0.14965
ORF19.2821	<i>ORF19.2821</i>	-0.13681
ORF19.267	<i>ORF19.267</i>	-0.13531
ORF19.6011	<i>ORF19.6011</i>	-0.13393
ORF19.242	<i>ORF19.242</i>	-0.13173
ORF19.7510	<i>ORF19.7510</i>	-0.12702
ORF19.194	<i>ORF19.194</i>	-0.11916
ORF19.7388	<i>ORF19.7388</i>	-0.11606
ORF19.2500	<i>ORF19.2500</i>	-0.11464
ORF19.403	<i>ORF19.403</i>	-0.11306
ORF19.942	<i>ORF19.942</i>	-0.11122
ORF19.7381	<i>AHR1</i>	-0.10994
ORF19.215	<i>ORF19.215</i>	-0.10721
ORF19.2115	<i>ORF19.2115</i>	-0.10255
ORF19.5994	<i>ORF19.5994</i>	-0.09978
ORF19.6018	<i>ORF19.6018</i>	-0.09945
ORF19.341	<i>ORF19.341</i>	-0.09843
ORF19.5338	<i>GAL4</i>	-0.09836
ORF19.641	<i>ORF19.641</i>	-0.09555
ORF19.682	<i>ORF19.682</i>	-0.09538
ORF19.10841	<i>ORF19.10841</i>	-0.09405
ORF19.5559	<i>ORF19.5559</i>	-0.09376
ORF19.173	<i>orf19.174</i>	-0.09285
ORF19.540	<i>ORF19.540</i>	-0.09254
ORF19.348	<i>ORF19.348</i>	-0.09229
ORF19.1625	<i>ORF19.1625</i>	-0.09224
ORF19.1747	<i>ORF19.1747</i>	-0.09221
ORF19.3417	<i>ORF19.3417</i>	-0.08999
ORF19.895	<i>ORF19.895</i>	-0.0897
ORF19.3753	<i>SEF1</i>	-0.08967
ORF19.3283	<i>ORF19.3283</i>	-0.08934
ORF19.5776	<i>ORF19.5776</i>	-0.08801
ORF19.3722	<i>ORF19.3722</i>	-0.08747
ORF19.7391	<i>ORF19.7391</i>	-0.08723
ORF19.548	<i>ORF19.548</i>	-0.08715
ORF19.3470	<i>ORF19.3470</i>	-0.087
ORF19.3710	<i>ORF19.3710</i>	-0.08451
ORF19.4758	<i>ORF19.4758</i>	-0.08306
ORF19.217	<i>orf19.218</i>	-0.08273
ORF19.726	<i>ORF19.726</i>	-0.08256
ORF19.3449	<i>ORF19.3449</i>	-0.08248
ORF19.433	<i>ORF19.433</i>	-0.08239
ORF19.3592	<i>ORF19.3592</i>	-0.08196
ORF19.6038	<i>UGA32</i>	-0.08052
ORF19.1317	<i>ORF19.1317</i>	-0.07941
ORF19.7247	<i>RIM101</i>	-0.0791

ORF19.4118	<i>ORF19.4118</i>	-0.07838
ORF19.2064	<i>ORF19.2064</i>	-0.07827
ORF19.255	<i>ZCF1</i>	-0.07785
ORF19.335	<i>ORF19.335</i>	-0.07659
ORF19.2133	<i>ORF19.2133</i>	-0.07651
ORF19.1411	<i>ORF19.1411</i>	-0.07578
ORF19.138	<i>ORF19.138</i>	-0.07467
ORF19.557	<i>ORF19.557</i>	-0.0745
ORF19.1373	<i>ORF19.1373</i>	-0.07416
ORF19.328	<i>ORF19.328</i>	-0.07365
ORF19.7086	<i>ORF19.7086</i>	-0.07267
ORF19.4567	<i>ORF19.4567</i>	-0.07252
ORF19.3395	<i>ORF19.3395</i>	-0.07198
ORF19.7023	<i>ORF19.7023</i>	-0.07179
ORF19.156	<i>ORF19.156</i>	-0.0714
ORF19.3693	<i>ORF19.3693</i>	-0.07059
ORF19.4856	<i>ORF19.4856</i>	-0.068
ORF19.5207	<i>ORF19.5207</i>	-0.06793
ORF19.3488	<i>ORF19.3488</i>	-0.06776
ORF19.431	<i>ZCF2</i>	-0.06773
ORF19.695	<i>ORF19.695</i>	-0.06689
ORF19.1497	<i>ZCF6</i>	-0.06685
ORF19.1576	<i>ORF19.1576</i>	-0.06678
ORF19.3207	<i>ORF19.3207</i>	-0.06663
ORF19.459	<i>ORF19.459</i>	-0.06574
ORF19.6607	<i>ORF19.6607</i>	-0.06547
ORF19.529	<i>ORF19.529</i>	-0.06498
ORF19.4312	<i>ORF19.4312</i>	-0.06446
ORF19.166	<i>ASG1</i>	-0.0641
ORF19.5662	<i>ORF19.5662</i>	-0.06396
ORF19.783	<i>ORF19.783</i>	-0.06385
ORF19.3212	<i>ORF19.3212</i>	-0.06327
ORF19.5673	<i>ORF19.5673</i>	-0.06316
ORF19.2156	<i>ORF19.2156</i>	-0.06308
ORF19.9470	<i>ORF19.9470</i>	-0.06297
ORF19.4844	<i>ORF19.4844</i>	-0.06237
ORF19.2805	<i>ORF19.2805</i>	-0.06227
ORF19.1471	<i>ORF19.1471</i>	-0.06153
ORF19.7214	<i>ORF19.7214</i>	-0.06087
ORF19.137	<i>ORF19.137</i>	-0.06085
ORF19.3374	<i>ORF19.3374</i>	-0.05994
ORF19.1364	<i>ORF19.1364</i>	-0.05949
ORF19.3384	<i>ORF19.3384</i>	-0.05872
ORF19.268	<i>ORF19.268</i>	-0.05865
ORF19.7314	<i>ORF19.7314</i>	-0.05855
ORF19.5547	<i>ORF19.5547</i>	-0.05833

ORF19.1041	<i>ORF19.1041</i>	-0.05761
ORF19.1567	<i>ORF19.1567</i>	-0.05761
ORF19.5593	<i>ORF19.5593</i>	-0.05759
ORF19.6985	<i>TEA1</i>	-0.05722
ORF19.757	<i>ORF19.757</i>	-0.05697
ORF19.3111	<i>ORF19.3111</i>	-0.05694
ORF19.6948	<i>ORF19.6948</i>	-0.05674
ORF19.419	<i>ORF19.419</i>	-0.05651
ORF19.1643	<i>ORF19.1643</i>	-0.05611
ORF19.5729	<i>FGR17</i>	-0.05604
ORF19.5760	<i>ORF19.5760</i>	-0.05597
ORF19.2108	<i>ORF19.2108</i>	-0.05561
ORF19.4831	<i>ORF19.4831</i>	-0.05552
ORF19.3396	<i>ORF19.3396</i>	-0.05538
ORF19.3404	<i>ORF19.3404</i>	-0.05511
ORF19.7318	<i>ORF19.7318</i>	-0.05481
ORF19.3226	<i>ORF19.3226</i>	-0.0548
ORF19.5352	<i>ORF19.5352</i>	-0.0547
ORF19.7098	<i>ORF19.7098</i>	-0.05442
ORF19.176	<i>ORF19.176</i>	-0.05437
ORF19.7313	<i>ORF19.7313</i>	-0.05435
ORF19.4933	<i>ORF19.4933</i>	-0.05419
ORF19.3412	<i>ORF19.3412</i>	-0.05417
ORF19.3203	<i>ORF19.3203</i>	-0.05404
ORF19.3345	<i>ORF19.3345</i>	-0.05394
ORF19.12108	<i>ORF19.12108</i>	-0.05386
ORF19.7590	<i>ORF19.7590</i>	-0.05362
ORF19.5509	<i>ORF19.5509</i>	-0.05354
ORF19.3453	<i>ORF19.3453</i>	-0.05325
ORF19.3575	<i>ORF19.3575</i>	-0.05318
ORF19.6842	<i>ORF19.6842</i>	-0.05278
ORF19.3720	<i>ORF19.3720</i>	-0.05237
ORF19.1760	<i>ORF19.1760</i>	-0.0523
ORF19.564	<i>ORF19.564</i>	-0.05195
ORF19.1443	<i>ORF19.1443</i>	-0.05185
ORF19.3237	<i>ORF19.3237</i>	-0.05182
ORF19.191	<i>ORF19.191</i>	-0.05175
ORF19.5942	<i>ORF19.5942</i>	-0.05169
ORF19.1185	<i>ORF19.1185</i>	-0.05146
ORF19.4189	<i>ORF19.4189</i>	-0.0514
ORF19.7282	<i>ORF19.7282</i>	-0.05111
ORF19.1623	<i>CAP1</i>	-0.05079
ORF19.1219	<i>ORF19.1219</i>	-0.05058

Appendix 1B. Cationic stress sensitive *C. albicans* mutants.

Alkaline pH stress sensitive mutants		
Transcription factor mutants		
ORF	Gene	SIS
ORF19.610	<i>EFG1</i>	-1.22501
ORF19.971	<i>SKN7</i>	-1.15977
ORF19.1623	<i>CAP1</i>	-0.97074
ORF19.7247	<i>RIM101</i>	-0.8086
ORF19.2842	<i>GZF3</i>	-0.73742
ORF19.3753	<i>SEF1</i>	-0.66057
ORF19.6514	<i>CUP9</i>	-0.59558
ORF19.2088	<i>ORF19.2089</i>	-0.55636
ORF19.6817	<i>FCR1</i>	-0.47498
ORF19.4998	<i>ROB1</i>	-0.46353
ORF19.2119	<i>NDT80</i>	-0.46316
ORF19.1187	<i>CPH2</i>	-0.4594
ORF19.909	<i>STP4</i>	-0.39474
ORF19.5343	<i>ASH1</i>	-0.39
ORF19.7381	<i>AHR1</i>	-0.37185
ORF19.4766	<i>ARG81</i>	-0.36552
ORF19.2476	<i>ORF19.2477</i>	-0.35094
ORF19.6874	<i>ORF19.6875</i>	-0.3499
ORF19.1718	<i>ZCF8</i>	-0.33315
ORF19.6781	<i>ZFU2</i>	-0.29942
ORF19.1253	<i>PHO4</i>	-0.27625
ORF19.2961	<i>orf19.2962</i>	-0.27331
ORF19.1926	<i>SEF2</i>	-0.26904
ORF19.2612	<i>ORF19.2612</i>	-0.25848
ORF19.3252	<i>DAL81</i>	-0.25528
ORF19.1499	<i>CTF1</i>	-0.24967
ORF19.4752	<i>MSN4</i>	-0.07114
ORF19.7401	<i>ISW2</i>	-0.03934

Noble deletion collection mutants		
ORF	Gene	SIS
ORF19.101	<i>ORF19.101</i>	-0.83809
ORF19.3829	<i>ORF19.3829</i>	-0.82388
ORF19.7247	<i>RIM101</i>	-0.74514
ORF19.3995	<i>ORF19.3995</i>	-0.67826
ORF19.4755	<i>ORF19.4755</i>	-0.46804
ORF19.2157	<i>ORF19.2157</i>	-0.38228
ORF19.5286	<i>ORF19.5286</i>	-0.3705
ORF19.5068	<i>ORF19.5068</i>	-0.33608
ORF19.7391	<i>ORF19.7391</i>	-0.27098
ORF19.1623	<i>CAP1</i>	-0.26686
ORF19.13064	<i>ORF19.13064</i>	-0.22299

ORF19.4002	<i>ORF19.4002</i>	-0.2041
ORF19.11257	<i>ORF19.11257</i>	-0.19922
ORF19.4036	<i>ORF19.4036</i>	-0.19858
ORF19.12247	<i>ORF19.12247</i>	-0.18609
ORF19.6736	<i>ORF19.6736</i>	-0.18502
ORF19.1471	<i>ORF19.1471</i>	-0.18159
ORF19.1267	<i>ORF19.1267</i>	-0.16964
ORF19.3753	<i>SEF1</i>	-0.16402
ORF19.3854	<i>ORF19.3854</i>	-0.14652
ORF19.7388	<i>ORF19.7388</i>	-0.13932
ORF19.2115	<i>ORF19.2115</i>	-0.13411
ORF19.942	<i>ORF19.942</i>	-0.132
ORF19.2484	<i>ORF19.2484</i>	-0.11662
ORF19.2020	<i>ORF19.2020</i>	-0.11525
ORF19.726	<i>ORF19.726</i>	-0.11306
ORF19.641	<i>ORF19.641</i>	-0.11226
ORF19.215	<i>ORF19.215</i>	-0.11125
ORF19.30	<i>ORF19.30</i>	-0.10642
ORF19.3417	<i>ORF19.3417</i>	-0.10609
ORF19.6011	<i>ORF19.6011</i>	-0.10017
ORF19.2941	<i>ORF19.2941</i>	-0.09814
ORF19.5200	<i>ORF19.5200</i>	-0.09758
ORF19.6637	<i>ORF19.6637</i>	-0.09696
ORF19.816	<i>ORF19.816</i>	-0.09495
ORF19.2699	<i>ORF19.2699</i>	-0.09342
ORF19.3395	<i>ORF19.3395</i>	-0.09325
ORF19.3534	<i>ORF19.3534</i>	-0.09283
ORF19.469	<i>ORF19.469</i>	-0.09278
ORF19.1373	<i>ORF19.1373</i>	-0.08972
ORF19.5559	<i>ORF19.5559</i>	-0.08907
ORF19.3418	<i>ORF19.3418</i>	-0.08811
ORF19.459	<i>ORF19.459</i>	-0.08802
ORF19.895	<i>ORF19.895</i>	-0.0865
ORF19.242	<i>ORF19.242</i>	-0.08623
ORF19.540	<i>ORF19.540</i>	-0.08537
ORF19.2378	<i>ORF19.2378</i>	-0.08319
ORF19.3283	<i>ORF19.3283</i>	-0.08246
ORF19.305	<i>ORF19.305</i>	-0.08162
ORF19.2703	<i>ORF19.2703</i>	-0.08129
ORF19.10004	<i>ORF19.10004</i>	-0.08127
ORF19.3693	<i>ORF19.3693</i>	-0.08118
ORF19.3618	<i>ORF19.3618</i>	-0.07913
ORF19.4312	<i>ORF19.4312</i>	-0.07883
ORF19.8477	<i>ORF19.8477</i>	-0.07845
ORF19.2245	<i>ORF19.2245</i>	-0.07797
ORF19.5207	<i>ORF19.5207</i>	-0.0775

ORF19.2975	<i>ORF19.2975</i>	-0.07691
ORF19.6738	<i>ORF19.6738</i>	-0.07615
ORF19.194	<i>ORF19.194</i>	-0.07587
ORF19.584	<i>ORF19.584</i>	-0.0757
ORF19.3592	<i>ORF19.3592</i>	-0.07531
ORF19.9470	<i>ORF19.9470</i>	-0.07474
ORF19.1567	<i>ORF19.1567</i>	-0.07467
ORF19.2961	<i>orf19.2962</i>	-0.07357
ORF19.3212	<i>ORF19.3212</i>	-0.07303
ORF19.2460	<i>ORF19.2460</i>	-0.07256
ORF19.2265	<i>ORF19.2265</i>	-0.06959
ORF19.3029	<i>ORF19.3029</i>	-0.06642
ORF19.1643	<i>ORF19.1643</i>	-0.06568
ORF19.3470	<i>ORF19.3470</i>	-0.06552
ORF19.2726	<i>ORF19.2726</i>	-0.06552
ORF19.3707	<i>ORF19.3707</i>	-0.06532
ORF19.3182	<i>GIS2</i>	-0.06516
ORF19.3438	<i>ORF19.3438</i>	-0.06467
ORF19.433	<i>ORF19.433</i>	-0.06467
ORF19.587	<i>ORF19.587</i>	-0.06377
ORF19.1317	<i>ORF19.1317</i>	-0.06377
ORF19.207	<i>ORF19.207</i>	-0.06367
ORF19.100	<i>ORF19.100</i>	-0.06342
ORF19.6327	<i>ORF19.6327</i>	-0.06293
ORF19.5635	<i>ORF19.5635</i>	-0.06242
ORF19.3396	<i>ORF19.3396</i>	-0.06229
ORF19.3722	<i>ORF19.3722</i>	-0.0622
ORF19.1490	<i>ORF19.1490</i>	-0.06148
ORF19.3012	<i>ARO80</i>	-0.06138
ORF19.2868	<i>ORF19.2868</i>	-0.06095
ORF19.137	<i>ORF19.137</i>	-0.06077
ORF19.217	<i>orf19.218</i>	-0.06075
ORF19.199	<i>ORF19.199</i>	-0.06072
ORF19.3112	<i>ORF19.3112</i>	-0.06011
ORF19.1497	<i>ZCF6</i>	-0.0599
ORF19.460	<i>ORF19.460</i>	-0.05924
ORF19.95	<i>ORF19.95</i>	-0.05868
ORF19.3845	<i>ORF19.3845</i>	-0.0584
ORF19.1397	<i>ORF19.1397</i>	-0.05719
ORF19.3453	<i>ORF19.3453</i>	-0.05715
ORF19.1092	<i>ORF19.1092</i>	-0.05645
ORF19.3615	<i>ORF19.3615</i>	-0.05624
ORF19.1920	<i>ORF19.1920</i>	-0.05611
ORF19.3384	<i>ORF19.3384</i>	-0.05588
ORF19.3434	<i>TRY5</i>	-0.05518
ORF19.5736	<i>ORF19.5736</i>	-0.05508

ORF19.3449	<i>ORF19.3449</i>	-0.05469
ORF19.206	<i>ORF19.206</i>	-0.05459
ORF19.3919	<i>ORF19.3919</i>	-0.05448
ORF19.2781	<i>ORF19.2781</i>	-0.05325
ORF19.2697	<i>ORF19.2697</i>	-0.05292
ORF19.341	<i>ORF19.341</i>	-0.05285
ORF19.3311	<i>ORF19.3311</i>	-0.05283
ORF19.449	<i>ORF19.449</i>	-0.05236
ORF19.348	<i>ORF19.348</i>	-0.05209
ORF19.6673	<i>ORF19.6673</i>	-0.05162
ORF19.2771	<i>ORF19.2771</i>	-0.05128

Appendix 1C. Cationic stress sensitive *C. albicans* mutants.

Wt genes upregulated in Pi deplete conditions				
Alias	FoldChange (WT-Pi vs. WT+Pi)	pho4-Pi vs. pho4+Pi	pho4+Pi vs. WT+Pi	pho4-Pi vs. WT-Pi
<i>PHO100</i>	847.65	-1.28571	1.35	-807.286
<i>BTA1</i>	378.789	1.16667	-3.16667	-1028.14
<i>PLB1</i>	320.75	1.25926	6.75	-37.7353
<i>PHO84</i>	289.744	2	-1.69565	-245.652
<i>C1_04800C_A</i>	149.667	1.33333	4	-28.0625
<i>C7_03310W_A</i>	134	-2	52	-5.15385
<i>C3_01540W_A</i>	66.6154	-11.6977	38.6923	-20.1395
<i>C3_02750W_A</i>	66.25	3.2	3.75	-5.52083
<i>RBT7</i>	58.8	1.5	1.4	-28
<i>C4_00530C_A</i>	55.5	?	?	-37
<i>C1_10060C_A</i>	44.8571	3.19565	6.57143	-2.13605
<i>PHO112</i>	42.3846	-1.76471	1.15385	-64.8235
<i>ASM3</i>	40.4	1.04926	4.06	-9.48357
<i>CR_10200W_A</i>	32.9286	1.10526	1.35714	-21.9524
<i>TRY6</i>	31.2	1.27273	2.2	-11.1429
<i>GIT1</i>	30.1456	1.22222	-1.0404	-25.6612
<i>PHO113</i>	26.4861	1.2766	-1.53191	-31.7833
<i>PGA28</i>	24	1.66667	12	-1.2
<i>GCV2</i>	23.7477	-1.04888	17.4486	-1.42753
<i>FET99</i>	21.3718	1.68159	2.57692	-4.93195
<i>SSU1</i>	20.1667	-1.29032	6.66667	-3.90323
<i>RNR1</i>	18.0955	-5.75394	10.2472	-10.1609
<i>MNN1</i>	18.0373	1.7631	3.27612	-3.12274
<i>XOG1</i>	16.2333	-1.76316	2.97778	-9.61184
<i>MSH6</i>	15.225	-2.06224	12.425	-2.52697
<i>MNN22</i>	15.0203	1.25254	3.98649	-3.00812
<i>C3_02140C_A</i>	14.8889	-2.8	4.04444	-10.3077
<i>CR_05800C_A</i>	12.5	-1.85185	6.25	-3.7037
<i>CR_03840C_A</i>	12.3333	-2	2.66667	-9.25
<i>BMT3</i>	11.5614	1.07692	2.50877	-4.27922
<i>CDC19</i>	11.1291	-2.10134	5.86235	-3.9892
<i>GIT4</i>	10.8	1	3.6	-3
<i>GIT3</i>	10.3651	1.12097	1.64021	-5.63741
<i>NAT4</i>	10.25	-3.25	1.625	-20.5
<i>C4_05730W_A</i>	10	1.0625	1.33333	-7.05882
<i>CR_01920W_A</i>	9.71429	3	-3.5	-11.3333
<i>BIO2</i>	9.69118	2.4	-1.51111	-6.10185
<i>C6_03320W_A</i>	9.34669	-1.68602	3.14228	-5.01505
<i>C4_03950C_A</i>	9.33333	-1.44444	4.33333	-3.11111

ALS4	9.15075	-1.12853	-1.77672	-18.348
BMT4	9.06504	1.37222	1.46341	-4.51417
C4_07080C_A	9.04762	-1.44211	6.52381	-2
DPB2	9	-1.84375	6.55556	-2.53125
POL1	8.71642	-1.74317	4.76119	-3.19126
PHO81	8.55747	1.11316	2.18391	-3.52009
GDE1	8.37838	1.16295	3.02703	-2.38004
CR_01910C_A	8	-1.4	3.5	-3.2
GIN1	8	-2.07273	5.18182	-3.2
PLB4.5	7.96279	-3.65385	3.09302	-9.40659
C3_04650W_A	7.71429	1.41509	2.52381	-2.16
C1_11080W_A	7.68889	-1.1583	1.66667	-5.34363
IFE1	7.54762	-1.38095	2.7619	-3.77381
KCS1	7.5	-1.06433	2.33333	-3.42105
ECM331	7.34783	-1.7619	6.43478	-2.0119
CR_07850W_A	7.07143	-1.22222	3.92857	-2.2
MDR1	7	-1.77778	5.33333	-2.33333
ALS2	6.87429	-1.29364	1.02628	-8.66517
UBC15	6.66667	-2.13793	4.13333	-3.44828
SRD1	6.51613	-1.5	4.35484	-2.24444
MCM3	6.50307	-1.75	3.2638	-3.48684
CR_03690W_A	6.40476	1.12152	1.88095	-3.03612
MCD1	6.36364	-2.66667	5.81818	-2.91667
C3_01310W_A	6.30303	-1.5873	3.0303	-3.30159
C7_01100C_A	6.22222	-1.61538	4.66667	-2.15385
CDC13	6.21053	-1.08511	5.36842	-1.25532
C3_03690W_A	6.14286	1.75	2.28571	-1.53571
UPC2	6.13725	-2.14286	3.82353	-3.43956
C3_01280W_A	5.97333	-1.33014	3.70667	-2.14354
C4_01800W_A	5.6	-2.875	2.3	-7
VTC3	5.44302	1.24691	1.78488	-2.44566
C7_04090C_A	5.42188	-1.50307	3.82813	-2.12883
C2_01800W_A	5.4	-1.38095	2.9	-2.57143
C2_08260W_A	5.32558	-1.09434	1.34884	-4.32075
TRY3	5.16438	-1.55752	2.41096	-3.33628
GAL4	5.10714	-1.77966	3.75	-2.42373
C1_04010C_A	5.1	-1.19048	-1.5	-9.10714
C3_05290C_A	5.08333	1.4	1.66667	-2.17857
C7_03140W_A	5.0625	-1.07692	-1.14286	-6.23077
MET13	5.03704	1.20548	1.68981	-2.47273
SMC1	5	-1.39785	3.29114	-2.12366
C6_02420W_A	4.97727	-1.12195	2.09091	-2.67073

SAM2	4.96687	-3.68053	2.0644	-8.85524
CR_03270W_A	4.94872	1.4	-1.56	-5.51429
CR_07480W_A	4.93173	-1.15913	2.45941	-2.32435
C7_00760C_A	4.66667	-3	6	-2.33333
C2_10650W_A	4.46429	-1.86047	2.85714	-2.90698
CHT1	4.41176	-3.20833	4.52941	-3.125
CR_09070C_A	4.32955	-1.37569	2.82955	-2.10497
RHD1	4.26006	-1.47403	1.40557	-4.46753
AMO1	4.10526	-1.10909	1.07018	-4.25455
THI13	4.07826	1.25	1.11304	-2.93125
CR_00910W_A	4.07258	-1.16677	2.22465	-2.13595
C2_04830W_A	4.02857	-1.25	1.42857	-3.525
GPD2	4.01449	1.00935	1.55072	-2.56481
MEP1	3.88764	2.25	-1.39062	-2.40278
HCM1	3.84615	-1.83333	3.38462	-2.08333
ZCF17	3.8	-1.61017	1.26667	-4.83051
EXO1	3.75676	-2.11111	3.59459	-2.20635
C5_03470C_A	3.68229	-1.22925	1.61979	-2.79447
C1_07360W_A	3.65263	-1.54313	2.54211	-2.21725
C2_09110C_A	3.6	-1.25	2	-2.25
C3_00170C_A	3.51579	-1.25	1.36842	-3.21154
C1_05520W_A	3.50633	1.20339	-1.33898	-3.90141
PDC11	3.49332	-2.63114	2.22941	-4.12281
C1_02730W_A	3.45455	1.11765	1.54545	-2
GDH3	3.41727	1.19761	1.35612	-2.1041
RHR2	3.37012	-3.075	1.25297	-8.27083
NTH1	3.35224	-1.37076	1.93134	-2.37924
C7_04340C_A	3.33333	-1.4	1.16667	-4
SUR2	3.30446	-1.54447	1.50394	-3.39353
ROD1	3.2657	-1.22165	1.14493	-3.48454
WSC4	3.25108	-2.01705	1.5368	-4.26705
HIS1	3.2243	-2.27273	-1.42667	-10.4545
FRE9	3.18421	-2.09091	1.81579	-3.66667
YMC1	3.125	-6.94737	2.75	-7.89474
C4_03960W_A	3.10825	-1.77778	-1.73214	-9.57143
RNR21	3.09258	-1.77527	2.57046	-2.13587
PST3	3.00298	-1.24046	1.61149	-2.31157
POL3	2.98256	1.19071	3.00291	1.19883
C2_07420W_A	2.9771	-1.59655	1.76718	-2.68966
ADE6	2.94498	-2.57916	2.2799	-3.33153
BMT1	2.91837	-1.34286	-1.04255	-4.08571
SYG1	2.88	-1.44231	1	-4.15385
APT1	2.86207	-1.75652	1.3931	-3.6087

RNR22	2.79259	-2.99573	1.15391	-7.25
C7_03860W_A	2.7883	-1.02062	1.12194	-2.53649
SLF1	2.76471	-1.75	1.44118	-3.35714
LSC2	2.6976	-1.49178	1.62974	-2.46924
C2_10740C_A	2.66605	-1.94974	1.35978	-3.82275
QDR1	2.62346	-2.42857	1.15432	-5.51948
IFD6	2.62051	1.03934	-2.4623	-6.2082
YWP1	2.4563	-2.5647	1.30523	-4.82647
C5_03920C_A	2.44444	-1.90323	2.18519	-2.12903
C1_10520W_A	2.44304	1.33113	1.91139	1.04145
C5_01260W_A	2.44	2.04211	1.9	1.59016
KCH1	2.4382	-1.03488	2	-1.26163
C2_01190C_A	2.43548	1.08621	1.87097	-1.19841
KIP4	2.43478	-1.36691	2.75362	-1.20863
RAD53	2.43478	1.06931	2.19565	-1.03704
LIG1	2.43172	1.08379	2.4185	1.0779
C4_05850C_A	2.42975	1.09677	2.81818	1.27211
SMI1B	2.42857	1.59036	2.96429	1.94118
PHM5	2.42779	-1.07937	1.11172	-2.35714
CR_01410C_A	2.4127	-1.86301	1.43915	-3.12329
C1_08900W_A	2.41104	1	-1.05844	-2.55195
C1_09790C_A	2.32669	-1.43682	1.58566	-2.1083
CR_00190W_A	2.32402	-1.71569	1.95531	-2.03922
MIG1	2.3119	1.03951	1.05788	-2.10234
SIT1	2.29843	-8.1	1.27225	-14.6333
C4_04090C_A	2.29539	-1.14929	1.31436	-2.00711
CAS4	2.24136	1.03221	1.07256	-2.02452
CR_01950W_A	2.22556	-2.11628	1.36842	-3.44186
C5_04030W_A	2.21061	1.69681	-1.65426	-2.15517
ARG5,6	2.20592	-1.40533	1.34859	-2.29874
KAR9	2.19333	-1.24786	-1.0274	-2.81197
CLA4	2.18954	-1.18634	1.24837	-2.08075
C2_10730W_A	2.16667	-2.8	-1.28571	-7.8
GDA1	2.1244	-3.12821	1.7512	-3.79487
MAE1	2.10254	-1.66253	1.70339	-2.05211
CR_07600W_A	2.08978	-1.29412	1.22601	-2.20588
MAK21	2.08818	-2.77073	1.00176	-5.77561
UBA4	2.05376	-1.77586	1.66129	-2.1954
DBP2	2.02961	-1.63529	1.26651	-2.62059
ORC3	2.01633	1.55672	1.94286	1.5
PRE9	2.0149	1.33501	1.85102	1.22643
MIM1	2.01471	1.44828	2.13235	1.53285
LAG1	2.01258	-1.31034	1.19497	-2.2069

ZCF20	2.00386	1.35794	1.72587	1.16956
STT4	2.00251	1.42866	1.36295	-1.02841
C3_03250W_A	2.0006	1.29321	1.73778	1.12332

Genes downregulated in the pho4Δ compared to WT in Pi deplete conditions					
Alias	p-value (pho4-Pi vs. WT-Pi)	Fold Change (pho4-Pi vs. WT-Pi)	WT-Pi vs. WT+Pi	pho4-Pi vs. pho4+Pi	pho4+Pi vs. WT+Pi
BTA1	0.000239329	-1028.14	378.789	1.16667	-3.16667
PHO100	0.000255069	-807.286	847.65	-1.28571	1.35
LEU2	6.65E-07	-295	1.53806	-2.2	-87.1818
PHO84	0.00012182	-245.652	289.744	2	-1.69565
PHO112	0.000187603	-64.8235	42.3846	-1.76471	1.15385
FGR2	0.000588333	-64.5	?	2	?
PLB1	0.000324426	-37.7353	320.75	1.25926	6.75
C4_00530C_A	0.000327596	-37	55.5	?	?
PHO113	0.000208752	-31.7833	26.4861	1.2766	-1.53191
C1_04800C_A	0.00037092	-28.0625	149.667	1.33333	4
RBT7	0.000259397	-28	58.8	1.5	1.4
GIT1	0.000287385	-25.6612	30.1456	1.22222	-1.0404
PGA12	0.000742289	-23	?	-2	?
CR_10200W_A	0.000313199	-21.9524	32.9286	1.10526	1.35714
NAT4	0.00606056	-20.5	10.25	-3.25	1.625
C3_01540W_A	0.00702695	-20.1395	66.6154	-11.6977	38.6923
ALS4	8.58E-05	-18.348	9.15075	-1.12853	-1.77672
UTP20	0.000262038	-15.5645	1.2356	-5.79032	-2.17549
SIT1	0.000103531	-14.6333	2.29843	-8.1	1.27225
C1_12910W_A	0.00459239	-14	?	-15	?
POL93	0.000663125	-11.6366	-1.25802	1.11111	-16.2656
CR_01920W_A	0.0016007	-11.3333	9.71429	3	-3.5
RDN18	0.00476298	-11.2097	-1.59005	-1.51775	-11.7437
TRY6	2.62E-05	-11.1429	31.2	1.27273	2.2
HIS1	9.49E-11	-10.4545	3.2243	-2.27273	-1.42667
C7_01030C_A	0.00154863	-10.4	1.29577	-5.57391	-1.43994
KTI12	0.00848235	-10.3571	1.26087	-5.42857	-1.51316
C3_02140C_A	0.00010583	-10.3077	14.8889	-2.8	4.04444
RNR1	0.00316546	-10.1609	18.0955	-5.75394	10.2472
XOG1	2.02E-05	-9.61184	16.2333	-1.76316	2.97778
C4_03960W_A	0.000155188	-9.57143	3.10825	-1.77778	-1.73214
ASM3	0.000266033	-9.48357	40.4	1.04926	4.06
PLB4.5	0.000456074	-9.40659	7.96279	-3.65385	3.09302
CR_03840C_A	0.000812051	-9.25	12.3333	-2	2.66667
C1_04590W_A	2.78E-05	-9.11111	1.74468	-3.11111	-1.67857
C1_04010C_A	0.00034154	-9.10714	5.1	-1.19048	-1.5
SAM2	0.000179322	-8.85524	4.96687	-3.68053	2.0644
ALS2	4.08E-05	-8.66517	6.87429	-1.29364	1.02628

RPA135	0.000668675	-8.5665	1.73207	-6.12315	1.23805
NOG1	0.00356725	-8.36792	1.35213	-3.83019	-1.61576
RHR2	5.51E-07	-8.27083	3.37012	-3.075	1.25297
KRR1	0.014344	-8.21429	1.35294	-4.57143	-1.32813
RPA190	0.000949526	-8.07865	1.18062	-4.6236	-1.47995
YMC1	0.000227338	-7.89474	3.125	-6.94737	2.75
C2_10730W_A	8.31E-05	-7.8	2.16667	-2.8	-1.28571
DRS1	0.00672321	-7.73228	2.43672	-4.82677	1.52109
RNR22	4.72E-06	-7.25	2.79259	-2.99573	1.15391
C4_05730W_A	6.09E-11	-7.05882	10	1.0625	1.33333
C4_01800W_A	0.00206677	-7	5.6	-2.875	2.3
ZRT2	0.00121062	-6.96373	-1.44048	-1.19689	-8.38095
UTP13	0.0142829	-6.8	1.44681	-5.3	1.12766
C3_06370C_A	0.00500967	-6.55814	1.86755	-4.4186	1.25828
C1_03790C_A	0.000545928	-6.51639	1.48321	-3.98361	-1.10288
ARX1	0.0107839	-6.40714	1.67351	-3.92143	1.02425
RPF2	0.0100005	-6.38462	1.44348	-3.34615	-1.32184
C2_02540W_A	0.00357418	-6.29958	1.37477	-3.52743	-1.29904
C7_03140W_A	0.00117263	-6.23077	5.0625	-1.07692	-1.14286
C5_04390C_A	4.94E-05	-6.21429	1.8913	1.55556	-5.11111
IFD6	0.000110158	-6.2082	2.62051	1.03934	-2.4623
C4_05010W_A	0.00287085	-6.13636	2.25	-4.09091	1.5
PES1	0.00435014	-6.13636	1.56716	-4.19481	1.07131
BIO2	0.00133931	-6.10185	9.69118	2.4	-1.51111
CR_04170W_A	0.00259089	-6.05056	1.7177	-3.59551	1.02073
SDA1	0.00597189	-6.02655	1.87088	-2.61947	-1.22973
C5_03910C_A	0.00489998	-6	3	?	?
RPA34	0.00944127	-5.95	1.91935	-4.5	1.45161
MAK5	0.003554	-5.78151	1.91111	-3.07563	1.01667
MAK21	0.000172554	-5.77561	2.08818	-2.77073	1.00176
C2_05160C_A	0.00626031	-5.7013	1.41613	-3.22078	-1.25
UTP5	0.0100621	-5.67033	1.5132	-3.85714	1.02933
GIT3	0.000162427	-5.63741	10.3651	1.12097	1.64021
C1_01640W_A	0.0109625	-5.63467	-1.60385	-2.83901	-3.18321
C1_00160C_A	0.000333383	-5.58663	1.9575	-4.39604	1.54033
CR_09740W_A	0.0124125	-5.57143	1.31461	-3.09524	-1.36923
C3_02750W_A	0.00169603	-5.52083	66.25	3.2	3.75
QDR1	0.000181825	-5.51948	2.62346	-2.42857	1.15432
CR_03270W_A	0.00159854	-5.51429	4.94872	1.4	-1.56
DBP8	0.00607132	-5.47945	2.5641	-3.23288	1.51282
C1_14080W_A	0.00012326	-5.3894	1.48132	-2.68894	-1.35304
BMS1	0.00589109	-5.35593	1.45287	-3.33051	-1.10687
C1_11080W_A	0.000289814	-5.34363	7.68889	-1.1583	1.66667
GAR1	0.00257133	-5.32558	1.2246	-4.86047	1.11765
SPB1	0.0124788	-5.24088	2.03977	-2.94891	1.14773
LEU4	0.00585357	-5.20588	2.22642	-3.16176	1.3522

C1_10620W_A	0.00566056	-5.19512	1.1246	-4.87805	1.05597
NOP13	0.00772151	-5.18333	1.96835	-3.08333	1.17089
C7_03310W_A	0.00243129	-5.15385	134	-2	52
NOC2	0.0111637	-5.09868	1.69214	-2.61842	-1.15075
C6_03320W_A	0.0020185	-5.01505	9.34669	-1.68602	3.14228
FET99	7.20E-07	-4.93195	21.3718	1.68159	2.57692
ZCF17	1.88E-05	-4.83051	3.8	-1.61017	1.26667
YWP1	1.51E-06	-4.82647	2.4563	-2.5647	1.30523
NAG3	0.00507464	-4.82569	-1.64259	-1.95413	-4.05634
MDN1	1.54E-05	-4.75	1.40023	-1.92739	-1.76005
MRT4	0.00182987	-4.72093	2.03	-2.4186	1.04
YOR1	3.13E-05	-4.61282	1.50544	-1.73077	-1.77037
FRE10	0.00169856	-4.56846	1.28284	-3.03942	-1.17167
BMT4	1.29E-06	-4.51417	9.06504	1.37222	1.46341
RHD1	1.07E-09	-4.46753	4.26006	-1.47403	1.40557
MPP10	0.0106934	-4.43939	1.64607	-3.15152	1.16854
C6_02480W_A	0.000500109	-4.42105	-1.21429	-2.47368	-2.17021
C2_00170C_A	0.0153932	-4.40278	-1.36593	-5.15278	-1.16712
URA2	0.00125773	-4.36877	1.12993	-3.08655	-1.25267
C1_04040C_A	0.0147249	-4.34091	1.86341	-2.39773	1.02927
C2_08260W_A	0.000176408	-4.32075	5.32558	-1.09434	1.34884
CR_03780C_A	0.00449927	-4.30769	2.66667	-2	1.2381
BMT3	0.000177604	-4.27922	11.5614	1.07692	2.50877
WSC4	0.000131721	-4.26705	3.25108	-2.01705	1.5368
CR_04240C_A	0.000719337	-4.25899	1.87046	-2.49281	1.09479
AMO1	0.000117433	-4.25455	4.10526	-1.10909	1.07018
GUA1	0.0119916	-4.25269	1.77753	-3.73656	1.5618
MET10	0.0146509	-4.23969	-1.24559	-3.36598	-1.56891
CWH8	0.000283891	-4.17969	1.16304	-3.0625	-1.17347
C1_01180C_A	0.00098879	-4.16667	1.92308	-1.16667	-1.85714
SYG1	0.000124963	-4.15385	2.88	-1.44231	1
SEN2	0.0073126	-4.13158	-1.03185	-2.52632	-1.6875
C2_04080W_A	8.38E-05	-4.12591	1.58555	-1.9635	-1.32528
PDC11	0.00458221	-4.12281	3.49332	-2.63114	2.22941
C1_05630C_A	0.0138199	-4.11538	-1.08965	-3.91738	-1.14473
BMT1	0.000110147	-4.08571	2.91837	-1.34286	-1.04255
C3_02350W_A	0.0148513	-4.08475	2.02521	-2.32203	1.15126
CEF3	0.0105401	-4.00764	1.13421	-4.4386	1.25617
C7_04340C_A	0.00563377	-4	3.33333	-1.4	1.16667
RRP15	0.0139538	-4	1.91667	-2.47826	1.1875
C7_03400C_A	0.000310672	-3.99612	1.82155	-2.23256	1.01767
CDC19	0.00939398	-3.9892	11.1291	-2.10134	5.86235
C3_05160C_A	0.0103785	-3.97512	2.62829	-2.20896	1.46053
C3_07800C_A	0.00672826	-3.94286	1.60465	-2.14286	-1.14667
C5_03450W_A	0.00524701	-3.94118	1.52273	-1.79412	-1.44262
SSU1	0.00221357	-3.90323	20.1667	-1.29032	6.66667

<i>C1_05520W_A</i>	0.00018379	-3.90141	3.50633	1.20339	-1.33898
<i>C2_10740C_A</i>	0.000135351	-3.82275	2.66605	-1.94974	1.35978
<i>GDA1</i>	0.000845056	-3.79487	2.1244	-3.12821	1.7512
<i>IFE1</i>	0.000349804	-3.77381	7.54762	-1.38095	2.7619
<i>C2_01070W_A</i>	0.00201303	-3.76923	1.58529	-2.11189	-1.12583
<i>CR_05800C_A</i>	0.0128297	-3.7037	12.5	-1.85185	6.25
<i>FRE9</i>	5.42E-06	-3.66667	3.18421	-2.09091	1.81579
<i>C2_00410C_A</i>	0.0110067	-3.65534	1.80576	-2.16505	1.06954
<i>CR_08500W_A</i>	0.00947916	-3.64324	1.6399	-2.55676	1.15085
<i>PGA53</i>	0.000638862	-3.6319	1.37196	-2.2362	-1.18381
<i>NMD3</i>	0.00685921	-3.62963	1.58065	-2.28571	-1.00463
<i>DBP7</i>	0.0110804	-3.61538	2.80132	-2.2906	1.77483
<i>APT1</i>	0.000112907	-3.6087	2.86207	-1.75652	1.3931
<i>CSH1</i>	0.000333515	-3.59104	1.20424	-1.2814	-2.32713
<i>FTR2</i>	1.87E-06	-3.57692	1.66071	1.81395	-3.90698
<i>C6_02430W_A</i>	0.000107525	-3.55833	1.38636	-1.69167	-1.51724
<i>C6_01890C_A</i>	0.0156618	-3.54054	2.51923	-1.72973	1.23077
<i>C2_04830W_A</i>	1.24E-05	-3.525	4.02857	-1.25	1.42857
<i>CPA2</i>	0.000941235	-3.52062	1.97685	-1.41237	-1.26095
<i>PHO81</i>	0.000728761	-3.52009	8.55747	1.11316	2.18391
<i>MLT1</i>	9.45E-05	-3.51374	1.14273	-1.85592	-1.65679
<i>C1_06820W_A</i>	0.000221402	-3.5	1.84211	-2.28571	1.20301
<i>MCM3</i>	7.93E-06	-3.48684	6.50307	-1.75	3.2638
<i>ROD1</i>	0.000362285	-3.48454	3.2657	-1.22165	1.14493
<i>PWP2</i>	0.00795823	-3.44724	2.3737	-2.23116	1.53633
<i>CR_01950W_A</i>	0.000363042	-3.44186	2.22556	-2.11628	1.36842
<i>UPC2</i>	0.00476739	-3.43956	6.13725	-2.14286	3.82353
<i>KCS1</i>	0.000139442	-3.42105	7.5	-1.06433	2.33333
<i>SUR2</i>	1.67E-05	-3.39353	3.30446	-1.54447	1.50394
<i>C5_01610W_A</i>	0.0117965	-3.36	1.66337	-2.14	1.05941
<i>SLF1</i>	0.000101031	-3.35714	2.76471	-1.75	1.44118
<i>TRY3</i>	7.47E-06	-3.33628	5.16438	-1.55752	2.41096
<i>ADE6</i>	0.000358539	-3.33153	2.94498	-2.57916	2.2799
<i>C3_01310W_A</i>	0.00228438	-3.30159	6.30303	-1.5873	3.0303
<i>C1_00270W_A</i>	0.000224722	-3.29231	-1.17103	1.52582	-5.88263
<i>C4_04990C_A</i>	0.000817848	-3.28205	1.93939	-1.30769	-1.29412
<i>C1_05550C_A</i>	0.00390553	-3.25	-1.22172	-1.64706	-2.41071
<i>OPT7</i>	0.0108485	-3.24084	1.84776	-2.71204	1.54627
<i>C2_09420W_A</i>	0.000206832	-3.23437	1.97143	-1.85937	1.13333
<i>C3_00170C_A</i>	0.000436715	-3.21154	3.51579	-1.25	1.36842
<i>CR_01910C_A</i>	0.00699715	-3.2	8	-1.4	3.5
<i>GIN1</i>	0.00598068	-3.2	8	-2.07273	5.18182
<i>POL1</i>	0.00204152	-3.19126	8.71642	-1.74317	4.76119
<i>C1_05230W_A</i>	0.00964465	-3.19048	1.91429	-2.42857	1.45714
<i>PTP3</i>	0.00131416	-3.18205	1.66801	-1.65128	-1.15528
<i>C2_04120C_A</i>	0.00846458	-3.15	2.48684	-1.39167	1.09868

C3_03210W_A	5.22E-05	-3.14954	1.06906	-1.36012	-2.16604
CHT1	0.0087271	-3.125	4.41176	-3.20833	4.52941
CR_01410C_A	0.00154198	-3.12329	2.4127	-1.86301	1.43915
MNN1	0.00106367	-3.12274	18.0373	1.7631	3.27612
C4_03950C_A	0.0112467	-3.11111	9.33333	-1.44444	4.33333
SOD3	5.03E-05	-3.08961	-1.27547	1.01324	-3.99291
CR_06570C_A	0.00624178	-3.06098	1.02869	-1.91463	-1.55414
CR_03690W_A	0.00256812	-3.03612	6.40476	1.12152	1.88095
C1_10350C_A	4.73E-05	-3.02874	1.56845	-1.7931	-1.07692
MNN22	0.000938051	-3.00812	15.0203	1.25254	3.98649
GIT4	0.000523034	-3	10.8	1	3.6
VRG4	0.00120888	-2.96053	1.15385	-1.77632	-1.44444
IMP4	0.0114837	-2.93252	1.43114	-2.21472	1.08084
THI13	0.00107968	-2.93125	4.07826	1.25	1.11304
C3_04370C_A	0.0114338	-2.92797	1.89315	-1.95763	1.26575
C2_02550C_A	0.00977425	-2.92308	2.59091	-1.05128	-1.07317
CR_09800C_A	0.0121329	-2.92275	1.75064	-1.24464	-1.34138
MCD1	0.00886482	-2.91667	6.36364	-2.66667	5.81818
ECM17	0.00577449	-2.91379	1.34984	-1.72701	-1.24992
C2_10650W_A	0.000853725	-2.90698	4.46429	-1.86047	2.85714
C6_00760W_A	4.30E-05	-2.90184	1.79167	-1.90798	1.17803
PMA1	0.00130311	-2.9018	1.55135	-1.07006	-1.74804
RPC10	0.00110921	-2.89655	1.6	-2.68966	1.48571
GDS1	7.86E-05	-2.88079	1.45242	-1.43377	-1.38337
IFH1	0.00161074	-2.86866	-1.08741	-1.5	-2.0796
HAS1	0.0140895	-2.84524	1.6176	-1.99107	1.13198
KAR9	2.78E-05	-2.81197	2.19333	-1.24786	-1.0274
C1_11160C_A	0.0058484	-2.80769	1.52083	-3.26923	1.77083
C5_03470C_A	7.74E-09	-2.79447	3.68229	-1.22925	1.61979
C2_07420W_A	0.00871918	-2.68966	2.9771	-1.59655	1.76718
C4_04230W_A	0.00123368	-2.6875	1.01575	-1.41667	-1.86765
CDR1	0.000127126	-2.67548	1.21499	-1.32468	-1.66234
C6_02420W_A	0.000918327	-2.67073	4.97727	-1.12195	2.09091
C2_00180C_A	2.67E-07	-2.64506	1.86304	1.35	-1.91667
C1_09710C_A	0.0130748	-2.63415	2.41791	-1.64634	1.51119
DBP2	0.00133292	-2.62059	2.02961	-1.63529	1.26651
URA7	0.0116982	-2.60417	1.34277	-2.78598	1.43652
ILV2	0.0139452	-2.60374	-1.09406	-2.31463	-1.23071
C2_08200W_A	0.000815666	-2.575	1.60937	-1.45	-1.10345
HIS5	0.00455353	-2.56923	2.02424	-2.03846	1.60606
RIO2	0.00626952	-2.56579	1.78082	-1.16447	-1.23729
GPD2	0.000145687	-2.56481	4.01449	1.00935	1.55072
NMD5	0.00190307	-2.55462	1.42389	-1.26471	-1.4186
C1_08900W_A	3.97E-05	-2.55195	2.41104	1	-1.05844
C7_03860W_A	0.0063992	-2.53649	2.7883	-1.02062	1.12194
DPB2	0.00776617	-2.53125	9	-1.84375	6.55556

C2_09000C_A	0.00299163	-2.5	1.36364	2	-3.66667
RAT1	0.00215781	-2.49645	1.80513	-1.7305	1.25128
TRX2	0.0132947	-2.48276	2.32258	1.61111	-1.72222
MET13	0.0031955	-2.47273	5.03704	1.20548	1.68981
LSC2	0.000126272	-2.46924	2.6976	-1.49178	1.62974
FLU1	0.00101698	-2.45312	-1.00425	-1.27083	-1.93852
VTC3	0.000919197	-2.44566	5.44302	1.24691	1.78488
MEP1	0.0105311	-2.40278	3.88764	2.25	-1.39062
C1_07990C_A	0.00750762	-2.39796	1.63763	-1.0051	-1.45685
GDE1	0.000942853	-2.38004	8.37838	1.16295	3.02703
NTH1	0.00721609	-2.37924	3.35224	-1.37076	1.93134
SGA1	0.0103578	-2.37791	1.3109	-2.23837	1.23397
C1_02240W_A	0.00684097	-2.37615	-1.01544	-1.33945	-1.80137
MSS116	0.012333	-2.37361	1.26812	-1.49814	-1.24938
RCL1	0.00516371	-2.37097	1.74308	-1.60753	1.18182
PHM5	0.000734566	-2.35714	2.42779	-1.07937	1.11172
MDR1	0.00881645	-2.33333	7	-1.77778	5.33333
RPC31	0.0133571	-2.33333	1.24051	-1.47619	-1.27419
CR_07480W_A	0.000113291	-2.32435	4.93173	-1.15913	2.45941
PST3	0.00466055	-2.31157	3.00298	-1.24046	1.61149
HGT8	1.03E-08	-2.30917	1.26433	-1.59611	-1.14427
ARG5,6	0.00661674	-2.29874	2.20592	-1.40533	1.34859
CHS4	0.00128764	-2.24339	1.26946	-1.1746	-1.5045
FCY21	0.000262458	-2.23757	1.35906	-1.09116	-1.50886
ZCF39	0.00288961	-2.23397	1.30769	1.06485	-1.81911
IHD2	0.0040265	-2.2234	1.91743	1.30556	-1.51389
C1_07360W_A	0.0106545	-2.21725	3.65263	-1.54313	2.54211
LAG1	0.00192555	-2.2069	2.01258	-1.31034	1.19497
EXO1	0.0135774	-2.20635	3.75676	-2.11111	3.59459
CR_07600W_A	0.00414619	-2.20588	2.08978	-1.29412	1.22601
CR_07850W_A	0.013444	-2.2	7.07143	-1.22222	3.92857
UBA4	0.00297761	-2.1954	2.05376	-1.77586	1.66129
CR_03600C_A	0.000898722	-2.16822	1.8125	-1.4486	1.21094
C3_04650W_A	0.00596927	-2.16	7.71429	1.41509	2.52381
C5_04030W_A	5.58E-06	-2.15517	2.21061	1.69681	-1.65426
C7_01100C_A	0.0112079	-2.15385	6.22222	-1.61538	4.66667
C3_01280W_A	0.00987633	-2.14354	5.97333	-1.33014	3.70667
SMF12	0.0147251	-2.1401	-1.20316	-1.34493	-1.91451
C5_03920C_A	0.0154326	-2.12903	2.44444	-1.90323	2.18519
C7_04090C_A	0.00117445	-2.12883	5.42188	-1.50307	3.82813
C4_04940W_A	0.00793296	-2.12821	1.88636	-1.17949	1.04545
C1_01910W_A	0.00983939	-2.11146	1.23925	-1.58917	-1.07214
C1_09790C_A	0.000628884	-2.1083	2.32669	-1.43682	1.58566
NMA111	0.00550915	-2.10565	1.71743	-1.61179	1.31463
MIG1	0.00943268	-2.10234	2.3119	1.03951	1.05788
C3_05320W_A	0.00153785	-2.08517	1.33266	-1.49842	-1.04421

CLA4	0.00410724	-2.08075	2.18954	-1.18634	1.24837
C3_06040W_A	0.000648572	-2.06338	1.83125	2	-2.25352
MAE1	0.000660832	-2.05211	2.10254	-1.66253	1.70339
RRP8	0.0135684	-2.05	1.54717	-1.1875	-1.11579
SNR52	0.00179362	-2.04596	1.36758	-1.6878	1.12818
CR_00190W_A	0.000399865	-2.03922	2.32402	-1.71569	1.95531
CAS4	0.000687466	-2.02452	2.24136	1.03221	1.07256
AGO1	0.0129535	-2.02338	1.24447	-1.08273	-1.50166
C1_12980W_A	0.00709026	-2.01961	1.02488	-1.33333	-1.47794
ECM331	0.0107268	-2.0119	7.34783	-1.7619	6.43478
C1_08110W_A	0.0157694	-2.01181	1.10268	-1.86835	1.02405
C4_04090C_A	0.00453198	-2.00711	2.29539	-1.14929	1.31436
C1_02830W_A	1.05E-05	2	1.57325	1.52941	2.05732
KIP2	0.00462075	2	4.21429	1.43902	5.85714
MAS1	3.84E-06	2	-1.10942	-1.01824	1.83562
C4_01840C_A	2.07E-05	2.00164	-1.2457	1.88872	-1.17543
CR_08290W_A	2.80E-08	2.00245	1.58755	1.47873	2.14981
C5_02730C_A	1.74E-05	2.00344	1.64407	1.22222	2.69492
CR_08710W_A	1.45E-07	2.00376	1.52828	1.32917	2.30393
CGR1	0.00132208	2.00495	-1.16337	1.35906	1.26809
STE11	1.48E-05	2.00581	1.43035	1.53333	1.8711
C2_05820W_A	0.000101959	2.0083	1.0905	1.17762	1.85973
TOK1	5.88E-06	2.00957	1.19429	1.30435	1.84
GPI8	0.00107343	2.01015	1.576	1.67797	1.888
C2_09710C_A	0.000114099	2.01074	1.40503	1.38642	2.03774
C7_02080W_A	0.000387283	2.01093	2.2875	1.46032	3.15
ERG8	0.000163115	2.01147	-1.00191	1.06586	1.88359
C4_04760C_A	0.000827918	2.01449	1.68293	1.32381	2.56098
FESUR1	0.000226071	2.01472	-1.19779	1.54334	1.08986
PRB1	1.92E-05	2.01472	1.52713	1.67186	1.84031
C5_01730W_A	0.00486058	2.01538	1.14035	1.25359	1.83333
NUO1	0.00137527	2.01685	-1.41501	1.6566	-1.16226
HPC2	0.00104127	2.01796	1.83516	1.42797	2.59341
C4_00070C_A	3.99E-08	2.01875	2.22538	1.25513	3.5793
C3_05760W_A	0.00173993	2.02092	-1.08787	1.38993	1.33654
HAP5	7.34E-05	2.0219	1.28638	1.25056	2.07981
C2_03910C_A	0.000348669	2.02193	1.2	1.08471	2.23684
C4_07210W_A	5.73E-05	2.02288	2.63793	1.45305	3.67241
MUC1	2.11E-05	2.02381	1.61538	1.08742	3.00641
RTT109	0.00333333	2.0241	-1.03614	-1.02381	2
CSE4	0.0139127	2.02542	2.74419	1.0042	5.53488
NUC2	0.00109421	2.02658	-1.34884	1.13225	1.32697
C3_02290W_A	0.000176614	2.02837	-1.12766	1.34272	1.33962
C2_00400C_A	0.000191064	2.02997	-1.00817	1.89728	1.06126
C6_00360C_A	4.60E-07	2.03354	-1.01829	1.50905	1.32335
C5_05250C_A	0.00332771	2.03371	-1.77903	1.11728	1.02316

GCF1	3.12E-05	2.03605	1.71315	1.569	2.22311
C7_01750W_A	0.00313009	2.03614	1.62745	1.34127	2.47059
C3_05510W_A	0.0028973	2.0367	1.75806	1.54167	2.32258
SRR1	0.00226853	2.04025	1.15771	1.25763	1.87814
C1_14530W_A	2.91E-05	2.04167	1.58491	1.75	1.84906
C3_03130C_A	0.00923739	2.04167	1.09091	1.75	1.27273
C5_04770W_A	7.13E-05	2.04202	1.10185	1.51875	1.48148
FGR15	5.03E-06	2.04332	1.92361	2.05072	1.91667
POT1	8.14E-07	2.04399	-1.21052	2.09455	-1.24046
SHE9	4.89E-05	2.04545	1.55435	1.75676	1.80978
RVS162	0.00272124	2.048	-1.032	1.55152	1.27907
C1_00970W_A	0.00030067	2.04819	2.51515	1.75258	2.93939
C1_04970W_A	0.00441829	2.04844	-1.74141	1.37062	-1.16519
IFF4	3.79E-06	2.05052	2.08727	1.59054	2.69091
MRPL19	0.000265875	2.05202	-1.04046	1.1794	1.67222
CAT8	2.49E-05	2.05236	1.12353	1.9122	1.20588
C5_00800C_A	1.10E-06	2.05323	1.25515	1.17232	2.19829
C1_10470W_A	0.00100761	2.05365	-1.7382	1.09748	1.07654
PHO8	0.00159287	2.05556	2.57143	1.7619	3
SAS2	0.000275406	2.05556	1.52542	1.39098	2.25424
C2_09870W_A	4.11E-05	2.0566	1.22308	1.54976	1.62308
VPS2	0.000207294	2.05882	1	1.56051	1.31933
CYT1	4.72E-05	2.06023	-1.13683	1.43401	1.26378
C2_00540W_A	7.64E-07	2.06033	1.13333	-1.11127	2.59487
SNO1	9.33E-05	2.0605	6.69048	1.43672	9.59524
SUA71	1.12E-07	2.06168	1.49687	1.53284	2.0133
C3_04410C_A	8.47E-06	2.06169	1.32757	1.34983	2.02768
CR_07670W_A	0.00859145	2.06218	-1.49223	1.46324	-1.05882
CR_05710C_A	0.0001514	2.0625	1.28736	1.26923	2.09195
C1_09620C_A	0.00201718	2.0625	-1.0625	1.91304	1.01471
CGT1	1.78E-05	2.06391	1.44565	1.30404	2.28804
C7_03280C_A	0.00015646	2.06591	1.87538	1.61418	2.4002
C2_01230W_A	0.014723	2.06667	1.31579	1.34783	2.01754
C1_07920W_A	0.0113557	2.06667	1.13924	1.43077	1.64557
SNM1	0.0070759	2.06667	-1.08889	1.69091	1.12245
C5_02850W_A	0.00050594	2.06731	1.27347	-1.69767	4.46939
MAD2	0.0102137	2.06897	1.07407	1.13208	1.96296
CR_03410W_A	8.18E-06	2.06912	1.0796	1.01584	2.199
MEF2	0.00012173	2.06977	1.32762	1.35993	2.02058
BUB1	4.14E-05	2.07061	2.63317	1.6874	3.23116
CR_07870W_A	5.61E-05	2.07179	2.40741	1.74138	2.8642
FAA2-1	7.24E-07	2.07194	1.00636	1.51328	1.37788
C4_03920W_A	0.000561965	2.07339	1.01869	1.29143	1.63551
CR_09500C_A	0.00280986	2.07407	1.0125	1.3125	1.6
C2_09610W_A	0.000113928	2.07692	1.625	1	3.375
C4_03500C_A	0.0127567	2.07692	?	13.5	?

HST6	0.00963186	2.07692	2.36364	1.35	3.63636
C2_07030C_A	0.00754097	2.07738	-1.72619	1.06079	1.13448
C2_00290W_A	0.000625205	2.07826	1.4557	1.62585	1.86076
C1_03170C_A	0.000883321	2.07865	1.58929	1.5812	2.08929
CAN2	5.13E-05	2.07869	2.31556	1.77396	2.71333
UGA4	0.0050218	2.08	1.47059	2	1.52941
PIM1	1.15E-05	2.08044	1.30705	1.69787	1.60155
ZCF23	0.000104801	2.08406	-1.21159	1.17101	1.4689
ADK1	0.000249061	2.0846	-1.84597	1.29307	-1.14505
USO5	0.00186916	2.08642	4.05	1.352	6.25
C1_11900C_A	0.00999131	2.08696	1.56818	2.36066	1.38636
C5_02370C_A	0.000107462	2.08955	-1.08955	1.26126	1.52055
UGA3	8.24E-07	2.09035	1.4837	1.46827	2.11232
C2_09690C_A	2.64E-05	2.09091	1.26923	1.60052	1.65812
C5_02190C_A	0.00515996	2.09328	-1.22343	1.29011	1.32624
C1_08680C_A	2.41E-05	2.09375	1.6	1.63415	2.05
C1_01390C_A	6.77E-05	2.09418	1.19536	1.45665	1.71854
ADA2	0.000476173	2.09848	2	1.3066	3.21212
C3_04790W_A	1.04E-06	2.09877	1.61355	1.36437	2.48207
C1_00450C_A	7.55E-05	2.09901	-1.19554	1.6466	1.06625
C5_04530W_A	0.00305822	2.10274	-1.69863	1.21344	1.02016
ROT2	4.21E-08	2.10523	1.43362	1.54706	1.95086
C1_04430C_A	8.31E-05	2.10985	1.89928	1.79677	2.23022
MAC1	1.28E-05	2.11354	1.86179	1.68056	2.34146
RIM1	7.82E-05	2.11549	2.84328	1.49536	4.02239
PEX11	0.00188536	2.1161	-1.05243	1.34204	1.49822
C4_00820W_A	0.00955092	2.11765	-1.56209	1.25097	1.08368
ISA1	6.29E-06	2.125	1.50986	1.72054	1.86479
TIM10	0.000776699	2.12879	-1.52273	1.61494	-1.15517
C3_04750W_A	7.50E-07	2.1308	1.54902	1.35027	2.44444
C1_02020W_A	0.00961521	2.13208	1.23256	1.29885	2.02326
C4_01960C_A	3.21E-05	2.1327	1.24852	1.49502	1.78107
ADR1	1.64E-06	2.13856	1.22032	1.93051	1.35184
NHP6A	0.000627724	2.13905	1.72669	1.08886	3.39208
C5_01490C_A	9.35E-05	2.1393	-1.02736	1.42149	1.46489
C7_01350C_A	0.00176574	2.14118	-1.18824	1.3	1.38614
TES1	0.00234452	2.14286	2.33333	1.30435	3.83333
SIP5	6.56E-06	2.14296	1.20536	1.49278	1.73036
RPM2	0.000173028	2.14346	-1.32738	1.72941	-1.07097
AGC1	0.00268818	2.14663	1.60849	1.06706	3.23585
CR_04460C_A	8.33E-05	2.14737	1.66667	1.35099	2.64912
C5_02040W_A	3.21E-06	2.14756	-1.15	1.06276	1.75716
C5_04410C_A	0.00011894	2.14919	1.34783	1.10352	2.625
VPS24	3.33E-05	2.14935	1.61257	1.61071	2.15183
C5_03490C_A	6.03E-05	2.15025	2.22205	1.32779	3.59843
C2_01030W_A	0.00041514	2.15135	-1.53514	1.29221	1.08451

C7_01150W_A	0.000237929	2.15455	-1.02727	1.3022	1.61062
CZF1	0.000267297	2.15512	1.93048	1.2062	3.4492
FKH2	3.37E-07	2.15517	1.35938	1.46484	2
C4_01710C_A	8.72E-05	2.15563	1.01684	1.36478	1.60606
XKS1	0.00207491	2.15567	-1.82058	1.23228	-1.04072
BUL4	2.07E-05	2.15596	1.42484	1.60136	1.9183
CR_09090C_A	0.000666443	2.15789	1.70149	1.35165	2.71642
YAH1	1.23E-05	2.15789	-1.06391	1.56403	1.29682
HMS1	0.00873617	2.15826	-1.96789	1.21263	-1.10567
PDE2	0.000100269	2.15909	-1.0803	1.42786	1.39972
CR_09670C_A	2.09E-05	2.15955	1.6146	1.41949	2.45639
IFK2	3.16E-07	2.16045	1.52273	1.31891	2.49432
OPT3	2.32E-08	2.16127	2.21749	2.09354	2.28924
YHB4	0.000129729	2.16388	1.67039	1.06942	3.37989
CR_02630C_A	0.000504846	2.16667	-1.08333	1.57576	1.26923
ARP1	0.00463061	2.16667	2.30769	1.16071	4.30769
RPB7	0.000568271	2.16667	2.23256	1.12432	4.30233
SAP5	0.00447094	2.16667	1.8	2.05263	1.9
C2_04030C_A	0.000207001	2.16776	-1.29934	1.57279	1.06076
CR_10420W_A	0.0081271	2.16801	-1.82553	1.47473	-1.24176
C2_08740W_A	0.00127716	2.17021	2.29268	1.41667	3.5122
SYS3	3.01E-06	2.17163	1.20975	1.75637	1.49576
CR_09620C_A	0.00093684	2.17172	-1.33333	1.51408	1.07576
C2_02300W_A	3.71E-05	2.17241	1.41463	1.43182	2.14634
C1_12650C_A	0.000302545	2.17273	1.13402	1.40588	1.75258
C2_07200W_A	0.00314415	2.17391	-1.19565	1.11111	1.63636
ZCF3	0.00305186	2.17447	1.51613	1.69205	1.94839
PAD1	0.00373567	2.17544	3	-1.04839	6.84211
C1_10410W_A	5.84E-05	2.17881	3.08163	1.47534	4.55102
C3_04630W_A	0.00132098	2.18072	-1.19277	1.71564	1.06566
MSM1	9.34E-07	2.18079	-1.06215	1.36396	1.50532
C1_13320C_A	2.59E-05	2.18268	1.08617	1.19577	1.98261
RIP1	0.00249108	2.18695	-1.30713	1.31955	1.26793
C7_01160C_A	0.000197798	2.18707	-1.50344	1.43243	1.01555
CR_04580W_A	0.00173106	2.18812	-1.61716	1.11242	1.21633
FGR10	0.000192173	2.18966	1.56757	1.29592	2.64865
CR_00570W_A	0.00362147	2.18994	-1.7095	1.22118	1.04902
NIP100	0.000500161	2.19048	2.11321	1.4347	3.22642
STN1	0.0112644	2.19048	1.3125	1.39394	2.0625
C4_01310W_A	0.0136932	2.19355	1.06897	1.17241	2
CR_10530W_A	0.000282903	2.19424	2.35593	1.40553	3.67797
PTC5	7.32E-06	2.1999	-1.11647	1.37295	1.43515
ZCF7	0.000456601	2.2	2	1.42593	3.08571
C4_00420C_A	2.13E-05	2.20232	1.10785	1.06931	2.28169
C5_01140C_A	0.00104822	2.20256	-1.53846	1.28401	1.115
C3_06940W_A	7.64E-05	2.20361	-1.013	1.31382	1.65574

C1_03280W_A	0.00081028	2.20637	-1.77948	1.3558	-1.09348
SLD5	0.0140745	2.20833	1	1.43243	1.54167
EPL1	5.16E-08	2.20989	1.1507	1.04469	2.43413
AFG1	6.82E-07	2.21143	1.49573	1.29431	2.55556
C2_07390C_A	0.000965317	2.21317	1.68783	1.10658	3.37566
SRT1	0.00172343	2.21569	-1.27451	1.11881	1.55385
CAT2	0.00053003	2.21969	-1.48337	1.91418	-1.2792
HSP104	2.92E-08	2.21974	1.64605	1.83701	1.98899
C2_07280W_A	0.00259067	2.22222	9	1.21212	16.5
C2_00600C_A	3.47E-05	2.22308	-1.34103	1.88478	-1.13696
CR_01360W_A	0.00111044	2.22449	1.48485	1.04808	3.15152
CR_04140W_A	0.000148354	2.22562	-1.6348	1.30201	1.04561
ARF1	2.25E-06	2.22618	2.51734	1.53645	3.6474
C1_13880C_A	3.12E-05	2.22627	-1.29736	1.54734	1.10901
C2_07800W_A	2.72E-05	2.22819	-1.50336	1.30196	1.13839
CR_10510W_A	2.71E-06	2.23077	1.3633	1.19062	2.55431
FRP2	1.37E-05	2.23404	3.43902	1.17537	6.53659
ABP1	0.000986704	2.23552	1.00834	1.08078	2.08569
SLA1	2.38E-06	2.24287	1.30134	1.11786	2.611
SAC6	3.34E-08	2.24291	1.56329	1.67069	2.09873
C3_02990C_A	6.24E-05	2.24299	1.38961	1	3.11688
TRS20	0.00046203	2.24444	1.36364	1.57813	1.93939
C1_05180C_A	8.18E-05	2.2459	-1.22951	1.24545	1.46667
CR_03250C_A	1.27E-06	2.24638	-1.23913	-1.00645	1.82456
HST3	5.64E-06	2.24654	1.65019	1.95	1.90114
PHB1	2.91E-08	2.24713	1.17369	1.59592	1.65261
OYE22	1.31E-06	2.24737	2.06522	1.4878	3.11957
C7_04010W_A	8.90E-08	2.24943	1.60949	1.44291	2.50912
RAS2	0.0089674	2.25	1.52381	1.41176	2.42857
CR_02300C_A	8.56E-07	2.25354	2.26531	1.71163	2.98251
C1_03120W_A	3.23E-06	2.25426	1.21642	1.67613	1.63599
C7_01590C_A	0.000533812	2.2562	-1.36364	1.25806	1.31515
C5_04520W_A	2.55E-06	2.25874	1.38835	1.11765	2.80583
C5_05140W_A	7.63E-06	2.26484	1.01389	1.32267	1.73611
C3_01950C_A	6.01E-05	2.26506	1.21168	1.27027	2.16058
CR_03240C_A	0.00186499	2.26506	1.25758	1.84314	1.54545
C7_01690W_A	0.00177063	2.26531	1.25641	1.3875	2.05128
C4_06240W_A	1.57E-05	2.26563	1.77778	1.71598	2.34722
SPL1	1.05E-09	2.26695	1.24866	1.61826	1.7492
C1_07220W_A	0.00561005	2.26813	-1.35168	1.21197	1.38452
PGM2	7.53E-06	2.26911	-1.00057	1.57371	1.44107
OPT2	0.000431677	2.27132	2.30357	1.51813	3.44643
C7_00190W_A	0.000103319	2.27138	3.05682	1.17274	5.92045
C3_00450C_A	0.000167951	2.27152	-1.74172	1.15655	1.12765
TRY5	0.000710778	2.27193	2.13084	1.47578	3.28037
C4_05360C_A	0.0133478	2.27273	1.1	1.25	2

CR_04410W_A	0.000887294	2.2766	1.80769	1.72581	2.38462
C6_03670C_A	0.00112045	2.27907	2.04762	1.28947	3.61905
C3_00620C_A	8.70E-05	2.28571	-1.1875	1.24272	1.54887
C2_05560W_A	3.94E-07	2.28634	1.74615	1.62188	2.46154
CTN3	0.00646178	2.28672	-1.62168	1.89789	-1.34593
BUB3	1.41E-06	2.28787	1.29329	1.61775	1.829
C7_03350C_A	0.000829506	2.29167	2.66667	1.48649	4.11111
C4_00910C_A	0.00153456	2.29167	-1.1	1.31579	1.58333
CR_03190C_A	0.00228136	2.29308	-1.08877	-1.1249	2.36916
C1_11880W_A	0.00199576	2.29687	-1.84375	1.32432	-1.06306
PET100	8.60E-08	2.29808	-1	1.75092	1.3125
BFA1	1.04E-05	2.29891	4	1.40066	6.56522
POX1-3	0.000113514	2.30128	-1.9421	2.53952	-2.14316
C5_02980C_A	0.000140425	2.30357	1.19149	2.38889	1.14894
ALI1	0.000139014	2.30499	-1.28745	1.77917	1.00629
URA3	0.00300196	2.30556	-1.44444	1.07792	1.48077
HSP21	0.000473298	2.3065	-1.0266	1.59365	1.4098
CAT1	2.83E-05	2.30713	-1.70954	1.59965	-1.18531
LYS142	5.69E-05	2.30861	1.1	1.38054	1.83947
C1_11020W_A	2.12E-05	2.30976	1.45588	1.44421	2.32843
C1_02490C_A	9.12E-05	2.31164	-1.11986	1.65037	1.25076
PGA38	5.12E-05	2.31381	2.16938	1.85887	2.70033
APM1	0.00417347	2.31618	1.97101	-1.27619	5.82609
MDJ1	2.06E-07	2.31835	-1.40262	1.21492	1.36048
C1_13130C_A	0.00341187	2.31892	-1.07387	1.20056	1.79866
C6_02460C_A	0.000108247	2.32022	-1.6236	1.30284	1.09689
C5_00320W_A	4.62E-05	2.32099	-1.01235	1.15337	1.9878
AOX1	8.15E-08	2.32283	1.71622	1.26068	3.16216
COX11	9.54E-09	2.32731	1.02259	1.38636	1.71663
C3_04080W_A	0.00256639	2.32799	-1.67007	1.61313	-1.15724
CAR2	4.57E-05	2.32799	-1.05491	1.01698	2.16997
C1_09440W_A	0.00010007	2.329	-1.00433	2.29424	1.01078
C1_07160C_A	0.00229278	2.33042	-1.03063	1.21391	1.8627
C5_03210C_A	0.00134943	2.33333	1	4.2	-1.8
C2_05400W_A	0.000663535	2.33333	1.1	1.30508	1.96667
HGT19	0.00363296	2.33383	1.07826	-1.02961	2.59099
C1_11970C_A	2.02E-05	2.34177	1.19697	1.35036	2.07576
BUB2	0.000306355	2.34211	4.22222	1.61818	6.11111
C5_02220C_A	1.60E-07	2.34946	1.17722	1.50172	1.84177
C3_03590W_A	2.73E-07	2.34973	1.00826	1.29909	1.82369
CPH1	1.04E-06	2.35211	1.57778	1.25564	2.95556
C5_00610C_A	1.00E-07	2.35625	1.36752	1.76168	1.82906
C3_01260C_A	0.00816826	2.36	-1.2	1.34091	1.46667
TOM6	0.00697501	2.36	-1.8	-1.32203	1.73333
NAT2	7.84E-07	2.36034	-1.07586	1.1085	1.97917
TEC1	0.000124894	2.36172	1.58635	1.28585	2.91365

C3_03270W_A	0.000693009	2.36667	-1.25	1.0597	1.78667
IMP2	7.67E-06	2.36905	1.2	1.16374	2.44286
FAA21	1.15E-05	2.37188	1.07349	1.82751	1.39325
CR_07120C_A	0.0111339	2.37255	3.92308	1.32967	7
CR_09340W_A	9.94E-06	2.375	1.3545	1.3913	2.31217
HAK1	0.00177036	2.375	3.42857	1.22581	6.64286
SNZ1	7.38E-06	2.37839	4.7121	1.81099	6.18846
C2_05300C_A	0.000240712	2.38005	-2.30189	1.08744	-1.05172
BRE1	3.59E-07	2.38206	-1.07532	1.68844	1.31198
HTA3	0.00537574	2.38511	2.91509	1.28397	5.41509
C2_08540C_A	8.84E-05	2.4	1.85714	1.90244	2.34286
C3_05440C_A	0.00133579	2.4	1.2963	2	1.55556
C4_00850C_A	0.000607452	2.40426	2.35	1.59155	3.55
C2_07540W_A	1.90E-05	2.40636	-1.02827	1.39406	1.67869
POT1-2	1.66E-06	2.40892	2.51402	1.52471	3.97196
C7_03640C_A	2.18E-05	2.41176	1.23188	1.72269	1.72464
C6_01050W_A	3.07E-06	2.41391	-1.24172	1.31826	1.47467
C1_05790W_A	1.73E-06	2.41667	-1.01667	1.13281	2.09836
CR_06430W_A	0.0131245	2.41667	1.5	1.16	3.125
ATX1	0.0118106	2.42105	1.11765	1.21053	2.23529
C5_02990W_A	1.17E-05	2.42188	1.23077	2.5	1.19231
C4_07240W_A	0.0116691	2.42308	1.08333	-1.1746	3.08333
C2_03560C_A	0.000928931	2.42369	-2.1754	1.18354	-1.06229
C1_07810C_A	1.13E-07	2.42381	4	1.82437	5.31429
CR_05970C_A	5.87E-08	2.42414	-1.01724	1.2355	1.92881
SMI1	2.52E-05	2.42593	1.27883	1.33586	2.32237
DUR35	3.06E-05	2.42857	3.11111	1.44681	5.22222
SDC1	0.0031821	2.42857	1.16667	1.65854	1.70833
FMT1	1.54E-07	2.42975	1.95161	1.36111	3.48387
C4_03880W_A	0.000134142	2.43243	1.85	1.52542	2.95
FDH3	1.39E-07	2.43546	1.80691	1.33593	3.29408
C4_02230C_A	0.00548507	2.4375	1.6	2.05263	1.9
PRM1	0.00144528	2.44	1	1.45238	1.68
VPH2	0.00172549	2.44	-1.26	-1.07377	2.07937
C3_03190C_A	6.08E-05	2.44667	-1.48667	1.53556	1.07175
UCF1	0.00541862	2.44701	-1.95762	1.2805	-1.0244
HOF1	0.00288457	2.44785	3.13462	1.3951	5.5
ZCF16	3.48E-05	2.44802	-1.09901	1.75666	1.26802
MRPL6	0.00631855	2.45045	-2.57658	1.07087	-1.12598
C1_10240C_A	2.57E-05	2.45532	-1.01277	1.58082	1.53361
BMT9	0.00258773	2.45679	2.31429	1.40141	4.05714
C4_05820W_A	4.65E-07	2.46	-1.2	1.43023	1.43333
C2_04790C_A	0.000440729	2.46296	-2.44444	1.37113	-1.36082
CR_03110W_A	7.12E-05	2.46328	-1.54802	1.06083	1.5
CR_03400W_A	2.86E-05	2.46455	-1.52323	1.05329	1.53612
EHD3	6.01E-07	2.46467	1.12893	1.82989	1.52055

CR_00660W_A	0.000295193	2.47368	1.35714	1.25333	2.67857
CR_08990C_A	0.0103554	2.47601	3.73793	-1.11252	10.2966
RK11	0.00112019	2.47619	-1.62857	1.12069	1.35673
CR_00700W_A	8.54E-06	2.47826	1.76923	1.60563	2.73077
ATO6	0.00290866	2.47826	1.91667	1.425	3.33333
YML6	0.000844604	2.47917	-1.92708	1.07692	1.19459
C7_01020C_A	0.000972555	2.48087	-1.60109	1.135	1.36519
C1_00880W_A	0.00254167	2.48276	1.07407	1.10769	2.40741
C1_01250W_A	6.19E-05	2.48405	-1.44465	1.49436	1.15065
C1_06840C_A	2.02E-07	2.48485	1.69231	1.72632	2.4359
SDH2	5.97E-05	2.48973	-1.41706	1.85466	-1.0556
MRPL8	0.00095544	2.49738	-2.06283	1.0021	1.20812
C4_03810W_A	4.48E-06	2.5	1.31852	1.59498	2.06667
C7_00630C_A	4.76E-05	2.5	1.46939	1.83673	2
C6_01200W_A	0.00245043	2.5	1.33333	1.72414	1.93333
DAD3	0.000744593	2.5	1.55556	2.05882	1.88889
ARG3	0.000397347	2.51107	-1.14576	2.35875	-1.07626
MSS51	2.12E-07	2.51289	-1.46991	1.27286	1.34308
CYC1	3.23E-05	2.51374	-1.56472	1.66745	-1.03793
C6_01980C_A	0.00144608	2.51724	-1.63793	1.05415	1.45789
C1_00980W_A	8.28E-08	2.51754	-1.5	1.34742	1.24561
DOG1	5.40E-08	2.51905	1.56716	1.59337	2.47761
C2_03970W_A	2.69E-07	2.51961	1.0625	1.49419	1.79167
C6_00550W_A	0.00120482	2.52323	-1.64792	1.72864	-1.12898
C6_00930C_A	2.03E-06	2.52386	-1.11543	1.93697	1.16816
C3_07730W_A	6.13E-05	2.52667	1.26761	-1.00264	3.21127
C1_11740W_A	0.000102154	2.52941	1	1	2.52941
C1_03950C_A	0.00419689	2.53333	-1.13333	2	1.11765
DOT5	2.21E-09	2.53411	1.31234	2.13643	1.55662
RER2	5.36E-08	2.53723	1.27027	1.07675	2.99324
C7_02120C_A	0.000233297	2.53846	-1.45299	1.57979	1.10588
C2_09250W_A	3.70E-06	2.53906	1.6	1.53302	2.65
C2_00920W_A	1.87E-05	2.54927	2.32203	1.75945	3.36441
CYC3	5.28E-08	2.54964	1.29467	1.56	2.11599
C5_04890C_A	4.41E-06	2.55	-1.06667	1.51485	1.57813
TFC4	2.03E-06	2.55145	1.64069	1.67591	2.49784
CR_07320C_A	0.000251742	2.5566	-1.88679	1.71519	-1.26582
C1_00460W_A	0.00184498	2.55789	-1.82105	1.01674	1.3815
C4_01910W_A	1.76E-06	2.5618	1.63303	1.59441	2.62385
LEU1	6.86E-05	2.56497	-1.12203	1.57639	1.45015
EHT1	1.24E-09	2.56515	2.08861	1.8584	2.88291
C6_03730C_A	0.00457844	2.57143	-2.42177	1.2	-1.13016
HEM3	0.000608049	2.57143	-1.27006	1.61823	1.25116
MED21	0.000439503	2.57143	1.75	2.07692	2.16667
YHM2	0.000133682	2.57637	1.21754	1.15355	2.7193
C1_02510W_A	5.00E-06	2.58	1.26582	1.73154	1.88608

CR_05360C_A	7.90E-05	2.5814	1.86957	1.83471	2.63043
C4_01470W_A	0.00034067	2.58333	1.62162	1.43519	2.91892
C1_07470C_A	3.72E-05	2.58442	1.45283	1.1988	3.13208
C2_07690W_A	1.73E-05	2.58696	1.7037	1.4	3.14815
C2_07680W_A	6.84E-05	2.59599	-1.86246	1.3811	1.00923
MST1	7.41E-09	2.5969	1.13158	1.4215	2.06725
C6_03200W_A	7.23E-07	2.59743	-1.00467	1.67494	1.54355
IFM1	2.54E-05	2.59885	-1.09742	1.2545	1.88773
C5_02350C_A	0.000485058	2.6	1.11111	1.2381	2.33333
C6_03530C_A	0.000749167	2.6	1.36364	1.48101	2.39394
FGR43	6.85E-05	2.6	-1.4	1.2381	1.5
C3_02720W_A	7.77E-05	2.60494	1.22727	1.39735	2.28788
TRY4	0.00320148	2.60861	-1.45597	1.70026	1.05376
C1_14320C_A	5.45E-05	2.61479	1.12227	1.52036	1.93013
C3_05940C_A	0.000935388	2.61538	-1.41026	1.25926	1.47273
C4_03080W_A	3.14E-07	2.6178	1.56557	1.80505	2.27049
C1_00790W_A	0.00245723	2.61905	1.4	1.57143	2.33333
NAM2	1.07E-06	2.61928	-1.16867	1.21453	1.84536
MRPS9	3.69E-05	2.62633	-2.44484	1.22388	-1.1393
MRPL33	2.00E-05	2.62745	-1.37255	1.54023	1.24286
MAM33	1.38E-05	2.6283	-1.54962	1.4995	1.13111
C2_03950W_A	0.000296739	2.63816	-2.15789	1.29355	-1.05806
C6_03620C_A	4.71E-12	2.64192	2.60227	1.63735	4.19886
PGA44	0.00347226	2.64286	-1.21429	-1.35135	2.94118
KGD2	6.79E-07	2.64325	-1.62784	1.4755	1.1005
PEX6	0.0103042	2.64531	1.38847	1.42976	2.56892
C2_04160W_A	5.58E-08	2.64796	1.50769	1.88043	2.12308
C4_04280C_A	2.34E-07	2.64835	1.78431	1.928	2.45098
HGT16	0.000339234	2.65873	1.14545	1.10927	2.74545
FMO2	0.000109286	2.65909	1.22222	1.28571	2.52778
MRP20	0.000421156	2.65915	-2	1.37209	-1.03198
C3_04620C_A	6.35E-05	2.66	-1.29	1.1982	1.72093
TUF1	0.00295694	2.66513	-2.46383	1.15493	-1.0677
C3_04720C_A	1.87E-06	2.66887	-1.14901	1.62828	1.42651
C1_03870C_A	7.36E-07	2.672	1.53374	2.081	1.96933
C1_05920W_A	0.000417983	2.67347	1.48485	1.52326	2.60606
HHT2	0.00841689	2.67801	20.3636	1.04667	52.1023
C5_04620C_A	8.76E-07	2.68093	-1.10117	1.50109	1.62191
NTG1	0.000147919	2.68293	-1.41463	1.35802	1.39655
C1_04460C_A	2.33E-06	2.69185	-1.26398	1.97055	1.08075
C1_02670C_A	0.00531001	2.69231	-1.15385	1.25	1.86667
PHHB	0.0033377	2.69388	-1.85714	1.0038	1.44505
MUM2	3.44E-07	2.69613	3.41509	1.10407	8.33962
PEA2	0.000170139	2.69663	1.23611	1.83206	1.81944
C2_07070W_A	7.02E-07	2.69673	-1.54602	1.33967	1.30204
C3_00230C_A	0.000696264	2.69767	-1.0814	1.56757	1.5914

C1_06980C_A	3.48E-11	2.69835	1.60265	1.39232	3.10596
C4_02930W_A	1.09E-06	2.7043	2.33962	1.63047	3.8805
PRP22	4.49E-08	2.70649	2.58389	1.22014	5.73154
CSO99	0.000435448	2.7087	-1.5913	1.61818	1.05191
OSM2	1.51E-11	2.71311	1.36319	1.82379	2.0279
C3_07670W_A	3.48E-06	2.71386	1.58411	1.21693	3.53271
CFL4	0.013185	2.71429	3.11111	1.16923	7.22222
C3_01230C_A	0.00811881	2.72727	-1.27273	2	1.07143
MSW1	1.57E-05	2.73103	-1.21379	1.62295	1.38636
ERV1	1.06E-07	2.73665	-1.00712	1.40073	1.93993
C2_01740C_A	0.0112475	2.74194	-2.48387	1.26866	-1.14925
C4_03460C_A	7.81E-08	2.75	1.34737	1.75124	2.11579
CR_08270W_A	0.00199384	2.75	5.33333	1.375	10.6667
C1_12110C_A	0.00824322	2.75	?	1.375	?
TLO34	0.0047218	2.75	1.14286	1.29412	2.42857
C1_08730W_A	7.79E-05	2.7513	-1.08808	1.69108	1.49524
CR_04150W_A	4.95E-05	2.75962	1.31646	1.58564	2.29114
C2_07430C_A	9.40E-05	2.76147	-1.43119	1.13158	1.70513
HTB1	0.00122863	2.76471	4.64898	1.71608	7.4898
C1_08690W_A	0.000172949	2.78151	-1.85714	1.77957	-1.18817
C3_07470W_A	5.32E-06	2.78182	2.97297	2.26667	3.64865
C2_10330C_A	0.00293692	2.78571	-1.32143	1.34483	1.56757
GCY1	1.68E-06	2.78699	2.93342	2.00849	4.07042
TIM17	1.99E-06	2.79487	-1.34615	1.41558	1.46667
ALD6	3.82E-06	2.79741	-1.3944	2.16694	-1.08013
MIA40	4.60E-06	2.79756	-1.49885	1.41609	1.31804
C4_03410W_A	0.000443377	2.79803	-2.37438	1.49474	-1.26842
CR_08440W_A	2.87E-08	2.80822	2.28125	1.35762	4.71875
C1_02270C_A	5.85E-08	2.80952	-1.71429	2.29417	-1.39983
C1_04370C_A	6.05E-05	2.81137	-1.69251	1.50276	1.10534
BNA4	8.16E-10	2.81242	1.08886	1.20449	2.54244
SDH12	3.63E-05	2.81758	-1.61298	1.96288	-1.12369
C2_02230C_A	0.00382802	2.81818	2.75	1.40909	5.5
COX19	7.76E-06	2.82895	-1.25	1.16216	1.94737
C4_06430C_A	9.58E-07	2.84	1.0479	2.09705	1.41916
C1_04600C_A	6.98E-07	2.84146	-1.99729	1.59954	-1.12433
MTW1	0.000395482	2.84615	-1.25641	1.63235	1.38776
CR_07820W_A	0.000434953	2.85	2.5	1.96552	3.625
C3_06240C_A	0.00314607	2.85185	-1.96296	1.7907	-1.23256
C1_05270C_A	1.73E-06	2.85326	-1.57609	1.45429	1.24483
C2_06270W_A	0.00782335	2.85714	4.66667	-1.075	14.3333
C3_02070C_A	0.00305999	2.85714	1.75	1.25	4
C1_07400C_A	6.52E-05	2.864	-1.096	1.58407	1.64964
INO4	0.000109508	2.87671	1.35185	1.75	2.22222
HHF1	0.00254702	2.8769	5.55274	1.23645	12.9198
C6_04510C_A	8.83E-11	2.88385	1.58296	1.63141	2.79821

DRE2	1.66E-07	2.88816	1.35111	2.48023	1.57333
C2_06280C_A	0.00218158	2.88889	4.5	2.36364	5.5
C5_02740W_A	1.65E-08	2.891	-1.00474	1.62667	1.76887
C5_05460C_A	0.000400217	2.89116	1.68966	-1.07529	5.25287
C1_11620W_A	2.72E-05	2.9	-1.25	1.70588	1.36
C6_02300C_A	0.00689186	2.9	5	4.14286	3.5
C1_07610C_A	0.0124753	2.9	1.42857	2.23077	1.85714
ALT1	0.000281776	2.90545	-2.57246	1.4135	-1.2515
C7_01440W_A	2.22E-05	2.91228	-1.19298	1.93023	1.26471
CR_00420W_A	0.000117874	2.92593	1.6875	1.26908	3.89063
CR_01020C_A	2.09E-05	2.92593	-1.01852	1.62887	1.76364
YHM1	6.33E-07	2.926	-1.97886	1.41658	1.0438
ATO1	0.0042989	2.92857	7	-1.37805	28.25
C2_04340C_A	0.0090268	2.93333	1	-1.04545	3.06667
MRPL40	2.13E-05	2.93662	-2.10211	1.40404	-1.00505
MSF1	3.23E-08	2.93884	-1.14526	1.60837	1.59546
PLB3	3.34E-07	2.94305	1.26725	2.41056	1.54718
GSY1	4.41E-08	2.94813	1.87418	1.83481	3.01138
CHT3	4.95E-06	2.95026	1.55285	2.18411	2.09756
PAM16	6.89E-06	2.95041	-2.04132	1.35227	1.06883
PRS	9.85E-07	2.96604	-1.67925	1.40357	1.25843
SAP3	0.000308612	2.97297	1.68182	1.48649	3.36364
C2_07250C_A	2.74E-06	2.97674	1.26471	1.33333	2.82353
C3_04690C_A	4.38E-07	2.97872	1.46875	1.67331	2.61458
C1_01580W_A	5.07E-06	2.97884	-1.98413	1.12151	1.33867
C1_14020W_A	0.00761715	3	1.28571	1	3.85714
C3_02200W_A	0.0098678	3	1	1.07143	2.8
C7_03690W_A	0.00337426	3	-2.28571	1	1.3125
C7_03470W_A	0.00714373	3	-1.375	1.45455	1.5
SWD3	2.38E-07	3	1.52632	1.45	3.15789
CR_07700W_A	9.65E-06	3.01326	1.34164	1.8623	2.17082
CYB2	1.85E-08	3.01503	1.53974	2.19921	2.11092
CDG1	7.55E-05	3.01961	1.73864	2.02632	2.59091
HHF22	0.00397877	3.02519	8.76623	1.13381	23.3896
C3_06050C_A	1.33E-06	3.02778	-1.37698	1.56996	1.40058
GAL10	6.18E-06	3.03134	-1.79157	1.70775	-1.00931
IDP2	0.000130124	3.03238	-2.9528	1.55809	-1.5172
C6_00920W_A	2.46E-07	3.0399	-1.08632	1.76501	1.58546
XYL2	0.000105219	3.0416	-1.16807	1.21299	2.14673
BLP1	1.20E-06	3.04323	-1.83535	1.74644	-1.05327
LEU42	4.19E-10	3.04547	-1.07346	1.92389	1.47466
C2_06760C_A	0.000446779	3.06122	4.45455	1.68539	8.09091
CR_01100C_A	1.02E-05	3.06667	1.18421	1.79221	2.02632
FUM12	3.41E-05	3.06683	-2.45429	1.61975	-1.29624
TOM7	0.000174808	3.06897	-1.75862	1.36923	1.27451
C2_01690W_A	6.11E-06	3.07463	-1.56219	2.16462	-1.09982

SAP6	0.00416638	3.09091	2.75	-1.02941	8.75
CHT4	0.000889003	3.10526	1.11765	1.11321	3.11765
HGT2	0.00170535	3.11092	1.08154	1.40356	2.39717
C1_05690C_A	0.00620584	3.11111	?	1.86667	?
OYE23	0.000617963	3.11765	1.54545	1.08163	4.45455
C2_07270W_A	3.35E-06	3.12409	1.37	1.49129	2.87
C5_05090W_A	9.01E-06	3.125	-1.8125	1.21951	1.41379
DUR3	0.00066116	3.125	1.6	1.35135	3.7
PHA2	0.000534212	3.125	-1.91667	1.1194	1.45652
C3_01890C_A	1.36E-07	3.12929	-1.05779	1.20023	2.46481
C1_06070W_A	0.000211017	3.14103	-2.34615	1.39205	-1.03977
CR_03670W_A	0.00606564	3.14286	7	1.69231	13
C5_00820W_A	1.52E-05	3.14365	-2.29834	1.30505	1.04808
C2_07190C_A	0.000803809	3.1448	-3.04525	-1.00288	1.03566
FGR41	1.37E-08	3.14876	2.08621	2.16477	3.03448
C1_14500C_A	1.82E-06	3.15981	-1.32446	-1.07969	2.57587
CHL4	0.000105873	3.16	5	2.46875	6.4
MRPL10	0.000407356	3.16379	-2.68966	-1.01362	1.19231
C5_03410C_A	0.00581579	3.16667	-2.88889	1.70149	-1.55224
C2_05330C_A	0.0112116	3.18182	1.375	1.45833	3
MLS1	8.20E-10	3.18848	-1.18493	2.79079	-1.03714
MAL2	0.000118669	3.22222	-4.11696	1.49322	-1.90786
CRG1	7.41E-06	3.2364	2.35841	1.92737	3.96018
AAT22	0.000221258	3.24771	-1.79817	-1.33616	2.41327
CR_03440W_A	0.015065	3.25	2.4	1	7.8
C5_01050C_A	2.23E-06	3.25287	-2.29885	1.06391	1.33
ECI1	4.12E-07	3.26217	1.33056	1.93843	2.2392
GAL1	1.84E-06	3.26667	-1.42487	1.6063	1.42726
MDM34	0.00199125	3.26931	-3.10193	1.85566	-1.76066
C1_10980W_A	0.000605728	3.28571	7	11.5	2
CR_07170W_A	4.12E-12	3.29503	6.25753	1.79633	11.4783
RIB5	1.08E-11	3.29735	1.23368	1.59061	2.55744
CSP1	0.0109687	3.3	-1.6	1.375	1.5
C6_00770C_A	7.66E-08	3.31868	-1.10989	1.77647	1.68317
C1_14090W_A	1.48E-08	3.32012	-1.48899	1.54124	1.44675
C5_03650C_A	0.000265996	3.33333	12	1.29032	31
C5_05240C_A	0.00238422	3.33333	-1.33333	1.07143	2.33333
SFC1	4.69E-09	3.34373	1.07351	1.97359	1.81878
CR_08400C_A	3.58E-07	3.35185	1.03846	2.12941	1.63462
CHA1	4.27E-05	3.35333	16.4063	1.24902	44.0469
HHT21	0.00866334	3.36983	23.6098	-1.01798	80.9919
CR_07680C_A	0.00245043	3.4	-1.6	-1.05882	2.25
WOR3	0.000997777	3.40196	-1.60784	1.46414	1.44512
C2_07410W_A	4.44E-08	3.41567	1.6808	2.01252	2.85268
HTA2	0.000687843	3.41588	5.04534	1.29265	13.3325
SOD5	0.00389521	3.41667	1	-1.14634	3.91667

C2_07180W_A	0.0130242	3.42857	1.16667	2	2
GDH2	1.09E-10	3.43918	1.05609	1.79054	2.02849
CR_08920W_A	2.74E-09	3.44046	-1.07288	2.81583	1.13883
C1_04820C_A	4.33E-05	3.44118	-1.94118	1.34483	1.31818
C6_02160W_A	4.27E-07	3.44444	1.63636	1.73427	3.25
C2_00760C_A	4.03E-05	3.45163	-2.15773	1.41037	1.13421
C4_04980W_A	3.18E-09	3.45283	1.03922	1.79412	2
C3_01420C_A	2.90E-06	3.45753	-2.19178	3.01193	-1.90931
IFM3	0.000121014	3.46296	1.17391	1.79808	2.26087
C5_04380C_A	0.00059576	3.46667	3.75	2.47619	5.25
C5_05360C_A	3.89E-09	3.4703	2.05224	1.50843	4.72139
CR_06790C_A	2.22E-07	3.5	1.07407	1.51493	2.48148
C5_01020C_A	0.00250725	3.5	-1.1875	1.86667	1.57895
FAR1	4.06E-05	3.5	2.4	1.16667	7.2
ACH1	3.12E-07	3.51917	-1.75197	1.54198	1.30268
HSP78	1.36E-11	3.51965	1.34551	2.2264	2.12707
MRPL37	0.0023622	3.53846	-3	1.29577	-1.09859
C1_01000C_A	1.83E-09	3.54396	-1.00549	1.56553	2.25137
HSP60	1.65E-06	3.54872	-2.34983	1.41505	1.06724
CR_03870W_A	0.00593773	3.57585	-2.50464	1.16431	1.22621
C7_01610W_A	1.09E-07	3.57971	-1.26087	1.23192	2.3046
PGA37	0.00280462	3.58065	2.58333	-1.00901	9.33333
C4_03780C_A	8.27E-07	3.60232	-1.82239	1.65426	1.19492
C4_02080W_A	0.00742148	3.625	2	-1.10345	8
C2_07370W_A	4.55E-07	3.6802	1.17964	1.48871	2.91617
CR_08130W_A	2.08E-08	3.68942	1.18623	1.64286	2.66397
DLD1	1.76E-14	3.6907	1.75667	1.9172	3.38167
C3_03440C_A	6.90E-08	3.69512	1.90698	1.56186	4.51163
STB3	1.62E-06	3.69945	-2.45902	1.15925	1.29778
GTT13	0.000406432	3.70588	1.54545	1.90909	3
FOX2	5.58E-06	3.72943	-2.27543	2.69217	-1.64257
CYT2	2.20E-08	3.73256	-1.18023	1.64194	1.92611
SOD1	0.0051091	3.73315	2.18405	-1.2611	10.2822
C5_04940W_A	0.00953184	3.73684	-4.43158	1.775	-2.105
SEF2	9.92E-06	3.74118	-1.10588	3.2449	1.04255
YFH1	2.57E-08	3.75207	-1.20661	1.40123	2.21918
HHO1	0.000178483	3.76609	6.12121	1.58986	14.5
SSC1	8.37E-09	3.77355	-1.89411	1.56027	1.27686
C4_04820C_A	5.09E-05	3.775	-2.8375	1.2636	1.05286
C1_04180W_A	0.000747323	3.77931	5.91837	1.54149	14.5102
STF2	1.81E-06	3.78445	-1.18173	2.22485	1.4394
NGT1	0.000144815	3.81818	1.83333	1.03704	6.75
C1_02780W_A	2.92E-10	3.82865	1.44715	1.1425	4.84959
SAP8	0.00010705	3.84615	1.52941	1.13636	5.17647
C1_02380C_A	0.00597243	3.85714	-1.57143	1.92857	1.27273
SOD6	3.90E-09	3.87678	3.57627	1.53759	9.01695

CR_06500C_A	3.00E-05	3.87879	-2.40909	1.3617	1.18239
C1_10170W_A	9.30E-06	3.88406	-1.20652	1.76606	1.82282
C2_05120C_A	5.00E-05	3.88889	1	2.05882	1.88889
CR_06510W_A	8.29E-05	3.90196	-1.88235	1.43165	1.44792
C7_02010C_A	9.00E-07	3.90476	2.47059	1.74468	5.52941
MED8	0.000158333	3.92308	-1.61538	1.7	1.42857
SCO1	1.21E-09	3.93323	-1.54213	1.41533	1.80206
YHB1	1.39E-06	3.98984	1.66385	1.26748	5.23756
FUS1	0.00402845	4	1.28571	2.11765	2.42857
C1_12140W_A	1.65E-10	4.04854	-1.18204	2.16062	1.58522
C2_02280W_A	1.88E-06	4.05108	-1.77419	1.507	1.51515
TIM13	8.04E-05	4.05263	-1.42105	1.01316	2.81481
FBP1	0.000310324	4.0632	-2.64312	-1.02882	1.58158
CR_00380W_A	0.000339969	4.09091	-1.09091	1.32353	2.83333
CTF5	0.000848526	4.14286	?	1.16	?
C6_01400W_A	1.05E-05	4.16279	1.48276	1.90426	3.24138
TES15	1.27E-07	4.18145	-1.09677	2.03333	1.875
C1_08610C_A	9.74E-09	4.24888	1.40505	2.0149	2.96286
C1_06860W_A	8.98E-06	4.42222	3.46154	3.43103	4.46154
MDH1-1	2.76E-09	4.42234	-1.32748	2.63981	1.26198
CR_04870C_A	7.93E-05	4.45455	-1.40909	1.58065	2
HMO1	1.39E-07	4.4618	1.50759	1.99026	3.37975
CR_05040W_A	1.85E-05	4.46875	-1.71875	2.30645	1.12727
FMA1	2.04E-08	4.55344	1.53816	3.46467	2.02153
HSP30	4.02E-07	4.55646	-1.15572	3.19485	1.23402
KGD1	8.14E-07	4.55729	-2.08542	1.70403	1.28244
C7_01510W_A	1.53E-07	4.61924	-2.17391	1.78332	1.19152
C4_03340C_A	1.01E-06	4.64286	2.33333	2.33333	4.64286
C1_07980C_A	2.04E-06	4.65714	-1.2	1.75269	2.21429
CRH11	1.35E-09	4.67114	-1.05705	1.64151	2.69206
C4_01140C_A	1.95E-05	4.68182	-2.09091	1.68852	1.32609
CRD2	6.66E-09	4.68966	1.8913	4.58427	1.93478
HGT1	1.35E-06	4.70422	-2.23176	1.52587	1.38141
C2_08580W_A	0.000982778	4.72727	1.375	2.08	3.125
CR_02880W_A	7.27E-08	4.76596	2.47368	1.44516	8.15789
PDC12	3.19E-05	4.85	1.33333	1.27632	5.06667
C7_02130W_A	1.36E-06	4.875	?	3.25	?
PRE1	1.08E-06	4.88359	1.60213	1.60708	4.86856
PEX4	7.14E-11	4.89394	-1.25758	1.76986	2.1988
C1_06430C_A	0.00238956	5	1	10	-2
C2_02390W_A	5.66E-07	5.02869	1.36313	1.90233	3.60335
IFE2	1.11E-10	5.04535	1.14894	2.40175	2.41357
C2_10070W_A	5.42E-06	5.05882	1.88889	1.65385	5.77778
C1_00190C_A	4.40E-07	5.29752	-2.66942	2.15825	-1.08754
C5_05060C_A	0.00605586	5.5	1	2.2	2.5
MGE1	1.71E-10	5.50072	-1.80186	1.73315	1.76141

GCA2	1.65E-08	5.5366	-1.33673	2.33065	1.77714
AGA1	0.00321293	5.66667	?	2.42857	?
COX15	5.42E-12	5.70309	-1.23951	1.70584	2.69724
JEN2	5.24E-08	5.70389	-1.54781	2.28635	1.6118
C6_02560W_A	7.71E-07	5.79972	1.21237	1.83006	3.84218
ICL1	5.09E-11	5.97523	-1.68451	3.2107	1.1048
C5_00810C_A	0.00606564	6	1	1.05882	5.66667
CTN1	3.26E-08	6.00892	-1.66412	2.99112	1.2072
C7_03380W_A	8.56E-08	6.175	-2.15	1.63576	1.75581
GCA1	2.30E-09	6.29175	-1.61752	2.02782	1.91819
CR_03120W_A	6.80E-08	6.36335	-1.76963	2.21707	1.62189
C1_12470W_A	2.38E-06	6.4	1.36364	1.92	4.54545
C4_01860C_A	1.15E-05	6.5	-2.44444	1.14706	2.31818
PGA4	1.70E-09	6.50976	1.39916	1.16218	7.83718
RHD3	1.45E-08	6.64549	1.47569	1.67351	5.85995
HGT17	0.00345737	6.67979	-1.20124	1.07357	5.17968
C2_08090W_A	1.07E-05	6.72973	-1.24324	1.77857	3.04348
C7_01770W_A	0.0151391	7	?	1.4	?
CAG1	0.00325431	7	?	2	?
PGA60	4.56E-08	7.375	2.28571	1.66197	10.1429
C4_01990W_A	0.00176543	7.5	1	1.66667	4.5
PXP2	0.000532646	7.72973	-12.2036	2.64897	-4.18215
CIT1	1.36E-12	7.73054	-1.6333	3.72898	1.26927
COX17	6.04E-07	8.3	-2.1	2.12821	1.85714
C5_02800C_A	2.95E-05	8.5	?	2.42857	?
CR_06870C_A	1.10E-05	9.16667	1.2	2.3913	4.6
ARO10	1.65E-08	9.37198	2.62025	1.98974	12.3418
C2_06060C_A	0.0130143	10	?	1.66667	?
HSP31	2.30E-06	10.1362	1.90769	1.78592	10.8274
C3_04450C_A	0.00626155	10.5	2	1.23529	17
OPT4	8.97E-14	12.5053	-2.45263	2.76923	1.8412
C5_03770C_A	2.43E-05	12.5455	1.375	1.55056	11.125
FDH1	1.70E-06	13.9617	-2.31826	2.47816	2.43023
CEK2	6.00E-06	18.75	?	2.08333	?
HPD1	3.46E-11	23.8864	-3.82576	3.24383	1.92475
C5_04980W_A	1.45E-07	28.2879	2.35714	3.32799	20.0357
C2_01630W_A	3.55E-08	75.2222	9	2.0209	335
TLO9	9.92E-06	184	?	1.26897	?

Genes down regulated in the pho4Δ compared to WT in Pi rich medium					
Alias	p-value (pho4+Pi vs. WT+Pi)	Fold Change (pho4+Pi vs. WT+Pi)	pho4-Pi vs. WT-Pi	WT-Pi vs. WT+Pi	pho4-Pi vs. pho4+Pi

<i>LEU2</i>	0.000175436	-87.1818	-295	1.53806	-2.2
<i>POL93</i>	4.35E-05	-16.2656	-11.6366	- 1.25802	1.11111
<i>RDN18</i>	5.85E-05	-11.7437	-11.2097	- 1.59005	-1.51775
<i>C2_00860C_A</i>	2.15E-05	-11.375	-7.90909	- 3.13793	-2.18182
<i>CR_09350C_A</i>	0.00247131	-9.75	-3.4	- 2.29412	1.25
<i>ZRT2</i>	1.84E-05	-8.38095	-6.96373	- 1.44048	-1.19689
<i>NAG4</i>	0.00574711	-8	?	- 1.77778	?
<i>C4_04190C_A</i>	0.0151391	-7	-6	- 1.16667	1
<i>C1_00270W_A</i>	4.06E-06	-5.88263	-3.29231	- 1.17103	1.52582
<i>C2_09880C_A</i>	0.000579153	-5.25362	1.46188	- 3.25112	2.36232
<i>PXP2</i>	1.46E-05	-4.18215	7.72973	- 12.2036	2.64897
<i>NAG3</i>	8.40E-05	-4.05634	-4.82569	- 1.64259	-1.95413
<i>SOD3</i>	5.05E-07	-3.99291	-3.08961	- 1.27547	1.01324
<i>FTR2</i>	0.000528316	-3.90698	-3.57692	1.66071	1.81395
<i>FET3</i>	2.80E-05	-3.88164	-2.93885	- 3.53244	-2.67446
<i>C2_09000C_A</i>	0.00703862	-3.66667	-2.5	1.36364	2
<i>CTR1</i>	0.000619013	-3.49269	-1.55925	- 1.45735	1.53702
<i>TNA1</i>	0.00127189	-3.375	-2.15625	- 1.95652	-1.25
<i>THI20</i>	3.90E-06	-3.31061	-1.64815	- 2.45506	-1.22222
<i>ADH2</i>	3.90E-09	-3.25264	-1.02594	- 1.32422	2.39417
<i>C1_01640W_A</i>	0.00126211	-3.18321	-5.63467	- 1.60385	-2.83901
<i>CSR1</i>	0.0102805	-3.15116	-3.12987	- 1.12448	-1.11688
<i>SUL2</i>	0.000409114	-3.14286	-2.93103	- 1.81176	-1.68966
<i>HGC1</i>	0.002803	-3.06452	1.41818	- 1.72727	2.51613
<i>C4_01220C_A</i>	0.00917896	-3	-1.2	-2.125	1.17647
<i>PTC8</i>	0.00893145	-2.7973	-1.83133	- 1.36184	1.12162
<i>HIP1</i>	2.13E-05	-2.77056	-1.6	- 1.90476	-1.1
<i>C3_03200C_A</i>	0.00947846	-2.7	1.11765	- 1.58824	1.9

<i>FRE30</i>	0.0100074	-2.46709	-1.25311	- 1.27235	1.54735
<i>C1_05550C_A</i>	0.00305747	-2.41071	-3.25	- 1.22172	-1.64706
<i>C6_02330W_A</i>	0.00725524	-2.3913	-1.82994	1.07164	1.40039
<i>C3_01900C_A</i>	0.000363981	-2.34653	-1.18552	- 1.80916	1.09406
<i>CSH1</i>	0.0102351	-2.32713	-3.59104	1.20424	-1.2814
<i>FRE7</i>	0.00976453	-2.32058	-1.28758	- 1.25783	1.43285
<i>ANP1</i>	0.00362367	-2.2	1.31667	-1.65	1.75556
<i>C7_00430W_A</i>	0.000599885	-2.18984	1.00144	- 1.18097	1.85695
<i>MET16</i>	0.00116702	-2.17857	-1.87342	- 1.64865	-1.41772
<i>C6_02480W_A</i>	0.00221323	-2.17021	-4.42105	- 1.21429	-2.47368
<i>C3_03210W_A</i>	0.00118329	-2.16604	-3.14954	1.06906	-1.36012
<i>C5_03440W_A</i>	0.00122484	-2.15625	1.06452	- 2.22581	1.03125
<i>POX1-3</i>	0.00110373	-2.14316	2.30128	-1.9421	2.53952
<i>SHA3</i>	0.000857346	-2.1233	-1.10916	- 1.70741	1.12118
<i>C3_05410W_A</i>	0.00960364	-2.09091	-1.4375	- 1.46667	-1.00833
<i>C2_01450C_A</i>	0.00225324	-2.08451	2.16667	- 3.08333	1.46479
<i>ZCF31</i>	0.000849422	-2.08108	-1.57979	- 1.03704	1.27027
<i>IFH1</i>	0.00493884	-2.0796	-2.86866	- 1.08741	-1.5
<i>ADH3</i>	0.0143547	-2.0625	1.47368	- 1.73684	1.75
<i>C2_03110W_A</i>	0.00360036	-2.05747	1.05405	- 2.41892	-1.11538
<i>MET14</i>	0.0111073	-2.0553	-2.87234	-3.3037	-4.61702
<i>SNX4</i>	0.00490376	2	1.3985	1.94634	1.36098
<i>C2_03760C_A</i>	0.00865075	2.00307	1.30332	1.68506	1.0964
<i>C5_04170W_A</i>	8.59E-06	2.00348	1.67087	1.37913	1.15017
<i>MNN10</i>	0.00427529	2.00407	1.07143	1.87805	1.00406
<i>C7_03970C_A</i>	1.06E-05	2.00442	1.53286	1.88496	1.4415
<i>TYS1</i>	0.00670927	2.00603	-1.03075	1.36501	-1.51481
<i>DFG5</i>	0.00324367	2.00702	-1.11185	2.33684	1.0472
<i>PUP2</i>	0.00993618	2.00825	1.06027	1.84742	-1.02526
<i>C5_01420W_A</i>	0.000250874	2.01083	1.33895	1.9278	1.28366
<i>C6_03520C_A</i>	0.000262005	2.01099	1.78889	1.48352	1.31967
<i>C2_01530C_A</i>	0.00983775	2.01132	1.23246	2.00755	1.23014
<i>RAD2</i>	0.00093429	2.01182	1.38807	1.95439	1.34845
<i>FGR32</i>	0.000267747	2.01233	1.28332	1.8083	1.1532
<i>SUA71</i>	5.28E-05	2.0133	2.06168	1.49687	1.53284

LIG4	6.11E-05	2.01521	1.48492	1.63878	1.20755
SAR1	0.000202541	2.01534	1.50775	1.58282	1.18417
LIP1	0.00129902	2.01639	1.68132	1.4918	1.2439
C3_05010C_A	0.00599513	2.01667	1.45408	1.63333	1.17769
SPT6	0.000137853	2.01789	1.12886	1.72138	-1.03843
LEM3	7.08E-07	2.01863	1.53855	1.54215	1.17538
NUP85	0.00478398	2.01918	1.05891	1.95342	1.02442
MEF2	0.0027447	2.02058	2.06977	1.32762	1.35993
ENG1	0.000387228	2.02118	1.82753	1.86838	1.68937
PCL7	0.011567	2.02252	-1.04545	2.40662	1.13818
NBN1	0.000127808	2.02381	-1.02825	2.16667	1.04118
C1_01590C_A	6.31E-05	2.02568	1.54057	1.52825	1.16226
SFI1	3.23E-06	2.02696	1.54161	1.85539	1.41112
C3_01190C_A	0.00356776	2.0274	-1.39597	2.84932	1.00676
C2_00570W_A	0.000539042	2.02749	1.43295	1.79381	1.2678
C3_04410C_A	0.000330516	2.02768	2.06169	1.32757	1.34983
OSM2	7.71E-06	2.0279	2.71311	1.36319	1.82379
GDH2	9.66E-05	2.02849	3.43918	1.05609	1.79054
PTR22	0.00592887	2.03229	1.23067	1.47084	-1.12274
SNF5	0.000399514	2.03234	1.27141	1.71393	1.07222
MGM101	0.000827333	2.03289	1.8371	1.45395	1.31392
C3_00570C_A	0.00385156	2.03529	1.47148	1.54706	1.1185
C2_02660W_A	0.00760373	2.03529	1.34	1.76471	1.16185
C2_10670W_A	0.000849825	2.03545	1.45365	1.08963	-1.28505
DOS2	0.00299509	2.03589	1.92821	1.43301	1.35723
TSC11	0.00185374	2.03636	1.90998	1.86818	1.75223
C6_00230W_A	0.0019343	2.03659	1.30769	1.58537	1.01796
C4_00100C_A	9.24E-06	2.03736	1.2	1.94684	1.14669
C2_09710C_A	0.00229138	2.03774	2.01074	1.40503	1.38642
C3_01690W_A	0.011592	2.03784	-1.30375	2.06486	-1.28669
RIA1	0.000418333	2.03927	-1.19872	2.26888	-1.07741
C1_09810W_A	0.0147945	2.04054	1.06818	1.18919	-1.60638
C1_06600W_A	0.000964634	2.04057	1.45719	1.67541	1.19642
CAF16	0.0155673	2.04061	-1.2533	2.88832	1.12935
SEC18	0.00419462	2.04138	1.22573	1.66207	-1.00203
C2_02870W_A	0.0100516	2.04167	1.49474	1.97917	1.44898
PGI1	0.00123911	2.04284	1.16107	2.06387	1.17302
C1_08240C_A	0.00754649	2.04396	1.18235	1.86813	1.08065
RIC1	0.00778423	2.04651	1.69424	1.61628	1.33807
PEX7	0.00494321	2.04878	1.32123	1.74634	1.12619
C3_07480W_A	0.0102812	2.04889	1.01587	1.96	-1.02902
C1_08680C_A	0.00378104	2.05	2.09375	1.6	1.63415
C2_00770W_A	7.52E-05	2.05085	1.32839	1.82712	1.18347
C1_09520C_A	7.74E-05	2.05212	1.5049	1.82899	1.34127
C1_14050C_A	6.40E-05	2.0522	1.32299	1.68189	1.08426
RPS14B	0.0115776	2.05299	1.67627	-1.6466	-2.01666

<i>C5_01880C_A</i>	0.0054309	2.05333	1.25263	1.9	1.15909
<i>SNP3</i>	0.00299069	2.05357	1.30986	1.26786	-1.23656
<i>CR_10610C_A</i>	0.0116818	2.05405	1.85714	1.7027	1.53947
<i>YEA4</i>	0.000993375	2.05556	1.74545	1.52778	1.2973
<i>CR_07200W_A</i>	0.00172107	2.05581	1.63221	1.93488	1.5362
<i>YMX6</i>	0.00375988	2.05607	-1.65289	1.86916	-1.81818
<i>C2_10630W_A</i>	0.000195714	2.0566	1.32653	2.21887	1.43119
<i>CEF1</i>	0.000189585	2.05672	1.23569	2.19104	1.3164
<i>PGA52</i>	0.0016597	2.05675	-1.83891	2.59836	-1.4556
<i>CR_04230W_A</i>	6.14E-06	2.05691	1.34659	1.43089	-1.06751
<i>C1_02830W_A</i>	0.000849572	2.05732	2	1.57325	1.52941
<i>C3_02770C_A</i>	0.000537889	2.06015	1.3172	1.3985	-1.11837
<i>C4_06440C_A</i>	0.00198257	2.0625	1.432	1.5625	1.08485
<i>GPM1</i>	0.0130902	2.06266	-1.54838	2.95029	-1.08253
<i>C2_09780C_A</i>	0.00129036	2.06375	1.85057	1.03984	-1.07246
<i>C5_04420W_A</i>	0.000543744	2.06466	1.53046	1.69828	1.25887
<i>RIM13</i>	0.000590275	2.06593	1.5625	1.75824	1.32979
<i>C4_03810W_A</i>	0.00315494	2.06667	2.5	1.31852	1.59498
<i>C1_08540C_A</i>	0.000179597	2.06681	1.33186	1.62787	1.04901
<i>MST1</i>	1.71E-05	2.06725	2.5969	1.13158	1.4215
<i>AHA1</i>	0.000170835	2.06857	1.29091	1.57143	-1.01972
<i>CR_10440W_A</i>	0.00994576	2.06863	1.12821	1.91176	1.04265
<i>C2_09860C_A</i>	0.000340954	2.06897	1.62439	1.76724	1.3875
<i>SPT14</i>	7.35E-05	2.06954	1.62698	1.25166	-1.01626
<i>C6_00680C_A</i>	0.00367731	2.07143	1.00645	1.84524	-1.11538
<i>CR_03710C_A</i>	0.010339	2.072	1.71168	2.192	1.81081
<i>SNG4</i>	0.00067339	2.07385	1.31443	1.79077	1.13501
<i>RVB2</i>	0.00191687	2.07429	-1.21744	1.59733	-1.58097
<i>C2_07650C_A</i>	0.00299636	2.07447	1.25685	1.55319	-1.06267
<i>C6_03880W_A</i>	0.00783314	2.07447	1.78797	1.68085	1.44872
<i>C1_01290C_A</i>	0.00769507	2.07477	-1.11282	2.02804	-1.13846
<i>RPN8</i>	0.0100656	2.07518	1.25906	1.95984	1.18908
<i>C2_00490W_A</i>	0.000351811	2.07532	1.80354	1.46753	1.27534
<i>STT3</i>	0.000110441	2.07561	1.15639	1.66098	-1.08063
<i>C1_11970C_A</i>	0.00138553	2.07576	2.34177	1.19697	1.35036
<i>ADE5,7</i>	0.00423381	2.07595	-1.24539	1.7741	-1.45728
<i>ORF298</i>	4.93E-05	2.07618	1.22796	1.53729	-1.09983
<i>RPR1</i>	3.20E-05	2.07742	1.57673	1.16448	-1.13144
<i>C4_00580W_A</i>	0.00660726	2.07843	-1.42647	1.90196	-1.55882
<i>ALG9</i>	6.09E-06	2.07865	1.39056	1.74532	1.16757
<i>TRM12</i>	0.00766435	2.07865	1.44538	1.33708	-1.07558
<i>VPH2</i>	0.00274762	2.07937	2.44	-1.26	-1.07377
<i>HAP5</i>	0.00057854	2.07981	2.0219	1.28638	1.25056
<i>CR_07250C_A</i>	0.0022348	2.08018	1.31354	2.26778	1.432
<i>ABP1</i>	0.0031179	2.08569	2.23552	1.00834	1.08078
<i>C2_00820W_A</i>	0.00312022	2.08661	1.11111	1.77165	-1.06

CR_09990W_A	0.00964553	2.08674	1.72712	2.2342	1.84917
PSD1	0.000133311	2.08902	1.96044	1.08754	1.0206
VPS28	0.00333106	2.09016	1.50811	1.51639	1.09412
BMT7	0.0166795	2.09091	1.86765	1.0303	-1.08661
C3_03510C_A	0.000556594	2.09148	1.04448	1.91483	-1.04574
CR_05710C_A	0.00135657	2.09195	2.0625	1.28736	1.26923
C4_02680C_A	0.00924404	2.09302	1.33333	1.18605	-1.32353
DFG16	1.32E-06	2.09302	1.54793	1.79535	1.32778
PAN3	0.00397896	2.09365	1.37271	2.01003	1.31789
C1_08470W_A	1.06E-06	2.09402	1.68977	1.29487	1.0449
MRS2	0.00448283	2.09459	1.30994	2.31081	1.44516
VPS36	0.00148195	2.09581	1.55294	1.52695	1.13143
C1_05790W_A	3.84E-05	2.09836	2.41667	-1.01667	1.13281
SAC6	8.69E-05	2.09873	2.24291	1.56329	1.67069
DCK2	3.67E-05	2.09915	1.41801	1.76204	1.19028
C1_04930C_A	0.0166604	2.1	1.31707	2.05	1.28571
NIK1	0.00806908	2.10182	-1.03522	2.99273	1.37543
C1_10420C_A	0.000623664	2.10213	1.5293	2.17872	1.58502
ARC40	3.06E-05	2.1022	1.64564	1.49677	1.17169
C5_03930C_A	0.0166261	2.10227	1.26389	1.63636	-1.01648
MED18	0.00798586	2.10256	1.1694	2.34615	1.30488
C7_00600C_A	7.95E-06	2.10265	1.51716	1.35099	-1.02585
C6_00390W_A	0.000353093	2.10309	1.78855	1.62113	1.37868
C1_03440C_A	0.000320881	2.10476	1.07561	1.67937	-1.1652
FPG1	7.44E-07	2.10496	1.53488	1.7551	1.27978
CR_00350W_A	0.00448055	2.10837	-1.18074	1.72167	-1.44595
SEC72	0.00173903	2.10863	1.51186	1.61661	1.15909
FRS2	0.00274898	2.10978	1.06801	1.08583	-1.81928
C4_01950W_A	0.000698609	2.11022	1.26945	1.86559	1.12229
NIT3	0.00379067	2.11086	-1.05263	2.1286	-1.04386
CR_03620C_A	3.33E-05	2.11087	1.64367	1.33913	1.04274
CYB2	0.00432352	2.11092	3.01503	1.53974	2.19921
C3_03930W_A	0.000159293	2.11207	1.70612	1.40805	1.13741
UGA3	0.000102394	2.11232	2.09035	1.4837	1.46827
C2_02500W_A	0.00281928	2.11297	1.74742	1.62343	1.34257
C4_03460C_A	0.000921366	2.11579	2.75	1.34737	1.75124
CYC3	0.000143517	2.11599	2.54964	1.29467	1.56
SHP1	0.0110664	2.11755	1.14844	2.22383	1.20608
DUR32	0.00103301	2.11842	1.77037	1.77632	1.48447
CTA6	0.000584508	2.11905	1.57669	1.94048	1.44382
GLC3	0.0143855	2.11965	-1.27597	2.87511	1.06304
C4_01830C_A	0.000936548	2.12131	-1.14091	2.46885	1.02009
C2_04160W_A	0.0011467	2.12308	2.64796	1.50769	1.88043
C6_02650C_A	0.00225684	2.12353	1.24757	1.21176	-1.40467
C1_10140C_A	0.00155151	2.12598	1.16574	1.88451	1.03333

<i>HSP78</i>	0.000201289	2.12707	3.51965	1.34551	2.2264
<i>CR_02590C_A</i>	0.00129615	2.128	1.44589	1.848	1.25564
<i>C6_03950C_A</i>	0.00292964	2.12987	1.34286	2.27273	1.43293
<i>MIM1</i>	0.00161291	2.13235	1.53285	2.01471	1.44828
<i>SRP101</i>	0.000256969	2.13289	1.26281	2.00997	1.19003
<i>GCV3</i>	1.07E-06	2.13565	1.7169	1.17887	-1.05516
<i>C1_06650W_A</i>	0.0012603	2.13672	1.75931	1.36328	1.12249
<i>C6_00210W_A</i>	0.00014583	2.13689	1.6938	1.18588	-1.06385
<i>C4_06090C_A</i>	0.0164298	2.13861	1.06637	2.23762	1.11574
<i>HGT4</i>	0.0131362	2.13861	-1.03393	1.91089	-1.15714
<i>C3_00790W_A</i>	0.00041617	2.14019	1.05291	1.76636	-1.15075
<i>C6_01450C_A</i>	0.00103482	2.14022	1.01119	1.64945	-1.28319
<i>C3_00380C_A</i>	2.27E-05	2.14103	1.5443	2.02564	1.46108
<i>CR_04600W_A</i>	0.00301282	2.14286	1.84924	1.74086	1.50233
<i>C1_03450C_A</i>	0.00160671	2.14465	1.77174	1.94367	1.60571
<i>C2_07760W_A</i>	0.000209325	2.14506	1.79972	2.2037	1.84892
<i>SEC24</i>	0.00460824	2.14511	1.25611	2.00537	1.17429
<i>C5_03690W_A</i>	0.00113116	2.14583	1.3128	2.19792	1.34466
<i>C1_01620C_A</i>	0.0113076	2.14607	1.88125	1.79775	1.57592
<i>CR_08650C_A</i>	5.59E-08	2.14621	1.69955	1.73803	1.37632
<i>C2_02300W_A</i>	0.00162042	2.14634	2.17241	1.41463	1.43182
<i>SAP10</i>	0.0134845	2.14634	-1.11953	3.12195	1.29924
<i>C5_03740W_A</i>	0.00629246	2.14667	1.29851	2.68	1.62112
<i>XYL2</i>	0.00493404	2.14673	3.0416	- 1.16807	1.21299
<i>GDB1</i>	0.00597293	2.14725	1.07958	2.3427	1.17784
<i>C6_01550C_A</i>	0.00121107	2.14793	1.15172	2.57396	1.38017
<i>C4_04860W_A</i>	0.013157	2.14943	-1.15126	3.14943	1.27273
<i>CR_08290W_A</i>	3.55E-06	2.14981	2.00245	1.58755	1.47873
<i>PGA18</i>	0.00166579	2.15029	1.94199	1.04624	-1.05832
<i>C5_02020C_A</i>	0.000982614	2.15068	1.26429	1.91781	1.12739
<i>VPS24</i>	0.00353918	2.15183	2.14935	1.61257	1.61071
<i>C1_13560W_A</i>	0.0138179	2.15217	1.5	2.34783	1.63636
<i>PRN3</i>	0.00124074	2.15217	1.1954	1.8913	1.05051
<i>C1_11300C_A</i>	1.28E-05	2.15284	1.46309	1.95197	1.32657
<i>C7_00260C_A</i>	0.00172602	2.15332	1.14514	2.14416	1.14028
<i>C2_07790C_A</i>	0.00871652	2.15385	1.10769	2.5	1.28571
<i>C2_10860C_A</i>	0.00323249	2.15486	1.03471	1.58793	-1.3115
<i>RPS30</i>	0.000569493	2.15505	1.44966	- 1.14759	-1.70599
<i>NAG6</i>	1.79E-06	2.15547	1.90886	1.63617	1.44897
<i>C5_00790C_A</i>	0.000734882	2.15725	1.44115	1.4916	-1.00355
<i>C1_00760W_A</i>	7.71E-05	2.15813	1.57201	1.65479	1.20537
<i>IFU5</i>	0.0146658	2.1598	1.36724	1.61944	1.02517
<i>C4_04660C_A</i>	0.000671623	2.16019	1.36816	1.95146	1.23596
<i>C3_01950C_A</i>	0.00104732	2.16058	2.26506	1.21168	1.27027
<i>C3_06290W_A</i>	0.000809811	2.16111	1.3821	1.92407	1.23051

C4_00680W_A	0.00231083	2.16129	-1.0661	2.68817	1.16667
C2_06230W_A	0.00323196	2.16316	1.35519	1.92632	1.20681
NPT1	0.00374421	2.16423	1.15832	2.25912	1.20911
APG7	0.00763663	2.16463	1.07634	2.39634	1.19155
C2_03450W_A	0.00173135	2.16484	1.58273	1.52747	1.11675
C3_07940W_A	0.000847393	2.16497	1.16575	1.53912	-1.20664
HEX1	1.70E-05	2.16766	1.19556	2.02096	1.11464
DOA4	0.00354539	2.1677	1.13896	2.2795	1.19771
C4_06940C_A	0.00140002	2.16883	1.39521	2.16883	1.39521
CAR2	0.000106	2.16997	2.32799	- 1.05491	1.01698
C2_06080C_A	7.31E-05	2.17	1.21495	1.605	-1.11282
PUP1	8.32E-05	2.17069	1.59881	1.16034	-1.17007
GSL1	4.68E-06	2.17259	1.54286	1.77665	1.26168
C3_03680W_A	2.52E-07	2.17274	1.48963	1.98237	1.35911
SET1	0.000388052	2.17406	1.57143	1.95904	1.41601
C3_00470W_A	3.90E-06	2.17466	1.19224	1.94178	1.06457
ACB1	0.0167873	2.17544	-1.44255	2.97368	-1.05532
UGA33	0.0048694	2.18033	1.05185	2.21311	1.06767
CR_03330W_A	0.000192607	2.1831	1.32963	1.90141	1.15806
C2_08900W_A	0.00596333	2.18421	1.29885	1.14474	-1.46903
C6_03310W_A	0.00183375	2.18537	-1.10222	2.41951	1.00446
C2_02820C_A	0.00974923	2.18696	-1.33509	2.2	-1.32718
CR_01770C_A	2.49E-05	2.18799	1.34763	1.70496	1.05012
MDL1	0.00620478	2.18803	1.49767	1.83761	1.25781
CRN1	0.00542296	2.18971	1.25138	2.12941	1.21692
CR_07190W_A	0.000209019	2.19004	1.67664	1.79554	1.37463
C6_02630C_A	0.00387196	2.19094	1.59691	1.88673	1.37518
MVD	0.00764871	2.19108	1.03382	- 1.13768	-2.41121
MID1	3.59E-05	2.19192	1.36	2.0202	1.25346
SAM4	0.0145774	2.19277	-1.82731	1.82731	-2.19277
ARH2	0.00575491	2.19512	1.05528	1.61789	-1.28571
AHR1	0.0118239	2.19565	1.38788	1.79348	1.13366
RAD53	0.00719648	2.19565	-1.03704	2.43478	1.06931
C1_07210C_A	5.87E-06	2.19601	1.36226	1.7608	1.09228
C2_00940W_A	5.40E-05	2.19634	1.6464	1.63613	1.22646
RAD14	0.00118689	2.19718	1.57143	1.87324	1.33974
C5_00800C_A	4.31E-06	2.19829	2.05323	1.25515	1.17232
POB3	0.000157105	2.19834	1.16575	2.02497	1.07382
C4_01280C_A	0.000794276	2.19872	1.29242	1.77564	1.04373
PEX4	0.000104605	2.1988	4.89394	- 1.25758	1.76986
CR_03410W_A	4.94E-06	2.199	2.06912	1.0796	1.01584
C6_00240C_A	3.99E-05	2.2	-1.00226	1.84583	-1.19457
C4_06410W_A	0.00254641	2.2	1.232	2.5	1.4
C4_00610W_A	3.16E-05	2.2	1.46468	1.68125	1.11932

MIT1	0.00380926	2.2029	-1.03883	2.58454	1.12939
C2_08960C_A	0.000354787	2.2043	1.44751	1.94624	1.27805
PEX5	0.00324909	2.20542	1.75881	1.89234	1.50913
C1_03140W_A	0.00136413	2.20635	1.24658	2.31746	1.30935
C6_04340W_A	0.00085545	2.20779	1.2446	1.80519	1.01765
C1_06890C_A	0.0058433	2.20833	1.26216	- 1.07227	-1.87611
C1_11580W_A	0.015783	2.21359	1.73451	1.09709	-1.16327
RDN5	0.0137457	2.21413	1.01637	1.03708	-2.10058
CR_02380C_A	0.0166215	2.21429	1.61538	- 1.07692	-1.47619
C1_07980C_A	0.0162278	2.21429	4.65714	-1.2	1.75269
C3_06520C_A	0.0111957	2.21429	1.18182	1.83333	-1.02198
C4_05350W_A	0.0132377	2.21495	1.36548	1.84112	1.13502
MNN15	0.000195249	2.21569	1.39318	1.72549	1.08496
LYS143	0.000457711	2.21739	1.17117	1.6087	-1.17692
DUR7	1.01E-05	2.21898	1.24906	1.93431	1.08882
YFH1	0.000135233	2.21918	3.75207	- 1.20661	1.40123
C5_04300C_A	0.000278479	2.2203	1.4646	1.7105	1.12831
C7_01230C_A	5.79E-05	2.22143	1.26036	2.15357	1.22186
MTM1	0.00253481	2.22152	1.70732	1.03797	-1.25357
GCF1	0.00147118	2.22311	2.03605	1.71315	1.569
C3_02080W_A	0.00366627	2.22517	1	3.49007	1.56845
C3_06810W_A	0.000117069	2.22642	1.72695	1.77358	1.37571
C2_10760C_A	1.72E-05	2.22693	1.11419	2.33666	1.16909
CR_08670C_A	0.000130283	2.22709	1.91587	1.65737	1.42576
C5_03840W_A	0.00407192	2.22727	1.13333	1.36364	-1.44118
MNL1	3.95E-07	2.22805	1.64965	1.87418	1.38765
C1_03690W_A	6.28E-06	2.22901	1.64503	1.25445	-1.08015
C1_04430C_A	0.0094681	2.23022	2.10985	1.89928	1.79677
PPS1	0.00284874	2.23077	1.13861	1.55385	-1.26087
CR_08610W_A	5.51E-05	2.23121	1.48667	1.7341	1.15544
APN1	3.28E-05	2.23239	1.66292	1.88028	1.40063
C6_02580W_A	0.00116191	2.23267	1.89831	1.75248	1.49002
C2_09810C_A	0.0116073	2.23404	1.05263	2.02128	-1.05
CR_03960C_A	0.00015174	2.23469	1.40704	2.03061	1.27854
PIKA	0.00309782	2.23507	1.00466	2.40299	1.08013
C3_02970C_A	1.16E-05	2.23529	1.61918	1.95187	1.41388
EAP1	0.0129729	2.23529	1.73585	- 1.28302	-1.65217
SEC23	7.34E-05	2.23623	1.24944	1.93478	1.08101
SER2	0.0148948	2.23636	1.32456	2.07273	1.22764
C2_03910C_A	0.000319867	2.23684	2.02193	1.2	1.08471
C1_09130W_A	0.0144711	2.2381	-1.01224	1.68707	-1.34286
ECI1	0.00661194	2.2392	3.26217	1.33056	1.93843
CR_05460W_A	0.000132159	2.24127	-1.02243	1.73651	-1.31963

ILS1	0.00198106	2.24277	1.15028	1.56235	-1.24796
C1_09000W_A	0.0123154	2.24299	1.28141	1.85981	1.0625
C4_00020W_A	6.18E-05	2.24617	1.6919	1.16037	-1.14412
SWI4	0.00273473	2.24631	1.14776	1.867	-1.04828
C3_01570W_A	0.000882656	2.24675	1.84	1.2987	1.06358
CR_07680C_A	0.00911962	2.25	3.4	-1.6	-1.05882
C1_01000C_A	5.34E-05	2.25137	3.54396	-1.00549	1.56553
POL2	0.000641847	2.25191	-1.49434	3.0229	-1.11321
NCB2	0.00515264	2.25263	1.18229	2.02105	1.06075
C2_05800C_A	0.000843836	2.25269	1.46173	2.17742	1.41289
SAS2	0.00266143	2.25424	2.05556	1.52542	1.39098
STE50	5.37E-05	2.25481	1.25392	1.53365	-1.1725
MOB2	2.62E-06	2.25498	1.32839	1.88048	1.10777
C2_00230W_A	1.04E-06	2.25651	1.31079	2.03346	1.18122
IML1	2.52E-05	2.25869	1.69898	2.27027	1.70769
C4_00470C_A	0.000558556	2.26	1.24532	2.405	1.32522
C2_07580W_A	0.0156419	2.26087	-1.08824	3.21739	1.30769
FAA2	0.000122994	2.26087	1.46414	2.06087	1.33462
DCR1	0.00145084	2.26389	-1.01667	1.69444	-1.35833
ECM42	0.00493761	2.26415	1.15873	2.77358	1.41944
C5_02690W_A	0.0126303	2.26571	1.80914	2.00359	1.59984
C5_00090C_A	0.000117833	2.26875	1.48111	1.65417	1.07989
C7_04260W_A	1.06E-06	2.26942	1.07151	2.03641	-1.04004
ZCF30	9.26E-05	2.26994	1.68966	2.13497	1.58919
C4_03080W_A	0.0012324	2.27049	2.6178	1.56557	1.80505
C1_06560W_A	0.0003652	2.27103	1.71271	1.69159	1.27572
C1_00470C_A	8.94E-06	2.27273	1.35417	2.07792	1.2381
CWH41	0.00030357	2.27386	1.39965	2.35685	1.45073
C1_07340W_A	0.00225333	2.27845	1.12903	2.10169	1.04145
PEP8	0.000410283	2.27907	1.27452	2.18439	1.22157
RBR3	0.000253824	2.27975	-1.01961	2.60543	1.12088
ADE6	0.0149351	2.2799	-3.33153	2.94498	-2.57916
CBP1	4.58E-07	2.28133	1.19987	2.07467	1.09117
C2_00830C_A	0.000371762	2.28139	1.31741	1.2684	-1.36528
CR_02570C_A	0.00745731	2.28169	1.40571	2.46479	1.51852
C4_00420C_A	3.41E-05	2.28169	2.20232	1.10785	1.06931
C2_09070C_A	0.00621246	2.28232	1.54802	1.40106	-1.05231
C5_05000C_A	0.000631608	2.28302	1.87742	1.46226	1.20248
C2_07110C_A	0.00178736	2.28351	-1.03785	2.68557	1.13318
SEC10	1.71E-05	2.28416	1.43922	1.75	1.10265
C3_04360W_A	0.00012992	2.28458	1.4738	1.73518	1.11938
DIT1	0.0167658	2.28571	1.82051	2.22857	1.775
FGR39	0.0108064	2.28571	1.54054	1.7619	1.1875
IFA4	5.34E-05	2.28571	1.46809	1.49206	-1.04348
CTA4	0.00015829	2.2872	1.29003	2.11765	1.1944

<i>C3_02720W_A</i>	0.00415777	2.28788	2.60494	1.22727	1.39735
<i>CGT1</i>	0.000141913	2.28804	2.06391	1.44565	1.30404
<i>OPT3</i>	0.000254113	2.28924	2.16127	2.21749	2.09354
<i>VID27</i>	0.00647892	2.29106	1.19173	2.25091	1.17085
<i>CR_04150W_A</i>	0.00953364	2.29114	2.75962	1.31646	1.58564
<i>LIP6</i>	0.00230491	2.29204	-1.10506	2.51327	-1.00778
<i>C1_10890C_A</i>	0.000752045	2.29612	1.44173	1.79126	1.12474
<i>RPT1</i>	0.0163562	2.29653	1.42728	2.41849	1.50307
<i>C4_05900C_A</i>	0.00692916	2.29861	1.58307	1.10764	-1.31089
<i>CR_05030W_A</i>	0.000450332	2.2992	1.88408	2.0704	1.69659
<i>C1_01460W_A</i>	7.65E-07	2.30221	1.39423	1.7887	1.08324
<i>CR_08710W_A</i>	1.59E-06	2.30393	2.00376	1.52828	1.32917
<i>TSM1</i>	8.49E-06	2.30426	1.51718	1.75286	1.15412
<i>C7_01610W_A</i>	5.18E-05	2.3046	3.57971	- 1.26087	1.23192
<i>C5_02050W_A</i>	0.00188777	2.3076	1.48517	2.09006	1.34516
<i>C2_06110W_A</i>	0.000148861	2.30769	1.09075	2.54299	1.20196
<i>NAG1</i>	0.000655924	2.31088	1.63924	1.63731	1.16143
<i>CR_09340W_A</i>	0.00052383	2.31217	2.375	1.3545	1.3913
<i>VPS23</i>	0.00950057	2.3125	1.70588	1.0625	-1.27586
<i>ZCF32</i>	3.69E-05	2.3125	1.67483	1.98611	1.43844
<i>C1_14560C_A</i>	0.000110236	2.31381	1.14724	2.04603	1.01447
<i>ERV46</i>	0.000145575	2.315	1.34085	1.775	1.02808
<i>C2_06520C_A</i>	0.000947463	2.31646	1.80899	1.12658	-1.13665
<i>C4_01860C_A</i>	0.00288352	2.31818	6.5	- 2.44444	1.14706
<i>CHO1</i>	0.00217964	2.31839	-1.2929	1.95964	-1.52959
<i>C4_04250W_A</i>	0.000139356	2.31844	1.88182	1.22905	-1.00242
<i>RGD3</i>	0.000407119	2.32114	1.90788	1.8313	1.50525
<i>CR_00130C_A</i>	0.00341223	2.32226	1.08296	2.20266	1.02718
<i>ECM3</i>	0.000576507	2.32237	1.3609	1.75	1.0255
<i>SMI1</i>	0.000799046	2.32237	2.42593	1.27883	1.33586
<i>PDX3</i>	1.68E-07	2.32248	1.6856	1.55581	1.12917
<i>CR_03220C_A</i>	0.000280604	2.32432	1.27551	2.64865	1.45349
<i>C6_00710W_A</i>	0.000347987	2.32432	1.86022	1.67568	1.34109
<i>C1_11020W_A</i>	0.00101298	2.32843	2.30976	1.45588	1.44421
<i>C7_02450W_A</i>	8.54E-05	2.32857	1.41667	2.14286	1.30368
<i>MSH2</i>	6.70E-05	2.3297	1.19243	2.59128	1.32632
<i>RDN58</i>	0.0104967	2.32988	-1.26744	1.32514	-2.22844
<i>CIS2</i>	9.35E-05	2.33019	1.77551	1.38679	1.05668
<i>C1_01190C_A</i>	0.000987882	2.33077	1.32721	2.09231	1.19142
<i>C4_06990W_A</i>	0.00198009	2.33333	1.15625	2.17687	1.07872
<i>CR_00880W_A</i>	0.000292449	2.33333	1.59794	2.30952	1.58163
<i>C5_05240C_A</i>	0.015422	2.33333	3.33333	- 1.33333	1.07143
<i>C5_02350C_A</i>	0.0054036	2.33333	2.6	1.11111	1.2381
<i>C3_06530W_A</i>	0.00238849	2.33333	-1.06173	2.20513	-1.12346

PGA33	0.00965721	2.33333	-1.19683	1.6982	-1.64444
C2_08850C_A	0.000210867	2.33533	1.6375	1.43713	1.00769
VPS33	0.000612941	2.33679	1.5601	2.02591	1.35255
CR_03520C_A	5.96E-06	2.33789	1.47805	1.60156	1.01253
IRS4	2.50E-06	2.33824	1.65266	1.75	1.2369
C5_02060W_A	0.000334011	2.33929	2	1.82143	1.55725
C1_09280W_A	0.000610403	2.33962	1.84122	1.86164	1.46505
CR_05310W_A	0.00908731	2.34146	1.04	1.82927	-1.23077
MAC1	0.00136841	2.34146	2.11354	1.86179	1.68056
C3_00890C_A	0.000339674	2.34286	1.47489	1.56429	-1.01548
CR_08980C_A	0.000739756	2.34426	1.93805	1.85246	1.53147
C4_06240W_A	0.00294892	2.34722	2.26563	1.77778	1.71598
ZCF2	2.85E-05	2.34901	1.58978	2.31563	1.56718
SOL1	0.00105533	2.35036	1.44541	1.67153	1.02795
CR_07910C_A	2.18E-06	2.35067	1.39484	2.39114	1.41885
SEC3	9.16E-07	2.35082	1.46996	1.52787	-1.04672
GLK1	0.00219814	2.35083	1.72473	1.74158	1.27775
C3_02090C_A	0.0137133	2.35268	-1.16795	2.70089	-1.01737
C6_00250W_A	3.89E-06	2.35335	1.25351	1.59218	-1.17915
C1_02440C_A	0.00128725	2.35484	1.38235	1.64516	-1.03546
HIS4	0.00711567	2.3552	-1.12224	1.4616	-1.80835
CR_00990W_A	0.00288494	2.35714	-1.22857	1.53571	-1.88571
LPT1	3.45E-06	2.35768	1.52906	1.86891	1.21207
C6_04420W_A	4.05E-08	2.35786	1.55421	2.92441	1.92766
C6_00260W_A	0.00107592	2.36318	1.08421	1.89055	-1.15291
C5_00580W_A	0.0130955	2.36508	1.34769	2.4881	1.41779
PRA1	0.000107374	2.36538	1.55952	1.61538	1.06504
SWD1	6.71E-05	2.36667	1.32597	2.01111	1.12676
SEC12	0.000708749	2.36758	1.2352	1.90738	-1.00491
NAB3	2.75E-06	2.3688	1.60385	1.51603	1.02646
CR_03190C_A	0.000657161	2.36916	2.29308	- 1.08877	-1.1249
C4_05640C_A	9.02E-05	2.36923	1.33735	1.91538	1.08117
CR_04120C_A	0.00181667	2.37143	1.22311	1.43429	-1.35179
CWT1	2.85E-07	2.37288	1.82068	1.60678	1.23286
ABC1	5.12E-06	2.37374	1.16096	2.41058	1.17897
ZCF9	4.55E-06	2.3758	1.78776	1.56051	1.17426
PXA1	0.0165272	2.37673	1.56925	1.93688	1.27884
FAA4	0.0030186	2.37901	1.11715	2.04711	-1.04026
MSK1	3.43E-06	2.38007	1.99761	1.54613	1.29767
NPR2	4.25E-08	2.38267	1.58659	1.93863	1.29091
GLK4	0.000610242	2.38273	1.62279	1.871	1.27427
TBF1	0.00299741	2.38514	-1.72146	2.5473	-1.61187
VPS34	0.000273052	2.38519	1.57377	2.25926	1.49068
TPS3	0.00286741	2.38607	1.00468	3.16655	1.33331
NRG1	3.95E-06	2.38619	1.85159	1.53375	1.19013

CR_06290C_A	5.38E-10	2.38764	1.80152	1.85393	1.39882
C5_00840W_A	0.00315154	2.38889	1.38158	2.11111	1.22093
C3_03100C_A	5.76E-06	2.38919	1.47368	1.84865	1.14027
PTC6	9.45E-08	2.38971	1.31648	1.96324	1.08154
RAD9	0.000357529	2.38974	1.74615	2	1.46137
C1_03490W_A	0.00376437	2.39063	-1.09653	1.47917	-1.7722
C4_02770C_A	0.00153835	2.39098	1.52459	2.29323	1.46226
C2_09580W_A	0.000635593	2.39516	1.95939	1.58871	1.29966
SPT20	1.90E-05	2.39552	1.45918	1.46269	-1.12238
C3_07490W_A	1.69E-06	2.39871	1.51437	1.70581	1.07692
C2_02290C_A	0.00335163	2.4	1.87324	1.57778	1.23148
C2_03340W_A	1.27E-05	2.4	1.36743	2.12889	1.21296
SAP1	0.000996449	2.4	-1.425	2.28	-1.5
C7_03280C_A	0.00398331	2.4002	2.06591	1.87538	1.61418
MRP8	0.000714966	2.40157	-1.05119	2.4252	-1.04096
C7_02780W_A	1.12E-06	2.40388	1.1768	1.75728	-1.16244
C7_01180W_A	0.000143244	2.40496	1.725	1.65289	1.18557
PRP13	4.44E-06	2.40569	1.70387	1.60485	1.13666
LEU5	4.33E-05	2.40717	1.44171	1.98371	1.18809
C1_00880W_A	0.00635969	2.40741	2.48276	1.07407	1.10769
TPS2	0.00109236	2.40861	1.69435	2.30373	1.62057
C2_02570W_A	0.0046735	2.40909	-1.18462	1.75	-1.63077
C1_04910C_A	7.15E-05	2.40909	1.7432	1.67172	1.20964
C3_00500C_A	0.000193313	2.41085	1.03352	2.77519	1.18971
ETR1	0.00131438	2.41085	1.49844	2.03453	1.26454
NOG2	0.00158889	2.41173	1.73347	- 1.09271	-1.52025
AAT22	5.69E-05	2.41327	3.24771	- 1.79817	-1.33616
IFE2	0.00144577	2.41357	5.04535	1.14894	2.40175
C7_04290W_A	0.00121133	2.41538	1.26667	2.42308	1.2707
LIG1	0.000270104	2.4185	1.0779	2.43172	1.08379
C3_02910W_A	0.00650778	2.42	-1.225	1.96	-1.5125
HGT3	0.00194154	2.42045	1.57534	1.65909	1.07981
SPT10	0.000144645	2.42056	1.45714	1.96262	1.18147
CR_05010W_A	0.000118822	2.42105	1.65537	2.32895	1.59239
C1_07650W_A	0.000404704	2.42149	1.80826	1.40083	1.04608
C1_08760W_A	0.000313931	2.42188	1.68224	1.67188	1.16129
CR_08430W_A	5.70E-07	2.42826	1.68871	1.56634	1.08929
SPC3	0.00291418	2.42857	1.18142	1.69925	-1.20974
C1_00570C_A	3.91E-05	2.4326	1.65369	2.25392	1.53222
EPL1	3.22E-08	2.43413	2.20989	1.1507	1.04469
UGA32	0.000879424	2.43529	1.3195	2.83529	1.53623
C1_06840C_A	0.00026942	2.4359	2.48485	1.69231	1.72632
C2_09680W_A	0.000569895	2.4375	1.84615	1.35417	1.02564
C2_10060C_A	0.0057314	2.43902	1.75	1.85366	1.33
HOL4	4.17E-06	2.44	-1.19668	2.16	-1.3518

C7_00270W_A	0.000243497	2.44019	-1.12808	2.19139	-1.25616
IMP2	3.91E-05	2.44286	2.36905	1.2	1.16374
C3_04750W_A	1.06E-05	2.44444	2.1308	1.54902	1.35027
C1_04840C_A	0.00438261	2.44444	1.51282	1.44444	-1.11864
C2_07440C_A	0.0092294	2.44482	1.09986	2.34448	1.05472
C6_00540W_A	0.00345953	2.4466	1.93269	2.01942	1.59524
TUS1	0.000160496	2.44752	1.49489	2.13848	1.30613
BUD6	5.72E-06	2.44838	1.77467	1.79351	1.3
C1_11430W_A	0.0046112	2.45	1.63415	2.05	1.36735
C4_04280C_A	0.00120274	2.45098	2.64835	1.78431	1.928
CR_09670C_A	0.000352338	2.45639	2.15955	1.6146	1.41949
NPL3	0.00177062	2.45647	1.12111	2.11765	-1.03469
ZCF18	4.98E-05	2.45665	1.67119	1.7052	1.16
C2_01920C_A	0.000753853	2.45669	1.48853	1.71654	1.04006
CR_05750W_A	6.69E-06	2.45909	1.69056	1.83909	1.26433
BRG1	0.00268359	2.46086	2.09434	- 1.00177	-1.17708
C2_05560W_A	0.00010799	2.46154	2.28634	1.74615	1.62188
C4_03720C_A	0.00214897	2.46226	1.28571	2.50943	1.31034
NPL6	0.000911645	2.46324	1.77528	1.96324	1.41493
OPT6	6.19E-05	2.46429	1.68391	2.07143	1.41546
VAM3	0.00400616	2.46429	1.86792	1.89286	1.43478
C3_01890C_A	1.22E-05	2.46481	3.12929	- 1.05779	1.20023
C1_10820C_A	0.0125324	2.46524	1.34146	1.53476	-1.1974
MED3	7.21E-05	2.46575	1.6746	1.72603	1.17222
C4_00030C_A	7.51E-05	2.46617	-1.31276	2.3985	-1.34979
CR_01670W_A	7.79E-05	2.46667	1.9899	1.65	1.33108
C7_03460W_A	2.84E-05	2.46939	1.07692	1.59184	-1.44048
C7_01750W_A	0.00830797	2.47059	2.03614	1.62745	1.34127
PDX1	0.00615145	2.47299	-1.13603	3.10277	1.10442
HPA2	0.00217677	2.475	1.06	2.5	1.07071
TCC1	0.00399289	2.47522	1.14374	1.41983	-1.52424
C1_09480W_A	0.000244523	2.47692	1.33796	1.66154	-1.11419
CR_00110W_A	1.50E-06	2.47717	1.57095	2.05936	1.30599
C5_05210W_A	0.00772352	2.47727	1.25153	2.77841	1.40367
DOG1	4.19E-05	2.47761	2.51905	1.56716	1.59337
RAD57	0.000993109	2.47945	1.45	2.19178	1.28177
CR_06790C_A	0.000408692	2.48148	3.5	1.07407	1.51493
MED16	0.000231765	2.48148	1.49742	1.7963	1.08396
C3_04790W_A	1.19E-05	2.48207	2.09877	1.61355	1.36437
MED20	0.00019054	2.48214	1.04425	2.01786	-1.17797
CR_05770W_A	9.46E-05	2.48485	1.5	2.90909	1.7561
GPI13	0.00044375	2.48649	1.48507	1.81081	1.08152
C3_07920W_A	1.32E-05	2.48701	1.65094	1.37662	-1.09429
C5_00180W_A	1.33E-05	2.48854	1.21715	2.57307	1.25849
SFT1	0.00246664	2.48889	1.29508	1.35556	-1.41772

ATC1	0.00424339	2.49037	1.27514	1.74374	-1.12002
HGT5	0.00125184	2.49138	1.20874	1.77586	-1.16064
C2_10720C_A	2.34E-06	2.49275	1.14327	1.68599	-1.29323
IFK2	3.48E-06	2.49432	2.16045	1.52273	1.31891
TFC4	0.000937118	2.49784	2.55145	1.64069	1.67591
C4_00840W_A	1.28E-05	2.49846	1.43218	2.31385	1.32635
PGA63	0.00144178	2.4987	1.10828	1.42358	-1.58374
C3_02340W_A	0.000123086	2.5	1.48936	1.38235	-1.21429
C1_02740C_A	4.08E-06	2.5	1.78788	1.13793	-1.22881
C2_04450W_A	0.0110996	2.5	1.17143	1.94444	-1.09756
C1_07100C_A	0.0106212	2.5	1.41667	1.875	1.0625
C1_14310W_A	0.000367141	2.5	1.09158	2.03731	-1.12416
RAP1	0.000203108	2.50376	1.96482	1.49624	1.17417
APE3	0.00843727	2.50774	-1.23565	3.13313	1.01111
C7_04010W_A	5.70E-06	2.50912	2.24943	1.60949	1.44291
C3_06600C_A	0.00454364	2.50943	1.61538	2.20755	1.42105
C7_03200C_A	0.0144529	2.51111	-1.37662	2.35556	-1.46753
PHR2	0.00332363	2.51119	-1.40641	2.26075	-1.56221
SUA72	4.32E-06	2.5125	1.54422	1.8375	1.12935
DES1	0.00126056	2.51646	-1.20267	2.22222	-1.36192
C3_00420W_A	0.00262749	2.51724	-1.3494	2.41379	-1.40723
BMT6	5.68E-06	2.5175	-1.12608	2.925	1.03178
C3_03670W_A	0.00850449	2.51754	-1.35115	3.10526	-1.09542
C1_00370W_A	0.00457055	2.51852	1.41667	2.66667	1.5
CR_04450C_A	2.04E-06	2.51869	1.48972	1.81776	1.07514
BBC1	0.000776386	2.52	1.95197	1.66545	1.29004
SIW14	0.00348987	2.52083	1.82143	1.75	1.26446
CDC23	0.000158346	2.52133	1.17864	2.30806	1.07895
ARO7	0.00148001	2.52174	1.87742	2.24638	1.67241
SRO77	4.61E-06	2.52222	1.52602	2.18889	1.32434
C6_01750C_A	0.00924509	2.52632	-1.17284	2.5	-1.18519
FMO2	0.00172466	2.52778	2.65909	1.22222	1.28571
C6_03810W_A	0.0142425	2.52857	1.0186	3.07143	1.23729
C1_11740W_A	0.000102154	2.52941	2.52941	1	1
CR_05450C_A	0.00544679	2.53191	1.40367	2.31915	1.28571
HOS1	0.000197968	2.53226	1.26744	2.77419	1.38854
ELA1	0.0121731	2.53333	-1.28788	2.83333	-1.15152
C1_10690W_A	2.45E-05	2.53846	1.89831	1.2967	-1.03125
MMS21	0.00220298	2.54054	1.60714	1.51351	-1.04444
DCW1	4.65E-06	2.54231	1.45396	1.79615	1.02723
BNA4	4.83E-08	2.54244	2.81242	1.08886	1.20449
C6_03960W_A	3.46E-06	2.54454	1.66196	1.72989	1.12987
PHR1	0.000126601	2.54472	-1.05882	1.90244	-1.41629
ERG26	0.00148711	2.54476	1.27454	1.66752	-1.19735
PPG1	0.00343656	2.54688	1.89011	1.42188	1.05521
FMO1	0.00537121	2.54762	-1.13913	3.11905	1.07477

<i>C1_06480C_A</i>	0.000307062	2.54839	-1.01449	2.25806	-1.14493
<i>ASH1</i>	0.00421738	2.55	1.20833	1.8	-1.17241
<i>C5_00750C_A</i>	0.00652282	2.55399	1.25724	2.67371	1.31618
<i>CR_10510W_A</i>	7.60E-06	2.55431	2.23077	1.3633	1.19062
<i>AFG1</i>	5.74E-06	2.55556	2.21143	1.49573	1.29431
<i>CDC15</i>	7.06E-06	2.55597	1.71262	1.92164	1.28759
<i>RIB5</i>	2.58E-07	2.55744	3.29735	1.23368	1.59061
<i>SEC13</i>	0.00111733	2.55837	1.162	2.22179	1.00913
<i>C7_00380W_A</i>	0.00149152	2.55963	-1.0493	1.36697	-1.96479
<i>C4_04760C_A</i>	0.00181569	2.56098	2.01449	1.68293	1.32381
<i>CR_07160C_A</i>	2.48E-05	2.56272	-1.32771	3.94982	1.16084
<i>CR_08470W_A</i>	0.000346004	2.56296	1.26593	2.67407	1.32081
<i>C1_11180C_A</i>	0.0114772	2.56897	-1.61972	1.98276	-2.09859
<i>MMD1</i>	2.52E-07	2.56899	1.53924	1.54109	-1.08301
<i>DAM1</i>	8.63E-05	2.56923	1.09735	1.73846	-1.34677
<i>C1_01360C_A</i>	0.000158899	2.56997	1.03704	2.31892	-1.06868
<i>ENO1</i>	0.00616667	2.57027	1.056	2.34784	-1.03668
<i>TLO13</i>	0.00472855	2.57143	-1.06522	1.75	-1.56522
<i>C5_05340W_A</i>	0.00924322	2.57209	1.00874	1.33023	-1.91681
<i>C4_06020C_A</i>	0.00116003	2.57216	1.62611	2.3299	1.47295
<i>C4_02160C_A</i>	0.000240925	2.57377	1.14379	2.5082	1.11465
<i>C4_02690W_A</i>	2.43E-06	2.57417	1.50498	1.92845	1.12746
<i>C7_03500W_A</i>	8.62E-07	2.57432	1.66445	2.03378	1.31496
<i>SER1</i>	0.000113241	2.57452	1.40999	1.77588	-1.02817
<i>FAD1</i>	0.00681646	2.57576	1.64122	1.98485	1.26471
<i>C1_14500C_A</i>	2.93E-06	2.57587	3.15981	- 1.32446	-1.07969
<i>FRP6</i>	0.00113462	2.57708	-1.24444	3.09881	-1.03492
<i>ORC1</i>	0.000340949	2.57995	1.7607	2.0271	1.3834
<i>SYN8</i>	0.00465841	2.58696	1.47706	2.36957	1.35294
<i>PUT4</i>	0.00247131	2.59091	1.25532	2.13636	1.03509
<i>HGT19</i>	0.00161835	2.59099	2.33383	1.07826	-1.02961
<i>C1_05010C_A</i>	2.98E-05	2.59223	-1.30374	2.70874	-1.24766
<i>ERG7</i>	0.000511129	2.5933	1.70906	1.50478	-1.00837
<i>HPC2</i>	0.00384309	2.59341	2.01796	1.83516	1.42797
<i>C2_00540W_A</i>	9.40E-09	2.59487	2.06033	1.13333	-1.11127
<i>FGR24</i>	0.00382933	2.59756	1.36872	2.18293	1.15023
<i>FAA2-3</i>	0.00914725	2.59854	1.53469	1.78832	1.05618
<i>C1_00200C_A</i>	0.0103373	2.6	1.17857	1.86667	-1.18182
<i>CET1</i>	3.07E-07	2.6	1.77372	1.73053	1.18057
<i>PKH3</i>	3.04E-05	2.60106	1.58357	1.87766	1.14315
<i>C3_04700W_A</i>	0.00111335	2.60577	1.97024	1.61538	1.2214
<i>C1_05920W_A</i>	0.0129216	2.60606	2.67347	1.48485	1.52326
<i>C1_00210C_A</i>	0.00913938	2.60612	1.0334	2.02323	-1.24646
<i>RAD1</i>	9.02E-06	2.60827	1.7131	2.0438	1.34235
<i>C5_01170W_A</i>	0.00153157	2.60976	1.91954	2.12195	1.56075

SLA1	2.51E-06	2.611	2.24287	1.30134	1.11786
C3_04690C_A	0.000593859	2.61458	2.97872	1.46875	1.67331
C1_07060C_A	0.000893095	2.61538	1.34211	1.46154	-1.33333
C1_02750C_A	0.00114014	2.62359	1.24187	1.937	-1.09066
C4_01910W_A	0.000402096	2.62385	2.5618	1.63303	1.59441
C5_04410C_A	6.93E-05	2.625	2.14919	1.34783	1.10352
TPT1	0.0165759	2.625	-1.34524	2.825	-1.25
C4_02570C_A	3.26E-05	2.62944	1.3379	2.22335	1.13127
CR_05360C_A	0.0130738	2.63043	2.5814	1.86957	1.83471
C6_00190W_A	0.000318816	2.63131	1.46389	1.81818	1.01152
C6_02980C_A	0.00485049	2.63134	1.11751	1.96083	-1.20084
OLE1	0.00016791	2.63351	-1.04186	1.72024	-1.59497
RPD31	0.00076424	2.6338	1.43232	2.32394	1.26381
CR_08620C_A	1.26E-05	2.63985	1.96699	1.97318	1.47025
C4_03230C_A	0.00688396	2.64058	1.31526	1.44348	-1.39084
SUC1	0.000129411	2.64286	1.44811	2.16327	1.18533
C4_03350C_A	0.00261541	2.64835	2.37879	- 1.37879	-1.53503
FGR10	0.000659743	2.64865	2.18966	1.56757	1.29592
CR_04460C_A	0.000401373	2.64912	2.14737	1.66667	1.35099
SST2	0.000105296	2.64912	1.62121	1.73684	1.06291
C2_09670C_A	3.30E-06	2.64984	1.00787	2.40379	-1.09375
C4_06280C_A	0.00021978	2.65	1.57746	1.775	1.0566
C2_09250W_A	0.000413179	2.65	2.53906	1.6	1.53302
C1_03040W_A	0.00553773	2.65217	-1.13235	2.23188	-1.34559
RPP1B	0.000916636	2.65408	2.07765	- 2.20644	-2.8186
COG4	0.00257869	2.65546	1.61806	2.42017	1.47468
HMI1	8.48E-07	2.65753	1.55556	2.03425	1.19072
SLD1	2.10E-06	2.65868	-1.02326	2.63473	-1.03256
SEH1	1.54E-05	2.66027	1.73522	2.13151	1.39032
VPS53	5.70E-06	2.66272	1.34591	2.35207	1.18889
CR_08130W_A	0.000153397	2.66397	3.68942	1.18623	1.64286
C2_05060C_A	0.016334	2.66667	1.39474	1.80952	-1.0566
GYP5	0.00157454	2.66667	1.3696	2.17014	1.11458
HFL1	0.00102519	2.66667	1.07865	2.11905	-1.16667
ZCF11	5.21E-06	2.66667	1.70039	2.19658	1.40064
PEX13	0.00920366	2.66841	1.10421	2.35509	-1.0261
C7_04280C_A	2.09E-06	2.672	1.90855	1.356	-1.03246
C5_02640W_A	0.00851407	2.67568	1.2716	2.18919	1.0404
SWI6	0.00581882	2.67647	1.07104	2.69118	1.07692
C1_11530C_A	0.00204091	2.67742	-1.25926	2.19355	-1.53704
CR_00660W_A	0.0015234	2.67857	2.47368	1.35714	1.25333
CDL1	0.000190753	2.67925	1.6391	1.25472	-1.30275
NUP159	1.87E-05	2.68079	1.21644	1.94139	-1.13517
C3_06630W_A	0.00198522	2.68421	1.92187	1.68421	1.20588
C7_03650W_A	9.89E-06	2.6875	1.78767	1.825	1.21395

IFF4	9.57E-05	2.69091	2.05052	2.08727	1.59054
CRH11	5.17E-05	2.69206	4.67114	- 1.05705	1.64151
C1_01750W_A	0.00998578	2.69231	-1.22115	1.95385	-1.68269
HMX1	6.95E-05	2.69288	-1.59524	2.63483	-1.63039
C5_02730C_A	1.23E-05	2.69492	2.00344	1.64407	1.22222
C4_01760W_A	0.000112808	2.69565	-1.35526	2.23913	-1.63158
COX15	2.92E-06	2.69724	5.70309	- 1.23951	1.70584
DIP5	7.12E-05	2.69914	1.27129	2.44771	1.15287
PGA38	0.00618817	2.70033	2.31381	2.16938	1.85887
CR_03260W_A	0.00111978	2.70513	1.99467	2.40385	1.77251
APL4	0.000113064	2.70707	1.74561	1.72727	1.11381
ARD	3.00E-08	2.71241	1.93478	1.947	1.38881
CAN2	0.00216811	2.71333	2.07869	2.31556	1.77396
CNH1	0.00783646	2.7138	1.16121	1.44108	-1.62173
CR_09090C_A	0.00222905	2.71642	2.15789	1.70149	1.35165
SEC20	0.00156961	2.71698	1.0625	2.41509	-1.05882
C3_07770C_A	0.00558315	2.71717	1.35458	2.53535	1.26394
C1_12120W_A	0.000443434	2.71875	1.92063	1.96875	1.3908
YHM2	0.000419709	2.7193	2.57637	1.21754	1.15355
C3_06440W_A	1.38E-07	2.72149	1.48875	1.68966	-1.0819
CR_08560C_A	0.000830481	2.72203	1.38013	1.83042	-1.07751
C2_07510W_A	3.80E-07	2.72289	1.7622	1.9759	1.27876
KSR1	7.58E-06	2.7234	1.62562	2.15957	1.28906
CRL1	0.000149773	2.72626	1.04381	2.1676	-1.20494
MCA1	3.24E-05	2.72642	1.44444	1.63443	-1.15485
CR_07310W_A	0.00543824	2.72662	1.04483	2.08633	-1.25083
CR_00700W_A	0.000845805	2.73077	2.47826	1.76923	1.60563
C1_02970W_A	0.00875731	2.73179	-1.00719	3.24834	1.18061
CR_08590W_A	0.000316208	2.73391	1.31858	1.93991	-1.06879
CMK1	0.0153238	2.73856	-1.38973	2.88998	-1.31692
RPN5	0.000401605	2.73868	1.99887	1.54704	1.12913
C7_04170W_A	0.00699847	2.73913	1.21053	2.47826	1.09524
C4_05970W_A	1.71E-06	2.74194	1.21053	2.58781	1.14248
HGT16	0.000770239	2.74545	2.65873	1.14545	1.10927
SAC7	0.00011992	2.7487	1.3646	1.46373	-1.37613
C2_08660C_A	0.000740614	2.75	1.78448	2.07143	1.34416
C2_05590C_A	0.000483643	2.75	1.91964	1.86667	1.30303
YMC1	0.00936314	2.75	-7.89474	3.125	-6.94737
RFC1	1.61E-05	2.75197	1.39657	2.3727	1.2041
KIP4	0.0011102	2.75362	-1.20863	2.43478	-1.36691
C7_01650W_A	0.00058264	2.75429	-1.23497	2.58286	-1.31694
C6_03580W_A	0.000128157	2.75439	1.97778	1.97368	1.4172
HET1	0.00461778	2.75462	-1.18672	2.49868	-1.30827
HGT14	0.000432132	2.75486	1.59158	1.57198	-1.10109
C7_00120W_A	9.69E-06	2.75625	1.85915	1.775	1.19728

CR_10630W_A	0.010155	2.76	1.71831	2.84	1.76812
C2_00650W_A	2.53E-05	2.76106	1.23893	2.86431	1.28526
C5_02200W_A	0.000150243	2.7619	1.42857	1.66667	-1.16
ADE1	4.41E-07	2.76322	1.16272	2.55416	1.07475
RSR1	0.01363	2.76596	-1.10945	2.37234	-1.29353
C7_01190W_A	0.00556836	2.77358	1.36842	1.79245	-1.13077
C1_10510W_A	0.00176504	2.77551	-1.4403	3.93878	-1.01493
KIN3	0.00357815	2.7757	1.344	2.33645	1.13131
HIR1	1.43E-06	2.7769	1.41816	2.77428	1.41682
ADE2	0.000607724	2.77778	-1.00124	2.35965	-1.17866
YPT7	0.000212845	2.77778	1.96629	1.97778	1.4
SET6	0.00157018	2.78125	-1.3625	4.54167	1.1985
SDH1	3.07E-08	2.7844	1.86337	1.94725	1.30313
C1_02030C_A	0.000163758	2.78571	1.04167	2.57143	-1.04
C7_00250C_A	0.000377949	2.78774	1.37709	1.97642	-1.02426
C3_00530C_A	0.000560761	2.78873	1.67105	2.14085	1.28283
PRD1	0.00172008	2.7931	1.71329	1.98046	1.21481
FGR34	0.00060765	2.79545	1.32212	2.36364	1.11789
C6_04510C_A	3.69E-07	2.79821	2.88385	1.58296	1.63141
C4_05810W_A	0.0019876	2.80044	1.6335	2.30479	1.34439
SKO1	0.000100707	2.80451	1.79931	2.17293	1.3941
C5_04520W_A	1.61E-06	2.80583	2.25874	1.38835	1.11765
AAF1	0.000870027	2.80687	1.26503	1.92704	-1.15141
MHP1	6.32E-05	2.80955	1.90334	1.92325	1.30291
C3_04260W_A	4.68E-08	2.81407	1.86327	1.87437	1.24107
TIM13	0.000476482	2.81481	4.05263	- 1.42105	1.01316
C4_05850C_A	1.16E-07	2.81818	1.27211	2.42975	1.09677
MCM6	0.000661098	2.8209	-1.31677	3.16418	-1.17391
C2_07250C_A	0.000136069	2.82353	2.97674	1.26471	1.33333
SFT2	1.36E-05	2.82456	1.5	2	1.06211
CR_03540W_A	0.000652833	2.825	1.64773	2.2	1.28319
C1_10500W_A	0.00197591	2.82569	1.24084	1.75229	-1.29958
ACF2	0.0040095	2.82813	-1.35052	2.04688	-1.86598
MLH3	0.00661818	2.82813	1.67516	1.22656	-1.37643
C1_00530C_A	0.000123362	2.832	1.58505	2.14	1.19774
C5_04540C_A	0.00502921	2.83333	1.95652	2.3	1.58824
CR_00380W_A	0.0113165	2.83333	4.09091	- 1.09091	1.32353
DFG10	4.53E-05	2.83333	1.42342	2.05556	1.03268
C4_03370C_A	4.96E-06	2.83621	1.89113	2.13793	1.42553
C7_03830C_A	0.000938785	2.83871	1.12264	3.41935	1.35227
TAZ1	0.000648778	2.84416	-1.5084	4.66234	1.08676
RBE1	0.00769491	2.84615	1.10256	4	1.54955
CTA3	3.02E-06	2.84974	1.74247	2.14875	1.31385
C2_07410W_A	0.000926218	2.85268	3.41567	1.6808	2.01252
C4_02040W_A	1.64E-05	2.85333	1.83537	2.18667	1.40654

<i>C1_02680C_A</i>	7.36E-07	2.85577	1.93671	1.51923	1.0303
<i>VID21</i>	0.00129772	2.85714	1.19444	1.71429	-1.39535
<i>CR_07870W_A</i>	0.00149737	2.8642	2.07179	2.40741	1.74138
<i>SHM2</i>	0.000754635	2.86438	-1.336	3.54633	-1.07909
<i>C2_07270W_A</i>	0.000578079	2.87	3.12409	1.37	1.49129
<i>PSF1</i>	0.00870588	2.88	1.8125	1.28	-1.24138
<i>C2_08380C_A</i>	0.0111519	2.8806	-1.16981	3.70149	1.09845
<i>EHT1</i>	6.00E-06	2.88291	2.56515	2.08861	1.8584
<i>C4_04920W_A</i>	5.60E-05	2.88525	1.06627	2.72131	1.00568
<i>VPS4</i>	0.0016339	2.88889	1.12346	3	1.16667
<i>C5_01070C_A</i>	0.0153347	2.8913	1.38017	1.31522	-1.59281
<i>CR_05440W_A</i>	2.07E-08	2.89189	1.48903	2.15541	1.10981
<i>DAL9</i>	0.000308332	2.89333	1.24138	3.09333	1.32719
<i>C2_07220W_A</i>	0.00428882	2.89431	-1.0574	2.84553	-1.07553
<i>CR_10430C_A</i>	0.00048532	2.89474	1.88372	2.26316	1.47273
<i>C2_00060C_A</i>	0.00225616	2.89815	1.32895	2.11111	-1.033
<i>C6_00660C_A</i>	0.000471312	2.90476	1.57732	1.53968	-1.19608
<i>PRN1</i>	0.00123518	2.90541	1.92746	2.60811	1.73023
<i>C6_02190C_A</i>	0.0135334	2.90741	-1.14815	3.44444	1.03185
<i>TEC1</i>	0.000440549	2.91365	2.36172	1.58635	1.28585
<i>C3_02620C_A</i>	0.00308476	2.91429	1.46269	1.91429	-1.04082
<i>C2_07370W_A</i>	0.000257073	2.91617	3.6802	1.17964	1.48871
<i>HUT1</i>	0.0161213	2.91667	1.03846	2.16667	-1.2963
<i>PLB5</i>	0.00848266	2.9171	-1.44264	3.68135	-1.14315
<i>C4_04010W_A</i>	2.53E-06	2.91803	1.66327	1.60656	-1.09202
<i>ERG24</i>	0.0121624	2.91837	-1.29719	2.19728	-1.72289
<i>C4_03580W_A</i>	0.00143679	2.91892	1.69892	2.51351	1.46296
<i>C4_01470W_A</i>	0.00428285	2.91892	2.58333	1.62162	1.43519
<i>MNT3</i>	0.000955058	2.92	-1.31507	3.84	1
<i>FAD2</i>	0.00353145	2.92068	1.04469	2.02833	-1.37834
<i>C3_03070W_A</i>	1.42E-05	2.92308	1.33333	1.80769	-1.21277
<i>C3_06400C_A</i>	1.10E-05	2.92857	1.12698	2.25	-1.15493
<i>MTR2</i>	0.00168834	2.92857	-1.57851	2.72857	-1.69421
<i>RAD59</i>	6.31E-06	2.92857	1.6	2.14286	1.17073
<i>VTC4</i>	0.0157699	2.93139	-1.19897	5.34435	1.52059
<i>C1_00970W_A</i>	0.00439426	2.93939	2.04819	2.51515	1.75258
<i>ATG9</i>	0.0162109	2.93976	-1.0169	4.3494	1.45492
<i>PGA44</i>	0.000121465	2.94118	2.64286	- 1.21429	-1.35135
<i>FRP3</i>	0.000590614	2.94299	-1.25412	3.07126	-1.20175
<i>C6_01090C_A</i>	0.0113892	2.94737	1.48649	1.94737	-1.01818
<i>C2_01240C_A</i>	0.000154297	2.94737	-1.58621	4.03509	-1.15862
<i>C1_05650W_A</i>	0.0123919	2.94872	-1.08397	3.64103	1.13913
<i>C4_03880W_A</i>	0.00243883	2.95	2.43243	1.85	1.52542
<i>C1_07830C_A</i>	0.0134055	2.95455	1.52	2.27273	1.16923
<i>CR_10800C_A</i>	0.000318017	2.95476	1.14064	2.30238	-1.12511

CPH1	3.53E-06	2.95556	2.35211	1.57778	1.25564
CR_05900W_A	1.75E-05	2.95798	1.08782	2.96639	1.09091
C7_00490C_A	0.0124657	2.96	-1.53571	3.44	-1.32143
C1_08610C_A	0.000673298	2.96286	4.24888	1.40505	2.0149
SMI1B	0.000518424	2.96429	1.94118	2.42857	1.59036
C3_05150W_A	0.00311697	2.97033	1.38889	1.57567	-1.35729
C4_00060W_A	0.00273732	2.97561	2.07018	1.39024	-1.0339
DAL8	6.64E-06	2.97802	1.77564	1.71429	1.02214
AAT1	0.000673621	2.97857	1.65118	2.12143	1.17602
CR_02300C_A	8.88E-05	2.98251	2.25354	2.26531	1.71163
C6_00890W_A	0.000242035	2.99063	1.66173	2.31875	1.2884
SGS1	1.38E-05	2.99275	1.06826	2.12319	-1.31949
RER2	3.87E-08	2.99324	2.53723	1.27027	1.07675
SOL3	0.00121818	2.99793	1.47907	2.32988	1.14948
C2_06430C_A	0.00070938	3	-1.10294	2.88462	-1.14706
C2_02950W_A	0.00708523	3	1.50877	2.375	1.19444
CR_10380C_A	0.00505444	3	1.04348	1.91667	-1.5
C5_00340W_A	0.00341183	3	1.33498	2.85915	1.2723
GPX2	0.0121393	3	2.17907	1.46758	1.06598
PHO8	0.0141034	3	2.05556	2.57143	1.7619
POL3	1.85E-07	3.00291	1.19883	2.98256	1.19071
MUC1	1.62E-06	3.00641	2.02381	1.61538	1.08742
GSY1	0.000140817	3.01138	2.94813	1.87418	1.83481
ACE2	0.00790734	3.01149	1.00415	2.77011	-1.08264
RAD18	5.19E-05	3.01408	1.15423	2.83099	1.08411
C4_04500C_A	0.0013266	3.01923	1.84021	1.86538	1.13694
PRO1	1.43E-05	3.02278	1.18447	2.08608	-1.22336
CCN1	0.00344807	3.02381	1.07634	3.11905	1.11024
C4_07220C_A	0.00408199	3.02532	1	2.16456	-1.39766
DEM1	3.83E-05	3.02597	1.34247	3.79221	1.6824
C4_02400C_A	0.00186814	3.02632	1.30986	1.86842	-1.23656
MLH1	0.00387077	3.02703	1.30769	3.16216	1.36607
FGR41	0.000490998	3.03448	3.14876	2.08621	2.16477
LAB5	8.66E-05	3.03627	1.05	3.52332	1.21843
C6_02540C_A	0.00909789	3.03659	1.52432	2.2561	1.13253
C2_08460C_A	0.000333873	3.03846	1.33784	2.84615	1.25316
NAT5	1.54E-07	3.04348	1.60355	1.83696	-1.03321
C2_07100W_A	6.53E-06	3.04364	1.51017	1.96727	-1.02448
C2_00270C_A	0.00011092	3.06061	-1.00855	1.78788	-1.7265
C3_05060W_A	0.000215546	3.06061	1.6506	2.51515	1.35644
C2_04340C_A	0.0057646	3.06667	2.93333	1	-1.04545
CR_00750C_A	4.20E-05	3.06849	1.77273	2.10959	1.21875
C1_13500C_A	0.0029034	3.07248	-1.04815	1.01076	-3.18614
C1_03270W_A	0.00121088	3.07435	1.9471	2.88104	1.82467
GYP1	0.00100669	3.07595	1.54868	2.21013	1.11276
C3_00910W_A	0.000533215	3.07692	1.60674	2.28205	1.19167

C6_01870C_A	8.16E-06	3.08046	1.1673	3.02299	1.14552
C4_07240W_A	0.00125895	3.08333	2.42308	1.08333	-1.1746
ZCF7	0.0016416	3.08571	2.2	2	1.42593
ECM38	0.000104304	3.0875	1.99237	1.6375	1.05668
C1_08490W_A	0.00187066	3.09058	1.41291	2.41304	1.10317
C3_06280W_A	9.12E-05	3.09167	-1.07505	2.3875	-1.39212
C4_04510W_A	4.91E-07	3.09266	1.89578	2.56643	1.57321
C3_00830C_A	0.000357261	3.10219	1.15704	3.16058	1.17882
C1_08960W_A	0.00297015	3.10481	1.25057	- 1.05232	-2.61262
C1_06980C_A	3.05E-09	3.10596	2.69835	1.60265	1.39232
C3_02990C_A	4.90E-06	3.11688	2.24299	1.38961	1
CHT4	0.00220402	3.11765	3.10526	1.11765	1.11321
SSA2	0.0103565	3.11946	-1.43757	1.67303	-2.68042
OYE22	1.79E-05	3.11957	2.24737	2.06522	1.4878
TLO4	0.00513629	3.12245	1.12097	2.53061	-1.10072
C2_00280C_A	4.04E-05	3.125	1.36047	2.6875	1.17
C4_02450W_A	0.000434527	3.125	1.39423	2.16667	-1.03448
CR_06430W_A	0.0131245	3.125	2.41667	1.5	1.16
C1_05320C_A	3.16E-05	3.12821	1.26136	2.25641	-1.0991
C1_07470C_A	9.07E-05	3.13208	2.58442	1.45283	1.1988
YCG1	0.00588579	3.13483	1.43062	2.34831	1.07168
ARO8	0.016341	3.13934	-1.55769	2.6045	-1.87756
APL2	0.0021824	3.14159	1.3029	2.13274	-1.13057
C2_01500W_A	0.000292165	3.14444	1.15245	2.15	-1.26906
PDB1	0.000296558	3.14799	-1.13142	3.08621	-1.15407
C2_07690W_A	0.000242988	3.14815	2.58696	1.7037	1.4
IPK2	0.000181793	3.14943	1.54404	2.21839	1.08759
C7_02080W_A	0.000779251	3.15	2.01093	2.2875	1.46032
CR_01360W_A	0.000217676	3.15152	2.22449	1.48485	1.04808
HSL1	0.00822665	3.15228	-1.2785	3.47208	-1.16075
C6_03040C_A	0.00165612	3.15464	1.81961	2.62887	1.51634
C6_04440C_A	1.25E-07	3.15517	1.81395	1.97701	1.13661
SWD3	2.78E-05	3.15789	3	1.52632	1.45
ACS2	0.0020265	3.15856	1.29925	1.81151	-1.34201
C4_05980C_A	5.42E-06	3.16049	1.40702	3.51852	1.56641
AOX1	1.73E-07	3.16216	2.32283	1.71622	1.26068
C5_04480C_A	0.00131118	3.16667	1.625	2	1.02632
SPC2	0.0137149	3.17647	-1.2449	3.58824	-1.10204
PDA1	0.000182593	3.18273	1.18573	2.37851	-1.12852
C2_00350W_A	2.28E-05	3.18321	-1.37127	3.8626	-1.13008
C6_04550C_A	4.25E-09	3.18398	1.39702	2.4697	1.08362
URA1	0.00196389	3.185	-1.58322	3.67482	-1.37219
GTR1	0.0110242	3.1875	1.88889	2.25	1.33333
MRR2	0.00800021	3.19298	1.66667	1.07895	-1.77561
RFA1	0.00153161	3.19902	1.03326	3.39803	1.09754

CR_02100C_A	0.000880884	3.20588	1.75862	2.55882	1.40367
YKU80	0.000739674	3.21111	1.29048	2.33333	-1.06642
C3_07730W_A	1.20E-05	3.21127	2.52667	1.26761	-1.00264
ADA2	0.000445229	3.21212	2.09848	2	1.3066
C3_00270C_A	1.10E-07	3.21244	1.86927	2.25907	1.31452
CR_05500C_A	0.0015056	3.22561	1.60847	2.30488	1.14934
NIP100	0.00152288	3.22642	2.19048	2.11321	1.4347
CTR2	0.000216101	3.22973	1.89231	1.75676	1.02929
BUB1	0.000515623	3.23116	2.07061	2.63317	1.6874
C2_07920W_A	0.000979803	3.23256	1.10112	2.06977	-1.41837
CR_05140W_A	0.00353579	3.23529	-1.57143	2.58824	-1.96429
AGC1	0.000494384	3.23585	2.14663	1.60849	1.06706
APC1	4.61E-05	3.24055	1.45455	2.72165	1.22163
C6_01400W_A	0.0113509	3.24138	4.16279	1.48276	1.90426
C6_02160W_A	0.000518634	3.25	3.44444	1.63636	1.73427
PPH3	0.000720929	3.25	1.50649	2.40625	1.11538
IML2	0.00449058	3.2521	1.3047	3.39916	1.3637
C3_02900W_A	4.37E-06	3.26087	1.71523	1.6413	-1.1583
MCM3	0.00869005	3.2638	-3.48684	6.50307	-1.75
C1_00510W_A	0.00158998	3.26804	1.30851	1.93814	-1.28862
TRY5	0.00310259	3.28037	2.27193	2.13084	1.47578
C4_02200C_A	0.00160228	3.28571	1.32653	2.33333	-1.06154
CBF1	0.00255592	3.28571	1.44726	2.82143	1.24275
BRN1	0.000127774	3.28736	1.58333	2.89655	1.3951
FDH3	8.67E-07	3.29408	2.43546	1.80691	1.33593
C1_11570W_A	0.0045589	3.29412	1.08511	2.76471	-1.09804
CAN3	0.00107807	3.3	-1.30387	3.93333	-1.09392
C1_12150C_A	0.00751495	3.30233	1.86957	2.67442	1.51408
SAC1	0.000602197	3.30303	1.30712	2.69697	1.06728
C7_04160W_A	0.000129627	3.30612	1.62595	2.67347	1.31481
ADE13	9.73E-10	3.30961	1.59019	2.33565	1.12222
C5_01440C_A	0.000175862	3.32203	1.6391	2.25424	1.11224
C4_02590C_A	0.00939984	3.32609	1.16216	3.21739	1.12418
C4_06950W_A	2.63E-06	3.32653	1.05263	2.71429	-1.16429
CR_03430W_A	0.00502577	3.33333	-1.02326	2.09524	-1.62791
C6_02760W_A	0.01025	3.33333	1.66667	2	1
ATO6	0.0112634	3.33333	2.47826	1.91667	1.425
SCW11	0.00478858	3.33333	1.90871	2.97531	1.7037
SWD2	1.06E-05	3.33333	1.66805	2.36275	1.18235
TLO5	0.0138414	3.33333	1.19672	4.06667	1.46
C4_00860C_A	2.37E-05	3.34043	1.00699	3.04255	-1.09028
INP51	0.00118965	3.34848	1.05238	3.18182	1
INN1	0.00352019	3.35535	-1.0073	2.60377	-1.29805
C3_02710W_A	0.000196566	3.36364	-1.57353	3.24242	-1.63235
SAP3	0.00563969	3.36364	2.97297	1.68182	1.48649
C2_00920W_A	0.00154481	3.36441	2.54927	2.32203	1.75945

RTA4	0.00955951	3.36842	3.05556	-1.05556	-1.16364
C2_09610W_A	2.52E-06	3.375	2.07692	1.625	1
C2_07390C_A	0.000227202	3.37566	2.21317	1.68783	1.10658
CR_03340C_A	0.00175432	3.37662	1.91414	2.57143	1.45769
C6_01380C_A	8.10E-05	3.37879	-1.01778	3.4697	1.00897
HMO1	0.00175875	3.37975	4.4618	1.50759	1.99026
YHB4	1.17E-05	3.37989	2.16388	1.67039	1.06942
DLD1	4.27E-09	3.38167	3.6907	1.75667	1.9172
HCM1	0.0152546	3.38462	-2.08333	3.84615	-1.83333
C1_13810W_A	0.000441661	3.38525	1.37592	3.33607	1.35593
DOA1	0.00417187	3.38745	-1.01882	3.49631	1.01307
CDC46	1.72E-05	3.38889	-1.07224	3.13333	-1.1597
C1_14410W_A	6.48E-05	3.38983	1.20192	1.76271	-1.6
RCH1	0.000275991	3.3913	1.18675	3.6087	1.26282
NHP6A	8.18E-05	3.39208	2.13905	1.72669	1.08886
QDR2	1.10E-08	3.39333	1.04754	3.92667	1.21218
C5_04310W_A	8.19E-05	3.4	1.47581	3.1	1.34559
C4_00750C_A	0.0146182	3.4	1.23529	2.26667	-1.21429
C3_06690C_A	0.00122985	3.40909	1.84783	2.09091	1.13333
CTA24	0.00237453	3.41837	1.84772	2.0102	1.08657
C6_00180C_A	0.00238785	3.42105	-1.04444	2.47368	-1.44444
C3_00440W_A	0.0017307	3.42105	1.17778	2.36842	-1.22642
CAP4	0.000215963	3.44318	1.42458	2.03409	-1.18824
OPT2	0.00217338	3.44643	2.27132	2.30357	1.51813
CZF1	9.75E-05	3.4492	2.15512	1.93048	1.2062
C1_01070C_A	0.000803926	3.45161	1.85906	2.40323	1.29439
PLD1	0.00139711	3.45273	-1.0109	4.04818	1.15982
C4_06860C_A	0.00279331	3.45455	1.84058	2.09091	1.11404
BMT5	0.000100959	3.45876	1.8135	2.90206	1.52161
DLD2	0.00161058	3.46552	1.58036	1.93103	-1.13559
STE13	8.83E-06	3.47887	1.05761	3.42254	1.04049
CR_01420W_A	5.58E-05	3.48095	1.75198	2.4	1.20793
FCY2	0.000368223	3.48148	-1.29596	3.5679	-1.26457
C3_07700W_A	0.000117956	3.48175	1.36957	2.0146	-1.2619
FMT1	8.71E-07	3.48387	2.42975	1.95161	1.36111
C5_04710W_A	0.000160056	3.48571	1.42197	2.47143	1.0082
C1_03460C_A	6.74E-07	3.5	-1.27044	4.3913	-1.01258
C4_00740W_A	0.0100209	3.5	-1.18868	3.15	-1.32075
FGR6-1	0.000723506	3.5	1.0125	3.63636	1.05195
C2_08740W_A	0.00222214	3.5122	2.17021	2.29268	1.41667
HOS3	4.90E-06	3.51316	1.52632	2.41667	1.04994
C4_07200C_A	6.68E-05	3.51366	1.954	2.25683	1.25505
MEC3	0.000694774	3.52	1.43529	3.4	1.38636
HAT1	0.00973355	3.53061	1.50388	2.63265	1.12139
C3_07670W_A	8.79E-06	3.53271	2.71386	1.58411	1.21693

CTA7	1.04E-07	3.5404	1.36325	2.36364	-1.09875
C1_04350C_A	0.002115	3.54286	-1.01562	3.71429	1.03226
C4_00850C_A	0.00516147	3.55	2.40426	2.35	1.59155
FCA1	0.000154173	3.56481	1.65185	1.25	-1.72646
C1_03180W_A	4.09E-05	3.56522	1.16923	2.82609	-1.07895
DAO2	1.39E-05	3.56667	1.85294	1.7	-1.13228
FGR6-10	0.0070097	3.57143	1.01493	4.78571	1.36
DAC1	1.12E-05	3.57225	1.08939	3.10405	-1.05641
C4_00070C_A	4.87E-09	3.5793	2.01875	2.22538	1.25513
EXO1	0.00271956	3.59459	-2.20635	3.75676	-2.11111
C5_03490C_A	4.97E-05	3.59843	2.15025	2.22205	1.32779
C3_07460W_A	0.00408338	3.59903	1.5986	2.76812	1.22953
C2_02390W_A	0.0027444	3.60335	5.02869	1.36313	1.90233
C3_02980C_A	0.000466898	3.60526	-1.51389	2.86842	-1.90278
SPC98	0.000525022	3.60784	1.21557	3.27451	1.10326
C6_01960W_A	0.000208426	3.61818	1.63492	2.29091	1.03518
C6_03670C_A	0.00112045	3.61905	2.27907	2.04762	1.28947
GPT1	0.000208751	3.62069	1.38462	3.13793	1.2
HST6	0.00766477	3.63636	2.07692	2.36364	1.35
GUT1	2.29E-06	3.64055	1.83272	2.50691	1.26203
ARF1	1.72E-05	3.6474	2.22618	2.51734	1.53645
C3_07470W_A	0.00603353	3.64865	2.78182	2.97297	2.26667
C6_00420W_A	0.0023846	3.65	1.7619	2.1	1.0137
ILV3	0.00142026	3.65106	1.64373	1.45819	-1.52326
C1_04640W_A	0.000532498	3.65217	1.39841	3.11801	1.19388
C5_01310W_A	0.000770086	3.65385	1.08824	3.92308	1.16842
SAP30	0.00168198	3.66667	1.85714	2.33333	1.18182
C4_07210W_A	6.40E-05	3.67241	2.02288	2.63793	1.45305
STD1	0.000965901	3.6754	1.41047	2.19556	-1.18685
CR_10530W_A	0.000463766	3.67797	2.19424	2.35593	1.40553
C3_06680C_A	0.00075687	3.68	1.92188	2.56	1.33696
MCT1	4.91E-05	3.68182	1.33548	3.52273	1.27778
RFA2	0.000579349	3.68702	-1.24581	3.40458	-1.34916
EBP7	0.000833367	3.69118	-1.01224	3.64706	-1.02449
PGA7	0.000675702	3.69168	1.5129	1.67318	-1.45838
C3_00410C_A	0.00344672	3.69231	1.25926	2.07692	-1.41176
C1_10540C_A	0.0110905	3.69444	1.4127	3.5	1.33835
C5_03080C_A	4.68E-05	3.69737	1.25098	3.35526	1.13523
DUR3	0.0045213	3.7	3.125	1.6	1.35135
MSB1	7.59E-05	3.70588	1.55303	2.58824	1.08466
MCM2	0.00674903	3.71429	-1.5914	7.04762	1.19231
C1_05950C_A	0.00724007	3.72222	1.66667	2.33333	1.04478
IFA14	0.00108481	3.72222	1.93478	2.55556	1.32836
C7_04240C_A	9.80E-06	3.72727	1.08456	2.74747	-1.25085
C1_04340C_A	0.000255648	3.73077	1.53333	2.30769	-1.05435
TERT	0.000589657	3.73438	1.88304	2.67188	1.34728

C2_06120C_A	0.000639425	3.73684	-1.08511	2.68421	-1.51064
CR_08450C_A	3.65E-07	3.73684	1.85366	2.15789	1.07042
C6_01130W_A	0.0101683	3.75	1.55556	1.125	-2.14286
C2_04110W_A	5.93E-05	3.75556	1.56618	3.02222	1.26036
C2_05510C_A	0.00100521	3.77778	1.60526	2.11111	-1.11475
C7_03210W_A	0.0109738	3.77778	-1.09804	3.11111	-1.33333
CDC20	0.0164343	3.78125	1.21762	3.01563	-1.02979
PGA32	0.000398905	3.78571	-1.6	2.28571	-2.65
C7_04090C_A	0.00135594	3.82813	-2.12883	5.42188	-1.50307
C3_00130C_A	6.74E-06	3.82822	1.57229	2.03681	-1.1954
RBT4	0.000416061	3.8296	1.46883	1.79821	-1.44992
MNN13	3.51E-05	3.83333	1.80972	2.42157	1.14322
TES1	0.00141424	3.83333	2.14286	2.33333	1.30435
C6_02560W_A	0.00256272	3.84218	5.79972	1.21237	1.83006
RDH54	0.00171533	3.85366	-1.09167	3.19512	-1.31667
C1_14020W_A	0.0036019	3.85714	3	1.28571	1
C2_07240C_A	0.000218187	3.86364	1.42623	2.77273	1.02353
C4_02930W_A	7.29E-05	3.8805	2.7043	2.33962	1.63047
ASE1	0.00663876	3.88889	1.63636	3.46296	1.45714
CR_00420W_A	0.000402151	3.89063	2.92593	1.6875	1.26908
EST1	4.89E-07	3.9	1.66171	1.92143	-1.22148
MUQ1	0.0051026	3.90306	-1.46759	5.42857	-1.05517
HTS1	0.000879133	3.90812	1.60331	- 1.34917	-3.28866
C1_12480W_A	0.00350035	3.90909	1.42308	2.36364	-1.16216
SOD5	0.000813617	3.91667	3.41667	1	-1.14634
C7_01910C_A	5.51E-06	3.92157	1.88571	2.7451	1.32
LYS14	0.000128816	3.92308	1.84848	2.53846	1.19608
GUT2	4.25E-06	3.92426	1.99236	2.57882	1.30927
C1_11270W_A	1.57E-07	3.93236	1.78134	1.7636	-1.25172
HOG1	1.78E-06	3.93237	1.63711	2.343	-1.02519
CR_10180W_A	0.000223547	3.93333	1.4878	2.73333	1.0339
C3_03160C_A	4.06E-05	3.96	1.45714	2.8	1.0303
CRG1	0.00310286	3.96018	3.2364	2.35841	1.92737
C6_00080C_A	4.56E-06	3.96429	1.07143	2.75	-1.34545
CR_01810C_A	1.16E-05	3.9697	1.38961	2.33333	-1.2243
POT1-2	1.73E-05	3.97196	2.40892	2.51402	1.52471
C2_09280C_A	5.34E-10	3.97253	1.78373	2.56593	1.15214
IRR1	0.00127399	3.98925	1.10979	3.62366	1.00809
SUN41	7.71E-07	3.99636	1.18099	2.96945	-1.13957
C3_02070C_A	0.00553374	4	2.85714	1.75	1.25
C5_02810W_A	0.000575315	4	1.33333	2.625	-1.14286
C1_12640W_A	0.000109447	4	1.85714	1.27273	-1.69231
RIM1	0.000133913	4.02239	2.11549	2.84328	1.49536
BMT9	0.00539705	4.05714	2.45679	2.31429	1.40141
GCY1	0.000865048	4.07042	2.78699	2.93342	2.00849

HAT2	1.01E-06	4.09184	1.61972	2.17347	-1.16232
C5_05440C_A	0.00187033	4.10596	-1.05367	2.4702	-1.75141
C7_03350C_A	0.00201188	4.11111	2.29167	2.66667	1.48649
ERG1	0.00771258	4.11364	-1.12956	2.26768	-2.04906
PGA59	4.03E-06	4.1163	1.74926	1.74563	-1.34803
PGA62	0.00010371	4.12716	1.2392	2.01543	-1.6525
C6_01490C_A	0.0083472	4.13333	2.93939	1.1	-1.27835
IQG1	0.00914696	4.14423	1.08961	3.70192	-1.02741
FGR50	0.000845042	4.14815	1.02679	4.14815	1.02679
C5_01230C_A	0.00127345	4.15238	1.44823	3.49524	1.21904
CAC2	1.16E-07	4.15385	1.8022	2.8	1.21481
ALG7	1.55E-05	4.16071	-1.07907	4.14286	-1.08372
GOR1	0.0095867	4.19178	-1.80794	5.20091	-1.45714
C6_03620C_A	8.19E-10	4.19886	2.64192	2.60227	1.63735
IHD1	0.000431458	4.22807	1.94643	1.96491	-1.1055
C3_07110W_A	0.00434837	4.23529	1.11719	3.76471	-1.00699
SCS7	1.38E-08	4.24514	1.15347	3.11015	-1.18332
REP1	0.000383266	4.25714	1.42395	5.00952	1.67562
C3_05720C_A	0.00128469	4.25926	1.38	3.7037	1.2
ELC1	0.00024155	4.26087	1.80597	2.91304	1.23469
C5_03000C_A	0.00592806	4.28125	1.05983	3.65625	-1.10484
RPB7	4.48E-05	4.30233	2.16667	2.23256	1.12432
C1_12880C_A	0.000479535	4.30303	1.8	2.82828	1.1831
ARP1	0.000857021	4.30769	2.16667	2.30769	1.16071
PRR2	0.00209208	4.32	1.15152	5.28	1.40741
C1_04250C_A	0.0152423	4.33333	-3	2	-6.5
CDC5	0.0132896	4.34911	-1.03149	4.84615	1.08027
C2_06160W_A	0.00179504	4.35714	1.775	2.85714	1.16393
ERG11	0.0146245	4.35821	-1.43719	3.20149	-1.95645
CHS2	0.00964541	4.36782	-1.45693	4.47126	-1.42322
CLB2	0.00231171	4.39604	1.86535	2.5	1.06081
CR_03020C_A	0.0154273	4.41935	-1.68421	4.12903	-1.80263
CR_00390W_A	6.10E-05	4.42029	-1.17343	4.6087	-1.12546
AFP99	0.00102365	4.42105	1.47945	3.84211	1.28571
C1_02370C_A	0.000183782	4.42424	1.17857	5.09091	1.35616
ACC1	0.000129443	4.42452	-1.25483	4.03542	-1.37582
OYE23	0.000364908	4.45455	3.11765	1.54545	1.08163
LAT1	0.000129849	4.4632	1.11546	2.43357	-1.64418
C5_02850W_A	1.24E-09	4.46939	2.06731	1.27347	-1.69767
C6_02990W_A	0.00166839	4.5	-1.37143	5.14286	-1.2
C3_03440C_A	1.56E-05	4.51163	3.69512	1.90698	1.56186
CHT1	0.00271717	4.52941	-3.125	4.41176	-3.20833
C3_01100W_A	0.00961539	4.53333	1.58182	3.66667	1.27941
C1_12470W_A	0.0051947	4.54545	6.4	1.36364	1.92
C1_10410W_A	7.58E-05	4.55102	2.17881	3.08163	1.47534
CR_06740W_A	6.99E-05	4.56522	1.36517	3.86957	1.15714

C1_06250W_A	0.00245357	4.57143	1.18182	3.14286	-1.23077
GCV1	4.17E-08	4.59244	1.60681	3.57983	1.25252
C1_14430C_A	0.000908778	4.6	1.61765	1.7	-1.67273
C4_01240C_A	0.000101765	4.61538	-1.30769	3.92308	-1.53846
FTH1	0.00155156	4.63768	-1.07547	2.47826	-2.01258
C4_03340C_A	0.00764198	4.64286	4.64286	2.33333	2.33333
MNN14	0.000317089	4.65385	1.72993	2.63462	-1.0211
C7_01100C_A	0.00599741	4.66667	-2.15385	6.22222	-1.61538
OPT5	0.00183972	4.66667	2.16667	2	-1.07692
TPO2	0.000106202	4.66667	1.57353	2.51852	-1.17757
RAD54	0.00551336	4.70909	1.02643	4.12727	-1.11159
FAV3	9.46E-05	4.71429	-1.02083	3	-1.60417
CR_08440W_A	1.46E-07	4.71875	2.80822	2.28125	1.35762
C5_05360C_A	5.14E-07	4.72139	3.4703	2.05224	1.50843
C5_03780C_A	0.00069157	4.75	-1.59091	5.83333	-1.29545
C7_01880C_A	0.000166196	4.75	-1.11765	2.375	-2.23529
C3_07540C_A	0.0128576	4.75	1.35417	4	1.14035
C2_02050C_A	0.0108356	4.81308	1.40845	3.98131	1.16505
CCE1	0.0147083	4.83333	2.11765	2.83333	1.24138
SMC2	0.00396235	4.84314	1.49756	4.01961	1.24291
C4_06960W_A	0.000301931	4.84615	1	4	-1.21154
C1_02780W_A	8.48E-10	4.84959	3.82865	1.44715	1.1425
C5_05200C_A	0.00175171	4.85882	1.63441	3.28235	1.10412
PRE1	0.000362927	4.86856	4.88359	1.60213	1.60708
C2_06550W_A	6.72E-06	4.88235	1.86667	3.08824	1.18072
PGA23	1.01E-05	4.9	-1.08867	2.7625	-1.93103
TOS1	0.000252019	4.91231	1.32103	3.88196	1.04394
DAL1	9.67E-05	4.92308	1	5.07692	1.03125
RTA2	3.84E-05	4.96571	-1.01651	3.16571	-1.5945
C1_11730W_A	0.00224228	5	-1.14324	3.81416	-1.49867
C2_09910C_A	0.00546845	5	-3	1.5	-10
C3_05080W_A	0.0142567	5	1.11765	2.42857	-1.84211
SAP4	0.00345155	5	?	?	-1.36364
GIN4	2.13E-06	5.02353	1.45892	4.15294	1.20609
PDC12	0.000413221	5.06667	4.85	1.33333	1.27632
C2_01260W_A	6.70E-07	5.08	1.41751	3.96	1.10499
CR_04650W_A	0.0144925	5.09091	2.04878	3.72727	1.5
C6_00120W_A	0.00234992	5.11111	1.83333	2.66667	-1.04545
RBT5	0.000538395	5.13811	1.26323	1.88325	-2.15979
C2_04390W_A	0.000126511	5.14286	1.70588	2.42857	-1.24138
CDC45	0.000266673	5.14286	1.41414	2.82857	-1.28571
SAP8	0.000168217	5.17647	3.84615	1.52941	1.13636
HGT17	0.00827709	5.17968	6.67979	-	1.07357
				1.20124	
C2_01420C_A	0.000411569	5.18182	-1.32692	6.27273	-1.09615
RAD52	0.002887	5.19355	1.16038	3.41935	-1.30894

<i>C6_02250W_A</i>	0.000485492	5.2	1.23529	3.4	-1.2381
<i>C5_05350W_A</i>	0.00023127	5.21429	1.99259	2.41071	-1.0855
<i>DUR35</i>	5.63E-05	5.22222	2.42857	3.11111	1.44681
<i>CDC47</i>	5.60E-05	5.2233	1.09216	4.95146	1.03532
<i>CDC54</i>	7.49E-05	5.23077	1.47253	3.5	-1.01493
<i>YHB1</i>	1.21E-05	5.23756	3.98984	1.66385	1.26748
<i>HXK2</i>	0.0136045	5.24266	1.77799	3.38822	1.14908
<i>C3_02790W_A</i>	0.00137134	5.25	2.55556	1.125	-1.82609
<i>C6_03420W_A</i>	0.00343111	5.25	1.64865	4.625	1.45238
<i>C5_05460C_A</i>	1.59E-05	5.25287	2.89116	1.68966	-1.07529
<i>CR_07470W_A</i>	0.00990154	5.27273	1.25	4.72727	1.12069
<i>C2_06130W_A</i>	0.00062723	5.30435	1.84043	4.08696	1.41803
<i>C1_07810C_A</i>	6.16E-06	5.31429	2.42381	4	1.82437
<i>CR_04680C_A</i>	0.00588929	5.33333	2.66667	1	-2
<i>MDR1</i>	0.00511122	5.33333	-2.33333	7	-1.77778
<i>CDC13</i>	0.00592654	5.36842	-1.25532	6.21053	-1.08511
<i>CR_06550C_A</i>	0.000232474	5.38889	1.79032	3.44444	1.14433
<i>YCS4</i>	0.0070506	5.3964	-1.20729	5.66667	-1.14971
<i>C1_01080W_A</i>	0.000302594	5.4	1.69697	3.3	1.03704
<i>C2_03890W_A</i>	0.00695305	5.4	1.30435	4.6	1.11111
<i>HTA3</i>	0.00275577	5.41509	2.38511	2.91509	1.28397
<i>FGR23</i>	0.0021956	5.41667	2.08696	1.91667	-1.35417
<i>C2_02230C_A</i>	0.00803655	5.5	2.81818	2.75	1.40909
<i>C4_02820W_A</i>	0.0054036	5.5	2.44444	2.25	1
<i>C6_00810C_A</i>	0.00230486	5.5	2.93333	1.5	-1.25
<i>HOF1</i>	0.00308216	5.5	2.44785	3.13462	1.3951
<i>C7_02010C_A</i>	0.00027368	5.52941	3.90476	2.47059	1.74468
<i>CSE4</i>	0.000314739	5.53488	2.02542	2.74419	1.0042
<i>C1_08140W_A</i>	7.34E-05	5.59091	1.88889	3.68182	1.2439
<i>C1_10920W_A</i>	2.97E-05	5.60976	1.99459	4.5122	1.60435
<i>C5_00810C_A</i>	0.00959985	5.66667	6	1	1.05882
<i>PRP22</i>	1.44E-08	5.73154	2.70649	2.58389	1.22014
<i>C4_04720W_A</i>	3.42E-06	5.73657	1.87063	4.68542	1.52786
<i>C2_10070W_A</i>	0.0010672	5.77778	5.05882	1.88889	1.65385
<i>SMC4</i>	0.000922284	5.79091	1.49225	4.69091	1.20879
<i>SSP96</i>	3.35E-05	5.79167	1.81818	4.125	1.29496
<i>MCD1</i>	0.00325731	5.81818	-2.91667	6.36364	-2.66667
<i>APM1</i>	7.03E-06	5.82609	2.31618	1.97101	-1.27619
<i>CHS8</i>	0.00831818	5.84615	-1.12736	6.89423	1.04605
<i>KIP2</i>	0.00150448	5.85714	2	4.21429	1.43902
<i>RHD3</i>	3.30E-05	5.85995	6.64549	1.47569	1.67351
<i>NRM1</i>	0.00694205	5.88889	1.26471	3.77778	-1.23256
<i>C7_00190W_A</i>	5.74E-06	5.92045	2.27138	3.05682	1.17274
<i>C7_00760C_A</i>	0.00091841	6	-2.33333	4.66667	-3
<i>BUB2</i>	0.000831293	6.11111	2.34211	4.22222	1.61818
<i>CAR1</i>	1.21E-06	6.12121	1.76059	4.76768	1.37129

<i>C1_06700W_A</i>	0.00924994	6.14286	-1.04274	4.97959	-1.28632
<i>SNZ1</i>	0.000112553	6.18846	2.37839	4.7121	1.81099
<i>C1_06000W_A</i>	0.00170913	6.2	1.66667	3	-1.24
<i>FGR29</i>	0.0051235	6.21875	-1.05233	5.65625	-1.15698
<i>MOB1</i>	0.00105148	6.23333	1.27907	5.73333	1.17647
<i>USO5</i>	0.000371805	6.25	2.08642	4.05	1.352
<i>C5_00050W_A</i>	0.0105769	6.27273	1.3	1.81818	-2.65385
<i>C2_01250W_A</i>	0.00737646	6.4	1.5	8.08	1.89375
<i>CHS1</i>	0.00986872	6.42963	-1.08654	6.6963	-1.04327
<i>YBL053</i>	0.00923722	6.43182	1.48848	4.93182	1.14134
<i>ECM331</i>	0.00050971	6.43478	-2.0119	7.34783	-1.7619
<i>C1_10710C_A</i>	0.00492099	6.46667	-1.61972	7.66667	-1.3662
<i>FRP2</i>	3.44E-07	6.53659	2.23404	3.43902	1.17537
<i>C3_07140C_A</i>	2.51E-05	6.53846	1.82979	3.61538	1.01176
<i>DPB2</i>	0.00678008	6.55556	-2.53125	9	-1.84375
<i>CR_07460C_A</i>	0.000661433	6.56	1.63636	4.69333	1.17073
<i>BFA1</i>	4.19E-06	6.56522	2.29891	4	1.40066
<i>HAK1</i>	0.000337403	6.64286	2.375	3.42857	1.22581
<i>C1_07850C_A</i>	0.00318495	6.75	1.14	6.25	1.05556
<i>NGT1</i>	4.29E-05	6.75	3.81818	1.83333	1.03704
<i>C6_00400C_A</i>	0.00300677	6.77778	1.11828	5.16667	-1.17308
<i>C5_00170W_A</i>	1.04E-07	6.83929	1.59864	2.625	-1.62979
<i>PAD1</i>	2.55E-05	6.84211	2.17544	3	-1.04839
<i>C2_06570C_A</i>	0.000196318	6.87105	1.03939	2.77237	-2.38447
<i>CHT2</i>	0.00901768	6.87135	-2.63043	5.66082	-3.19293
<i>ASK1</i>	0.0101652	6.89286	1.57143	5.75	1.31088
<i>CDC21</i>	0.0153556	6.95918	1.18868	4.32653	-1.35317
<i>C3_04170W_A</i>	0.0031821	7	2.88889	2.25	-1.07692
<i>C6_00090W_A</i>	0.0140562	7	1.24	3.125	-1.80645
<i>C7_00230W_A</i>	0.0157258	7	-1.3083	7.69767	-1.18972
<i>CR_07120C_A</i>	0.00543732	7	2.37255	3.92308	1.32967
<i>SPO1</i>	7.86E-06	7	1.92857	3.5	-1.03704
<i>tG(CCC)1</i>	0.0118771	7	4	1	-1.75
<i>tP(AGG)1</i>	0.00155906	7	-3	2	-10.5
<i>CYK3</i>	0.00926944	7.09375	1.04054	6.9375	1.01762
<i>HTA1</i>	0.00284275	7.18458	1.60977	5.89452	1.32072
<i>FAR1</i>	2.73E-05	7.2	3.5	2.4	1.16667
<i>CFL4</i>	0.00477709	7.22222	2.71429	3.11111	1.16923
<i>C6_01780C_A</i>	5.78E-07	7.35135	1.88235	3.67568	-1.0625
<i>HTB1</i>	0.00747938	7.4898	2.76471	4.64898	1.71608
<i>DUN1</i>	0.000355537	7.63636	1.28205	7.09091	1.19048
<i>C7_00310C_A</i>	0.00168146	7.66154	2.12581	2.38462	-1.51138
<i>CR_03440W_A</i>	0.00319925	7.8	3.25	2.4	1
<i>PGA4</i>	1.26E-08	7.83718	6.50976	1.39916	1.16218
<i>HGT20</i>	3.07E-07	7.9	1.375	3.2	-1.79545
<i>PGA54</i>	5.03E-06	7.92187	1.34867	4.41406	-1.33071

HGT13	0.0165109	7.92727	2.16462	2.46667	-1.48468
C4_02080W_A	0.000751592	8	3.625	2	-1.10345
SOU2	0.000240385	8.05556	2.48889	2.5	-1.29464
C2_06760C_A	0.00411238	8.09091	3.06122	4.45455	1.68539
CR_02880W_A	3.49E-06	8.15789	4.76596	2.47368	1.44516
C1_04490W_A	0.00883494	8.26829	1.02756	6.19512	-1.29885
MUM2	8.27E-09	8.33962	2.69613	3.41509	1.10407
C6_00110C_A	9.18E-05	8.38462	-1.09322	9.92308	1.08257
CR_04220C_A	0.0015709	8.65789	-1.15113	9.42105	-1.05788
SWE1	0.00019477	8.68627	1.45802	7.70588	1.29345
SAP6	0.000304674	8.75	3.09091	2.75	-1.02941
RAD51	0.0038965	8.92727	1.07163	6.6	-1.26221
PGA46	0.00204383	9	1.75	4	-1.28571
POX18	0.0153005	9	1.5	4	-1.5
tA(UGC)3mt	0.00204383	9	2	1	-4.5
SOD6	2.11E-07	9.01695	3.87678	3.57627	1.53759
FAS1	3.91E-05	9.32997	-1.42856	8.98175	-1.48395
PGA37	0.000385691	9.33333	3.58065	2.58333	-1.00901
C2_06920C_A	3.85E-06	9.4	1.13174	8.35	1.00532
PHO13	0.00335686	9.5	2.22222	4.5	1.05263
SPO22	0.00153283	9.5	-1.4	3.5	-3.8
SNO1	9.10E-06	9.59524	2.0605	6.69048	1.43672
C4_06200W_A	0.000240727	9.66667	-1.13333	5.66667	-1.93333
RHD2	0.00388148	9.66667	1.1978	3.79167	-2.12844
C2_10300C_A	0.00115606	9.75	1.5	4.5	-1.44444
CR_00060C_A	0.00422584	9.92308	1.70417	3.69231	-1.57702
DUT1	0.00656984	9.95455	-2.57143	5.72727	-4.46939
YVC1	0.00506684	10.1084	-1.34025	11.6747	-1.16044
PGA60	3.24E-05	10.1429	7.375	2.28571	1.66197
SOD1	8.88E-05	10.2822	3.73315	2.18405	-1.2611
ESP1	0.000924151	10.2963	1.4181	8.59259	1.18345
CR_08990C_A	0.000117417	10.2966	2.47601	3.73793	-1.11252
MPS1	0.0145898	10.3333	1.17391	5.75	-1.53086
CR_08270W_A	0.00148464	10.6667	2.75	5.33333	1.375
HSP31	0.00147674	10.8274	10.1362	1.90769	1.78592
C1_04470C_A	0.000220947	10.8889	1.27642	13.6667	1.60204
CR_06310W_A	0.00642349	11	1.28571	7	-1.22222
C5_03770C_A	0.00236256	11.125	12.5455	1.375	1.55056
C2_06140C_A	0.000166985	11.3333	2.06667	5	-1.09677
C5_01220W_A	0.00513135	11.4286	1.58621	12.4286	1.725
CR_07170W_A	1.12E-09	11.4783	3.29503	6.25753	1.79633
PCL2	0.00850589	12	1.52632	6.33333	-1.24138
ARO10	0.000144156	12.3418	9.37198	2.62025	1.98974
MSH6	0.0120022	12.425	-2.52697	15.225	-2.06224
HHF1	0.00080409	12.9198	2.8769	5.55274	1.23645
C6_03280W_A	0.0132609	13	4.66667	3	1.07692

<i>MRV1</i>	0.00932455	13	2.66667	6	1.23077
<i>TOS4</i>	0.00519206	13	1.09333	8.82353	-1.34756
<i>MLC1</i>	0.00884672	13.1667	1.55797	7.66667	-1.10233
<i>HTA2</i>	0.000615918	13.3325	3.41588	5.04534	1.29265
<i>HXT5</i>	0.00293169	13.3333	3.68627	1.7	-2.12766
<i>PMS1</i>	0.00260387	13.4	-1.13559	6.7	-2.27119
<i>C2_06270W_A</i>	0.000196261	14.3333	2.85714	4.66667	-1.075
<i>HHO1</i>	0.00156409	14.5	3.76609	6.12121	1.58986
<i>C1_04180W_A</i>	0.00388285	14.5102	3.77931	5.91837	1.54149
<i>FAS2</i>	1.71E-05	14.6688	-1.18658	11.7833	-1.47715
<i>CDC14</i>	0.000898843	15.4783	1.94388	8.52174	1.07022
<i>MRV2</i>	0.000536918	15.6667	2.64286	4.66667	-1.27027
<i>C2_07280W_A</i>	9.77E-05	16.5	2.22222	9	1.21212
<i>PGA45</i>	0.00078564	16.5294	-1.00885	6.70588	-2.48673
<i>GCV2</i>	0.000830913	17.4486	-1.42753	23.7477	-1.04888
<i>CFL2</i>	5.72E-05	17.5	-1.0625	8.5	-2.1875
<i>CTF8</i>	0.000356767	18	1.28571	14	1
<i>RBT1</i>	0.000131902	20	2.03448	5.8	-1.69492
<i>PGA10</i>	0.00505279	20.5313	-1.02158	13.3125	-1.57554
<i>PGA6</i>	0.0112555	20.7143	-4.80769	17.8571	-5.57692
<i>HHF22</i>	0.000552732	23.3896	3.02519	8.76623	1.13381
<i>CR_09050C_A</i>	0.002784	24.5	1.78571	14	1.02041
<i>C4_02210W_A</i>	0.00645617	25	-1.81818	20	-2.27273
<i>C1_01510W_A</i>	0.00849713	26.7857	6.62745	3.64286	-1.10947
<i>ATO1</i>	2.46E-06	28.25	2.92857	7	-1.37805
<i>C5_03650C_A</i>	0.000127712	31	3.33333	12	1.29032
<i>C3_04210W_A</i>	0.000705803	35	3.16667	6	-1.84211
<i>CHA1</i>	1.11E-05	44.0469	3.35333	16.4063	1.24902
<i>HHT2</i>	0.000295652	52.1023	2.67801	20.3636	1.04667
<i>RNH35</i>	0.00348969	62.5	-1.89796	46.5	-2.55102
<i>HHT21</i>	0.000483944	80.9919	3.36983	23.6098	-1.01798
<i>C2_01630W_A</i>	0.000336897	335	75.2222	9	2.0209

Genes upregulated in the WT in Pi deplete conditions					
Alias	p-value (WT-Pi vs. WT+Pi)	Fold Change (WT-Pi vs. WT+Pi)	pho4-Pi vs. pho4+Pi	pho4+Pi vs. WT+Pi	pho4-Pi vs. WT-Pi
<i>PHO100</i>	0.000254914	847.65	-1.28571	1.35	-807.286
<i>BTA1</i>	0.00024352	378.789	1.16667	-3.16667	-1028.14
<i>PLB1</i>	0.000254489	320.75	1.25926	6.75	-37.7353

<i>PHO84</i>	0.000120989	289.744	2	- 1.69565	- 245.652
<i>C1_04800C_A</i>	0.000274884	149.667	1.33333	4	- 28.0625
<i>C7_03310W_A</i>	0.000374063	134	-2	52	- 5.15385
<i>C3_01540W_A</i>	0.0054864	66.6154	-11.6977	38.6923	- 20.1395
<i>C3_02750W_A</i>	0.000305103	66.25	3.2	3.75	- 5.52083
<i>RBT7</i>	0.000212336	58.8	1.5	1.4	-28
<i>C4_00530C_A</i>	0.000298338	55.5	?	?	-37
<i>C1_10060C_A</i>	0.000339367	44.8571	3.19565	6.57143	- 2.13605
<i>PHO112</i>	0.000204892	42.3846	-1.76471	1.15385	- 64.8235
<i>ASM3</i>	0.000105422	40.4	1.04926	4.06	- 9.48357
<i>CR_10200W_A</i>	0.000266521	32.9286	1.10526	1.35714	- 21.9524
<i>TRY6</i>	1.21E-05	31.2	1.27273	2.2	- 11.1429
<i>GIT1</i>	0.00027019	30.1456	1.22222	-1.0404	- 25.6612
<i>PHO113</i>	0.000223533	26.4861	1.2766	- 1.53191	- 31.7833
<i>PGA28</i>	4.01E-05	24	1.66667	12	-1.2
<i>GCV2</i>	2.56E-05	23.7477	-1.04888	17.4486	- 1.42753
<i>FET99</i>	4.75E-08	21.3718	1.68159	2.57692	- 4.93195
<i>SSU1</i>	0.000227884	20.1667	-1.29032	6.66667	- 3.90323
<i>RNR1</i>	0.00218517	18.0955	-5.75394	10.2472	- 10.1609
<i>MNN1</i>	3.37E-05	18.0373	1.7631	3.27612	- 3.12274
<i>RBR1</i>	0.00288359	17.4	2.68692	10.7	1.6523
<i>XOG1</i>	1.13E-05	16.2333	-1.76316	2.97778	- 9.61184
<i>MSH6</i>	0.0025911	15.225	-2.06224	12.425	- 2.52697
<i>MNN22</i>	2.63E-05	15.0203	1.25254	3.98649	- 3.00812
<i>C3_02140C_A</i>	7.33E-05	14.8889	-2.8	4.04444	- 10.3077
<i>CTF8</i>	0.00373653	14	1	18	1.28571
<i>C1_04470C_A</i>	1.23E-05	13.6667	1.60204	10.8889	1.27642
<i>CR_09060W_A</i>	0.011118	13	3	3	- 1.44444
<i>CR_05800C_A</i>	0.00256852	12.5	-1.85185	6.25	-3.7037

<i>C5_01220W_A</i>	0.00257118	12.4286	1.725	11.4286	1.58621
<i>CR_03840C_A</i>	0.000614316	12.3333	-2	2.66667	-9.25
<i>FAS2</i>	0.000259183	11.7833	-1.47715	14.6688	- 1.18658
<i>YVC1</i>	0.00145463	11.6747	-1.16044	10.1084	- 1.34025
<i>BMT3</i>	2.35E-05	11.5614	1.07692	2.50877	- 4.27922
<i>CDC19</i>	0.00230709	11.1291	-2.10134	5.86235	-3.9892
<i>GIT4</i>	1.69E-05	10.8	1	3.6	-3
<i>GIT3</i>	5.68E-05	10.3651	1.12097	1.64021	- 5.63741
<i>NAT4</i>	0.00863403	10.25	-3.25	1.625	-20.5
<i>C4_05730W_A</i>	2.60E-11	10	1.0625	1.33333	- 7.05882
<i>C6_00110C_A</i>	9.23E-06	9.92308	1.08257	8.38462	- 1.09322
<i>CR_01920W_A</i>	0.00183523	9.71429	3	-3.5	- 11.3333
<i>BIO2</i>	0.000712398	9.69118	2.4	- 1.51111	- 6.10185
<i>CR_04220C_A</i>	0.000671242	9.42105	-1.05788	8.65789	- 1.15113
<i>C6_03320W_A</i>	0.000777287	9.34669	-1.68602	3.14228	- 5.01505
<i>C4_03950C_A</i>	0.00150535	9.33333	-1.44444	4.33333	- 3.11111
<i>ALS4</i>	0.000165725	9.15075	-1.12853	- 1.77672	-18.348
<i>BMT4</i>	1.80E-07	9.06504	1.37222	1.46341	- 4.51417
<i>C4_07080C_A</i>	0.00981178	9.04762	-1.44211	6.52381	-2
<i>DPB2</i>	0.000312376	9	-1.84375	6.55556	- 2.53125
<i>FAS1</i>	6.46E-05	8.98175	-1.48395	9.32997	- 1.42856
<i>POL1</i>	0.000186808	8.71642	-1.74317	4.76119	- 3.19126
<i>ESP1</i>	0.0047969	8.59259	1.18345	10.2963	1.4181
<i>PHO81</i>	8.34E-05	8.55747	1.11316	2.18391	- 3.52009
<i>GDE1</i>	9.33E-06	8.37838	1.16295	3.02703	- 2.38004
<i>C2_06920C_A</i>	2.18E-05	8.35	1.00532	9.4	1.13174
<i>CRZ2</i>	6.80E-06	8.2381	1.52632	3.61905	- 1.49138
<i>C2_01250W_A</i>	0.000870103	8.08	1.89375	6.4	1.5
<i>CR_01910C_A</i>	0.00106012	8	-1.4	3.5	-3.2
<i>GIN1</i>	0.000862195	8	-2.07273	5.18182	-3.2
<i>PLB4.5</i>	0.000563269	7.96279	-3.65385	3.09302	- 9.40659

<i>C5_04260W_A</i>	0.000413257	7.79245	1.72189	3.18868	-1.41924
<i>C3_04650W_A</i>	7.13E-05	7.71429	1.41509	2.52381	-2.16
<i>SWE1</i>	0.000755418	7.70588	1.29345	8.68627	1.45802
<i>C7_00230W_A</i>	0.0079835	7.69767	-1.18972	7	-1.3083
<i>C1_11080W_A</i>	0.000141647	7.68889	-1.1583	1.66667	-5.34363
<i>C1_10710C_A</i>	0.000989252	7.66667	-1.3662	6.46667	-1.61972
<i>IFE1</i>	5.80E-05	7.54762	-1.38095	2.7619	-3.77381
<i>KCS1</i>	1.26E-05	7.5	-1.06433	2.33333	-3.42105
<i>ECM331</i>	0.00010101	7.34783	-1.7619	6.43478	-2.0119
<i>DPP1</i>	0.000536671	7.27778	1.21739	3.83333	-1.55952
<i>DUN1</i>	0.000811102	7.09091	1.19048	7.63636	1.28205
<i>CR_07850W_A</i>	0.000376265	7.07143	-1.22222	3.92857	-2.2
<i>MCM2</i>	1.51E-06	7.04762	1.19231	3.71429	-1.5914
<i>ESC4</i>	0.00121789	7	-1.05556	4.75	-1.55556
<i>MDR1</i>	0.000308348	7	-1.77778	5.33333	-2.33333
<i>CYK3</i>	0.0109207	6.9375	1.01762	7.09375	1.04054
<i>ATF1</i>	7.53E-05	6.92105	1.39382	3.40789	-1.45706
<i>CHS8</i>	0.0019571	6.89423	1.04605	5.84615	-1.12736
<i>ALS2</i>	6.13E-05	6.87429	-1.29364	1.02628	-8.66517
<i>C5_03950W_A</i>	0.000235282	6.82609	-1.08092	4.06522	-1.81503
<i>CHS1</i>	0.0072154	6.6963	-1.04327	6.42963	-1.08654
<i>SNO1</i>	0.000881041	6.69048	1.43672	9.59524	2.0605
<i>UBC15</i>	0.00674152	6.66667	-2.13793	4.13333	-3.44828
<i>TUB1</i>	0.0111185	6.58238	1.06959	6.11111	-1.00703
<i>SRD1</i>	0.00460174	6.51613	-1.5	4.35484	-2.24444
<i>GFA1</i>	0.0015021	6.5125	-1.28917	4.6625	-1.80069
<i>MCM3</i>	7.44E-07	6.50307	-1.75	3.2638	-3.48684
<i>CR_03690W_A</i>	0.000322689	6.40476	1.12152	1.88095	-3.03612
<i>NIT2</i>	0.00718523	6.37931	1.33882	5.24138	1.1
<i>MCD1</i>	0.00135629	6.36364	-2.66667	5.81818	-2.91667

<i>C3_01310W_A</i>	0.000423131	6.30303	-1.5873	3.0303	- 3.30159
<i>C2_01420C_A</i>	3.22E-05	6.27273	-1.09615	5.18182	- 1.32692
<i>CR_07170W_A</i>	3.21E-05	6.25753	1.79633	11.4783	3.29503
<i>C1_07850C_A</i>	0.00619264	6.25	1.05556	6.75	1.14
<i>PHO114</i>	1.03E-05	6.22951	1.09524	3.09836	- 1.83575
<i>C7_01100C_A</i>	0.000291404	6.22222	-1.61538	4.66667	- 2.15385
<i>CDC13</i>	0.00151282	6.21053	-1.08511	5.36842	- 1.25532
<i>C3_03690W_A</i>	0.00772093	6.14286	1.75	2.28571	- 1.53571
<i>UPC2</i>	0.00127238	6.13725	-2.14286	3.82353	- 3.43956
<i>C3_01280W_A</i>	0.000246168	5.97333	-1.33014	3.70667	- 2.14354
<i>CR_08830W_A</i>	5.76E-05	5.85279	2.57705	1.54822	- 1.46692
<i>SGO1</i>	0.00586455	5.84211	1.37895	5	1.18018
<i>C5_03780C_A</i>	4.71E-05	5.83333	-1.29545	4.75	- 1.59091
<i>PYC2</i>	0.000195179	5.79628	2.35519	1.36059	- 1.80882
<i>MOB1</i>	0.00246076	5.73333	1.17647	6.23333	1.27907
<i>SRB1</i>	0.00266162	5.68454	-1.41732	4.09621	- 1.96689
<i>YCS4</i>	0.00464092	5.66667	-1.14971	5.3964	- 1.20729
<i>FGR29</i>	0.010961	5.65625	-1.15698	6.21875	- 1.05233
<i>C4_01800W_A</i>	0.00290599	5.6	-2.875	2.3	-7
<i>VTC3</i>	2.98E-05	5.44302	1.24691	1.78488	- 2.44566
<i>MUQ1</i>	0.000109807	5.42857	-1.05517	3.90306	- 1.46759
<i>C7_04090C_A</i>	1.09E-05	5.42188	-1.50307	3.82813	- 2.12883
<i>C2_01800W_A</i>	0.00540573	5.4	-1.38095	2.9	- 2.57143
<i>VTC4</i>	8.38E-06	5.34435	1.52059	2.93139	- 1.19897
<i>C2_08260W_A</i>	9.63E-05	5.32558	-1.09434	1.34884	- 4.32075
<i>PRR2</i>	0.000193008	5.28	1.40741	4.32	1.15152
<i>GOR1</i>	0.00120409	5.20091	-1.45714	4.19178	- 1.80794
<i>TRY3</i>	1.07E-06	5.16438	-1.55752	2.41096	- 3.33628
<i>C6_02450W_A</i>	0.00890948	5.15385	2.55	3.07692	1.52239

<i>C6_02990W_A</i>	0.000351654	5.14286	-1.2	4.5	- 1.37143
<i>CR_03480W_A</i>	0.00166156	5.11111	1.91176	3.77778	1.41304
<i>GAL4</i>	0.00402292	5.10714	-1.77966	3.75	- 2.42373
<i>C1_04010C_A</i>	0.000906677	5.1	-1.19048	-1.5	- 9.10714
<i>C1_02370C_A</i>	2.38E-05	5.09091	1.35616	4.42424	1.17857
<i>C3_05290C_A</i>	0.0015284	5.08333	1.4	1.66667	- 2.17857
<i>DAL1</i>	6.24E-05	5.07692	1.03125	4.92308	1
<i>DYN1</i>	0.00788314	5.06827	-1.07432	4.26707	- 1.27604
<i>C7_03140W_A</i>	0.00172926	5.0625	-1.07692	- 1.14286	- 6.23077
<i>C3_06920W_A</i>	0.000361807	5.04918	-1.14627	3.14754	- 1.83881
<i>MET13</i>	0.00021539	5.03704	1.20548	1.68981	- 2.47273
<i>REP1</i>	3.93E-05	5.00952	1.67562	4.25714	1.42395
<i>SMC1</i>	0.0026684	5	-1.39785	3.29114	- 2.12366
<i>C6_02420W_A</i>	7.47E-05	4.97727	-1.12195	2.09091	- 2.67073
<i>SAM2</i>	0.000521002	4.96687	-3.68053	2.0644	- 8.85524
<i>CDC47</i>	0.000119043	4.95146	1.03532	5.2233	1.09216
<i>CR_03270W_A</i>	0.00198107	4.94872	1.4	-1.56	- 5.51429
<i>CR_07480W_A</i>	1.63E-06	4.93173	-1.15913	2.45941	- 2.32435
<i>C3_02390W_A</i>	0.00497794	4.84615	1.6129	2.38462	-1.26
<i>CDC5</i>	0.00539896	4.84615	1.08027	4.34911	- 1.03149
<i>FGR6-10</i>	0.000261901	4.78571	1.36	3.57143	1.01493
<i>CAR1</i>	6.45E-05	4.76768	1.37129	6.12121	1.76059
<i>SNZ1</i>	0.00268658	4.7121	1.81099	6.18846	2.37839
<i>SMC4</i>	0.00719879	4.69091	1.20879	5.79091	1.49225
<i>CR_02060W_A</i>	0.00138695	4.68627	1.38188	3.02941	- 1.11944
<i>C4_04720W_A</i>	7.93E-05	4.68542	1.52786	5.73657	1.87063
<i>C7_00760C_A</i>	0.00990354	4.66667	-3	6	- 2.33333
<i>INO2</i>	0.00183972	4.66667	1.44444	3	- 1.07692
<i>TAZ1</i>	1.14E-07	4.66234	1.08676	2.84416	-1.5084
<i>C6_03420W_A</i>	0.0103438	4.625	1.45238	5.25	1.64865
<i>CR_00390W_A</i>	3.23E-05	4.6087	-1.12546	4.42029	- 1.17343
<i>TLO1</i>	6.80E-05	4.60377	1.82051	1.4717	- 1.71831

<i>C4_02420C_A</i>	0.00727645	4.6	-1.58333	3.8	- 1.91667
<i>SET6</i>	4.96E-07	4.54167	1.1985	2.78125	-1.3625
<i>BAT21</i>	0.00777654	4.52381	-1.15027	4.00952	- 1.29781
<i>C1_10920W_A</i>	0.00057068	4.5122	1.60435	5.60976	1.99459
<i>CHS2</i>	0.00792627	4.47126	-1.42322	4.36782	- 1.45693
<i>DBF2</i>	0.00524167	4.46512	1.17178	3.7907	- 1.00524
<i>C2_10650W_A</i>	0.000160256	4.46429	-1.86047	2.85714	- 2.90698
<i>PGA54</i>	0.00644003	4.41406	-1.33071	7.92187	1.34867
<i>CHT1</i>	0.00353238	4.41176	-3.20833	4.52941	-3.125
<i>C7_02140W_A</i>	0.00890509	4.4	1.77273	2.2	- 1.12821
<i>C1_03460C_A</i>	5.68E-09	4.3913	-1.01258	3.5	- 1.27044
<i>C1_08780W_A</i>	0.000166531	4.36816	1.32488	2.1592	- 1.52696
<i>ATG9</i>	0.000202466	4.3494	1.45492	2.93976	-1.0169
<i>CR_09070C_A</i>	0.00238812	4.32955	-1.37569	2.82955	- 2.10497
<i>C3_01180C_A</i>	0.00285446	4.32778	-1.0782	2.52778	- 1.84597
<i>C2_09030W_A</i>	7.34E-05	4.30556	1.66279	2.38889	- 1.08392
<i>RHD1</i>	1.36E-09	4.26006	-1.47403	1.40557	- 4.46753
<i>C4_03710C_A</i>	0.00119649	4.22581	1.7561	2.64516	1.09924
<i>GIN4</i>	4.92E-05	4.15294	1.20609	5.02353	1.45892
<i>FGR50</i>	0.000845042	4.14815	1.02679	4.14815	1.02679
<i>C7_01390W_A</i>	0.00146007	4.14286	-1.11765	2.71429	- 1.70588
<i>ALG7</i>	1.67E-05	4.14286	-1.08372	4.16071	- 1.07907
<i>SSP96</i>	0.00243893	4.125	1.29496	5.79167	1.81818
<i>AMO1</i>	0.00013286	4.10526	-1.10909	1.07018	- 4.25455
<i>PGA57</i>	0.00159445	4.09677	1.49412	2.74194	1
<i>C2_06130W_A</i>	0.00877743	4.08696	1.41803	5.30435	1.84043
<i>THI13</i>	0.000294525	4.07826	1.25	1.11304	- 2.93125
<i>CR_00910W_A</i>	0.00558391	4.07258	-1.16677	2.22465	- 2.13595
<i>C4_05790W_A</i>	0.00130176	4.06897	-1.45213	3.13793	- 1.88298
<i>TLO5</i>	0.002028	4.06667	1.46	3.33333	1.19672
<i>PLD1</i>	0.00017099	4.04818	1.15982	3.45273	-1.0109
<i>ACC1</i>	0.000452357	4.03542	-1.37582	4.42452	- 1.25483

<i>C2_01240C_A</i>	5.18E-07	4.03509	-1.15862	2.94737	- 1.58621
<i>C2_04830W_A</i>	6.61E-06	4.02857	-1.25	1.42857	-3.525
<i>GPD2</i>	1.25E-05	4.01449	1.00935	1.55072	- 2.56481
<i>ANT1</i>	0.00404156	4.01299	1.23437	3.32468	1.02265
<i>C1_07810C_A</i>	0.00041713	4	1.82437	5.31429	2.42381
<i>C4_06960W_A</i>	0.00282662	4	-1.21154	4.84615	1
<i>C2_06740W_A</i>	0.00584516	4	1.01087	3.06667	-1.29032
<i>BFA1</i>	0.0030478	4	1.40066	6.56522	2.29891
<i>RBE1</i>	0.000105444	4	1.54955	2.84615	1.10256
<i>C2_01260W_A</i>	4.69E-05	3.96	1.10499	5.08	1.41751
<i>C7_00240W_A</i>	0.000324686	3.95	1.36	2.5	- 1.16176
<i>CR_07160C_A</i>	1.98E-09	3.94982	1.16084	2.56272	- 1.32771
<i>C1_10510W_A</i>	7.77E-06	3.93878	-1.01493	2.77551	-1.4403
<i>CAN3</i>	9.31E-05	3.93333	-1.09392	3.3	- 1.30387
<i>QDR2</i>	3.65E-10	3.92667	1.21218	3.39333	1.04754
<i>C5_01310W_A</i>	0.000300987	3.92308	1.16842	3.65385	1.08824
<i>C4_01240C_A</i>	0.000878678	3.92308	-1.53846	4.61538	- 1.30769
<i>C1_10750C_A</i>	0.00716198	3.91667	1.39394	2.75	- 1.02174
<i>UME7</i>	0.00223235	3.91667	1.55814	1.79167	- 1.40299
<i>ECM18</i>	0.00523337	3.90909	1.25714	3.18182	1.02326
<i>MEP1</i>	0.00182872	3.88764	2.25	- 1.39062	- 2.40278
<i>TOS1</i>	0.0038297	3.88196	1.04394	4.91231	1.32103
<i>CR_06740W_A</i>	0.000673457	3.86957	1.15714	4.56522	1.36517
<i>C2_00350W_A</i>	5.80E-07	3.8626	-1.13008	3.18321	- 1.37127
<i>HCM1</i>	0.00484858	3.84615	-1.83333	3.38462	- 2.08333
<i>AFP99</i>	0.00460268	3.84211	1.28571	4.42105	1.47945
<i>MNT3</i>	1.34E-05	3.84	1	2.92	- 1.31507
<i>FCR1</i>	0.000334276	3.80055	-1.1626	2.37673	- 1.85908
<i>ZCF17</i>	4.58E-05	3.8	-1.61017	1.26667	- 4.83051
<i>DEM1</i>	5.22E-07	3.79221	1.6824	3.02597	1.34247
<i>PHO4</i>	3.36E-08	3.78322	?	?	?
<i>C1_07480C_A</i>	0.00312422	3.77778	1.375	2.66667	-1.0303
<i>C3_04740C_A</i>	0.00189085	3.775	1.38532	2.725	1
<i>C1_09670C_A</i>	0.000747718	3.77143	1.45745	2.68571	1.03788
<i>EXO1</i>	0.00165757	3.75676	-2.11111	3.59459	- 2.20635

<i>C7_01830W_A</i>	0.0102885	3.75	1.98214	3.5	1.85
<i>C5_03370C_A</i>	0.00907924	3.75	2.66667	1.5	1.06667
<i>C1_04350C_A</i>	0.00121655	3.71429	1.03226	3.54286	- 1.01562
<i>C3_05720C_A</i>	0.0055904	3.7037	1.2	4.25926	1.38
<i>C2_08380C_A</i>	0.000676625	3.70149	1.09845	2.8806	- 1.16981
<i>C5_03470C_A</i>	9.24E-10	3.68229	-1.22925	1.61979	- 2.79447
<i>C1_08140W_A</i>	0.0087703	3.68182	1.2439	5.59091	1.88889
<i>PLB5</i>	0.000579536	3.68135	-1.14315	2.9171	- 1.44264
<i>C6_01780C_A</i>	0.0066082	3.67568	-1.0625	7.35135	1.88235
<i>URA1</i>	0.000304929	3.67482	-1.37219	3.185	- 1.58322
<i>C1_07360W_A</i>	0.00133361	3.65263	-1.54313	2.54211	- 2.21725
<i>EBP7</i>	0.000968643	3.64706	-1.02449	3.69118	- 1.01224
<i>C1_05650W_A</i>	0.00133797	3.64103	1.13913	2.94872	- 1.08397
<i>FGR6-1</i>	0.000435037	3.63636	1.05195	3.5	1.0125
<i>IRR1</i>	0.00367946	3.62366	1.00809	3.98925	1.10979
<i>RCH1</i>	0.00010891	3.6087	1.26282	3.3913	1.18675
<i>C2_09110C_A</i>	0.00577446	3.6	-1.25	2	-2.25
<i>SPC2</i>	0.00436168	3.58824	-1.10204	3.17647	-1.2449
<i>GCV1</i>	5.40E-06	3.57983	1.25252	4.59244	1.60681
<i>KAR3</i>	0.00225046	3.57895	1.71111	2.36842	1.13235
<i>FCY2</i>	0.000260063	3.5679	-1.26457	3.48148	- 1.29596
<i>C2_01540W_A</i>	7.38E-05	3.56044	1.49275	1.51648	- 1.57282
<i>C5_04850W_A</i>	0.00672381	3.55556	1.84211	2.11111	1.09375
<i>SHM2</i>	2.63E-05	3.54633	-1.07909	2.86438	-1.336
<i>LAB5</i>	6.20E-06	3.52332	1.21843	3.03627	1.05
<i>MCT1</i>	9.91E-05	3.52273	1.27778	3.68182	1.33548
<i>C4_05980C_A</i>	6.33E-07	3.51852	1.56641	3.16049	1.40702
<i>C3_00170C_A</i>	0.000297357	3.51579	-1.25	1.36842	- 3.21154
<i>C1_05520W_A</i>	0.000278043	3.50633	1.20339	- 1.33898	- 3.90141
<i>CR_04560C_A</i>	0.000385819	3.5	-1.27778	2.46429	- 1.81481
<i>CDC54</i>	0.00823334	3.5	-1.01493	5.23077	1.47253
<i>DOA1</i>	0.00297423	3.49631	1.01307	3.38745	- 1.01882
<i>C5_01230C_A</i>	0.00765437	3.49524	1.21904	4.15238	1.44823
<i>PDC11</i>	0.00695704	3.49332	-2.63114	2.22941	- 4.12281
<i>C3_02080W_A</i>	1.66E-06	3.49007	1.56845	2.22517	1

<i>C5_04050W_A</i>	1.25E-05	3.4781	1.46501	1.61679	- 1.46841
<i>HSL1</i>	0.00305417	3.47208	-1.16075	3.15228	-1.2785
<i>C6_01380C_A</i>	5.25E-05	3.4697	1.00897	3.37879	- 1.01778
<i>C1_02730W_A</i>	0.00213283	3.45455	1.11765	1.54545	-2
<i>C6_02190C_A</i>	0.00241343	3.44444	1.03185	2.90741	- 1.14815
<i>C7_00490C_A</i>	0.00272564	3.44	-1.32143	2.96	- 1.53571
<i>FRP2</i>	0.00372604	3.43902	1.17537	6.53659	2.23404
<i>C6_01560W_A</i>	0.00735408	3.42857	1.46053	2.71429	1.15625
<i>STE13</i>	1.19E-05	3.42254	1.04049	3.47887	1.05761
<i>C3_07430W_A</i>	4.48E-05	3.41981	1.52198	1.71698	- 1.30866
<i>C7_03830C_A</i>	5.45E-05	3.41935	1.35227	2.83871	1.12264
<i>GDH3</i>	0.00371818	3.41727	1.19761	1.35612	-2.1041
<i>MUM2</i>	0.0055673	3.41509	1.10407	8.33962	2.69613
<i>RFA2</i>	0.00157789	3.40458	-1.34916	3.68702	- 1.24581
<i>DUO1</i>	0.00257497	3.4	1.66667	2.1	1.02941
<i>MEC3</i>	0.00108487	3.4	1.38636	3.52	1.43529
<i>IML2</i>	0.00277952	3.39916	1.3637	3.2521	1.3047
<i>RFA1</i>	0.000705996	3.39803	1.09754	3.19902	1.03326
<i>RHR2</i>	1.19E-05	3.37012	-3.075	1.25297	- 8.27083
<i>XUT1</i>	0.00822623	3.35714	-1.36667	2.92857	- 1.56667
<i>C5_03080C_A</i>	0.00021248	3.35526	1.13523	3.69737	1.25098
<i>NTH1</i>	0.00170404	3.35224	-1.37076	1.93134	- 2.37924
<i>C4_06710W_A</i>	0.000405557	3.34203	1.30478	2.06377	- 1.24112
<i>C1_13810W_A</i>	0.000540773	3.33607	1.35593	3.38525	1.37592
<i>C7_04340C_A</i>	0.00897049	3.33333	-1.4	1.16667	-4
<i>C5_04360C_A</i>	0.000697989	3.31953	1.17112	2.21302	- 1.28082
<i>SAP99</i>	8.05E-05	3.31034	1.14583	1.65517	- 1.74545
<i>SUR2</i>	1.92E-05	3.30446	-1.54447	1.50394	- 3.39353
<i>C1_02910C_A</i>	0.000579829	3.30303	1.875	2.30303	1.30734
<i>SPC98</i>	0.0017972	3.27451	1.10326	3.60784	1.21557
<i>ROD1</i>	0.000474621	3.2657	-1.22165	1.14493	- 3.48454
<i>WSC4</i>	0.000376868	3.25108	-2.01705	1.5368	- 4.26705
<i>C1_02970W_A</i>	0.00119998	3.24834	1.18061	2.73179	- 1.00719

<i>C3_02710W_A</i>	0.00033856	3.24242	-1.63235	3.36364	-1.57353
<i>HIS1</i>	9.82E-09	3.2243	-2.27273	-1.42667	-10.4545
<i>CR_06230W_A</i>	7.21E-08	3.2193	1.18378	1.62281	-1.6758
<i>C2_07580W_A</i>	0.000155781	3.21739	1.30769	2.26087	-1.08824
<i>CAN1</i>	0.000434992	3.20812	1.89607	2.00254	1.18354
<i>FRE9</i>	1.17E-05	3.18421	-2.09091	1.81579	-3.66667
<i>INP51</i>	0.00221788	3.18182	1	3.34848	1.05238
<i>TPS3</i>	3.40E-05	3.16655	1.33331	2.38607	1.00468
<i>RTA2</i>	0.00947816	3.16571	-1.5945	4.96571	-1.01651
<i>MCM6</i>	0.00011267	3.16418	-1.17391	2.8209	-1.31677
<i>MLH1</i>	0.00234452	3.16216	1.36607	3.02703	1.30769
<i>C3_00830C_A</i>	0.00027049	3.16058	1.17882	3.10219	1.15704
<i>C4_04860W_A</i>	5.61E-05	3.14943	1.27273	2.14943	-1.15126
<i>GPT1</i>	0.00145917	3.13793	1.2	3.62069	1.38462
<i>CDC46</i>	6.71E-05	3.13333	-1.1597	3.38889	-1.07224
<i>APE3</i>	0.000514982	3.13313	1.01111	2.50774	-1.23565
<i>C1_04580C_A</i>	0.00995288	3.13043	-1.5119	2.76087	-1.71429
<i>YMC1</i>	0.0023027	3.125	-6.94737	2.75	-7.89474
<i>SAP10</i>	6.62E-05	3.12195	1.29924	2.14634	-1.11953
<i>CCN1</i>	0.00240632	3.11905	1.11024	3.02381	1.07634
<i>FMO1</i>	0.000370196	3.11905	1.07477	2.54762	-1.13913
<i>C1_04640W_A</i>	0.00366365	3.11801	1.19388	3.65217	1.39841
<i>SCS7</i>	8.10E-06	3.11015	-1.18332	4.24514	1.15347
<i>C4_03960W_A</i>	0.00215236	3.10825	-1.77778	-1.73214	-9.57143
<i>PFK2</i>	0.000397306	3.10744	1.0008	2.15626	-1.43997
<i>C3_03670W_A</i>	0.000628633	3.10526	-1.09542	2.51754	-1.35115
<i>DAC1</i>	0.000123591	3.10405	-1.05641	3.57225	1.08939
<i>PDX1</i>	0.000295403	3.10277	1.10442	2.47299	-1.13603
<i>C5_04310W_A</i>	0.000341972	3.1	1.34559	3.4	1.47581
<i>FRP6</i>	6.11E-05	3.09881	-1.03492	2.57708	-1.24444
<i>KAR2</i>	0.00872472	3.09524	1.05796	2.81494	-1.03934
<i>DAL9</i>	0.000105854	3.09333	1.32719	2.89333	1.24138

RNR21	0.00458944	3.09258	-1.77527	2.57046	- 2.13587
C2_06550W_A	0.00404969	3.08824	1.18072	4.88235	1.86667
PDB1	0.000397753	3.08621	-1.15407	3.14799	- 1.13142
C1_10410W_A	0.0087363	3.08163	1.47534	4.55102	2.17881
C2_03700W_A	0.00602723	3.08	1.63793	2.32	1.23377
C4_02510W_A	0.00116271	3.07463	-1.0146	2.07463	- 1.50365
C6_03810W_A	0.00163594	3.07143	1.23729	2.52857	1.0186
FRP3	0.000314935	3.07126	-1.20175	2.94299	- 1.25412
RME1	5.92E-05	3.0493	1.94872	1.09859	- 1.42434
C4_00860C_A	0.000116291	3.04255	-1.09028	3.34043	1.00699
CTA26	0.00221404	3.032	1.51095	1.096	- 1.83092
C6_01870C_A	1.17E-05	3.02299	1.14552	3.08046	1.1673
POL2	2.32E-06	3.0229	-1.11321	2.25191	- 1.49434
C2_04110W_A	0.00136344	3.02222	1.26036	3.75556	1.56618
ARE2	2.45E-05	3.00901	1.08286	1.57658	- 1.76253
PST3	0.00128139	3.00298	-1.24046	1.61149	- 2.31157
C4_03160C_A	0.00766912	3	1.16981	2.65	1.03333
VPS4	0.0009921	3	1.16667	2.88889	1.12346
NIK1	3.31E-05	2.99273	1.37543	2.10182	- 1.03522
MIH1	0.00514989	2.985	-1.04244	1.965	- 1.58355
POL3	2.17E-07	2.98256	1.19071	3.00291	1.19883
C2_07420W_A	0.00600121	2.9771	-1.59655	1.76718	- 2.68966
C1_08840W_A	0.00069902	2.97561	-1.04819	2.12195	- 1.46988
ACB1	0.000288597	2.97368	-1.05532	2.17544	- 1.44255
C3_02060W_A	0.00357043	2.9697	1.52	2.27273	1.16327
SUN41	0.000159529	2.96945	-1.13957	3.99636	1.18099
CR_05900W_A	1.66E-05	2.96639	1.09091	2.95798	1.08782
ISC1	0.000111539	2.95522	1.32171	1.92537	- 1.16129
GPM1	6.90E-05	2.95029	-1.08253	2.06266	- 1.54838
ADE6	0.000630487	2.94498	-2.57916	2.2799	- 3.33153
PEX22	0.00251699	2.93846	1.22297	2.27692	- 1.05525
PMT2	0.00349014	2.93228	-1.29853	2.50709	- 1.51876

<i>C7_00870W_A</i>	0.00286336	2.925	2.27869	1.525	1.18803
<i>BMT6</i>	1.89E-07	2.925	1.03178	2.5175	- 1.12608
<i>C6_04420W_A</i>	1.13E-10	2.92441	1.92766	2.35786	1.55421
<i>C3_05800W_A</i>	0.00435068	2.92157	1.14912	2.23529	-1.1374
<i>PDS5</i>	0.00481959	2.92	-1.11878	2.025	- 1.61326
<i>BMT1</i>	0.000468491	2.91837	-1.34286	- 1.04255	- 4.08571
<i>CR_05770W_A</i>	4.20E-06	2.90909	1.7561	2.48485	1.5
<i>BMT5</i>	0.00129452	2.90206	1.52161	3.45876	1.8135
<i>BRN1</i>	0.000842236	2.89655	1.3951	3.28736	1.58333
<i>C2_07040W_A</i>	0.00014198	2.89333	-1.19091	1.74667	- 1.97273
<i>CMK1</i>	0.009213	2.88998	-1.31692	2.73856	- 1.38973
<i>CAF16</i>	0.000109526	2.88832	1.12935	2.04061	-1.2533
<i>C2_06430C_A</i>	0.00121549	2.88462	-1.14706	3	- 1.10294
<i>C1_03270W_A</i>	0.00273572	2.88104	1.82467	3.07435	1.9471
<i>SYG1</i>	0.000588836	2.88	-1.44231	1	- 4.15385
<i>GLC3</i>	0.000224606	2.87511	1.06304	2.11965	- 1.27597
<i>C3_02980C_A</i>	0.00716529	2.86842	-1.90278	3.60526	- 1.51389
<i>C2_00650W_A</i>	1.24E-05	2.86431	1.28526	2.76106	1.23893
<i>APT1</i>	0.000343748	2.86207	-1.75652	1.3931	-3.6087
<i>C5_00340W_A</i>	0.00581797	2.85915	1.2723	3	1.33498
<i>C3_01190C_A</i>	8.23E-06	2.84932	1.00676	2.0274	- 1.39597
<i>C2_08460C_A</i>	0.000865473	2.84615	1.25316	3.03846	1.33784
<i>C2_07220W_A</i>	0.00518128	2.84553	-1.07553	2.89431	-1.0574
<i>RIM1</i>	0.00939878	2.84328	1.49536	4.02239	2.11549
<i>DPB4</i>	0.00108314	2.84091	1.43976	1.88636	- 1.04603
<i>CR_10630W_A</i>	0.00761337	2.84	1.76812	2.76	1.71831
<i>UGA32</i>	6.99E-05	2.83529	1.53623	2.43529	1.3195
<i>ELA1</i>	0.0036117	2.83333	-1.15152	2.53333	- 1.28788
<i>RAD18</i>	0.000152006	2.83099	1.08411	3.01408	1.15423
<i>C1_03180W_A</i>	0.00134943	2.82609	-1.07895	3.56522	1.16923
<i>TPT1</i>	0.00815166	2.825	-1.25	2.625	- 1.34524
<i>C3_03160C_A</i>	0.00470189	2.8	1.0303	3.96	1.45714
<i>C6_01480W_A</i>	0.00562959	2.8	1.89474	1.26667	- 1.16667
<i>CAC2</i>	0.000186854	2.8	1.21481	4.15385	1.8022
<i>RNR22</i>	0.000167877	2.79259	-2.99573	1.15391	-7.25

GLT1	0.000198724	2.79047	1.50286	1.39241	- 1.33349
C7_03860W_A	0.00426097	2.7883	-1.02062	1.12194	- 2.53649
FBA1	0.00807266	2.78172	-1.06208	2.31494	- 1.27623
C5_05210W_A	0.00194139	2.77841	1.40367	2.47727	1.25153
C3_00500C_A	1.32E-05	2.77519	1.18971	2.41085	1.03352
HIR1	1.46E-06	2.77428	1.41682	2.7769	1.41816
HOS1	3.79E-05	2.77419	1.38854	2.53226	1.26744
ECM42	0.0002564	2.77358	1.41944	2.26415	1.15873
SLF1	0.000280432	2.76471	-1.75	1.44118	- 3.35714
C6_00080C_A	0.00152931	2.75	-1.34545	3.96429	1.07143
CR_07500W_A	0.00661692	2.75	1.04494	2.02273	- 1.30108
C7_04240C_A	0.00124207	2.74747	-1.25085	3.72727	1.08456
C7_01910C_A	0.00155984	2.7451	1.32	3.92157	1.88571
MTR2	0.0040211	2.72857	-1.69421	2.92857	- 1.57851
C2_02930C_A	0.000214836	2.72492	-1.29036	1.99191	-1.7652
APC1	0.00074384	2.72165	1.22163	3.24055	1.45455
C4_04920W_A	0.000155502	2.72131	1.00568	2.88525	1.06627
C4_06950W_A	0.000118067	2.71429	-1.16429	3.32653	1.05263
C6_01300W_A	0.000132635	2.71053	1.19014	1.86842	- 1.21893
C1_05010C_A	1.24E-05	2.70874	-1.24766	2.59223	- 1.30374
C3_02090C_A	0.00285612	2.70089	-1.01737	2.35268	- 1.16795
HST2	8.38E-06	2.69767	1.92517	1.7093	1.21983
LSC2	6.73E-05	2.6976	-1.49178	1.62974	- 2.46924
SAC1	0.00713392	2.69697	1.06728	3.30303	1.30712
SWI6	0.00547231	2.69118	1.07692	2.67647	1.07104
CR_07140C_A	0.01049	2.69048	1.80882	1.61905	1.0885
C4_00680W_A	5.82E-05	2.68817	1.16667	2.16129	-1.0661
C2_00280C_A	0.000489532	2.6875	1.17	3.125	1.36047
C2_07110C_A	0.000128777	2.68557	1.13318	2.28351	- 1.03785
C5_03740W_A	0.000233754	2.68	1.62112	2.14667	1.29851
CR_08470W_A	0.000169574	2.67407	1.32081	2.56296	1.26593
C5_00750C_A	0.00383104	2.67371	1.31618	2.55399	1.25724
C7_04160W_A	0.00265811	2.67347	1.31481	3.30612	1.62595
C1_00370W_A	0.00223274	2.66667	1.5	2.51852	1.41667
C2_10740C_A	0.000731809	2.66605	-1.94974	1.35978	- 3.82275
C7_00850W_A	0.000516243	2.65487	1.44882	1.12389	- 1.63043

<i>C4_05390W_A</i>	0.00432834	2.65089	1.16533	2.21893	- 1.02517
<i>CR_03220C_A</i>	2.36E-05	2.64865	1.45349	2.32432	1.27551
<i>PHO91</i>	1.82E-06	2.64719	-1.28025	1.74026	- 1.94745
<i>C4_07210W_A</i>	0.00586042	2.63793	1.45305	3.67241	2.02288
<i>HMX1</i>	0.000103219	2.63483	-1.63039	2.69288	- 1.59524
<i>SLD1</i>	2.57E-06	2.63473	-1.03256	2.65868	- 1.02326
<i>BUB1</i>	0.00668552	2.63317	1.6874	3.23116	2.07061
<i>THI4</i>	0.000516543	2.63248	1.41139	1.35043	- 1.38117
<i>GST2</i>	0.00023968	2.63092	1.86254	- 1.17419	- 1.65859
<i>SNQ2</i>	1.22E-05	2.62424	1.34225	1.35909	- 1.43854
<i>QDR1</i>	0.00246854	2.62346	-2.42857	1.15432	- 5.51948
<i>IFD6</i>	0.0020801	2.62051	1.03934	-2.4623	-6.2082
<i>C1_01400C_A</i>	3.04E-06	2.62014	1.22541	1.1167	- 1.91472
<i>C3_01940C_A</i>	0.0025921	2.61161	2.09454	2.125	1.70427
<i>PRN1</i>	0.00478734	2.60811	1.73023	2.90541	1.92746
<i>RBR3</i>	1.90E-05	2.60543	1.12088	2.27975	- 1.01961
<i>GAT1</i>	0.000563439	2.60256	1.73913	1.47436	-1.015
<i>C6_03620C_A</i>	2.62E-05	2.60227	1.63735	4.19886	2.64192
<i>PGA52</i>	2.23E-05	2.59836	-1.4556	2.05675	- 1.83891
<i>C5_03700C_A</i>	0.0100095	2.59574	-1.09278	2.25532	- 1.25773
<i>MSH2</i>	7.29E-06	2.59128	1.32632	2.3297	1.19243
<i>MSB1</i>	0.00866975	2.58824	1.08466	3.70588	1.55303
<i>C4_05970W_A</i>	6.09E-06	2.58781	1.14248	2.74194	1.21053
<i>C3_00310C_A</i>	0.00765565	2.58621	-1.22917	2.03448	-1.5625
<i>C3_07230W_A</i>	0.00293766	2.58519	1.17939	1.94074	- 1.12945
<i>MIT1</i>	0.000340209	2.58454	1.12939	2.2029	- 1.03883
<i>PRP22</i>	0.00625962	2.58389	1.22014	5.73154	2.70649
<i>YCP4</i>	0.00186001	2.58386	-1.03772	1.7086	- 1.56931
<i>CR_03470W_A</i>	4.78E-05	2.58333	1.36146	2	1.05403
<i>C7_01650W_A</i>	0.00147834	2.58286	-1.31694	2.75429	- 1.23497
<i>GUT2</i>	0.00303284	2.57882	1.30927	3.92426	1.99236
<i>C6_01550C_A</i>	4.70E-05	2.57396	1.38017	2.14793	1.15172
<i>C5_00180W_A</i>	6.51E-06	2.57307	1.25849	2.48854	1.21715

<i>C4_01300W_A</i>	0.000891684	2.57179	1	1.84635	- 1.39291
<i>C1_02030C_A</i>	0.000597936	2.57143	-1.04	2.78571	1.04167
<i>C3_01780C_A</i>	0.00350235	2.57143	1.07407	1.92857	- 1.24138
<i>C4_04510W_A</i>	2.49E-05	2.56643	1.57321	3.09266	1.89578
<i>C2_09280C_A</i>	1.02E-05	2.56593	1.15214	3.97253	1.78373
<i>ADE1</i>	2.69E-06	2.55416	1.07475	2.76322	1.16272
<i>TBF1</i>	0.00119791	2.5473	-1.61187	2.38514	- 1.72146
<i>C2_06110W_A</i>	2.18E-05	2.54299	1.20196	2.30769	1.09075
<i>C4_01420W_A</i>	0.00162401	2.53659	-1.10818	1.70732	- 1.64644
<i>ARF1</i>	0.00434093	2.51734	1.53645	3.6474	2.22618
<i>YDC1</i>	0.000962901	2.51697	1.25055	1.8004	- 1.11791
<i>MET6</i>	6.71E-05	2.51573	1.3077	1.5258	- 1.26084
<i>C3_05060W_A</i>	0.00346714	2.51515	1.35644	3.06061	1.6506
<i>POT1-2</i>	0.00974313	2.51402	1.52471	3.97196	2.40892
<i>C4_03580W_A</i>	0.00858787	2.51351	1.46296	2.91892	1.69892
<i>LIP6</i>	0.000572316	2.51327	-1.00778	2.29204	- 1.10506
<i>C4_03720C_A</i>	0.00165097	2.50943	1.31034	2.46226	1.28571
<i>C4_02160C_A</i>	0.000371726	2.5082	1.11465	2.57377	1.14379
<i>GUT1</i>	0.00132739	2.50691	1.26203	3.64055	1.83272
<i>C4_06410W_A</i>	0.000341328	2.5	1.4	2.2	1.232
<i>C2_07790C_A</i>	0.00117858	2.5	1.28571	2.15385	1.10769
<i>C6_01750C_A</i>	0.0103244	2.5	-1.18519	2.52632	- 1.17284
<i>EAF6</i>	0.0028001	2.5	-1.02521	1.96774	- 1.30252
<i>HPA2</i>	0.00189588	2.5	1.07071	2.475	1.06
<i>PIR1</i>	0.00021424	2.49818	1.25	1.94187	- 1.02919
<i>STP1</i>	3.63E-05	2.49765	1.35863	1.57746	- 1.16539
<i>C2_06780C_A</i>	0.000203968	2.49306	1.47009	1.625	-1.0436
<i>C5_00580W_A</i>	0.00759363	2.4881	1.41779	2.36508	1.34769
<i>C6_04550C_A</i>	1.94E-06	2.4697	1.08362	3.18398	1.39702
<i>SAH1</i>	1.31E-05	2.46918	-1.15232	1.83847	- 1.54763
<i>C4_01830C_A</i>	5.73E-05	2.46885	1.02009	2.12131	- 1.14091
<i>PFK26</i>	0.000589848	2.4656	1.26807	1.25344	- 1.55123
<i>CR_02570C_A</i>	0.00282899	2.46479	1.51852	2.28169	1.40571
<i>CR_05550C_A</i>	0.0044547	2.45833	-1.36748	2.06127	- 1.63089

YWP1	6.39E-05	2.4563	-2.5647	1.30523	- 4.82647
C1_04960C_A	0.000147189	2.45614	1.39037	1.64035	- 1.07692
C1_11990W_A	0.0101571	2.45588	1.51111	1.98529	1.22156
DIP5	0.000395068	2.44771	1.15287	2.69914	1.27129
C5_03920C_A	0.00790545	2.44444	-1.90323	2.18519	- 2.12903
LIP5	0.00121716	2.44444	1.23478	1.59722	- 1.23944
C1_10520W_A	0.000198447	2.44304	1.33113	1.91139	1.04145
C5_01260W_A	0.00719672	2.44	2.04211	1.9	1.59016
KCH1	0.00162087	2.4382	-1.03488	2	- 1.26163
C2_01190C_A	0.00127737	2.43548	1.08621	1.87097	- 1.19841
KIP4	0.00548131	2.43478	-1.36691	2.75362	- 1.20863
RAD53	0.00182616	2.43478	1.06931	2.19565	- 1.03704
LIG1	0.000245423	2.43172	1.08379	2.4185	1.0779
C4_05850C_A	3.82E-06	2.42975	1.09677	2.81818	1.27211
SMI1B	0.00701184	2.42857	1.59036	2.96429	1.94118
PHM5	0.000601631	2.42779	-1.07937	1.11172	- 2.35714
MRP8	0.000610857	2.4252	-1.04096	2.40157	- 1.05119
C7_04290W_A	0.00115484	2.42308	1.2707	2.41538	1.26667
C4_05800C_A	0.00271059	2.42149	1.79126	1.70248	1.25939
COG4	0.00786742	2.42017	1.47468	2.65546	1.61806
C6_03310W_A	0.000350349	2.41951	1.00446	2.18537	- 1.10222
RPT1	0.00951254	2.41849	1.50307	2.29653	1.42728
HOS3	0.0023442	2.41667	1.04994	3.51316	1.52632
SEC20	0.00686728	2.41509	-1.05882	2.71698	1.0625
C3_00420W_A	0.00449848	2.41379	-1.40723	2.51724	-1.3494
CR_01410C_A	0.00497552	2.4127	-1.86301	1.43915	- 3.12329
C1_08900W_A	6.23E-05	2.41104	1	- 1.05844	- 2.55195
ABC1	3.58E-06	2.41058	1.17897	2.37374	1.16096
CR_02910W_A	0.00183989	2.40934	1.41926	1.8544	1.09236
PCL7	0.00106202	2.40662	1.13818	2.02252	- 1.04545
C4_00470C_A	0.000185723	2.405	1.32522	2.26	1.24532
CR_03260W_A	0.00528006	2.40385	1.77251	2.70513	1.99467
C2_09670C_A	2.68E-05	2.40379	-1.09375	2.64984	1.00787
C4_05160C_A	0.000188329	2.40351	1.21359	1.80702	-1.096
PIKA	0.00107226	2.40299	1.08013	2.23507	1.00466

CR_01420W_A	0.00941128	2.4	1.20793	3.48095	1.75198
C4_07060W_A	2.81E-06	2.39916	-1.00622	1.85893	- 1.29864
C4_00030C_A	0.000127446	2.3985	-1.34979	2.46617	- 1.31276
ADH1	0.000245129	2.39772	-1.063	1.89068	- 1.34807
APG7	0.00197981	2.39634	1.19155	2.16463	1.07634
IFF5	3.98E-05	2.3951	1.42495	1.79371	1.06715
DNA2	0.0034125	2.39286	-1.18012	1.69643	-1.6646
CR_07910C_A	1.44E-06	2.39114	1.41885	2.35067	1.39484
C3_06280W_A	0.00414699	2.3875	-1.39212	3.09167	- 1.07505
SMC6	0.000731606	2.38723	1.3133	1.98298	1.09091
PDA1	0.00903289	2.37851	-1.12852	3.18273	1.18573
LIP7	0.0073149	2.375	1.7931	1.20833	- 1.09615
APS3	0.00321568	2.37405	1.24498	1.90076	- 1.00323
RFC1	0.000264321	2.3727	1.2041	2.75197	1.39657
MNN11	0.00698025	2.37037	-1.07273	2.18519	- 1.16364
CTA7	0.000328766	2.36364	-1.09875	3.5404	1.36325
FGR34	0.00583272	2.36364	1.11789	2.79545	1.32212
SWD2	0.00281964	2.36275	1.18235	3.33333	1.66805
C1_10730W_A	5.94E-08	2.35967	1.05457	1.84741	- 1.21119
ADE2	0.00555488	2.35965	-1.17866	2.77778	- 1.00124
CWH41	0.000156658	2.35685	1.45073	2.27386	1.39965
C1_05160C_A	0.00578896	2.35551	1.40596	2.07625	1.23928
VPS53	7.39E-05	2.35207	1.18889	2.66272	1.34591
C1_13560W_A	0.00495984	2.34783	1.63636	2.15217	1.5
RCK2	2.58E-07	2.34707	-1.02807	1.39303	- 1.73216
MED18	0.00180072	2.34615	1.30488	2.10256	1.1694
PET127	0.00826261	2.34392	-1.16288	1.62434	- 1.67803
HOG1	0.00638133	2.343	-1.02519	3.93237	1.63711
GDB1	0.00179275	2.3427	1.17784	2.14725	1.07958
DFG5	0.000253224	2.33684	1.0472	2.00702	- 1.11185
C2_10760C_A	5.67E-06	2.33666	1.16909	2.22693	1.11419
ADE13	4.70E-06	2.33565	1.12222	3.30961	1.59019
C4_06020C_A	0.00447052	2.3299	1.47295	2.57216	1.62611
CR_05010W_A	0.000243499	2.32895	1.59239	2.42105	1.65537
C1_09790C_A	0.000282221	2.32669	-1.43682	1.58566	-2.1083
CR_00190W_A	0.000124729	2.32402	-1.71569	1.95531	- 2.03922

<i>RPD31</i>	0.00436784	2.32394	1.26381	2.6338	1.43232
<i>C3_01770C_A</i>	0.000633426	2.31959	1.46392	2	1.26222
<i>C1_01360C_A</i>	0.000897374	2.31892	-1.06868	2.56997	1.03704
<i>C6_00890W_A</i>	0.00787393	2.31875	1.2884	2.99063	1.66173
<i>C1_03140W_A</i>	0.0006133	2.31746	1.30935	2.20635	1.24658
<i>C1_03990W_A</i>	0.000739392	2.31579	1.13761	1.43421	- 1.41935
<i>ZCF2</i>	3.86E-05	2.31563	1.56718	2.34901	1.58978
<i>C4_00840W_A</i>	6.33E-05	2.31385	1.32635	2.49846	1.43218
<i>C1_11790W_A</i>	0.00933156	2.3125	-1.27273	1.75	- 1.68182
<i>MIG1</i>	0.00554677	2.3119	1.03951	1.05788	- 2.10234
<i>MRS2</i>	0.00103771	2.31081	1.44516	2.09459	1.30994
<i>CR_00880W_A</i>	0.00035099	2.30952	1.58163	2.33333	1.59794
<i>CDC23</i>	0.000722489	2.30806	1.07895	2.52133	1.17864
<i>C6_02810C_A</i>	0.000656727	2.30769	-1.13287	1.66154	- 1.57343
<i>FGR17</i>	0.00144179	2.30682	-1.32	1.875	-1.624
<i>ATG1</i>	0.000579392	2.30653	1.87289	1.6407	1.33224
<i>TPS2</i>	0.00211418	2.30373	1.62057	2.40861	1.69435
<i>CR_10800C_A</i>	0.00902702	2.30238	-1.12511	2.95476	1.14064
<i>CR_08350W_A</i>	0.00118207	2.30197	1.11425	1.78118	- 1.15987
<i>SIT1</i>	0.00839116	2.29843	-8.1	1.27225	- 14.6333
<i>C1_08860C_A</i>	0.000984632	2.29832	1.55965	1.93697	1.31444
<i>C4_04090C_A</i>	0.00180859	2.29539	-1.14929	1.31436	- 2.00711
<i>C4_07130W_A</i>	5.62E-05	2.29517	-1.01256	1.44781	- 1.60518
<i>C4_02770C_A</i>	0.00279428	2.29323	1.46226	2.39098	1.52459
<i>C6_02200C_A</i>	0.0107033	2.29167	1.89474	1.58333	1.30909
<i>VRP1</i>	0.00369515	2.29032	-1.35	1.74194	-1.775
<i>C3_07330W_A</i>	0.00395259	2.28571	1.67925	1.51429	1.1125
<i>MCD4</i>	0.00303227	2.28571	-1.28395	1.65079	- 1.77778
<i>SAP1</i>	0.00214831	2.28	-1.5	2.4	-1.425
<i>DOA4</i>	0.00170669	2.2795	1.19771	2.1677	1.13896
<i>PFK1</i>	0.00216665	2.27858	1.15867	1.46044	- 1.34654
<i>C4_06690C_A</i>	0.00934251	2.2754	1.29502	1.90519	1.08433
<i>C4_05650W_A</i>	0.000639503	2.27419	-1.06322	1.49194	- 1.62069
<i>C6_03950C_A</i>	0.00108408	2.27273	1.43293	2.12987	1.34286
<i>IML1</i>	2.25E-05	2.27027	1.70769	2.25869	1.69898
<i>SLU7</i>	0.0100984	2.27027	1.2	1.89189	1
<i>RIA1</i>	4.82E-05	2.26888	-1.07741	2.03927	- 1.19872

CR_07250C_A	0.000540869	2.26778	1.432	2.08018	1.31354
C6_02210W_A	0.00409861	2.26667	1.84375	- 1.40625	- 1.72881
CR_02300C_A	0.0053941	2.26531	1.71163	2.98251	2.25354
C2_08060W_A	0.000272433	2.26471	1.17054	1.89706	- 1.01987
PRC3	5.72E-08	2.26378	1.32805	1.1601	- 1.46934
VPS34	0.000696173	2.25926	1.49068	2.38519	1.57377
NPT1	0.00202081	2.25912	1.20911	2.16423	1.15832
C3_00270C_A	0.000186308	2.25907	1.31452	3.21244	1.86927
C1_06480C_A	0.00206435	2.25806	-1.14493	2.54839	- 1.01449
CR_04180C_A	3.97E-05	2.2579	1.29189	1.88686	1.07959
C1_05320C_A	0.00501088	2.25641	-1.0991	3.12821	1.26136
TDH3	0.00580079	2.25591	1.06226	1.83851	- 1.15512
C1_00570C_A	0.000176711	2.25392	1.53222	2.4326	1.65369
VID27	0.00801352	2.25091	1.17085	2.29106	1.19173
C3_06400C_A	0.00121688	2.25	-1.15493	2.92857	1.12698
ARO7	0.00683738	2.24638	1.67241	2.52174	1.87742
PTP1	0.000657886	2.24576	-1.22396	1.99153	- 1.38021
CR_06090W_A	0.0013774	2.24537	1.05732	1.4537	- 1.46084
ARG8	0.00582161	2.24352	1.51186	1.5285	1.03002
MRR1	0.000677856	2.24312	1.68649	- 1.17838	- 1.56731
CAS4	0.000283713	2.24136	1.03221	1.07256	- 2.02452
HSE1	0.00182189	2.241	1.50147	1.88366	1.26205
C4_04160W_A	0.000205983	2.24099	1.17463	1.50901	- 1.26429
C4_01760W_A	0.00227154	2.23913	-1.63158	2.69565	- 1.35526
C1_07440W_A	6.15E-07	2.23847	1.1372	1.9062	- 1.03264
C4_06090C_A	0.00996441	2.23762	1.11574	2.13861	1.06637
CR_03230W_A	0.00286935	2.23669	1.55752	1.33728	- 1.07386
C4_02520C_A	0.00707831	2.23611	1.66942	1.68056	1.25466
PGK1	0.00460186	2.2354	1.10581	1.37924	- 1.46566
CR_09990W_A	0.00401191	2.2342	1.84917	2.08674	1.72712
SCH9	1.87E-06	2.23182	1.27513	1.71818	- 1.01867
C5_01930W_A	0.000226778	2.23171	1.30408	1.94512	1.13661
C2_05810W_A	0.00163846	2.22667	-1.0723	1.60667	-1.4861
CR_01950W_A	0.00338161	2.22556	-2.11628	1.36842	- 3.44186

<i>C4_00070C_A</i>	0.000161619	2.22538	1.25513	3.5793	2.01875
<i>SHP1</i>	0.00609861	2.22383	1.20608	2.11755	1.14844
<i>C4_02570C_A</i>	0.000705372	2.22335	1.13127	2.62944	1.3379
<i>DES1</i>	0.0067245	2.22222	-1.36192	2.51646	- 1.20267
<i>SEC13</i>	0.00738763	2.22179	1.00913	2.55837	1.162
<i>C2_10630W_A</i>	3.91E-05	2.21887	1.43119	2.0566	1.32653
<i>OPT3</i>	0.000452309	2.21749	2.09354	2.28924	2.16127
<i>UGA33</i>	0.00398372	2.21311	1.06767	2.18033	1.05185
<i>SET3</i>	0.00046782	2.21203	-1.12295	1.73418	- 1.43238
<i>C1_06910C_A</i>	1.83E-06	2.21065	1.301	1.86111	1.09529
<i>C5_04030W_A</i>	4.18E-06	2.21061	1.69681	- 1.65426	- 2.15517
<i>BNR1</i>	0.00667455	2.21019	-1.09859	1.49045	- 1.62911
<i>TRK1</i>	6.79E-06	2.20741	1.1319	1.60988	- 1.21138
<i>ARG5,6</i>	0.00824991	2.20592	-1.40533	1.34859	- 2.29874
<i>NDE1</i>	0.00369686	2.20526	1.4238	1.95132	1.25984
<i>C3_06530W_A</i>	0.00514281	2.20513	-1.12346	2.33333	- 1.06173
<i>C2_07760W_A</i>	0.000122275	2.2037	1.84892	2.14506	1.79972
<i>ULP3</i>	0.000392424	2.20308	1.47705	1.54154	1.03352
<i>CR_00130C_A</i>	0.00676236	2.20266	1.02718	2.32226	1.08296
<i>C2_02820C_A</i>	0.00909101	2.2	-1.32718	2.18696	- 1.33509
<i>C5_03690W_A</i>	0.000755885	2.19792	1.34466	2.14583	1.3128
<i>ZCF11</i>	0.000266132	2.19658	1.40064	2.66667	1.70039
<i>DAL5</i>	0.00176567	2.19565	1.43956	1.97826	1.29703
<i>KAR9</i>	0.000191622	2.19333	-1.24786	-1.0274	- 2.81197
<i>CR_03710C_A</i>	0.00507166	2.192	1.81081	2.072	1.71168
<i>RAD57</i>	0.00560171	2.19178	1.28177	2.47945	1.45
<i>C7_00270W_A</i>	0.00146901	2.19139	-1.25616	2.44019	- 1.12808
<i>CEF1</i>	4.97E-05	2.19104	1.3164	2.05672	1.23569
<i>CPA1</i>	0.00147	2.19048	1.95281	1.17725	1.04952
<i>CLA4</i>	0.00291738	2.18954	-1.18634	1.24837	- 2.08075
<i>SRO77</i>	9.76E-05	2.18889	1.32434	2.52222	1.52602
<i>C4_02040W_A</i>	0.0017617	2.18667	1.40654	2.85333	1.83537
<i>PEP8</i>	0.000853292	2.18439	1.22157	2.27907	1.27452
<i>CDC48</i>	0.005672	2.18011	1.45069	1.62354	1.08033
<i>C1_10420C_A</i>	0.000322908	2.17872	1.58502	2.10213	1.5293
<i>CR_08050C_A</i>	2.27E-06	2.17813	1.06199	1.96296	- 1.04484
<i>C2_05800C_A</i>	0.00146236	2.17742	1.41289	2.25269	1.46173

<i>C4_06990W_A</i>	0.0051686	2.17687	1.07872	2.33333	1.15625
<i>CWC22</i>	0.00040551	2.17647	1.2	1.52941	-1.1859
<i>CR_06030C_A</i>	1.94E-05	2.17391	1.05352	1.92935	- 1.06952
<i>BUL1</i>	0.00300174	2.17352	1.21538	1.18721	- 1.50633
<i>SKO1</i>	0.0051283	2.17293	1.3941	2.80451	1.79931
<i>CTA1</i>	0.000882896	2.17054	1.73684	1.76744	1.41429
<i>C4_06940C_A</i>	0.00140002	2.16883	1.39521	2.16883	1.39521
<i>C1_01920W_A</i>	0.00287428	2.16867	-1.03153	1.37952	- 1.62162
<i>PHO88</i>	0.000609472	2.16854	-1.22846	1.8427	- 1.44569
<i>VPS8</i>	0.00171315	2.16779	1.16797	1.71812	- 1.08027
<i>CRL1</i>	0.00499458	2.1676	-1.20494	2.72626	1.04381
<i>C3_02760C_A</i>	1.85E-05	2.16702	1.28844	1.57388	- 1.06864
<i>C2_10730W_A</i>	0.00650346	2.16667	-2.8	- 1.28571	-7.8
<i>NBN1</i>	2.81E-05	2.16667	1.04118	2.02381	- 1.02825
<i>CR_00290W_A</i>	0.00895066	2.16601	1.03963	1.29644	- 1.60704
<i>FHL1</i>	0.000961068	2.16541	-1.43539	1.92105	- 1.61798
<i>CR_08720W_A</i>	0.00148412	2.16477	1.26613	1.40909	- 1.21338
<i>POL32</i>	0.00570785	2.16438	-1.2233	1.72603	- 1.53398
<i>C1_04990C_A</i>	0.00113139	2.16327	1.15789	1.16327	- 1.60606
<i>SUC1</i>	0.00321552	2.16327	1.18533	2.64286	1.44811
<i>ISN1</i>	0.00829004	2.1625	-1.03521	1.53125	- 1.46197
<i>QDR3</i>	1.55E-05	2.16239	1.11304	1.96581	1.01186
<i>C3_07350W_A</i>	0.0106366	2.16234	-1.02583	1.80519	- 1.22878
<i>C3_07660W_A</i>	0.00113093	2.16088	-1.2398	1.53312	- 1.74745
<i>C5_03670C_A</i>	0.00438566	2.16071	-1.0099	1.82143	- 1.19802
<i>LAP41</i>	0.00322348	2.16022	1.20608	1.68232	- 1.06467
<i>HOL4</i>	6.31E-05	2.16	-1.3518	2.44	- 1.19668
<i>KSR1</i>	0.000666704	2.15957	1.28906	2.7234	1.62562
<i>CR_08450C_A</i>	0.0051588	2.15789	1.07042	3.73684	1.85366
<i>C1_05120W_A</i>	0.00363574	2.15625	1.08163	1.8375	- 1.08491
<i>SLY41</i>	0.000199894	2.15566	1.41108	1.61792	1.05908

CR_05440W_A	2.46E-05	2.15541	1.10981	2.89189	1.48903
C7_01230C_A	0.000110826	2.15357	1.22186	2.22143	1.26036
C1_02220C_A	0.00804356	2.15123	1.48231	1.65741	1.14204
CTA3	0.00074352	2.14875	1.31385	2.84974	1.74247
GLO1	8.33E-05	2.1456	1.1991	1.37546	-1.3009
C7_00260C_A	0.00184497	2.14416	1.14028	2.15332	1.14514
C7_02450W_A	0.000420695	2.14286	1.30368	2.32857	1.41667
MAK32	0.000345685	2.14286	1.13077	1.42857	- 1.32653
RAD59	0.00181888	2.14286	1.17073	2.92857	1.6
RLM1	0.00365457	2.14286	-1.2	1.54286	- 1.66667
C1_00530C_A	0.00785259	2.14	1.19774	2.832	1.58505
CR_00280C_A	0.00464152	2.13889	1.32308	1.80556	1.11688
TUS1	0.00161454	2.13848	1.30613	2.44752	1.49489
C4_03370C_A	0.00105761	2.13793	1.42553	2.83621	1.89113
C4_02700W_A	0.00359143	2.13725	-1.02186	1.83333	- 1.19126
ZCF30	0.000308158	2.13497	1.58919	2.26994	1.68966
C1_01210W_A	0.00387727	2.13278	1.26479	1.47303	- 1.14477
CR_04720C_A	1.74E-05	2.13276	1.41611	1.54138	1.02344
SEH1	0.000983021	2.13151	1.39032	2.66027	1.73522
C6_03910C_A	0.00337664	2.13043	1.35075	1.94203	1.23129
CRN1	0.00774714	2.12941	1.21692	2.18971	1.25138
C2_03340W_A	0.00016084	2.12889	1.21296	2.4	1.36743
NIT3	0.00336198	2.1286	-1.04386	2.11086	- 1.05263
C6_04470C_A	0.000537346	2.12785	1.16142	1.9217	1.04891
C4_04930C_A	1.09E-05	2.125	1.1791	1.675	- 1.07595
GDA1	0.010619	2.1244	-3.12821	1.7512	- 3.79487
SGS1	0.0043164	2.12319	-1.31949	2.99275	1.06826
C7_00340C_A	9.90E-06	2.12116	1.62835	1.9324	1.48344
C2_09760W_A	0.0103809	2.12069	1.38596	1.96552	1.28455
DBF4	0.00061652	2.11864	-1.40157	1.50847	-1.9685
CTA4	0.00065889	2.11765	1.1944	2.2872	1.29003
TLO10	0.00294397	2.11765	1.43571	- 1.21429	- 1.79104
CRP1	0.00202809	2.11743	-1.06795	1.57355	- 1.43708
YPT53	8.06E-05	2.11504	1.81633	1.73451	1.48954
C2_10460C_A	0.00444356	2.11082	-1.21685	1.79156	- 1.43369
SIR2	0.00165018	2.10989	1.28662	1.72527	1.05208
CR_00750C_A	0.0111119	2.10959	1.21875	3.06849	1.77273
MAE1	0.00053315	2.10254	-1.66253	1.70339	- 2.05211

C1_07340W_A	0.00681936	2.10169	1.04145	2.27845	1.12903
C2_02920W_A	0.00135857	2.09984	1.32903	1.74718	1.10583
C5_02820C_A	0.00173959	2.09375	1.22222	1.125	- 1.52273
C1_01190C_A	0.00488075	2.09231	1.19142	2.33077	1.32721
C5_02050W_A	0.0073741	2.09006	1.34516	2.3076	1.48517
CR_07600W_A	0.00582141	2.08978	-1.29412	1.22601	- 2.20588
CR_10620C_A	0.00214992	2.08922	-1.03448	1.67286	- 1.29195
EHT1	0.00216039	2.08861	1.8584	2.88291	2.56515
MAK21	0.00884767	2.08818	-2.77073	1.00176	- 5.77561
GPH1	0.000642131	2.08733	1.25484	1.71032	1.02819
IFF4	0.00536154	2.08727	1.59054	2.69091	2.05052
C3_00300W_A	0.000156395	2.0871	1.04577	1.83226	- 1.08923
PRO1	0.00623846	2.08608	-1.22336	3.02278	1.18447
TRS33	4.48E-05	2.0855	1.12526	1.78067	- 1.04082
RAD23	0.0016686	2.08171	-1.11547	1.37599	- 1.68757
C1_00470C_A	6.86E-05	2.07792	1.2381	2.27273	1.35417
TVP18	6.53E-05	2.07692	-1.16993	1.96703	- 1.23529
C4_07100C_A	6.97E-05	2.07541	1.0046	1.24836	-1.6549
UGA1	0.00456516	2.07482	2.06315	1.91886	1.90808
CBP1	5.46E-06	2.07467	1.09117	2.28133	1.19987
C1_12400C_A	0.00118074	2.07407	1.10236	1.5679	-1.2
JEM1	1.74E-05	2.07407	1.31132	1.57037	- 1.00719
IRO1	7.56E-05	2.07143	1.58427	1.58929	1.21552
OPT6	0.00144345	2.07143	1.41546	2.46429	1.68391
C1_09980C_A	0.000880456	2.07116	1.44963	1.52434	1.06691
SGE1	7.88E-06	2.07101	1.3808	1.91124	1.27429
C5_03510C_A	0.000511003	2.07054	-1.10156	1.17012	- 1.94922
CR_05030W_A	0.00251563	2.0704	1.69659	2.2992	1.88408
CYM1	0.00191548	2.0694	1.17358	1.67192	- 1.05466
C2_07610C_A	0.00181339	2.06613	1.10128	1.56313	- 1.20023
OYE22	0.0108014	2.06522	1.4878	3.11957	2.24737
C3_01690W_A	0.00987561	2.06486	-1.28669	2.03784	- 1.30375
PGI1	0.00103833	2.06387	1.17302	2.04284	1.16107
FAA2	0.000712224	2.06087	1.33462	2.26087	1.46414
CSC25	0.00021689	2.05959	1.48272	1.74329	1.25501
CR_00110W_A	0.000102212	2.05936	1.30599	2.47717	1.57095

<i>DFG10</i>	0.0073432	2.05556	1.03268	2.83333	1.42342
<i>KRE5</i>	0.00253001	2.05385	1.36351	1.84103	1.22222
<i>UBA4</i>	0.00465594	2.05376	-1.77586	1.66129	-2.1954
<i>PRE3</i>	0.00469697	2.05222	1.12572	1.80679	- 1.00899
<i>C2_00640W_A</i>	0.00197457	2.04861	1.51653	1.68056	1.24407
<i>C5_01920C_A</i>	0.000479912	2.04667	1.06186	1.94	1.00651
<i>C5_04350C_A</i>	0.00111413	2.04605	-1.0036	1.83553	- 1.11871
<i>C1_14560C_A</i>	0.00107686	2.04603	1.01447	2.31381	1.14724
<i>C7_03680W_A</i>	0.000885272	2.04487	1.71154	2	1.67398
<i>CMK2</i>	0.0039052	2.04451	1.37	1.78042	1.19303
<i>RAD1</i>	0.00104776	2.0438	1.34235	2.60827	1.7131
<i>PRC2</i>	0.000421542	2.04379	1.54978	1.91361	1.45107
<i>VPS70</i>	0.000792622	2.03852	-1.00236	1.36437	- 1.49764
<i>C1_14310W_A</i>	0.00776723	2.03731	-1.12416	2.5	1.09158
<i>C7_04260W_A</i>	1.63E-05	2.03641	-1.04004	2.26942	1.07151
<i>C6_00850W_A</i>	0.000805834	2.03531	1.49405	1.3065	- 1.04269
<i>HMI1</i>	0.000294908	2.03425	1.19072	2.65753	1.55556
<i>C4_06740C_A</i>	0.00836848	2.03421	1.56658	1.93684	1.49159
<i>C7_03500W_A</i>	0.000175039	2.03378	1.31496	2.57432	1.66445
<i>C2_00230W_A</i>	1.47E-05	2.03346	1.18122	2.25651	1.31079
<i>C6_00290W_A</i>	0.00263796	2.03248	-1.19059	1.29393	- 1.87016
<i>CR_03960C_A</i>	0.000915126	2.03061	1.27854	2.23469	1.40704
<i>KTR4</i>	0.00386982	2.0303	-1.18182	1.9697	- 1.21818
<i>DBP2</i>	0.00622486	2.02961	-1.63529	1.26651	- 2.62059
<i>C1_01290C_A</i>	0.010258	2.02804	-1.13846	2.07477	- 1.11282
<i>ORC1</i>	0.0110142	2.0271	1.3834	2.57995	1.7607
<i>C1_10560C_A</i>	0.000340904	2.02649	1.4216	1.90066	1.33333
<i>GSL2</i>	0.00241388	2.02626	1.12991	1.61707	- 1.10898
<i>VPS33</i>	0.00545597	2.02591	1.35255	2.33679	1.5601
<i>C3_00380C_A</i>	8.04E-05	2.02564	1.46108	2.14103	1.5443
<i>POB3</i>	0.00075341	2.02497	1.07382	2.19834	1.16575
<i>HEX1</i>	8.46E-05	2.02096	1.11464	2.16766	1.19556
<i>MID1</i>	0.000207266	2.0202	1.25346	2.19192	1.36
<i>C4_03680C_A</i>	0.00868845	2.01818	1.37824	1.75455	1.1982
<i>MED20</i>	0.00525996	2.01786	-1.17797	2.48214	1.04425
<i>ORC3</i>	0.0035707	2.01633	1.55672	1.94286	1.5
<i>PRE9</i>	0.00426435	2.0149	1.33501	1.85102	1.22643
<i>MIM1</i>	0.00386831	2.01471	1.44828	2.13235	1.53285
<i>LAG1</i>	0.00372111	2.01258	-1.31034	1.19497	-2.2069

<i>SWD1</i>	0.00139418	2.01111	1.12676	2.36667	1.32597
<i>PAN3</i>	0.00700095	2.01003	1.31789	2.09365	1.37271
<i>SRP101</i>	0.000790417	2.00997	1.19003	2.13289	1.26281
<i>C2_01530C_A</i>	0.0100732	2.00755	1.23014	2.01132	1.23246
<i>SEC24</i>	0.0110562	2.00537	1.17429	2.14511	1.25611
<i>ZCF20</i>	0.00371508	2.00386	1.35794	1.72587	1.16956
<i>STT4</i>	0.00680878	2.00251	1.42866	1.36295	- 1.02841
<i>C3_03250W_A</i>	8.88E-05	2.0006	1.29321	1.73778	1.12332
<i>PAM16</i>	0.00434008	-2.04132	1.35227	1.06883	2.95041
<i>C2_08100W_A</i>	0.0012218	-2.04151	1.1263	- 1.19918	1.91744
<i>MRPL40</i>	0.00517997	-2.10211	1.40404	- 1.00505	2.93662
<i>PET9</i>	0.00202111	-2.1155	-1.09499	- 1.41579	1.36459
<i>C2_03950W_A</i>	0.0057961	-2.15789	1.29355	- 1.05806	2.63816
<i>C2_03560C_A</i>	0.0044531	-2.1754	1.18354	- 1.06229	2.42369
<i>C3_01420C_A</i>	0.00546447	-2.19178	3.01193	- 1.90931	3.45753
<i>C4_00660W_A</i>	0.00305536	-2.22289	1.09251	- 1.62555	1.49398
<i>C5_03440W_A</i>	0.000966075	-2.22581	1.03125	- 2.15625	1.06452
<i>FOX2</i>	0.00969007	-2.27543	2.69217	- 1.64257	3.72943
<i>C5_00820W_A</i>	0.00263915	-2.29834	1.30505	1.04808	3.14365
<i>C5_01050C_A</i>	0.00119561	-2.29885	1.06391	1.33	3.25287
<i>C2_05300C_A</i>	0.000434142	-2.30189	1.08744	- 1.05172	2.38005
<i>C1_06070W_A</i>	0.0101399	-2.34615	1.39205	- 1.03977	3.14103
<i>GRE3</i>	0.000975346	-2.34833	1.19643	- 1.76566	1.59125
<i>HSP60</i>	0.00204958	-2.34983	1.41505	1.06724	3.54872
<i>C3_01850W_A</i>	0.00366935	-2.36129	-1.07407	- 1.26207	1.74194
<i>C4_03410W_A</i>	0.00441037	-2.37438	1.49474	- 1.26842	2.79803
<i>C5_03710C_A</i>	0.00957827	-2.39759	1.62802	- 1.92271	2.03012
<i>C2_03110W_A</i>	0.00122376	-2.41892	-1.11538	- 2.05747	1.05405
<i>C6_03730C_A</i>	0.00909322	-2.42177	1.2	- 1.13016	2.57143
<i>C2_04790C_A</i>	0.000499069	-2.44444	1.37113	- 1.36082	2.46296
<i>MRPS9</i>	0.000142744	-2.44484	1.22388	-1.1393	2.62633

<i>FUM12</i>	0.00130929	-2.45429	1.61975	- 1.29624	3.06683
<i>THI20</i>	3.19E-05	-2.45506	-1.22222	- 3.31061	- 1.64815
<i>STB3</i>	0.00170783	-2.45902	1.15925	1.29778	3.69945
<i>TUF1</i>	0.00750592	-2.46383	1.15493	-1.0677	2.66513
<i>C1_09020W_A</i>	0.00875056	-2.49786	1.32365	- 1.54425	2.14103
<i>ALT1</i>	0.00169125	-2.57246	1.4135	-1.2515	2.90545
<i>MRPL6</i>	0.00345191	-2.57658	1.07087	- 1.12598	2.45045
<i>MNN4</i>	0.00796292	-2.57711	1.0591	-1.6112	1.69403
<i>RPS3</i>	0.0028294	-2.58212	-1.97019	- 1.51256	- 1.15411
<i>MRP7</i>	0.0043297	-2.62437	1.05336	- 1.19954	2.30457
<i>C1_00190C_A</i>	0.00997715	-2.66942	2.15825	- 1.08754	5.29752
<i>C1_08920W_A</i>	0.0111143	-2.67568	1.05738	- 1.62295	1.74324
<i>C5_03530C_A</i>	0.0107422	-2.68182	-1.68421	- 1.84375	- 1.15789
<i>PCK1</i>	0.00752043	-2.68614	-1.64045	- 1.08786	1.50519
<i>MRPL10</i>	0.00352767	-2.68966	-1.01362	1.19231	3.16379
<i>C7_01600W_A</i>	0.00632068	-2.79412	-1.14286	- 1.23698	1.97647
<i>C4_04820C_A</i>	0.00285873	-2.8375	1.2636	1.05286	3.775
<i>MRP17</i>	0.0073934	-2.84	-1.23529	- 1.69048	1.36
<i>CDA2</i>	0.00246206	-2.85714	-1.5	- 1.66667	1.14286
<i>TIM12</i>	9.26E-05	-2.87097	-1.21053	- 1.93478	1.22581
<i>MRPL3</i>	0.00584603	-2.94186	-1.3133	- 1.65359	1.35465
<i>IDP2</i>	0.000199978	-2.9528	1.55809	-1.5172	3.03238
<i>C2_07190C_A</i>	0.00123233	-3.04525	-1.00288	1.03566	3.1448
<i>C2_01450C_A</i>	0.000196583	-3.08333	1.46479	- 2.08451	2.16667
<i>MDM34</i>	0.00364614	-3.10193	1.85566	- 1.76066	3.26931
<i>C2_00860C_A</i>	0.000536637	-3.13793	-2.18182	-11.375	- 7.90909
<i>C2_09880C_A</i>	0.00229767	-3.25112	2.36232	- 5.25362	1.46188
<i>MET14</i>	0.00112295	-3.3037	-4.61702	-2.0553	- 2.87234
<i>MPRL36</i>	0.000366845	-3.44872	-1.2125	-1.3866	2.05128
<i>FET3</i>	4.26E-05	-3.53244	-2.67446	- 3.88164	- 2.93885

YNK1	0.00238046	-3.59839	-2.56182	- 1.90774	- 1.35818
MAL2	1.67E-06	-4.11696	1.49322	- 1.90786	3.22222
C5_04940W_A	0.00181067	-4.43158	1.775	-2.105	3.73684
C2_00890W_A	0.00566429	-4.57143	-1.08	- 1.18519	3.57143
PXP2	1.16E-06	-12.2036	2.64897	- 4.18215	7.72973

Genes upregulated in the pho4Δ in minus Pi compared to Pi rich medium					
Alias	p-value (pho4-Pi vs. pho4+Pi)	Fold Change (pho4-Pi vs. pho4+Pi)	pho4+Pi vs. WT+Pi	pho4-Pi vs. WT- Pi	WT-Pi vs. WT+Pi
C1_12140W_A	4.81E-08	2.16062	1.58522	4.04854	-1.18204
CR_08920W_A	1.33E-08	2.81583	1.13883	3.44046	-1.07288
C1_08610C_A	5.14E-06	2.0149	2.96286	4.24888	1.40505
C2_07410W_A	6.45E-06	2.01252	2.85268	3.41567	1.6808
C2_01630W_A	0.000264676	2.0209	335	75.2222	9
C5_04980W_A	1.35E-05	3.32799	20.0357	28.2879	2.35714
C1_03870C_A	9.57E-06	2.081	1.96933	2.672	1.53374
C1_02270C_A	4.44E-07	2.29417	- 1.39983	2.80952	-1.71429
C7_02130W_A	8.91E-06	3.25	?	4.875	?
CR_03120W_A	2.80E-05	2.21707	1.62189	6.36335	-1.76963
C3_07470W_A	3.04E-05	2.26667	3.64865	2.78182	2.97297
C4_03340C_A	6.27E-05	2.33333	4.64286	4.64286	2.33333
CR_08400C_A	1.70E-05	2.12941	1.63462	3.35185	1.03846
C6_02110W_A	4.49E-06	2.06707	1.53271	1.71212	1.85047
C4_06430C_A	1.72E-05	2.09705	1.41916	2.84	1.0479
C1_06860W_A	2.73E-05	3.43103	4.46154	4.42222	3.46154
C3_01940C_A	7.46E-05	2.09454	2.125	1.70427	2.61161
C5_02990W_A	8.85E-06	2.5	1.19231	2.42188	1.23077
C1_00190C_A	9.77E-05	2.15825	- 1.08754	5.29752	-2.66942
C3_01420C_A	6.70E-06	3.01193	- 1.90931	3.45753	-2.19178
C5_04790C_A	0.000295419	2	2.42857	1.94286	2.5
CR_06870C_A	0.00113562	2.3913	4.6	9.16667	1.2
C5_02800C_A	0.00187086	2.42857	?	8.5	?
C1_06410W_A	3.39E-05	2.1102	1.16667	1.78276	1.38095
C2_01690W_A	9.80E-05	2.16462	- 1.09982	3.07463	-1.56219
CR_06320C_A	7.15E-05	2.21429	1.22807	1.38393	1.96491
C1_10980W_A	3.20E-05	11.5	2	3.28571	7
C5_01260W_A	0.000538063	2.04211	1.9	1.59016	2.44
C5_02980C_A	0.000104275	2.38889	1.14894	2.30357	1.19149
CR_05040W_A	0.000598167	2.30645	1.12727	4.46875	-1.71875

C2_05120C_A	0.00197348	2.05882	1.88889	3.88889	1
C4_03500C_A	8.97E-05	13.5	?	2.07692	?
C1_09440W_A	0.000113681	2.29424	1.01078	2.329	-1.00433
C5_04380C_A	0.00277068	2.47619	5.25	3.46667	3.75
CR_09100C_A	0.00469631	2.04981	-	-	1.67221
			1.61303	1.31589	
C5_03210C_A	7.51E-05	4.2	-1.8	2.33333	1
C1_03620C_A	0.00039274	-2.02644	1.6478	1.12906	-1.3885
CR_04820W_A	0.000375886	2.08915	1.08861	1.47268	1.5443
C7_00870W_A	0.0025862	2.27869	1.525	1.18803	2.925
CR_01430W_A	0.00307994	2.16822	2.01887	1.49677	2.92453
C6_02450W_A	0.00336585	2.55	3.07692	1.52239	5.15385
C1_12910W_A	0.00261384	-15	?	-14	?
C7_01880C_A	0.00417274	-2.23529	4.75	-	2.375
				1.11765	
CR_08480C_A	0.000891071	-2.88571	1.58087	1.04651	-1.9103
C6_02300C_A	0.00232275	4.14286	3.5	2.9	5
C1_00160C_A	0.00451475	-4.39604	1.54033	-	1.9575
				5.58663	
C1_06430C_A	0.000869564	10	-2	5	1
CR_07610C_A	0.000869564	10	-2	2.5	2
C4_03770W_A	0.000417851	3.28571	-	1.76923	-1.05769
			1.96429		
C1_11160C_A	0.000949133	-3.26923	1.77083	-	1.52083
				2.80769	
C2_00170C_A	0.00416873	-5.15278	-	-	-1.36593
			1.16712	4.40278	
C1_13500C_A	0.00253751	-3.18614	3.07248	-	1.01076
				1.04815	
C1_11900C_A	0.00504715	2.36066	1.38636	2.08696	1.56818
CR_05160C_A	0.00523975	2	1.15	1.35294	1.7
C2_09910C_A	0.00223824	-10	5	-3	1.5
C1_02330C_A	0.00340773	-3.12033	1.90139	-	-1.50667
				1.08921	
C3_07050W_A	0.00211663	3.46154	-	1.875	1.26316
			1.46154		
C5_04010C_A	0.00514769	2.72727	1.1	1.57895	1.9
C6_00630W_A	0.00261731	4	-1.75	2.28571	1
ACO2	0.00547299	-4.27154	1.04203	-2.6236	-1.56246
ADH2	5.66E-06	2.39417	-	-	-1.32422
			3.25264	1.02594	
ALD6	3.66E-05	2.16694	-	2.79741	-1.3944
			1.08013		
ARG3	0.000607246	2.35875	-	2.51107	-1.14576
			1.07626		
ASC1	0.00153591	-4.45835	1.25574	-2.0488	-1.7329
CCC1	4.98E-05	2.49861	-1.1727	1.69245	1.25891
CDG1	0.00124549	2.02632	2.59091	3.01961	1.73864

<i>CEF3</i>	0.00423763	-4.4386	1.25617	- 4.00764	1.13421
<i>CEK2</i>	0.00323999	2.08333	?	18.75	?
<i>CHL4</i>	0.000452459	2.46875	6.4	3.16	5
<i>CHT3</i>	5.94E-05	2.18411	2.09756	2.95026	1.55285
<i>CIT1</i>	3.24E-11	3.72898	1.26927	7.73054	-1.6333
<i>COX17</i>	0.000330711	2.12821	1.85714	8.3	-2.1
<i>CRD2</i>	7.39E-09	4.58427	1.93478	4.68966	1.8913
<i>CTA9</i>	1.61E-05	2.09067	1.13196	1.88993	1.2522
<i>CTN1</i>	9.98E-07	2.99112	1.2072	6.00892	-1.66412
<i>CYB2</i>	4.37E-07	2.19921	2.11092	3.01503	1.53974
<i>DAD3</i>	0.00279089	2.05882	1.88889	2.5	1.55556
<i>DDC1</i>	0.000461749	3.58824	- 1.58824	1.84848	1.22222
<i>DOT5</i>	1.89E-08	2.13643	1.55662	2.53411	1.31234
<i>DRE2</i>	6.49E-07	2.48023	1.57333	2.88816	1.35111
<i>DRG1</i>	0.00410843	-3.02016	1.17031	- 2.03226	-1.26984
<i>FDH1</i>	0.000359095	2.47816	2.43023	13.9617	-2.31826
<i>FGR15</i>	4.80E-06	2.05072	1.91667	2.04332	1.92361
<i>FGR41</i>	5.52E-07	2.16477	3.03448	3.14876	2.08621
<i>FMA1</i>	8.88E-08	3.46467	2.02153	4.55344	1.53816
<i>FOX2</i>	3.83E-05	2.69217	- 1.64257	3.72943	-2.27543
<i>GAP2</i>	0.000471759	2.50751	1.70187	1.62346	2.62862
<i>GCA1</i>	5.32E-06	2.02782	1.91819	6.29175	-1.61752
<i>GCA2</i>	3.73E-06	2.33065	1.77714	5.5366	-1.33673
<i>GCY1</i>	4.06E-05	2.00849	4.07042	2.78699	2.93342
<i>GSG1</i>	5.30E-05	2	1.93056	1.89116	2.04167
<i>HCH1</i>	0.00282565	-2.00781	1.43575	- 1.03906	-1.34586
<i>HPD1</i>	9.61E-09	3.24383	1.92475	23.8864	-3.82576
<i>HSP30</i>	2.51E-06	3.19485	1.23402	4.55646	-1.15572
<i>HSP78</i>	1.39E-09	2.2264	2.12707	3.51965	1.34551
<i>HTS1</i>	0.00158563	-3.28866	3.90812	1.60331	-1.34917
<i>ICL1</i>	1.41E-09	3.2107	1.1048	5.97523	-1.68451
<i>IFE2</i>	2.43E-08	2.40175	2.41357	5.04535	1.14894
<i>IMH3</i>	0.00378562	-4.78279	1.46241	- 3.07787	-1.06258
<i>JEN2</i>	1.27E-05	2.28635	1.6118	5.70389	-1.54781
<i>KRS1</i>	0.00362451	-3.96605	1.38619	- 2.44753	-1.16898
<i>MDH1-1</i>	9.77E-08	2.63981	1.26198	4.42234	-1.32748
<i>MED21</i>	0.00194135	2.07692	2.16667	2.57143	1.75
<i>MLS1</i>	2.58E-09	2.79079	- 1.03714	3.18848	-1.18493
<i>MVD</i>	0.00457212	-2.41121	2.19108	1.03382	-1.13768
<i>OPT3</i>	3.66E-08	2.09354	2.28924	2.16127	2.21749

<i>OPT4</i>	7.35E-11	2.76923	1.8412	12.5053	-2.45263
<i>PGA32</i>	0.00183067	-2.65	3.78571	-1.6	2.28571
<i>PLB3</i>	1.92E-06	2.41056	1.54718	2.94305	1.26725
<i>POT1</i>	5.83E-07	2.09455	- 1.24046	2.04399	-1.21052
<i>POX1-3</i>	5.13E-05	2.53952	- 2.14316	2.30128	-1.9421
<i>RBR1</i>	0.00130615	2.68692	10.7	1.6523	17.4
<i>RPC10</i>	0.00290757	-2.68966	1.48571	- 2.89655	1.6
<i>RPL11</i>	0.00258723	-3.01647	1.30579	- 1.10368	-2.09306
<i>RPL14</i>	0.00486613	-2.14989	1.73807	1.32826	-1.64298
<i>RPL23A</i>	0.00259554	-2.53787	1.44929	1.06581	-1.86635
<i>RPL3</i>	0.00401666	-3.20171	1.32105	-1.0619	-2.28233
<i>RPL30</i>	0.00265244	-3.27287	1.55057	1.01631	-2.14519
<i>RPL37B</i>	0.00101121	-2.68247	1.54605	1.06011	-1.83934
<i>RPP1B</i>	0.000665219	-2.8186	2.65408	2.07765	-2.20644
<i>RPP2B</i>	0.00344511	-4.1741	1.56924	1.22126	-3.24849
<i>RPS21</i>	0.00299635	-3.61481	- 1.02652	- 1.54716	-2.39838
<i>SEF2</i>	2.06E-05	3.2449	1.04255	3.74118	-1.10588
<i>SOU1</i>	0.00534969	-3.0481	1.96091	- 2.21772	1.42671
<i>STF2</i>	7.34E-05	2.22485	1.4394	3.78445	-1.18173
<i>TES15</i>	3.35E-05	2.03333	1.875	4.18145	-1.09677
<i>TIF34</i>	0.00130419	-2.69186	1.51555	- 1.76163	-1.00825
<i>tP(AGG)1</i>	0.00097059	-10.5	7	-3	2
<i>UGA1</i>	6.34E-06	2.06315	1.91886	1.90808	2.07482
<i>YMC1</i>	0.000958963	-6.94737	2.75	- 7.89474	3.125

Appendix 2. Entire RNA Seq Dataset.

Romanowski, K., Zaborin, A., Valuckaite, V., Rolfes, R.J., Babrowski, T., Bethel, C., Olivas, A., Zaborina, O. and Alverdy, J.C. (2012) 'Candida albicans isolates from the gut of critically ill patients respond to phosphate limitation by expressing filaments and a lethal phenotype', *PLoS One*, 7(1), p. e30119.